Sustainable synthesis of 2-pyrones and application of biobased 2-pyrones

Atypical reactivity of anthracene derivatives

Dissertation

Zur Erlangung des Doktorgrades der Naturwissenschaften

Dr. rer. nat.

der Fakultät für Chemie und Pharmazie

der Universität Regensburg

vorgelegt von

Michael Leitner

aus Prien am Chiemsee

Regensburg 2020

Die Arbeit wurde angeleitet von: Prof. Dr. Oliver Reiser

Promotionsgesuch eingereicht am: 02.07.2020

Promotionskolloqium am:

Prüfungsauschuss:	Vorsitz:	Prof. Dr. Oliver Tepner
	1. Gutachter:	Prof. Dr. Oliver Reiser
	2. Gutachter:	Prof. Dr. Alexander Breder
	3. Gutachter:	Prof. Dr. Frank-Michael Matysik

Der experimentelle Teil der vorliegenden Arbeit wurde im Zeitraum von November 2016 bis Januar 2020 unter der Anleitung von Prof. Dr. Oliver Reiser am Institut für Organische Chemie der Universität Regensburg angefertigt.

Besonders bedanken möchte ich mich bei Herrn Prof. Dr. Oliver Reiser für die Aufnahme in seinen Arbeitskreis, die Überlassung des interessanten Themas, die anregenden Diskussionen und die stete Unterstützung.

Für meine Familie

Table of contents

A Introduction....1
1 2-Pyrone – a privileged heterocycle and widespread motif in nature....1
2 Synthesis of 2-pyrones....3
2.1 Synthesis from renewable resources....3
2.2 Transition metal-catalyzed synthesis....5
2.3 Transition metal-free synthesis....18
3 Reactivity of 2-pyrones....25
3.1 Ring-opening....25
3.2 [2+2]-Cycloaddition....28
3.3 [4+2]-Cycloaddition....29
3.4 Other cycloadditions....33
3.5 Lactamization....35
3.6 Conjugate addition....36
3.7 Cross-coupling reactions....39
3.8 C-H activation....42
3.9 2-Pyrone ligands....45
B Main part....47
1 Sustainable synthesis of 2-pyrones....47
1.1 Introduction....47
1.2 Big-scale synthesis of unsubstituted 2-pyrone....50
1.3 Synthesis of naturally occurring 6-alkyl 2-pyrones....55
1.4 Investigations towards the synthesis of 6-alkyl-4-methoxy-2-pyrones....58
2 Application of 2-pyrones derived from renewable resources....61
2.1 Synthesis of 3-substituted phthalides....61
2.1.1 Introduction....61
2.1.2 Synthesis of 3-substituted phthalides by Diels-Alder reaction of pyrones....63

2.2 [4+2]-Cycloaddition of 6-acetyl 2-pyrone with alkenes 70
2.3 Visible light-mediated [4+2]-cycloaddition of 2-pyrones 73
2.4 Cyclopropanation of 2-pyrone and 2-pyridinone and follow-up transformation 77
2.4.1 Cyclopropanation of 2-pyrone and 2-pyridinone 77
2.4.2 Follow-up transformations of cyclopropanated pyrone 85
3 Atypical reactivity of anthracene derivatives 93
3.1 Diels-Alder reaction with atypical regioselectivity 93
3.1.1 Diels-Alder reaction of anthracene derivatives 93
3.1.2 Computational studies 102
3.2 Atypical regioselectivity in electrophilic aromatic substitution reactions 108
3.3 Investigation of the photodimerization of pyrrolidine substituted anthracenes 111
C Summary 115
D Zusammenfassung 119
E Experimental Part 123
1 General information 123
2 Sustainable synthesis of 2-pyrones 126
3 Application of 2-pyrones derived from renewable resources 137
4 Atypical reactivity of anthracene derivatives 148
5 Computational details 161
5.1 Thermodynamic data 162
5.2 Bond orders 164
5.3 Marcus Analysis 168
5.4 FMO Analysis 170
5.5 NBO Analysis 171
5.6 IRC plots with DMAD as dienophile 173
5.7 IRC plots with maleic anhydride as dienophile 176
F Appendix 182
1 NMR-spectra 182

2 GC-spectra....246
3 Chiral HPLC data....247
4 X-ray data....250
5 Curriculum Vitae....255
G References....257
H Acknowledgment....272
I Declaration....275

Abbreviations

Ac	acetyl
acac	acetylacetone
Ac_2O	acetic anhydride
AcO	acetoxy
Am	amyl
APCI	atmospheric pressure chemical ionization
aq.	aqueous
Ar	aryl
atm	atmosphere
BEP	Bell-Evans-Polanyi
BINOL	1,1-binaphthol
BO	bond order
Boc	*tert*-butyloxycarbonyl
Box	bis(oxazoline)
bpy	bipyridine
BQ	benzoquinone
brine	saturated NaCl solution
Bu	butyl
c	concentration
cat.	catalyst
CDI	1,1‘-carbonyldiimidazole
ClBcat	*B*-chlorocatecholborane
cod	1,5-cyclooctadiene
Cp*	pentamethylcyclopentadiene
Cy	cyclohexyl
Cyp	cyclopentyl
d	day(s)
DABCO	1,4-diazabicyclo[2.2.2]octane
dap	2,9-bis(*para*-anisyl)-1,10-phenanthroline
dba	dibenzylideneacetone
DBU	1,8-diazabicyclo[5.4.0]undec-7-ene
DCC	*N*,*N*‘-dicyclohexylcarbodiimide
DCM	dichloromethane
dcype	1,2-bis(dicyclohexylphosphino) ethane
DEPT	distortionless enhancement by polarization transfer
dF(CF_3)ppy	(2-(2,4-difluorophenyl)-5(trifluoromethyl)pyridine
DIBAL-H	diisobutylaluminium hydride
DIPEA	*N*,*N*-diisopropylethylamine
DMAD	dimethyl acetylenedicarboxylate
DMAP	4-dimethylaminopyridine
DMDO	dimethyldioxirane
DMF	dimethylformamide
DMSO	dimethyl sulfoxide

dppf	1,1‘-bis(diphenylphosphino) ferrocene
dr	diastereomeric ratio
dtp-bpy	4,4‘-di-t*ert*-butyl-2,2‘-dipyridyl
DuanPhos	2,2‘-di-*tert*-butyl-2,3,2‘,3‘-tetrahydro-1*H*,1’*H*-(1,1‘) biisophosphindolyl
EA	ethyl acetate
EDC	1-ethyl-3-(3-dimethyl-aminopropyl)carbodiimide
EDG	electron-donating group
ee	enantiomeric excess
EI	electron impact
equiv	equivalent(s)
ESI	electrospray ionization
ET	energy transfer
Et	ethyl
et al.	and others
Et_2O	diethyl ether
EWG	electron-withdrawing group
Fc	ferrocene
FDA	U.S. Food and Drug Administration
FID	flame ionization detector
FMO	frontier molecular orbital
FT	Fourier transform
FVT	flash vacuum thermolysis
GC	gas chromatography
h	hour(s)
Hept	heptyl
HFIP	hexafluoroisopropanol
HOBT	1-hydroxybenzotriazole
HOMO	highest occupied molecular orbital
HPLC	high-performance liquid chromatography
HRMS	high-resolution mass spectrometry
hν	light
i-	*iso*-
IEDDA	inverse electron-demand Diels-Alder
IPr	1,3-bis(2,6-diisopropylphenyl) -1,3-dihydro-2*H*-imidazol-2-ylidene
IR	infrared
IRC	intrinsic reaction coordinate
ISC	intersystem crossing
L	undefined ligand
LA	Lewis acid
LB	Lewis base
LDA	lithium diisopropylamide
LED	light-emitting diode
LiHMDS	lithium bis(trimethylsilyl) amide

LG	leaving group
LOT	level of theory
LUMO	lowest unoccupied molecular orbital
M	molar
m-CPBA	*meta*-chloroperoxybenzoic acid
Me	methyl
MeCN	acetonitrile
MEP	minimum energy pathway
min	minute(s)
mp.	melting point
MS	mass spectrometry or molecular sieves
Ms	mesyl
MTAD	4-methyl-1,2,4-triazoline-3,5-dione
MW	microwave
m/*z*	mass-to-charge ratio
n-	*normal*-
NBO	natural bond orbital
NBS	*N*-bromosuccinimide
NHC	*N*-heterocyclic carbene
NMP	*N*-methyl-2-pyrrolidone
NMR	nuclear magnetic resonance
Nu	nucleophile
Oct	octyl
OLED	organic light-emitting diode
OTf	triflate
p	pressure
p-	*para*-
PE	petroleum ether
Pent	pentyl
Ph	phenyl
pin	pinacolyl
Piv	pivalate
ppy	2-phenylpyridine
Pr	propyl
Py	pyridine
Q-Phos	1,2,3,4,5-pentaphenyl-1‘-(di-*tert*-butylphosphino)ferrocene
R	arbitrary rest
rds	rate-determining step
R_f	retention factor
RMS	root mean square
rt	room temperature
s	second(s)
SCF	Self-Consistent-Field
Solphos	(7,7’-bis(diarylphosphino)-3,3’,4,4’-tetrahydro-4,4‘-dimethyl-8,8‘-bis-2*H*-1,4-benzooxazine
SPhos	2-dicyclohexylphosphino-2‘,6‘-dimethoxybiphenyl

T	temperature
t	time
t-	*tert*-
TBAB	tetrabutylammonium bromide
TBAF	tetrabutylammonium fluoride
TBMDS	*tert*-butyldimethylsilyl
THF	tetrahydrofuran
TLC	thin layer chromatography
TMS	trimethylsilyl
TS	transition state
Ts	tosyl
UV	ultraviolet
Vis	visible
vs.	versus
WHO	World Health Organization
X	arbitrary moiety

A Introduction

1 2-Pyrone – a privileged heterocycle and widespread motif in nature

Nature is an inimitable source of myriad heterocyclic molecules that are involved in all kinds of biochemical processes, exhibiting precious biological activities. Research of these natural products is one of the cornerstones of medicinal chemistry and plays a vital role in the discovery of new drugs. Consequently, the vast majority of drugs marketed over the past 35 years originate from various natural products either by consisting directly of naturally occurring compounds or are inspired by these entities.[1] 2-Pyrone (**1**), an unsaturated six-membered cyclic ester, constitutes a renowned representative of naturally occurring heterocycles which can be found in all domains of life, e.g., bacteria, fungi, microbes, marine organisms, insects, plants or animals (Figure 1).[2–4] In these systems, 2-pyrones fulfill important functions as intermediates or products in metabolism, as well as signaling molecules or defensive agents against predators.[3,5] But most importantly, natural 2-pyrones evince an extensive range of biological activities with immense therapeutic importance like HIV protease inhibiting, telomerase inhibiting, antifungal, anti-inflammatory, antimicrobial, cardiotonic, cytotoxic and neurotoxic effects.[2–7]

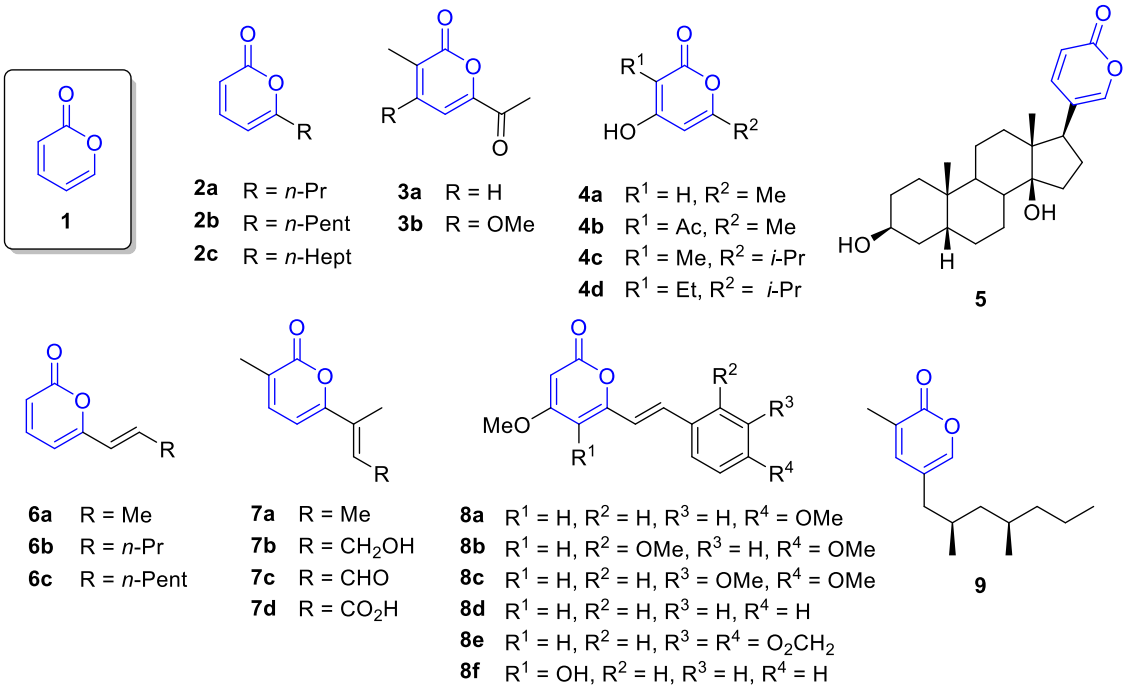

Figure 1. Selected examples of natural occurring 2-pyrones.[3–8]

Moreover, the privileged heterocyclic structure of 2-pyrones, accommodating the chemical behavior of conjugated dienes, lactones and arenes (30−35% resonance energy of benzene[7]), has been widely exploited for the synthesis of value-added products in synthetic organic chemistry, polymer chemistry and medicinal chemistry.[9,10] Herein, the versatile reactivity of pyrones reaches from cycloadditions to ring-opening reactions and cross-coupling reactions (Figure 2). Remarkably, functionalized pyrones show also interesting photophysical properties that can be delicately tuned by variation of donor-acceptor substituents indicating promising applications for organic light-emitting diode (OLED) displays and solid-state lightings.[11] Owing to their exquisite chemical and physical properties, 2-pyrones have attracted considerable attention to their synthesis and functionalization over the past decades (Figure 2). This review highlights synthetic strategies to the greatest extent divergent from traditional methods. Beyond that, the versatile reactivity of 2-pyrones is discussed encompassing their application in the synthesis of valuable products.

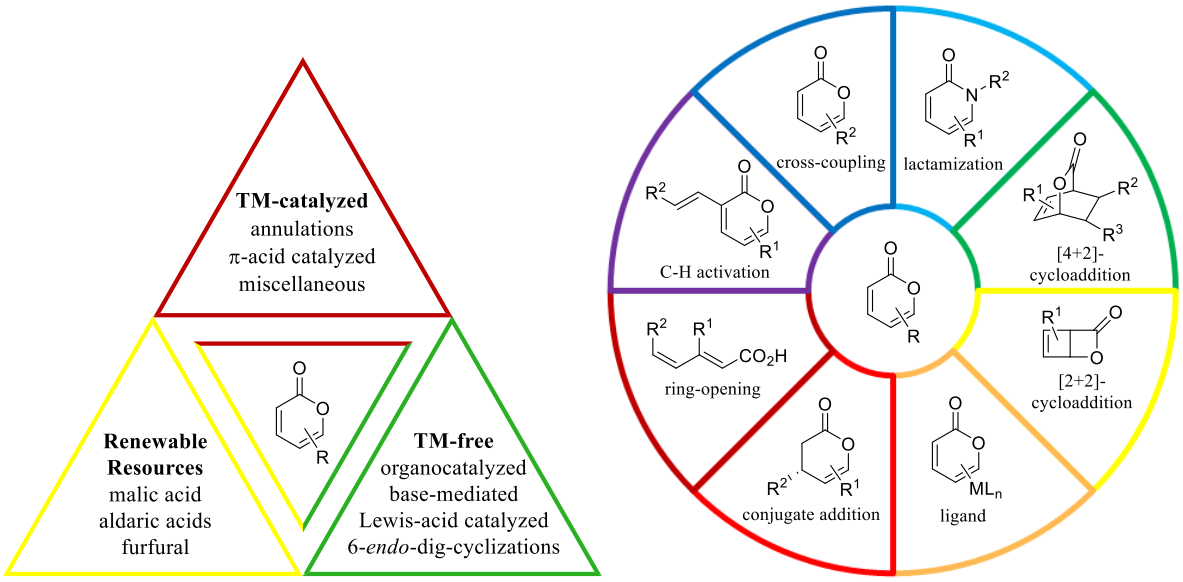

Figure 2. Overview of the synthetic strategies and versatile chemistry of 2-pyrones.

2 Synthesis of 2-pyrones

2.1 Synthesis from renewable resources

The growing endeavor of reducing fossil-based feedstocks has encouraged research for sustainable strategies to convert renewable resources into valuable chemicals. In 1891, one of the first documented syntheses of the 2-pyrone scaffold already utilized malic acid (**10**) as starting material, a renewable resource readily derived from the fermentation of glucose (Scheme 1).[12] The acid-catalyzed dehydration/decarboxylation of malic acid (**10**) afforded coumalic acid (**12**) via self-condensation of in situ formed formyl acetic acid (**11**). Coumalates are important platform molecules and until today several big-scale batch conditions[13] as well as continuous flow processes[14] have been developed for the synthesis of coumalic acid (**12**) from malic acid (**10**).

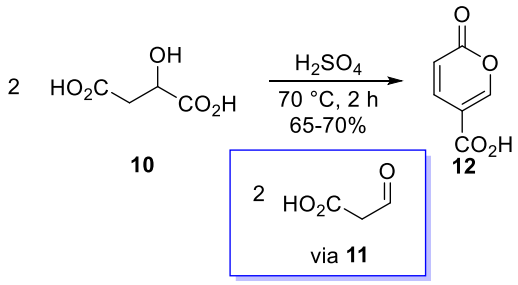

Scheme 1. Acid-catalyzed synthesis of coumalic acid (**12**) from malic acid (**10**).[12,13]

Recently, Sebastiano and co-workers reported a sustainable procedure toward the synthesis of pyrones starting from various biomass-based C6 sugar acids, also known as aldaric acids **13**.[15] Treatment of mucic acid (**13**, R = H) with acetic anhydride in a buffered medium yielded either 3-acetoxy-pyrone-6-carboxylic acid or the corresponding sodium salt **15** in good yields depending on the employed buffer base (NaOH, pyridine or NaOAc) (Scheme 2). This procedure was also verified for the conversion of two salts of glucaric acid (**13**, R = Ca, K). In both cases, the reaction was performed without the presence of a base, since the carboxylate anions were able to promote the reaction via intermediate **14** themselves (Scheme 2). Moreover, pyrones **15** were quantitatively converted with HCl to 3-hydroxy-2-oxo-2*H*-pyran-6-carboxylic acid (**16**) which afforded 3-hydroxy-pyrone derivative **17** by subsequent thermal decarboxylation under quite mild reaction conditions (Scheme 2).

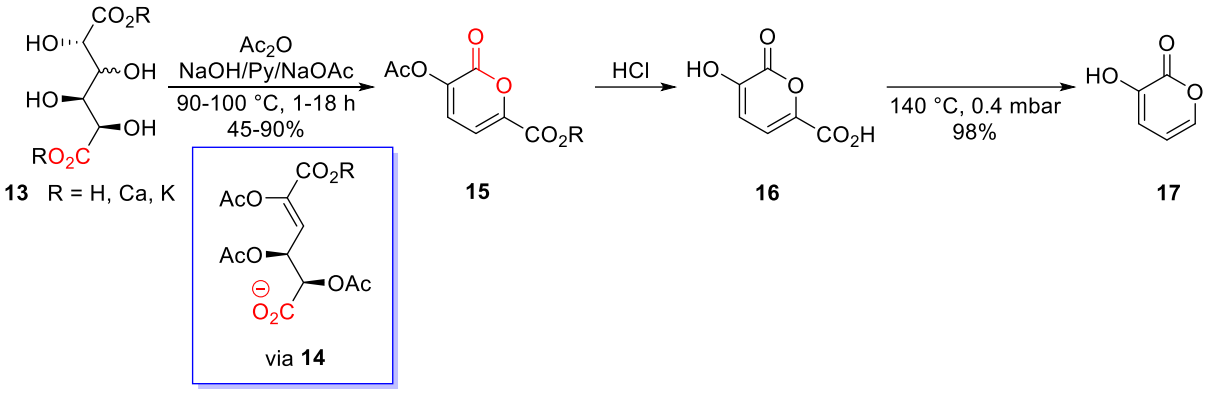

Scheme 2. Sustainable synthesis of 2-pyrones **15** and **17** from aldaric acids (**13**).[15]

Likewise, Reiser *et al.* developed an atom-economic reaction sequence to 6-substituted hydroxyalkyl pyrones **26** starting from furfuryl alcohol (**18**), a renewable resource derived from inexpensive agricultural waste products like bran and bagasse (Scheme 3).[16] A range of hydroxyalkyl substituents were introduced by Baylis-Hillman reaction of enone **22** and various aldehydes **23**. The thermal rearrangement of epoxides **25**, which were utilized as stable cyclopentenone epoxide surrogates, constituted the key step of this sequence. Elimination of the hydroxy group also enabled the synthesis of naturally occurring 6-alkenyl pyrones **27**.

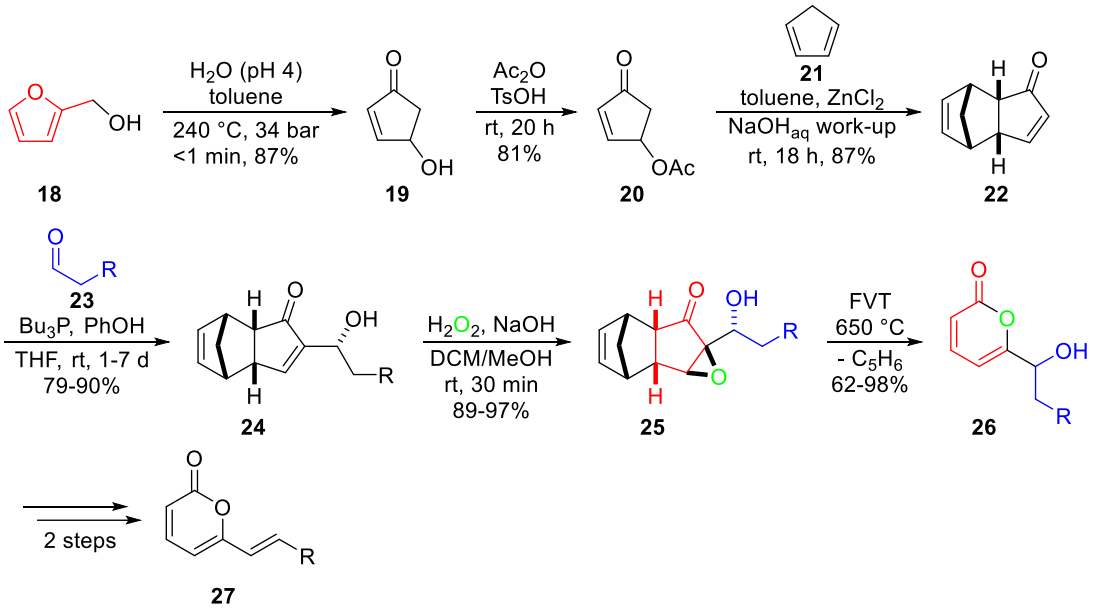

Scheme 3. Synthesis of 6-substituted pyrones **26** from furfuryl alcohol (**18**).[16]

2.2 Transition metal-catalyzed synthesis

Progresses in transition metal-catalysis paved the way for some elegant and efficient pathways towards 2-pyrones, being an attractive extension to traditional methods that often require harsh reaction conditions, thus making them unfavorable for the synthesis of sensitive target compounds. Particularly, the late transition metals proved to be very efficient catalysts for the preparation of 2-pyrone derivatives.

Conceptually, the synthesis of pyrones via the formation of 7-membered metallacycles **28** has moved into the spotlight and a plethora of strategies have been developed to forge these intermediates **28** by transition metal-catalyzed annulation that selectively yield the pyrone scaffold **29** after reductive elimination (Scheme 4).

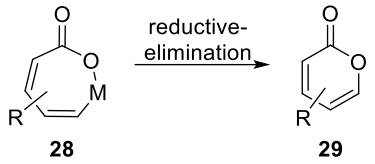

Scheme 4. Pyrone synthesis via 7-membered metallacycles **28**.

Nickel-catalyzed [2+2+2]-cycloaddition of diynes **30** and CO_2, giving rise to pyrone derivatives **32**, represents one of the oldest transition metal-catalyzed strategies, however, the reaction suffered from the employment of high CO_2-pressure (Scheme 5).[17] Louie and co-workers discovered that application of a *N*-heterocyclic carbene ligand (IPr-ligand) allows the performance of this reaction at atmospheric CO_2 pressure with excellent regioselectivity.[18] Analogously, a rhodium-catalyzed version developed by Tanaka *et al*. yielded carbocyclic as well as heterocyclic fused pyrones under atmospheric CO_2 pressure and even at room temperature.[19] Mechanistically, an initial [2+2]-cycloaddition of CO_2 and the sterically less hindered alkynyl unit leads to the formation of intermediate **31**. Subsequent insertion of the second alkyne followed by reductive elimination furnishes pyrones **32** via the intermediacy of a 7-membered metallacycle and regenerates the catalyst.

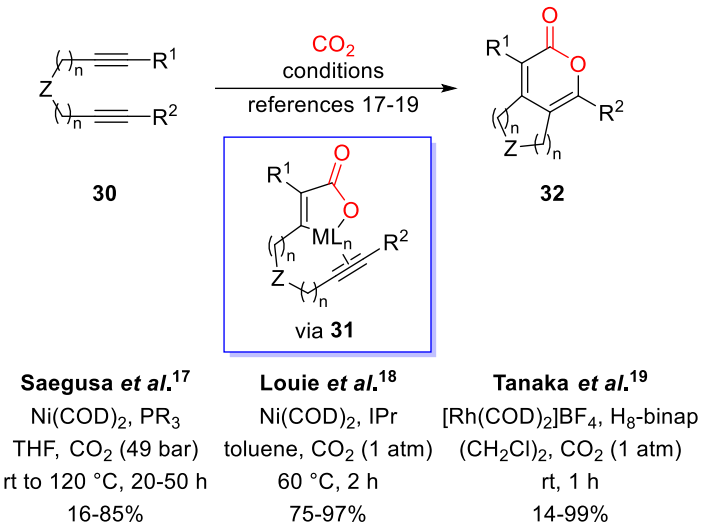

Scheme 5. Transition metal-catalyzed [2+2+2]-cycloaddition of diynes **30** and CO_2.[17–19]

A rare example of a 2-pyrone synthesis via intermolecular [2+2+2]-cycloaddition between two terminal alkynes **33** and CO_2 at ambient pressure and temperature was reported by Wu and co-workers.[20] An iridium/cobalt dual catalytic system provided access to 4,6-disubstituted pyrones **35** under irradiation with visible light (Scheme 6). Herein, the photocatalytic system is utilized to generate an active Co^I species by a visible light-mediated reductive quenching cycle of the Ir^{III}-catalyst and *i*-Pr_2NEt. Similarly to the intramolecular [2+2+2]-cycloadditions, the Co^I species reacts with CO_2 and alkyne **33** to produce the five-membered cobaltacycle intermediate **34**. Insertion of a second alkyne **33** into the cobaltacyle **34** gives rise to pyrones **35** after reductive elimination.

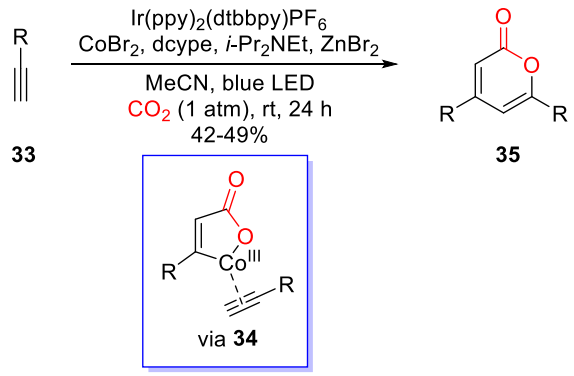

Scheme 6. Visible-light mediated [2+2+2]-cycloaddition of alkynes **33** with CO_2.[20]

Moreover, homo- and heterodimerization of substituted propiolates **36** proved to be an efficient method for the construction of the pyrone skeleton (Scheme 7).[21] Ruthenium-catalyzed homodimerization of propiolate **36** yielded trisubstituted pyrones **40**, whereas disubstituted pyrones **41** were obtained by heterodimerization with terminal propiolate **37**. Remarkably, by

using acetic acid as solvent no homodimerization of the respective propiolates was observed in the latter case. Depending on the residue of alkyne **36** either 5-carboxylate- or 6-carboxylate-substituted pyrones **40-41** are formed regioselectively which can be attributed to selective formation of 5-membered metallacycles **38**. Aryl substituents coordinate strongly with ruthenium thus preferring the formation of 5-carboxylate substituted pyrones **40-41**. Selective protonation of intermediate **38** again gives rise to a 7-membered metallacycle and followingly to pyrones **40-41** by nucleophilic attack of the ester in **39**.

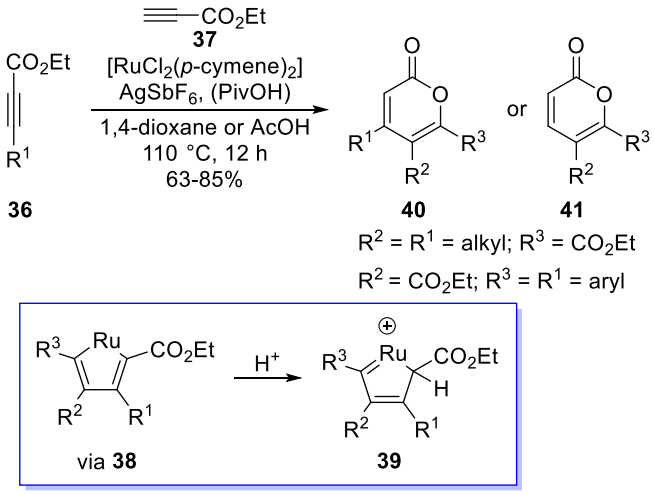

Scheme 7. Homo- and heterodimerization of propiolates **36-37**.[21]

In addition to the processes utilizing only alkynes as starting materials, other approaches investigated the formation of pyrone derivatives via 7-membered metallacycles **28** by transition metal-catalyzed insertion of α,β-unsaturated acids or esters to alkynes.

For instance, a range of aryl-, alkyl- and silyl-substituted pyrones **45** were regioselectively prepared by Larock and co-workers through palladium-catalyzed annulation of halogen- or triflate-containing α,β-unsaturated esters **42** and internal alkynes **43** (Scheme 8).[22] The regiochemistry of the reaction seems to be controlled by steric factors in the apparent seven-membered palladacyclic transition product being formed by attack of the carbonyl oxygen on the vinylpalladium intermediate **44**. Consequently, unsymmetrical alkynes **43** give rise to pyrones **45** having the larger residue in 6-position.

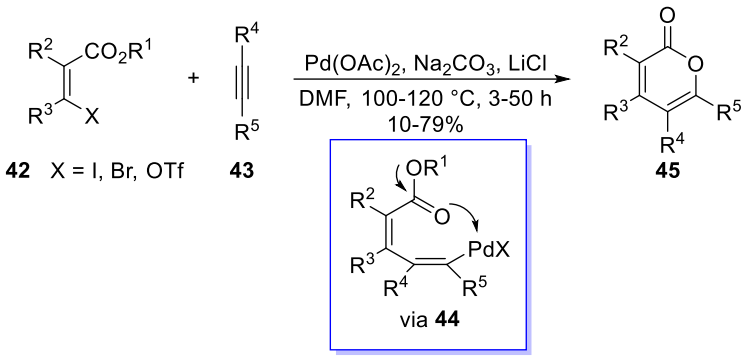

Scheme 8. Palladium-catalyzed annulation of α,β-unsaturated esters **42** and internal alkynes **43**.[22]

The development of transition metal-catalyzed reactions proceeding via C-H bond activation allowed to circumvent initial halogen- or triflate-functionalization of acrylic acids. Miura and co-workers were the first to demonstrate that pyrones **49** can be directly prepared from acrylic acid and derivatives **46** by rhodium-catalyzed oxidative coupling/annulation with alkynes **47** (Scheme 9).[23] Key step is the cyclometallation of acrylic acid **46** in 3-position to afford the 5-membered intermediate **48** that further undergoes insertion into the alkyne **47**. Since then, several oxidative annulation strategies have been described for the synthesis of 2-pyrones **49** from readily available acrylic acids **46**. Palladium-catalysis enabled the utilization of oxygen as oxidant under mild conditions[24], whereas cinnamic acid derivatives could be converted into multisubstituted pyrones by applying an inexpensive ruthenium-catalyst.[25] In addition, Mei and co-workers reported the first example of an iridium-catalyzed electrochemical version.[26] Herein, anodic oxidation was necessary to release the pyrone product **49** from a stable, coordinatively saturated 18-electron iridium complex. Recently, the combination of acrylic acids with 4-hydroxy-2-alkynoates yielded fused heterocyclic pyrone derivatives under rhodium-catalysis.[27] In all cases, the reaction with unsymmetrical alkynes **47** proceeded regioselectively and again large substituents and especially aryl- or heteroaryl groups are located in 6-position of the final product.

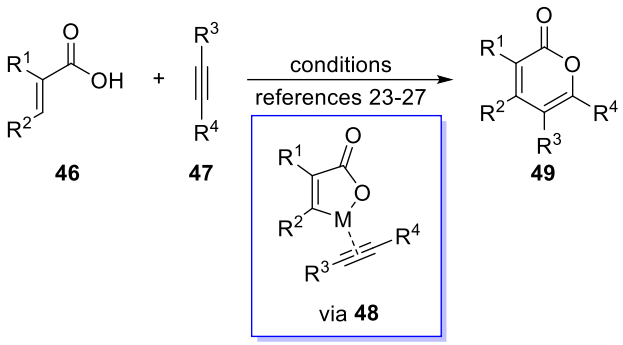

Miura *et al.*[23]	**Jiang *et al.*[24]**	**Gogoi *et al.*[25]**	**Mei *et al.*[26]**	**Prabhu *et al.*[27]**
$[Cp^*RhCl_2]_2$, Ag_2CO_3	$Pd(OAc)_2$, $CuBr_2$	$[RuCl_2(p\text{-cymene})]_2$	$(Cp^*IrCl_2)_2$	$[RhCp^*Cl_2]_2$, $AgSbF_6$
DMF, 120 °C, 4-10 h	NEt_3, O_2 (1 atm)	$Cu(OAc)_2 \cdot H_2O$	*n*-Bu_4NOAc	Ag_2CO_3, LiOAc
22-96%	$AcOH:Ac_2O$	*t*-AmOH	MeOH, 1.5 mA	EtOAc
	90 °C, 12 h, 13-94%	90 °C, 12 h, 30-92%	60 °C, 12 h, 12-96%	100 °C, 16 h, 15-98%

Scheme 9. Transition metal-catalyzed oxidative annulation of acrylic acids **46** and alkynes **47**.[23–27]

Analogous to these oxidative annulations of acrylic acids, decarbonylative- or decarboxylative coupling provides an additional elegant route from simple starting materials proceeding also via formation of a 5-membered metallacycle **52**. Decarbonylative coupling of anhydrides **50** to alkynes **47** was first investigated by Matsubara and co-workers using a nickel catalyst in association with a Lewis acid cocatalyst.[28] Later, the scope of anhydrides **50** and alkynes **47** was widely extended by applying a rhodium catalytic system, yielding tri- or tetra-substituted pyrones **53** regioselectively (Scheme 10).[29] However, in both cases coupling of the parent maleic anhydride failed and by using terminal alkynes only oligomerization was observed. While the first issue could be solved by a modified protocol under ruthenium-catalysis developed by Boruah *et al.*, the latter remained an insuperable challenge.[30]

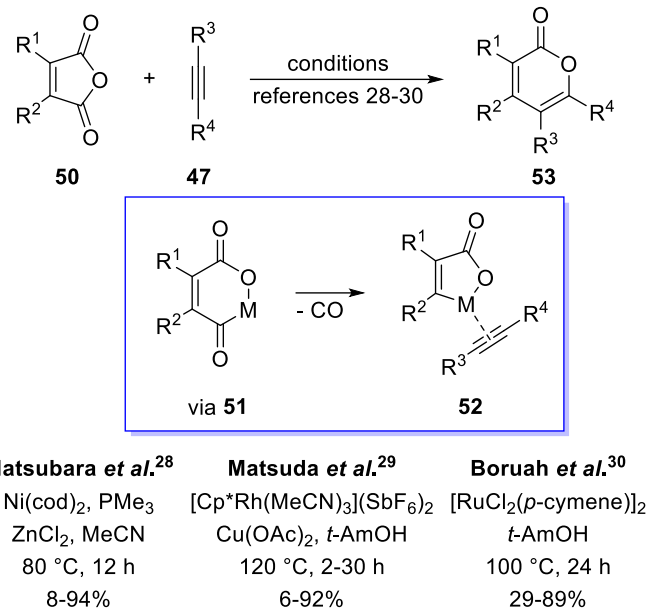

Scheme 10. Dercarbonylative coupling of maleic anhydrides **50** and alkynes **47**.[28–30]

In a similar vein, the decarboxylative coupling of readily available maleic acids **54** with internal alkynes **55** furnished aryl-, heteroaryl-, alkyl- and carboxyl-substituted pyrones **58** smoothly under rhodium-catalysis with excellent regioselectivity (Scheme 11).[31] By using 2-substituted maleic acids, the decarboxylation takes place at the C3-position to selectively form metallacycle **57**.

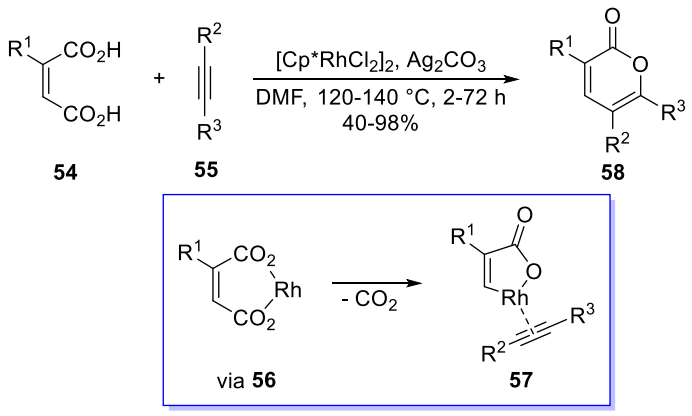

Scheme 11. Decarboxylative coupling of maleic acids **54** and alkynes **55**.[31]

During the past few decades, the directing-group-assisted C-H activation has become a pivotal strategy for the production of diversely substituted molecules. In this context, tunable tandem oxidative cyclization of *N*-tosylacrylamides **59** and diazo compounds **60** furnished either highly substituted pyrone derivatives **63** or furans depending on the applied reaction conditions (Scheme 12).[32] In absence of an external oxidant, the rhodium-catalyzed reaction again takes place via an acylsulfonamide group directed formation of a 5-membered rhodacycle **61**. This

complex **61** can coordinate the diazo compound **60** and after protonation intermediate **62** is obtained selectively. Finally, keto-enol tautomerization and lactonization afford pyrone **63** under C-N cleavage. Aromatic- as well as aliphatic substituents are well tolerated in the respective starting materials.

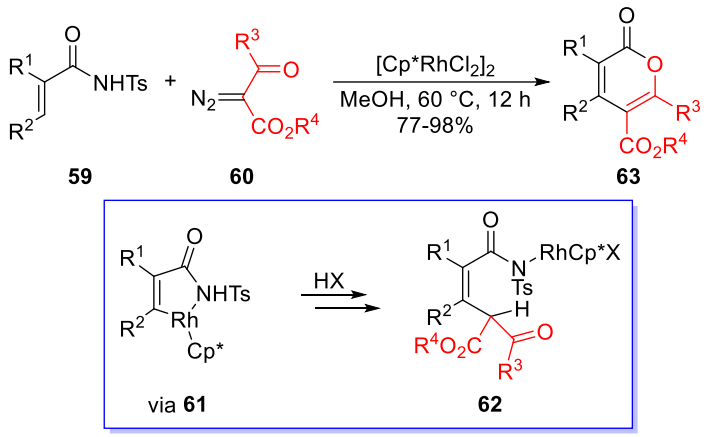

Scheme 12. Oxidative cyclization of acrylamides **59** and diazo compounds **60**.[32]

A different annulation strategy utilizing sulfoxonium ylides **65** as reliable and practical substitutes for diazo compounds has been reported by Jiang and co-workers.[33] By application of a rhodium-catalyst they observed [3+3]-annulation between cyclopropenones **64** and β-ketosulfoxonium ylides **65** having only DMSO as a major byproduct. The proposed catalytic cycle involves cyclometallation of cyclopropenone **64** and transmetallation with substrate **65** delivering a 4-membered rhodacycle intermediate **66**. The complex **66** releases DMSO to yield the 7-membered metallacyle **67** and ultimately, pyrone **68** by reductive elimination. (Scheme 13).

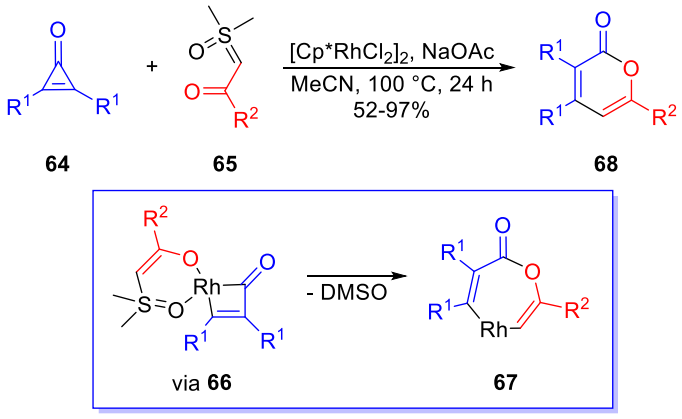

Scheme 13. Rhodium-catalyzed [3+3]-annulation of cyclopropenones **64** and sulfoxonium ylides **65**.[33]

A large part of traditional pyrone synthesis relies on carbonyl condensation reactions.[6,7] Since carbon atoms of a carbonyl compound and an alkyne have the same formal oxidation state, alkynes can be used as stable ketone surrogates which can be activated by π-acid catalysts. Therefore, π-acid catalysis and particularly gold catalysis has emerged as a powerful tool for a systematic exploration of the pyrone estate.

Gold-catalyzed cycloisomerization of strained β-alkynylpropiolactones **69** triggered by π-acid coordination to the alkyne moiety furnished 2-pyrones **71** (Scheme 14).[34] In some cases, by-product formation of acyclic acids was observed as a consequence of simultaneous σ-coordination of the catalyst to the lactone **69**. Noteworthy, derivatives with a substituent adjacent to the β-lactone moiety proved far less reactive with a concomitant increase in reaction time.

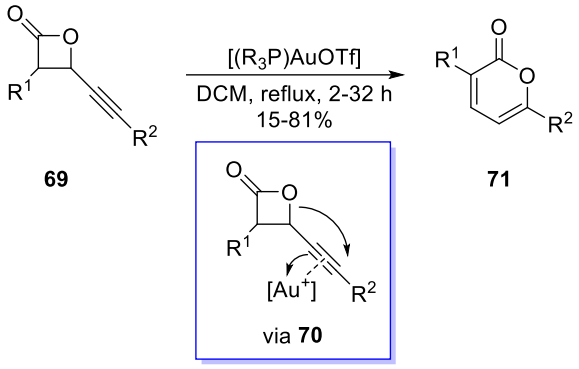

Scheme 14. Gold-catalyzed cycloisomerization of β-alkynylpropiolactones **69**.[34]

A facile π-acid-catalyzed route towards 2-pyrones was developed by Fürstner and co-workers. The ability to manipulate alkynes **72** by the pronounced carbophilicity of [LAu$^+$]-fragments, enables the 6-*endo*-dig attack of a tethered ester carbonyl group onto the transient alkyne-gold complex **73** to forge the pyrone ring in a fully regiocontrolled manner. During the total synthesis of the marine natural product Neurymenolide A **75** the power of this approach was showcased with the synthesis of various 4-hydroxy-2-pyrones **74** from ynonates **72** (Scheme 15).[35]

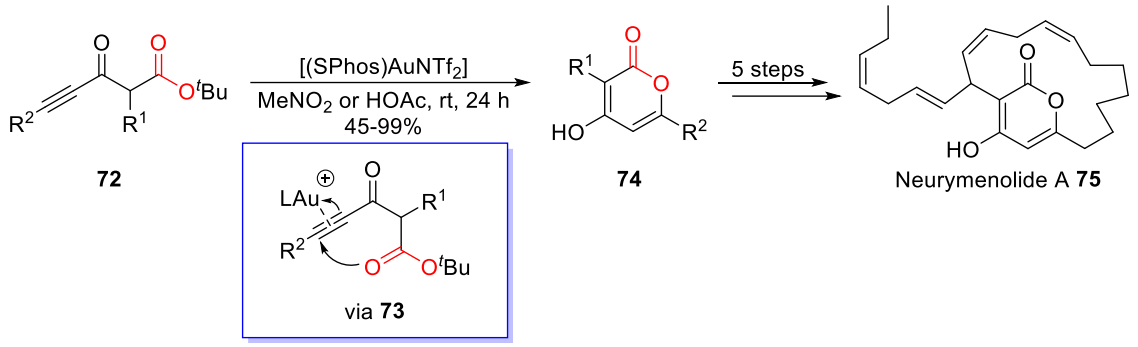

Scheme 15. Synthesis of 4-hydroxy-2-pyrones **74** by gold-π-acid catalysis.[35]

A different approach starting from propargyl propiolates **76** was described by Schreiber *et al* (Scheme 16).[36] Upon addition of a gold-catalyst, the [3,3]-sigmatropic rearrangement of propiolate **76** to enyne allene intermediate **77** is induced. Activation of the alkyne moiety by π-coordination again instigates a 6-*endo*-dig cyclization to oxocarbenium intermediate **78**, which either eliminates a proton to give rise to vinyl pyrones **79** or can be trapped by external heteroarene nucleophiles to obtain pyrones **80**. Olefinic- as well as aromatic residues are well tolerated without interfering with the cascade reaction. Moreover, Schreiber's strategy has also been adapted for the total synthesis of a ring A aromatic congener of urbalactone **81**.[37]

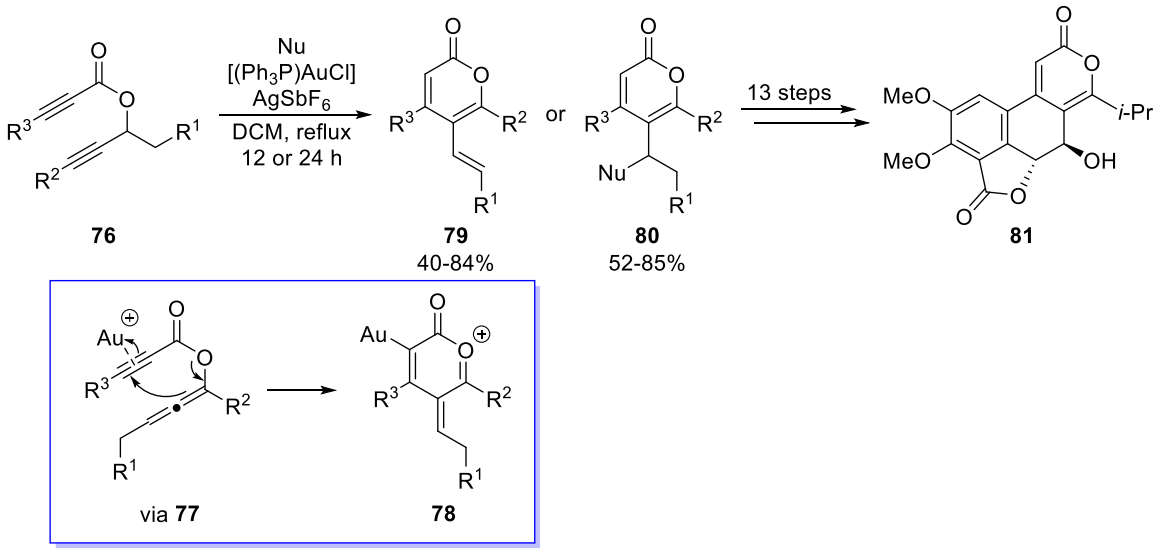

Scheme 16. Gold-catalyzed cascade process for the conversion of propargyl propiolates **76**.[36,37]

In addition to their earlier work, Schreiber and co-workers investigated the synthesis of disubstituted pyrones **85** directly from propiolic acids **82** and terminal alkynes **83** via a cascade reaction based on alkyne coupling and subsequent 6-*endo* cyclization of intermediate **84** (Scheme 17).[38] Several functional groups like ester, halide and alkynes are compatible with the

reaction conditions. However, sterically hindered alkynes **83** gave lower yields and phenylacetylene reacted only at elevated reaction temperature.

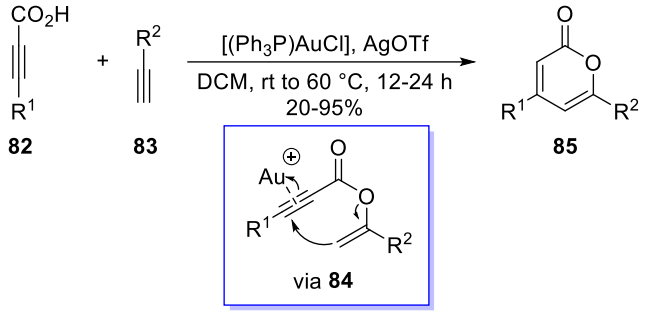

Scheme 17. Synthesis of disubstituted 2-pyrones **85** from propiolic acids **82**.[38]

Previous examples have shown that π-acid-catalyzed intramolecular 6-*endo*-dig cyclization can provide the 2-pyrone framework in a very reliable way. The enormous value of these transformations has been further undergirded by pioneering work in palladium-catalyzed methodologies combining cross-coupling and π-acid features of the transition metal and thus, enabling the construction of highly functionalized pyrone derivatives.

Burton and Wang reported the synthesis of 3,4-difluoro-6-substituted pyrones **89** by Sonogashira coupling of 2,3-difluoro-3-iodoacrylic acid (**86**) and terminal alkynes **87** (Scheme 18).[39] The resulting enyoic acid intermediate **88** undergoes further palladium-catalyzed cyclization to fluorinated pyrone **89**. Aromatic, aliphatic as well as heterocyclic acetylenes **87** worked well at ambient temperature and the presence of neither an electron-withdrawing nor an -donating group on the aromatic rings affected the yield of the products **89**.

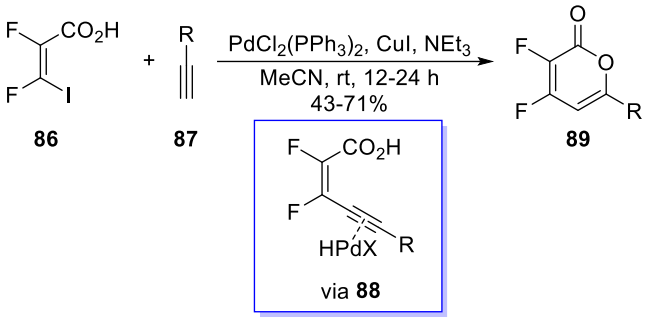

Scheme 18. Synthesis of 3,4-difluoro-6-substituted pyrones **89**.[39]

Accordingly, formation of the pyrone scaffold was achieved by tandem Stille coupling and selective 6-*endo*-dig oxacyclization of iodovinylic acids **90** and allenyl-tributyltin reagents **91**.[40] By this convenient method, alkyl-, aryl- and silyl-substituted pyrone derivatives **93** were obtained in good yields (Scheme 19).

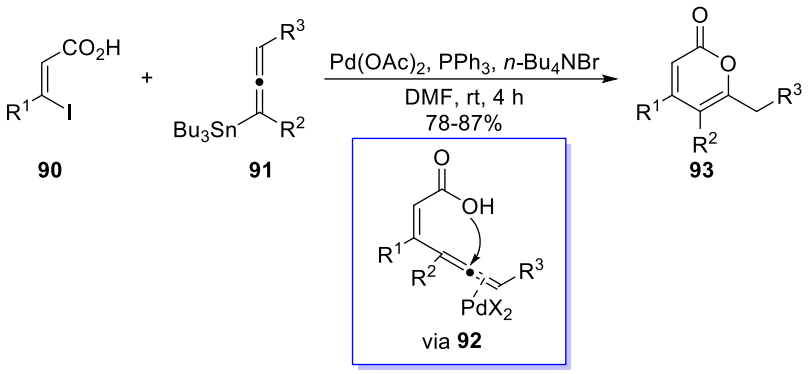

Scheme 19. Tandem Stille coupling/oxacyclization of iodovinylic acids **90** and allenyl-tributyltin reagents **91**.[40]

A strategy utilizing an opposite chronology of reaction events was developed by Loh and co-workers. Pd(II)-catalyzed 6-*endo*-dig cyclization of enynoates **94** in the first step allowed the introduction of various substituents in 5-position of pyrones **97** by subsequent cross-coupling reactions with alkenes **95** (Scheme 20).[41–43] The generality of this method was showcased by formation of alkenyl[41], alkenone[42]- or allyl pyrones **97a-c**[43] employing either electron-deficient alkenes **95a** or allylic alcohols **95b-c**. While pyrones **97a-b** are formed by β-hydride elimination in the final step, $CuCl_2$ assisted the β-hydroxyl elimination to pyrones **97c**. Oxidants like $Cu(OAc)_2$, O_2 and benzoquinone (BQ) are necessary to regenerate the active Pd(II)-catalyst species for a new catalytic cycle.

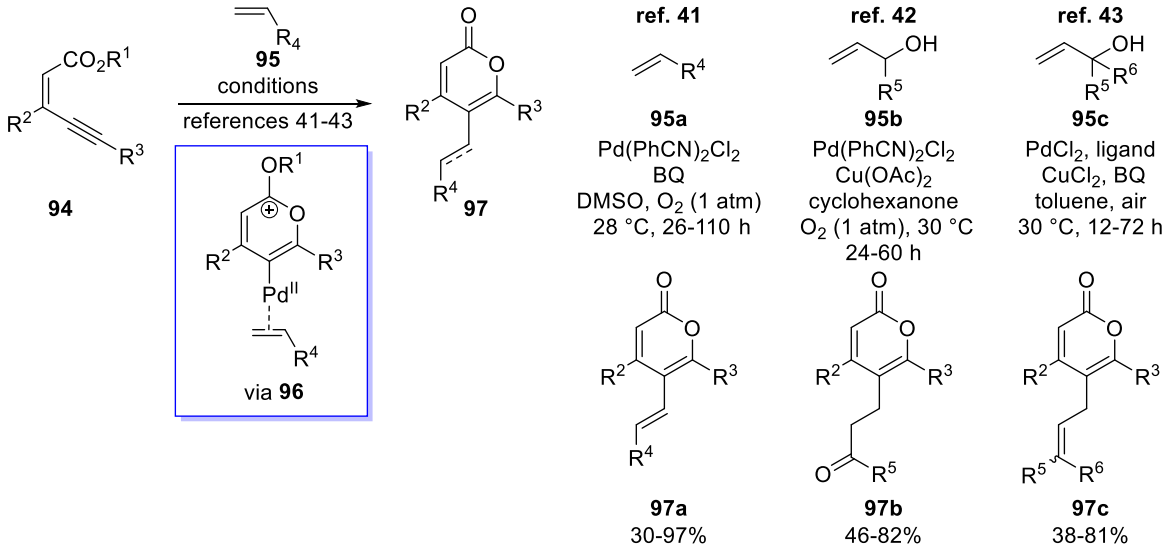

Scheme 20. Synthesis of pyrones **97a-c** by subsequent 6-*endo*-dig cyclization/cross-coupling.[41–43]

Besides the pyrone synthesis via annulation and π-acid catalysis, miscellaneous transition metal-catalyzed approaches were investigated yielding the pyrone scaffold also in very intriguing ways.

In addition to aforementioned [2+2+2]-cycloaddition strategies, for instance, a ruthenium-catalyzed carbonylative [3+2+1]-cycloaddition method, using silylacetylenes **98**, α,β-unsaturated ketones **99** and CO as starting materials, was described by Ryu *et al*. (Scheme 21).[44] Initially, an in situ formed ruthenium hydride reacts with methyl vinyl ketone **99** to yield a ruthenium enolate, which undergoes carboruthenation with silylacetylene **98** to a vinyl ruthenium complex **100**. Following CO insertion, cyclization via acyl ruthenium complex **101** and β-hydride elimination, the respective tetra-substituted pyrone **102** is obtained

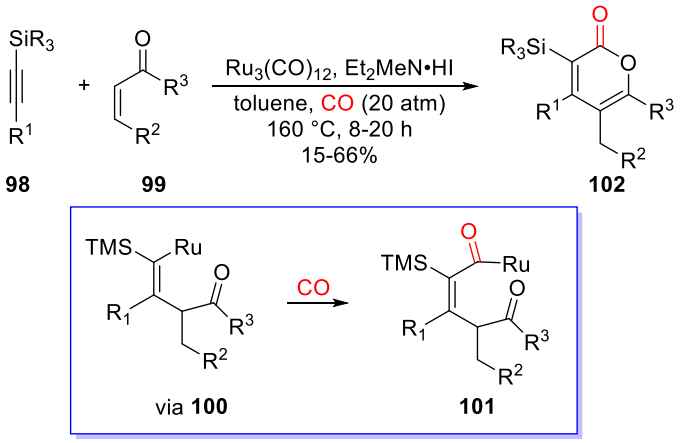

Scheme 21. [3+2+1]-cycloaddition towards silyl-substituted pyrones **102**.[44]

A synthetic strategy utilizing rather unusual rhenium- or manganese-catalysts was developed by Takai e*t al*.[45] Mechanistically, the formation of pyrones **107** is divided into two parts. The metal complexes are catalyzing the insertion of acetylenes **104** into β-ketoesters **103** leading to the formation of δ-keto esters **106** after retro-aldol reaction of 5-membered metallacycle **105** and subsequent reductive elimination. Finally, the cyclization of δ-keto esters **106** to pyrones **107** under mild reaction conditions is triggered by TBAF (Scheme 22). Remarkably, the sterically demanding substituents of unsymmetrical alkynes **104** are exclusively installed in 4-position of the pyrone skeleton. In contrast to the rhenium-catalyst, the cheaper manganese-catalyst did not give pyrones **107** in the reaction with internal acetylenes **104**.

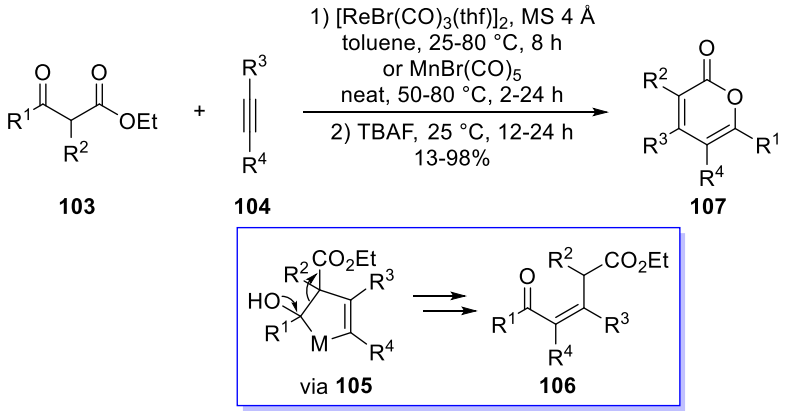

Scheme 22. Rhenium-and manganese-catalyzed synthesis of pyrones **107**.[45]

In other approaches, the use of alkynes as starting materials is obviated. Helquist and co-workers obtained trisubstituted pyrones **111** by a palladium-catalyzed three-component reaction in a single-flask (Scheme 23).[46] The reaction proceeded via α-arylation of ketone **108** with an aryl bromide in the first step. Subsequent α-alkenylation of the resulting intermediate with β-bromoacrylate **109** gives rise to key enolate **110** that readily cyclizes to pyrone **111** after alkene isomerization. Palladium was found to have beneficial roles in all of the key steps.

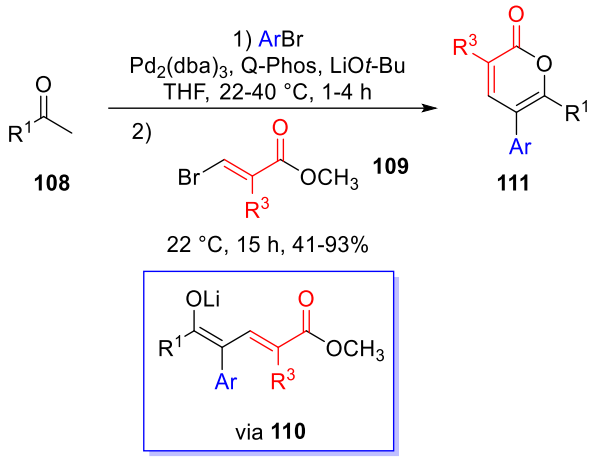

Scheme 23. Palladium-catalyzed multicomponent synthesis of pyrones **111**.[46]

Zhou and co-workers developed a synthesis of various 3-aryl pyrones **114** by palladium-catalyzed cross-coupling of aryl iodides and cyclic vinyldiazo ester **112** that was easily prepared from commercially available 3,5-dihydro 2-pyrone (Scheme 24).[47] Oxidative addition with aryl iodide affords a palladium(II) complex that reacts with diazo compound **112** to carbene **113**. The aryl group inserts into the carbenic carbon and palladatropic rearrangement to C-5 followed by β-hydride elimination furnishes the aryl-substituted pyrone **114**. Electron-withdrawing-, electron-donating- as well as halogen (F, Cl, Br) substituents on the aryl moiety are compatible

with the reaction conditions. The preservation of the bromo group in aryl pyrones **114** was attributed to the lower reactivity of bromobenzene under these mild reaction conditions.

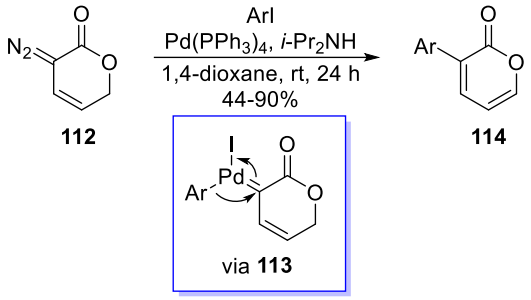

Scheme 24. Palladium-catalyzed synthesis of 3-aryl pyrones **114**.[47]

2.3 Transition metal-free synthesis

Alongside traditional carbonyl condensation-cyclization protocols, a number of novel transition metal-free methods have been developed for the construction of 2-pyrones utilizing various starting materials and strategies. Some selected examples are listed herein.

Even before to transition metal-catalyzed approaches, enyoic acids and enynoates **115** served as important starting materials in transition metal-free electrophilic 6-*endo*-dig oxacyclization protocols. In 2001, Rossi and co-workers demonstrated that 5-iodo-2-pyrones **118a** are readily available by iodolactonization of enyoic acids **115** via iodonium ion **116** (Scheme 25).[48] However, butenolides were observed as minor byproducts due to competitive 5-*exo*-dig cyclization of acid **115**. The 5-iodo pyrones **118a** were further derivatized by Stille coupling with organotin compounds. Analogously, electrophilic cyclization of enynoates **115** was performed by Larock *et al*., using different electrophiles like ICl, I_2, *p*-$O_2NC_6H_4SCl$ or PhSeCl.[49] Also here the reaction suffered from unselective 5-*exo*-dig cyclization in some cases. Furthermore, Blum and co-workers developed a catalyst-free oxyboration of enynoates **115** with *B*-chlorocatecholborane (ClBcat) and the resulting 5-borylated 2-pyrones were isolated as pincacolboronate esters **118c**, providing a variety of bench-stable organoboron building blocks for downstream functionalization.[50] Equally, oxyindation with indium trihalides furnished 5-metalated pyrones that enabled easy access to various multi functionalized 2-pyrones **118d** by subsequent halogenations or cross-coupling reactions.[51] In contrast to the first two reports, no competitive 5-*exo*-dig cyclization was observed in the boron- and indium-mediated protocols which can be rationalized by selective formation of intermediate **117**.

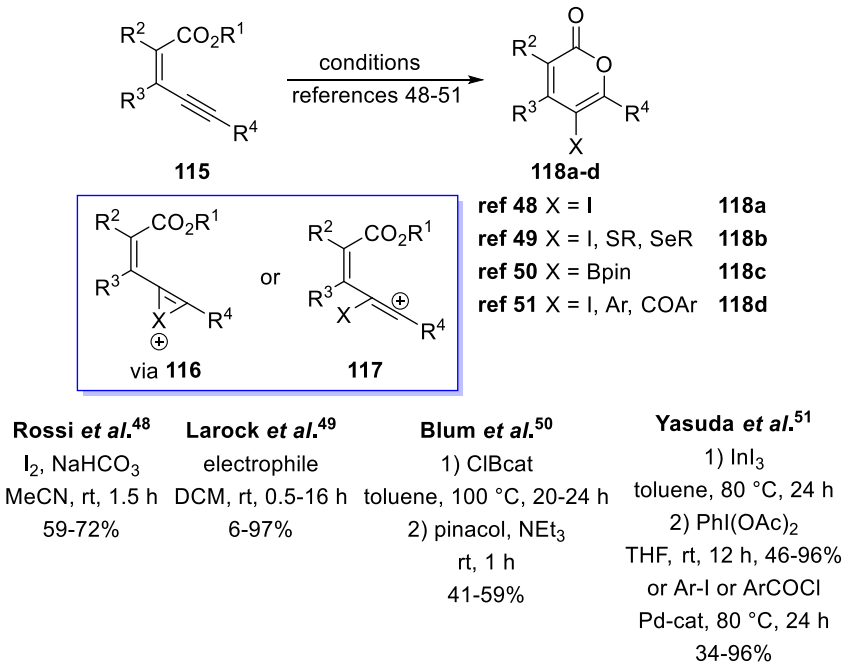

Scheme 25. Electrophilic oxycyclization of enynoates **115**.[48–51]

Historically, catalytic organic synthesis has been dominated by transition metal catalysis. Since its discovery, organocatalysis, however, has grown explosively to become one of the most exciting research areas in current organic chemistry. Groundbreaking principles to form heterocycles were recognized and among these entities 2-pyrones have been organocatalytic target molecules as well.

In this way, one-step phosphine-catalyzed synthesis of 6-alkyl- or aryl-substituted pyrones **122** from commercially available aldehydes **119** and ethyl allenoate (**120**) was achieved by Kwon *et al.* (Scheme 26).[52] After addition to the allenoate **120**, sterically demanding trialkylphosphines are shifting the equilibrium towards the *E*-isomer of the zwitterionic intermediate **121** which is required to form pyrones **122** in further steps by γ-addition of vinylphosphonium salt **121** to aldehyde **119** and subsequent lactonization.

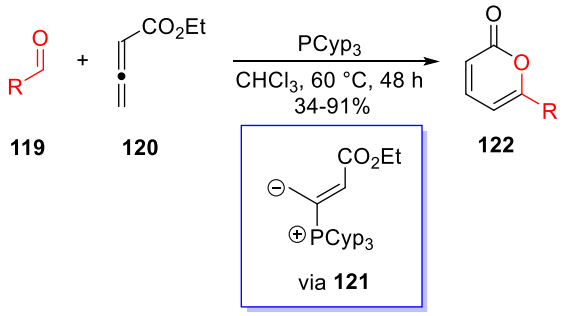

Scheme 26. Phosphine-catalyzed synthesis of 6-substituted pyrones **122**.[52]

An elegant one-pot isothiourea-mediated cascade sequence towards valuable trifluoromethyl substituted pyrones **127** including bioactive COX-2 inhibitors was developed by Smith and co-workers. By addition of pivaloyl chloride and DIPEA, acid **123** is converted in situ to the corresponding mixed anhydride. The organocatalyst **125** is acylated by this reactive species and a base-mediated Michael-addition to enone **124** leads to the formation of intermediate **126**. Then, trifluoromethylated pyrone **127** is obtained by lactonization and thiophenol elimination (Scheme 27).[53] The utilization of alternate Lewis bases than isothiourea-catalyst **125** resulted in a poor conversion of the starting materials.

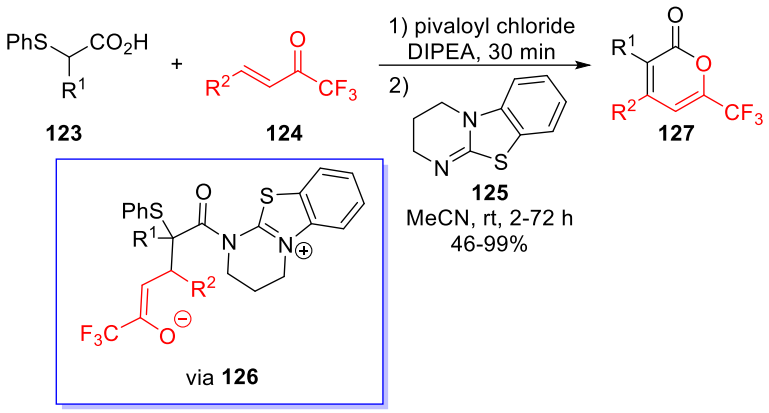

Scheme 27. Isothiourea-catalyzed synthesis of trifluoromethyl substituted pyrones **127**.[53]

Moreover, *N*-heterocyclic carbene (NHC) catalysts have developed into a powerful tool for the organocatalytic synthesis of pyrone derivatives.[54] Ma and co-workers presented a flexible protocol for the synthesis of either 2-pyrones **133** or chiral dihydro pyranones from 3-bromoenals **128** and 1,3-dicarbonyl compounds **129** upon NHC-catalyzed oxidative transformation (Scheme 28).[55] By addition of an external oxidant, pyrones **133** were selectively formed in yields up to 90%, whereas dihydropyrones are obtained in the absence of an oxidant. The postulated mechanism explained this observation by generation of an oxidized β-bromo Breslow intermediate **131** that is attacked by a deprotonated dicarbonyl compound **129** to furnish 1,4-adduct **132**. Cyclization of intermediate **132** and bromide elimination yields pyrone **133** with liberation of the carbene catalyst. Notably, the bigger residues of diketone **129** are selectively introduced in 6-position of pyrone **133** which can be attributed to electronic and steric factors in the Michael-addition of the corresponding enolate to Breslow intermediate **131**.

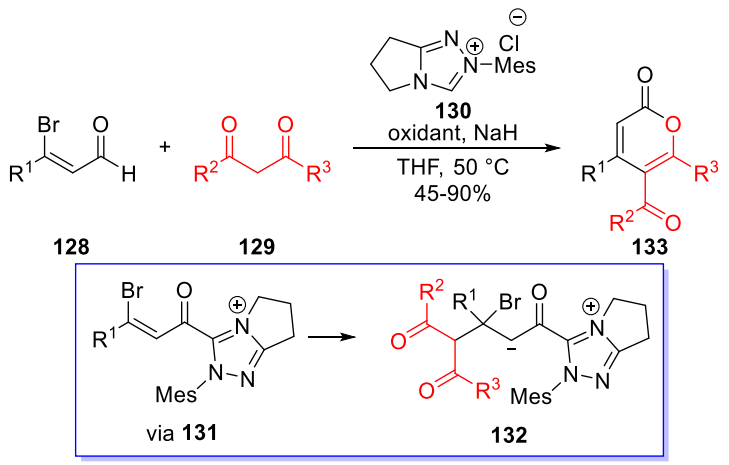

Scheme 28. NHC-catalyzed oxidative transformation of 3-bromoenals **128**.[55]

A novel thiazolium salt-catalyzed [3+2+1]-cyclization of acetylene dicarboxylates **134** with arylglyoxals **135** via umpolung and C-C bond cleavage was reported by Jiang *et al.* (Scheme 29).[56] According to the proposed mechanism, a whole series of reaction events are leading to the formation of trisubstituted pyrone derivatives **140**. Starting from arylglyoxal **135** a base-mediated elimination of water gives an aldehyde that is attacked by carbene-catalyst **136**. After an umpolung process to intermediate **137**, nucleophilic attack to alkyne **134** furnishes the zwitterionic intermediate **138**. Aldol-type reaction between zwitterion **138** and a second in situ prepared aldehyde of arylglyoxal **135** yields intermediate **139** by following proton transfer and elimination of an aryl acid. Finally, **139** is converted into pyrone **140** through a continuous intramolecular nucleophilic addition/elimination and dehydration sequence. Herein, the arylglyoxals **135** played dual roles in the formation of trisubstituted pyrones **140**. Besides serving as a ring component, glyoxal derivatives **135** possessed additional importance as a carbonyl source for this particular transformation.

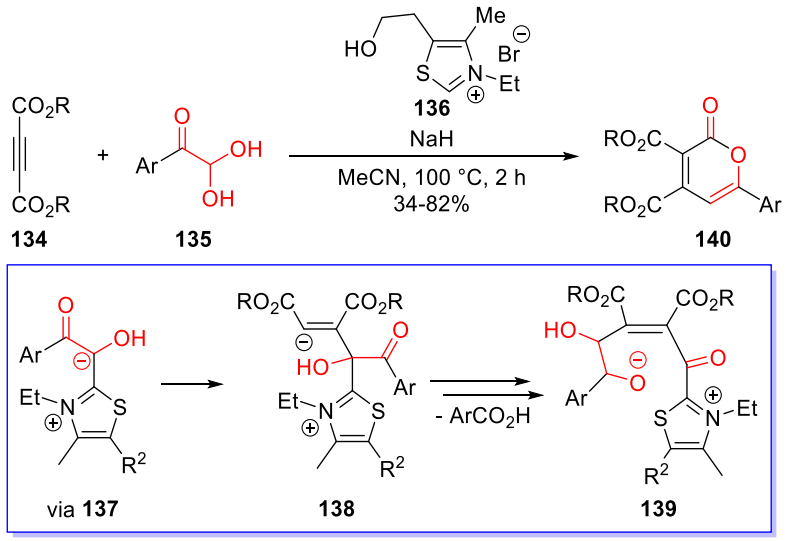

Scheme 29. Thiazolium salt-catalyzed [3+2+1]-cyclization.[56]

Due to their rich chemical reactivity, cyclopropanes have been demonstrated to be useful synthetic building blocks in organic chemistry. Especially, the ring-opening reaction of activated cyclopropanes via 1,3-dipoles provides versatile access to a plethora of cyclic and acyclic compounds.

In line with this, donor-acceptor cyclopropanes **141** underwent sequential ring-opening, fragmentation, recombination and lactonization into highly substituted pyrones **144** upon treatment with $AlCl_3$ (Scheme 30).[57] Since no cross-over products were observed by having different cyclopropanes **141** in the reaction mixture, the fragmentation/recombination-step of zwitterion **142** to **143** was assigned to be intramolecular in nature. Alternatively, by switching the Lewis acid to $TiCl_4$, substituted 1-indanones were obtained.

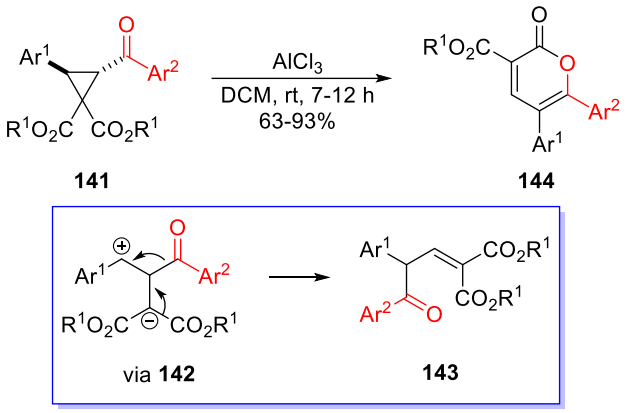

Scheme 30. Lewis acid-mediated transformation of donor-acceptor cyclopropanes **141**.[57]

Starting from 2-acyl-1-chloro cyclopropane carboxylates **145** and aliphatic amines, a base-promoted domino reaction yielded 2-pyrone derivatives **148** (Scheme 31).[58] The substitution of

the chlorine in cyclopropane **145** instantly triggers ring-opening of the resulting donor-acceptor cyclopropane to iminium intermediate **146**. Deprotonation and lactonization gives 3-amine substituted pyrones **148** in up to excellent yields. Several compounds that were obtained by this simple and transition metal-free method exhibited interesting photophysical properties.

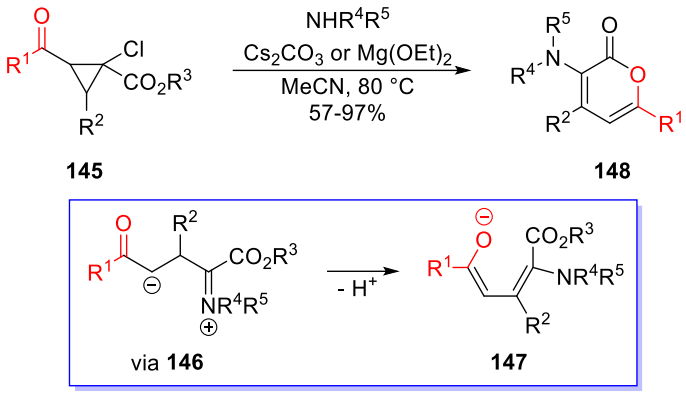

Scheme 31. Base-promoted domino reaction of cyclopropanes **145** and amines.[58]

Another base-mediated synthesis has been accomplished by direct conjugate addition of imino esters **150** to β-chlorovinyl ketones **149**.[59] Remarkably, only substoichiometric amounts of a hard base are required since an in situ generated species **151** is acting in an autocatalytic way to convert the imino esters **150** to its corresponding enolates. The resulting neutral addition product of **151** readily eliminates HCl and MeOH to give pyrone **152** with the help of molecular sieves. Thereby, a broad range of 2-imino-pyranones **152** were obtained in good to excellent yields (Scheme 32).

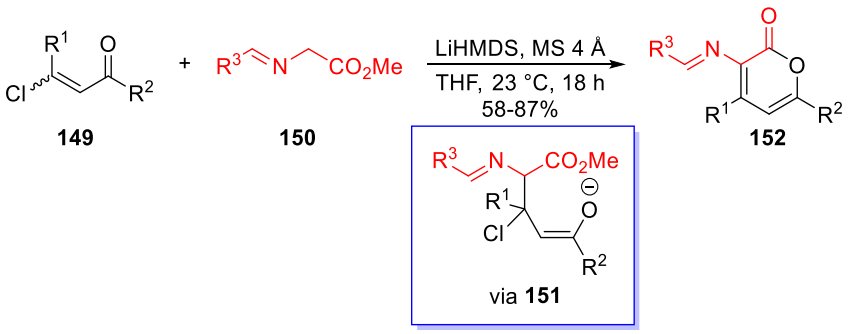

Scheme 32. Conjugate addition approach to 2-imino-pyrones **152**.[59]

With respect to the concept of Green Chemistry, the utilization of abundant reagents like CO_2 and O_2 plays a vital role in modern synthetic chemistry. Consequently, a base-mediated approach utilizing CO_2 as abundant, non-toxic and renewable C1 building block was developed by Lu and co-workers.[60] The carboxylative cyclization of propenyl ketones **153** with CO_2 afforded pyrones **155** simply and efficiently (Scheme 33). Experiments using ^{18}O-labeled CO_2

revealed that only one oxygen atom of pyrone **155** comes from CO_2. Therefore, the cyclization of **154** presumably proceeds via an intramolecular attack of carbonyl oxygen into the carboxylate group.

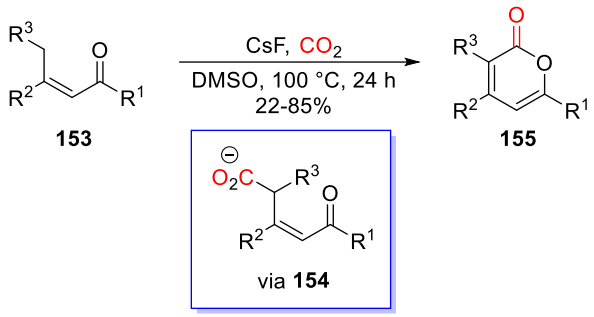

Scheme 33. Carboxylative cyclization of propenyl ketones **153** and CO_2.[60]

Likewise, a catalyst- and additive-free Baeyer-Villiger-type oxidation of α-iodocyclopentenones **156** to pyrones **158** using air as a green oxidant was reported by Rao e*t al*. (Scheme 34).[61] This reaction exhibits an excellent functional group tolerance and the synthetic utility was demonstrated by a large-scale synthesis of a pyrone derivative **158**. Control experiments indicated that the role of molecular oxygen as the oxidant is crucial for the success of the Baeyer-Villiger-type oxidation. On the basis of these experiments, it was proposed that cyclopentenone **156** undergoes thermally driven homolysis of C-I and the resulting radical is trapped by oxygen. Intramolecular attack on the carbonyl gives intermediate **157** that rearranges to the 6-membered lactone scaffold.

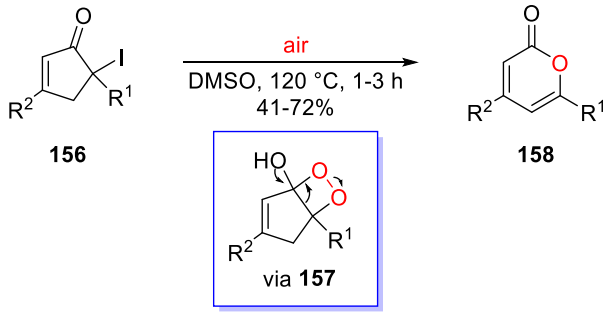

Scheme 34. Catalyst- and additive-free Baeyer-Villiger oxidation of iodocyclopentenones **156**.[61]

3 Reactivity of 2-pyrones

3.1 Ring-opening

In common with other lactones, 2-pyrones can be easily hydrolyzed or opened to the corresponding acyclic products by nucleophilic attack of aqueous alkali- or Grignard reagents at the C-2 carbon.[62] However, due to the inherent unsaturated lactone structure, ring-opened products can also be obtained by nucleophilic attack at the C-6 position. The nucleophilic ring--opening of 2-pyrone (**1**) by 1,6-addition of cyanide was already discovered by Vogel in 1965 (Scheme 35).[63] After attack of the nucleophile, resonance-stabilized intermediate **159** is formed, subsequently collapsing to acid **160** by 6-π electrocyclic ring-opening.

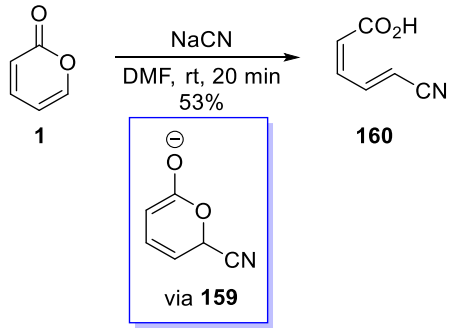

Scheme 35. Nucleophilic ring opening of 2-pyrone (**1**).[63]

Fürstner and co-workers were able to supersede the conventional reactivity mode of Grignard reagents by iron-catalysis.[64] In presence of an iron-catalyst, pyrones **161** underwent formal cross-coupling reactions at C-6 in which the lactone moiety gained a new role as a nontraditional leaving group (Scheme 36). The unconventional reactivity mode can be assigned to the formation of a complex **162** in which 2-pyrone **161** serves as an η^4-bound diene ligand. Critical delivery of the nucleophile occurs by an inner-sphere mechanism. This method opened access to di-unsaturated acid derivatives **163** or **164** with high functional group tolerance and the stereochemistry (2*E*,4*E* **163** vs. 2*Z*,4*E* **164**) being easily controlled by variation of the temperature before work-up. Interestingly, the power of this transformation has been illustrated in the synthesis of several diene containing natural products. The total synthesis of cytotoxic Granulatamide B (**165**) was accomplished in two steps from pyrone **161**, which was readily available in multigram amounts by condensation of cheap 3-methyl-crotonate and octanoyl chloride. Moreover, the 2-pyrone ring-opening proved to be very efficient in late-stage incorporation of dienoates (Scheme 36, red) into a macrocyclic core. Thus, macrodiolides Pateamine A (**166a**) and its simplified designer analog DMDA-Pat A (**166b**), possessing potent

cytotoxic and in vivo anticancer activities, were synthesized by the same working-group unveiling the dienoate motif just before macrocyclization.[65,66]

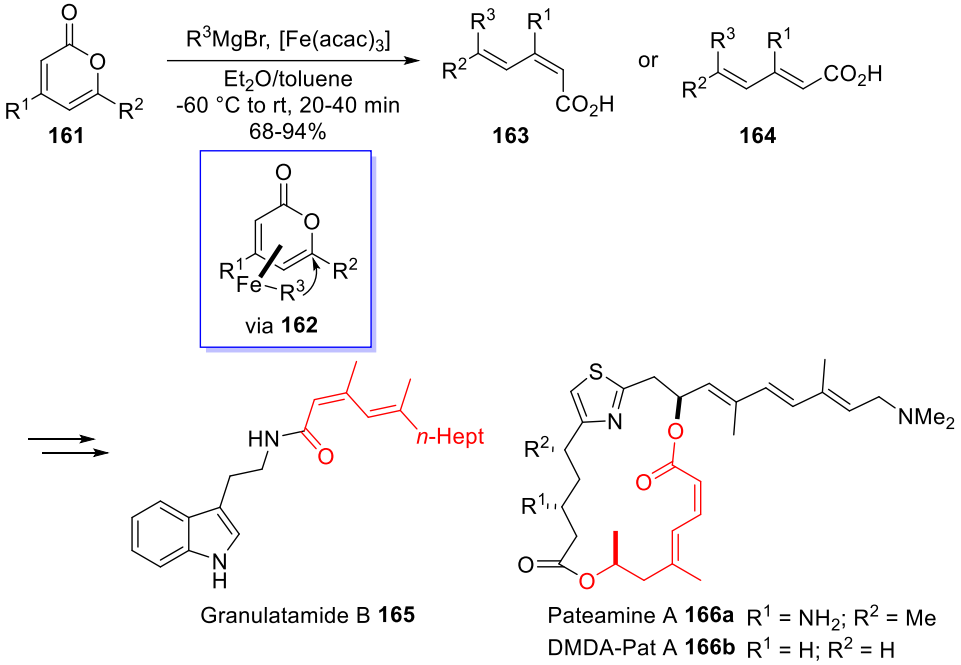

Scheme 36. Iron-catalyzed ring-opening reaction.[64–66]

An uncatalyzed ring-opening of methyl coumalate (**167**) through 1,6-addition of Grignard reagents was reported by Dechoux *et al.* yielding 2*Z*,4*Z* or 2*Z*,4*E* dienoics acids **169** with high chemo- and stereoselectivity (Scheme 37).[67] In this case, the presence of an ester in 5-position on the pyrone modified the regioselectivity of the nucleophile addition. The nature of the Grignard reagent played a key role on the outcome of the reaction. While alkenyl-, alkynyl- and aromatic reagents mainly furnished dienoic acids **169**, the additional formation of unsaturated lactones **170** was observed using alkyl Grignards. The selective formation of conjugated acids **169** using alkenyl-, alkynyl- and aromatic reagents can be easily rationalized by invoking the stabilization by π-conjugation in these acids.

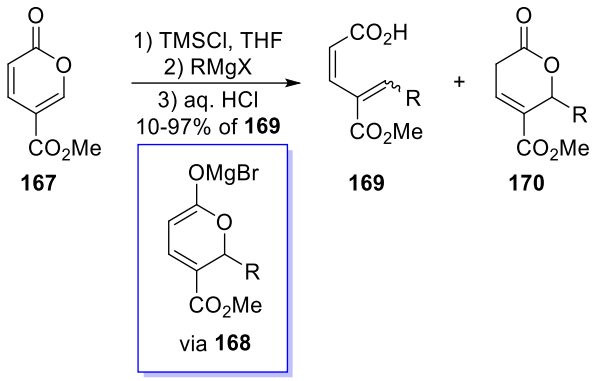

Scheme 37. Synthesis of dienoic acids **169** by nucleophilic ring-opening of methyl coumalate **167**.[67]

Later, the same working-group described a sequential double 1,6-addition of Grignard reagents to methyl coumalate (**167**) to afford β,γ-unsaturated acids **173** in a highly regio-, chemo- and stereoselective manner (Scheme 38).[68] The excellent stereoselectivity of the reaction can be explained by formation of a chair-like bicyclic transition state **172** after addition of the second Grignard reagent via complex **171**.

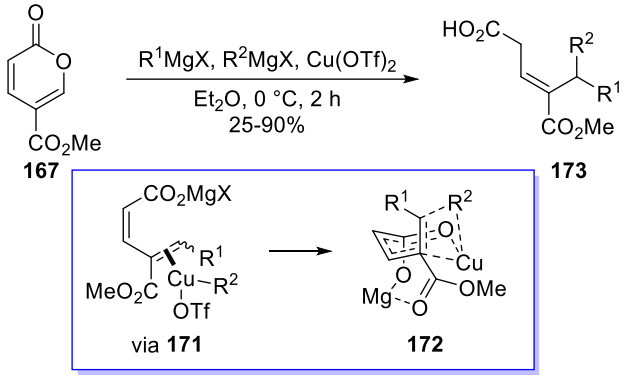

Scheme 38. Sequential double 1,6-addition to methyl coumalate (**167**).[68]

Differently, Tunge *et al.* engaged pyrone **174** in an unique palladium-catalyzed double-decarboxylative addition of allyl carbonates and carbamates **175**, forming valuable dienoic esters **177** (Scheme 39).[69] In contrast to previous strategies, ring-opening proceeds through allylation of pyrone **174** at C-3 by a π-allyl-Pd complex in a first step to form intermediate **176**. Afterward, intermediate **176** undergoes further palladium-catalyzed decarboxylation to ester **177**.

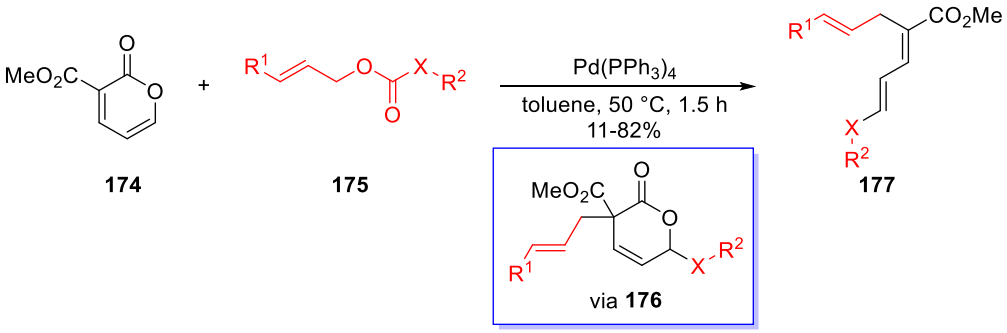

Scheme 39. Palladium-catalyzed double-decarboxylative addition to pyrone **174**.[69]

3.2 [2+2]-Cycloaddition

Examples of inter- and intramolecular [2+2]-cycloadditions of pyrones with alkenes are quite rare in literature and especially the intermolecular reactions are facing grave regio- and chemoselectivity issues making, these transformations unattractive for applications in synthetic chemistry.[70] However, the intramolecular [2+2]-cycloaddition of the 2-pyrone scaffold itself has attracted considerable attention in organic chemistry. Already in 1964, Corey *et al.* discovered that UV-light irradiation of 2-pyrone **178** furnishes cyclobutene lactones **179** in almost quantitative yield (Figure 3).[71] Lately, the working-groups of Kappe and Maulide demonstrated in collaboration the first continuous flow synthesis of lactone **179**, achieving a roughly ten-fold productivity increase compared to batch conditions.[72] Maulide *et al.* also recognized the enormous potential of bicyclic lactones **179** as versatile building blocks resulting in intriguing synthetic approaches for cyclobutene and diene derivatives. Palladium-catalyzed allylic alkylation of **179** enabled rapid access to functionalized cyclobutenes **180** or **181** with high and unusual diastereo- and enantioselectivities (Figure 3).[73,74] Besides stabilized nucleophiles like malonates and azlactones, nonstabilized allylpinacaol boronates were employed to afford cyclobutene derivatives **182**.[75] Simple alkyl- **183** or halogen-substituted cyclobutene derivatives **184** were obtained by reaction with organocopper reagents[76] or alkali halide salts.[77] Noteworthy, these cyclobutenes can be further opened by 4π-electrocyclic ring-opening reactions giving rise to various diene frameworks, which themselves were extensively exploited for the synthesis of polyenic natural products, e.g. the southeastern fragment of Macrolactin A (**185**) and Inthomycin C (**186**) (Figure 3).[76–78] Furthermore, the

photoisomerization of pyrones has been utilized in the total synthesis of natural products by other working groups as well.[79]

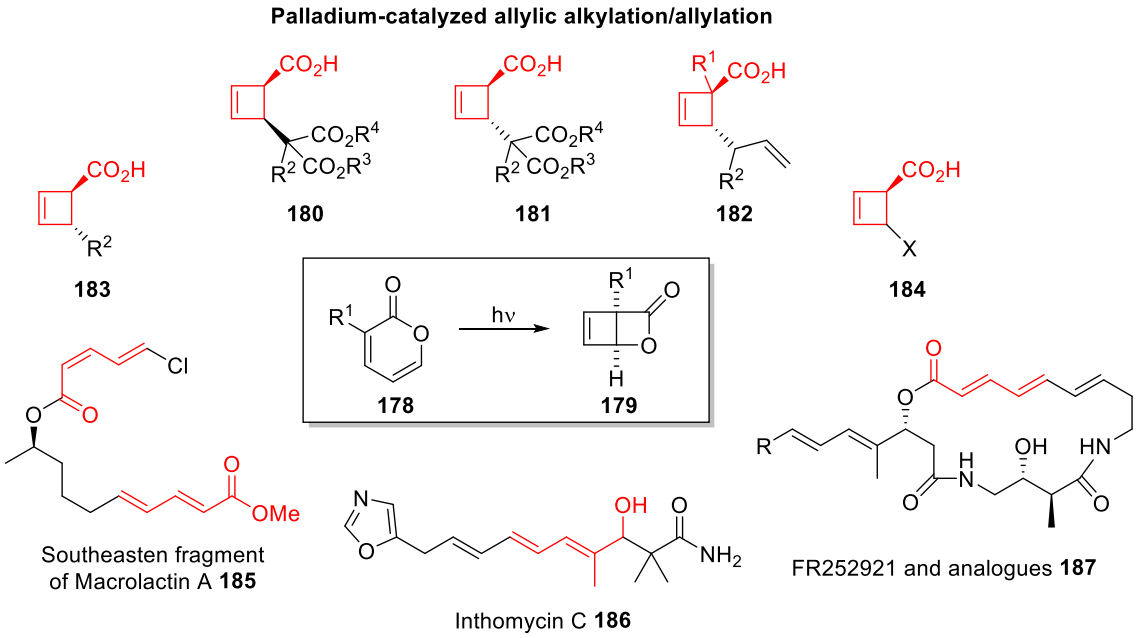

Figure 3. Synthesis and versatile chemistry of cyclobutene lactones **179**.[71,73–78]

3.3 [4+2]-Cycloaddition

The [4+2]-cycloaddition of a conjugated diene and a dienophile (an alkene or alkyne) – commonly known as the Diels-Alder reaction – is an exceptionally reliable and atom-economic pericyclic reaction for the construction of complex structures in a regio- and stereoselective fashion. Interestingly, 2-pyrones can act as both diene and dienophile in Diels-Alder reactions. However, just a few examples for the latter are reported in literature.[80,81] Generally, electron-withdrawing substituents in 5-position are necessary, as demonstrated in the reaction of methyl coumalate (**167**) and electron-rich dienes **188** (Scheme 40) – the first example for the usage of 2-pyrone as dienophile.[81]

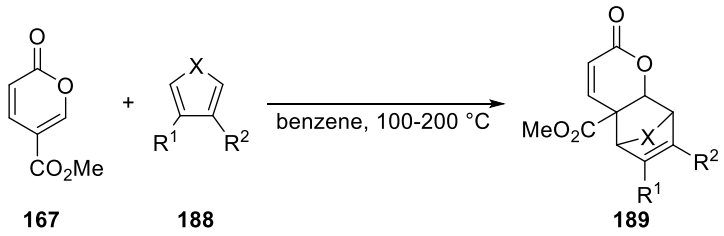

Scheme 40. Pyrone **167** as dienophile in Diels-Alder reactions.[81]

Classically, pyrones take part as dienes in [4+2]-cycloadditions with alkenes and alkynes (Scheme 41). Depending on the substitution pattern of pyrones, the cycloaddition can proceed

through a normal- or inverse electron-demand Diels-Alder (IEDDA) reaction. The [4+2]-cycloaddition with alkynes **190** gives rise to highly strained bicyclooctadiene intermediates **191**, which readily form aromatic products **192** after extrusion of CO_2. In contrast, cycloaddition with alkenes **193** yields isolable adducts **194**, representing useful synthetic intermediates due to their structural and stereochemical inimitability.[82]

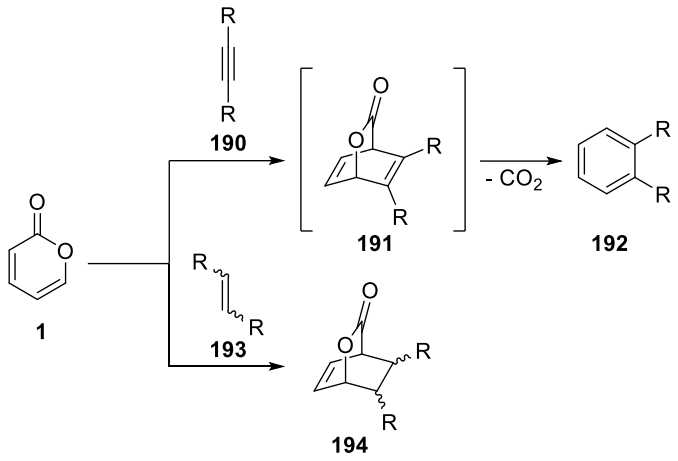

Scheme 41. 2-Pyrone (**1**) as diene in Diels-Alder reactions.[82]

Since Diels and Alder published in 1931 that 2-pyrones could function as a diene component in [4+2]-cycloadditions[83], this strategy has emerged as a powerful tool for the synthesis of aromatics, heteroaromatics and natural products.[82] Especially, the ability to form aromatic products from pyrones has been widely exploited. For instance, Garg *et al.* demonstrated, that an additional benzene ring can be easily introduced to oxygen-or nitrogen-containing strained alkynes **196** (Scheme 42).[84,85]

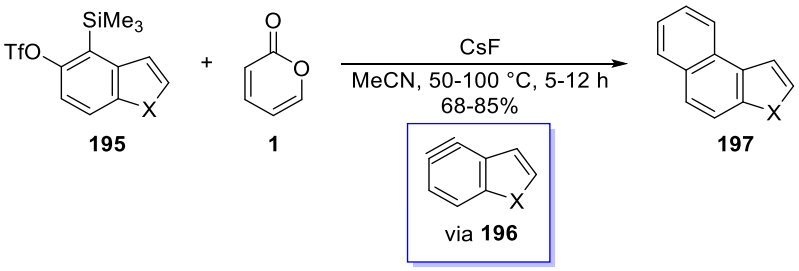

Scheme 42. [4+2]-cycloaddition of strained alkynes **196** and 2-pyrone (**1**).[84,85]

A substrate-directed cycloaddition of pyrones **198** and alkynyl boronates **199** was developed by Harrity and co-workers.[86] By activation of pyrone **198** with a Lewis acid the cycloaddition proceeded smoothly under mild reaction conditions and various synthetically useful motifs such as pyridines, azoles or amides could be used as directing groups. To demonstrate the utility of

this reaction the boronated products **201** were further functionalized by C-O, C-C and C-N bond-forming reactions (Scheme 43).

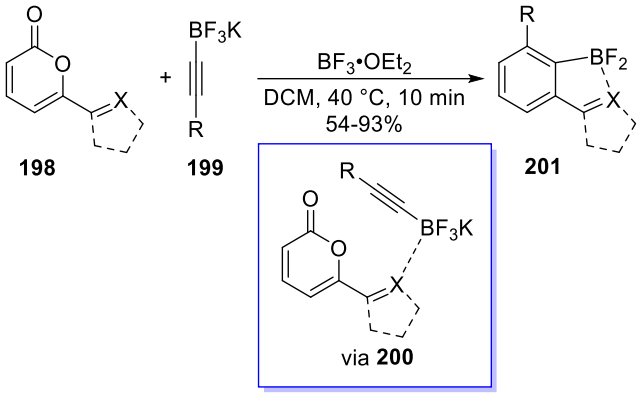

Scheme 43. Substrate-directed cycloaddition of pyrones **198** and alkynyl boronates **199**.[86]

Additionally, heteroaromatic compounds like phosphinines **203** – the higher homologs of pyridines – can be easily prepared by Diels-Alder reaction of 2-pyrone (**1**) with phosphoalkynes **202** (Scheme 44).[87,88] The silyl-phosphinine product **203** has been utilized for the preparation of a Cu(I)- and the first crystallographically characterized phosphinine-Ag(I) complex.

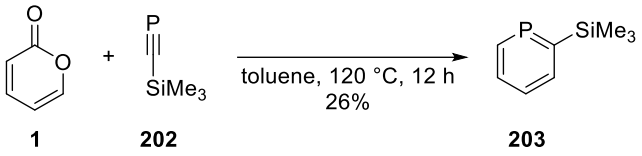

Scheme 44. Synthesis of phosphinines **203**.[87]

Although 2-pyrones were regarded as challenging dienes in asymmetric Diels-Alder reactions due to their inherent electron-deficient properties of aromatic character, some examples have been reported for the reaction with alkenes. In 2007, Deng *et al.* explored cinchona alkaloid-based bifunctional organic catalysts **206** for the asymmetric [4+2]-cycloaddition of 3-hydroxy pyrones **204** and electron-deficient alkenes **205**.[89] Thereby, valuable bicyclic adducts **208** were obtained with high enantio- and diastereoselectivity (Scheme 45). Herein, the cinchona alkaloid catalyst **206** simultaneously raises the energy of the HOMO of pyrone **204** and lowers the energy of the LUMO of the dienophile **205** by H-bonding interactions while orienting the two reactants to exert stereochemistry control.

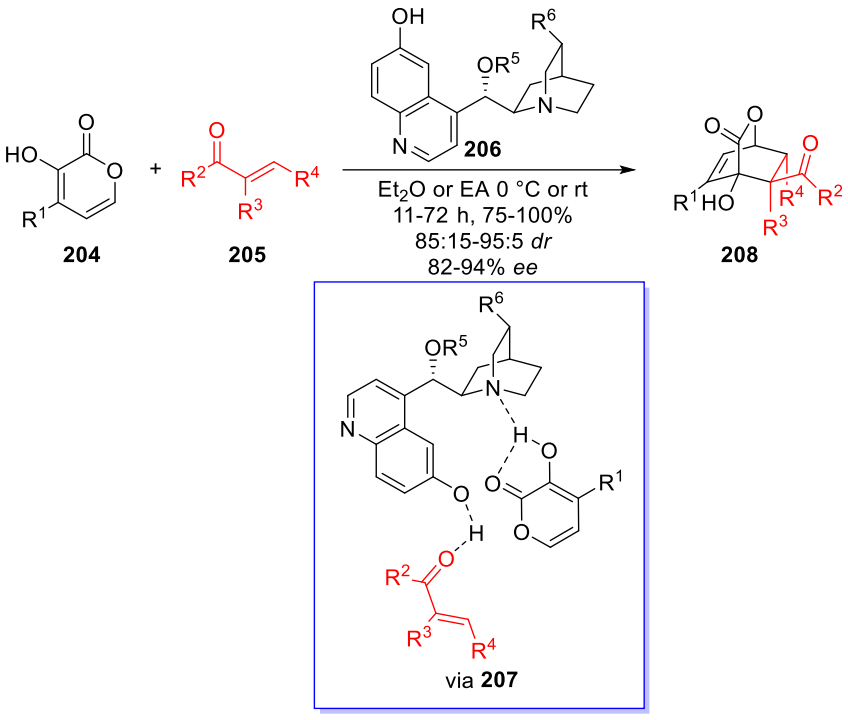

Scheme 45. Asymmetric Diels-Alder reaction of 3-hydroxy pyrones **204**.[89]

Besides further organocatalyzed methods employing chinchona alkaloid[90,91]- or Jørgensen-Hayashi-type catalysts[92], also some Lewis acid-catalyzed asymmetric IEDDA reaction of 2-pyrones have been developed.[93] Recently, an ytterbium-catalyzed IEDDA reaction of pyrones **209** with 2,2-dimethyl-1,3-dioxole (**210**) enabled the total synthesis of bioactive natural product (+)-MK7607 (**213**) in total three steps (Scheme 46).[94] By coordination to both carbonyls of pyrone **209**, the chiral catalyst is forcing the alkene **210** to a stereoselective cycloaddition due to steric shielding.

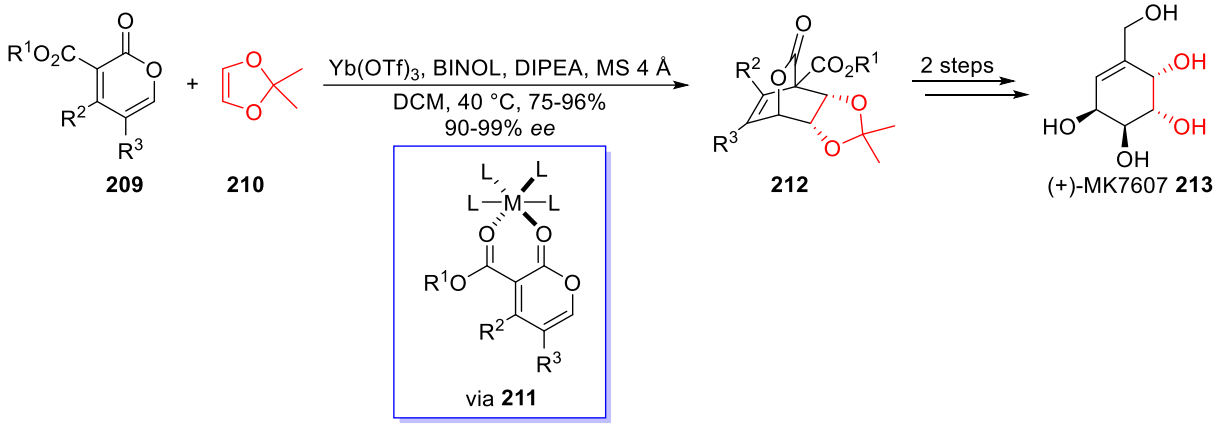

Scheme 46. Ytterbium-catalyzed asymmetric IEDDA reaction of pyrones **209**.[94]

Likewise, intramolecular [4+2]-cycloaddition of pyrones has been established as a reliable method for the synthesis of otherwise elusive natural or pharmacological important products,

even in late stages.[91,95,96] By combining the diene and dienophile moiety in one molecule, the cycloadditions can proceed regioselectively without employing catalysts due to the predefined coordination of the reactants. Snyder and co-workers, for instance, demonstrated the simple and elegant route to hydroindolines **215** which underwent subsequent hydrolysis to compounds **216**, a widespread motif in natural products (Scheme 47).[97] As an illustration of the power of this strategy, natural products Δ^7-Mesembrenone (**217**) and Gracilamine (**218**) have been obtained either formally or by total synthesis.

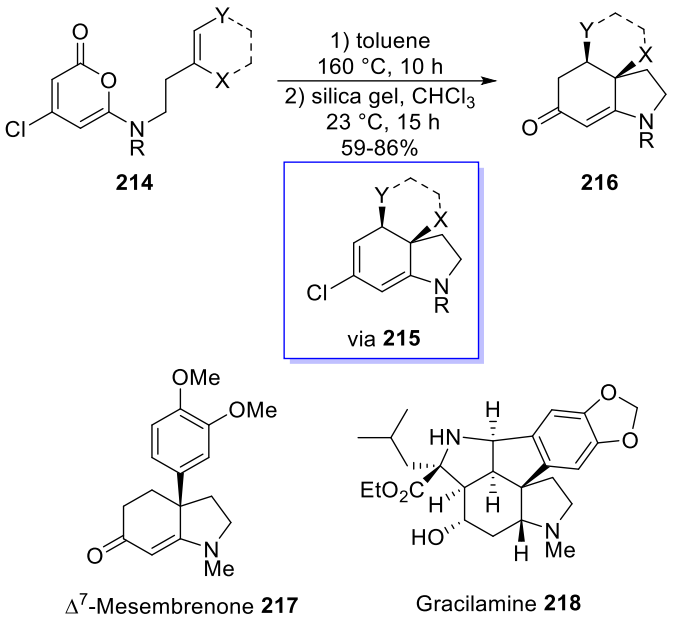

Scheme 47. Intramolecular Diels-Alder reaction to hydroindolines **215**.[97]

3.4 Other cycloadditions

The versatility of pyrones is also reflected in their ability to serve as a substrate in other cycloaddition reactions, e.g. [3+2]-[98] or [4+3]-cycloadditions[99], to give rise to otherwise elusive medium-sized ring systems. Guo *et al.* reported an enantioselective synthesis of medium-sized bicyclic compounds **222** via tandem [3+2]-cycloaddition of vinyl ethylene carbonates **219** and pyrones bearing electron-withdrawing substituents in 5-position **220** followed by Cope rearrangement of intermediate **221** (Scheme 48).[100] Noteworthy, the presence of aryl and at least vinyl-substituted substituents on carbonates **219** is necessary for a successful reaction. Based on control experiments and detailed computational studies product formation via direct [5+4]-cycloaddition pathway was excluded.

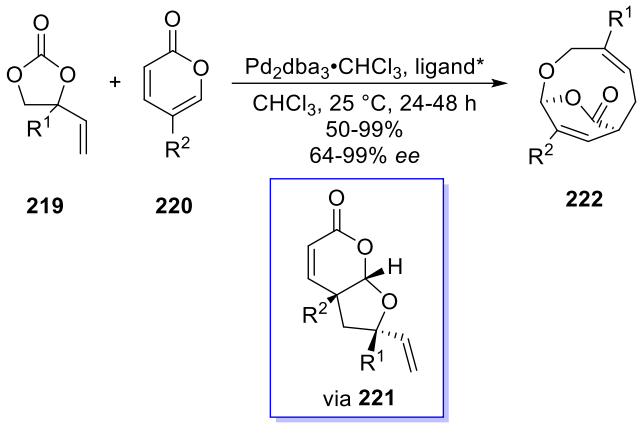

Scheme 48. Tandem [3+2]-cycloaddition/Cope rearrangement of pyrones **220**.[100]

In contrast, [4+3]-cycloaddition of 5-substituted pyrones **223** and imine esters **224** furnished functionalized azepine derivatives **226** after decarboxylation of bicyclic intermediate **225** and [1,5]-H-shift (Scheme 49).[101] The tandem reaction only requires NEt_3 as a mild base to provide biologically important azepine derivatives. However, again only pyrones with electron-withdrawing substituents worked in this reaction type, whereas no conversion of unsubstituted 2-pyrone was observed.

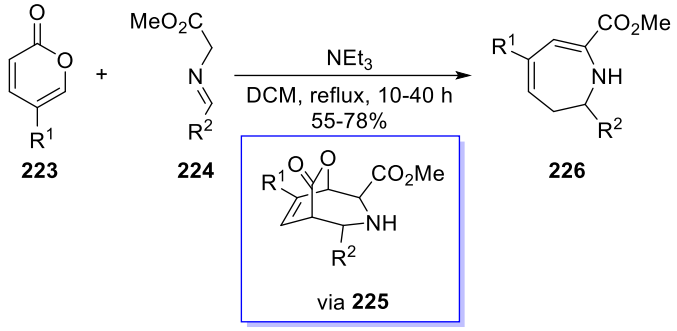

Scheme 49. [4+3]-cycloaddition of pyrones **223** and imine esters **224**.[101]

A quite unusual [10+4]-cycloaddition strategy for the synthesis of azulenes **231** has been investigated by Jørgensen and co-workers.[102] Application of a bifunctional thiourea catalyst **229** allowed the performance of the [10+4]-cycloaddtion of indene-2-carbaldehydes **227** and ethyl coumalate (**228**) under mild reaction conditions (Scheme 50). Herein, the 10π-reactant, which undergoes cycloaddition with pyrone **228**, is formed in situ by condensation of carbaldehyde **227** and catalyst **229**. Deprotonation of the resulting intermediate **230** concomitantly releases the catalyst and CO_2. The introduction of additional substituents to pyrone **228** proved to be unsuccessful.

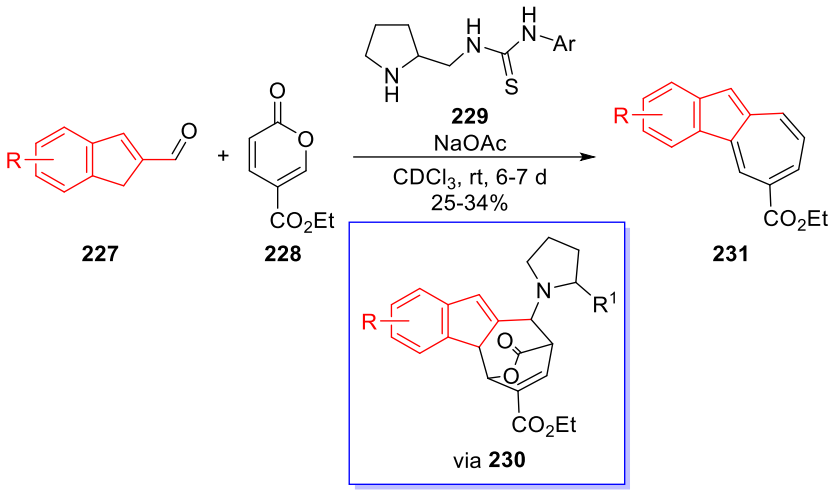

Scheme 50. Organocatalyzed [10+4]-cycloaddition.[102]

3.5 Lactamization

The structural motif of 2-pyridinone **232** is ubiquitous in nature and a wide range of 2-pyridinone derivatives exhibit important bioactivities (Figure 4).[103–109] Similarly to pyrones, pyridinones are useful starting materials in organic and medicinal chemistry possess interesting properties like dimer formation of the two existing tautomers of 2-pyridinone **232** and **233** (Figure 4).[110,111]

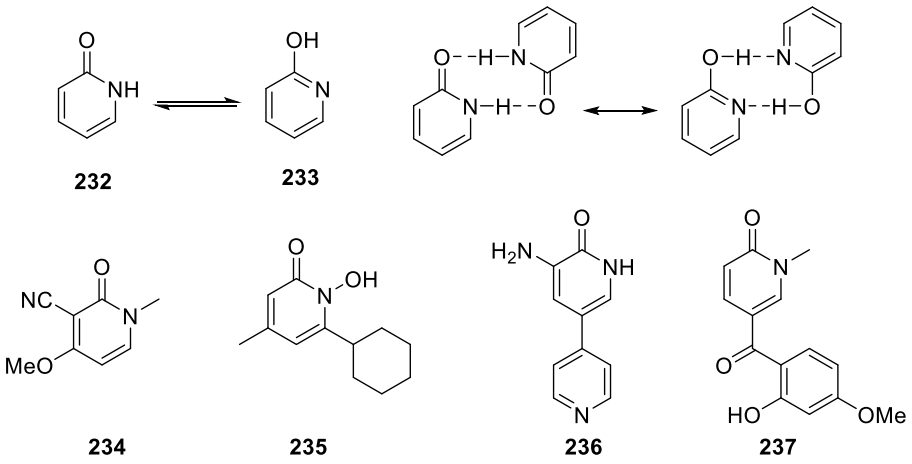

Figure 4. Dimerization of 2-pyridinone tautomers **232-233** and bioactive derivatives **234-237**.[103–111]

2-pyrones are easily converted into the corresponding lactams via 1,6-addition of amines. Reaction with ammonia yields *N*-unsubstituted 2-pyridinones, whereas *N*-substituted derivatives are obtained by reaction with primary amines.[112] The transfer of 2-pyrones to 2-pyridinones is frequently used in research. Moloney and co-workers developed a three-step

synthetic sequence to triazolo pyridines **241** enclosing the lactamization of methyl coumalate (**167**) to dihydrazide intermediate **240** as key step (Scheme 51).[113]

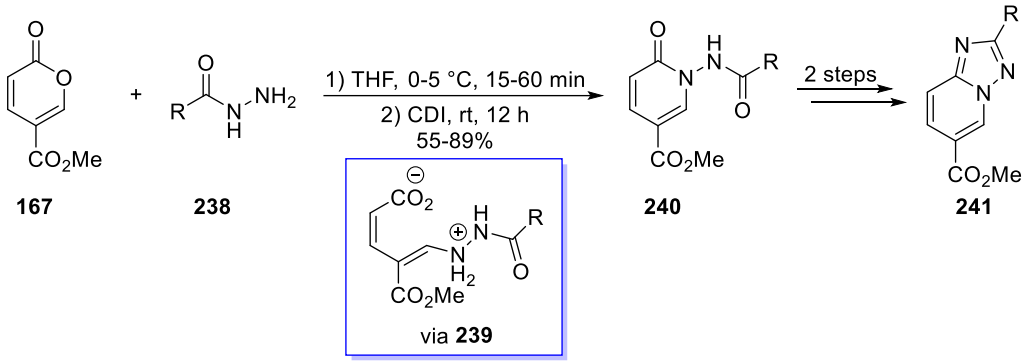

Scheme 51. Synthesis of triazolo pyridines **241** by lactamization of pyrone **167**.[113]

A different lactamization approach for the synthesis of bicyclic 2-pyridinones **245** was lately investigated by Disadee *et al.* (Scheme 52).[114] The novel double cyclization of 2-pyrones **242** bearing a tethered, homochiral α-amino acid proceeded through deprotection, enamine **243** formation, decarboxylation and lactamization of **244** with retention of the chirality. This strategy required no special reagents for the multichemical transformations. Only ethylene glycol was added to improve the solubility of pyrones **242** in water.

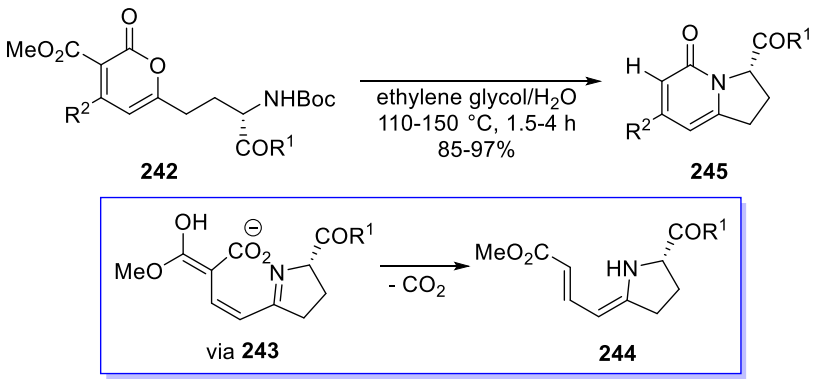

Scheme 52. Synthesis of bicyclic 2-pyridinones **245**.[114]

3.6 Conjugate addition

The α,β-unsaturated carbonyl structure present in 2-pyrones offers the opportunity for 1,4-nucleophilic additions resulting in synthetic valuable 3,4-dihydro-2-pyrones or allowing the introduction of additional substituents into the 2-pyrone ring system.[115,116] During the formal synthesis of antibacterial agent Lasalocid A **249**, Ireland *et al.* found that Grignard reagent **246** effectively underwent conjugate addition to pyrone **174**, while organocuprates surprisingly failed (Scheme 53).[117] The regioselective 1,4-addition of the Grignard reagent **246** was

attributed to the stabilization of the carbanion generated at 3-position by the methoxycarbonyl group.

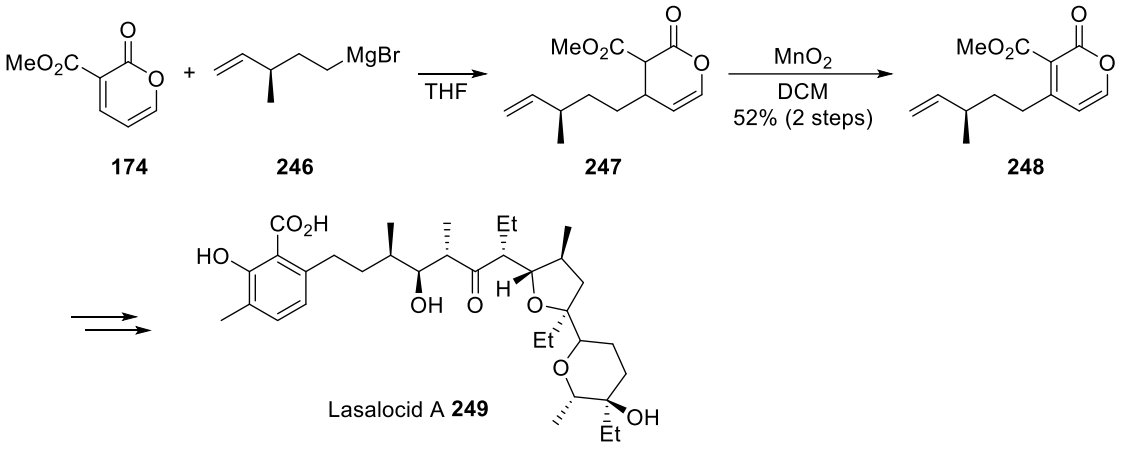

Scheme 53. Conjugate addition of pyrone **174** with Grignard reagent **246**.[117]

However, the reactivity of 2-pyrones **250** towards organocopper reagents could be increased by silylation with *tert*-butyldimethylsilyl triflate (TBDMSOTf) forming the corresponding pyrylium salt **251**.[115] After silylation, several substituents were introduced by conjugate addition, whereby a selective attack at 4-position was especially preferred by soft and bulky organocuprates. Moreover, lithium diorganocuprates reacted more efficiently than the cuprates prepared from Grignard reagents. Finally, hydrolysis of silylated adducts **252** afforded substituted dihydro pyrones **253** (Scheme 54).

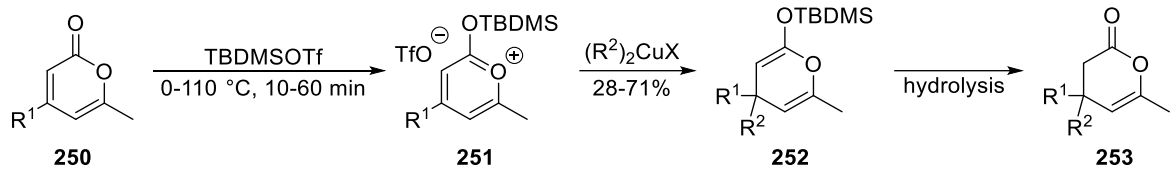

Scheme 54. Conjugate addition of organocuprates.[115]

Due to the increased electron delocalization compared to acyclic unsaturated esters, the stereoselective addition to pyrones is quite challenging. However, an efficient copper-catalyzed asymmetric conjugate addition of Grignard reagents to unsubstituted 2-pyrone (**1**) has been developed by Feringa and co-workers.[116] In the presence of a chiral ferrocenyl-based diphosphine ligand **254**, various 3,4-dihydro-pyrones **255** were obtained with excellent enantioselectivity (Scheme 55). Further transformations of these products **255** allowed to access highly versatile building blocks with high stereocontrol.

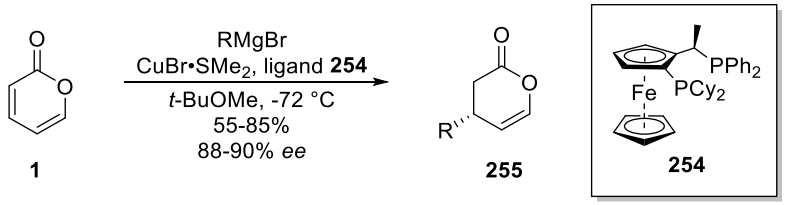

Scheme 55. Asymmetric conjugate addition to 2-pyrone (**1**).[116]

The development of organocatalytic conjugate-addition protocols plays also a pivotal role in the functionalization of pyrones. The first example of a sequential Mukaiyama-Michael/Mukaiyama aldol reaction of pyrones **256** with silicon enolate **257** and acetone **258** was published by Yanai and Matsumoto in 2016 (Scheme 56).[118] Moreover, the strong acid catalyst was able to promote a second Mukaiyama-Michael reaction to dihydropyrone **262** by adding a further Michael-acceptor **259** to the reaction mixture without overreacting to polymeric byproducts.

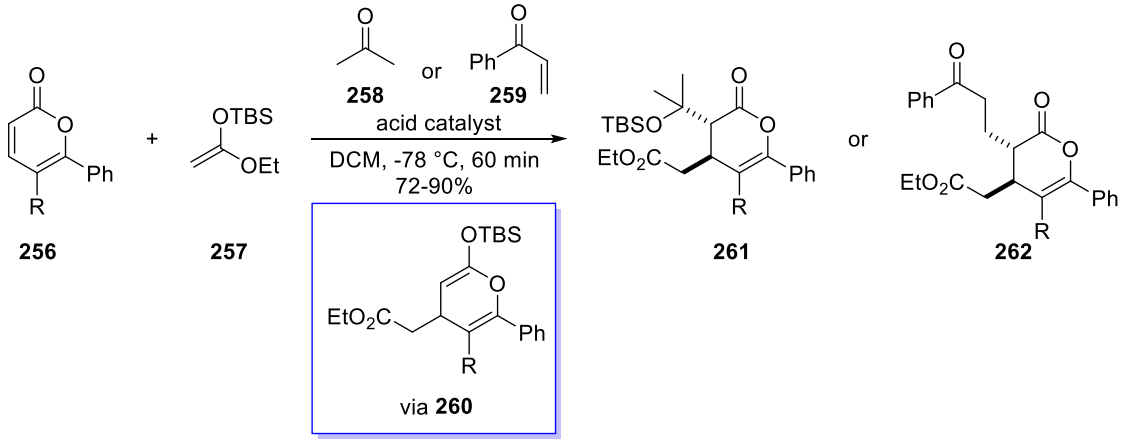

Scheme 56. Subsequential Mukaiyama-Michael/Mukaiyama aldol reaction of pyrones **256**.[118]

As previous illustrations of ring-opening reactions showed, conjugate additions can also take place at the 6-position of 2-pyrones. Consequently, Zu *et al.* reported an organocatalyzed enantioselective Rauhut-Currier reaction of methyl coumalate (**167**) with α,β-unsaturated aldehydes **263**.[119] The enals **263** were activated by iminium catalysis to serve as Michael-acceptors, while 1,6-addition of a nucleophile to pyrone **167** generated the latent enolate. The latter is also facilitated by activation of pyrone **167** by the organocatalyst **264**. Ultimately, elimination of the nucleophile in intermediate **265** furnished 3-substituted pyrones **266** in yields up to 99% with high levels of enantioselectivity (Scheme 57).

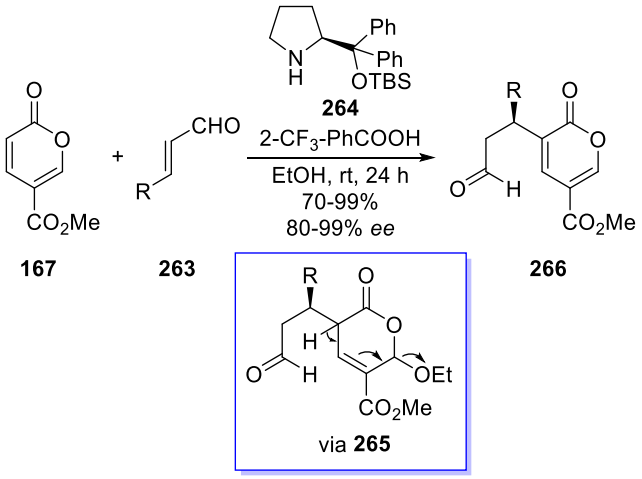

Scheme 57. Enantioselective Rauhut-Currier reaction of methyl coumalate (**167**).[119]

In conformity with this approach, Dechoux and co-workers demonstrated the functionalization of methyl coumalate (**167**) with various aldehydes or imines **267** by an organocatalyzed Morita-Baylis-Hillman reaction (Scheme 58).[120] In contrast to common Baylis-Hillman reactions, the transformation occurs via an unprecedented 1,6-conjugate addition of the Lewis base to pyrone **167**.

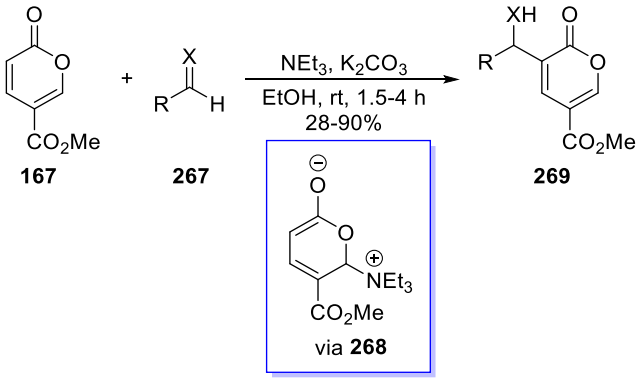

Scheme 58. Morita-Baylis-Hillman reaction of methyl coumalate (**167**).[120]

3.7 Cross-coupling reactions

Cross-coupling reactions constitute an important tool for the premeditated derivatization of pyrones in the total synthesis of natural products and biologically active compounds.[96,121–123] Owing to the merging aromatic and alkenic character, the pyrone scaffold can be used as the organometallic component as well as the organic halide/pseudohalide component in several renowned coupling reactions.

Meinwald *et al.* investigated the synthesis of the core structure of steroidal pyrone substrates by direct Stille coupling of 5-stannyl pyrone **270a** with various cyclic enol triflates.[124] The

5-stannyl pyrone **270a** was easily prepared from 5-bromo pyrone (Scheme 59) and this concept was also applicable to the synthesis of 3-substituted pyrones and 3-substituted 5-bromo-pyrones.[125] The analogous conversion of 5-bromo pyrone into 5-boronate ester **270b** and subsequent Suzuki coupling with a range of aryl- and heteroaryl halides and triflates was reported by Jones and co-workers (Scheme 59)[126]. Similarly, a facile route to 5,6-disubstituted pyrones via Negishi coupling of 5-iodozinc pyrones **270c** with organic electrophiles was developed by Rossi *et al*. (Scheme 59).[127] The required iodo pyrones **270c** can be obtained by iodolactonization as discussed earlier (Scheme 25).[48]

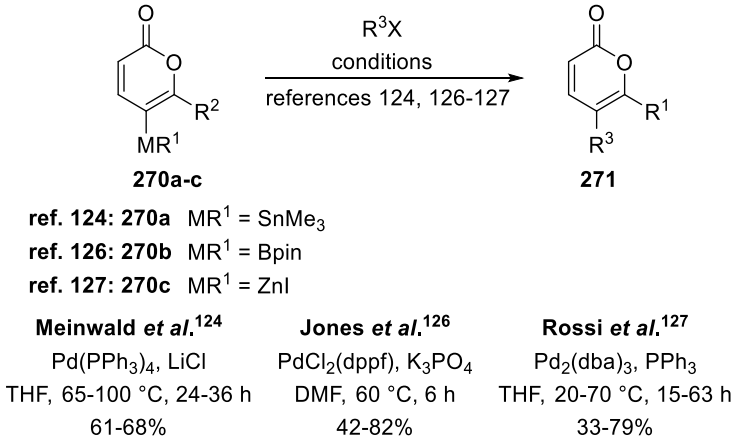

Scheme 59. Cross-coupling of 5-metallated pyrones **270a-c**.[124,126,127]

Although the conversion of halogenated pyrones into organometallic compounds proved to be successful, the direct engagement of halogenated- or pseudohalogenated pyrones in cross-couplings has been established as a more efficient strategy. In 2002, Cho *et al.* demonstrated the regioselective palladium-catalyzed Sonogashira coupling of 3,5-dibromo-2-pyrone (**272**) with alkynes **273** to give rise to 3-alkynyl-5-bromo-2-pyrones **274** (Scheme 60).[128] Later, the same strategy found application in the formal synthesis of the steroidal tricyclic lactone (+)-Aplykurodinone-1 (**275**).[96]

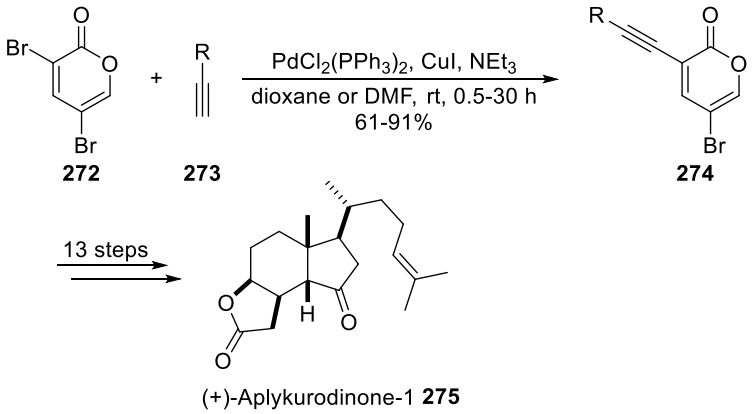

Scheme 60. Regioselective Sonogashira coupling of dibromo pyrone **272**.[96,128]

The same working-group found that dibromo pyrone **272** undergoes Stille coupling with stannanes regioselectively at either C-3 or C-5, depending on the employed reaction conditions (Scheme 61).[129] Usually, cross-couplings proceed preferred at the 3-position of dibromo pyrone **272** due to the lower electron density at C3. However, conducting the reaction in DMF a switch in regioselectivity was observed, which could not be explained with the level of current mechanistic understanding. Moreover, in DMF the ratio of **278** to **277** increases in proportion to the equivalents of CuI. Sarpong and co-workers exploited this strategy for an one-pot sequential Stille-Stille coupling in the total synthesis of Delavatine A (**279**).[121]

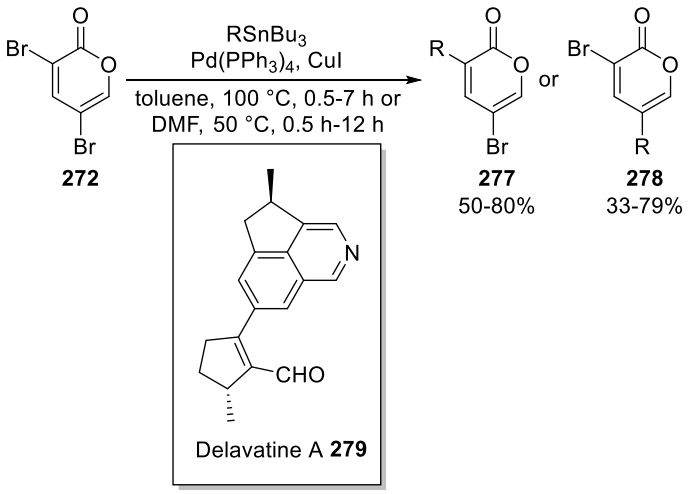

Scheme 61. Regioselective Stille coupling of dibromo pyrone **272**.[121,129]

Along these lines, Suzuki coupling of pyrones has established as a reliable functionalization method.[130] Recently, a synthetic pathway to natural products **283** isolated from fungus *Phellinus igniarius* has been developed by Ohyoshi *et al.* enclosing Suzuki couplings of 3-brominated pyrone **280** with boronate **281** as key step (Scheme 62).[123]

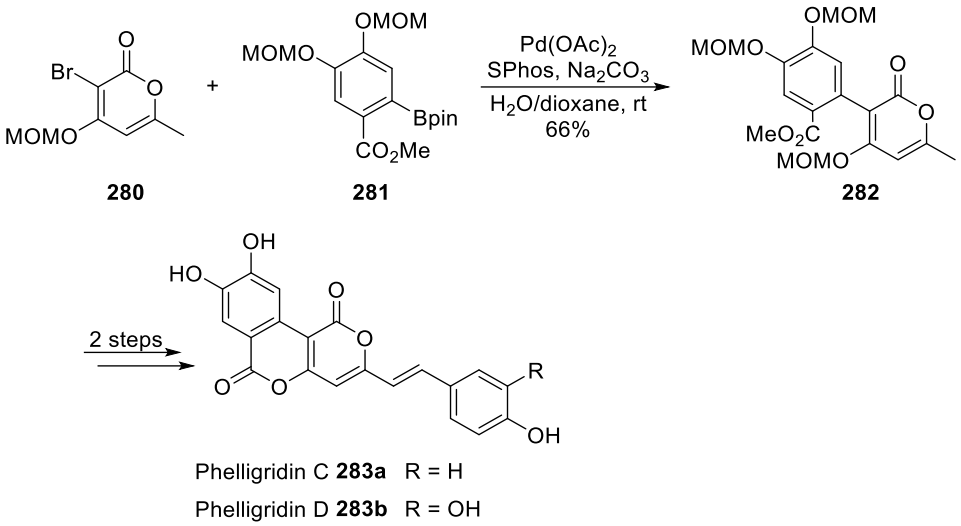

Scheme 62. Suzuki coupling pyrone **280** with boronate **281**.[123]

A novel intramolecular direct arylation of 3-bromo 2-pyrones **284** was developed by McGlacken and co-workers (Scheme 63).[131] Herein, intramolecular coupling was achieved by C-H activation of the phenoxy substituent and subsequent cross-coupling reaction. Both electron-donating and withdrawing substituents were tolerated on the aryl moiety. Surprisingly, the employment of iodo-substituted pyrone derivatives failed and no conversion of these substrates was observed.

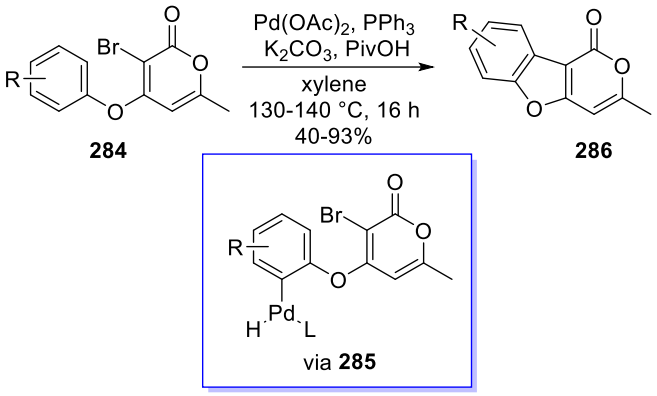

Scheme 63. Intramolecular direct arylation of 3-bromo 2-pyrones **284**.[131]

3.8 C-H activation

Direct coupling methods, involving at least one C-H activation step, offer several advantages over traditional cross-couplings. In general, the production of waste is reduced by avoiding suitable prefunctionalization of substrates with activating groups and ideally, both coupling partners are unactivated. Generally, pyrones have higher electron-density at their 3- or 5-position and these positions are also liable for palladium activation. The first catalytic protocol

for a C-H functionalization of 2-pyrones was described by Fairlamb and co-workers.[132] Pyrones **287** were regioselectively activated at the 3-position to yield fused products **289** (Scheme 64). Control experiments revealed the oxidative addition of palladium to the aryl substituent to be the first step in the reaction events. The reaction worked with iodo- and bromo-substituted aryls and the yield decreased significantly by employing substrates that bear electron-withdrawing substituents on the aryl moiety.

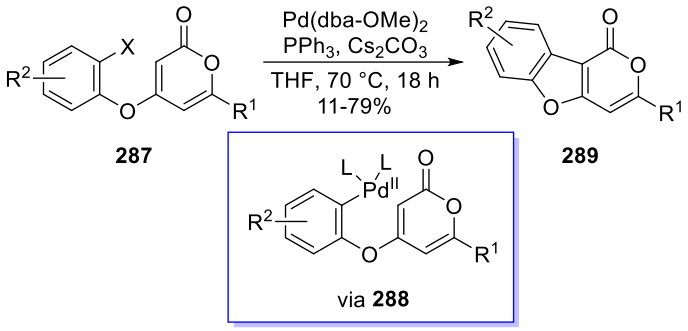

Scheme 64. Palladium-catalyzed C-H functionalization of pyrones **287**.[132]

In collaboration with McGlacken, the same working group also extended the scope to six-membered fused cycles **292** by varying the length of the tethered side-chain.[133] However, the formation of C-5 activated byproducts was observed in some cases. Later, regioselective functionalization at C-3 has been optimized by McGlacken and co-workers (Scheme 65).[134] The use of pivalic acid was proved to be necessary for a successful reaction since a concerted metalation-deprotonation via intermediate **291** was determined as a crucial key step.

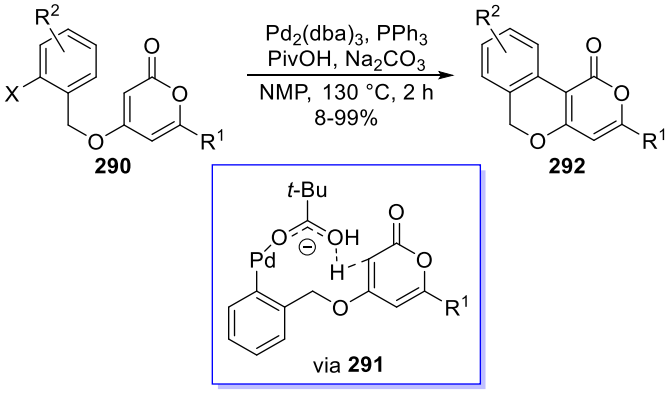

Scheme 65. Regioselective C-H functionalization at C-3.[134]

In addition, McGlacken and co-workers were able to circumvent the preferential reactivity at the 3-position and developed a direct arylation protocol for the intramolecular coupling at C-5 by blocking C-3 with an unreactive chlorine atom.[135] The retained chlorine atom at C-3 in pyrones **294** allows further derivatization of the pyrone scaffold (Scheme 66).

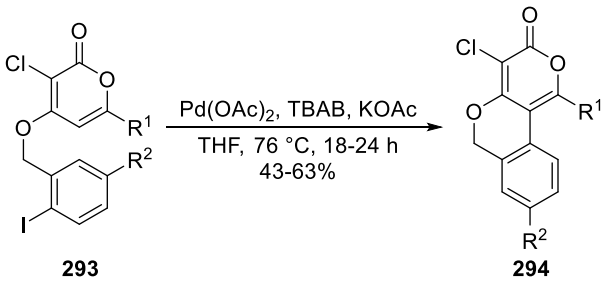

Scheme 66. Regioselective C-H functionalization at C-5.

As part of their pioneering work in this research field, McGlacken *et al.* also investigated the aryl-heteroaryl coupling via double C-H activation of compound **295**, thus avoiding the preinstallation of any activating group (Scheme 67). Based on mechanistic studies, the excellent regioselectivity towards cyclized products **297** was rationalized by initial C-H activation of the 2-pyrone skeleton at C-3.[136] Equally, double C-H activations of 4-aniline[137] or 4-thioaryl[138] substituted pyrones led to the formation of indole- or benzothiophene fused products, respectively.

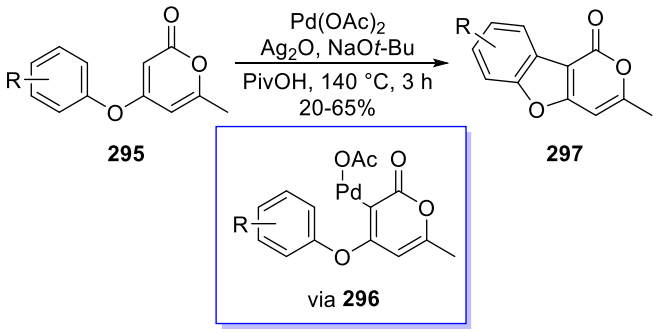

Scheme 67. Double C-H activation of pyrone **295**.[136]

A heretofore unprecedented intermolecular C-H activation approach was developed by Yusuf and co-workers (Scheme 68).[139] The palladium-catalyzed ligand-free alkenylation of pyrones **298** with various alkenes **299** proceeded smoothly under mild reaction conditions with high regioselectivity. Besides hydroxy or methoxy groups, also chlorine was tolerated as substituent in 4-position furnishing valuable pyrone derivatives **301** without forming classical Heck-type products. Moreover, styrenes **299** with both electron-donating, electron-withdrawing groups and halogen-substituents reacted efficiently to generate the corresponding alkenylated products **301**. The excellent chemo- and regioselectivity again can be explained by C-H activation of pyrone **298** in 3-position by the palladium catalyst in the first mechanistic step.

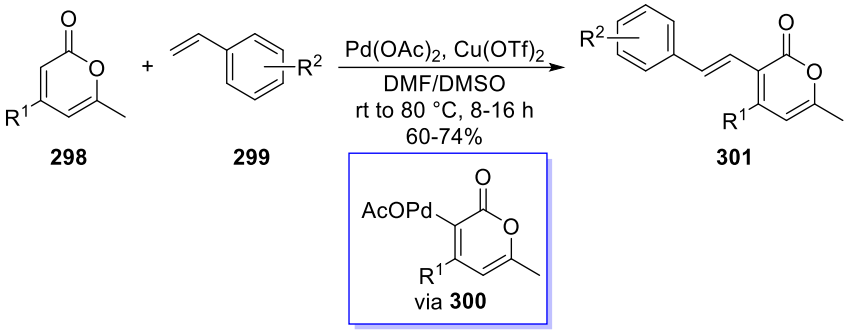

Scheme 68. Palladium-catalyzed direct alkenylation of pyrones **298**.[139]

3.9 2-Pyrone ligands

The multifaceted nature of 2-pyrones appears not only in their versatile reactivity but also in their vein to complex various metals. The preparation of new complexes is an important research field in catalysis. Alternatively, coordination of organic molecules to metal fragments can have pronounced effects on their reactivity as observed in the iron-catalyzed ring-opening reactions of 2-pyrones **161** (Scheme 36).[64] Pyrone complexes with various metals, e.g. Fe[140,141], Os[142], Co[143], Re[144], Mo[145,146] or Ir[26], have been reported in which the 2-pyrone unit is bound either in a η^4-diene- or η^1-like fashion (Figure 5).

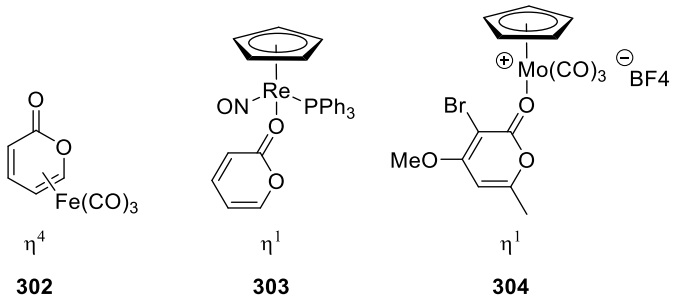

Figure 5. 2-Pyrone complexes.[140,144,146]

Furthermore, pyrone complexes like **302** and **304** show interesting CO-releasing properties.[146–148] Those CO-releasing molecules are capable of delivering controlled amounts of CO within a cellular environment having potential therapeutic applications. Herein, the intrinsic stability of the complexes, which can be controlled by appropriate substituents on the pyrone scaffold, influences the extent and rate of the CO release.[147]

In conclusion, 2-pyrones are a privileged class of heterocycles exhibiting an extensive range of biological activities with immense therapeutic importance, which attracted considerable attention in recent years for the synthesis of this specific molecular scaffold by either transition metal-catalyzed or transition metal-free methods. Due to their versatile reactivity, 2-pyrones

exert a vast potential to generate molecular complexity being showcased in the synthesis of numerous natural or pharmacologically active products. Moreover, the ability to form metal complexes could enable the development of new catalytic systems and CO-releasing molecules, whose intrinsic stability can be delicately tuned by a plethora of diverse substitution patterns located on the pyrone moiety. Therefore, the development of novel strategies for the synthesis and functionalization of 2-pyrones remains an important field of research in organic chemistry.

B Main part

1 Sustainable synthesis of 2-pyrones

1.1 Introduction

Processes for the production of carbon-based chemicals are nowadays predominantly based on non-renewable feedstocks like oil, natural gas and coal (Figure 6).[149] However, the predictable depletion of fossil raw materials as well as the increasing environmental awareness of society are progressively forcing the chemical industry to replace fossil-based chemicals by commodities that can be derived from renewable resources. With advances in its conversion technologies, biomass has become the most promising renewable carbon source.[150] All organic materials, that are assigned to biomass, are originally produced by biological photosynthesis using CO_2, water and light and therefore, abundant carbon-neutral renewable resources.[151] Accordingly, research is especially focused on the development of new synthetic strategies for the production of valuable products based on biomass. Among these, fine chemicals, which demonstrate a variety of reactivities and thus enabling access to value-added molecules are of particular interest.

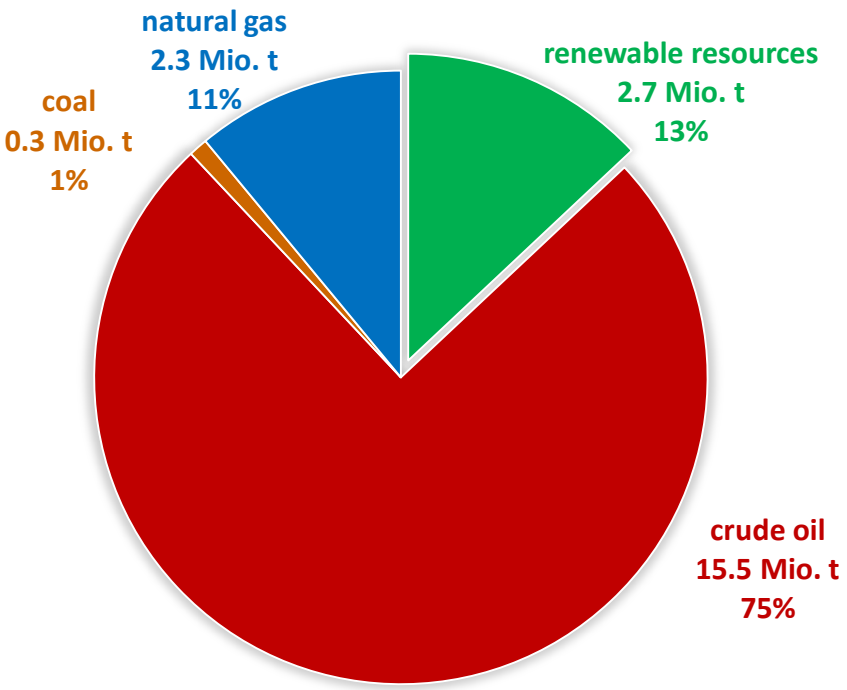

Figure 6. Used resources (Mio. t) in the organic chemical industry in Germany 2017.[152]

2-pyrones, for instance, are versatile starting materials in synthetic organic chemistry and several methods have been developed over the years to access this class of substrates (see introduction A2). Recently, Reiser *et al.*[16] reported the synthesis of 6-hydroxyalkyl 2-pyrones **26** starting from renewable resources (Scheme 69). The key step of this synthetic sequence is the thermal rearrangement of cyclopentenone epoxide **307** through a 6π-electrocyclic reaction via the intermediacy of a vinyl ketene **308** (Scheme 69).[153]

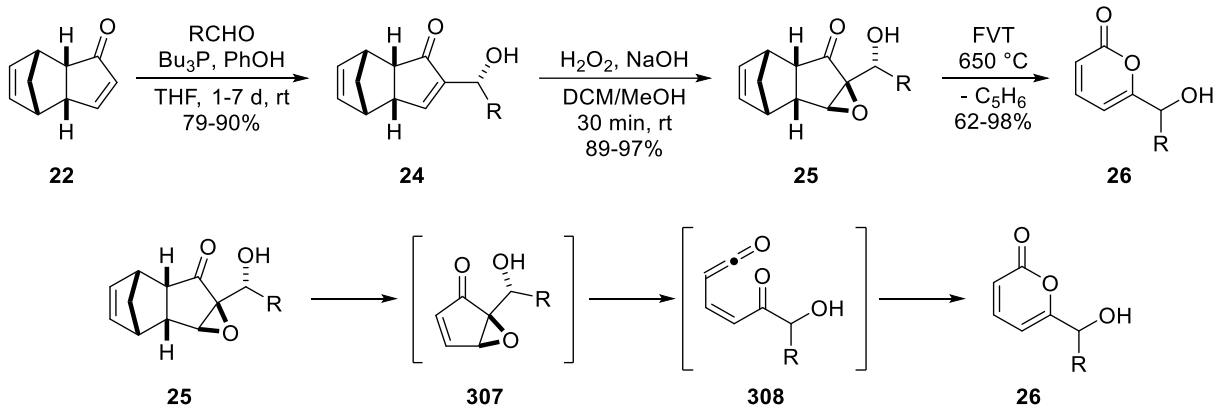

Scheme 69. Synthesis of 6-hydroxyalkyl 2-pyrones **26** from renewable resources via thermal rearrangement of epoxide **307**.[16]

Since cyclopentenone epoxides cannot be directly obtained from cyclopentadienones due to the high tendency of the latter to dimerize, enone **22** was envisioned as a suitable cyclopentadienone precursor[154] for the synthesis of hydroxyalkyl 2-pyrone derivatives **26**. Enone **22** was readily available by a reaction sequence starting from furfuryl alcohol (**18**) (Scheme 70) which itself can be prepared by catalytic reduction of furfural (**310**) on ton scale (Scheme 71).

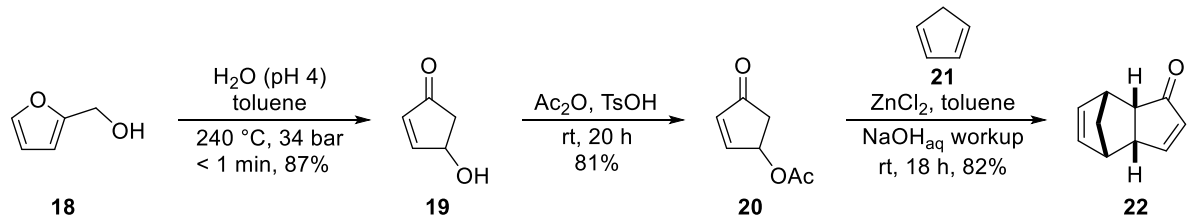

Scheme 70. Synthesis of enone **22** from renewable resources.[16]

Furfural (**310**) is the most frequent chemical derived from hemicellulosic biomass in industry and used as an important platform chemical for the production of biofuels, solvents and other valuable products.[155,156] Hemicellulose, a polysaccharide of different sugar monomers, e.g. xylose, arabinose, mannose and galactose, is an abundant and inexpensive renewable resource based on non-edible waste products like bagasse and bran.[155–157] Treatment of

hemicellulose with acids gives rise to xylose (**309**), the major component of this polysaccharide and by further dehydration furfural (**310**) is obtained (Scheme 71).

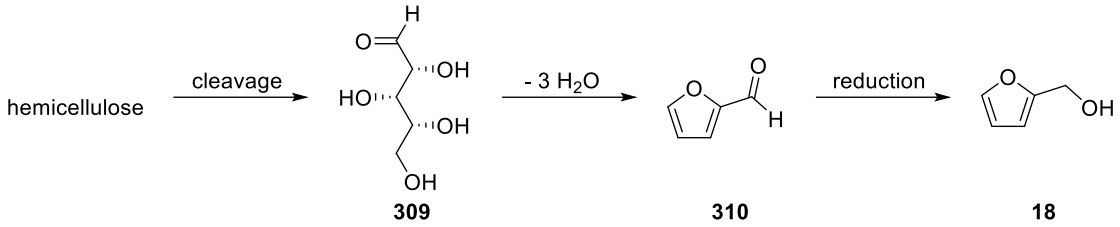

Scheme 71. Synthesis of furfuryl alcohol (**18**) starting from renewable resources.

The ready availability of furfuryl alcohol (**18**) by the aforementioned process and its versatile reactivity[158] offer outstanding opportunities for the production of valuable chemicals and drugs. In the synthesis of 6-hydroxyalkyl pyrones **26,** the acid-catalyzed Piancatelli rearrangement of alcohol **18**[159] was used to get access to 4-hydroxy-2-cyclopentenone (**19**), a precursor for key compound enone **22** (Scheme 70). In 2010, Reiser *et al.*[160] were successful in transferring this rearrangement to a continuous flow setup making a large scale synthesis and high yields possible (Figure 7).

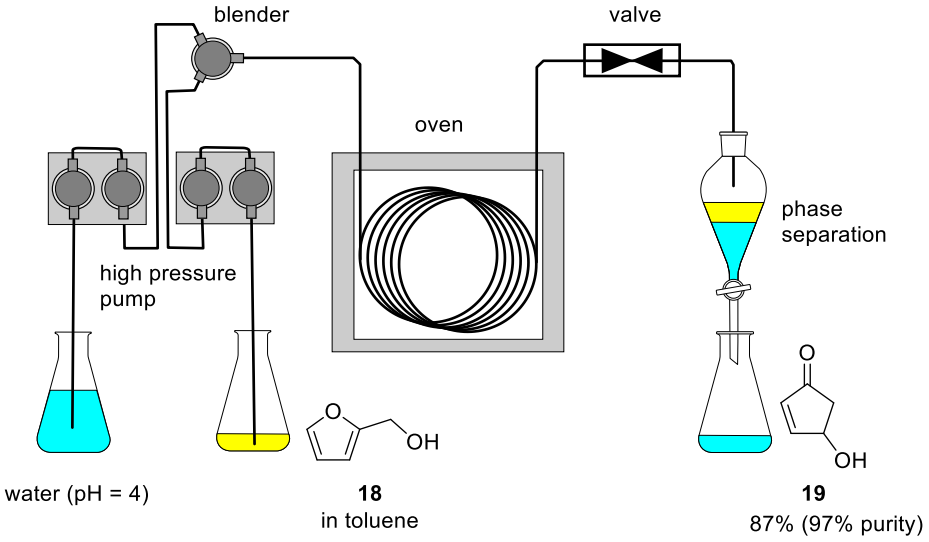

Figure 7. Continuous flow setup for the Piancatelli rearrangement of furfuryl alcohol (**18**).[160,161]

A solution of furfuryl alcohol (**18**) in toluene and water (pH = 4) are separately injected via a high-pressure pump and mixed with a blender. After passing the mixture through an oven at 240 °C and 34 bar in less than 1 min two layers are obtained, with 4-hydroxy-2-cyclopentenone (**19**) dissolved in the aqueous phase and polymeric byproducts in the organic layer. Water is evaporated and hydroxy cyclopentenone **19** can be obtained in 87% yield and 97% purity. This

strategy allowed the synthesis of key compound enone **22** (Scheme 70) and therefore, of 2-pyrone derivatives **26** from readily available renewable resources (Scheme 69).

Based on this previous work of Reiser *et al.*[16,161] the first part of the present thesis constitutes the development of a sustainable big-scale process towards unsubstituted 2-pyrone (**1**) from furfuryl alcohol (**18**). Additionally, the synthesis of 6-alkyl pyrones was investigated which could enable access to natural products. The utility of biobased pyrone compounds should be showcased in various follow-up transformations.

1.2 Big-scale synthesis of unsubstituted 2-pyrone[a]

Unsubstituted 2-pyrone (**1**) is a versatile starting material in organic chemistry and has been used for the synthesis of a variety of natural products and pharmacologically active substances e.g. (-)-Leodomycin D (**311**) or Rosiglitazone (**312**) (Scheme 72).[10,76] Nevertheless, only few methods for the synthesis of pyrone **1** have been reported in literature to date[162] which is associated with quite high prices at commercial suppliers for this valuable chemical.

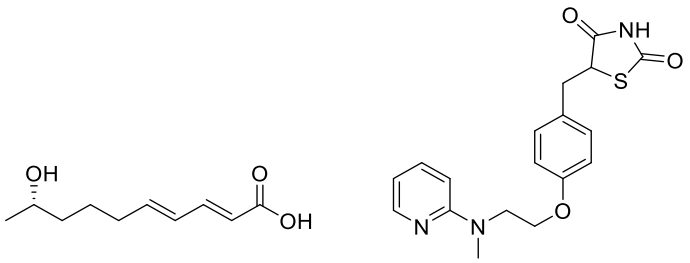

(-)-Leodomycin D **311** Rosiglitazone **312**

Scheme 72. Examples of substances derived from 2-pyrone (**1**).[10,76]

Targeting the synthesis of unsubstituted 2-pyrone (**1**) on a big-scale the thermal rearrangement of epoxide **313** should provide an exceptional atom economic and efficient route (Scheme 73). Due to aforementioned processes, acetate **20** can be obtained on a large scale from inexpensive, biomass-based furfuryl alcohol (**18**).[16] However, upscaling of the following Diels-Alder reaction to enone **22** and thermal rearrangement to pyrone **1** created some issues.

[a] This chapter includes parts from a manuscript which has been prepared in collaboration with D. Dobler (University of Regensburg)[161].

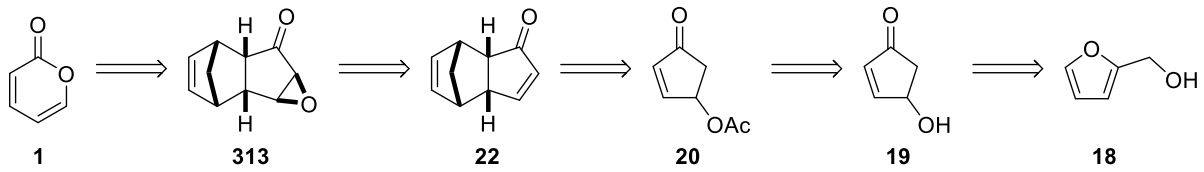

Scheme 73. Envisioned retrosynthetic strategy towards 2-pyrone (**1**).

In literature, the Diels-Alder/elimination reaction of acetate **20** with cyclopentadiene **21** is generally performed by using superstoichiometric amounts of $ZnCl_2$ as Lewis acid and dry benzene or toluene as solvent making these conditions unfavorable for a multigram synthesis of enone **22** (Table 1, entry 1 and 2).[16,163] In addition, significant amounts of inorganic waste are formed herein leading to a quite challenging reaction work-up. Therefore, different cycloaddition conditions were investigated to obviate the usage of stoichiometric amounts of reagents and toxic solvents in this synthetic step (Table 1).

Table 1. [4+2]-cycloaddition of acetate **20** with cyclopentadiene **21**.

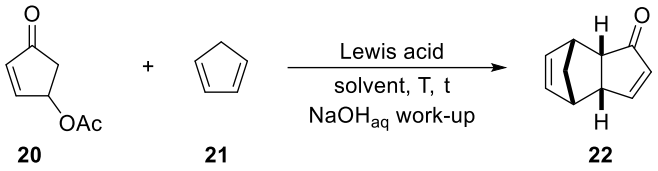

entry[a]	Lewis acid	equiv LA	solvent	T	t [h]	yield [%]
1	$ZnCl_2$	3.0	benzene	rt	17	89 (95)[163]
2	$ZnCl_2$	3.0	toluene	rt	18	86 (87)[16]
3	$ZnCl_2$	1.0	Et_2O	rt	18	86
4	$ZnCl_2$	0.25	Et_2O	rt	18	70
5	$BF_3{\cdot}OEt_2$	0.10	Et_2O	0 °C	18	72
6[b]	$BF_3{\cdot}OEt_2$	0.10	Et_2O	0 °C	18	82

[a] conditions: acetate **20** (10.0 mmol, 1.0 equiv), cyclopentadiene **21** (3.0 equiv) in solvent (65 mL); [b] conditions: acetate **20** (200 mmol, 1.0 equiv), cyclopentadiene **21** (2.0 equiv) in Et_2O (650 mL).

Comparable yields to those obtained under literature conditions (Table 1, entry 1 and 2) could be achieved by switching the solvent to Et_2O allowing a better solubility and thus equimolar amounts of the used Lewis acid (86%, Table 1, entry 3). A further decrease of Lewis acid led to a significantly lower yield of 70% after 18 h (entry 4). Additional [4+2]-cycloaddition of the product **22** with cyclopentadiene **21** was observed when a stronger Lewis acid was applied and

the reaction furnished enone **22** in 72% yield (entry 5). In this case, the OAc-elimination of the primarily Diels-Alder intermediate is already partially catalyzed by the Lewis acid. This issue was overcome by lowering the equivalents of cyclopentadiene **21** in the reaction mixture and enone **22** was obtained in very good yields of 82% (Table 1, entry 6). Notably, by using this method the reaction workup is substantially facilitated and pure enone **22**, itself a valuable starting material in organic synthesis[164], is readily available in multigram scale and very good yields just by recrystallization.

In the following, the Diels-Alder adduct **22** was epoxidized with hydrogen peroxide to yield epoxide **313** in 84% yield (Scheme 74). The retro-Diels-Alder reaction of epoxide **313** and subsequent rearrangement to unsubstituted 2-pyrone (**1**), the key step of the synthetic sequence, was performed by using a flash vacuum thermolysis (FVT) setup (Figure 8). The apparatus of the FVT consists of a quartz tube containing the starting material on one end, an oven in the middle and a cooling trap on the other end. The starting material is usually evaporated and then sucked through the high-temperature area of the oven by a vacuum (0.02 mbar). The following transformation towards the respective product is induced by thermal excitation occurring mainly by molecule-wall collisions. The high-temperature exposure periods are only very short (ca. 10^{-3}–1 s) and therefore, very high temperatures between 400 and 1100 °C can be used without destroying the compounds. In this way, products can be obtained by unique transformations that are not accessible by other strategies.[165,166]

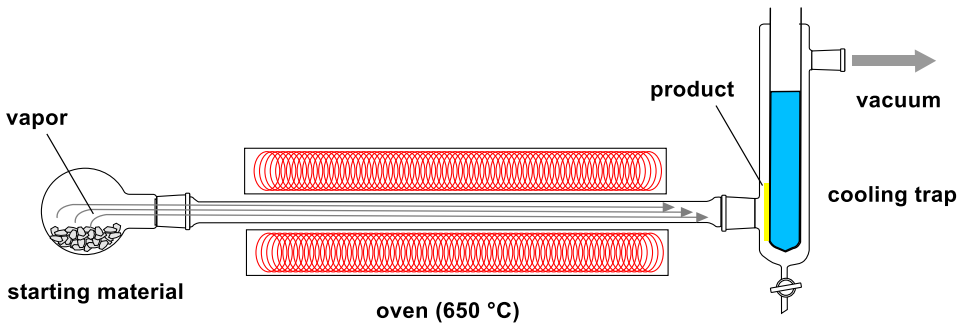

Figure 8. Flash vacuum thermolysis setup.[161]

Although, the FVT is an elegant and atom-economic method for the rearrangement of epoxide **313** towards 2-pyrone (**1**), upscaling remained a big challenge because there are several issues to face. The steady-state concentration, the concentration of the substrate **313** in the hot temperature zone, has to be controlled avoiding incomplete conversion or undesirable side

reactions.[166] Additionally, the temperature of the cooling trap features prominently in the big-scale pyrolysis. Too low temperatures could lead to freezing of the product **1** and thus blocking of the quartz tube and the vacuum. Whereas, product loss could be observed by an insufficient trapping temperature. Several conditions for the FVT of epoxide **313** were examined to make this process reliable for a big-scale synthesis of pyrone **1** (Table 2).

Table 2. Upscaling of the flash vacuum thermolysis setup.

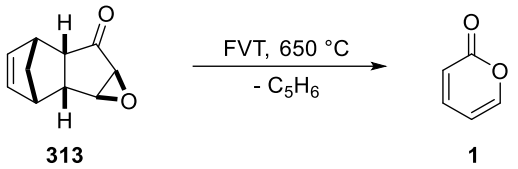

313 **1**

entry[a]	extern heating	T [°C]	p [mbar]	cooling trap	yield [%]	observation
1	pyrolysis oven	650	0.02	liquid nitrogen	60	incomplete conversion
2	Kugelrohr oven	130	0.02	liquid nitrogen	98	frozen product
3	Kugelrohr oven	130	0.02	water	88	product loss
4	Kugelrohr oven	130	0.02	cryostat (−10 °C)	94	frozen product
5[b]	Kugelrohr oven	130	0.02	ice/water	96	perfect conditions

[a] conditions: epoxide **313** (15 mmol) was used; [b] conditions: epoxide **313** (123 mmol) was used.

Incomplete conversion of epoxide **313**, caused by a too high steady-state concentration, was observed when the flask with starting material was directly heated in the pyrolysis oven at 650 °C and pyrone **1** was obtained in moderate yield of 60% (Table 2, entry 1). To control the steady-state concentration, the sublimation temperature of epoxide **313** was ascertained at first. The experiment revealed that the amount of starting material **313** in the high-temperature zone may be controlled by slowly sublimating the compound at 110 °C and 0.02 mbar pressure. Indeed, complete conversion and excellent yield of pyrone **1** was achieved by extern heating at 130 °C using an upstream Kugelrohr distillation oven (98%, entry 2). However, freezing of the product **1** at the cooling trap filled with liquid nitrogen was observed in this case. On the opposite, using only water cooling led to a product loss (88%, entry 3) and by connecting the trap to a cryostat, setting the temperature to −10 °C, again an excellent yield of 94% but also

only frozen 2-pyrone (**1**) was obtained (entry 4). The freezing of the product finally could be circumvented at a cooling trap temperature of 0 °C (entry 5). With this optimized condition in hand, a big-scale pyrolysis of epoxide **313** (20.0 g, 123 mmol) was performed yielding the desired product **1** in excellent 96% yield and >99% purity (GC-analysis) without any further purification (Figure 9). This FVT setup would allow running even bigger scales and is only limited to the size of the used extern heater and cooling trap. In addition, dicyclopentadiene, which is formed after the extrusion of cyclopentadiene **21** by the retro-Diels-Alder reaction, is collected at the cooling trap of the high vacuum pump and can be reused for a new reaction cycle of pyrone synthesis.

Figure 9. Big-scale FVT setup (Kugelrohr oven left, high-temperature oven in the middle and cooling trap right).

Remarkably, the multigram synthesis of unsubstituted pyrone **1** is achieved without any chromatographic workup step during the sequence. Hydroxy cyclopentenone **19** and acetate **20** were distilled, enone **22** was recrystallized and epoxide **313** was extracted after completion of the reaction (Scheme 74).

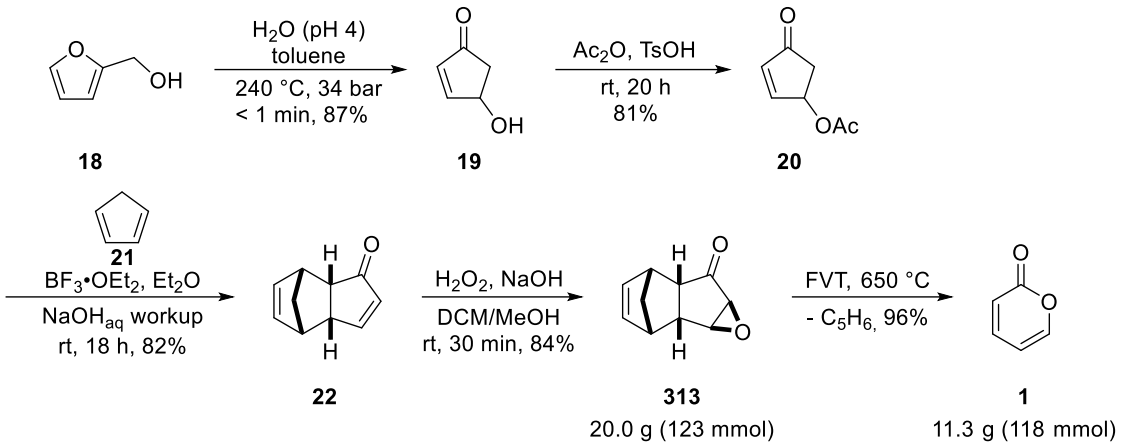

Scheme 74. Big-scale synthesis of 2-pyrone (**1**) from renewable resources.

The novel big-scale FVT setup is not only applicable for the multigram synthesis of unsubstituted pyrone (**1**) but also 6-(1-hydroxyethyl)-2*H*-pyran-2-one (**26a**)[16] was obtained in excellent yield by slow distillation of epoxide **25a** (3.1 g, 15 mmol) at 170 °C extern oven temperature (Scheme 75).

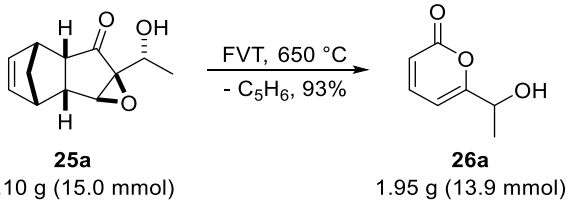

Scheme 75. Synthesis of hydroxyalkyl pyrone **26a** by the established FVT setup.

1.3 Synthesis of naturally occurring 6-alkyl 2-pyrones[b]

The established synthetic strategy towards 2-pyrones starting from furfuryl alcohol (**18**) should also be adopted for the introduction of further substituents into the pyrone skeleton. Herein, the introduction of alkyl substituents in 6-position is from particular interest. This structural motif is present in many naturally occurring 2-pyrone derivatives, e.g. 6-*n*-propyl, -*n*-pentyl or *n*-heptyl 2-pyrone **2a-c**, which were isolated from strains of *Trichoderma viride* and possess fragrant aromas (Scheme 76).[8,167]

[b] This chapter includes parts from a manuscript which has been prepared in collaboration with D. Dobler (University of Regensburg).[161].

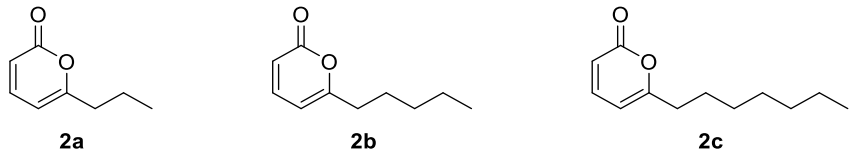

Scheme 76. 2-Pyrone natural products **2a-c** isolated from *Trichoderma viride*.[8]

The synthesis of the desired pyrones **2a-c** should be accomplished from furfuryl alcohol derivatives **314a-c**. The required alkyl substituents can be easily introduced by a Grignard reaction with furfural (**310**) and the reaction of the respective Grignard reagents yielded the furfuryl alcohol derivatives **314a-c** in excellent yields (92-98%, Scheme 77). Piancatelli rearrangement to 5-substituted 4-hydroxy cyclopentenone derivatives **315a-c** was performed under microwave conditions in a water/acetone mixture (40-75%, Scheme 77). In case of the heptyl derivative **315c**, considerable amounts of polymeric byproduct were formed and the yield dropped drastically to 45%. A continuous flow setup as for the synthesis of unsubstituted 4-hydroxy-cyclopentenone **19** might be also beneficial for this synthetic step. The subsequent acetylation gave the corresponding acetates **316a-c** again in excellent yields (89-94%, Scheme 77).

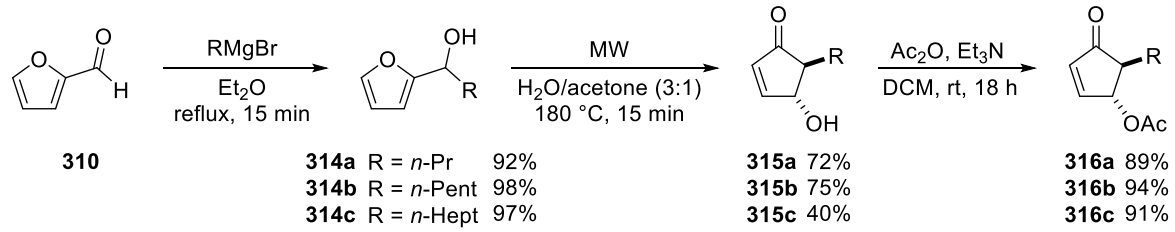

Scheme 77. Synthesis of 5-substituted acetates **316a-c** from furfural (**310**).

Analogously to the synthesis of unsubstituted 2-pyrone (**1**) the Diels-Alder/elimination step of acetates **316a-c** had to be investigated in greater detail (Table 3).

Table 3. Diels-Alder/elimination reaction of 5-substituted acetates **316a-c**.

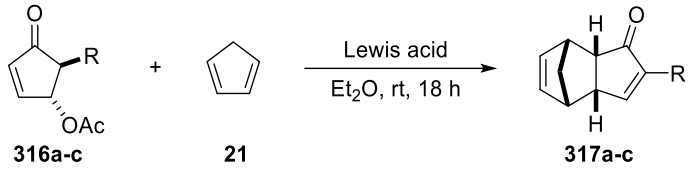

entry[a]	R	Lewis acid	equiv LA	equiv 21	yield [%]
1	*n*-Pr	$ZnCl_2$	1.0	3.0	79
2	*n*-Pr	$BF_3{\cdot}OEt_2$	0.10	2.0	70
3	*n*-Pr	$BF_3{\cdot}OEt_2$	0.10	3.0	82
4	*n*-Pr	$BF_3{\cdot}OEt_2$	0.20	3.0	94
5	*n*-Pr	$BF_3{\cdot}OEt_2$	0.20	1.5	76
6	*n*-Pent	$BF_3{\cdot}OEt_2$	0.20	3.0	95
7	*n*-Hept	$BF_3{\cdot}OEt_2$	0.20	3.0	94

[a] conditions: acetate **316a-c** (10 mmol, 1.0 equiv) in Et_2O (30 mL).

Reaction of propyl acetate **316a** using stoichiometric amounts of $ZnCl_2$ as Lewis acid furnished the Diels-Alder adduct **317a** in 79% yield (Table 3, entry 1). Applying previously optimized conditions for the synthesis of unsubstituted enone **22** slightly decreased the yield to 70% (entry 2). The yield of desired product **317a** could be improved by increasing the equivalents of cyclopentadiene **21** in a following experiment (82%, entry 3). Finally, an excellent yield of 94% could be achieved by using 20 mol% of $BF_3{\cdot}OEt_2$ as Lewis acid and 3.0 equivalents of cyclopentadiene **21** (Table 3, entry 4), whereas lower equivalents of cyclopentadiene **21** again dropped the yield to 76% (entry 5). Under the optimized conditions also the *n*-pentyl- and *n*-heptyl substituted derivatives **317b-c** were obtained in excellent yields (94-95%, entry 6 and 7). The sterically demanding alkyl substituents prevent further cycloaddition with cyclopentadiene as it is observed with unsubstituted acetate **20** (Table 1).

In the last steps, enones **317a-c** were epoxidized (97-98%) and subjected to FVT to yield the natural 6-alkyl 2-pyrone products **2a-c** in nearly quantitative yield (Scheme 78).

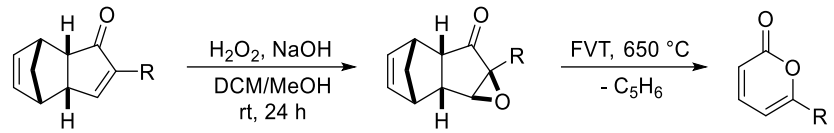

317a R = *n*-Pr
317b R = *n*-Pent
317c R = *n*-Hept

318a 98%
318b 98%
318c 97%

2a >99%
2b >99%
2c >99%

Scheme 78. Synthesis of naturally occurring 6-alkyl 2-pyrones **2a-c**.

1.4 Investigations towards the synthesis of 6-alkyl-4-methoxy-2-pyrones

The 6-alkyl-4-methoxy-2-pyrone structure is present in many natural products with interesting biological properties. Among them, the kavalactones **8** (Figure 10) isolated from the kava-kava plant (*piper methysticum*) are the most prominent representatives and especially known for their anxiolytic, sedative and antidepressant effects.[168,169]

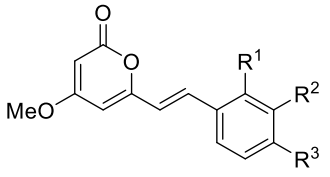

$R^1 = R^2 = H, R^3 = OMe$	yangonin **8a**
$R^1 = R^3 = OMe, R^2 = H$	10-methoxyangonin **8b**
$R^1 = H, R^2 = R^3 = OMe$	11-methoxyangonin **8c**
$R^1 = R^2 = R^3 = H$	desmethoxyangonin **8d**
$R^1 = H, R^2, R^3 = O(CH_2)O$	5,6-dehydromethysticin **8e**

Figure 10. Naturally occurring kavalactones **8**.[169]

Having previously shown that 6-hydroxyalkyl[16] **26** or 6-alkyl pyrones[161] **2** are easily accessible from renewable resources the further introduction of a methoxy group in 4-position could give rise to such interesting compounds. With consideration of the retrosynthesis, the additional alkoxy/hydroxy-group has to be introduced at the γ-position to the carbonyl group, between the 6- and 5-membered ring of enone **317** (Scheme 79).

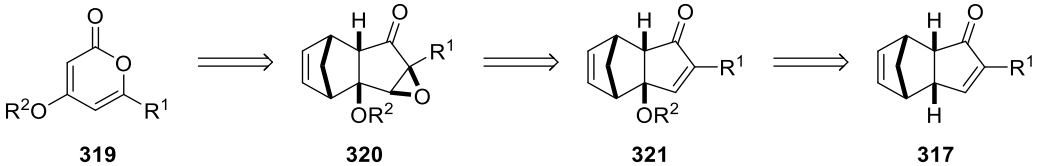

319 **320** **321** **317**

Scheme 79. Envisioned retrosynthesis of 4-alkoxy-6-alkyl 2-pyrones (**319**).

For this purpose, allylic oxidation was intended as the preferred strategy. The allylic oxidation of olefins can be generally performed by the well-known Riley oxidation using SeO_2 as the

oxidant. Unfortunately, under conventional heating as well as microwave conditions no conversion of the starting material **317a** was observed, which could be ascribed to steric hindrance of substrate and oxidant (Scheme 80).

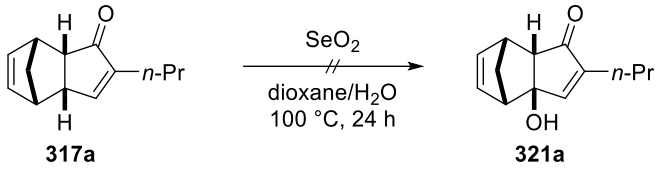

Scheme 80. Investigation of the Riley oxidation of enone **317a**.

Consequently, a different approach had to be pursued. Zwanenburg *et al.* demonstrated that the γ-bromo enone compound **322** can be transformed into the methoxy derivative **324** within few minutes (Scheme 81).[170] Interestingly, the reaction is reported to take place via elimination of the bromide to dienone **323** and subsequent conjugate addition of a methoxide.

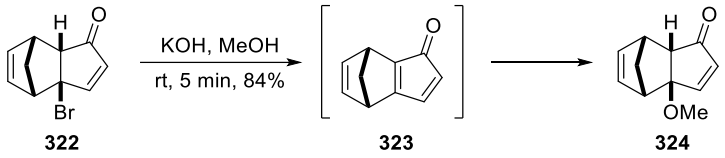

Scheme 81. Introduction of methoxy group according to Zwanenburg *et al.*[170]

The introduction of a bromine in γ-position of enone **317a** is quite impossible by standard methods. Therefore, we questioned if bromination of the enone **317a** in δ-position would allow for the same transformation by the intermediacy of a dienone **323**.

The methylation of enones **317** in δ-position, for instance, can be achieved by using LDA as base to generate the enolate and MeI as electrophile.[161] Accordingly, these reaction conditions should be applied for the analogous introduction of bromine (Table 4).

Table 4. Attempts for the introduction of an α-bromo atom.

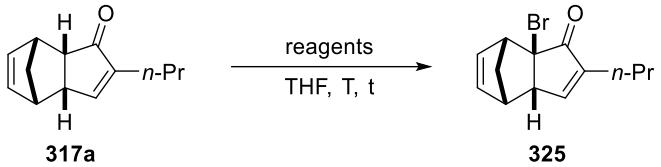

entry	reagents	T	t [h]	yield [%]
1	LDA, NBS	−78 °C	1	decomposition
2	1) LDA, TMSCl 2) NBS, NaOAc	−78 °C to 0 °C	2	decomposition
3	TMSOTf, NBS	rt	24	---

However, similar conditions as for the methylation but using NBS as electrophile led only to decomposition (Table 4, entry 1). This might be due to further elimination of the initially introduced bromo-atom by the strong base. In an attempt to avoid elimination by protecting the enolate in the first step and brominating in the second step also decomposition was observed (Table 4, entry 2). By applying more gentle conditions using TMSOTf the starting material **317a** was completely recovered after one day (Table 4, entry 3). Since all attempts for the synthesis of 4-methoxy 2-pyrones **319** failed, the next focus of this thesis was placed on the application and functionalization of biobased 2-pyrone derivatives.

In summary, a multigram synthesis of unsubstituted 2-pyrone (**1**) was achieved in high yields and excellent purity from biobased and inexpensive furfuryl alcohol (**18**). The Diels-Alder reaction of acetate **20**, a key step of the synthetic strategy, could be performed with catalytic amounts of Lewis acid without using toxic solvents. Furthermore, a FVT setup was developed that enabled us to run the thermal rearrangement of epoxide **313** on every scale and with various substrates. Naturally occurring 6-alkyl 2-pyrones **2a-c** were also synthesized from renewable resources by this strategy, whereas the introduction of a hydroxy/methoxy group in 4-position was unsuccessful.

2 Application of 2-pyrones derived from renewable resources

2.1 Synthesis of 3-substituted phthalides

2.1.1 Introduction

The structure of 3*H*-isobenzofuran-1-ones, also called phthalides, is characterized by the fusion of a benzene- and γ-lactone-ring. This framework is present in a large number of natural products displaying a broad range of bioactivities like anticonvulsant, anesthesia, anti-HIV, antibacterial and antibiotic effects (Figure 11).[171,172] Most of the naturally occurring and pharmacologically active compounds belong to the group of 3-substituted phthalides. 3-Butylphthalide (**326b**) is the best-known representative of this class and, despite its structural simplicity, possesses interesting physiological properties. The major constituent of celery oil can be used as an antiplatelet drug for ischemia-cerebral apoplexy and has been approved as an anti-ischemic stroke drug by the China Food and Drug Administration (CFDA).[171,173] Besides their interesting biological activities, phthalides are also used as versatile building blocks in organic and medical chemistry.[171,174]

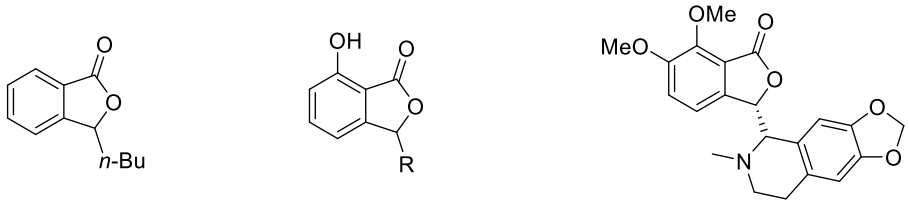

3-butylphthalide **326b** | R = CH_2CO_2H isoochracinic acid **327a** | (-)-hydrastine **328**
R = *n*-Oct paecilocin A **327b**
R = CH_2Ph typhaphthalide **327c**
R = 2-thienyl chrycolide **327d**

Figure 11. Selected examples of naturally occurring 3-substituted phthalides.[171]

Over the years, various methods have been developed for the racemic and asymmetric synthesis of 3-substituted phthalide derivatives.[171] Most of them rely on a lactone formation on the benzene ring. One of the simplest strategies for an enantiomeric pure synthesis of phthalides is the catalytic reduction/lactonization of 2-acylarylcarboxylates **329**.[174,175] In 2017, Zhang co-workers reported a general method for the stereoselective synthesis of various 3-substituted phthalides **330** using a Ru-diphosphine catalytic system (Scheme 82).[176]

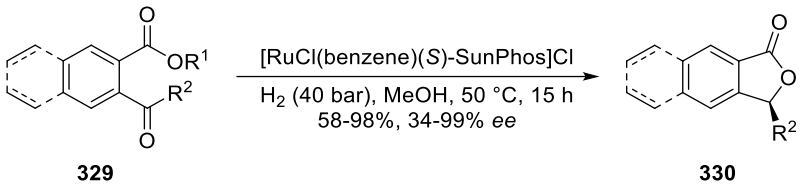

Scheme 82. Stereoselective reduction/lactonization approach by Zhang *et al.*[176]

In addition, progress in transition metal-catalyzed C-H bond functionalization paved the way for a rhodium-catalyzed intramolecular hydroacylation of 2-ketobenzaldehydes **331** developed by Dong *et al*. (Scheme 83).[177] By appropriate choice of the counterion of AgX the enantioselectivity could be controlled for each substrate.

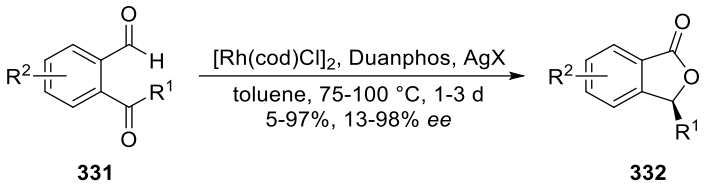

Scheme 83. Intramolecular hydroacylation by Dong *et al.*[177]

Transition metal-catalyzed [2+2+2]-cycloadditions of ester-linked diynes **333** with monoalkynes **334** have also been described for the synthesis of 3-substituted phthalide derivatives **335**. In presence of a chiral phosphine ligand a one-pot transesterification and cycloaddition process gave rise to enantioenriched tricyclic 3,3-disubstituted derivatives **335** (Scheme 84).[178]

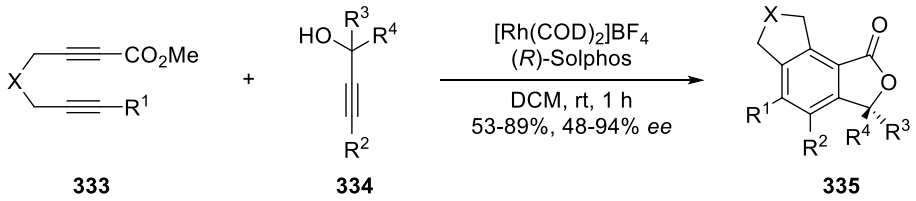

Scheme 84. Transesterification/[2+2+2]-cycloaddition of diynes **333** with tertiary propargylic alcohols **334**.[178]

The only method that was developed starting from renewable resources is based on a [4+2]-cycloaddition of furfuryl alcohol (**18**) and dimethyl acetylenedicarboxylate (DMAD **D**) followed by a ring-opening/aromatization with $IrCl_3$ (Scheme 85).[179] However, no substituents were introduced in 3-position.

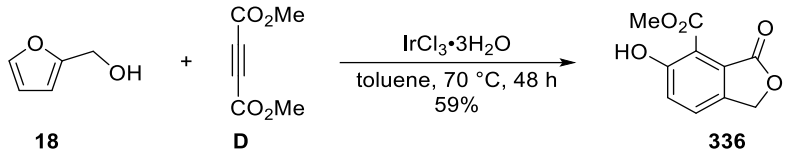

Scheme 85. Synthesis of 3-unsubstituted phthalide **336** from renewable resource.[179]

Hence, the utilization of starting materials that were derived from renewable resources would be a heretofore unprecedented strategy for the synthesis of 3-substituted phthalides.

2.1.2 Synthesis of 3-substituted phthalides by Diels-Alder reaction of pyrones

2-pyrones are well known to undergo [4+2]-cycloadditions with various alkenes and alkynes. Depending on the substitution pattern of the pyrones the cycloaddition can proceed through a normal or inverse electron demand Diels-Alder (IEDDA) reaction.[180] The latter is usually evoked by electron-withdrawing substituents on the pyrone moiety. Generally, the cycloaddition of pyrones with alkynes gives rise to benzene derivatives after extrusion of CO_2 due to instability of the highly strained bicyclooctadiene intermediate **338**. Therefore, the aforementioned 6-hydroxyalkyl 2-pyrones **26**, reported by Reiser *et al.*[16], seem to be suitable precursors for the synthesis of phthalide derivatives **340**. It was envisioned, that the electron-rich pyrones **26** undergo normal Diels-Alder reaction with electron-poor acetylenecarboxylate derivatives **337** and after extrusion of CO_2 a transesterification in intermediate **339** should lead to the lactone ring formation (Scheme 86).

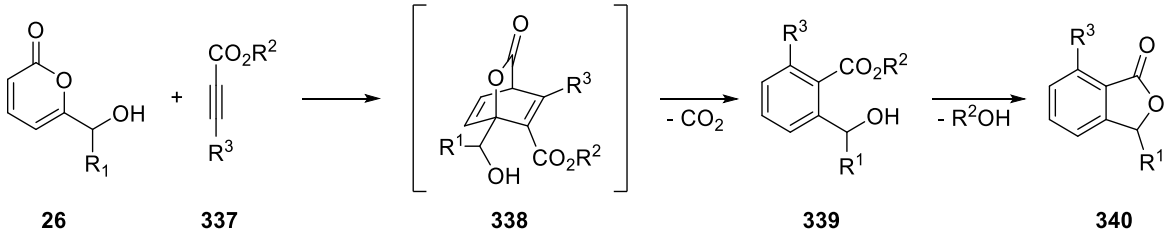

Scheme 86. Envisioned transformation of 6-hydroxyalkyl pyrones **26** towards 3-substituted phthalides **340**.

Initially, the reaction was investigated using a symmetrical alkyne ester **341** to prevent the formation of regioisomers in the [4+2]-cycloaddition step (Table 5).

Table 5. Investigation of the synthesis of 3-substituted phthalide derivative **342a** by Diels-Alder reaction of pyrone **26a**.

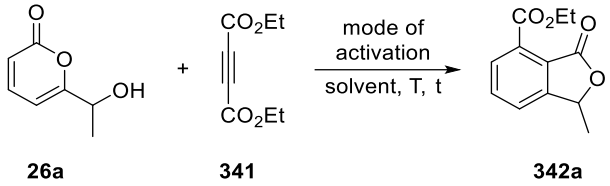

26a **341** **342a**

entry[a]	mode of activation	solvent	c [M]	T [°C]	t [h]	yield [%]
1	Δ	xylene	1.0	200	24	58
2	Δ	xylene	2.0	200	24	74
3	Δ	neat	-	200	24	56
4	MW	xylene	2.0	150	7	64
5	MW	neat	-	150	7	80

[a] conditions: pyrone **26a** (1.00 mmol, 1.0 equiv), dienophile **341** (1.4 equiv).

Indeed, the reaction of 6-hydroxyethyl 2-pyrone (**26a**) with diethyl acetylenedicarboxylate (**341**) afforded the phthalide derivative **342a** in fair yield by conventional heating (58%, Table 5, entry 1). In 2004, Loupy *et al.* demonstrated, that the yields and selectivities of pyrone cycloadditions can be improved by using more concentrated reaction conditions and/or microwave irradiation.[181] In case of conventional heating, a higher concentration led to increased yield of product **342a** (74%, entry 2), whereas under neat conditions a drop in the yield to 56% was observed (entry 3). Microwave irradiation in the presence of a solvent slightly decreased the yield (64%, entry 4) compared to conventional heating. This could be rationalized by the poor excitability of xylene by microwave irradiation.[182] Consequently, microwave activation under neat conditions gave the best result with 80% yield of phthalide **342a** and additionally, shorter reaction times than under conventional heating could be achieved (Table 5, entry 5).

With the optimized conditions in hand, other 2-pyrone derivatives **26b-c** and one enantiomerically pure substrate **(*S*)-26a** (99% *ee*)[16] were subjected to the cycloaddition reactions with alkyne **341** (Scheme 87). As expected, no change of enantiomeric excess was observed during the cycloaddition/lactonization approach and enantiomerically pure phthalide **(*S*)-342a** is easily accessible in very good yield (81%, 99% *ee*). Furthermore, a derivative **342b** of the biological active 3-butylphthalide (**326b**) was obtained in a good yield of 70%. Due to

the inferior solubility of the phenyl substituted pyrone **26c** in alkyne **341** the yield dropped drastically and the corresponding phthalide **342c** was obtained in fair yield (50%, Scheme 87).

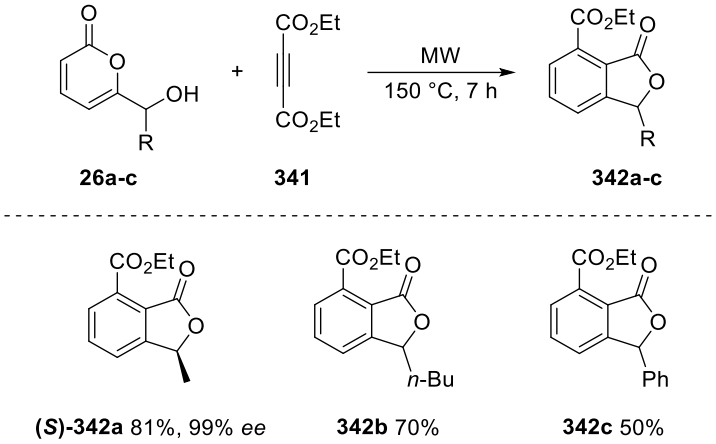

Scheme 87. Synthesis of 3-substituted phthalide derivatives **342a-c**.

It was demonstrated that chiral phthalide derivatives **342** can be synthesized from enantiomeric pure pyrones **26** by this strategy. Nevertheless, another methodology starting directly from racemic pyrones **26** should be investigated as well. In 2005, a catalytic enantioselective Diels-Alder reaction of 2,4-hexadienol (**343**) with methyl acrylate (**344**) was developed (Scheme 88).[183] Chirality was induced by applying a binuclear Lewis-acid template derived from (*R*)-BINOL.

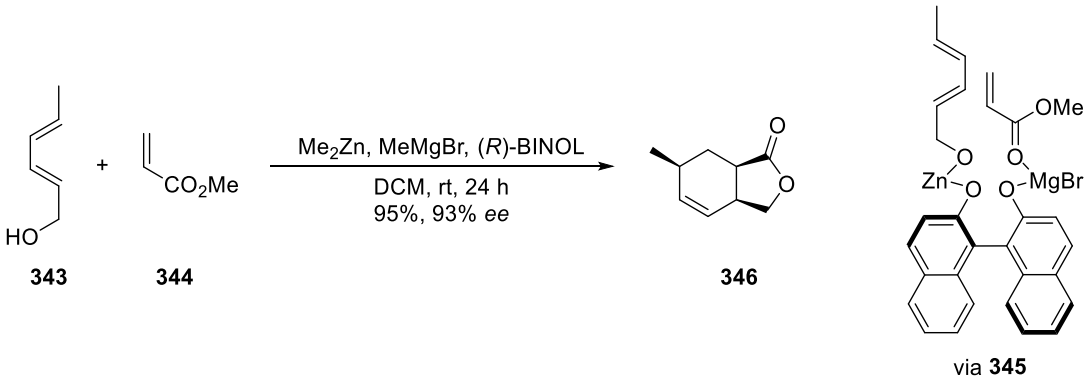

Scheme 88. Enantioselective cycloaddition of 2,4-hexadienol (**343**) and methyl acrylate (**344**).[183]

By possessing the same dienol structure 2-pyrones **26** appeared to be convenient substrates for a similar transformation. Herein, a kind of kinetic resolution should give the enantiomerically pure product **347a**, whereas the other enantiomer of **26a** remains unreacted (Table 6).

Table 6. Investigation of the stereoselective synthesis of **347a**.

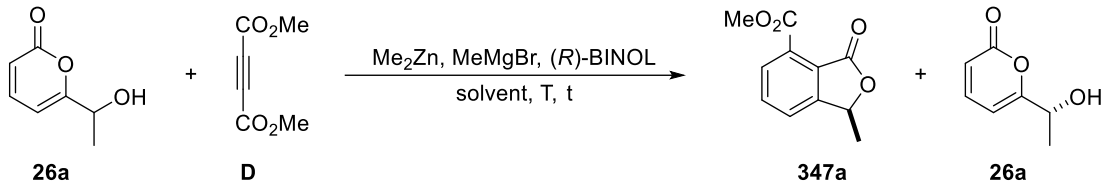

26a **D** **347a** **26a**

entry[a]	solvent	T [°C]	t [h]	yield [%]
1	DCM	rt	48	---
2	DCM	70	48	---
3	toluene	150	48	---

[a] conditions: Pyrone **26a** (0.5 mmol, 1.0 equiv), dienophile **D** (1.4 equiv), catalyst (1.0 equiv).

However, by investigating different solvents and temperatures no conversion was observed and the starting material was recovered (Table 6). This could be attributed to the presence of the lactone moiety in pyrone **26a** which also can be coordinated by the Lewis acid, thus preventing coordination of the dienophile **D** or creating an electronical mismatch.

Considering the significance of simple 3-substituted phthalides **326** as versatile substrates in organic chemistry as well as important drugs like 3-butylphthalide (**326b**) for instance, the cycloaddition approach was also examined for the synthesis of phthalides **326** bearing no substituents on the benzene moiety (Table 7).

Table 7. Diels-Alder reaction of pyrone **26a** with dienophile **37**.

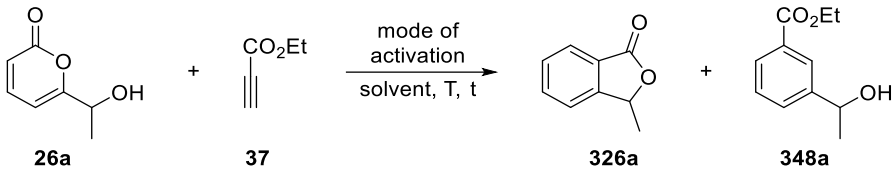

26a **37** **326a** **348a**

entry[a]	mode of activation	solvent	c [M]	T [°C]	t [h]	yield 326a [%]	yield 348a [%]
1	Δ	xylene	0.5	200	24	30	33
2	Δ	xylene	2.0	200	24	27	51
3[b]	Δ	xylene	2.0	200	48	---	---
4	MW	neat	-	150	7	20	59

[a] conditions: Pyrone **26a** (1.0 mmol, 1.0 equiv), dienophile **37** (1.4 equiv); [b] $ZnCl_2$ (1.0 equiv) was added.

Intermolecular Diels-Alder reaction with ethyl propiolate (**37**) was performed to afford the desired phthalide **326a**, but utilization of an asymmetric alkyne furnished two different regioisomers **326a** (30%) and **348a** (33%) in almost equal yields (Table 7, entry 1). A higher concentrated reaction mixture favored the formation of the benzene derivative **348a** (51%, entry 2) compared to phthalide **326a** (27%), which could be explained by steric repulsion of the hydroxyalkyl and ester group. Additionally, a larger orbital coefficient of the HOMO of pyrone **26a** in 6-position than in 3-position due to the electron-donating substituent and smaller orbital coefficient in the LUMO at the β-position of alkyne **37** could prefer product **348a**. The attempt to control the ratio by adding a Lewis acid failed and starting material **26a** was completely recovered after 48 h (entry 3). The previously optimized neat microwave condition also rather promoted the synthesis of **348a** (59%, Table 7, entry 4) than of phthalide **326a** (20%).

Therefore, a different approach for the selective synthesis of phthalides **326** had to be examined. Intramolecular cycloaddition should prevent the formation of regioisomers due to the predefined orientation of the dienophile and diene. For this purpose, hydroxyalkyl 2-pyrones **26** had to be coupled with propiolic acid (**349**). Screening revealed that the solvent had a big impact on the outcome of the respective reaction (Table 8).

Table 8. Coupling of pyrones **26a-c** with propiolic acid (**349**).

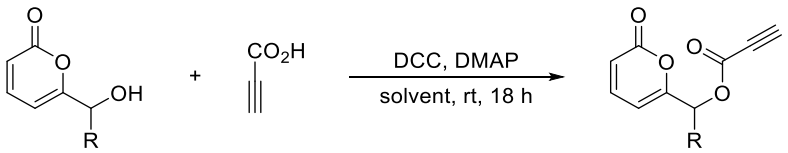

26a-c **349** **350a-c**

entry[a]	R	solvent	yield [%]
1	Me	THF	24
2	Me	Et_2O	42
3	Me	DCM	56
4	*n*-Bu	DCM	62
5	Ph	DCM	54

[a] conditions: Pyrone **26a-c** (1.0 equiv), propiolic acid (**349**) (2.0 equiv), DCC (1.13 equiv), DMAP (7 mol%).

The reaction in Et_2O and especially THF provided the ester **350a** in poor yields of 24% and 42%, respectively (Table 8, entry 1 and 2). The use of DCM proved to be beneficial and the yield was increased to 56% (entry 3). No influence of steric factors in the yield was observed,

when the reaction was conducted with the *n*-butyl (62%) or phenyl (54%) substituted 2-pyrone derivative **26b** and **26c** (Table 8, entry 4 and 5).

Subsequently, the intramolecular Diels-Alder reaction of the methyl derivative **350a** was initially investigated under conventional heating conditions (Table 9).

Table 9. Synthesis of 3-substituted phthalides **326a-c** by intramolecular cycloaddition.

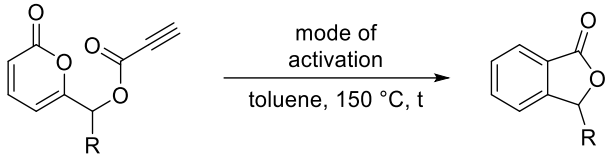

350a-c **326a-c**

entry	R	mode of activation	c [M]	t [h]	yield [%]
1	Me	Δ	0.025	20	82
2	Me	MW	0.025	3	>99
3	Me	MW	0.10	5	>99
4[a]	*n*-Bu	MW	0.10	5	>99, 74% *ee*[b]
5	Ph	MW	0.10	5	>99

[a] starting from enantioenriched 2-pyrone **26b** (74% *ee*); [b] determined by chiral HPLC analysis of the isolated product.

The reaction provided phthalide **326a** in a very good yield of 82% after 24 h (Table 9, entry 1). Satisfyingly, microwave activation again was superior to conventional heating and furnished product **326a** quantitatively (>99%) in much shorter reaction time (entry 2). Furthermore, the concentration could be increased at least four times without observing byproducts by intermolecular cycloaddition (entry 3). Likewise, *n*-butyl and phenyl derivative **326b** and **326c** were obtained in quantitative yield (>99%, entry 4 and 5). Additionally, starting from enantioenriched butyl 2-pyrone **(*R*)-26b** (74% *ee*[16]) the enantiomeric excess remained unchanged over the two synthetic steps giving rise to enantioenriched naturally occurring 3-butylphthalide **(*R*)-326b** (>99%, 74% *ee*, entry 4).

After validating the inter- and intramolecular cycloaddition as an atom-economic synthetic strategy towards phthalides, the research was concentrated on the synthesis of 7-hydroxy 3-substituted phthalides **327**. This structural motif can be found in many naturally occurring substances, e.g. isoochracinic acid (**327a**), paecilocin A (**327b**), typhaphthalide

(**327c**) and chrycolide (**327d**) (Figure 11). During the total synthesis of 8-deshydroxyajudazol B, Rizzacasa and co-workers[184] made use of Buchwald's condition[185] for the borylation of aryl halides **351** and after subsequent oxidation/hydrolysis the corresponding phenol derivative **352** was obtained (Scheme 89).

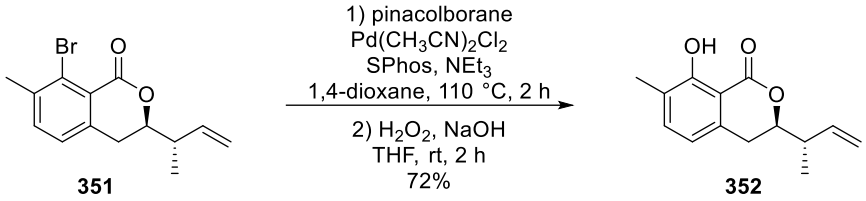

Scheme 89. Borylation/oxidation of **351** to alcohol **352** by Rizzacasa *et al.*[184]

Thus, an analogous transformation should give rise to the aforementioned natural products using 7-bromo substituted phthalides **354**. However, the introduction of bromine in 7-position by intermolecular Diels-Alder reaction with ethyl 3-bromopropiolate (**353**) was unsuccessful and only starting material **26a** was recovered (Scheme 90).

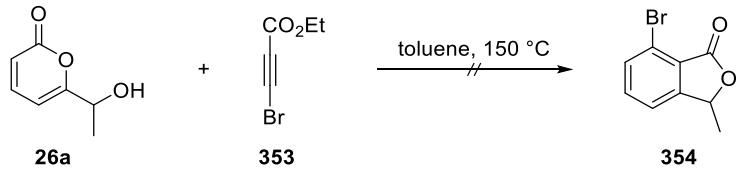

Scheme 90. Attempted intermolecular cycloaddition of pyrone **26a** with ethyl 3-bromopropiolate (**353**).

In contrast, bromination of the terminal alkyne **350a** using NBS and $AgNO_3$ followed by intramolecular [4+2]-cycloaddition furnished the bromo phthalide **354** in excellent yield over two steps. Unfortunately, the borylation and oxidation step afforded mainly unsubstituted phthalide **326a** and the desired phenol derivative **327** was only obtained in traces (Scheme 91).

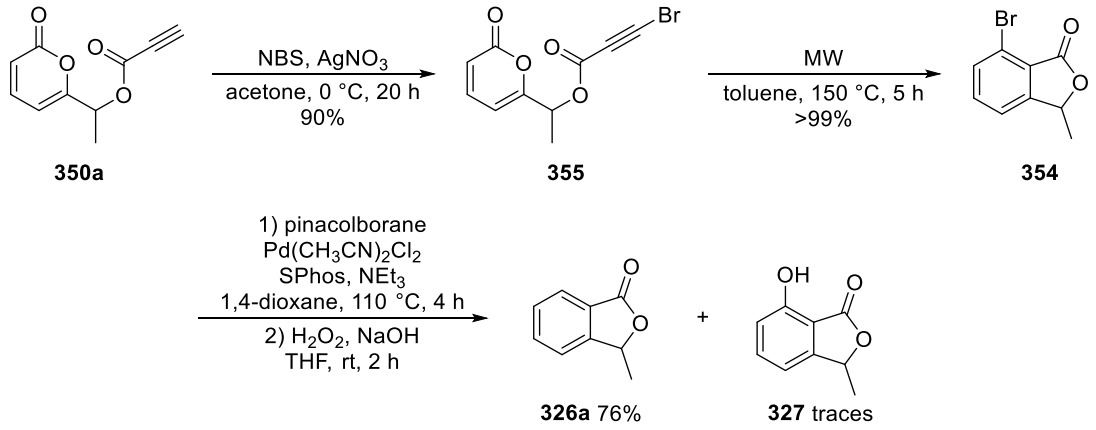

Scheme 91. Investigation of the synthesis of 7-hydroxy phthalide **327** via intramolecular cycloaddition.

Although there are still some methods described in literature that could allow converting the bromo-phthalide **354** into the hydroxy derivative **327**, further investigations could not be conducted due to limited time left in the lab.

2.2 [4+2]-Cycloaddition of 6-acetyl 2-pyrone with alkenes

As stated above (B.2.1.2), 2-pyrones can also undergo cycloaddition reactions with alkenes leading generally to isolable bicycloadducts **359**. These structurally and stereochemically rich compounds **359** are useful synthetic intermediates, for instance, in the stereoselective synthesis of cyclohexane derivatives **360** (Scheme 92).[180,186]

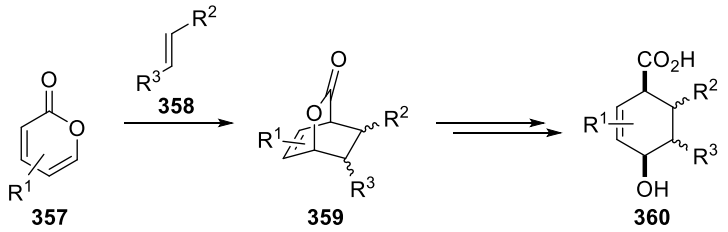

Scheme 92. Diels-Alder reaction of pyrones with alkenes.

Accordingly, bicycloadducts **363** derived from cycloadditions with pyrone **361** would possess valuable functional groups enabling their further elaboration towards value-added products. 6-Hydroxyalkyl pyrones **26** have been previously demonstrated to participate in normal Diel-Alder reactions with electron-poor alkynes. Consequently, pyrone **361** bearing an α-carbonyl group in 6-position was considered as an electron-poor diene due to the electron-withdrawing character of the substituent. For this reason, compound **361**, readily available by

oxidation of the respective α-hydroxy pyrone **26a**[161], was investigated in an inverse electron demand Diels-Alder reaction using ethyl vinyl ether (**362**) as dienophile (Table 10).

Table 10. Investigation of the IEDDA of α-carbonyl pyrone **361**.

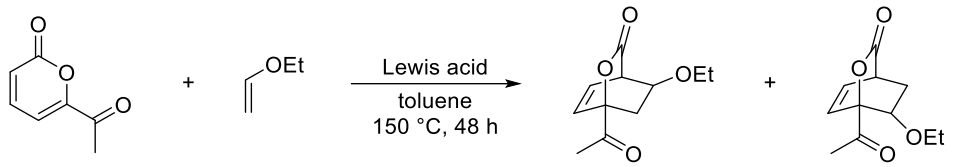

361 **362** **363a** **363b**

entry[a]	Lewis acid	yield 363a [%]	yield 363b [%]
1	-	---	---
2	$ZnCl_2$	---	---
3	$BF_3{\cdot}OEt_2$	---	---

[a] conditions: pyrone **361** (1.0 mmol, 1.0 equiv), ethyl vinyl ether (**362**) (2.0 equiv), toluene (2.0 M).

Surprisingly, pyrone **361** did not react with the electron-rich dienophile **362** upon heating at 150 °C for 48 h (Table 10, entry 1). Also, activation of the pyrone **361** with a Lewis acid did not lead to a successful conversion of the starting material (Table 10, entry 2 and 3).

These results indicated, that pyrone **361**, despite the electron-withdrawing substituent, is a rather electron-rich diene and hence the cycloaddition had to be performed with an electron-poor dienophile like methyl acrylate (**344**) (Table 11).

Table 11. Investigation of the Diels-Alder reaction of α-carbonyl pyrone **361** with methyl acrylate (**344**).

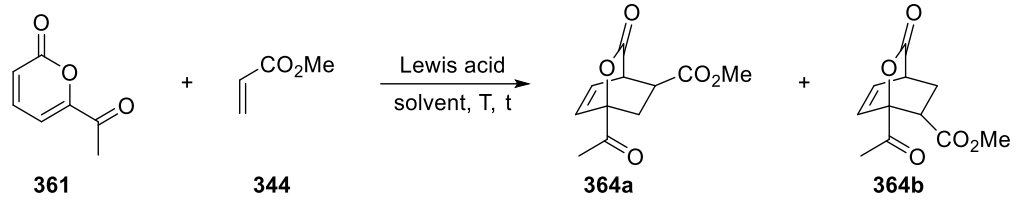

361 **344** **364a** **364b**

entry[a]	Lewis acid	equiv 344	solvent	T [°C]	t [h]	yield 364a [%]	yield 364b [%]
1	-	2.0	toluene	150	24	complex mixture	
2	-	1.0	toluene	150	24	complex mixture	
3	-	1.0	DCM	60	48	---	
4	$ZnCl_2$	1.0	DCM	60	48	---	
5	$BF_3{\cdot}OEt_2$	1.0	DCM	60	48	---	

[a] conditions: pyrone **361** (1.0 mmol, 1.0 equiv), Lewis acid (1.0 equiv) in solvent (2.0 M).

In fact, pyrone **361** underwent facile cycloaddition with methyl acrylate (**344**), but bicycloadducts **364** could not be isolated in any case. Under the thermal conditions extrusion of CO_2 in adducts **364** and further cycloaddition of the corresponding cyclohexadiene intermediates with methyl acrylate (**344**) occurred leading to a complex mixture of various products (Table 11, entry 1). The attempt to isolate the initial cyclohexadiene intermediates by lowering the amount of alkene **344** (entry 2) was unsuccessful since the second cycloaddition was more favored than in the first step with pyrone **361**. In order to circumvent the thermal extrusion of CO_2 in bicycloadducts **364**, the reaction was also performed at a lower reaction temperature (entry 3). However, this experiment showed that higher temperatures are necessary for an uncatalyzed Diels-Alder reaction and only starting material **361** was recovered. Upon addition of Lewis acids for the preactivation of dienophile **344** also no conversion was observed (Table 11, entry 4 and 5). Herein, again an electronic mismatch due to simultaneous coordination of both reagents to the Lewis acid could be the major reason. Thus, the selectivity issues of the reaction could not be solved with the given materials and therefore, other applications for the biomass-derived pyrones were investigated.

To sum up, a heretofore unprecedented transition metal-free synthetic strategy towards 3-substituted phthalides **326** and derivatives **342** was developed starting from pyrones **26** derived from renewable resources. During the inter- and intramolecular cycloadditions no change in

enantiomeric excess was observed and enantioenriched products were obtained. In addition, the capability to introduce a bromine atom in 7-position of the phthalide by this method could pave the way to some natural products in future work. In contrast, desired bicycloadducts **364** could not be isolated by cycloaddition of 6-substituted pyrone **361** with alkenes.

2.3 Visible light-mediated [4+2]-cycloaddition of 2-pyrones

The eclectic photochemistry of 2-pyrone (**1**) has been discovered early and these photoinduced transformations provide appealing entities that are elusive by other methods (Scheme 93). In 1964, Corey[71] reported that direct irradiation of 2-pyrone (**1**) in diethyl ether furnished bicyclic lactone **365** by 4π-photocyclization, while an acyclic ester **366** was obtained by irradiation in methanol.[187] In contrast, by addition of acetophenone as sensitizer the formation of two [4+2]-cycloadducts **367a** and **367b** was observed, which constitutes a rare example of photochemical [4+2]-cycloaddition.[187] Whereas the latter reaction seems to arise via the triplet 2-pyrone excited state (T_1, Figure 12), the cyclobutene lactone **365** and acyclic ester **366** are formed via the singlet excited state (S_1, Figure 12).

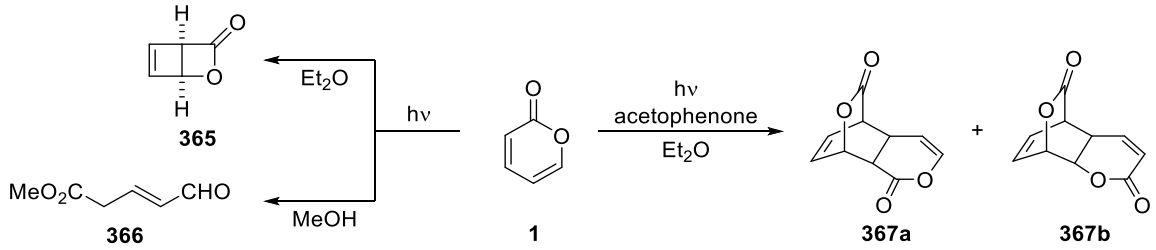

Scheme 93. Versatile photochemistry of 2-pyrone (**1**).

As discussed earlier in the introduction (see chapter A3.2 and A3.3) lactone **365** and structurally rich cycloadducts like **367a** and **367b** are very potent building blocks. However, established synthetic protocols still make use of UV-mediated processes entailing some drawbacks. UV-light requires a high input of energy and specialized equipment for its safe generation. The concentration of substrates has to be kept low in order to allow efficient light penetration and prevent undesired intermolecular reactions. Moreover, up-scaling of UV-mediated reactions is a big challenge. Concerning a more sustainable process, the UV-light source should be replaced by an environmentally friendly visible light-emitting diode (LED).

Transformations proceeding via singlet excited transition states (S_1) can not be accomplished by direct irradiation with visible light in this case. Therefore, the focus was placed on the triplet-catalyzed reaction of 2-pyrone (**1**). Generally, energy transfer (ET) from another photoexcited

molecule (sensitizer) can be applied to generate the first triplet state of a substrate (T_1), from which the reaction takes place (Figure 12).

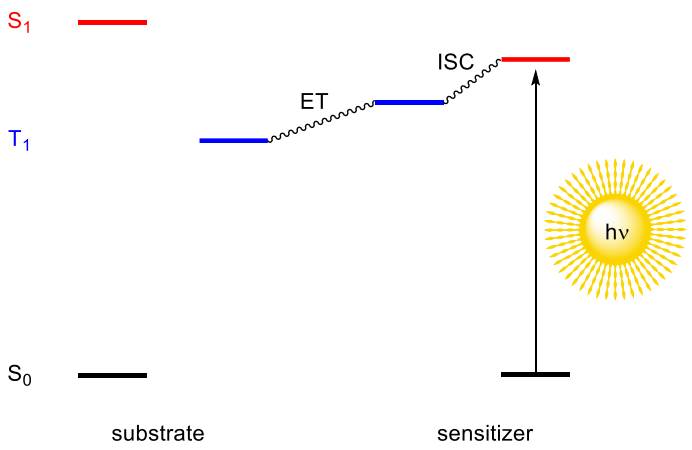

Figure 12. Energy transfer of a sensitizer to a substrate.

Over the years, several transition metal catalysts have been developed that absorb in the visible region of light promoting various chemical processes either by photoredox or energy transfer mechanisms. In 2019, Reiser *et al.* developed a visible light-mediated, intramolecular [2+2]-photocycloaddition of amide linked dienes catalyzed by $[Ir(dtb\text{-}bpy)(dF(CF_3)ppy)_2]PF_6$ as triplet sensitizer.[188]

Encouraged by this work, an iridium-sensitized protocol was considered as a promising strategy to replace the UV-mediated [4+2]-cycloaddition of 2-pyrone (**1**) (Table 12).

Table 12. Investigation of the photocatalyzed cycloaddition of 2-pyrone (**1**).

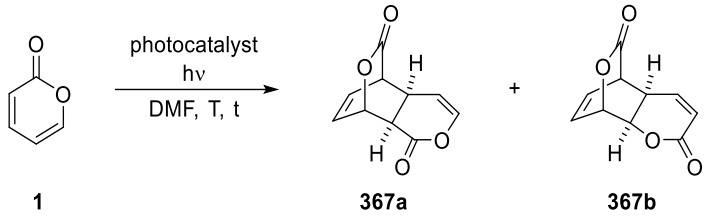

entry[a]	catalyst	hν [nm]	c [M]	T [°C]	t [h]	yield 367a [%]	yield 367b [%]
1	[Ir(dtb-bpy)(dF(CF$_3$)ppy)$_2$]PF$_6$	455	0.05	rt	3	43	42
2	[Ir(dtb-bpy)(dF(CF$_3$)ppy)$_2$]PF$_6$	455	0.50	rt	0.5	46	46
3	-	-	0.50	150	48	---	
4	-	455	0.50	rt	48	---	
5	Cu(dap)$_2$Cl	530	0.50	rt	48	---	
6	Ru(bpy)$_3$Cl$_2$	455	0.50	rt	48	---	

[a] conditions: pyrone **1** (1.0 mmol, 1.0 equiv), catalyst (1.0 mol%).

Gratifyingly, the iridium-catalyzed reaction furnished both regioisomers **367a** and **367b** in equal amounts after 3 h (Table 12, entry 1). The reaction took place in a complete diastereoselective fashion and for both products only the *exo*-diastereomer was obtained. In contrast to the earlier report[187], structures of **367a** and **367b** could be unambiguously characterized by spectroscopic and single-crystal X-ray analysis (Figure 13). Moreover, the reaction time could be reduced by tenfold concentrated reaction conditions and cycloadducts **367a** and **367b** were formed in an excellent overall yield of 92% (entry 2). In order to exclude the transformation to proceed through thermal (entry 3) or light-induced (entry 4) excitation, the conditions were examined in further experiments, but pyrone **1** was recovered in both cases. Other photocatalysts did not promote the reaction (entry 5 and 6), indicating unsuccessful energy transfer.

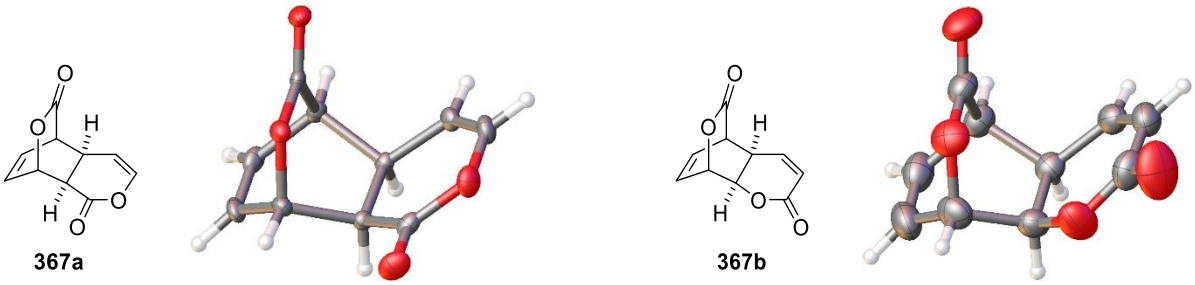

Figure 13. Crystal structure of **367a** and **367b** (50% thermal probability).

Having identified excellent conditions for a visible light-catalyzed [4+2]-cycloaddition of 2-pyrone (**1**) it was examined if an additional substituent could prevent the formation of one regioisomer. Hence, pyrones **2a** and **26a** were employed having an alkyl or hydroxyalkyl substituent, which might induce selectivity by steric reasons or additionally through H-bond interactions. But the reactions of alkyl pyrone **2a** and hydroxyalkyl pyrone **26a** provided a complex reaction mixture of different products that were not separable by standard column chromatography. NMR- and mass-analysis of the crude reaction mixture revealed the formation of [4+2]-cycloadducts and their corresponding products after elimination of the CO_2-bridgehead. (Scheme 94). In addition, [2+2]-cycloaddition products of two pyrone molecules were observed, as well.

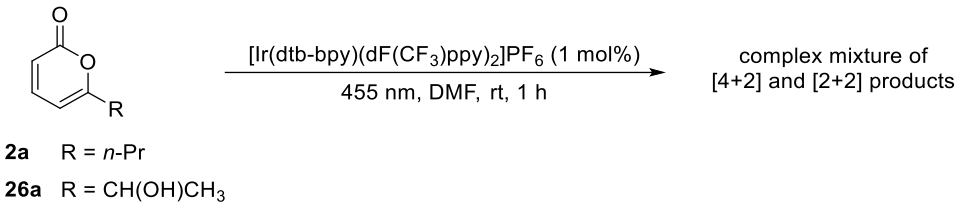

Scheme 94. Triplett sensitized reaction of alky pyrone **2a** and hydroxyalkyl pyrone **26a**.

All in all, the UV-mediated [4+2]-cycloaddition of 2-pyrone (**1**) was successfully replaced by a visible light catalyzed process giving rise to structurally and stereochemically rich cycloadducts **367a** and **367b** in a diastereoselective manner. The structures of both cycloadducts were unambiguously characterized by X-ray analysis. By introduction of substituents no selectivity of this reaction type could be obtained and only a complex mixture of various products was formed.

2.4 Cyclopropanation of 2-pyrone and 2-pyridinone and follow-up transformation

2.4.1 Cyclopropanation of 2-pyrone and 2-pyridinone

In general, 2-pyrones represent valuable starting materials in synthetic organic chemistry, however, besides versatile reactivities, that have been reported in recent literature, enantioselective functionalization of pyrones is still a remaining challenge. So far, only few methods have been developed in this field, e.g. asymmetric conjugate addition of Grignard reagents[116] or enantioselective hydrogenation of pyrone derivatives[189] accessing chiral 3,4- or 5,6-dihydro 2-pyrone derivatives – again precious synthetic building blocks.[190] Among the various known catalytic processes, transition metal-catalyzed cyclopropanation deems to be a promising strategy for stereoselective functionalization of 2-pyrones. Cyclopropanation reactions have already been established for the stereoselective elaboration of heterocycles like furan, pyrrole and indole[191,192] and the utility of these transformations have been showcased through the synthesis of many biologically relevant compounds (Figure 14).[193–198]

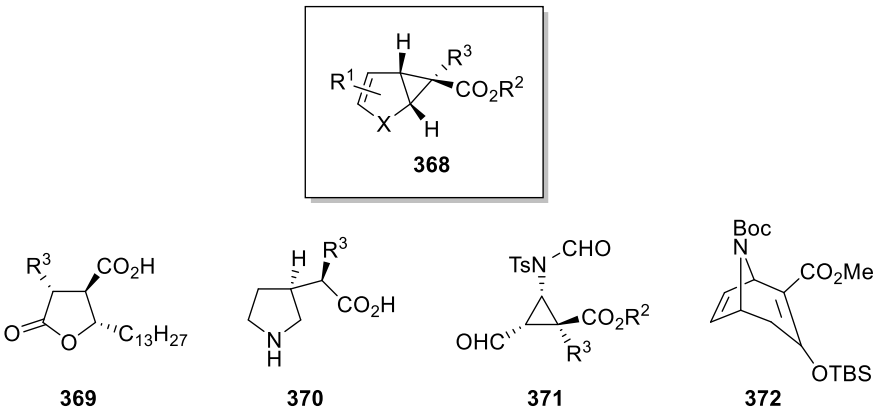

Figure 14. Selected examples of synthetic applications out of cyclopropanated heterocycles **368**.[193,194,196,198]

Commonly, cyclopropanation of olefinic compounds proceeds via copper or rhodium carbenoids as key reaction intermediates readily generated by metal-catalyzed decomposition of diazoacetates. In contrast to free carbenes, metal carbenoids provide higher stability and tunable reactivity/selectivity dependent on the carbenoid structure. The letter can be categorized in three classes – acceptor/acceptor- **373**, acceptor- **374** and donor/acceptor-carbenoids **375** (Figure 15). Due to their electrophilic character, the reactivity of carbenoids can be increased by acceptor substituents, while at the same time selectivity gets decreased. Introduction of donor substituents reverses these reactivity trends.[191,192]

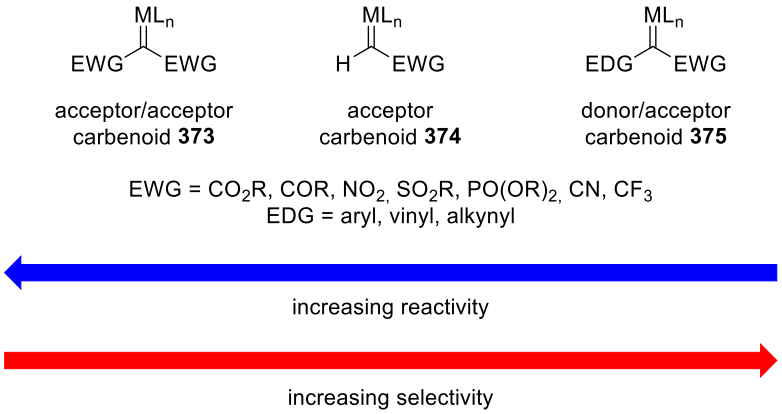

Figure 15. Classification and reactivity pattern of metal carbenoids.

Although transition metal-catalyzed cyclopropanation has been already applied to a number of heterocycles, to the best of our knowledge 2-pyrones have not been investigated as substrates in literature so far. Considering the electrophilic character of metal carbenoids, functionalization should occur on the more electron-rich double bond in 5,6-position next to the ring oxygen of pyrone **1** remaining an interesting α,β-unsaturated lactone moiety. Thus, the enantioselective formation of cyclopropanated pyrones would enable further follow-up transformations to access value-added compounds under high stereochemical control. Consequently, unsubstituted 2-pyrone (**1**) was at first investigated in racemic cyclopropanation using an achiral rhodium(II) catalyst and a donor/acceptor-diazoacetate **376** (Table 13).

Table 13. Racemic cyclopropanation of 2-pyrone (**1**) with diazoacetate **376**.

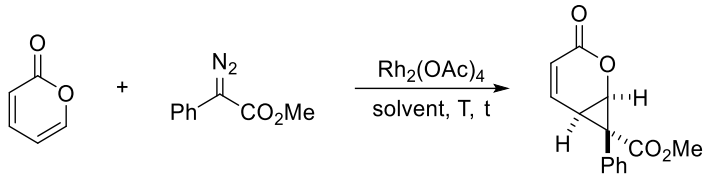

1 **376** **377a**

entry[a]	solvent	cat. [mol%]	equiv 376	T	t [h]	yield [%]
1	toluene	5.0	3.0	rt	1.5	74
2	toluene	1.0	3.0	rt	1.5	49
3[b}	toluene	2.5	3.0	rt	1.5	75
4	toluene	2.5	1.5	rt	1.5	55
5	toluene	2.5	3.0	60 °C	1.5	66
6	toluene	2.5	3.0	rt	3.0	72
7	DCM	2.5	3.0	rt	1.5	59
8	hexanes	2.5	3.0	rt	1.5	24
9	trifluorotoluene	2.5	3.0	rt	1.5	67
10[c]	DCM	-	0.2	rt	24	---

[a] conditions: to a solution of pyrone **1** (1.00 mmol, 1.0 equiv) and catalyst in solvent (0.5 M) was added dropwise a solution of diazoacetate **376** in solvent (1.1 M) over the indicated time; [b] pyrone **1** (5.00 mmol, 1.0 equiv) was used; [c] pyrone **1** (1.00 mmol) and diazoacetate **376** in DCM (0.5 M) were stirred under irradiation with a blue LED (λ = 455 nm) for 24 h.

Encouragingly, in a first experiment, using 5.0 mol% of $Rh_2(OAc)_4$, the expected reactivity could be confirmed and 2-pyrone (**1**) was regioselectively cyclopropanated in 5,6-position in good yields of 74% (Table 13, entry 1). Remarkably, no additional double cyclopropanated product was observed though the aromatic character of pyrone **1** is broken. In addition, cyclopropanation furnished only one diastereomer **377a** whose structure was unambiguously characterized by single-crystal X-ray analysis (Figure 16). This promising result initiated further research to optimize the reaction conditions. Screening of the amount of catalyst revealed that a catalyst loading of at least 2.5 mol% is necessary to achieve good yields of 75% (Table 13, entry 3), while a lower catalyst loading of 1.0 mol% significantly decreased the yield to 49% (entry 2). Likewise, reduction of the equivalents of diazoacetate **376** led to a drop in yield to 55% (entry 4). Furthermore, increasing the reaction temperature (entry 5) or addition

time of **376** (entry 6) did not improve the yield. Next, solvents commonly used in cyclopropanation reactions were screened. DCM (59%, entry 7) and hexanes (24%, entry 8) had adverse effects on the outcome of the reaction. In some cases, toluene, bearing a benzylic CH bond, shows unwanted side reactions with metal carbenoids and therefore, inert trifluorotoluene was also tested as solvent (Table 13, entry 9). However, utilization of trifluorotoluene slightly decreased the yield of **377a** to 67% indicating that the aforementioned side reactivity is no issue in this case. In 2018, Davies *et al*. reported that aryldiazoacetates **376** undergo photolysis by irradiation with blue light enabling cyclopropanation with a variety of substrates.[199] Irradiation of diazoacetate **376** with a blue LED (λ = 455 nm) in presence of pyrone **1** only gave dimers of **376** and 2-pyrone (**1**) was completely recovered (entry 10).

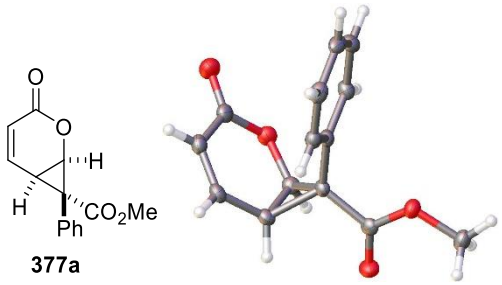

Figure 16. Crystal structure of **377a** (50% thermal probability).

Having identified the optimized conditions for a racemic cyclopropanation of unsubstituted 2-pyrone (**1**), next, the scope of this transformation should be investigated using 2-pyridinone derivative **378** as substrate (Table 14), which is readily available by a reaction of 2-hydroxypyridine **233** with *n*-butyllithium and *p*-toluenesulfonyl chloride.[200]

Table 14. Racemic cyclopropanation of 2-pyridinone **378** with diazoacetate **376**.

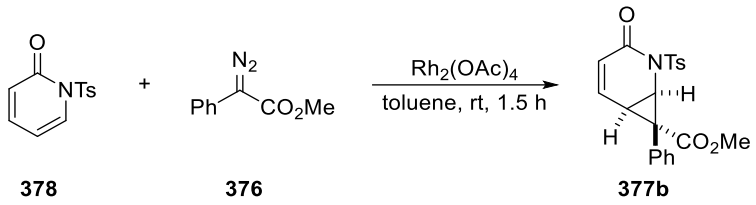

378 **376** **377b**

entry[a]	cat. [mol%]	equiv 376	yield [%]
1	2.5	3.0	97
2	2.5	1.5	89
3	1.0	3.0	96
4	1.0	2.0	95

[a] conditions: to a solution of pyridinone **378** (5.0 mmol, 1.0 equiv) and catalyst in toluene (0.5 M) was added dropwise a solution of diazoacetate **376** in toluene (1.1 M) over 1.5 h.

Interestingly, under previously determined reaction conditions, cyclopropanated pyridinone **377b** was isolated in almost quantitative yield of 97% (Table 14, entry 1). On the analogy of 2-pyrone (**1**), only one diastereomer was formed and the structure of the α,β-unsaturated lactam **377b** could be characterized by X-ray analysis (Figure 17). Further experiments showed, that the catalyst loading could be even reduced to 1.0 mol% and 2.0 equivalents of diazoacetate **376** were still sufficient to furnish **377b** in excellent yields of 95% (entry 4). The increased reactivity of pyridinone **378** compared to 2-pyrone (**1**) could be assigned to the powerful electron-donating ability of the nitrogen lone-pair leading to a more electron-rich heterocycle.

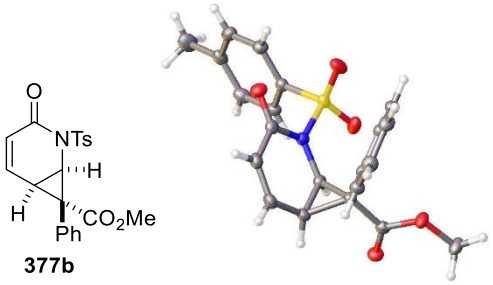

377b

Figure 17. Crystal structure of **377b** (50% thermal probability).

After proving pyrone **1** and pyridinone **378** as suitable substrates in transition metal-catalyzed cyclopropanations, the focus was then turned to the asymmetric transformation. A variety of chiral dirhodium catalysts have been developed for the reactions with donor/acceptor carbenes and they have been already applied for the enantioselective cyclopropanation of several

heterocycles.[193–195,198,201] Therefore, a short catalyst screening using 2-pyrone (**1**) as model substrate and DCM as solvent was conducted at the beginning (Table 15).

Table 15. Catalyst screening for the enantioselective cyclopropanation of 2-pyrone (**1**).

entry[a]	Rh(II) catalyst	yield [%]	*ee* [%][b]	$[\alpha]_D^{20}$
1	Rh_2(*S*-TCPTTL)$_4$	52	50	−165
2	Rh_2(*R*-*p*-BrTPCP)$_4$	46	57	−190
3	Rh_2(*S*-PTAD)$_4$	94	87	281

[a] conditions: to a solution of pyrone **1** (0.5 mmol, 1.0 equiv) and catalyst (1.0 mol%) in DCM (0.5 M) was added dropwise a solution of **376** (3.0 equiv) in DCM (1.1 M) over 1.5 h at room temperature; [b] determined by chiral HPLC analysis of the isolated product.

The initially tested phthalimido catalyst Rh_2(*S*-TCPTTL)$_4$ gave the cyclopropanated pyrone **377a** in moderate yield (52%) and low enantiomeric excess (50% *ee*, Table 15, entry 1). Utilization of the triarylcyclopropane carboxylate catalyst Rh_2(*R*-*p*-BrTPCP)$_4$ furnished **377a** in even lower yield (46%) but slightly increased *ee* (58% *ee*, entry 2). The Rh_2(*S*-PTAD)$_4$ catalyst proved to be very efficient and **377a** was isolated in an excellent yield of 94% with a high level of enantioselectivity (87% *ee*, entry 3).

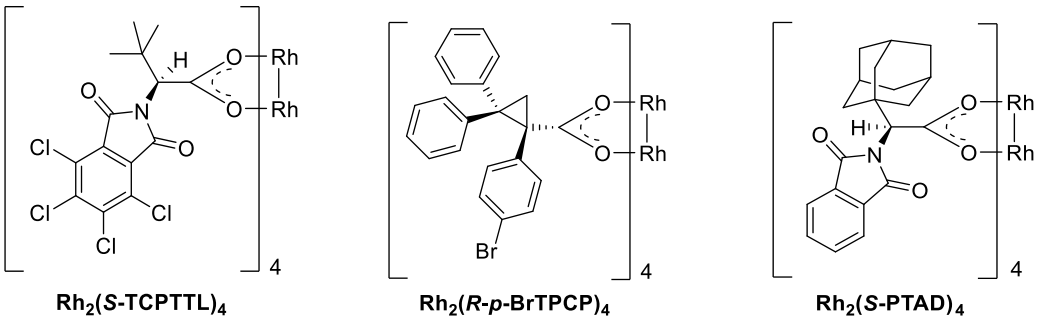

Figure 18. Structures of chiral rhodium catalysts used.

Encouraged by the satisfying performance of Rh_2(*S*-PTAD)$_4$, further screening of the reaction conditions was conducted in collaboration with Jiantao Fu, a member of the research group of Professor Huw M. L. Davies at the Emory University in Atlanta. For this purpose, trichloroethyl *p*-bromophenyldiazoacetate (**379**) was used as donor/acceptor carbenoid (Table 16).

Table 16. Screening of reaction conditions for the enantioselective cyclopropanation of pyrone **1**.

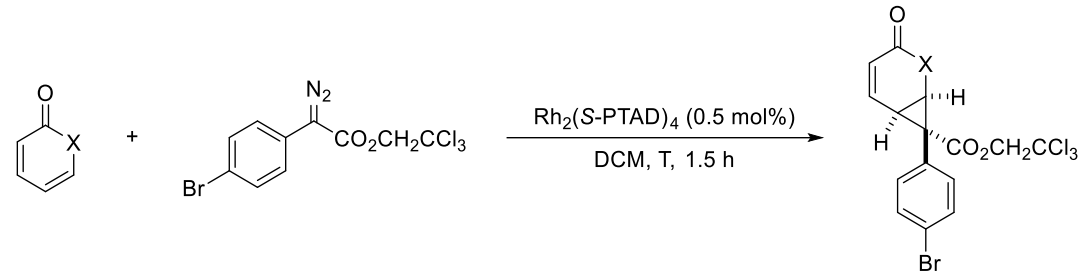

1 X = O
378 X = NTs

379

380a-b

entry[a]	starting material	equiv 379	T	yield [%]	*ee* [%][b]
1	X = O	0.5	rt	33	90
2	X = O	0.5	40 °C	60	86
3	X = O	2.0	rt	98	90
4	X = O	2.0	0 °C	98	93
5	X = NTs	2.0	0 °C	99	95

[a] conditions: to a solution of pyrone **1** or pyridinone **378** (0.5 mmol, 1.0 equiv) and Rh_2(*S*-PTAD)$_4$ (0.5 mol%) in DCM (0.5 M) was added dropwise a solution of **379** in DCM (1.1 M) over 1.5 h at the indicated temperature; [b] determined by chiral HPLC analysis of the isolated product.

Using a twofold excess of pyrone **1**, like it is reported for chiral cyclopropanations of furans and pyrroles[193,194], gave cycloproduct **380a** in poor yield of 33% but with excellent *ee* of 90% (Table 16, entry 1). Under reflux conditions (40 °C) the yield could be increased to 60%, however, a marginally decrease in enantioselectivity (86% *ee*) was observed (entry 2). A much better result was obtained, when diazoacetate **379** was added in excess (entry 3 and 4). Reaction at room temperature furnished **380a** in almost quantitative yield (98%) with an excellent *ee* of 90% (Table 16, entry 3). Enantioselectivity could be even slightly increased (93% *ee*) by performing the reaction at 0 °C (entry 4). Notably, lowering the catalyst loading to 0.5 mol% is still sufficient to achieve chiral functionalization with great results. In addition, pyridinone **378** was cyclopropanated under the same conditions in almost quantitative yield of 99% and with excellent enantiomeric excess of 95% (entry 5). With optimized conditions in hand, the scope of pyrones **381**, pyridinones **382** and aryl diazoacetates **383** is currently investigated in enantioselective cyclopropanation reactions by Jiantao Fu (Scheme 95).

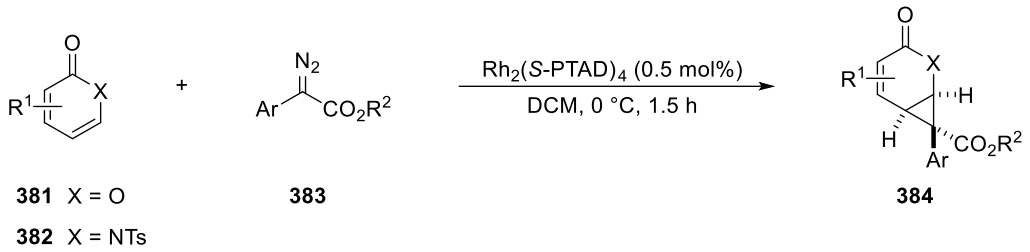

381 X = O
382 X = NTs
383
384

Scheme 95. Planned scope of enantioselective cyclopropanation of pyrones **381**, pyridinones **382** and diazoacetates **383**.

Besides donor/acceptor-carbenes, acceptor-diazoacetate **385** should also be employed for a cyclopropanation of pyrone **1** (Table 17). Routinely, reactions of acceptor-only carbenes under dirhodium tetracarboxylate catalysis give poor results in terms of selectivity and reactivity.[193,202] Hence, metal carbenoids derived from copper salts or copper(I)-bis(oxazoline) complexes are used for cyclopropanation reactions.[196,203]

Table 17. Attempts towards cyclopropanation of pyrone **1** with diazoacetate **385**.

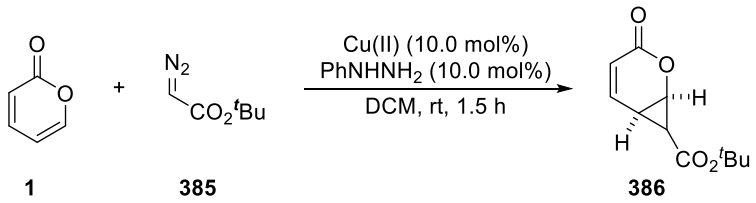

1 **385** **386**

entry[a]	Cu catalyst	ligand	yield [%]
1	$Cu(OTf)_2$	-	---
2	$Cu(OTf)_2$	*i*-Pr-Box	---
3	$Cu(acac)_2$	-	---
4	$Cu(acac)_2$	*i*-Pr-Box	---

[a] conditions: pyrone **1** (1.00 mmol, 1.0 equiv), catalyst (10.0 mol%), ligand (20.0 mol%), $PhNHNH_2$ (10.0 mol%), diazoacetate **385** (3.0 equiv).

Disappointingly, under several conditions tested, no conversion of pyrone **1** was observed and only dimers of diazoacetate **385** were obtained (Table 17, entry 1-4). Upon addition of *i*-Pr-bis(oxazoline) ligand, usually increasing the reactivity of copper carbenoids, also only dimerization was observed in both cases (entry 2 and 4). The inefficient reactivity of **1** with these types of electrophilic carbenoids in contrast to heterocycles like furan and pyrrole could be attributed to the less electron-rich character of pyrone heterocycles, thus creating an electronical mismatch. Since all attempts to a cyclopropanation of pyrone **1** with acceptor

diazoacetate **385** were unsuccessful, the focus was then turned to the follow-up transformations of cyclopropanated pyrone **377a**.

2.4.2 Follow-up transformations of cyclopropanated pyrone

As already mentioned in the previous chapter (B.2.4.1), cyclopropanated 2-pyrone **377a** contains an α,β-unsaturated lactone moiety clearly offering the possibility for further stereoselective transformations. The same structural motif can be found in 5,6-dihydro pyrones **387** displaying versatile reactivities in synthetic organic chemistry, e.g. in cycloadditions[204], 1,4-additions[118,205], Baylis-Hillman reactions[206], and hence, presenting a powerful tool for building up molecular complexity (Figure 19).

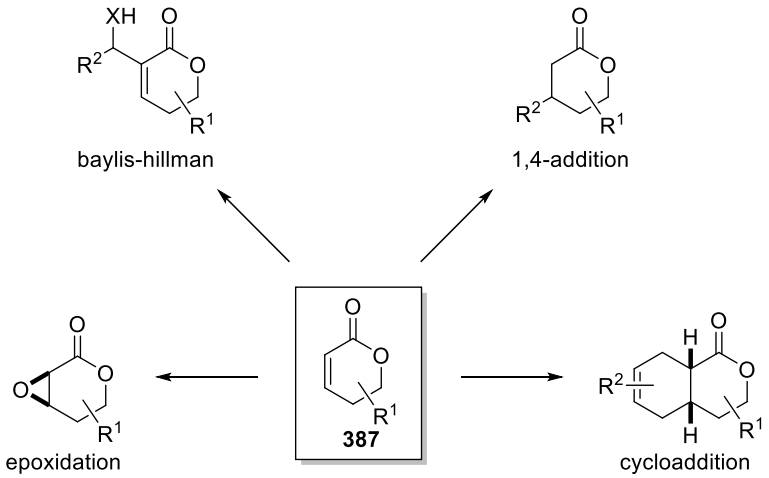

Figure 19. Reactivity of 5,6-dihydro 2-pyrones **387**.[207,208,209]

Lately, the research of our working group was focused on the stereoselective synthesis of 6-membered heterocycles by endocyclic ring-opening of cyclopropanated pyrones and furans, which is much more challenging than the well-known exocyclic ring-opening reaction.[210] Besides selective cleavage of the non-activated endocyclic C-C bond through palladium-catalyzed Heck coupling[211], introduction of a good leaving group (e.g. OMs) next to the cyclopropane moiety provided these valuable products after trapping of the resulting cation with a nucleophile (Scheme 96).[c]

[c] This research is currently part of the Ph.D. thesis of Robert Eckl (Working group of Prof. Reiser, University of Regensburg).

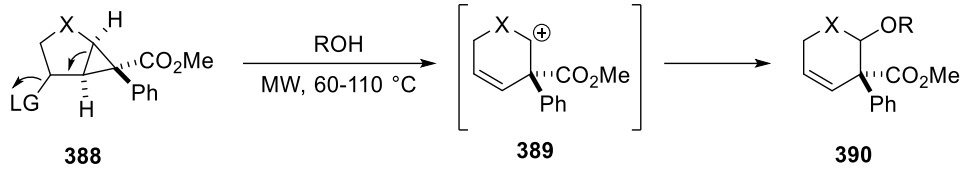

388 389 390

Scheme 96. Endocyclic ring expansion of cyclopropanated heterocycles by introduction of a leaving group.

Inspired by this work, the question arose whether an endocyclic ring expansion of cyclopropanated pyrone **377a** could enable access to 7-membered heterocycles, whose selective construction is still an important and challenging task in organic synthesis.[212] Therefore, the aforementioned reactivity of unsaturated lactones in Baylis-Hillman reactions should be utilized for the in situ introduction of a leaving group next to the cyclopropane ring. Generally, Baylis-Hillman reactions proceed via 1,4-addition of a Lewis base (LB) forming enolate **392**. Consequently, an aldol reaction gives rise to intermediate **393** and after proton abstraction, which is the rate-determining step (rds), product **395** is formed and the Lewis base catalyst is recovered (Scheme 97).

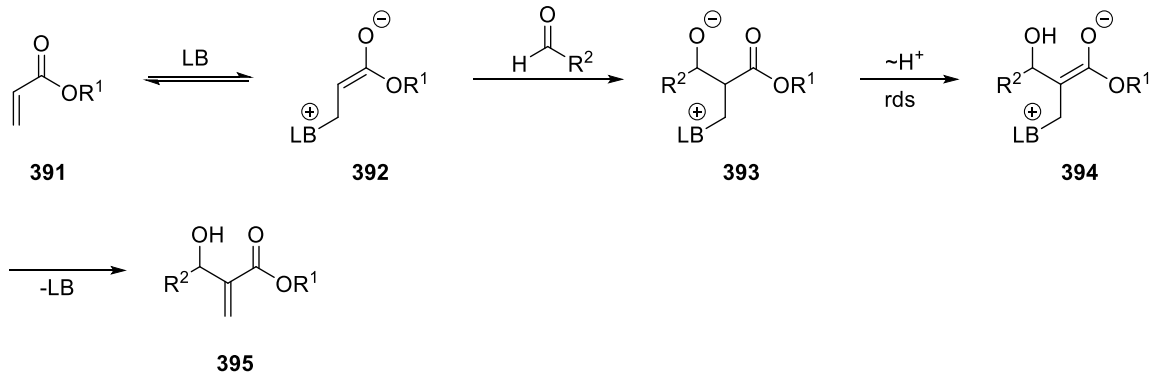

391 392 393 394 395

Scheme 97. General mechanism of a Baylis-Hillman reaction.

Following this mechanism, it was envisioned that 1,4-addition of a Lewis base could lead to in situ introduction of a valuable leaving group next to the cyclopropane moiety of unsaturated lactone **377a**. Hence, after endocyclic ring-opening, the corresponding cation **397** could be trapped by a nucleophile accessing 7-membered ring systems **398** (Scheme 98).

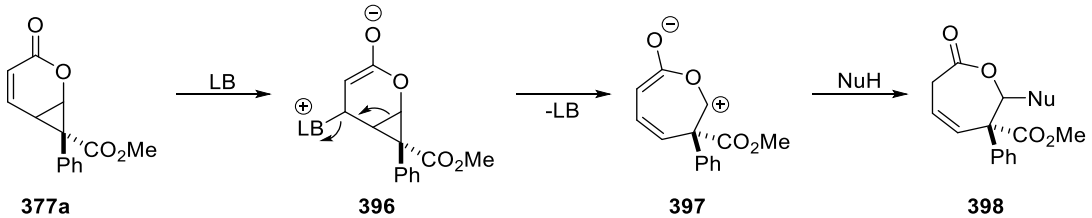

377a 396 397 398

Scheme 98. Envisioned strategy for an endocyclic ring expansion of **377a**.

Lewis base-catalyzed ring-opening of cyclopropanes via Michael-addition has already been applied by Zhang *et al.* for the construction of 2,3-dihydrofurans **401** (Scheme 99).[213] Herein, DABCO provides both the electron source as well as the electron sink.

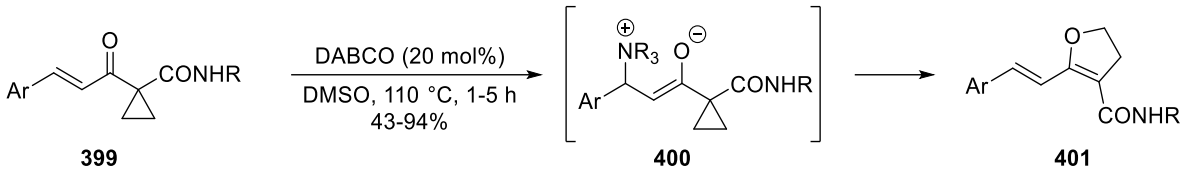

399 400 401

Scheme 99. Synthesis of 2,3-dihydrofurans **401** by Lewis-base-catalyzed ring-opening.[213]

In a first experiment, the reaction was performed using DABCO as Lewis base and a polar protic solvent (MeOH) to stabilize anionic intermediates by H-bond interactions and simultaneously acting as the nucleophile (Table 18, entry 1).

Table 18. Attempts to a Lewis base mediated endocyclic ring-opening of **377a**.

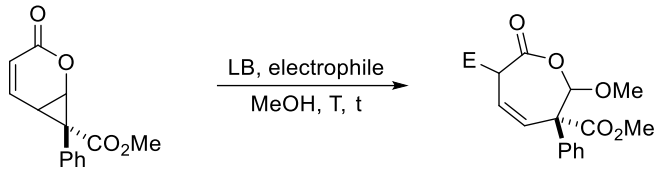

377a **402**

entry[a]	Lewis base	electrophile	T	t [h]	yield [%]
1	DABCO	-	rt to 80 °C	48	decomposition
2	Bu_3P	-	rt	24	decomposition
3	DABCO	benzaldehyde	rt to 80 °C	48	decomposition
4	Bu_3P	benzaldehyde	rt	24	traces, decomposition

[a] conditions: cyclopropanated pyrone **377a** (1.00 mmol, 1.0 equiv), Lewis base (40 mol%), electrophile (1.5 equiv) in MeOH (0.2 M).

However, when running the reaction at room temperature, no conversion of the starting material **377a** was observed. Hence, the reaction temperature was increased to 80 °C, but under reflux condition the starting material **377a** decomposed (Table 18, entry 1). The same trend was observable for tributylphosphine as Lewis base (entry 2). In order to stabilize the potential enolate intermediate **396** by an aldol reaction, benzaldehyde was added as an electrophile in further reactions (Table 18, entry 3 and 4). Again, no starting material **377a** was converted at room temperature using DABCO and upon heating decomposition was observed (entry 3). In contrast to the reaction with DABCO, tributylphosphine already reacted at room temperature

with cyclopropanated pyrone **377a** (entry 4). Mass spectrometry of the crude product revealed some formation of **402** besides mainly decomposition, but the ring expansion product **402** could not be isolated after column chromatography.

A further attempt to achieve Lewis base mediated ring-expansion was conducted by adding trimethylsilyl azide to trap the possible enolate intermediate **396** as silyl ether. Additionally, azide should act as the nucleophile. Unfortunately, decomposition of **377a** was also observed in this case (Scheme 100).

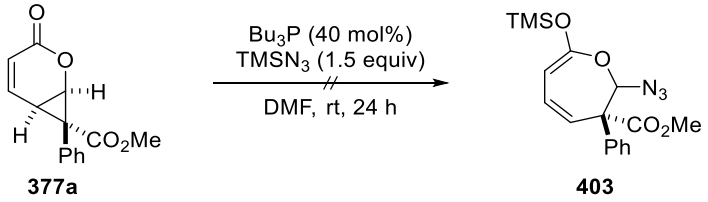

Scheme 100. Investigation of the ring expansion of **377a** by addition of $TMSN_3$.

This led to the decision to pursue a different strategy for the ring-opening of bicyclic lactone **377a**. A variety of reaction conditions have been developed for the epoxidation of unsaturated δ-lactone systems. After epoxidation of cyclopropanated pyrone **377a,** the corresponding epoxide **404** should be investigated in a Brønsted- or Lewis acid-catalyzed ring-extension via cationic intermediate **405**. (Scheme 101). This concept was already successfully applied to cyclopropanated piperidine substrates in our research group.[d]

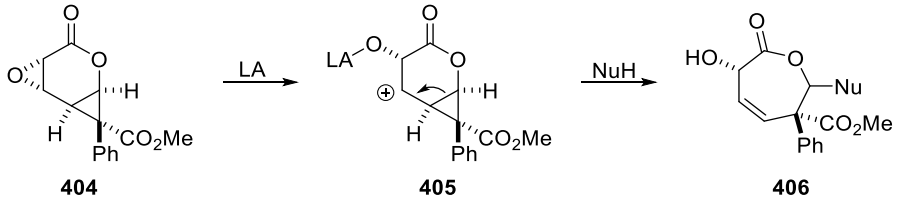

Scheme 101. Envisioned strategy for a ring-opening of pyrone **377a** by epoxidation.

In the following, cyclopropanated substrate **377a** was investigated in different epoxidation reactions (Table 19).

[d] This research is currently part of the Ph.D. thesis of Tobias Babl (Working group of Prof. Reiser, University of Regensburg).

Table 19. Investigation of the epoxidation of cyclopropanated pyrone **377a**.

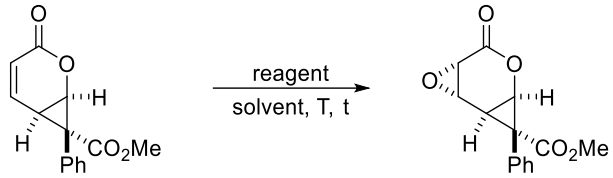

377a **404**

entry	reagent	solvent	T	t [h]	yield [%]
1	H_2O_2/NaOH	DCM/MeOH	rt	24	decomposition
2	DMDO	acetone/H_2O	0 °C to 80 °C	72	---
3	*m*CPBA	DCM	rt to 40 °C	72	---
4	*m*CPBA, $NaHCO_3$	DCM	rt to 40 °C	24	---
5	*t*-BuOOH, DBU	DCM	rt	24	decomposition

Due to the electron-deficient character of the targeted double bond in **377a**, a nucleophilic epoxidation as for the synthesis of 2-pyrones was performed at first (Table 19, entry 1). Under basic reaction conditions, starting material **377a** completely decomposed, which could be rationalized by a lactone opening leading to further unselective reactions. Consequently, rather neutral conditions were tested (entry 2-4). However, the electrophilic epoxidation reagents DMDO and *m*CPBA did not convert **377a** even under reflux conditions (entry 2-4). DBU-catalyzed conjugated addition of *tert*-butyl-hydroperoxide, specifically developed for the epoxidation of base sensitive α,β-unsaturated lactones by Kapoor and co-workers[209], again showed decomposition of cyclopropanated pyrone **377a**. Like reported for other base sensitive lactones, the electron-withdrawing cyclopropane ring seems to facilitate opening of the lactone ring thus prevent selective epoxide formation.[208,209]

The unsuccessful epoxidation of pyrone **377a** ultimately led to the end of the endocyclic ring-opening efforts. Nevertheless, the previously observed tendency of cyclopropanated pyrone **377a** to undergo easily lactone opening should be exploited for another kind of transformation. The presence of a vinylcyclopropane moiety in cyclopropanated pyrone **377a** provides further opportunities for its application as chiral building blocks. Vinylcyclopropanes can undergo several rearrangements that have been used for the synthesis of valuable complex molecules.[198,214] Among them, the 1,3-sigmatropic rearrangement giving rise to cyclopentane

derivatives has been studied in detail.[215,216] For instance, Davies *et al*. showed Et_2AlCl catalyzed 1,3-sigmatropic rearrangement of vinylcyclopropane **407** exhibiting excellent stereoselectivity (Scheme 102).

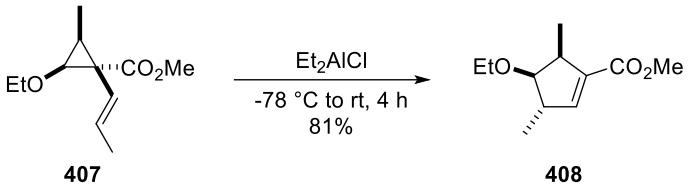

407 **408**

Scheme 102. Et_2AlCl catalyzed 1,3-sigmatropic rearrangement of vinylcyclopropane **407**.[216]

Applying this reaction pattern on cyclopropanated pyrone **377a**, may give rise to derivatives of hydroxymethyl cyclopentenol **409** with high stereocontrol. This important substrate and the corresponding dihydroxymethyl derivatives have found application in the synthesis of valuable natural occurring substances and drugs, e.g. entecavir (**410**), hexacyclinol or (+)-ophiobolin A.[217,218] Entecavir (**410**) is a nucleoside analog and has been approved by the U.S. FDA for the treatment of hepatitis B virus (HBV) infected patients, thus being listed on WHO's list of essential medicines. It was first discovered and synthesized by chemists from Bristol-Myers Squibb starting from enantiomerical pure (1*S*,2*R*)-2-(hydroxymethyl)cyclopent-3-en-1-ol (**409**) (Scheme 103).

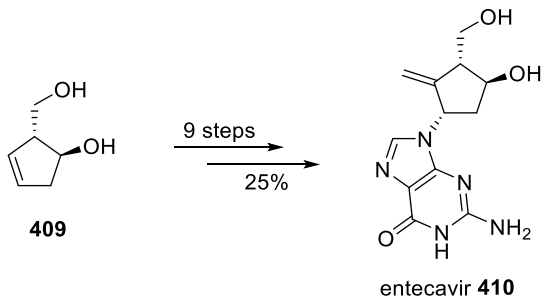

409 entecavir **410**

Scheme 103. Synthesis of entecavir (**410**) according to Bristol-Myers Squibb.[217]

Lactone opening of cyclopropanated pyrone **377a** should provide an acyclic vinylcyclopropane undergoing a further sigmatropic rearrangement towards cyclopentenol derivative **411**. Moreover, ring-opening by applying reductive conditions could lead to the simultaneous formation of a hydroxymethyl substituent next to the secondary alcohol. Therefore, DIBAL-H was used as reductive agent for the lactone opening/rearrangement approach (Scheme 104).

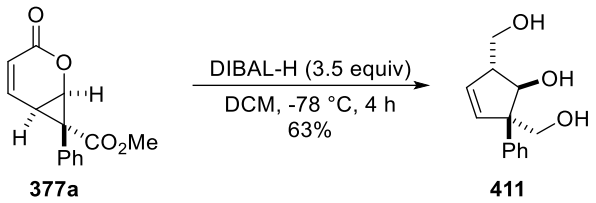

Scheme 104. Synthesis of cyclopentenol **411** by reductive ring-opening/rearrangement of **377a**.

Pleasingly, first attempts under reductive conditions furnished cyclopentenol derivative **411** in 63% yield. Further optimization of the aforementioned reaction remains to be determined. Therefore, increasing the amount of DIBAL-H or varying the reduction agent seems to be a promising starting point since a not complete reduced aldehyde derivative of **411** was observed as a side-product. Noteworthy, the reductive ring-opening/rearrangement of **377a** proceeded with excellent stereoselectivity and only one diastereomer of **411** was obtained. On closer consideration of the mechanism (Scheme 105), the excellent stereocontrol can be explained by the suprafacial 1,3-sigmatropic rearrangement of intermediate **412** leading to a retention of the configuration.[216]

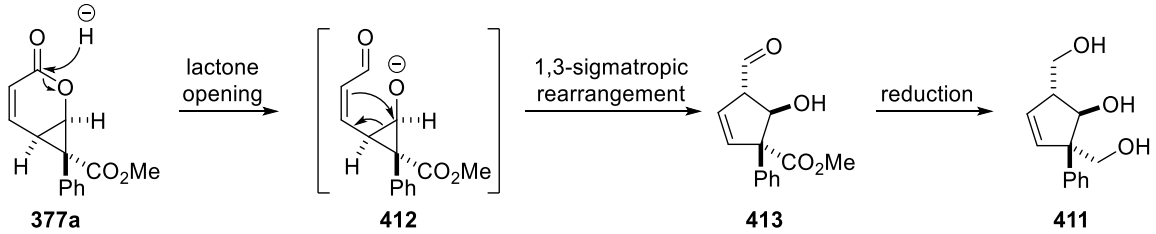

Scheme 105. Proposed mechanism for the ring-opening/rearrangement of **377a**.

Starting from enantiopure cyclopropanated pyrone **377a** this process enables access to chiral hydroxymethyl cyclopentenol derivatives **411** being a valuable precursor for the synthesis of highly biologically active products like entecavir derivatives. Additionally, the same transformation of cyclopropanated pyridinone **377b** could give rise to chiral derivatives of hydroxymethyl cyclopentene amines **414** which have been proved as important intermediates in organic synthesis (Figure 20).[219,220] Reaction optimization, scope investigation and application of this process is part of the Ph.D. thesis of Natalija Moor, a member of our research group.

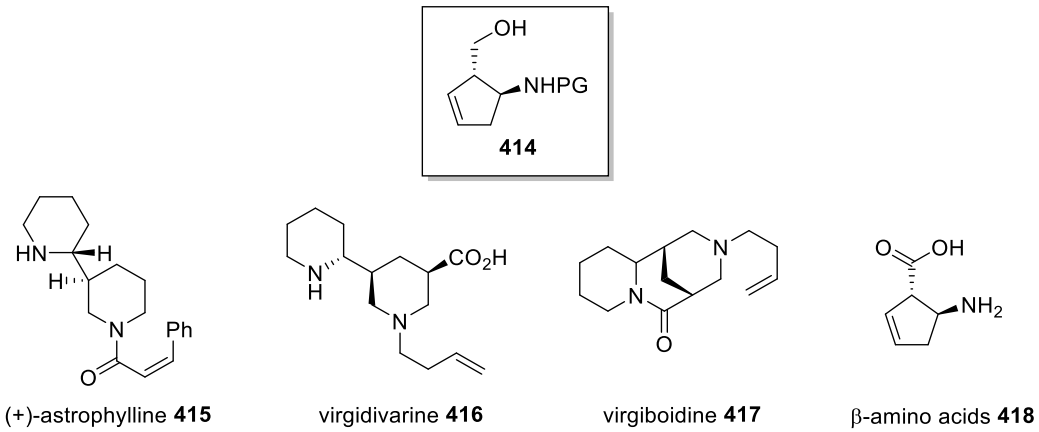

Figure 20. Selected samples of valuable products derived from hydroxymethyl cyclopentene amine **414**.[219,220]

In conclusion, 2-pyrone (**1**) and pyridinone **378** were successfully functionalized by transition metal-catalyzed cyclopropanation using donor/acceptor-carbenoids. Moreover, catalyst screening revealed that chiral Rh_2(*S*-PTAD)$_4$ proved to be an efficient catalyst giving rise to cyclopropanated pyrone **380a** and pyridinone **380b** in excellent yields and enantiomeric excess. The scope of substrates and diazoacetates is currently investigated by Jiantao Fu, a member of the research group of Professor Huw Davies in Atlanta. Unfortunately, attempts to use acceptor-carbenoids were unsuccessful. The following endocyclic ring expansion of cyclopropanated pyrone **377a** to 7-membered heterocycles failed under applied strategies. In contrast, the development of a reductive lactone ring-opening/rearrangement strategy enabled access to a cyclopentenol derivative **411** that could find application in the synthesis of precious compounds like, e.g., entecavir derivatives. Further investigations on this project and additional follow-up transformations like 1,4-additions and cycloadditions are already in progress in the Reiser group.

3 Atypical reactivity of anthracene derivatives[e]

3.1 Diels-Alder reaction with atypical regioselectivity

3.1.1 Diels-Alder reaction of anthracene derivatives

The [4+2]-cycloaddition of a conjugated diene with 4 π-electrons and a dienophile (an alkene or alkyne) with 2 π-electrons – commonly known as the Diels-Alder reaction – is one of the most emblematic pericyclic reactions. It is deservedly celebrated due to its synthetic reliability and atom-economic approach for the facile construction of complex 6-membered ring systems in a regio- and stereoselective fashion. Being an easily available conjugated π-electron-rich carbocyclic system, anthracene (**419a**) has been widely exploited as a classic diene for Diels-Alder reactions wherein its chemical reactivity and transformational effectiveness are subsidized by the partial loss of aromaticity. Extensive synthetic and mechanistic studies reveal that the natural preference for [4+2]-cycloadditions of unsubstituted anthracene (**419a**) is at its 9,10-positions (red, Figure 21).[221] The selectivity is governed by thermodynamic factors given that the twofold stabilization energy of benzene (2 × 35 = 70 kcal/mol) is greater compared to that of the naphthalene moiety (50 kcal/mol) as well as kinetic factors for having the largest frontier molecular orbital coefficients at the 9,10-positions (red sphere, Figure 21) in the Highest Occupied Molecular Orbitals (HOMO) of **419a** (Figure 21).[222]

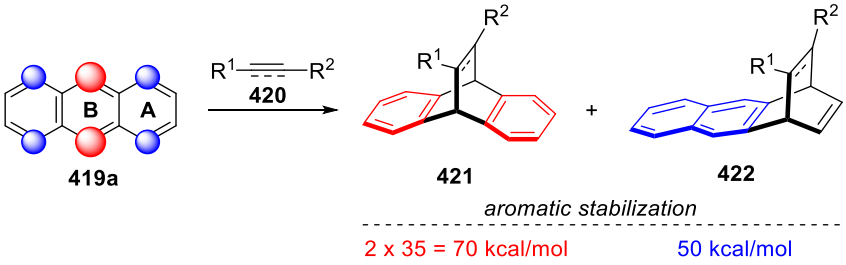

Figure 21. Inherent reactivity mode of anthracene (**419a**) with dienophiles.[222]

Considering the significance of the transformation, tuning the regioselectivity of the Diels-Alder reaction of anthracenes is an attractive problem. However, until today, only very few approaches have been successful to indirectly circumvent the inherent 9,10-preference of anthracenes in [4+2]-cycloaddition reactions and almost all of these studies relied on premeditated engagement of the 9,10-positions either sterically or electronically. Installation of

[e] This chapter includes parts from a manuscript which has been prepared in collaboration with V. Ngoc, A. Bhattacharyya, P. Kreimeier, P. Sarkrausky, J. Rehbein and O. Reiser. Experimental results obtained from the Ph.D. thesis of V. Ngoc are highlighted.

voluminous and/or electron-withdrawing substituents at the 9- and 10-positions indirectly deactivates the central B-ring for steric and electronic reasons, thereby allowing the formation of the corresponding cycloadducts with the terminal A-ring (Figure 22).

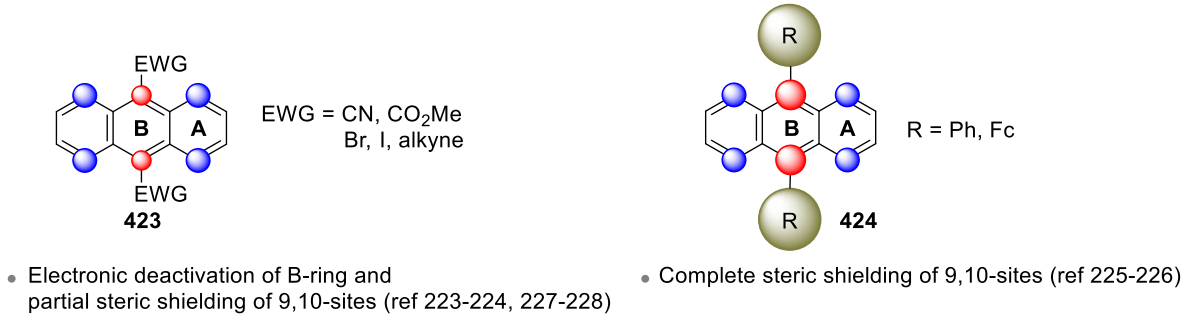

Figure 22. Previous approaches for 1,4-selective [4+2]-cycloadditions by electronic and steric maneuvers at the 9,10-positions.[223–228]

For example, 9,10-dicyanoanthracene in the reaction with benzyne furnishes a 1:1 mixture of the corresponding 1,4- and 9,10- adducts, albeit only in low yield (8%).[223] Moreover, in the total synthesis of molecular gyroscopes with triptycyl frames, Garcia-Garibay *et al.* observed the formation of 1,4-cycloadducts as byproducts (maximal ratio 9,10/1,4 = 1:1) during the Diels-Alder reaction of anthracenes bearing alkyne groups in 9-position with benzynes.[224] Likewise, sterically more demanding 9,10-diphenyl- or 9,10-diferrocenyl-substituted anthracenes were found to yield exclusively the corresponding A-ring adducts with DMAD in 50% and 38% yield, respectively.[225,226] More recently, a 1,4-selective cycloaddition with sterically bulky *N*-2,6-difluorophenylmaleimide[227] or with *N*-substituted maleimides activated by superstoichiometric amounts of $AlCl_3$[228] was reported with anthracene derivatives. However, yet again blocking of both, the 9- and / or the 10-position by ester, halide and/or phenyl groups was necessary.

The only example so far that is reported to be exclusively 1,4-selective with an anthracene moiety unsubstituted at the 9,10-positions is the reaction between anthracene (**419a**) itself and *N*-cyclohexylmaleimide confined as an inclusion complex of a supramolecular octahedral organopalladium host.[229] It was assumed that the unusual regioselectivity stemmed from an external topochemical control by the way the substrate bind to the host which made it geometrically impossible to attack the 9,10-positions with the dienophile (Figure 23).

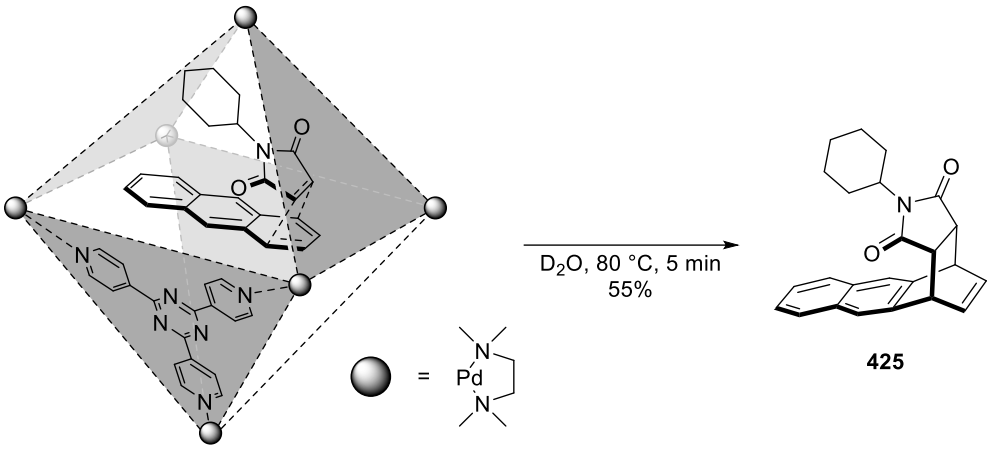

Figure 23. 1,4-Selective [4+2]-cycloaddition of anthracene (**419a**) by external topochemical control.[229]

More recently, an anthracene derivative with fused carbocyclic moieties in 2,3- and 6,7-positions was found to undergo a cycloaddition at both 9,10- and 1,4-positions (ratio 9,10/1,4 = 1:2) with 4,5-dimethoxybenzyne in 33% yield.[230] The unusual reactivity was explained by electronic activation of the outer rings that outweighs the steric hindrance.

Motivated by this literature void, the question was asked whether the A-ring of the anthracene could be sufficiently electronically enriched by placing donor substituents on it so that corresponding 1,4-cycloadducts would directly form with electron-deficient dienophiles without the necessity of blocking the 9,10-positions (Figure 24).

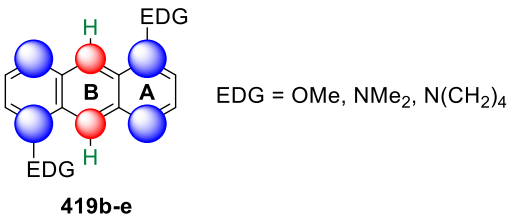

Figure 24. Direct electronic activation of the A-ring with unblocked 9,10-sites.

In order to assess the validity of the hypothesis, 1,5-disubstituted anthracenes **419b-d** were synthesized from readily available anthraquinones **426-428** (Scheme 106)[231,232] and employed in a series of thermal [4+2]-cycloaddition reactions.

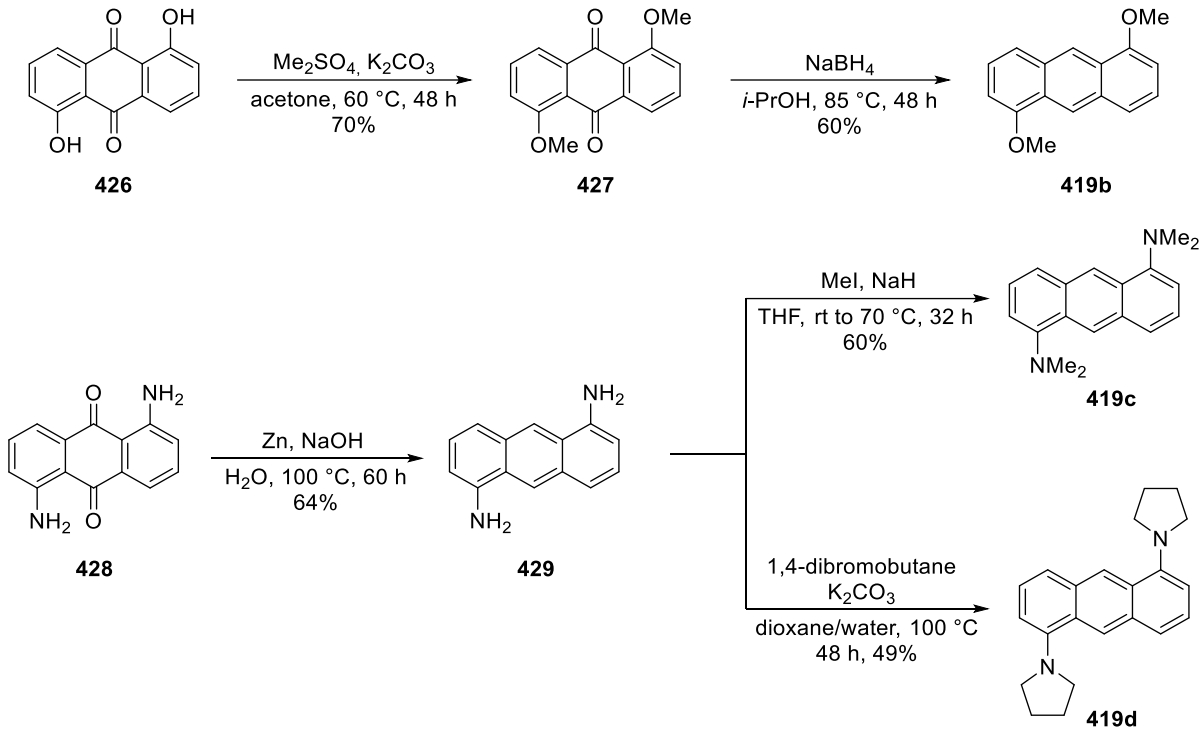

Scheme 106. Synthesis of 1,5-disubstituted anthracenes **419b-d**.[231,232]

A range of electron-deficient alkene dienophiles such as dimethyl fumarate (**A**), maleic anhydride (**B**) and *N*-phenylmaleimide (**C**) were investigated at first (Table 20).

Table 20. Diels-Alder reactions of disubstituted anthracenes **419b-d** and dienophiles **A-C**.

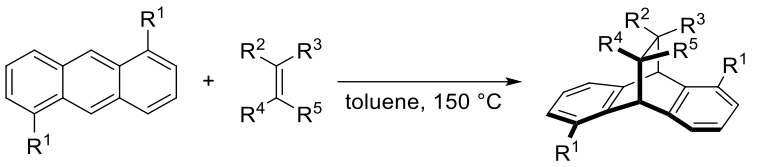

419b R^1 = OMe
419c R^1 = NMe_2
419d R^1 = $N(CH_2)_4$

A-C

430A-C

entry[a]	R^1	dienophile	product[b]
1 2[233] 3[233]	OMe NMe_2 $N(CH_2)_4$	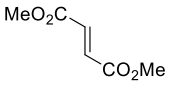 **A**	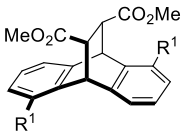 ***syn*-430bA: R^1 = OMe; 95%** ***syn*-430cA: R^1 = NMe_2; 40%** ***syn*-430dA: R^1 = $N(CH_2)_4$; 55%**
			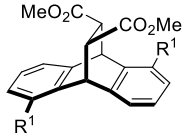 ***anti*-430cA: R^1 = NMe_2; 28%** ***anti*-430dA: R^1 = $N(CH_2)_4$; 31%**
4 5[233] 6[233]	OMe NMe_2 $N(CH_2)_4$	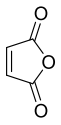 **B**	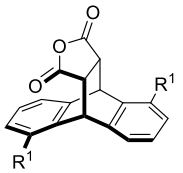 **430bB: R^1 = OMe; 97%** **430cB: R^1 = NMe_2; 88%** **430dB: R^1 = $N(CH_2)_4$; 75%**
7 8 9	OMe NMe_2 $N(CH_2)_4$	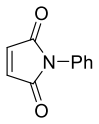 **C**	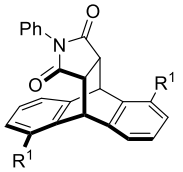 **430bC: R^1 = OMe; 99%** **430cC: R^1 = NMe_2; 98%** **430dC: R^1 = $N(CH_2)_4$; 92%**

[a] conditions: anthracene (**419b-d**, 1.0 equiv) and dienophile (**A-C**, 1.1 equiv) in toluene (0.5 M) in a sealed tube at 150 °C (for details on reaction times see experimental part); [b] isolated yield.

However, only the formation of 9,10-cycloadducts **430A-C** was observed in 68-99% yield (Table 20), even in the case of substrates **419c** (entry 2, 5 and 8) and **419d** (entry 3, 6 and 9) with increased π-electron density. Notably, the reaction of dimethoxy anthracene **419b** and dimethyl fumarate (**A**) furnished selectively the *syn*-cycloadduct **430bA** (Table 20, entry 1), because steric effects are negligible for **419b** and the electronic secondary orbital interactions predominate in every reaction. Next, the attention was turned to evaluate alkyne dienophiles (Table 21) such as dimethylacetylene dicarboxylate (DMAD, **D**)[233] which are also known for being exclusively 9,10-selective for unsubstituted anthracene[234] (**419a**, Table 21, entry 1).

Table 21. Diels-Alder between 1,5-disubstituted anthracenes **419a-d** and alkynes **D-F**.

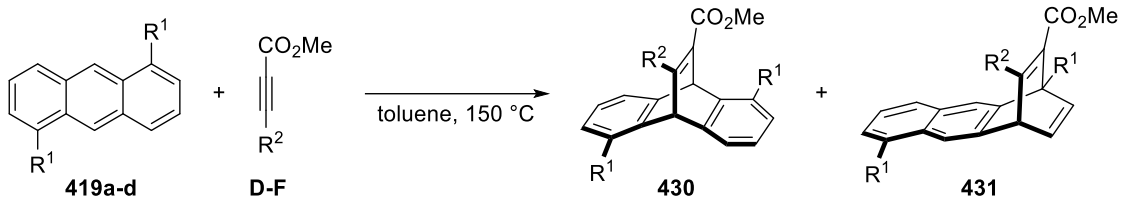

entry[a]	R^1	dienophile	product[b]	430 : 431[c]
1[233]	H	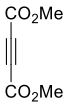 D	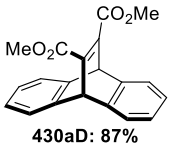 430aD: 87%	>99 : 1
2[233]	OMe	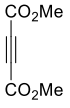 D	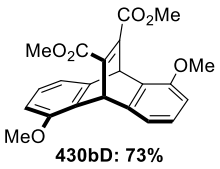 430bD: 73% 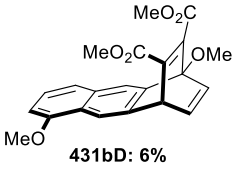 431bD: 6%	90 : 10
3[233]	NMe_2	 D	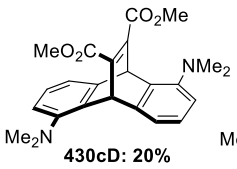 430cD: 20% 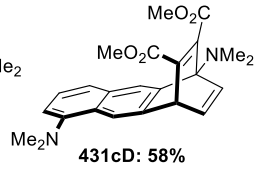 431cD: 58%	30 : 70
4[233]	$N(CH_2)_4$	 D	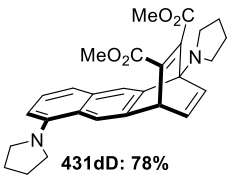 431dD: 78%	1 : >99
5	$N(CH_2)_4$	 E	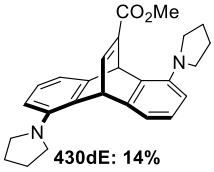 430dE: 14% 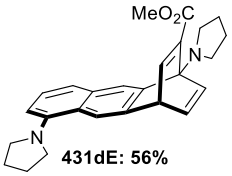 431dE: 56%	17 : 83
6[233]	$N(CH_2)_4$	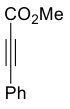 F	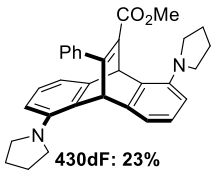 430dF: 23%	>99 : 1

[a] conditions: anthracene (**419a-d**, 1.0 equiv) and dienophile (**D-E**, 1.1 equiv; **F** 5.0 equiv) in toluene (0.5 M) in a sealed tube at 150 °C (for details on reaction times see experimental part); [b] isolated yield; [c] determined by ^{1}H NMR.

When **419b** was reacted with **D** under thermal reaction conditions, the first indication of the change in trend of regioselectivity was pleasingly observed, as 6% of the corresponding 1,4-

cycloadduct **431bD** formed alongside the formation of the usual 9,10-cycloadduct **430bD** (73%, Table 21, entry 2). Subsequently, when dimethylamino-group bearing 1,5-disubstituted anthracene **419c** was subjected to the [4+2]-cycloaddition with DMAD (**D**), the corresponding 1,4-cycloadduct **431cD** turned out to be the major product (58% yield) dominating over the usual 9,10-cycloadduct **430cD** which was obtained in only 20% yield (Table 21, entry 3). Inspired by the observation that the donor strength of the substitutions on the A-ring indeed affected the regioselectivity of [4+2]-cycloaddition reactions of anthracene derivatives, the dipyrrolidino 1,5-disubstituted anthracene **419d** was next investigated, following the lead of Zipse *et al.*[235] who demonstrated that a pyrrolidine substituted pyridine is more nucleophilic than dimethylaminopyridine (DMAP). When **419d** was engaged in the thermal [4+2]-cycloaddition with **D**, gratifyingly, the reaction yielded the 1,4-adduct **431dD** exclusively in 78% yield (Table 21, entry 4), representing the first example for a 1,4-selective [4+2]-cycloaddition of an anthracene derivative in which the 9,10-positions are not blocked with substituents or shielded by any other means. Interestingly, when methyl propiolate (**E**) bearing a single ester group on the alkyne functionality was employed as the dienophile and reacted with **419d**, a drop in regioselectivity was observed and the corresponding 1,4-cycloadduct **431dE** as a single isomer was obtained in 56% yield along with the formation of the corresponding 9,10-cycloadduct **430dE** in 14 % yield (entry 5). The regioselectivity was again found to be entirely reversed when methyl phenylpropiolate (**F**) was reacted with **419d** and the 9,10-cycloadduct **430dF** formed exclusively, albeit with poor yield even after 72 h (23%, Table 21, entry 6).

After establishing a definite relationship between the donor strength of the substituents at the 1,5-positions and the regioselective outcomes of the [4+2]-cycloadditions of anthracenes with alkene and alkyne dienophiles, the extent of the electron-donating effect on the regioselectivity of the transformations should be investigated next. Accordingly, monosubstituted pyrrolidino anthracene derivative **419e** was synthesized (Scheme 107).[236]

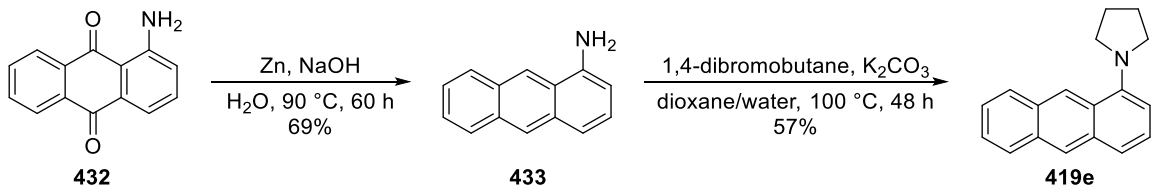

Scheme 107. Synthesis of 1-pyrrolidine anthracene (**419e**).[236]

The monosubstituted anthracene derivative **419e** was also investigated in a series of cycloaddition reactions with alkenes **A-C** and alkyne dienophiles **D-G** (Table 22).

Table 22. Diels-Alder reaction of pyrrolidine anthracene **419e** and dienophiles **A**-**G**.

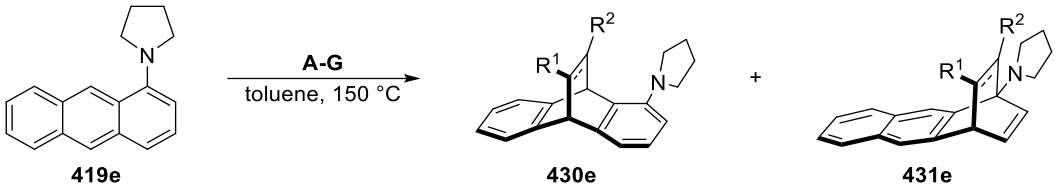

entry[a]	dienophile	product[b]	430e : 431e[c]
1	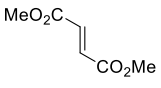 A	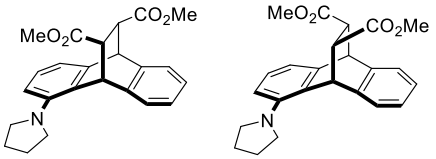 *syn*-430eA: 46% *anti*-430eA: 50%	>99 : 1
2	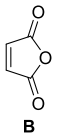 B	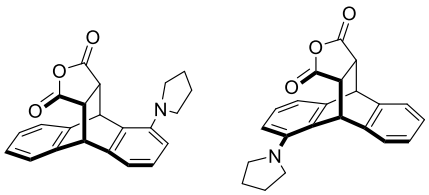 *exo*-430eB/*endo*-430eB (33:67): 99%[c]	>99 : 1
3	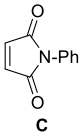 C	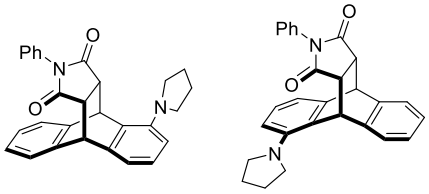 *exo*-430eC/*endo*-430eC (33:67): 95%	>99 : 1
4[d]	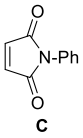 C	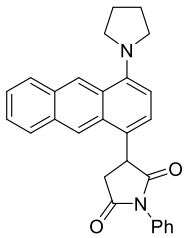 434: 62%	---
5	 D	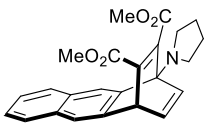 431eD: 90%	1 : >99
6	 E	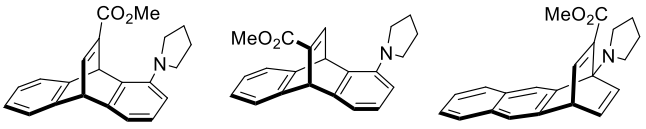 *syn*-430eE *anti*-430eE 431eE: 72% *syn*-430eE/*anti*-430eE (55:45): 25%	23 : 77

7	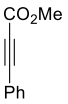 **F**	---	---
8	 **G**	decomposition	---

[a] conditions: anthracene (**419e**, 1.0 equiv) and dienophile (**A-E**, 1.1 equiv; **F-G** 5.0 equiv) in toluene (0.5 M) in a sealed tube at 150 °C (for details on reaction times see experimental part); [b] isolated yield; [c] determined by ^{1}H NMR; [d] conditions: anthracene (**419e**, 1.0 equiv), dienophile (**C**, 1.1 equiv) and $AlCl_3$ (3.0 equiv) in $CHCl_3$ (0.08 M) in a sealed tube at room temperature for 3 h.

Analogous to the disubstituted anthracenes **419b-d**, when **419e** was employed in the thermal [4+2]-cycloaddition with alkene dienophiles **A-C**, the respective 9,10-cycloadducts **430eA-C** exclusively formed in every case in 95-99% yields (Table 22, entry 1-3). On the contrary, activation of dienophile **C** by a Lewis acid ($AlCl_3$) furnished Friedel-Crafts type product **434** exclusively in *para*-position of the pyrrolidine substituent (62%, Table 22, entry 4). The reaction seems to take place through a Michael-addition in the first step. Subsequent rearomatization of the zwitterionic intermediate by proton abstraction proceeds faster than ring closure to the corresponding cycloadduct. Satisfyingly, when DMAD (**D**) was used as dienophile, the selective formation of the 1,4-cycloadduct **431eD** was observed in excellent yield (90%, entry 5). Likewise, methyl propiolate (**E**) yielded preferentially the corresponding 1,4-cycloadduct **431eE** as a single regioisomer in 72% yield along with the formation of the corresponding 9,10-cycloadducts **430eE** as a *syn*/*anti* (*syn*/*anti* = 55:45) isomeric mixture (25%, entry 6). In contrast, methyl phenylpropiolate (**F**) did not undergo any cycloaddition reaction with **419e** (entry 7). The reaction of **419e** with in situ prepared benzyne (**G**), a reagent that has been studied in 1,4-cycloadditions with anthracene derivatives[223,224,230], led only to decomposition of the starting material (Table 22, entry 8). The structure of 1,4-cycloadduct **431eD** was unambiguously assigned by NMR spectroscopy and was confirmed by single-crystal X-ray diffraction analysis (Figure 25). It is noteworthy to mention that all 1,4- and 9,10-cycloadducts were examined at high-temperature conditions (reflux, 24 h, 160 °C), however, no crossover between the products was observed in any case.

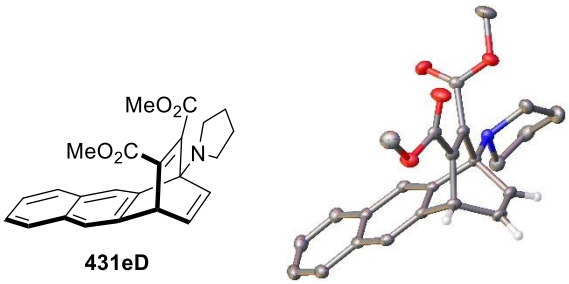

Figure 25. Crystal structure of **431eD** (50% thermal probability).

3.1.2 Computational studies

With a view to completely comprehending the atypical regioselectivity demonstrated by the anthracenes **419b-e** in aforementioned [4+2]-cycloadditions with alkyne dienophiles **D-E**, extensive theoretical calculations were performed in cooperation with Prof. J. Rehbein. The theoretical calculations were conducted by Patrick Sakrausky (Ph.D. student of AK Rehbein).

The fundamental question arose, what governs the 9,10- vs. 1,4-selectivity in the reaction of the various dienophile and anthracene combinations. The two dienophiles maleic anhydride (**B**) and DMAD (**D**) were picked as they show a stark contrast in their position-selectivity in the reaction with the dienes **419a-e**. Whereas **D** followed a smooth trend from 9,10- to 1,4-selectivity with the variation of the electronics of the dienes, **B** apparently was insensitive to this and showed expected 9,10-selectivity only.

The analyses went beyond the simple comparison of calculated activation barriers ($\Delta G^{\neq}$) and driving forces ($\Delta_R G$) to achieve a fundamental understanding of the variation in product selectivities. On the same note, the concepts by Fukui (frontier molecular orbital analysis, FMO) and Bell-Evans-Polanyi (BEP) that are commonly used to predict relative reactivities, i.e. selectivities in Diels-Alder reactions, were re-evaluated in their applicability for the observed peculiar position-selectivities.

A judgment about the minimum energy pathway (MEP, concerted vs. stepwise) was based on the intrinsic reaction coordinate (IRC) calculations and analysis of the root mean square (RMS) gradient. In a subsequent step, Marcus theory was employed to differentiate the kinetic (intrinsic barrier) and thermodynamic contributions to the overall activation barrier ($\Delta G^{\neq}$). To understand why the intrinsic barriers of the (first) σ-bond formation govern the product ratios, the electronics of the starting materials and transition state structures were analyzed by natural bond orbital (NBO) analysis. The calculations have been run with the Gaussian09.E01 suite of programs using the B3LYP-D3/6-31G** level of theory. For further details and citations see experimental part (E5).

The combination of dienophile DMAD (**D**) with five different anthracenes (**419a-e**, R = H, OMe, NMe_2, bis-pyrrolidine, mono-pyrrolidine) was used to establish the choice of the level of theory (LOT). The calculated activation barriers reproduced the experimentally observed trend of 9,10- to 1,4-cycloaddition selectivity as a function of the electron donor substituent (EDG) at the diene (Table 23). Therefore, this LOT was used for a more detailed analysis.

Table 23. Summary of calculated vs experimental selectivities of the reaction between anthracenes **419a-e** and DMAD (**D**).

anthracene	**$\Delta\Delta G^{\neq}_{9,10\text{-}1,4}$ [kcal/mol]**	**calculated selectivity 9,10 : 1,4**	**experimental selectivity 9,10 : 1,4**
419a (R = H)	–6.2	9,10 only	>99 : 1
419b (R = OMe)	–1.4	10 : 1	9 : 1
419c (R = NMe_2)	0	1 : 1	1 : 2.5
419d (R = bis-($N(CH_2)_4$)	1.5	1 : 13	1 : >99
419e (R = mono-($N(CH_2)_4$)	6	quant. 1,4	1 : >99

To determine the extent of concertedness, the transition state (TS) structures were analyzed with respect to the extent of bond reorganization (Figure 26) and most importantly the minimum energy pathway (MEP) of the respective transformations were scanned by IRC calculations and the RMS gradient was analyzed (for details see IRC plots in experimental part E5.6 and E5.7).

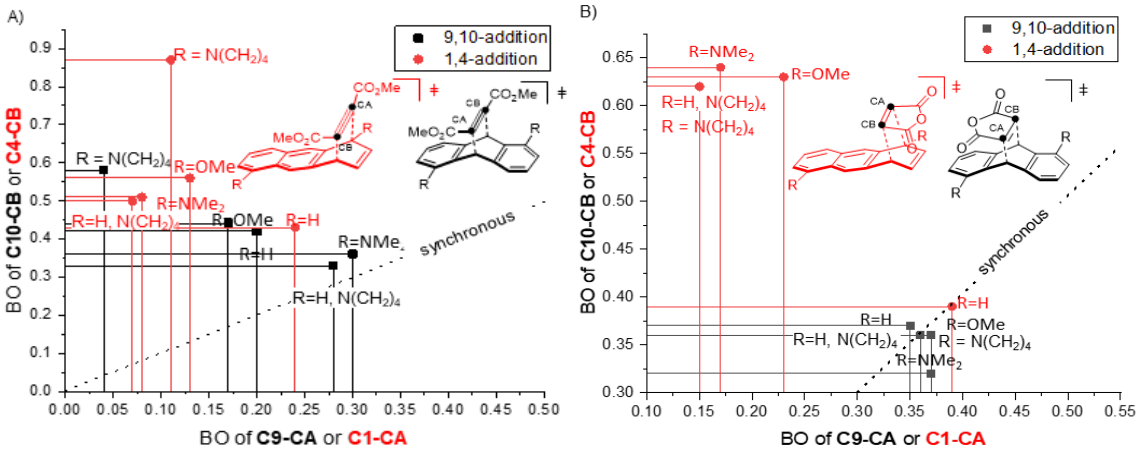

Figure 26. Bond orders (BOs) according to Pauling characterizing the mechanisms in the computationally analyzed Diels-Alder reactions.

Interestingly, in the cycloaddition of **D** even with the parent anthracene (**419a**) the TS structures of the 9,10-additions, as well as the 1,4-addition, are asynchronous, with the 1,4-addition slightly more so (Figure 26A). This is contrary to the TS structures with maleic anhydride (**B**, Figure 26B) that remained insensitive to changes in the electronics for the 9,10-additions and only showed asynchronicity for the 1,4-additions process. Adding electron donor groups (EDGs) in 1-and/or 5-position of the anthracenes a trend towards higher asynchronicity is consistently observed for reactions with **D**. Based on the analysis of the RMS gradient along with the calculated IRC a stepwise mechanism was identified to be in operation for the 1,4-additions of **D** with **419d** and **B** with **419b-d**. And for the 9,10-addition in case of **D** with **419d** (for details see IRC plots in experimental part E5.6 and E5.7). With the help of this energy and force related differentiation of concerted vs. two-step mechanism in the reactions of **D** also a geometric parameter of the transition state structures was defined as an indicator for a change in mechanism: A difference in bond orders (ΔBO^{237}) of the two-forming σ-bonds of $\Delta BO \geq 0.63$ is characteristic for the stepwise pathway.

Based on the MEP-analysis the comparison of the Gibbs free activation barriers of the 9,10- vs. 1,4-addition were conducted with respect to either the concerted pathways or the first σ-bond formation step that is occurring. In case of the addition reaction with **D,** the 1,4-addition is consistently facilitated by increasingly electron-donating substituents, whereas the 9,10-addition barrier is significantly less sensitive to changes in the diene electronic (Table 24) and in addition, shows no consistent correlation.

Table 24. Thermodynamic data for the reaction of anthracenes **419a-e** with DMAD **D**.

anthracene	9,10-addition				1,4-addition			
	$\Delta G^{\neq}$[a]	$\Delta H^{\neq}$[a]	$\Delta_R G$[a]	$\Delta_R H$[a]	$\Delta G^{\neq}$[a]	$\Delta H^{\neq}$[a]	$\Delta_R G$[a]	$\Delta_R H$[a]
419a	25.7	13.5	–24.6	–39.6	31.9	19.5	–12.4	–27.2
419b	26.7	13.6	–22.7	–38.0	28.1	14.3	–6.9	–22.7
419c	25.0	11.9	–25.6	–41.4	25.0	10.2	–5.1	–21.7
419d	24.4	8.2	–26.8	–42.9	21.6	5.4	–5.0	–21.0
419e[b]	29.1	14.8	–24.8	–40.9	23.1	7.0	–19.7	–2.3

[a] values in [kcal/mol], [b] values in [kcal/mol] for 5,8-addition: $\Delta G^{\neq} = 36.1$; $\Delta H^{\neq} = 22.0$; $\Delta_R G = -10.8$; $\Delta_R H = -42.3$; for details on thermodynamic data with maleic anhydride (**B**) see Table S2 + S3 in the experimental part (E5.1).

The relative thermodynamic contributions ($\Delta_R G$) to the activation barrier of the reaction with **D** based on the Marcus analysis[238] do not explain the observed product selectivities. On the contrary, the 1,4-addition product is thermodynamically significantly less stable than the 9,10-addition product and moreover, the driving force for the 1,4-product formation decreases with increasing strength of the electron donor (EDG, see Figure 27, Table 25).

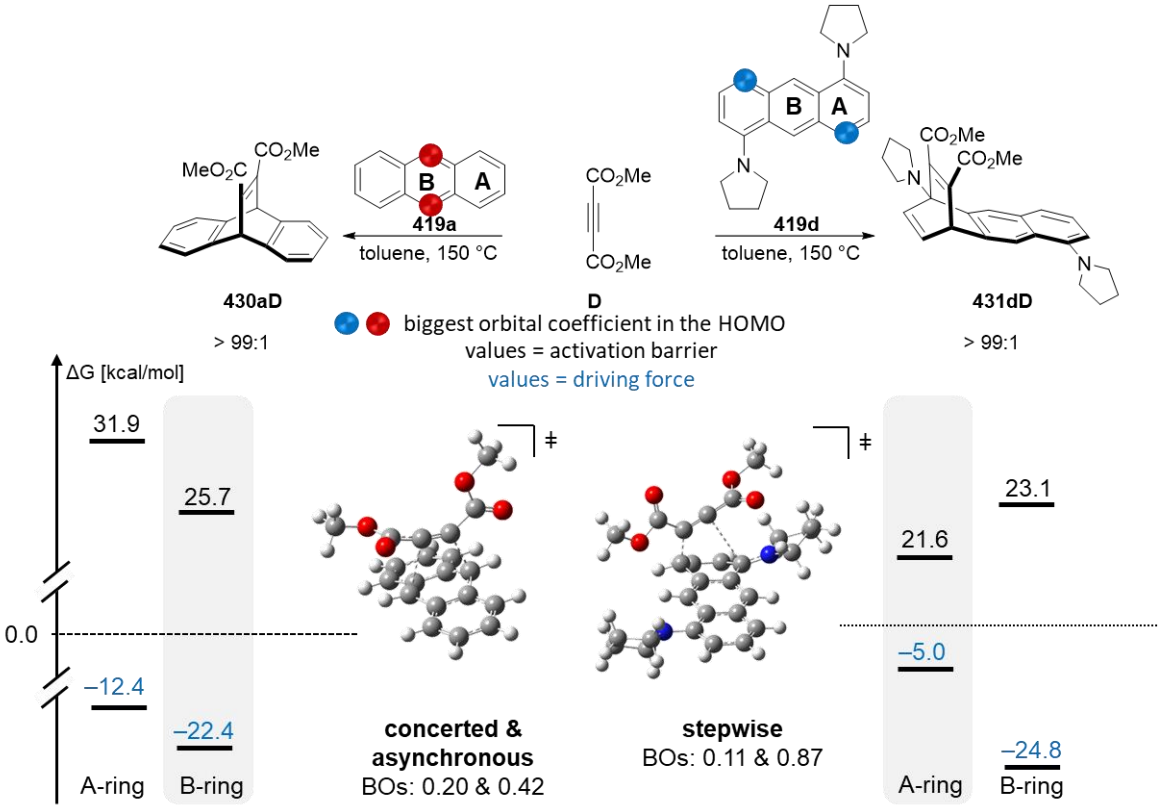

Figure 27. Summary of the experimental results and their computational rational based on FMO-analysis, activation barriers, mechanism (concerted vs. stepwise) and thermodynamics.

Clearly, there is no linear free energy relationship in operation. In addition, analysis of intrinsic activation barriers $\Delta G^{\neq\circ}$ according to Marcus confirmed this conclusion: the observed product selectivities are kinetic in nature (Table 25).

Table 25. Calculated intrinsic barriers for the reaction of anthracenes **419a-e** with DMAD (**D**).

$$\Delta G^{\neq}=\Delta G^{\neq\circ}+0.5\Delta_R G+\frac{\Delta_R G^2}{16\Delta G^{\neq\circ}}$$

$\Delta G^{\neq}$ representing the activation barrier, $\Delta G^{\neq\circ}$ representing the intrinsic barrier and $\Delta_R G$ representing the driving force.

anthracene	$\Delta G^{\neq}_{9,10}$[a]	$\Delta_R G_{9,10}$[a]	$\Delta G^{\neq\circ}_{9,10}$[a]	$\Delta G^{\neq}_{1,4}$[a]	$\Delta_R G_{1,4}$[a]	$\Delta G^{\neq\circ}_{1,4}$[a]
419a	25.7	–24.6	37.0	31.9	–12.4	37.9
419b	26.7	–22.7	37.2	28.1	–6.9	31.5
419c	25.0	–25.6	35.7	25.0	–5.1	27.5
419d	23.1	–26.8	36.6	21.6	–5.0	24.0
419e[b]	29.1	–24.8	40.6	23.1	–2.3	24.2

[a]values in [kcal/mol]; [b] values in [kcal/mol] for 5,8 position: $\Delta G^{\neq}_{5,8}$ = 36.1 ; $\Delta_R G_{5,8}$ = –10.8, $\Delta G^{\neq\circ}_{5,8}$ = 41.3; for details on calculations of intrinsic barriers for maleic anhydride (**B**) see Table S11 + S12 in the experimental part (E5.3).

Kinetic control of the product formation may be rationalized by a maximal orbital overlap in the rate-determining step. Therefore, the analysis was focused on the understanding of how the amino substituents change the electronic (FMO) and nuclear structure of the transition states (TSs) and the dienes in favor of the 1,4-addition process. This analysis is based on the frontier molecular orbitals (FMOs), and the natural bond orbital (NBO) analysis (partial charges).

Although the 1,4-addition pathway is shifting from a concerted to a stepwise bond reorganization in the series of **419a** to **419d** the FMO analysis of the anthracenes turned out to correctly predict the position selectivity in the reactions with **D**. The relative size of the orbital coefficients in the anthracenes provided a mean for a quick estimate where the first bonding interaction will take place (Figure 27). On the other hand, the HOMO-LUMO gap $\Delta\varepsilon$ of the reactants reflects the increased ease of the 1,4-addition in the series R = H to $N(CH_2)_4$ surprisingly well (Table 26). Whereas, there is no correlation between the activation barriers of the 9,10-addition and $\Delta\varepsilon$. This observation can be read in support of the results obtained by the Marcus-analysis, i.e. only the 1,4-addition is a kinetically preferred process in the reactions of **D**.

Table 26. FMO analysis for anthracenes **419a-e** and DMAD (**D**).

anthracene	normal electron demand			inverse electron demand		
	e_{HOMO} (419) (eV)	e_{LUMO}(D) (eV)	$\Delta_{HOMO-LUMO}$ (eV)	e_{HOMO} (D) (eV)	e_{LUMO} (419) (eV)	$\Delta_{HOMO-LUMO}$ (eV)
419a	−5.23		3.74		−1.65	6.24
419b	−4.82		3.33		−1.27	6.62
419c	−4.81	−1.49	3.32	−7.89	−1.40	6.49
419d	−4.37		2.88		−1.12	6.77
419e	−4.68		3.19		−1.38	6.51

For details on FMO analysis for maleic anhydride (**B**) see Table S14 in the experimental part (E5.4).

Since the bond reorganization is approaching the stepwise limit in the reaction of **D** and **419d-e** charge separation and its stabilization by the substituents is deemed to be the second important player in the kinetically controlled Diels-Alder reaction in anthracene derivatives **419b-e**. With an increasing asymmetry, one would expect a built-up of a partial positive charge at C1 and a partial negative charge at CA (see Figure 26 for nomenclature). Indeed, significant charge separation in the TS structures was confirmed by NBO analysis (Table 27).

Table 27. Partial charges at the reaction centers for the reaction with DMAD (**D**).

anthr.	1,4-addition				9,10-addition			
	CA	**CB**	**C1**	**C4**	**CA**	**CB**	**C9**	**C10**
419a	−0.023	−0.130	0.049	0.076	−0.132	−0.013	0.074	0.102
419b	−0.025	−0.153	0.410	0.005	−0.130	−0.022	0.083	0.119
419c	−0.060	−0.131	0.269	−0.012	−0.103	−0.052	0.077	0.091
419d	−0.058	−0.148	0.283	−0.022	−0.173	−0.047	0.019	0.125
419e[a]	−0.103	−0.138	0.282	−0.032	−0.123	−0.086	0.068	0.096

[a] Values for 5,8-addition: CA = −0.106, CB = −0.110, C5 = 0.074, C8 = 0.056; for details on NBO analysis for maleic anhydride (**B**) see Table S16 + S17 in the experimental part (E5.5).

The comparison of the aforementioned parameters also provided a clue for the apparent insensitivity of maleic anhydride (**B**) to the electronic changes in **419a-e**. The computed activation barriers and driving forces indicated that in the reaction of **B** with all five analyzed

dienes, the 1,4-addition is still kinetically favored, but the transformation is thermodynamically inhibited (endergonic, Figure 28), Hence, the 9,10-adduct is predicted to be the only product being formed in case of **B** independent of the electronic situation in the diene (Figure 28, for more details see computational details experimental part E5).

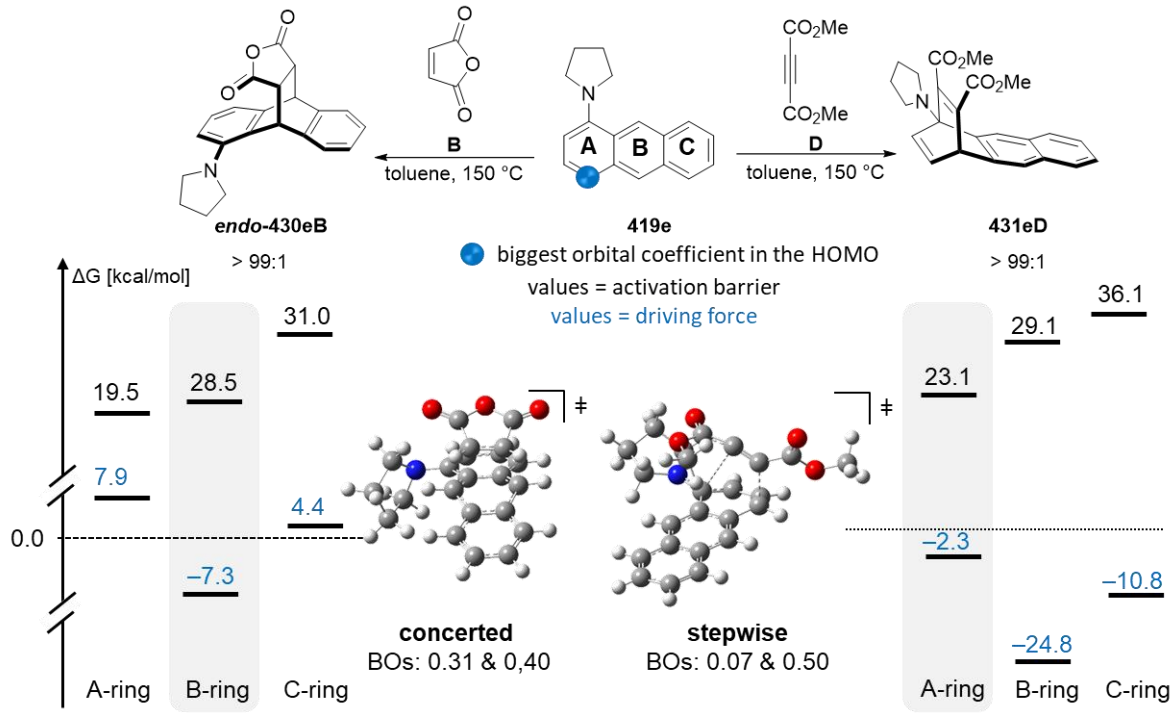

Figure 28. Summary of the experimental results and their computational rational based on FMO-analysis, activation barriers, mechanism (concerted vs. stepwise) and thermodynamics.

3.2 Atypical regioselectivity in electrophilic aromatic substitution reactions

The effect of the pronounced electronic perturbations exerted by the amine substitution in 1- and/or 5-position favoring their terminal ring functionalization in Diels-Alder reaction with electron-deficient alkynes was also investigated for the reactions with various electrophiles. Analogous to the cycloaddition reactions, electrophilic aromatic substitution of anthracenes generally takes place in the central B ring as a consequence of maximizing the aromatic stabilization energies in the transition state and by harboring the largest orbital coefficients of the HOMO at the 9,10-positions.[239] Therefore, mono-pyrrolidine substituted anthracene **419e** was examined in a bromination reaction (Table 28) that is also reported to be 9,10-selective for anthracene (**419a**) and derivatives.[240]

Table 28. Investigation of the bromination of anthracene **419e**.

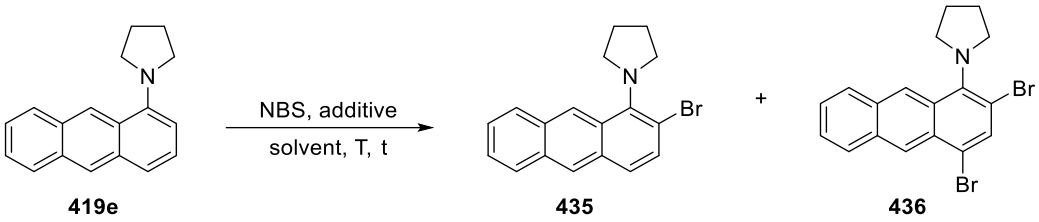

419e **435** **436**

entry[a]	equiv NBS	additive	solvent	T	t [h]	yield 435 [%]	yield 436 [%]
1	1.0	-	MeCN	rt	5	decomposition	
2	1.0	NH_4OAc (10 mol%)	MeCN	rt	1	14	4
3	1.0	-	DCM	0 °C	5	18	10
4	2.5	-	DCM	0 °C	5	decomposition	
5	2.0	NEt_3 (2.0 equiv)	DCM	0 °C	5	30	41
6	6.0	NEt_3 (6.0 equiv)	DCM	0 °C	5	-	58

[a] conditions: to anthracene **419e** (1.0 equiv) dissolved in solvent (0.08 M) was added NBS.

When **419e** was reacted with NBS in a polar solvent, usually promoting bromination reactions, only decomposition was observed (Table 28, entry 1). It was demonstrated that the addition of NH_4OAc had advantageous impacts in the bromination of phenol and aniline derivatives leading to excellent yields in short reaction times.[241] Similar reaction conditions furnished *ortho*-brominated anthracene **435** together with *ortho/para*-brominated product **436** albeit in low yield (14% and 4%, entry 2). The same products were obtained in slightly increased yields (18% and 10%) when **419e** was reacted with NBS in DCM at 0 °C (entry 3). Hence, in a further attempt, the synthesis of only *ortho/para*-product **436** should be achieved exclusively by adding more equivalents of NBS (entry 4). However, decomposition was also observed in this case. During NMR-analysis it was observed that brominated products **435** and **436** are sensitive to traces of acids and decomposition occurred in deuterated $CHCl_3$. Therefore, NEt_3 was added as an acid scavenger to the reaction mixture to prevent the decomposition of products by HBr and to facilitate deprotonation of the initially brominated intermediate. Indeed, yields of **435** and **436** could be significantly improved to 30% and 41% respectively (entry 5). Moreover, by further increasing the amount of NBS and NEt_3 only *ortho/para*-brominated anthracene **436**

could be synthesized in 58% yield (entry 6). Satisfyingly, in every reaction no 9- and/or 10-brominated product was observed indicating that the electronic perturbation also directs the selectivity of electrophilic aromatic substitutions towards the outer A-ring system.

In addition to the bromination, 4-methyl-1,2,4-triazoline-3,5-dione (MTAD, **437**) was employed in the reaction with **419e** (Table 29). MTAD (**437**) has been reported to react with anthracene (**419a**) in the dark to produce the corresponding 9,10-cycloadduct within three minutes quantitatively, while under acid catalysis also the formation of a Friedel-Crafts type product in 9-position was observed.[242]

Table 29. Reaction of anthracene **419e** with MTAD (**437**).

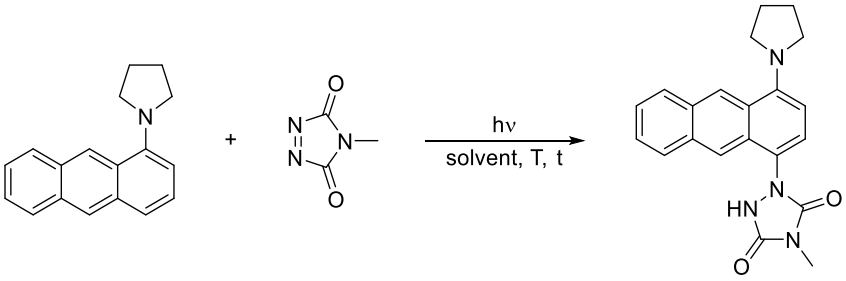

419e **437** **438**

entry[a]	equiv 437	hν	solvent	T	t [h]	yield [%]
1	1.0	dark	$CHCl_3$	rt	24	---
2	1.1	dark	HFIP	rt	2	polymerization
3	0.5	530 nm	acetone	−78 °C	5	42%
4	1.0	530 nm	acetone	−78 °C	5	34%
5	3.0	530 nm	acetone	−78 °C	5	decomposition
6[a]	0.5	530 nm	acetone	−78 °C	5	60

[a] conditions: anthracene **419e** (1.0 mmol, 1.0 equiv) was dissolved in solvent (0.2 M) and MTAD (**437**) was added; [b] NEt_3 (4.0 equiv) was added to the reaction mixture.

Under the same reaction conditions, no conversion of **419e** was observed even after 24 h (Table 29, entry 1). In 2017, Crousse *et al.* found that hexafluoro-2-propanol (HFIP) effectively promotes the *para*-selective C-H amination of various anilines with azodicarboxylate derivatives such as MTAD (**437**).[243] However, the reaction of **419e** and MTAD (**437**) in HFIP led to the formation of a polymeric product that was not dissolvable in any solvent (entry 2). Hence, the ability of MTAD (**437**) to undergo a [4+2]-cycloaddition with benzene and naphthalene by irradiation with visible light[244] was exploited. In contrast to the benzene and

naphthalene derivatives, the activation of MTAD by irradiation with a green LED (λ = 530 nm) and subsequent reaction with **419e** furnished a *para*-Friedel-Crafts type product **438** in 42% yield wherein again the terminal ring was functionalized exclusively (Table 29, entry 3). In order to improve the yield of **438** further reactions with increased amounts of MTAD (**437**) were conducted but in course of this the yield decreased (entry 4) or only decomposition was observed (entry 5). As in the bromination reactions, the product **438** was very sensitive towards acids. By addition of NEt_3, the yield of **438** could be increased to 60% (Table 29, entry 6). Mechanistically, as observed in the Lewis acid-mediated reaction of anthracene **419e** and *N*-phenylmaleimide (**C**, Table 22, entry 4), again a kind of Michael-addition to the electrophile **437** leads to the formation of a zwitterionic intermediate that performs proton abstraction faster than the respective ring-closing furnishing a Friedel-Crafts type product **438**. In conclusion, it was demonstrated that the selectivity of electrophilic aromatic substitution reactions switched from the inner ring system to the outer A-ring by installing electron donating-substituents in 1-position enabling further interesting transformations in future work.

3.3 Investigation of the photodimerization of pyrrolidine substituted anthracenes

The photodimerization of anthracenes is one of the oldest known photochemical reactions and can be considered as a (4π + 4π)-photocycloaddition (Scheme 108). Generally, the dimerization of anthracene (**419a**) occurs across the 9,10-positions and the resulting photodimer **439** reverts to the monomers by photochemical (wavelengths <300 nm) or thermal dissociation. By irradiation, an anthracene molecule is excited to its singlet excited state ^{1}**419a*** and combines with a nonexcited molecule to form an excimer [**419a** · **419a**]*. Excimer decay via cycloaddition affords the photodimer **439**.[245] Cross-dimerization of two different anthracene derivatives is only efficient, in case if one anthracene molecule can be excited separately at a distinguished wavelength, however, itself has to be inert towards homodimerization due to steric constraints for instance.[246]

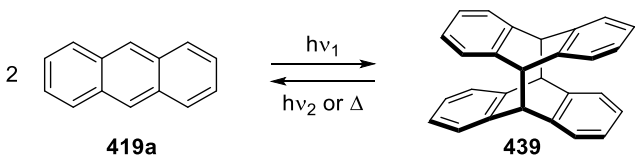

Scheme 108. Photodimerization of anthracene (**419a**).

Although anthracenes are prone to dimerize across the 9,10-position, again guided by relative aromatic stabilization energies and orbital coefficients of the HOMO, a few dissymmetrical exceptions have been reported in the literature. Photocycloaddition occurring through

9,10/1,4-positions have been observed for 2,6-bis(didecyloxy)anthracene[247], 1-acetylanthracene and methyl anthracene-1-carboxylate[248], but always as mixtures with the respective 9,10/9,10-dimers.

As the computational studies revealed pyrrolidine anthracenes **419d** and **419e** harbor the largest orbital coefficients in the HOMO at the 4-positions and therefore, it was envisioned that these anthracene derivatives might undergo selective ($4\pi + 4\pi$)-photocycloaddition across the unusual 9,10/1,4-positions (product **440**, Table 30) or even 1,4/1,4-positions (product **441**, Table 30). Initially, the UV/Vis spectra of anthracene (**419a**) and pyrrolidine substituted derivatives **419d-e** were measured to determine the appropriate wavelengths for their irradiation (Figure 29). Compared to anthracene (**419a**, blue) the absorption maxima of the pyrrolidine derivatives (**419d**, red and **419e**, green) are significantly bathocromically shifted, ranging widely into the visible region of light.

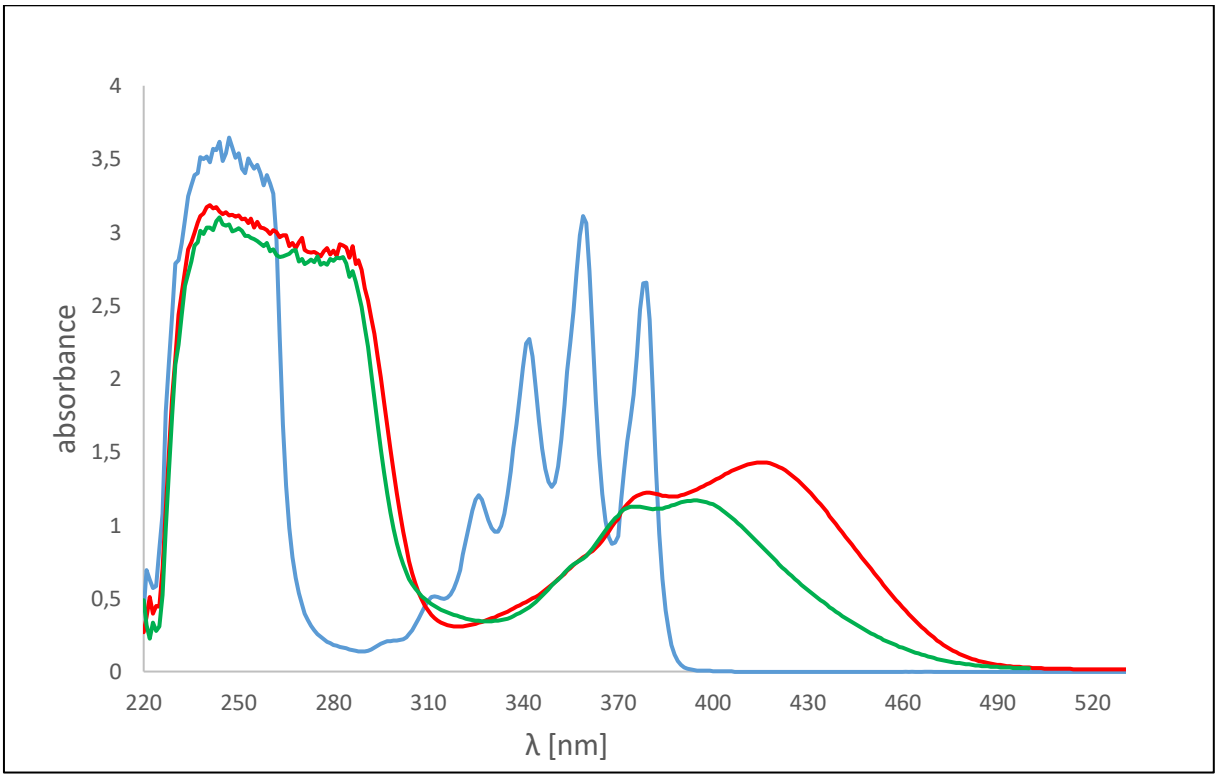

Figure 29. UV/Vis spectra of anthracene (**419a**, blue), 1,5-diyprrolidine anthracene (**419d**, red) and 1-pyrrolidine anthracene (**419e**, green).

In the following, the pyrrolidine substituted derivatives were investigated in a series of photodimerization reactions using LEDs for irradiation at 403 nm or 455 nm wavelength, respectively (Table 30).

Table 30. Investigation of the photodimerization of anthracene **419d** and **419e**.

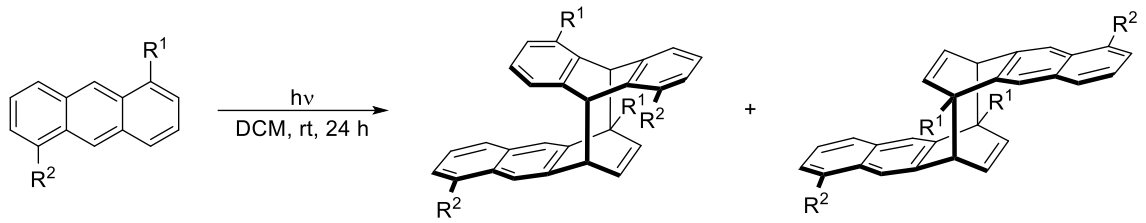

419d $R^1 = R^2 = N(CH_2)_4$

419e $R^1 = N(CH_2)_4$, $R^2 = H$

440 **441**

entry[a]	anthracene	additional reactant	hν [nm]	yield [%]
1	**419d**	-	403	---
2	**419d**	-	455	---
3	**419d**	anthracene (**419a**)	403	---
4	**419d**	anthracene (**419a**)	455	---
5	**419e**	-	403	---
6	**419e**	anthracene (**419a**)	403	---

[a] conditions: anthracene (**419d-e**, 1.0 equiv) and additional reactant (**419a**, 2.0 equiv) in degassed DCM (0.0125 M) were stirred under irradiation with a LED for 24 h at room temperature.

The pyrrolidine anthracenes **419d-e** showed no homodimerization by irradiation at the respective wavelengths (Table 30, entry 1,2 and 5) and the starting materials were completely recovered. Since no homodimerization was observed, the anthracene derivatives were also examined in a cross-dimerization reaction with anthracene (**419a**). However, again no conversion of the pyrrolidine anthracenes **419d** (entry 4-5) and **419e** (entry 6) was observed. Obviously, the (4π + 4π)-photocycloadditions of pyrrolidine substituted anthracenes **419d-e** are prevented by steric repulsion. Therefore, no further attempts for photodimerizations of **419d** and **419e** were performed.

To conclude a longstanding problem in controlling and accessing atypical regioselectivity in the Diels-Alder reaction of anthracenes has been addressed by a simple yet highly effective electronic manipulation of the terminal rings by installing substituents of varying electron-donating abilities at the 1- or 1,5-positions. This synthetic approach obviates any premeditated engagement of the 9,10-positions with either any sterically bulky or electron-withdrawing substituents. Consequently, a functionally diverse range of 1,4-cycloadducts could be obtained in up to excellent yields and regioselectivity. In addition, atypical regioselectivity was also

observed in aromatic substitution reactions with various electrophiles. The computational studies revealed the origin of the atypical regioselectivity to be of kinetic nature, being reflected by the largest orbital coefficient in the HOMO at the 4-position imposed by the electron-donating ability of the substituents in the terminal rings and the highly asynchronous transition states leading to the products.

C Summary

The first chapter of the present thesis deals with the synthesis of 2-pyrones starting from renewable resources (Scheme 109). The synthetic sequences started from furfuryl alcohol (**18**) and its corresponding derivatives **314**, which were readily available from inexpensive furfural (**310**) – a platform chemical that is derived from agricultural waste products. Initially, the big-scale synthesis of unsubstituted 2-pyrone (**1**) was described. Key step was the development of a FVT setup that allowed to perform the thermal rearrangement of epoxide **313** on a multigram scale. Herein, 20 g (123 mmol) of epoxide **313** were converted to the desired pyrone **1**. Similarly, a reaction sequence starting from furfuryl alcohol derivatives **314** furnished naturally occurring 6-substituted alkyl-pyrones **2**.

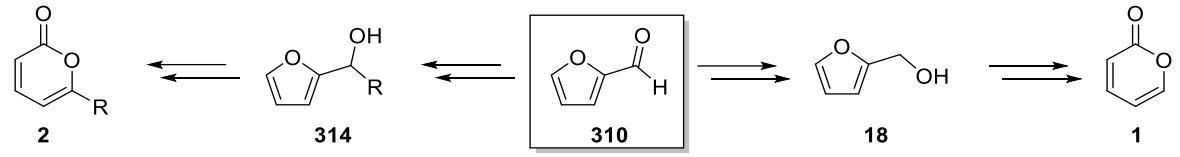

2 **314** **310** **18** **1**

Scheme 109. Overview of the sustainable synthesis of 2-pyrones.

The second chapter focused on further applications and functionalizations of the biobased 2-pyrone derivatives. Utilizing 6-hydroxyalkyl-2-pyrones **26** that have also been obtained from furfuryl alcohol (**18**) in a previous work of Reiser *et al.*[16], several 3,7-substituted phthalide derivatives **342** were synthesized by an intermolecular Diels-Alder reaction with diethyl acetylenedicarboxylate (**341**) (Scheme 110). Likewise, intramolecular [4+2]-cycloaddition yielded 3-substituted phthalides **326**, including the anti-ischemic stroke drug *n*-butyl phthalide **326b** (Scheme 110). Moreover, starting from enantioenriched pyrones **26** the stereoselective synthesis of respective phthalides **326** and **342** was accomplished.

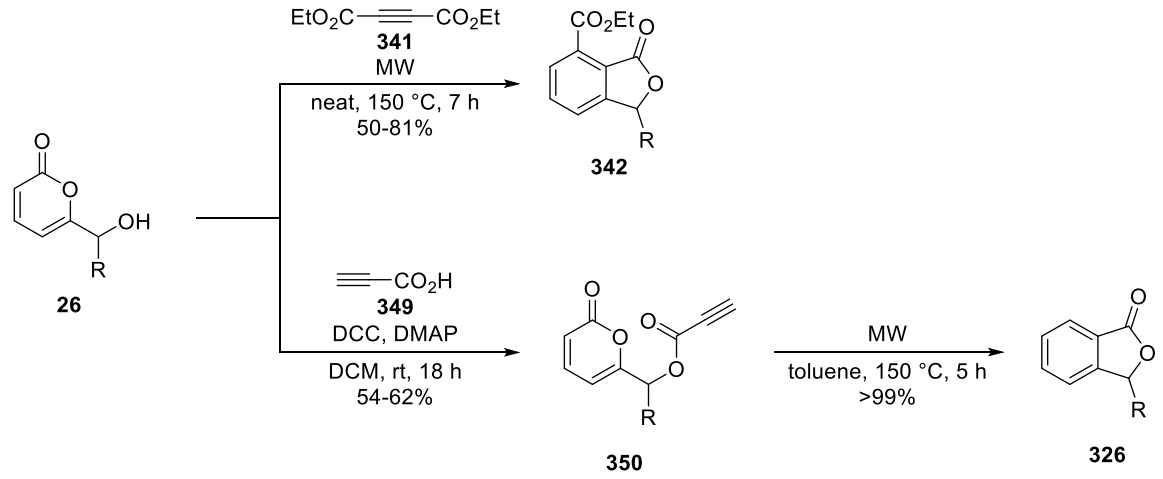

Scheme 110. Synthesis of 3-substituted phthalides **342** and **326** by Diels-Alder reaction.

In addition, the UV-mediated [4+2]-cycloaddition of 2-pyrone (**1**), an extremely rare example of a photocatalyzed [4+2]-cycloaddition in organic chemistry, was replaced by sustainable conditions using visible light-emitting diodes (Scheme 111). By employing the $[Ir(dtb\text{-}bpy)(dF(CF_3)ppy)_2]PF_6$ energy transfer catalyst, two structural and stereochemical rich regioisomers **367a-b** were obtained diastereoselectively in short reaction time and overall excellent yield.

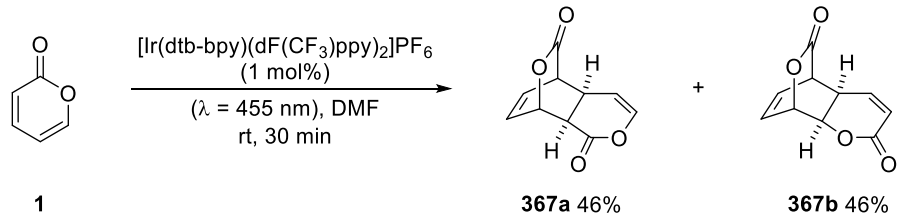

Scheme 111. Visible light mediated [4+2]-cycloaddition of 2-pyrone (**1**).

Lastly, a transition metal-catalyzed cyclopropanation with donor-acceptor diazoacetate **376** furnished cyclopropanated pyrone **377a** and pyridinone **377b** in regioselective and diastereoselective fashion. Furthermore, the functionalization of these substrates was achieved with high levels of enantioselectivity by applying a chiral rhodium-catalyst – usually representing a major challenge in pyrone chemistry (Scheme 112). The scope of further pyrone and pyridinone derivatives as well as diazoacetates is currently investigated as a part of the Ph.D. thesis of Jiantao Fu, a member of the research group of Professor Huw Davies in Atlanta. The high functional group density displayed in these products offers the opportunity for further stereoselective follow-up transformations to build-up molecular complexity in future work as it was demonstrated in the synthesis of hydroxymethyl cyclopentenol derivatives **411** (Scheme 112).

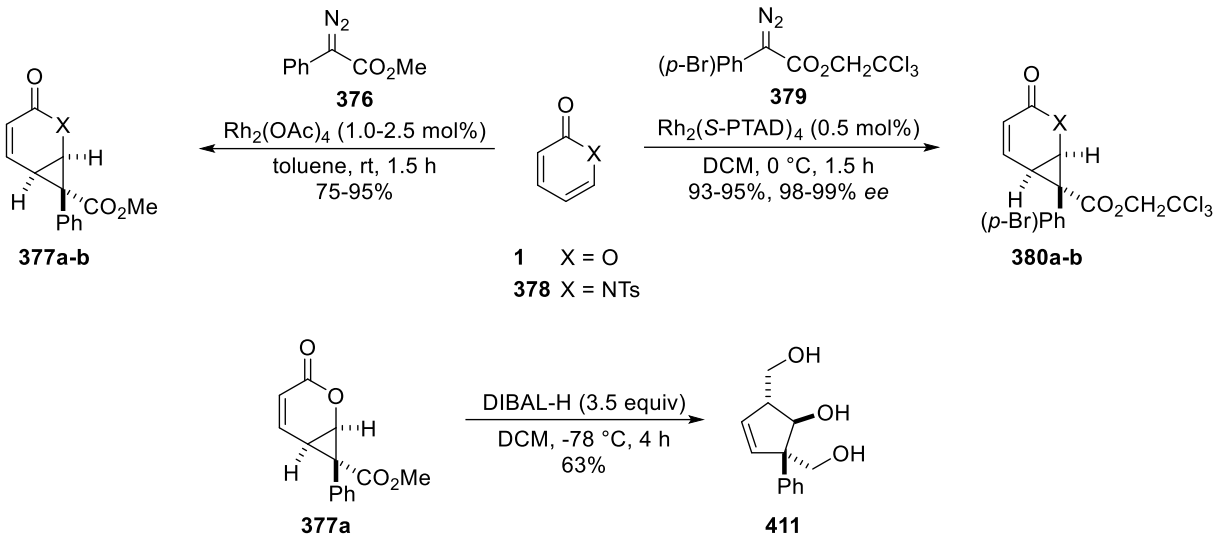

Scheme 112. Cyclopropanation of pyrone **1** and pyridinone **378** and elaboration towards enol **411**.

The last chapter was devoted to the atypical reactivity of anthracene derivatives **419b-e**. The natural 9,10-preference of anthracenes in [4+2]-cycloaddition was successfully circumvented by simple yet effective installation of electron-donating substituents at the 1- or 1,5-positions. Consequently, a functionally diverse range of 1,4-cycloadducts **431** was obtained in up to excellent yields and regioselectivity without any premeditated blocking of the 9,10-positions (Scheme 113). However, employment of alkene dienophiles **A-C** yielded ordinary 9,10-cycloadducts **430** exclusively (Scheme 113). In cooperation with the working group of Prof. J. Rehbein (University of Regensburg), extensive computational studies were conducted investigating the influence of substituents and dienophiles on the regioselectivity of the [4+2]-cycloaddition. These studies revealed the origin of the atypical selectivity to be of kinetic nature, being reflected by the largest orbital coefficient in the HOMO at the 4-position (blue sphere, Scheme 113) imposed by the electron-donating ability of the substituents in the terminal rings. Moreover, highly asynchronous transition states are leading to the products **431**. In contrast, computed activation barriers and driving forces of the reaction with alkene dienophile **B** indicated that 1,4-addition is still kinetically favored, but the transformation is thermodynamically inhibited yielding only 9,10-products **430**.

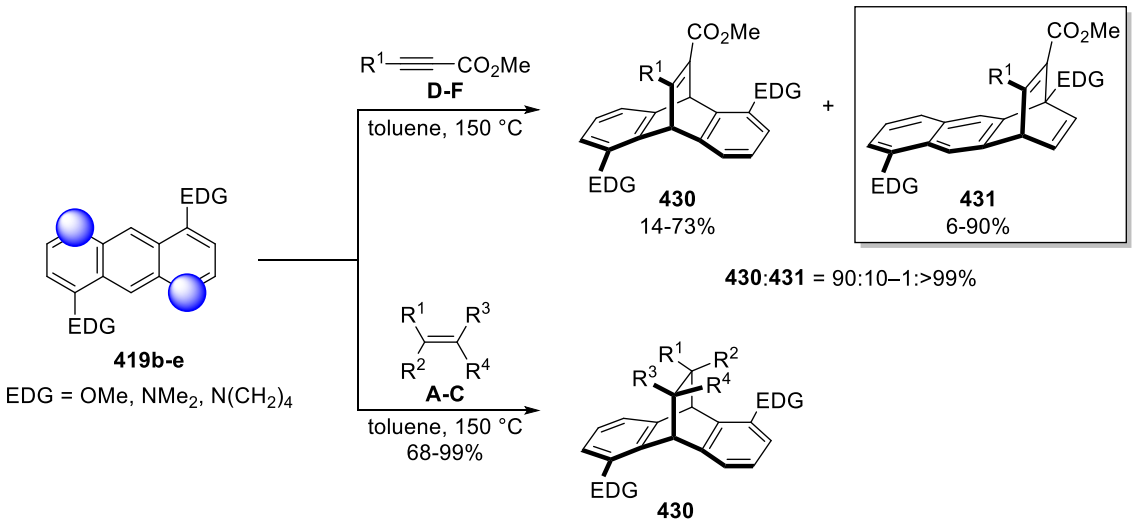

Scheme 113. Overview of the [4+2]-cycloaddition of anthracenes **419b-e** with alkynes **D-F** and alkenes **A-C**.

Additionally, electronic manipulation of a terminal ring by installation of a pyrrolidine group in 1-position allowed to override the inherent 9,10-preference in aromatic substitution reactions with various electrophiles, leading to the exclusive functionalization of the outer ring in all cases (Scheme 114).

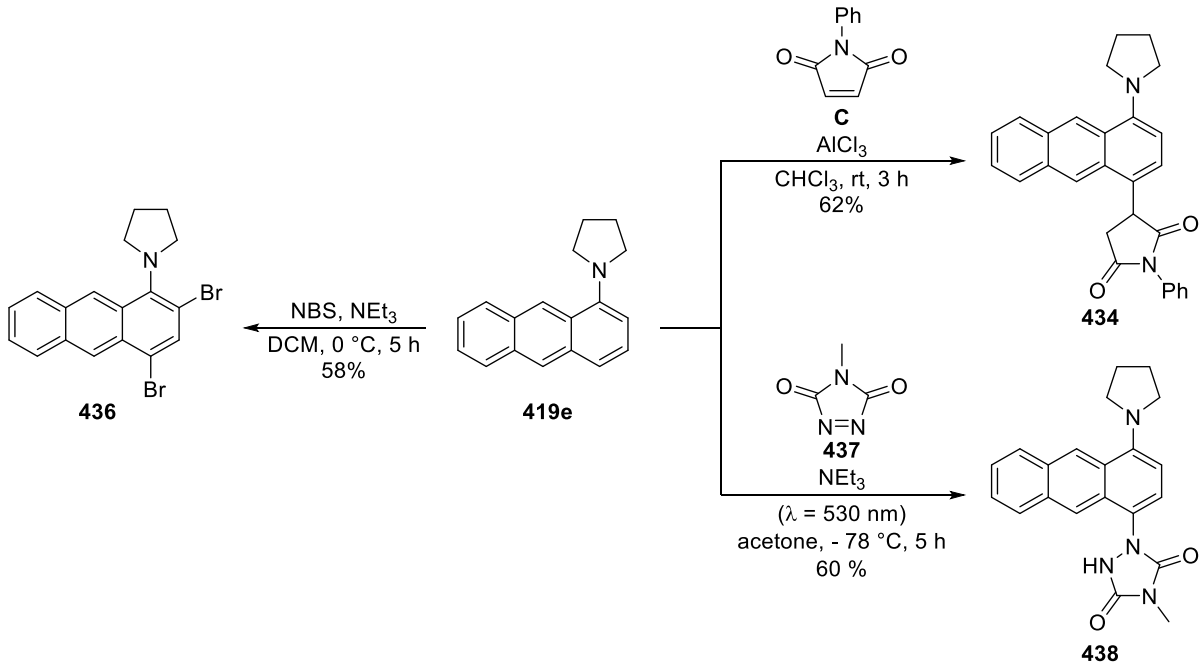

Scheme 114. Overview of the electrophilic aromatic substitution of anthracene **419e**.

D Zusammenfassung

Das erste Kapitel der vorliegenden Arbeit beschäftigt sich mit der Synthese von 2-Pyronen ausgehend von erneuerbaren Rohstoffen (Abbildung 1). Die Synthesesequenzen gingen von Furfurylalkohol (**18**) und dessen Derivaten **314** aus, welche leicht aus kostengünstigem Furfural (**310**) erhältlich sind – einer Plattformchemikalie, die aus landwirtschaftlichen Abfallprodukten gewonnen wird. Zunächst wurde die Synthese von unsubstituiertem 2-Pyron (**1**) in großem Maßstab beschrieben. Der Schlüsselschritt war die Entwicklung eines FVT-Aufbaus, der es ermöglichte, die thermische Umlagerung von Epoxid **313** im Multigramm-Maßstab durchzuführen. Hierbei wurden 20 g (123 mmol) des Epoxids **313** in das gewünschte Pyron **1** umgesetzt. In ähnlicher Weise lieferte eine Reaktionssequenz ausgehend von Furfurylalkoholderivaten **314** natürlich vorkommende 6-substituierte Alkylpyrone **2**.

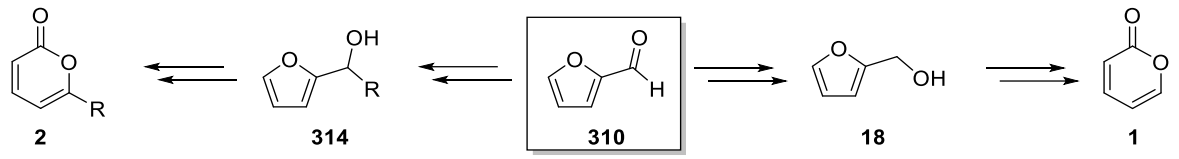

Abbildung 1. Übersicht der nachhaltigen Synthese von 2-Pyronen.

Das zweite Kapitel befasste sich mit den weiteren Anwendungen und Funktionalisierungen der biobasierten 2-Pyron-Derivate. Unter Verwendung von 6-Hydroxyalkyl-2-Pyronen **26**, welche in vorangegangener Arbeit von Reiser *et al.* ebenfalls aus Furfurylalkohol (**18**) erhalten wurden, wurden einige 3,7-substituierte Phthalidderivate **342** durch intermolekulare Diels-Alder-Reaktion mit Diethylacetylendicarboxylat (**341**) synthetisiert (Abbildung 2). Gleichermaßen ergab eine intramolekulare [4+2]-Cycloaddition 3-substituierte Phthalide **326**, einschließlich des antiischämischen Schlaganfallmedikaments *n*-Butylphthalid (**326b**) (Abbildung 2). Darüber hinaus wurde ausgehend von enantiomerenangereicherten Pyronen **26** die stereoselektive Synthese der jeweiligen Phthalide **326** und **342** erreicht.

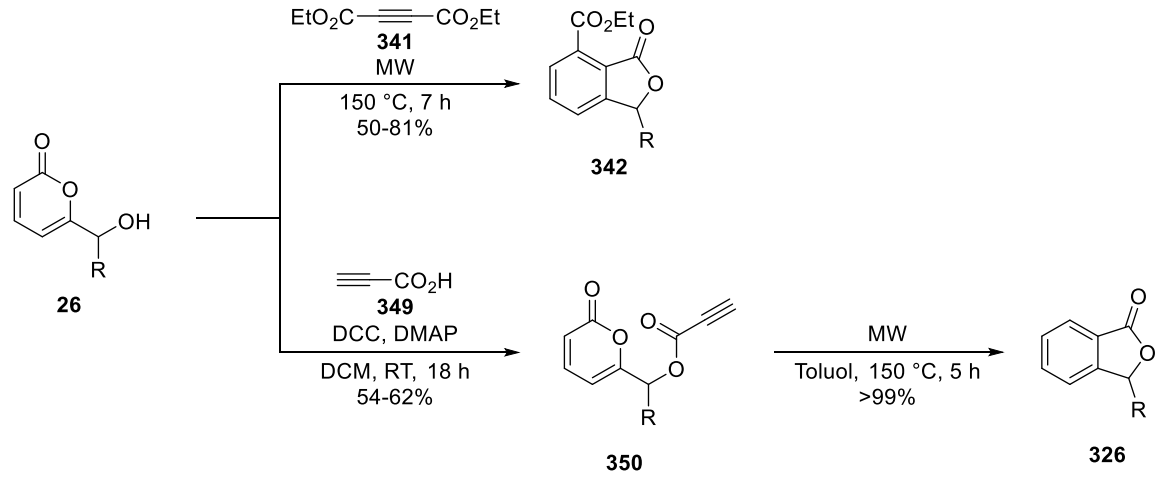

Abbildung 2. Synthese von 3-substituierten Phthaliden **342** und **326** durch Diels-Alder-Reaktion.

Des Weiteren konnte die mittels UV-Licht induzierte [4+2]-Cycloaddition von 2-Pyron (**1**), ein äußerst seltenes Beispiel für eine photokatalysierte [4+2]-Cycloaddition in der organischen Chemie, durch nachhaltige Bedingungen unter Verwendung von Dioden, die sichtbares Licht emittieren, ersetzt werden (Abbildung 3). Durch die Verwendung eines $[Ir(dtb\text{-}bpy)(dF(CF_3)ppy)_2]PF_6$ Energieübertragungskatalysators wurden zwei strukturell und stereochemisch reiche Regioisomere **367a-b** diastereoselektiv in kurzer Reaktionszeit und insgesamt ausgezeichneter Ausbeute erhalten.

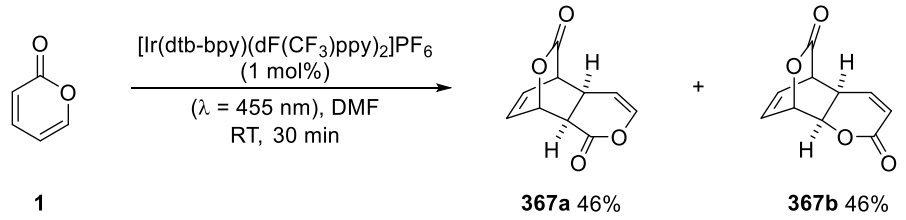

Abbildung 3. [4+2]-Cycloaddition von 2-Pyron (**1**) mittels sichtbarem Licht.

Zuletzt lieferte die übergangsmetallkatalysierte Cyclopropanierung mit Donor-Akzeptor-Diazoacetat **376** cyclopropaniertes Pyron **377a** und Pyridinon **377b** auf regioselektive und diastereoselektive Weise. Außerdem wurde durch die Anwendung eines chiralen Rhodiumkatalysators die Funktionalisierung dieser Substrate mit hoher Enantioselektivität erreicht – was gewöhnlich eine große Herausforderung in der Pyronchemie darstellt (Abbildung 4). Der Anwendungsbereich weiterer Pyron- und Pyridinonderivate sowie Diazoacetate wird derzeit im Rahmen der Doktorarbeit von Jiantao Fu, einem Mitglied der Forschungsgruppe von Professor Huw Davies in Atlanta, untersucht. Die hohe Dichte an funktionellen Gruppen in diesen Produkten bietet die Möglichkeit für weitere stereoselektive Folgetransformationen zum

Aufbau molekularer Komplexität in zukünftigen Arbeiten, wie es bei der Synthese von Hydroxymethylcyclopentenolderivat **411** gezeigt wurde (Abbildung 4).

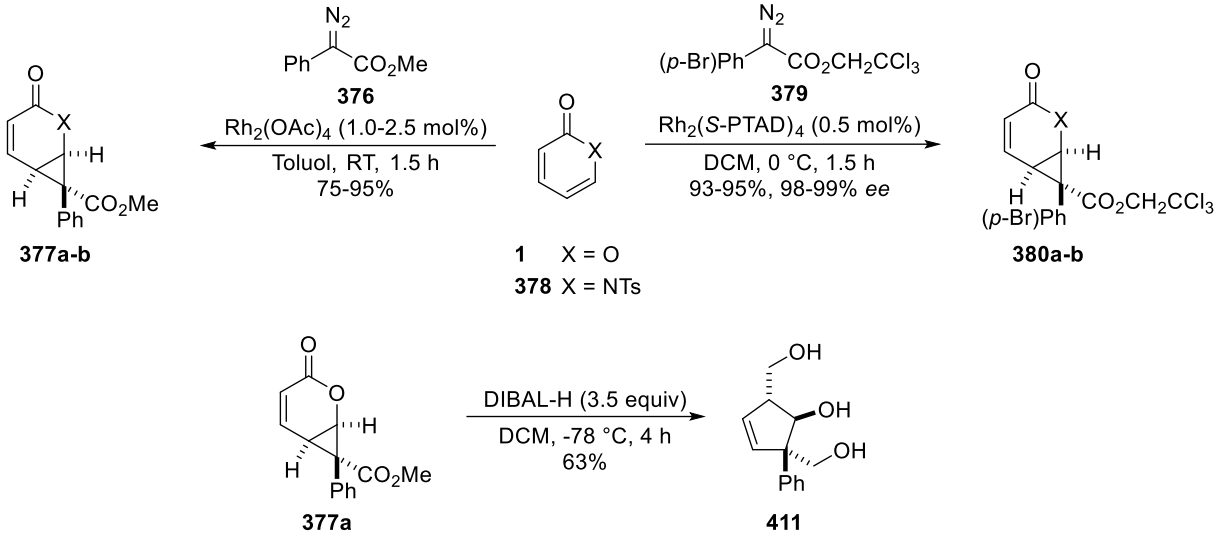

Abbildung 4. Enantioselektive Cyclopropanierung von Pyron **1** und Pyridinon **378** und Umwandlung zu Enol **411**.

Das letzte Kapitel widmete sich der atypischen Reaktivität von Anthracenderivaten **419b-e**. Die natürliche 9,10-Präferenz von Anthracenen in [4+2]-Cycloadditionen wurde erfolgreich durch einfache, aber effektive Installation elektronendonierender Substituenten an den 1- oder 1,5-Positionen umgangen. Infolgedessen wurde eine vielfältige Palette an 1,4-Cycloaddukten **431** erhalten, ohne dass die 9,10-Positionen vorsätzlich blockiert wurden (Abbildung 5). Die Verwendung von Alkendienophilen **A-C** ergab jedoch ausschließlich gewöhnliche 9,10-Cycloaddukte **430** (Abbildung 5). In Zusammenarbeit mit der Arbeitsgruppe von Prof. J. Rehbein (Universität Regensburg) wurden umfangreiche Computerstudien durchgeführt, in denen der Einfluss der Substituenten und Dienophilen auf die Regioselektivität der [4+2]-Cycloaddition untersucht wurde. Diese Studien ergaben, dass der Ursprung der atypischen Selektivität kinetischer Natur ist, was sich in dem größten Orbitalkoeffizienten im HOMO an der 4-Position (blaue Kugel, Abbildung 5) widerspiegelt und durch die Elektronendonorfähigkeit der Substituenten im terminalen Ring bedingt ist. Zudem führen stark asynchrone Übergangszustände zu den Produkten **431**. Im Gegensatz wiesen berechnete Aktivierungsbarrieren und Triebkräfte der Reaktion mit Alkendienophil **B** darauf hin, dass die 1,4-Addition immer noch kinetisch bevorzugt ist, die Umwandlung jedoch thermodynamisch gehemmt ist und nur 9,10-Produkte **430** ergibt.

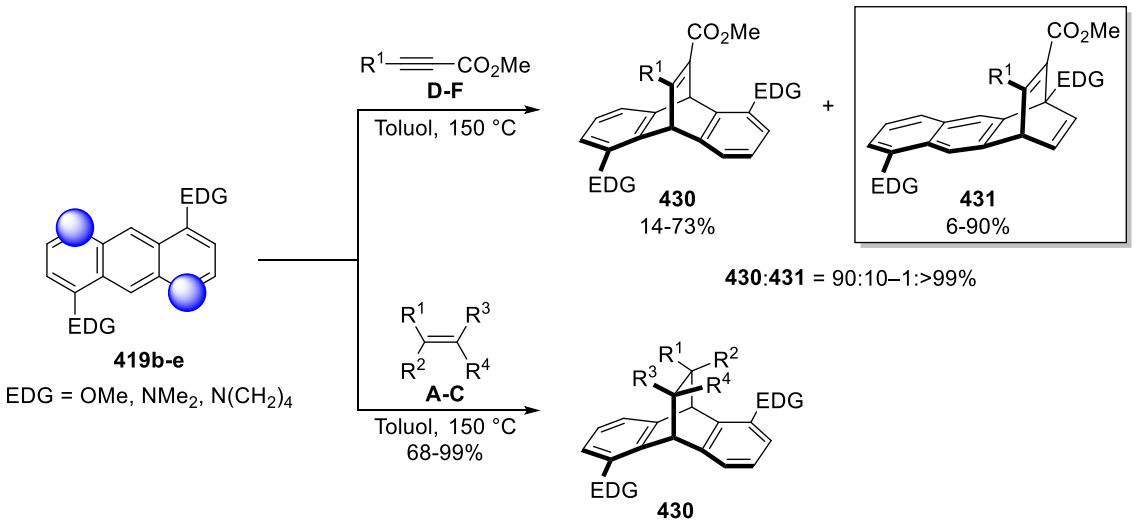

Abbildung 5. Überblick über die [4+2]-Cycloadditionen der Anthracene **419b-e** mit Alkinen **D-F** und Alkenen **A-C**.

Zusätzlich ermöglichte die elektronische Manipulation eines terminalen Rings durch Installation einer Pyrrolidingruppe in 1-Position sich über die inhärente 9,10-Präferenz bei aromatischen Substitutionen mit verschiedenen Elektrophilen hinwegzusetzen und in jedem Fall eine ausschließliche Funktionalisierung des äußeren Rings zu erreichen (Abbildung 6).

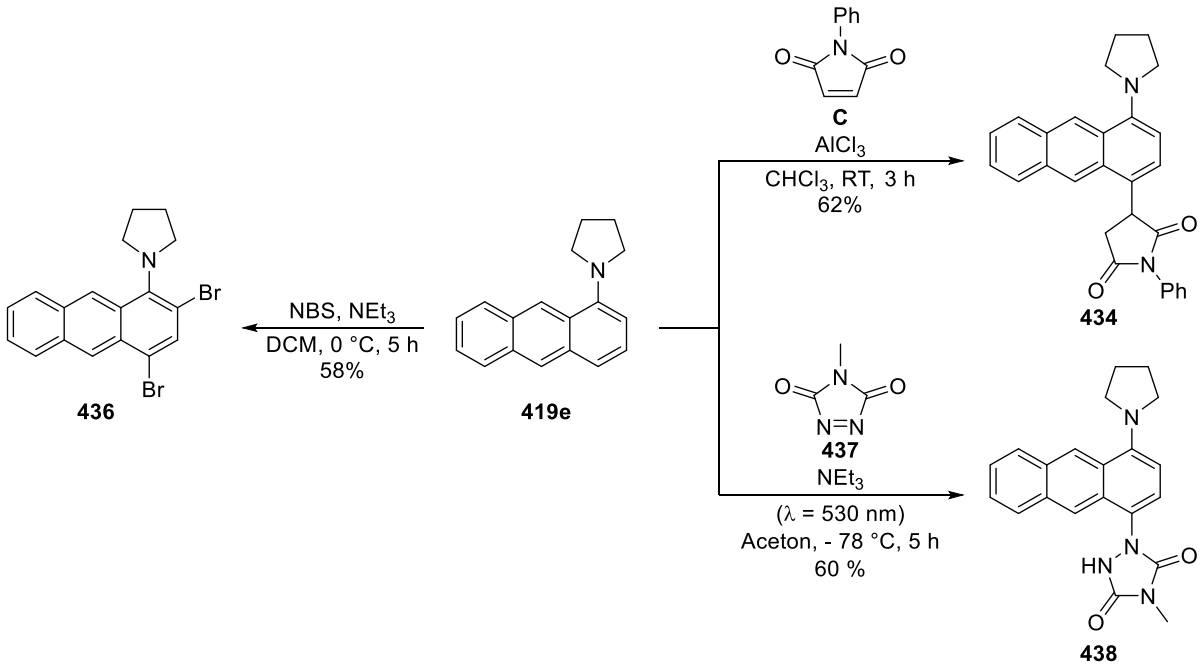

Abbildung 6. Überblick über die elektrophile aromatische Substitution von Anthracen **419e**.

E Experimental Part

1 General information

Synthesis

All chemicals were used as received or purified according to Purification of Laboratory Chemicals[249] if necessary. Glassware was dried in an oven at 110 °C or flame-dried prior to use. Solvents were applied in puriss p. a. grade and absolute solvents were prepared by established laboratory procedures. Larger quantities of dried solvents were purchased from a MB-SPS solvent purification system. Ethyl acetate, hexanes (40/60) and DCM for chromatography were distilled prior to use. Reactions with moisture and oxygen sensitive reagents were carried out in flame-dried glassware under an atmosphere of pre-dried nitrogen.

^{1}H- and ^{13}C-NMR

^{1}H-NMR spectra were recorded on a BRUKER Avance 400 (400 MHz) and a BRUKER Avance 300 (300 MHz) spectrometer at ambient temperature. ^{13}C-NMR spectra were recorded on a BRUKER Avance 300 (75 MHz) and BRUKER Avance 400 (101 MHz). Chemical shifts are reported in δ [ppm] relative to the signal of the solvent as the internal standard. Characterization of signals: s = singlet, bs = broad singlet, d = doublet, t = triplet, q = quartet, sext = sextet, m = multiplet, dd = doublet of doublet, dt = doublet of triplet, dq = doublet of quartet, td = triplet of doublet, ddd = doublet of doublet of doublet. Integration is determined as the relative number of atoms, and the coupling constants (*J*) are given in Hertz [Hz]. In addition, DEPT 135 spectra (primary or tertiary carbon (positive signal), secondary carbon (negative signal), quaternary carbon (no signal)) were recorded.

Column Chromatography

Column Chromatography was performed using Merck Gerduran 60 silica gel (0.063-0.200 mm) or Merck flash silica gel (0.040-0.063 mm).

Gas chromatography

Gas chromatography was carried out on a Fisons GC 8000 Series with flame ionization detector (FID). As stationary phase DB-1 (100% dimethylpolysiloxane, 30 m, ID 0.25 mm, 0.25 µm Film) was used. GC instrument conditions: Inlet temperature = 250 °C; detector

temperature = 300 °C. GC method: starting temperature 80 °C, then temperature ramp (5 °C/min) for 24 min to 200 °C followed by an isothermal period at 200 °C for 5 min.

HPLC

HPLC was performed on a Varian 920-LC with a photodiode array (PDA) detector. Phenomenex Lux Cellulose-1 and 2, Chiracel OD-H and AS served as chiral stationary phase and mixtures of *n*-heptane and *i*-PrOH were used for elution.

IR spectroscopy

IR spectroscopy was carried out on a Cary 630 FTIR Spectrometer (Agilent Technology) with ZnSe windows and Diamond Single Reflection Accessory. Solid and liquid compounds were measured neatly, and the wavenumbers are reported in cm^{-1}.

Mass spectrometry

Mass spectrometry was performed on a Finnigan MAT95, Agilent Q-TOF 6540 UHD, Finnigan MAT SSQ 710 A, ThermoQuest Finnigan TSQ 7000 at the Central Analytical Department of the University of Regensburg.

Melting points

The melting points were measured automatically on a MPA 100 Optimelt (Automated Melting Point System, Digital Image Processing Technology). Values thus obtained were not corrected.

Microwave

Microwave reactions were carried out on an Anton-Paar Monowave 300 microwave using pressure stable sealed 10 mL or 25 mL vessels.

Optical rotations

The optical rotation was determined on an Anton Paar MCP 500 polarimeter at 589 nm wavelength (sodium-d-line) in a 1.0 dm measuring cell.

Thin layer chromatography

Thin layer chromatography was done using Merck silica gel 60 F254 coated with 0.2 mm silica. Visualization was accomplished by UV light (254 nm) and staining was performed with vanillin or potassium permanganate solutions followed by heating.

X-ray-crystallography

X-ray crystallography was done by the crystallography laboratory of the University of Regensburg.

Synthesis of literature known compounds

The following compounds were synthesized according to literature known procedures and spectroscopic data matched well with those reported:

4-hydroxycyclopent-2-en-1-one (**19**)[160], 4-oxocyclopent-2-en-1-yl acetate (**20**)[16], 6a-(1-hydroxyethyl)-1a,1b,2,5,5a,6a-hexahydro-6*H*-2,5-methanoindeno[1,2-*b*]oxiren-6-one (**25a**)[16], (*S*)-6-(1-hydroxyethyl)-2*H*-pyran-2-one (**(*S*)-26a**)[16], 6-(1-hydroxypentyl)-2*H*-pyran-2-one (**26b**)[16], (*R*)-6-(1-hydroxypentyl)-2*H*-pyran-2-one (**(*R*)-26b**)[16], 6-(hydroxy(phenyl)methyl)-2*H*-pyran-2-one (**26c**)[16], 6-acetyl-2*H*-pyran-2-one (**361**)[161], $[Ir(dtb\text{-}bpy)(dF(CF_3)ppy)_2]PF_6$[250], $Cu(dap)_2Cl$[251], 1-tosylpyridin-2(1*H*)-one (**350**)[200], methyl 2-diazo-2-phenylacetate (**376**)[252], 2,2,2-trichloroethyl 2-(4-bromophenyl)-2-diazoacetate (**379**)[253], Rh_2(*S*-TCPTTL)$_4$[254], Rh_2(*R*-*p*-BrTPCP)$_4$[255], Rh_2(*S*-PTAD)$_4$[256], 1,5-dimethoxyanthracene (**419b**)[231], anthracene-1,5-diamine (**429**)[232], anthracen-1-amine (**433**)[236], 4-methyl-3*H*-1,2,4-triazole-3,5(4*H*)-dione (**437**)[257].

2 Sustainable synthesis of 2-pyrones

3a,4,7,7a-Tetrahydro-1*H*-4,7-methanoinden-1-one (22)[163]

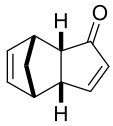

In an oven dried round-bottom flask acetate **20** (28.0 g, 200 mmol, 1.0 equiv) was dissolved in dry Et_2O (650 mL) and the flask was sealed with a drying tube. After stirring the solution for 30 min at 0 °C in an ice bath, $BF_3{\cdot}OEt_2$ (2.50 mL, 20.0 mmol, 10 mol%) and freshly distilled cyclopentadiene **21** (33.5 mL, 400 mmol, 2.0 equiv) were added. The resulting mixture was stirred at 0 °C for 18 h. The reaction mixture was quenched by slow addition of water (50 mL) and stirred for 30 min. After phase separation, 3 M NaOH solution (100 mL) was added to the organic phase and intensively stirred for 1 h. The phases were separated and the organic phase was concentrated to 250 mL under reduced pressure. The aqueous phase was extracted by using the previously distilled Et_2O (3×) and the combined organic phases were washed with brine (1×) and dried over Na_2SO_4. The solvent was removed under reduced pressure and the crude product was dried under a vacuum (20.0 mbar) for 30 min. Afterward, PE (35 mL) and ethyl acetate (0.5 mL) were added to the oily residue and the solution was carefully heated to 60 °C using a water bath. The solution was allowed to rest at room temperature until crystallization was observed and finally stored in the fridge for complete crystallization overnight. The resulting solid was filtered off, washed with cold PE (2×) and dried under vacuum to give **22** as a white solid (23.8 g, 163 mmol, 82%).

^{1}H NMR (400 MHz, $CDCl_3$) δ_H = 7.29 (dd, *J* = 5.7, 2.6 Hz, 1H), 5.86 – 5.78 (m, 2H), 5.67 (dd, *J* = 5.7, 3.0 Hz, 1H), 3.35 – 3.29 (m, 1H), 3.12 – 3.07 (m, 1H), 2.89 – 2.84 (m, 1H), 2.69 (t, *J* = 5.1 Hz, 1H), 1.64 (dt, *J* = 8.4, 1.9 Hz, 1H), 1.52 (dt, *J* = 8.4, 1.5 Hz, 1H); **^{13}C NMR** (101 MHz, $CDCl_3$) δ_C = 210.5 , 164.5, 136.7, 132.33, 132.31, 52.5, 50.0, 48.1, 44.8, 43.9.

1a,1b,2,5,5a,6a-Hexahydro-6*H*-2,5-methanoindeno[1,2-*b*]oxiren-6-one (313)[258]

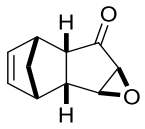

In a flask equipped with a reflux condenser enone **22** (24.7 g, 169 mmol, 1.0 equiv) was dissolved in DCM:MeOH (1:1, 500 mL) and the resulting solution was cooled by stirring in an ice/salt bath for 15 min. 2 M NaOH solution (101 mL, 203 mmol, 1.2 equiv) and H_2O_2 (34% in

water, 90.0 mL, 912 mmol, 5.4 equiv) were added and the mixture was stirred at 0 °C for 15 min before the ice/salt bath was removed and stirred for further 15 min at ambient temperature. The reaction mixture was poured into DCM (300 mL) and washed with brine (1×). The aqueous phase was extracted with DCM (3×). The combined organic phases were dried over $MgSO_4$ and the solvent was removed under reduced pressure to yield pure **313** as a white solid (23.1 g, 142 mmol, 84%).

^{1}H NMR (400 MHz, $CDCl_3$) δ_H = 6.05 (dd, *J* = 5.8, 2.6 Hz, 1H), 5.98 (dd, *J* = 5.8, 2.9 Hz, 1H), 3.55 (t, *J* = 1.9 Hz, 1H), 3.23 – 3.16 (m, 1H), 3.17 (d, *J* = 2.2 Hz, 1H), 3.11 – 3.02 (m, 2H), 2.76 – 2.68 (m, 1H), 1.58 (dt, *J* = 8.6, 1.7 Hz, 1H), 1.42 (dt, *J* = 8.7, 1.4 Hz, 1H); **^{13}C NMR** (101 MHz, $CDCl_3$) δ_C = 209.7, 135.4, 133.6, 60.5, 58.3, 51.7, 49.2, 45.7, 44.4, 43.6.

2*H*-Pyran-2-one (1)[259]

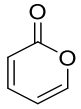

A high-quality glass tube (length 90 cm, diameter 1 cm) was fixed horizontally in a tube furnace. On one end the tube was connected to a cooling trap filled with ice/water and on the other end to a flask containing epoxide **313** (20.0 g, 123 mmol). The cooling trap was connected to a high-vacuum line at $2 \cdot 10^{-2}$ mbar and the tube furnace was heated to 650 °C. Epoxide **313** was slowly sublimed through the furnace by extern heating at 130 °C using a Kugelrohr distillation oven and the product was collected in the cooling trap. The product was washed off the cooling trap with MeOH, the solvent was removed under reduced pressure to yield the pure pyrone **1** as a brownish liquid (11.3 g, 118 mmol, 96%).

^{1}H NMR (400 MHz, $CDCl_3$) δ_H = 7.47 (ddd, *J* = 5.2, 2.2, 1.2 Hz, 1H), 7.30 (ddd, *J* = 9.5, 6.4, 2.2 Hz, 1H), 6.30 (dt, *J* = 9.5, 1.2 Hz, 1H), 6.20 (ddd, *J* = 6.3, 5.2, 1.1 Hz, 1H); **^{13}C NMR** (101 MHz, $CDCl_3$) δ_C = 161.7, 152.0, 142.9, 116.8, 106.0.

6-(1-Hydroxyethyl)-2*H*-pyran-2-one (26a)[16]

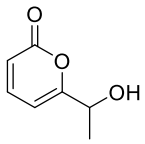

A high-quality glass tube (length 90 cm, diameter 1 cm) was fixed horizontally in a tube furnace. On one end the tube was connected to a cooling trap filled with ice/water and on the other end to a flask containing epoxide **25a** (3.10 g, 15.0 mmol). The cooling trap was

connected to a high-vacuum line at $2 \cdot 10^{-2}$ mbar and the tube furnace was heated to 650 °C. Epoxide **25a** was slowly distilled through the furnace by extern heating at 170 °C using a Kugelrohr distillation oven and the product was collected in the cooling trap. The product was washed off the cooling trap with DCM, the solvent was removed under reduced pressure to yield the pure pyrone **26a** as a brownish liquid (1.95 g, 13.9 mmol, 96%).

^{1}H NMR (300 MHz, $CDCl_3$) δ_H = 7.34 (dd, *J* = 9.4, 6.6 Hz, 1H), 6.29 (dt, *J* = 6.5, 0.8 Hz, 1H), 6.21 (dd, *J* = 9.3, 0.9 Hz, 1H), 4.60 (q, *J* = 6.6 Hz, 1H), 1.51 (d, *J* = 6.6 Hz, 3H); **^{13}C NMR** (75 MHz, $CDCl_3$) δ_C = 167.7, 162.3, 144.0, 114.3, 100.6, 66.8, 21.4.

General procedure A. Grignard reaction of 310 to 314

In a two necked Schlenk flask magnesium shavings (2.27 g, 93.6 mmol, 1.3 equiv) were suspended in dry Et_2O (37 mL) and a catalytic amount of iodine was added under nitrogen atmosphere. A solution of alkyl bromide (115 mmol, 1.6 equiv) in dry Et_2O (92 mL) was added dropwise via a dropping funnel. After complete addition, the reaction mixture was heated under reflux conditions for 1 h until complete consumption of magnesium was observed. The resulting solution was cooled to 0 °C in an ice bath and a solution of furfural **310** (72.0 mmol, 1.0 equiv) in dry Et_2O (58 mL) was added dropwise. The mixture was stirred for 15 min at 0 °C and finally quenched with water and saturated NH_4Cl solution. The aqueous phase was extracted with Et_2O (3×) and the combined organic phases were dried over $MgSO_4$. The solvent was removed under reduced pressure and the crude product was purified by flash column chromatography (PE:EA = 19:1 to 9:1).

General procedure B. Piancatelli rearrangement of 314 to 315

In a microwave vessel furfuryl alcohol **314** (5.0 mmol, 1.0 equiv.) was dissolved in acetone (5.0 mL) and water (15 mL). The mixture was stirred under microwave irradiation at 180 °C for 15 min. Depending on the employed alcohol **314**, this procedure was repeated multiple times in order to achieve the desired reaction scale (42.5−65.0 mmol). The reaction mixtures were combined and extracted with DCM (3×). The organic phase was dried over $MgSO_4$ and the solvent was removed under reduced pressure. The crude product was purified by flash column chromatography (PE:EA = 2:1).

General procedure C. Acetylation of 315 to 316

5-substituted 4-hydroxy-2-cyclopentenone **315** (1.0 equiv) was dissolved in DCM (0.17 M). NEt_3 (5.0 equiv) and Ac_2O (5.0 equiv) were added and the mixture was stirred at room

temperature for 20 h. Water was added and the phases were separated. The aqueous phase was extracted with DCM (3×) and the combined organic phases were dried over $MgSO_4$. The crude product was purified by flash column chromatography (PE:EA = 9:1).

General procedure D. Diels-Alder/elimination reaction of 316 to 317

5-substituted acetate **316** (10 mmol, 1.0 equiv) was dissolved in dry Et_2O (30 mL) and the solution was cooled to 0 °C in an ice bath. $BF_3 \cdot OEt_2$ (0.25 mL, 2.0 mmol, 20 mol%) and freshly distilled cyclopentadiene **21** (2.5 mL, 30 mmol, 3.0 equiv) were added at 0 °C. The mixture was allowed to warm up to room temperature and stirred for 18 h. The solvent was removed under reduced pressure and the residue was dissolved in DCM:MeOH (1:1, 90 mL). 10 M NaOH solution (15 mL) was added and stirred for 1 h at room temperature. The mixture was washed with brine (1×) and the phases were separated. The aqueous phase was extracted with DCM (3×) and the combined organic phases were dried over $MgSO_4$. The solvent was removed under reduced pressure and the crude product was purified by flash column chromatography (PE:EA = 19:1 to 9:1).

General procedure E. Epoxidation of 317 to 318

Enone **317** (3.00 mmol, 1.0 equiv) was dissolved in DCM:MeOH (1:1, 15 mL). 2 M NaOH solution (1.80 mL, 3.60 mmol, 1.2 equiv) and H_2O_2 (34% in water, 1.46 mL, 16.2 mmol, 5.4 equiv) were added and the reaction mixture was stirred for 24 h at room temperature. The reaction mixture was poured into DCM (90 mL) and washed with brine (1x). The organic layer was dried over $MgSO_4$ and concentrated under vacuum to yield the pure compound.

General procedure F. Flash vacuum thermolysis of 318 to 2

A high-quality glass tube (length 90 cm, diameter 1 cm) was fixed horizontally in a tube furnace. On one end the tube was connected to a cooling trap filled with liquid nitrogen and on the other end to a flask containing epoxide **318**. The cooling trap was connected to a high-vacuum line at $2 \cdot 10^{-2}$ mbar and the furnace was heated to 650 °C. Epoxide **318** (500 µmol, 1.0 equiv) was slowly evaporated through the tube furnace and the product was collected in a trap cooled with ice/water. The product was washed off the cooling trap with DCM and the solvent was removed under reduced pressure to yield the pure compound.

1-(Furan-2-yl)butan-1-ol (314a)[260]

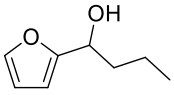

Following general procedure **A**, reaction of magnesium shavings (2.27 g, 93.6 mmol, 1.3 equiv), 1-bromopropane (10.5 mL, 115 mmol, 1.6 equiv) and furfural **310** (5.96 mL, 72.0 mmol, 1.0 equiv) afforded **314a** as a yellowish liquid (9.28 g, 66.0 mmol, 92%).

^{1}H NMR (300 MHz, $CDCl_3$) δ_H = 7.37 (dd, *J* = 1.9, 0.8 Hz, 1H), 6.32 (dd, *J* = 3.2, 1.8 Hz, 1H), 6.22 (dt, *J* = 3.2, 0.8 Hz, 1H), 4.68 (t, *J* = 6.9 Hz, 1H), 1.92 (bs, 1H), 1.87 – 1.79 (m, 2H), 1.51 – 1.28 (m, 2H), 0.94 (t, *J* = 7.4 Hz, 3H); **^{13}C NMR** (75 MHz, $CDCl_3$) δ_C = 157.0, 142.0, 110.2, 105.8, 67.6, 37.7, 18.9, 13.9.

1-(Furan-2-yl)hexan-1-ol (314b)[261]

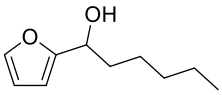

Following general procedure **A**, reaction of magnesium shavings (2.27 g, 93.6 mmol, 1.3 equiv), 1-bromopentane (14.3 mL, 115 mmol, 1.6 equiv) and furfural **310** (5.96 mL, 72.0 mmol, 1.0 equiv) afforded **314b** as a yellowish liquid (11.9 g, 70.9 mmol, 98%).

^{1}H NMR (300 MHz, $CDCl_3$) δ_H = 7.37 (dd, *J* = 1.8, 0.8 Hz, 1H), 6.33 (dd, *J* = 3.2, 1.8 Hz, 1H), 6.22 (dt, *J* = 3.2, 0.8 Hz, 1H), 4.67 (t, *J* = 6.8 Hz, 1H), 1.96 – 1.80 (m, 3H), 1.45 – 1.27 (m, 6H), 0.92 – 0.85 (m, 3H); **^{13}C NMR** (75 MHz, $CDCl_3$) δ_C = 157.0, 142.0, 110.2, 105.9, 67.9, 35.6, 31.7, 25.3, 22.7, 14.1.

1-(Furan-2-yl)octan-1-ol (314c)[262]

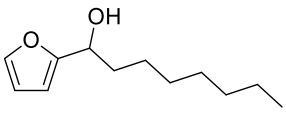

Following general procedure **A**, reaction of magnesium shavings (2.27 g, 93.6 mmol, 1.3 equiv), 1-bromoheptane (18.1 mL, 115 mmol, 1.6 equiv) and furfural **310** (5.96 mL, 72.0 mmol, 1.0 equiv) afforded **314c** as a yellowish liquid (13.7 g, 69.8 mmol, 97%).

^{1}H NMR (300 MHz, $CDCl_3$) δ_H = 7.37 (dd, *J* = 1.9, 0.9 Hz, 1H), 6.33 (dd, *J* = 3.2, 1.8 Hz, 1H), 6.22 (dt, *J* = 3.2, 0.7 Hz, 1H), 4.67 (t, *J* = 6.8 Hz, 1H), 1.92 – 1.79 (m, 3H), 1.37 – 1.20 (m,

10H), 0.90 – 0.85 (m, 3H); **^{13}C NMR** (75 MHz, $CDCl_3$) δ_C = 157.0, 141.9, 110.2, 105.8, 67.9, 35.6, 31.9, 29.5, 29.3, 25.6, 22.7, 14.2.

4-Hydroxy-5-propylcyclopent-2-en-1-one (315a)

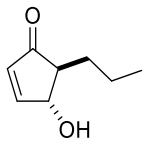

According to general procedure **B** furfuryl alcohol **314a** (5.96 g, 42.5 mmol (8.5 × 5.0 mol)) was employed to yield **315a** as a yellowish liquid (4.30 g, 30.6 mmol, 72%).

^{1}H NMR (300 MHz, $CDCl_3$) δ_H = 7.49 (dd, *J* = 5.8, 2.2 Hz, 1H), 6.17 (dd, *J* = 5.8, 1.3 Hz, 1H), 4.70 – 4.65 (m, 1H), 2.61 (bs, 1H), 2.27 – 2.20 (m, 1H), 1.87 – 1.74 (m, 1H), 1.53 – 1.39 (m, 3H), 0.95 (t, *J* = 7.1 Hz, 3H); **^{13}C NMR** (75 MHz, $CDCl_3$) δ_C = 208.2, 161.7, 134.4, 76.9, 55.3, 30.8, 20.7, 14.2.

4-Hydroxy-5-pentylcyclopent-2-en-1-one (315b)[160]

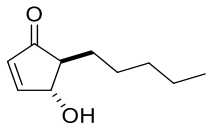

According to general procedure **B** furfuryl alcohol **314b** (10.1 g, 60.0 mmol (12 × 5.0 mol)) was employed to yield **315b** as a yellowish liquid (7.60 g, 45.2 mmol, 75%).

^{1}H NMR (400 MHz, $CDCl_3$) δ_H = 7.49 (dd, *J* = 5.8, 2.2 Hz, 1H), 6.19 (dd, *J* = 5.8, 1.3 Hz, 1H), 4.72 – 4.65 (m, 1H), 2.28 – 2.16 (m, 2H), 1.91 – 1.80 (m, 1H), 1.49 – 1.41 (m, 3H), 1.35 – 1.28 (m, 4H), 0.91 – 0.86 (m, 3H); **^{13}C NMR** (75 MHz, $CDCl_3$) δ_C = 208.2, 161.6, 134.5, 76.9, 55.6, 32.0, 28.7, 27.1, 22.6, 14.1.

5-Heptyl-4-hydroxycyclopent-2-en-1-one (315c)[262]

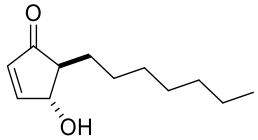

According to general procedure **B** furfuryl alcohol **314c** (12.8 g, 65.0 mmol (13 × 5.0 mol)) was employed to yield **315c** as a yellowish liquid (5.08 g, 25.9 mmol, 40%).

^{1}H NMR (300 MHz, $CDCl_3$) δ_H = 7.49 (dd, *J* = 5.8, 2.2 Hz, 1H), 6.19 (dd, *J* = 5.8, 1.3 Hz, 1H), 4.71 – 4.66 (m, 1H), 2.25 – 2.19 (m, 1H), 1.90 – 1.78 (m, 1H), 1.51 – 1.40 (m, 3H), 1.33 – 1.24

(m, 8H), 0.89 – 0.84 (m, 3H); **^{13}C NMR** (75 MHz, $CDCl_3$) δ_C = 208.1, 161.5, 134.5, 77.0, 55.6, 31.9, 29.7, 29.2, 28.7, 27.5, 22.7, 14.2.

4-Oxo-5-propylcyclopent-2-en-1-yl acetate (316a)

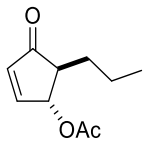

Following general procedure **C**, reaction of 5-substituted 4-hydroxycyclopent-2-enone **315a** (4.29 g, 30.6 mmol, 1.0 equiv), NEt_3 (21.3 mL, 153 mmol, 5.0 equiv) and Ac_2O (14.5 mL, 153 mmol, 5.0 equiv) afforded acetate **316a** as a yellowish oil (4.96 g, 27.2 mmol, 89%).

R_f = 0.32 (PE:EA = 9:1); **^{1}H NMR** (300 MHz, $CDCl_3$) δ_H = 7.49 (dd, *J* = 5.8, 2.3 Hz, 1H), 6.28 (dd, *J* = 5.8, 1.2 Hz, 1H), 5.66 – 5.61 (m, 1H), 2.38 (ddd, *J* = 8.5, 5.0, 2.4 Hz, 1H), 2.10 (s, 3H), 1.85 – 1.73 (m, 1H), 1.55 – 1.34 (m, 3H), 0.92 (t, *J* = 7.2 Hz, 3H); **^{13}C NMR** (75 MHz, $CDCl_3$) δ_C = 207.1, 170.6, 157.8, 136.3, 77.6, 51.4, 30.8, 21.1, 20.2, 14.1; **IR** (ν/cm^{-1}): 2960, 2937, 2874, 1715, 1595, 1485, 1372, 1327, 1230, 1170, 1088, 1025, 954, 924, 895, 857, 798, 734; **HRMS** (APCI) *m/z* calculated for $C_{10}H_{15}O_3$ [MH^+]: 183.1016, found: 183.1026.

4-Oxo-5-pentylcyclopent-2-en-1-yl acetate (316b)

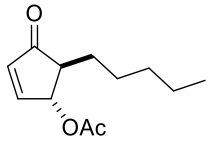

Following general procedure **C**, reaction of 5-substituted 4-hydroxycyclopent-2-enone **315b** (5.99 g, 35.6 mmol, 1.0 equiv), NEt_3 (24.8 mL, 178 mmol, 5.0 equiv) and Ac_2O (16.8 mL, 178 mmol, 5.0 equiv) afforded acetate **316b** as a yellowish oil (7.02 g, 33.4 mmol, 94%).

R_f = 0.38 (PE:EA = 9:1); **^{1}H NMR** (300 MHz, $CDCl_3$) δ_H = 7.49 (dd, *J* = 5.8, 2.3 Hz, 1H), 6.29 (dd, *J* = 5.8, 1.2 Hz, 1H), 5.66 – 5.62 (m, 1H), 2.38 (ddd, *J* = 8.4, 4.9, 2.4 Hz, 1H), 2.10 (s, 3H), 1.86 – 1.75 (m, 1H), 1.58 – 1.46 (m, 1H), 1.37 – 1.24 (m, 6H), 0.90 – 0.84 (m, 3H); **^{13}C NMR** (75 MHz, $CDCl_3$) δ_C = 207.1, 170.7, 157.8, 136.3, 77.6, 51.6, 31.8, 28.6, 26.5, 22.5, 21.1, 14.1; **IR** (ν/cm^{-1}): 2929, 2862, 1714, 1595, 1461, 1371, 1226, 1095, 1021, 924, 868, 793, 726; **HRMS** (APCI) *m/z* calculated for $C_{12}H_{19}O_3$ [MH^+]: 211.1329, found: 211.1330.

5-Heptyl-4-oxocyclopent-2-en-1-yl acetate (316c)

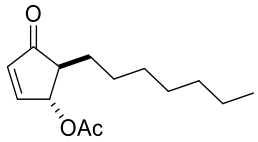

Following general procedure **C**, reaction of 5-substituted 4-hydroxycyclopent-2-enone **315c** (3.14 g, 16.0 mmol, 1.0 equiv), NEt_3 (11.2 mL, 80.0 mmol, 5.0 equiv) and Ac_2O (7.56 mL, 80.0 mmol, 5.0 equiv) afforded acetate **316c** as a yellowish oil (3.49 g, 14.6 mmol, 91%).

R_f = 0.42 (PE:EA = 9:1); **^{1}H NMR** (300 MHz, $CDCl_3$) δ_H = 7.49 (dd, *J* = 5.8, 2.3 Hz, 1H), 6.29 (dd, *J* = 5.8, 1.2 Hz, 1H), 5.67 – 5.62 (m, 1H), 2.37 (ddd, *J* = 8.5, 4.9, 2.4 Hz, 1H), 2.10 (s, 3H), 1.87 – 1.75 (m, 1H), 1.57 – 1.46 (m, 1H), 1.34 – 1.23 (m, 10H), 0.89 – 0.84 (m, 3H); **^{13}C NMR** (75 MHz, $CDCl_3$) δ_C = 207.1, 170.6, 157.8, 136.3, 77.6, 51.6, 31.9, 29.6, 29.1, 28.7, 26.8, 22.7, 21.1, 14.2; **IR** (ν/cm^{-1}): 2926, 2855, 1718, 1595, 1581, 1372, 1230, 1170, 1096, 1021, 976, 906, 794, 723; **HRMS** (APCI) *m/z* calculated for $C_{14}H_{23}O_3$ [MH^+]: 239.1642, found: 239.1641.

2-Propyl-3a,4,7,7a-tetrahydro-1*H*-4,7-methanoinden-1-one (317a)

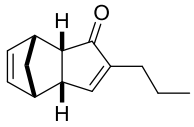

According to general procedure **D** acetate **316a** (1.82 g, 10.0 mmol, 1.0 equiv) was employed to yield **317a** as a colorless liquid (1.77 g, 9.39 mmol, 94%).

R_f = 0.48 (PE:EA = 9:1); **^{1}H NMR** (300 MHz, $CDCl_3$) δ_H = 7.02 – 6.94 (m, 1H), 5.86 (dd, *J* = 5.6, 2.9 Hz, 1H), 5.74 (dd, *J* = 5.6, 3.0 Hz, 1H), 3.28 – 3.22 (m, 1H), 3.22 – 3.17 (m, 1H), 2.93 – 2.89 (m, 1H), 2.83 – 2.79 (m, 1H), 2.08 – 1.92 (m, 2H), 1.73 (dt, *J* = 8.4, 1.8 Hz, 1H), 1.62 – 1.57 (m, 1H), 1.39 (sext, *J* = 7.3 Hz, 2H), 0.85 (t, *J* = 7.3 Hz, 3H); **^{13}C NMR** (75 MHz, $CDCl_3$) δ_C = 210.3, 157.7, 149.3, 132.6, 132.3, 52.7, 50.9, 45.4, 45.2, 44.1, 26.8, 21.2, 13.9; **IR** (ν/cm^{-1}): 3064, 2960, 2933, 2870, 1692, 1625, 1454, 1338, 1230, 1204, 1126, 1074, 828, 738, 712; **HRMS** (EI) *m/z* calculated for $C_{13}H_{16}O$ [M^+]: 188.1195, found: 188.1200.

2-Pentyl-3a,4,7,7a-tetrahydro-1*H*-4,7-methanoinden-1-one (317b)[263]

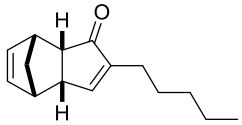

According to general procedure **D** acetate **316b** (2.10 g, 10.0 mmol, 1.0 equiv) was employed to yield **317b** as a colorless liquid (2.06 g, 9.52 mmol, 95%).

R_f = 0.51 (PE:EA = 9:1); **^{1}H NMR** (400 MHz, $CDCl_3$) δ_H = 7.01 – 6.94 (m, 1H), 5.87 (dd, *J* = 5.6, 2.9 Hz, 1H), 5.74 (dd, *J* = 5.6, 3.0 Hz, 1H), 3.27 – 3.22 (m, 1H), 3.22 – 3.17 (m, 1H), 2.93 – 2.88 (m, 1H), 2.81 (t, *J* = 5.1 Hz, 1H), 2.08 – 1.95 (m, 2H), 1.73 (dt, *J* = 8.4, 1.8 Hz, 1H), 1.60 (dt, *J* = 8.4, 1.5 Hz, 1H), 1.39 – 1.20 (m, 6H), 0.86 (t, *J* = 7.0 Hz, 3H); **^{13}C NMR** (75 MHz, $CDCl_3$) δ_C = 210.3, 157.5, 149.6, 132.6, 132.3, 52.7, 50.9, 45.4, 45.2, 44.2, 31.5, 27.6, 24.7, 22.5, 14.1; **IR** (ν/cm^{-1}): 3063, 2929, 2862, 1695, 1625, 1457, 1338, 1203, 1125, 909, 738, 711; **HRMS** (APCI) *m/z* calculated for $C_{15}H_{21}O$ [MH^+]: 217.1587, found: 217.1586.

2-Heptyl-3a,4,7,7a-tetrahydro-1*H*-4,7-methanoinden-1-one (317c)

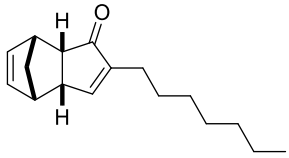

According to general procedure **D** acetate **316c** (2.38 g, 10.0 mmol, 1.0 equiv) was employed to yield **317c** as a colorless oil (2.29 g, 9.37 mmol, 94%).

R_f = 0.57 (PE:EA = 9:1); **^{1}H NMR** (300 MHz, $CDCl_3$) δ_H = 7.02 – 6.92 (m, 1H), 5.86 (dd, *J* = 5.6, 2.9 Hz, 1H), 5.74 (dd, *J* = 5.7, 3.0 Hz, 1H), 3.28 – 3.22 (m, 1H), 3.22 – 3.17 (m, 1H), 2.93 – 2.88 (m, 1H), 2.81 (t, *J* = 5.1 Hz, 1H), 2.11 – 1.91 (m, 2H), 1.72 (dt, *J* = 8.4, 1.8 Hz, 1H), 1.62 – 1.56 (m, 1H), 1.39 – 1.19 (m, 10H), 0.90 – 0.82 (m, 3H); **^{13}C NMR** (75 MHz, $CDCl_3$) δ_C = 210.3, 157.5, 149.6, 132.6, 132.4, 52.7, 50.9, 45.4, 45.2, 44.2, 31.9, 29.3, 29.1, 28.0, 24.7, 22.7, 14.2; **IR** (ν/cm^{-1}): 3064, 2926, 2855, 1696, 1625, 1461, 1338, 1293, 1230, 1126, 910, 738, 716; **HRMS** (EI) *m/z* calculated for $C_{17}H_{24}O$ [M^+]: 244.1821, found: 244.1816.

6a-Propyl-1a,1b,2,5,5a,6a-hexahydro-6*H*-2,5-methanoindeno[1,2-*b*]oxiren-6-one (318a)[161]

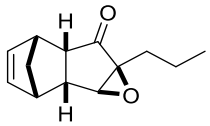

According to general procedure **E** enone **317a** (565 mg, 3.00 mmol, 1.0 equiv) was used to afford **318a** as a colorless oil (598 mg, 2.93 mmol, 98%).

R_f = 0.47 (PE:EA = 10:1); **^{1}H NMR** (300 MHz, $CDCl_3$) δ_H = 6.04 (dd, *J* = 5.7, 2.8 Hz, 1H), 5.99 (dd, *J* = 5.7, 2.8 Hz, 1H), 3.46 (d, *J* = 1.7 Hz, 1H), 3.25 – 3.19 (m, 1H), 3.09 – 3.04 (m, 1H), 3.01 – 2.95 (m, 1H), 2.85 – 2.78 (m, 1H), 1.85 – 1.71 (m, 1H), 1.60 (dt, *J* = 8.5, 1.8 Hz, 1H), 1.57 – 1.47 (m, 1H), 1.47 – 1.42 (m, 1H), 1.34 – 1.20 (m, 2H), 0.89 (t, *J* = 7.3 Hz, 3H); **^{13}C NMR** (75 MHz, $CDCl_3$) δ_C = 210.5, 135.2, 133.8, 67.0, 65.5, 51.9, 50.1, 45.9, 43.6, 43.4, 27.0, 17.9, 14.5; **IR** (ν/cm^{-1}): 3064, 2963, 2874, 1733, 1457, 1338, 1200, 1126, 1029, 910, 835, 775, 723; **HRMS** (EI) *m/z* calculated for $C_{13}H_{16}O_2$ [M^+]: 204.1145, found: 204.1145.

6a-Pentyl-1a,1b,2,5,5a,6a-hexahydro-6*H*-2,5-methanoindeno[1,2-*b*]oxiren-6-one (318b)[161]

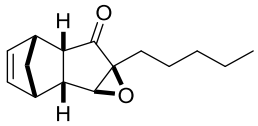

According to general procedure **E** enone **317b** (649 mg, 3.00 mmol, 1.0 equiv) was used to afford **318b** as a colorless oil (684 mg, 2.94 mmol, 98%).

R_f = 0.54 (PE:EA = 10:1); **^{1}H NMR** (300 MHz, $CDCl_3$) δ_H = 6.04 (dd, *J* = 5.6, 2.8 Hz, 1H), 5.99 (dd, *J* = 5.6, 2.8 Hz, 1H), 3.46 (d, *J* = 1.6 Hz, 1H), 3.26 – 3.17 (m, 1H), 3.10 – 3.04 (m, 1H), 3.02 – 2.95 (m, 1H), 2.85 – 2.79 (m, 1H), 1.84 – 1.72 (m, 1H), 1.62 – 1.43 (m, 3H), 1.34 – 1.19 (m, 6H), 0.86 (t, *J* = 6.8 Hz, 3H); **^{13}C NMR** (75 MHz, $CDCl_3$) δ_C = 210.6, 135.2, 133.8, 67.1, 65.5, 51.9, 50.1, 45.9, 43.6, 43.4, 32.1, 24.8, 24.1, 22.5, 14.1; **IR** (ν/cm^{-1}): 3064, 2933, 2862, 1737, 1461, 1420, 1338, 1252, 1126, 1088, 1044, 910, 842, 775, 723; **HRMS** (EI) *m/z* calculated for $C_{15}H_{20}O_2$ [M^+]: 232.1458, found: 232.1452.

6a-Heptyl-1a,1b,2,5,5a,6a-hexahydro-6*H*-2,5-methanoindeno[1,2-*b*]oxiren-6-one (318c)[161]

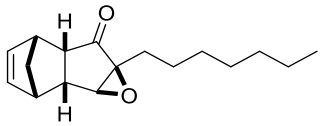

According to general procedure **E** enone **317c** (733 mg, 4.00 mmol, 1.0 equiv) was used to afford **318c** as a colorless oil (758 mg, 2.91 mmol, 97%).

R_f = 0.54 (PE:EA = 10:1); **^{1}H NMR** (300 MHz, $CDCl_3$) δ_H = 6.04 (dd, *J* = 5.7, 2.8 Hz, 1H), 5.99 (dd, *J* = 5.6, 2.8 Hz, 1H), 3.46 (d, *J* = 1.7 Hz, 1H), 3.25 – 3.19 (m, 1H), 3.09 – 3.04 (m, 1H), 3.01 – 2.95 (m, 1H), 2.84 – 2.79 (m, 1H), 1.84 – 1.71 (m, 1H), 1.60 (dt, *J* = 8.5, 1.8 Hz, 1H), 1.58 – 1.48 (m, 1H), 1.45 (dt, *J* = 8.5, 1.6 Hz, 1H), 1.31 – 1.18 (m, 10H), 0.90 – 0.83 (m, 3H); **^{13}C NMR** (75 MHz, $CDCl_3$) δ_C = 210.6, 135.2, 133.8, 67.1, 65.5, 51.9, 50.1, 45.9, 43.6, 43.4, 31.8, 29.9, 29.1, 24.8, 24.4, 22.7, 14.2; **IR** (ν/cm^{-1}): 3064, 2930, 2855, 1737, 1461, 1338, 1200, 1126, 1088, 1044, 910, 842, 775, 723; **HRMS** (EI) *m/z* calculated for $C_{17}H_{24}O_2$ [M^+]: 260.1771, found: 260.1765.

6-Propyl-2*H*-pyran-2-one (2a)[161,167]

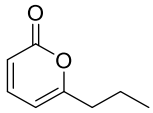

Following general procedure **F**, epoxide **318a** (102 mg, 500 µmol, 1.0 equiv) was employed to yield **2a** as a colorless oil (68.8 mg, 498 µmol, >99%).

^{1}H NMR (300 MHz, $CDCl_3$) δ_H = 7.26 (dd, *J* = 9.4, 6.5 Hz, 1H), 6.15 (d, *J* = 9.4 Hz, 1H), 5.97 (dd, *J* = 6.6, 0.8 Hz, 1H), 2.46 (t, *J* = 7.5 Hz, 2H), 1.69 (sext, *J* = 7.5 Hz, 2H), 0.96 (t, *J* = 7.4 Hz, 3H); **^{13}C NMR** (75 MHz, $CDCl_3$) δ_C = 166.6, 163.1, 143.8, 113.2, 102.8, 35.8, 20.3, 13.6.

6-Pentyl-2*H*-pyran-2-one (2b)[8,161]

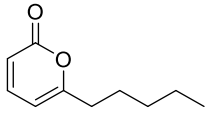

Following general procedure **F**, epoxide **318b** (116 mg, 500 µmol, 1.0 equiv) was employed to yield **2b** as a colorless oil (82.4 mg, 496 µmol, >99%).

^{1}H NMR (300 MHz, $CDCl_3$) δ_H = 7.25 (dd, *J* = 9.4, 6.5 Hz, 1H), 6.14 (d, *J* = 9.4 Hz, 1H), 5.97 (dd, *J* = 6.6, 0.7 Hz, 1H), 2.47 (t, *J* = 7.6 Hz, 2H), 1.69 – 1.60 (m, 2H), 1.36 – 1.27 (m, 4H), 0.89 (t, *J* = 6.9 Hz, 3H); **^{13}C NMR** (75 MHz, $CDCl_3$) δ_C = 166.9, 163.1, 143.8, 113.2, 102.7, 33.9, 31.2, 26.7, 22.4, 14.0.

6-Heptyl-2*H*-pyran-2-one (2c)[161,167]

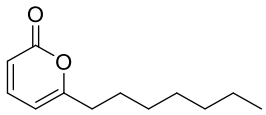

Following general procedure **F**, epoxide **318c** (130 mg, 500 µmol, 1.0 equiv) was employed to yield **2c** as a colorless oil (970 mg, 499 µmol, >99%).

^{1}H NMR (300 MHz, $CDCl_3$) δ_H = 7.25 (dd, *J* = 9.4, 6.6 Hz, 1H), 6.15 (d, *J* = 9.4 Hz, 1H), 5.96 (dd, *J* = 6.6, 0.8 Hz, 1H), 2.47 (t, *J* = 7.5 Hz, 2H), 1.70 – 1.60 (m, 2H), 1.35 – 1.22 (m, 8H), 0.87 (t, *J* = 6.8 Hz, 3H); **^{13}C NMR** (75 MHz, $CDCl_3$) δ_C = 166.9, 163.1, 143.8, 113.2, 102.7, 33.9, 31.7, 29.07, 29.05, 27.0, 22.7, 14.2.

3 Application of 2-pyrones derived from renewable resources

General procedure G. Intermolecular Diels-Alder reactions of 26 with alkynes

A microwave vessel was charged with pyrone **26** (1.0 equiv) and alkyne (1.4 equiv). The mixture was heated in the microwave at 150 °C for 7 h. The resulting crude product was purified by flash column chromatography (PE:EA).

Ethyl (*S*)-1-methyl-3-oxo-1,3-dihydroisobenzofuran-4-carboxylate ((*S*)-342a)

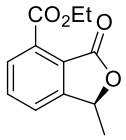

Following general procedure **G**, reaction of pyrone **(*S*)-26a** (72.6 mg, 518 µmol, 1.0 equiv) and diethyl acetylenedicarboxylate (**341**) (115 µL, 725 µmol, 1.4 equiv) afforded **(*S*)-342a** after purification by flash column chromatography (PE:EA = 4:1) as a yellowish oil (93.2 mg, 420 µmol, 81%).

R_f = 0.16 (PE:EA = 4:1); **^{1}H NMR** (400 MHz, $CDCl_3$) δ_H = 7.77 – 7.68 (m, 2H), 7.54 (dt, *J* = 7.3, 1.0 Hz, 1H), 5.53 (q, *J* = 6.7 Hz, 1H), 4.47 (q, *J* = 7.1 Hz, 2H), 1.64 (d, *J* = 6.7 Hz, 3H), 1.42 (t, *J* = 7.1 Hz, 3H); **^{13}C NMR** (101 MHz, $CDCl_3$) δ_C = 167.4, 166.0, 152.3, 133.8, 132.3,

129.4, 124.1, 123.5, 76.8, 62.3, 20.5, 14.2; **IR** (ν/cm^{-1}): 2981, 2937, 1766, 1722, 1595, 1446, 1371, 1289, 1144, 1025, 946, 745, 700; **HRMS** (EI) *m/z* calculated for $C_{12}H_{12}O_4$ [M^+]: 220.0730, found: 220.0723; **Chiral HPLC** 99% *ee* (t_R minor, major = 39.9, 43.0 min, Chiralpak AS-H 4.6 × 250 mm 10 µm, *n*-heptane:*i*-PrOH 90:10, 0.5 mL/min).

Ethyl 1-butyl-3-oxo-1,3-dihydroisobenzofuran-4-carboxylate (342b)

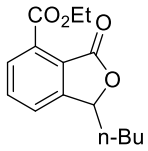

Following general procedure **G**, reaction of pyrone **26b** (182 mg, 1.00 mmol, 1.0 equiv) and diethyl acetylenedicarboxylate (**341**) (223 µL, 1.40 mmol, 1.4 equiv) afforded **342b** after purification by flash column chromatography (PE:EA = 7:1) as a yellowish oil (183 mg, 700 µmol, 70%).

R_f = 0.17 (PE:EA = 7:1); **^{1}H NMR** (300 MHz, $CDCl_3$) δ_H = 7.78 – 7.66 (m, 2H), 7.53 (ddd, *J* = 7.3, 1.4, 0.8 Hz, 1H), 5.44 (dd, *J* = 8.0, 4.0 Hz, 1H), 4.47 (q, *J* = 7.2 Hz, 2H), 2.10 – 1.97 (m, 1H), 1.82 – 1.67 (m, 1H), 1.49 – 1.34 (m, 7H), 0.90 (t, *J* = 7.1 Hz, 3H); **^{13}C NMR** (101 MHz, $CDCl_3$) δ_C = 167.6, 166.1, 151.3, 133.7, 132.3, 129.3, 124.2, 123.8, 80.5, 62.2, 34.5, 27.0, 22.5, 14.2, 13.9; **IR** (ν/cm^{-1}): 2983, 2934, 1766, 1722, 1595, 1447, 1370, 1289, 1144, 1025, 946, 700; **HRMS** (ESI) *m/z* calculated for $C_{15}H_{19}O_4$ [MH^+]: 263.1278, found: 263.1286.

Ethyl 3-oxo-1-phenyl-1,3-dihydroisobenzofuran-4-carboxylate (342c)

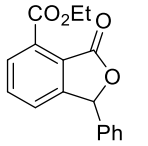

Following general procedure **G**, reaction of pyrone **26c** (202 mg, 1.00 mmol, 1.0 equiv) and diethylacetylenedicarboxylate (**341**) (223 µL, 1.40 mmol, 1.4 equiv) afforded **342c** after purification by flash column chromatography (PE:EA = 7:1) as a yellowish oil (142 mg, 500 µmol, 50%).

R_f = 0.15 (PE:EA = 7:1); **^{1}H NMR** (300 MHz, $CDCl_3$) δ_H = 7.82 – 7.76 (m, 1H), 7.68 (t, *J* = 7.6 Hz, 1H), 7.45 – 7.34 (m, 4H), 7.32 – 7.26 (m, 2H), 6.37 (s, 1H), 4.50 (q, *J* = 7.1 Hz, 2H), 1.45 (t, *J* = 7.1 Hz, 3H); **^{13}C NMR** (75 MHz, $CDCl_3$) δ_C = 167.5, 165.9, 150.9, 136.1, 134.1, 132.1, 129.8, 129.5, 129.1, 127.1, 125.5, 123.2, 81.9, 62.3, 14.2; **IR** (ν/cm^{-1}): 2983, 2934, 2923,

1766, 1722, 1595, 1447, 1370, 1289, 1144, 1025, 946, 700; **HRMS** (ESI) *m/z* calculated for $C_{17}H_{15}O_4$ [MH^+]: 283.0965, found: 283.0973.

Ethyl 3-(1-hydroxyethyl)benzoate (348a)/3-Methylisobenzofuran-1(3*H*)-one (326a)[176]

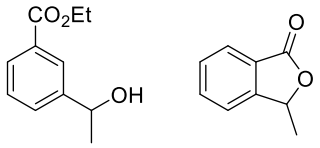

Following general procedure **G**, reaction of pyrone **26a** (280 mg, 2.00 mmol, 1.0 equiv) and ethyl propiolate (**37**) (286 µL, 2.80 mmol, 1.4 equiv) afforded after purification by flash column chromatography (PE:EA = 7:1 to 4:1) **348a** as a colorless oil (229 mg, 1.18 mmol, 59%) and **326a** as a colorless oil (59.6 mg, 400 µmol, 20%).

348a: $\mathbf{R_f}$ = 0.37 (PE:EA = 2:1); **^{1}H NMR** (400 MHz, $CDCl_3$) δ_H = 8.02 (t, *J* = 1.8 Hz, 1H), 7.93 (dt, *J* = 7.7, 1.5 Hz, 1H), 7.57 (dt, *J* = 7.7, 1.5 Hz, 1H), 7.40 (t, *J* = 7.7 Hz, 1H), 4.94 (q, *J* = 6.5 Hz, 1H), 4.36 (q, *J* = 7.1 Hz, 2H), 2.21 (s, 1H), 1.50 (d, *J* = 6.5 Hz, 3H), 1.38 (t, *J* = 7.1 Hz, 3H); **^{13}C NMR** (101 MHz, $CDCl_3$) δ_C = 166.7, 146.3, 130.7, 129.9, 128.7, 128.6, 126.6, 70.0, 61.1, 25.4, 14.4; **IR** (ν/cm^{-1}): 3418, 3071, 2974, 2933, 2903, 1714, 1587, 1446, 1367, 1278, 1192, 1017, 756, 697; **HRMS** (EI) *m/z* calculated for $C_{11}H_{14}O_3$ [M^+]: 194.0937, found: 194.0931.

326a: $\mathbf{R_f}$ = 0.78 (PE:EA = 2:1); **^{1}H NMR** (400 MHz, $CDCl_3$) δ_H = 7.90 (d, *J* = 7.7 Hz, 1H), 7.68 (td, *J* = 7.5, 1.1 Hz, 1H), 7.53 (t, *J* = 7.5 Hz, 1H), 7.44 (dd, *J* = 7.6, 0.9 Hz, 1H), 5.57 (q, *J* = 6.7 Hz, 1H), 1.64 (d, *J* = 6.7 Hz, 3H); **^{13}C NMR** (101 MHz, $CDCl_3$) δ_C = 170.6, 151.3, 134.1, 129.1, 125.9, 125.8, 121.6, 77.8, 20.5.

General procedure H. Coupling of 6-hydroxyalkyl pyrones 26 with propiolic acid 349

Under nitrogen atmosphere 6-hydroxyalkyl pyrone **26** (1.0 equiv) and propiolic acid (**349**) (2.0 equiv) were dissolved in dry DCM (2.0 M). The mixture was cooled to −20 °C and a solution of DCC (1.1 equiv) and DMAP (7.0 mol%) in dry DCM (0.45 M) was added dropwise. After complete addition, the reaction mixture was allowed to warm up to room temperature and stirred for 18 h. The solvent was removed under reduced pressure and cold EA was added. The dicyclohexylurea solid was filtered off and washed with cold EA. The organic filtrate was washed with 1 M HCl (1×) and brine (1×). The organic phase was dried over $MgSO_4$ and the solvent was removed under reduced pressure. The crude product was purified by flash column chromatography (PE:EA).

General procedure I. Intramolecular Diels-Alder reaction of 350 to 326

In a microwave vessel pyrone **350** was dissolved in toluene (0.1 M) and the solution was stirred under microwave irradiation at 150 °C for 5 h. The crude reaction mixture was filtered through a short pad of silica and washed with PE:EA = 1:1. The solvent was removed under reduced pressure to yield the pure product.

1-(2-Oxo-2*H*-pyran-6-yl)ethyl propiolate (350a)

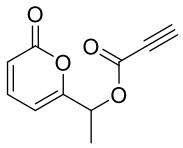

Following general procedure **H**, reaction of pyrone **26a** (1.05 g, 7.52 mmol, 1.0 equiv), propiolic acid (**349**) (932 µL, 15.0 mmol, 2.0 equiv), DMAP (68.9 mg, 564 µmol, 7.0 mol%) and DCC (1.75 g, 8.46 mmol, 1.1 equiv) afforded **350a** after purification by flash column chromatography (PE:EA = 4:1) as a yellowish oil (807 mg, 4.20 mmol, 56%).

R_f = 0.17 (PE:EA = 4:1); **^{1}H NMR** (300 MHz, $CDCl_3$) δ_H = 7.32 (dd, *J* = 9.4, 6.5 Hz, 1H), 6.31 – 6.21 (m, 2H), 5.66 (q, *J* = 6.7 Hz, 1H), 2.97 (s, 1H), 1.61 (d, *J* = 6.7 Hz, 3H); **^{13}C NMR** (101 MHz, $CDCl_3$) δ_C = 161.3, 161.2, 151.4, 143.0, 116.0, 102.6, 76.2, 74.1, 70.1, 18.1; **IR** (ν/cm^{-1}): 3239, 3093, 2993, 2937, 2858, 2117, 1710, 1640, 1561, 1453, 1367, 1207, 1039, 801, 752; **HRMS** (ESI) *m/z* calculated for $C_{10}H_9O_4$ [MH^+]: 193.0495, found: 193.0500.

(*R*)-1-(2-Oxo-2*H*-pyran-6-yl)pentyl propiolate) ((*R*)-350b)

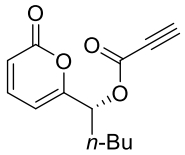

Following general procedure **H**, reaction of pyrone **(*R*)-26b** (434 mg, 2.38 mmol, 1.0 equiv), propiolic acid (**349**) (295 µL, 4.76 mmol, 2.0 equiv), DMAP (21.8 mg, 179 µmol, 7.0 mol%) and DCC (552 mg, 2.68 mmol, 1.1 equiv) afforded **(*R*)-350b** after purification by flash column chromatography (PE:EA = 7:1 to 2:1) as a yellowish oil (345 mg, 1.47 mmol, 62%).

R_f = 0.18 (PE:EA = 7:1); **^{1}H NMR** (300 MHz, $CDCl_3$) δ_H = 7.30 (dd, *J* = 9.4, 6.5 Hz, 1H), 6.26 (dd, *J* = 9.4, 1.0 Hz, 1H), 6.21 (dt, *J* = 6.6, 0.9 Hz, 1H), 5.52 (t, *J* = 6.7 Hz, 1H), 2.98 (s, 1H), 2.00 – 1.88 (m, 2H), 1.41 – 1.27 (m, 4H), 0.93 – 0.87 (m, 3H); **^{13}C NMR** (101 MHz, $CDCl_3$) δ_C = 161.3, 160.8, 151.7, 143.0, 115.8, 103.3, 76.3, 74.1, 73.8, 31.8, 27.0, 22.3, 13.9; **IR** (ν/cm^{-}

[1]): 3235, 3090, 2959, 2933, 2866, 2117, 1714, 1640, 1558, 1464, 1207, 1095, 954, 805, 752; **HRMS** (ESI) *m/z* calculated for $C_{13}H_{15}O_4$ [MH^+]: 235.0965, found: 235.0970.

(2-Oxo-2*H*-pyran-6-yl)(phenyl)methyl propiolate (350c)

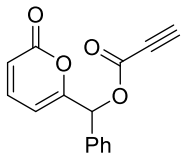

Following general procedure **H**, reaction of pyrone **26c** (1.02 g, 5.03 mmol, 1.0 equiv), propiolic acid (**349**) (624 µL, 10.1 mmol, 2.0 equiv), DMAP (46.0 mg, 377 µmol, 7.0 mol%) and DCC (1.17 g, 5.66 mmol, 1.1 equiv) afforded **350c** after purification by flash column chromatography (PE:EA = 4:1 to 2:1) as a yellowish oil (691 mg, 2.72 mmol, 54%).

R_f = 0.11 (PE:EA = 4:1); **^{1}H NMR** (300 MHz, $CDCl_3$) δ_H = 7.46 – 7.38 (m, 5H), 7.30 (dd, *J* = 9.4, 6.6 Hz, 1H), 6.53 (s, 1H), 6.28 – 6.22 (m, 2H), 3.00 (s, 1H); **^{13}C NMR** (75 MHz, $CDCl_3$) δ_C = 161.0, 160.4, 151.1, 142.8, 134.4, 129.7, 129.1, 127.7, 115.9, 103.3, 76.7, 74.9, 74.0; **IR** (ν/cm^{-1}): 3257, 3067, 2937, 2117, 1714, 1640, 1558, 1453, 1207, 1095, 801, 745, 697; **HRMS** (ESI) *m/z* calculated for $C_{15}H_{11}O_4$ [MH^+]: 255.0652, found: 255.0659.

3-Methylisobenzofuran-1(3*H*)-one (326a)[176]

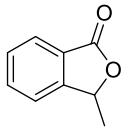

According to general procedure **I** pyrone **350a** (100 mg, 520 µmol, 1.0 equiv) was used to yield phthalide **326a** as a colorless oil (76.9 mg, 519 µmol, >99%).

R_f = 0.78 (PE:EA = 2:1); **^{1}H NMR** (400 MHz, $CDCl_3$) δ_H = 7.90 (d, *J* = 7.7 Hz, 1H), 7.68 (td, *J* = 7.5, 1.1 Hz, 1H), 7.53 (t, *J* = 7.5 Hz, 1H), 7.44 (dd, *J* = 7.6, 0.9 Hz, 1H), 5.57 (q, *J* = 6.7 Hz, 1H), 1.64 (d, *J* = 6.7 Hz, 3H); **^{13}C NMR** (101 MHz, $CDCl_3$) δ_C = 170.6, 151.3, 134.1, 129.1, 125.9, 125.8, 121.6, 77.8, 20.5.

(*R*)-3-Butylisobenzofuran-1(3*H*)-one ((*R*)-326b)[176]

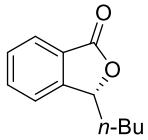

According to general procedure **I** pyrone **(*R*)-350b** (121 mg, 517 µmol, 1.0 equiv) was used to yield phthalide **(*R*)-326b** as a colorless oil (97.9 mg, 515 µmol, >99%).

R_f = 0.78 (PE:EA = 2:1); **^{1}H NMR** (400 MHz, $CDCl_3$) δ_H = 7.87 (dd, *J* = 7.6, 0.9 Hz, 1H), 7.66 (td, *J* = 7.5, 1.1 Hz, 1H), 7.50 (t, *J* = 7.5 Hz, 1H), 7.43 (dd, *J* = 7.7, 0.9 Hz, 1H), 5.46 (dd, *J* = 7.9, 4.1 Hz, 1H), 2.08 – 1.99 (m, 1H), 1.79 – 1.70 (m, 1H), 1.49 – 1.32 (m, 4H), 0.89 (t, *J* = 7.1 Hz, 3H); **^{13}C NMR** (101 MHz, $CDCl_3$) δ_C = 170.7, 150.2, 134.0, 129.1, 126.2, 125.7, 121.8, 81.5, 34.5, 26.9, 22.5, 13.9; **Chiral HPLC** 74% *ee* (t_R minor, major = 14.0, 19.4 min, Chiralcel AS-H 4.6 × 250 mm 10 µm, *n*-heptane:*i*-PrOH 95:5, 1.0 mL/min).

3-Phenylisobenzofuran-1(3*H*)-one (326c)[176]

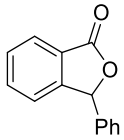

According to general procedure **I** pyrone **350c** (127 mg, 500 µmol, 1.0 equiv) was used to yield phthalide **326c** as a yellowish solid (104 mg, 500 µmol, >99%).

R_f = 0.32 (PE:EA = 4:1); **^{1}H NMR** (400 MHz, $CDCl_3$) δ_H = 7.85 (d, *J* = 7.6 Hz, 1H), 7.54 (td, *J* = 7.5, 1.1 Hz, 1H), 7.44 (t, *J* = 7.5 Hz, 1H), 7.29 – 7.21 (m, 4H), 7.17 (dd, *J* = 6.6, 3.0 Hz, 2H), 6.30 (s, 1H); **^{13}C NMR** (101 MHz, $CDCl_3$) δ_C = 170.6, 149.7, 136.4, 134.4, 129.4, 129.3, 129.0, 127.0, 125.6, 125.5, 122.9, 82.7.

1-(2-Oxo-2*H*-pyran-6-yl)ethyl 3-bromopropiolate (355)

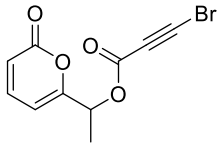

Pyrone propiolate **350a** (659 mg, 3.43 mmol, 1.0 equiv) was dissolved in acetone (70 mL) and the solution was cooled to 0 °C in an ice bath. Subsequently, $AgNO_3$ (291 mg, 1.72 mmol, 0.5 equiv) and NBS (917 mg, 5.15 mmol, 1.5 equiv) were added and the mixture was stirred at 0 °C for 20 h. The reaction mixture was diluted with Et_2O (30 mL) and quenched with H_2O

(40 mL). After phase separation, the aqueous phase was extracted with Et_2O (3×). The organic phase was washed with H_2O (1×), brine (1×) and dried over $MgSO_4$. The solvent was concentrated under vacuum and the crude product was filtered over a short pad of silica (washed with PE:EA = 2:1). The solvent was removed under reduced pressure to yield the pure product **355** as a yellowish oil (838 mg, 3.09 mmol, 90%).

R_f = 0.43 (PE:EA = 2:1); **^{1}H NMR** (400 MHz, $CDCl_3$) δ_H =7.30 (dd, *J* = 9.4, 6.6 Hz, 1H), 6.24 (dd, *J* = 10.2, 8.0 Hz, 2H), 5.61 (q, *J* = 6.7 Hz, 1H), 1.57 (d, *J* = 6.7 Hz, 3H); **^{13}C NMR** (101 MHz, $CDCl_3$) δ_C = 161.3, 161.1, 151.1, 143.0, 115.9, 102.7, 72.2, 70.2, 54.7, 18.1; **IR** (ν/cm^{-1}): 3090, 2989, 2937, 2191, 1707, 1640, 1558, 1215, 1080, 980, 801, 738; **HRMS** (ESI) *m/z* calculated for $C_{10}H_8BrO_4$ [MH^+]: 270.9600, found: 270.9604.

7-Bromo-3-methylisobenzofuran-1(3*H*)-one (354)

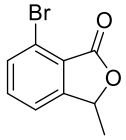

According to general procedure **I** pyrone **355** (195 mg, 720 µmol, 1.0 equiv) was used to yield phthalide **354** as a yellowish solid (164 mg, 718 µmol, >99%).

R_f = 0.59 (PE:EA = 2:1); **mp** 80 − 81 °C; **^{1}H NMR** (400 MHz, $CDCl_3$) δ_H = 7.57 (d, *J* = 7.8 Hz, 1H), 7.43 (t, *J* = 7.7 Hz, 1H), 7.32 (d, *J* = 7.6 Hz, 1H), 5.41 (q, *J* = 6.7 Hz, 1H), 1.53 (d, *J* = 6.7 Hz, 3H); **^{13}C NMR** (101 MHz, $CDCl_3$) δ_C = 167.7, 153.6, 135.1, 133.7, 126.9, 124.0, 120.7, 76.0, 20.3; **IR** (ν/cm^{-1}): 3082, 2993, 2933, 2184, 1707, 1636, 1558, 1215, 1066, 801; **HRMS** (EI) *m/z* calculated for $C_9H_7BrO_2$ [M^+]: 225.9624, found: 225.9624.

(*Exo*)-4a,5,8,8a-tetrahydro-1*H*-8,5-(epoxymethano)isochromene-1,10-dione (367a)[187]

(*Exo*)-4a,5,8,8a-tetrahydro-2*H*-8,5-(epoxymethano)chromene-2,10-dione (367b)[187]

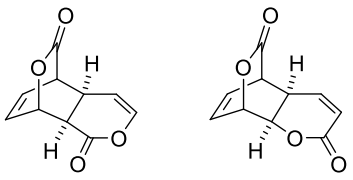

Under nitrogen atmosphere 2-pyrone (**1**) (96.1 mg, 1.00 mmol, 1.0 equiv) and $[Ir(dtb\text{-}bpy)(dF((CF_3)ppy)_2]PF_6$ (11.2 mg, 10.0 µmol, 1.0 mol%) were dissolved in dry degassed DMF (2.0 mL). The reaction mixture was stirred under irradiation with a blue LED (λ = 455 nm) at room temperature for 30 min. The solvent was removed under reduced pressure

and the crude product was purified by flash column chromatography (PE:EA = 1:1 to 1:3) to afford **367a** as a yellow solid (44.5 mg, 230 µmol, 46%) and **367b** as a yellow solid (43.9 mg, 230 µmol, 46%).

367a: $\mathbf{R_f}$ = 0.36 (PE:EA = 1:3); **^{1}H NMR** (400 MHz, $CDCl_3$) δ_H = 6.66 – 6.61 (m, 2H), 6.53 (dd, *J* = 6.4, 1.8 Hz, 1H), 5.75 – 5.68 (m, 1H), 5.15 (dd, *J* = 6.4, 3.6 Hz, 1H), 3.60 – 3.56 (m, 1H), 3.09 (dd, *J* = 11.3, 1.6 Hz, 1H), 2.82 – 2.76 (m, 1H); **^{13}C NMR** (101 MHz, $CDCl_3$) δ_C = 170.6, 165.4, 140.6, 132.8, 132.3, 103.8, 77.0, 46.8, 41.5, 31.0.

367b: $\mathbf{R_f}$ = 0.11 (PE:EA = 1:3); **^{1}H NMR** (400 MHz, $CDCl_3$) δ_H = 6.68 – 6.60 (m, 2H), 6.55 (ddd, *J* = 7.7, 5.1, 1.6 Hz, 1H), 6.08 (dd, *J* = 10.2, 2.1 Hz, 1H), 5.39 (dt, *J* = 5.2, 1.9 Hz, 1H), 4.91 (dd, *J* = 9.9, 1.8 Hz, 1H), 3.61 (dt, *J* = 6.2, 1.9 Hz, 1H), 2.88 – 2.83 (m, 1H); **^{13}C NMR** (101 MHz, $CDCl_3$) δ_C = 169.7, 159.6, 141.8, 133.7, 130.5, 120.8, 78.0, 75.3, 46.2, 29.3.

General procedure J. Racemic cyclopropanation of pyrone 1 or pyridinone 378

Under nitrogen atmosphere pyrone **1** or pyridinone **378** (1.0 equiv) and $Rh_2(OAc)_4$ (2.5 mol% or 1.0 mol%) were dissolved in dry toluene (0.5 M). A solution of methyl 2-diazo-2-phenylacetate (**376**) (3.0 equiv or 2.0 equiv) in dry toluene (1.1 M) was added dropwise at room temperature for the duration of 1.5 h using a syringe pump. After complete addition, the mixture was stirred at room temperature for 30 min. The reaction mixture was filtered through a short pad of silica and washed with EA. The solvent was removed under reduced pressure and the crude product was purified by flash column chromatography (PE:EA = 4:1 to 2:1).

Methyl 3-oxo-7-phenyl-2-oxabicyclo[4.1.0]hept-4-ene-7-carboxylate (377a)

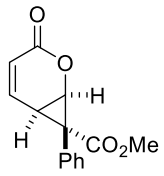

Following general procedure **J**, reaction of 2-pyrone (**1**) (480 mg, 5.00 mmol, 1.0 equiv), $Rh_2(OAc)_4$ (55.2 mg, 125 µmol, 2.5 mol%) and methyl 2-diazo-2-phenylacetate (**376**) (2.64 g, 15.0 mmol, 3.0 equiv) yielded **377a** as a white solid (916 mg, 3.75 mmol, 75%).

$\mathbf{R_f}$ = 0.33 (PE:EA = 2:1); **mp** 121 − 122 °C; **^{1}H NMR** (400 MHz, $CDCl_3$) δ_H = 7.35 – 7.27 (m, 3H), 7.25 – 7.05 (m, 2H), 6.90 (ddd, *J* = 10.0, 5.5, 1.0 Hz, 1H), 5.60 (d, *J* = 10.0 Hz, 1H), 4.99 (dd, *J* = 7.0, 1.0 Hz, 1H), 3.66 (s, 3H), 2.84 (dd, *J* = 7.0, 5.6 Hz, 1H); **^{13}C NMR** (101 MHz, $CDCl_3$) δ_C = 171.9, 159.3, 141.9, 133.8, 128.7, 128.5, 127.9, 121.0, 65.2, 53.3, 36.8, 25.4; **IR**

(ν/cm^{-1}): 3030, 2955, 1714, 1435, 1330, 1244, 1136, 1062, 864, 820, 700; **HRMS** (APCI) *m/z* calculated for $C_{14}H_{13}O_4$ [MH$^+$]: 245.0808, found: 245.0810.

Methyl 3-oxo-7-phenyl-2-tosyl-2-azabicyclo[4.1.0]hept-4-ene-7-carboxylate (377b)

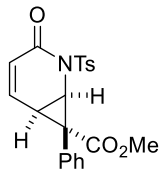

Following general procedure **J**, reaction of 2-pyridinone (**378**) (1.25 g, 5.00 mmol, 1.0 equiv), $Rh_2(OAc)_4$ (22.1 mg, 50.0 µmol, 1.0 mol%) and methyl 2-diazo-2-phenylacetate (**376**) (1.76 g, 10.0 mmol, 2.0 equiv) yielded **377b** as a white solid (1.89 g, 4.76 mmol, 95%).

R$_f$ = 0.28 (PE:EA = 2:1); **mp** 178 − 179 °C; **^{1}H NMR** (400 MHz, $CDCl_3$) δ_H =7.98 (d, *J* = 8.3 Hz, 2H), 7.35 – 7.20 (m, 7H), 6.80 (dd, *J* = 9.9, 5.2 Hz, 1H), 5.52 (d, *J* = 9.9 Hz, 1H), 4.81 (d, *J* = 9.0 Hz, 1H), 3.69 (s, 3H), 3.00 (dd, *J* = 9.0, 5.3 Hz, 1H), 2.43 (s, 3H); **^{13}C NMR** (101 MHz, $CDCl_3$) δ_C = 172.5, 159.5, 145.4, 139.8, 135.7, 133.7, 129.5, 129.0, 128.5, 128.47, 128.43, 125.7, 53.4, 46.7, 35.3, 26.9, 21.8; **IR** (ν/cm^{-1}): 3063, 2955, 1692, 1595, 1435, 1360, 1252, 1170, 1092, 991, 820, 708; **HRMS** (ESI) *m/z* calculated for $C_{21}H_{20}NO_5S$ [MH$^+$]: 398.1057, found: 398.1062.

General procedure K. Enantioselective cyclopropanation of pyrone 1 and pyridinone 378

Pyrone **1** or pyridinone **378** (500 µmol, 1.0 equiv) and Rh_2(*R*-PTAD)$_4$ (3.90 mg, 2.50 µmol, 0.5 mol%) were dissolved in dry DCM (1.0 mL) under nitrogen atmosphere. The mixture was cooled to 0 °C and a solution of 2,2,2-trichloroethyl 2-(4-bromophenyl)-2-diazoacetate (**379**) (372 mg, 1.00 mmol, 2.0 equiv) in dry DCM (0.9 mL) was added dropwise for the duration of 1.5 h using a syringe pump. After complete addition, the solvent was removed under reduced pressure and the crude product was purified by flash column chromatography (PE:EA = 4:1 to 2:1).

2,2,2-Trichloroethyl 7-(4-bromophenyl)-3-oxo-2-oxabicyclo[4.1.0]hept-4-ene-7-carboxylate (380a)

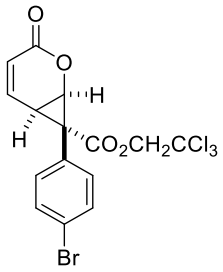

Following the general procedure **K**, pyrone **1** (48.0 mg, 500 µmol, 1.0 equiv) was employed to afford **380a** as a white solid (216 mg, 490 µmol, 98%).

R_f = 0.39 (PE:EA = 2:1); **^{1}H NMR** (400 MHz, $CDCl_3$) δ_H =7.50 – 7.41 (m, 2H), 7.08 (d, *J* = 8.0 Hz, 2H), 6.92 (ddd, *J* = 10.0, 5.5, 1.0 Hz, 1H), 5.69 (d, *J* = 10.0 Hz, 1H), 5.08 (dd, *J* = 7.1, 1.0 Hz, 1H), 4.73 (d, *J* = 11.9 Hz, 1H), 4.66 (d, *J* = 11.9 Hz, 1H), 2.93 (dd, *J* = 7.1, 5.5 Hz, 1H); **^{13}C NMR** (101 MHz, $CDCl_3$) δ_C = 169.2, 158.6, 141.1, 135.4, 132.0, 126.2, 123.2, 121.7, 94.4, 74.7, 65.0, 36.2, 25.5; **Chiral HPLC** 93% *ee*.[f]

2,2,2-Trichloroethyl 7-(4-bromophenyl)-3-oxo-2-tosyl-2-azabicyclo[4.1.0]hept-4-ene-7-carboxylate (380b)

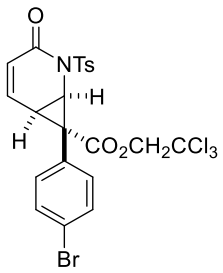

Following general procedure **K**, pyridinone **379** (125 mg, 500 µmol, 1.0 equiv) was employed to afford **380b** as a white solid (294 mg, 495 µmol, 99%).

R_f = 0.37 (PE:EA = 2:1); **^{1}H NMR** (400 MHz, $CDCl_3$) δ_H =7.97 (d, *J* = 8.4 Hz, 2H), 7.47 – 7.42 (m, 2H), 7.36 – 7.31 (m, 2H), 7.14 (d, *J* = 8.0 Hz, 2H), 6.82 (ddd, *J* = 9.9, 5.3, 0.8 Hz, 1H), 5.61 (d, *J* = 9.9 Hz, 1H), 4.87 (dd, *J* = 9.1, 0.7 Hz, 1H), 4.78 (d, *J* = 11.9 Hz, 1H), 4.72 (d, *J* = 11.9 Hz, 1H), 3.10 (dd, *J* = 9.1, 5.2 Hz, 1H), 2.44 (s, 3H); **^{13}C NMR** (101 MHz, $CDCl_3$) δ_C =

[f] The complete characterization and HPLC chromatogram of this molecule can be viewed in the Ph.D. thesis of Jiantao Fu (Working group of Prof. Huw Davies, Emory University, Atlanta, USA).

170.0, 159.1, 145.7, 139.0, 135.3, 131.9, 129.6, 129.0, 126.7, 126.4, 123.1, 94.5, 74.8, 47.0, 34.8, 27.0, 21.8; **Chiral HPLC** 95% *ee*.[g]

(2-Hydroxy-1-phenylcyclopent-4-ene-1,3-diyl)dimethanol (411)

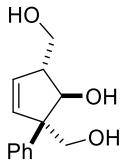

Under nitrogen atmosphere cyclopropanated pyrone **377a** (100 mg, 409 µmol, 1.0 equiv) was dissolved in dry DCM (8.0 mL) and cooled to −78 °C. DIBAL-H solution (1.2 M in toluene, 1.19 mL, 1.43 mmol, 3.5 equiv) was added dropwise and the mixture was stirred at −78 °C for 4 h. The reaction mixture was allowed to warm up to ambient temperature and quenched with saturated $NaHCO_3$ solution (4.0 mL). Saturated Rochelle salt solution (6.0 mL) was added and the mixture was stirred for 30 min at room temperature. The phases were separated and the aqueous phase was extracted with EA (6×). The combined organic phases were dried over Na_2SO_4 and the solvent was removed under reduced pressure. The crude product was purified by flash column chromatography (DCM:MeOH = 19:1 to 9:1) to yield **411** as yellowish oil (56.6 mg, 257 µmol, 63%).

R_f = 0.44 (DCM:MeOH = 19:1); **^{1}H NMR** (300 MHz, $CDCl_3$) δ_H = 7.42 – 7.29 (m, 5H), 6.06 (dd, *J* = 6.1, 2.5 Hz, 1H), 5.95 (dd, *J* = 6.0, 2.0 Hz, 1H), 4.49 (d, *J* = 6.1 Hz, 1H), 3.85 – 3.65 (m, 4H), 3.16 – 3.04 (m, 1H), 2.76 (s, 1H), 2.03 (s, 1H), 1.93 (s, 1H); **^{13}C NMR** (101 MHz, $CDCl_3$) δ_C = 138.9, 133.5, 133.3, 128.9, 128.3, 127.5, 77.3, 68.7, 64.4, 61.8, 51.8; **IR** (ν/cm^{-1}): 3377, 3056, 2926, 2881, 1703, 1420, 1360, 1222, 1062, 1021, 760, 700; **HRMS** (APCI) *m/z* calculated for $C_{13}H_{17}O_3$ [MH^+]: 221.1172, found: 221.1171.

[g] The complete characterization and HPLC chromatogram of this molecule can be viewed in the Ph.D. thesis of Jiantao Fu (Working group of Prof. Huw Davies, Emory University, Atlanta, USA).

4 Atypical reactivity of anthracene derivatives

1,5-Dimethoxy-9,10-anthraquinone (427)[264]

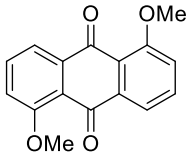

1,5-dihydroxy-9,10-anthraquinone (**426**) (8.00 g, 33.3 mmol, 1.0 equiv) and K_2CO_3 (13.4 g, 96.6 mmol, 2.9 equiv) were dissolved in acetone (42 mL). Dimethyl sulfate (9.24 g, 73.2 mmol, 2.2 equiv) was added and the mixture was stirred under reflux conditions for 48 h. The solvent was removed under reduced pressure and the crude product was purified by flash column chromatography (DCM) to afford **427** as a yellow solid (6.26 g, 23.3 mmol, 70%).

^{1}H NMR (300 MHz, $CDCl_3$) δ_H = 8.01 – 7.78 (m, 2H), 7.77 – 7.51 (m, 2H), 7.38 – 7.09 (m, 2H), 4.13 – 3.82 (m, 6H); **^{13}C NMR** (75 MHz, $CDCl_3$) δ_C = 182.8, 159.8, 137.5, 135.1, 120.9, 119.8, 116.8, 56.6.

1,5-Bis(*N*,*N*-dimethylamino)anthracene (419c)

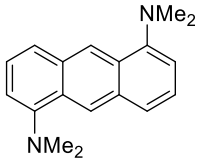

Under nitrogen atmosphere 1,5-diaminoanthracene (**429**) (2.00 g, 9.60 mmol, 1.0 equiv) and methyl iodide (5.98 mL, 96.0 mmol, 10 equiv) were dissolved in dry THF (100 mL) and the resulting solution was cooled to 0 °C. At this temperature NaH (60% dispersion in mineral oil, 3.84 g, 96.0 mmol, 10 equiv) was added in portions and the reaction mixture was stirred at room temperature for 14 h, followed by stirring under reflux conditions for 18 h. The mixture was cooled to 0 °C and carefully quenched with water (50 mL). THF was removed under reduced pressure and the remaining aqueous phase was extracted with DCM (3×). The combined organic phases were washed with brine and dried over $MgSO_4$. The solvent was removed under reduced pressure and the crude product was purified by flash column chromatography (PE:DCM = 3:1) to yield **419c** as a yellow solid (1.52 g, 5.75 mmol, 60%).

R_f = 0.50 (PE:DCM = 7:3); **mp** 144 − 145 °C; **^{1}H NMR** (300 MHz, $CDCl_3$) δ_H =8.78 (d, *J* = 3.5 Hz, 2H), 7.75 (d, *J* = 8.5 Hz, 2H), 7.39 (dd, *J* = 10.4, 5.2 Hz, 2H), 7.02 (d, *J* = 7.2 Hz, 2H), 3.01 (s, 12H); **^{13}C NMR** (75 MHz, $CDCl_3$) δ_C = 150.6, 132.7, 127.5, 125.1, 123.7, 123.5, 112.6,

45.2; **IR** (ν/cm^{-1}): 3049, 2981, 2944, 2862, 2832, 2788, 1610, 1543, 1453, 1349, 1189, 1140, 1077, 916, 793, 730; **HRMS** (ESI) *m/z* calculated for $C_{18}H_{21}N_2$ [MH$^+$]: 265.1699, found: 265.1702.

1,5-Di(pyrrolidin-1-yl)anthracene (419d)

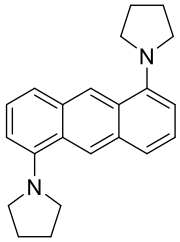

1,5-Diaminoanthracene (**429**) (2.00 g, 9.60 mmol, 1.0 equiv) and K_2CO_3 (5.31 g, 38.4 mmol, 4.0 equiv) were dissolved in dioxane/water (1:1, 40 mL) and 1,4-dibromobutane (3.40 mL, 28.8 mmol, 3.0 equiv) was added. The reaction mixture was stirred under reflux conditions for 24 h. Additional 1,4-dibromobutane (3.40 mL,28.8 mmol, 3.0 equiv) was appended and the mixture was stirred under reflux conditions for 24 h. The reaction solution was cooled to ambient temperature and water (40 mL) was added. The phases were separated and the aqueous phase was extracted with DCM (3×). The combined organic phases were dried over $MgSO_4$ and the solvent was removed under reduced pressure. The crude product was purified by flash column chromatography (PE:DCM = 9:1 to 7:3) to afford **419d** as a yellow solid (1.49 g, 4.71 mmol, 49%).

R$_f$ = 0.58 (PE:DCM = 7:3); **mp** 194 − 195 °C; **^{1}H NMR** (300 MHz, $CDCl_3$) δ_H = 8.74 (s, 2H), 7.65 (d, *J* = 8.4 Hz, 2H), 7.45 – 7.28 (m, 2H), 6.91 (d, *J* = 7.3 Hz, 2H), 3.58 – 3.39 (m, 8H), 2.17 – 2.01 (m, 8H); **^{13}C NMR** (75 MHz, $CDCl_3$) δ_C = 147.3, 132.4, 127.1, 125.1, 123.9, 122.1, 109.7, 52.8, 25.0; **IR** (ν/cm^{-1}): 3067, 2948, 2873, 2821, 1610, 1539, 1453, 1353, 1110, 920, 793, 730; **HRMS** (ESI) *m/z* calculated for $C_{22}H_{25}N_2$ [MH$^+$]: 317.2012, found: 317.2013.

1-(Pyrrolidine-1-yl)anthracene (419e)

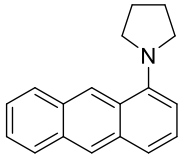

1-Aminoanthracene (**433**) (9.79 g, 50.7 mmol, 1.0 equiv) and K_2CO_3 (14.0 g, 101 mmol, 2.0 equiv) were dissolved in dioxane/water (1:1, 210 mL) and 1,4-dibromobutane (8.97 mL, 76.0 mmol, 1.5 equiv) was added. The reaction mixture was stirred under reflux conditions for 24 h. Additional 1,4-dibromobutane (8.97 mL, 76.0 mmol, 1.5 equiv) was appended and the

mixture was stirred under reflux conditions for 24 h. The reaction solution was cooled to ambient temperature and water (100 ml) was added. The phases were separated and the aqueous phase was extracted with DCM (6×). The combined organic phases were dried over $MgSO_4$ and the solvent was removed under reduced pressure. The crude product was purified by flash column chromatography (PE:DCM = 9:1 to 7:3 to 1:1) to give rise to **419e** as a bright yellow solid (7.14 g, 28.9mmol, 57%).

R_f = 0.24 (PE:DCM = 7:3); **mp** 60 − 61 °C; **^{1}H NMR** (400 MHz, $CDCl_3$) δ_H = 8.85 (s, 1H), 8.41 (s, 1H), 8.13 – 7.96 (m, 2H), 7.66 (d, *J* = 8.4 Hz, 1H), 7.54 – 7.45 (m, 2H), 7.39 (dd, *J* = 8.4, 7.3 Hz, 1H), 6.95 (d, *J* = 7.3 Hz, 1H), 3.56 – 3.44 (m, 4H), 2.17 – 2.06 (m, 4H); **^{13}C NMR** (101 MHz, $CDCl_3$) δ_C = 147.5, 133.3, 131.4, 130.8, 128.8, 127.7, 127.4, 126.3, 125.5, 125.0, 123.7, 121.7, 109.9, 52.9, 24.9; **IR** (ν/cm^{-1}): 3049, 2996, 2967, 2870, 2810, 1613, 1535, 1453, 1394, 1349, 1230, 1129, 887, 749; **HRMS** (EI) *m/z* calculated for $C_{18}H_{17}N$ [M^+]: 247.1355, found: 247.1350.

General procedure L. [4+2]-Cycloaddition of anthracenes

In a pressure tube anthracene **419** (1.0 equiv) and dienophile **A**-**E** (1.1 equiv) were dissolved in toluene (0.5 M) and the reaction mixture was stirred at 150 °C until complete conversion of starting material was observed (monitored by TLC). The solvent was removed under reduced pressure and the crude product was purified by flash column chromatography.

***Syn*-dimethyl-1,5-dimethoxy-9,10-dihydro-9,10-ethanoanthracene-11,12-dicarboxylate (430bA)**

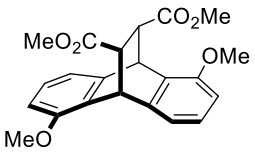

Following general procedure **L**, reaction of anthracene **419b** (80.0 mg, 335 µmol, 1.0 equiv) and dimethyl fumarate (**A**) (53.0 mg, 369 µmol, 1.1 equiv) for 24 h afforded **430bA** after purification by flash column chromatography (DCM to DCM:EA = 99:1) as a white solid (122 mg, 318 µmol, 95%).

R_f = 0.52 (DCM:EA = 99:1); **mp** 162 − 163 °C; **^{1}H NMR** (400 MHz, $CDCl_3$) δ_H = 7.10 – 6.99 (m, 3H), 6.91 (d, *J* = 7.3 Hz, 1H), 6.68 (d, *J* = 8.2 Hz, 2H), 5.22 – 5.17 (m, 2H), 3.85 (s, 3H), 3.82 (s, 3H), 3.64 (s, 3H), 3.63 (s, 3H), 3.37 (dt, *J* = 5.5, 1.3 Hz, 2H); **^{13}C NMR** (101 MHz, $CDCl_3$) δ_C = 173.18, 173.15, 155.1, 154.0, 144.2, 142.5, 129.9, 128.2, 127.2, 127.0, 117.5,

116.6, 109.1, 108.9, 55.7, 55.5, 52.2, 52.1, 47.5, 47.4, 40.0, 39.5; **IR** (ν/cm^{-1}): 3000, 2952, 2840, 1729, 1587, 1483, 1438, 1263, 1200, 1095, 1021, 909, 782, 730; **HRMS** (ESI) *m/z* calculated for $C_{22}H_{23}O_6$ [MH^+]: 383.1489, found: 383.1490.

1,5-Dimethoxy-9,10-dihydro-9,10-[3,4]furanoanthracene-12,14-dione (430bB)

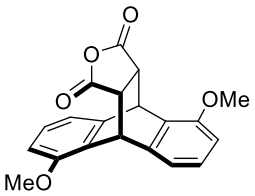

Following general procedure **L**, reaction of anthracene **419b** (80.0 mg, 335 µmol, 1.0 equiv) and maleic anhydride (**B**) (36.0 mg, 369 µmol, 1.1 equiv) for 2 h afforded **430bB** after recrystallization from DCM as a white solid (109 mg, 324 µmol, 97%).

R_f = 0.69 (DCM:EA = 99:1); **mp** 263 − 264 °C; **^{1}H NMR** (400 MHz, $CDCl_3$) δ_H = 7.14 (ddd, *J* = 8.3, 7.4, 4.2 Hz, 2H), 7.03 (d, *J* = 7.4 Hz, 1H), 6.98 (d, *J* = 7.4 Hz, 1H), 6.75 (ddd, *J* = 8.4, 5.7, 0.9 Hz, 2H), 5.33 (dd, *J* = 17.1, 3.0 Hz, 2H), 3.86 (s, 3H), 3.84 (s, 3H), 3.50 – 3.41 (m, 2H); **^{13}C NMR** (101 MHz, $CDCl_3$) δ_C = 170.7, 170.6, 155.0, 154.6, 142.8, 140.2, 128.6, 128.5, 127.8, 126.4, 117.9, 117.0, 110.2, 109.5, 55.9, 55.6, 47.8, 47.7, 38.5, 38.4; **IR** (ν/cm^{-1}): 3011, 2959, 2922, 2840, 1863, 1781, 1587, 1483, 1267, 1215, 1099, 939, 786, 726; **HRMS** (EI) *m/z* calculated for $C_{20}H_{16}O_5$ [M^+]: 336.0992, found: 336.0998.

1,5-Dimethoxy-13-phenyl-9,10-dihydro-9,10-[3,4]epipyrroloanthracene-12,14-dione (430bC)

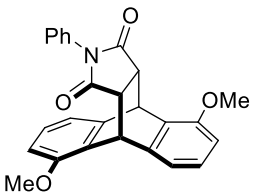

Following general procedure **L**, reaction of anthracene **419b** (80.0 mg, 335 µmol, 1.0 equiv) and *N*-phenylmaleimide (**C**) (64.0 mg, 369 µmol, 1.1 equiv) for 2 h afforded **430bC** after recrystallization from DCM as a white solid (137 mg, 333 µmol, 99%).

R_f = 0.41 (DCM:EA = 99:1); **mp** 274 − 275 °C; **^{1}H NMR** (400 MHz, $CDCl_3$) δ_H = 7.35 – 7.27 (m, 3H), 7.16 (ddd, *J* = 8.1, 7.3, 4.6 Hz, 2H), 7.08 (d, *J* = 7.3 Hz, 1H), 7.01 (d, *J* = 7.3 Hz, 1H), 6.77 (ddd, *J* = 8.2, 5.8, 0.9 Hz, 2H), 6.60 – 6.52 (m, 2H), 5.42 (d, *J* = 3.3 Hz, 1H), 5.38 (d, *J* = 3.3 Hz, 1H), 3.88 (s, 3H), 3.81 (s, 3H), 3.32 (dq, *J* = 8.4, 3.3 Hz, 2H); **^{13}C NMR** (101 MHz,

$CDCl_3$) δ_C = 176.3, 176.1, 155.1, 154.6, 143.5, 140.8, 131.7, 129.3, 129.1, 128.7, 127.8, 127.5, 127.1, 126.6, 118.0, 117.0, 109.8, 109.2, 56.1, 55.6, 46.9, 46.7, 38.8; **IR** (ν/cm^{-1}): 3067, 2996, 2937, 2899, 2836, 2255, 1777, 1707, 1584, 1479, 1382, 1263, 1095, 909, 723; **HRMS** (ESI) *m/z* calculated for $C_{26}H_{22}NO_4$ [MH^+]: 412.1543, found: 412.1547.

1,5-Bis(dimethylamino)-13-phenyl-9,10-dihydro-9,10-[3,4]epipyrroloanthracene-12,14-dione (430cC)

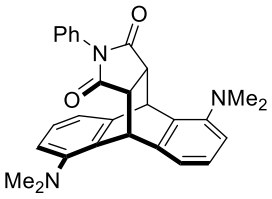

Following general procedure **L**, reaction of anthracene **419c** (132 mg, 500 µmol, 1.0 equiv) and *N*-phenylmaleimide (**C**) (95.0 mg, 550 µmol, 1.1 equiv) for 30 min afforded **430cC** after purification by flash column chromatography (DCM:EA = 99:1 to 1:1) as a white solid (215 mg, 492 µmol, 98%).

R_f = 0.46 (DCM:EA = 99:1); **mp** 209 − 210 °C; **^{1}H NMR** (400 MHz, $CDCl_3$) δ_H = 7.43 – 7.37 (m, 3H), 7.28 – 7.22 (m, 3H), 7.17 (dd, *J* = 7.3, 1.1 Hz, 1H), 7.07 (dd, *J* = 8.1, 1.1 Hz, 1H), 7.03 (dd, *J* = 6.4, 2.8 Hz, 1H), 6.68 – 6.60 (m, 2H), 5.54 (d, *J* = 3.1 Hz, 1H), 5.41 (d, *J* = 3.0 Hz, 1H), 3.45 – 3.37 (m, 2H), 2.90 (s, 6H), 2.84 (s, 6H); **^{13}C NMR** (101 MHz, $CDCl_3$) δ_C = 176.3, 175.9, 150.6, 150.1, 142.6, 139.6, 135.2, 133.5, 131.7, 129.0, 128.6, 127.3, 126.9, 126.6, 119.8, 118.6, 117.2, 116.5, 47.0, 46.8, 45.1, 44.9, 41.5, 41.2; **IR** (ν/cm^{-1}): 3063, 2985, 2944, 2862, 2784, 2251, 1777, 1710, 1584, 1483, 1382, 1319, 1189, 909, 790, 726; **HRMS** (ESI) *m/z* calculated for $C_{28}H_{28}N_3O_2$ [MH^+]: 438.2176, found: 438.2181.

13-Phenyl-1,5-di(pyrrolidin-1-yl)-9,10-dihydro-9,10-[3,4]epipyrroloanthracene-12,14-dione (430dC)

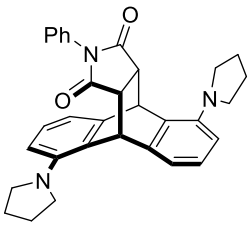

Following general procedure **L**, reaction of anthracene **419d** (158 mg, 500 µmol, 1.0 equiv) and *N*-phenylmaleimide (**C**) (95.0 mg, 550 µmol, 1.1 equiv) for 30 min afforded **430dC** after

purification by flash column chromatography (DCM:EA = 99:1 to 1:1) as a white solid (223 mg, 460 µmol, 92%).

R_f = 0.52 (DCM:EA = 99:1); **mp** 225 − 226 °C; **^{1}H NMR** (400 MHz, $CDCl_3$) δ_H =7.31 – 7.22 (m, 3H), 7.08 – 6.98 (m, 2H), 6.94 (d, *J* = 7.2 Hz, 1H), 6.79 (d, *J* = 7.2 Hz, 1H), 6.71 (d, *J* = 8.2 Hz, 1H), 6.64 (d, *J* = 8.3 Hz, 1H), 6.60 – 6.51 (m, 2H), 5.44 (d, *J* = 2.7 Hz, 1H), 5.22 (d, *J* = 2.3 Hz, 1H), 3.58 – 3.46 (m, 2H), 3.46 – 3.38 (m, 2H), 3.31 – 3.17 (m, 6H), 2.03 – 1.90 (m, 6H), 1.90 – 1.77 (m, 2H); **^{13}C NMR** (101 MHz, $CDCl_3$) δ_C = 176.6, 176.4, 146.7, 146.4, 143.7, 140.5, 131.8, 130.4, 129.0, 128.5, 127.2, 126.8, 126.69, 126.65, 115.8, 115.6, 113.94, 113.91, 52.0, 51.8, 47.1, 47.0, 43.2, 42.8, 25.6, 25.4; **IR** (ν/cm^{-1}): 3063, 2967, 2870, 2825, 2251, 1774, 1710, 1580, 1476, 1382, 1356, 1185, 909, 726; **HRMS** (ESI) *m/z* calculated for $C_{32}H_{32}N_3O_2$ [MH^+]: 490.2489, found: 490.2496.

Methyl 1,5-di(pyrrolidin-1-yl)-9,10-dihydro-9,10-ethenoanthracene-11-carboxylate (430dE)

Methyl 1,5-di(pyrrolidin-1-yl)-1,4-dihydro-1,4-ethenoanthracene-2-carboxylate (431dE)

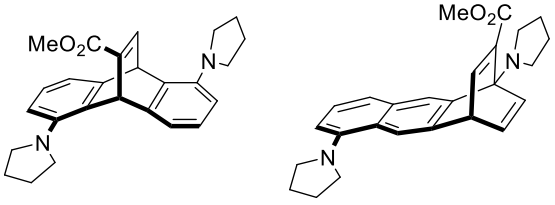

Following general procedure **L**, reaction of anthracene **419d** (200 mg, 632 µmol, 1.0 equiv) and methyl propiolate (**E**) (62.0 µL, 695 µmol, 1.1 equiv) for 24 h afforded after purification by flash column chromatography (DCM:EA = 19:1 to 3:2) **430dE** as a white solid (34.9 mg, 87.0 µmol, 14%) and **431dE** as a white solid (142 mg, 355 µmol, 56%).

430dE: R_f = 0.56 (DCM:EA = 19:1); **mp** 118 − 119 °C; **^{1}H NMR** (400 MHz, $CDCl_3$) δ_H =7.87 (dd, *J* = 6.3, 1.9 Hz, 1H), 6.98 (d, *J* = 7.2 Hz, 1H), 6.91 – 6.83 (m, 3H), 6.55 (dd, *J* = 8.3, 1.0 Hz, 1H), 6.51 (d, *J* = 8.2 Hz, 1H), 6.20 (d, *J* = 1.9 Hz, 1H), 5.69 (d, *J* = 6.4 Hz, 1H), 3.70 (s, 3H), 3.49 – 3.38 (m, 6H), 3.31 – 3.24 (m, 2H), 2.03 – 1.95 (m, 8H); **^{13}C NMR** (101 MHz, $CDCl_3$) δ_C = 165.5, 150.5, 147.7, 146.6, 146.2, 146.0, 144.9, 133.5, 132.9, 125.4, 125.3, 116.0, 114.9, 112.7, 112.5, 52.2, 51.9, 51.7, 49.1, 47.8, 25.8, 25.5.; **IR** (ν/cm^{-1}): 3034, 2944, 2866, 1710, 1625, 1580, 1461, 1330, 1237, 1092, 730; **HRMS** (ESI) *m/z* calculated for $C_{26}H_{29}N_2O_2$ [MH^+]: 401.2224, found: 401.2233.

431dE: $\mathbf{R_f}$ = 0.18 (DCM:EA = 3:2); **mp** 201 − 202 °C; **^{1}H NMR** (400 MHz, $CDCl_3$) δ_H =7.89 (s, 2H), 7.43 (d, *J* = 6.3 Hz, 1H), 7.39 (d, *J* = 8.1 Hz, 1H), 7.29 (t, *J* = 7.8 Hz, 1H), 7.00 (d, *J* = 3.8 Hz, 2H), 6.96 (d, *J* = 7.5 Hz, 1H), 4.95 – 4.85 (m, 1H), 3.70 (s, 3H), 3.37 – 3.21 (m, 8H), 2.08 – 1.98 (m, 8H); **^{13}C NMR** (101 MHz, $CDCl_3$) δ_C = 166.7, 148.7, 147.4, 146.0, 143.8, 141.2, 139.6, 138.5, 132.5, 125.7, 125.4, 122.2, 121.7, 117.5, 112.5, 52.8, 52.0, 51.3, 48.0, 26.0, 24.7; **IR** (ν/cm^{-1}): 3052, 2948, 2866, 2817, 1714, 1621, 1580, 1457, 1364, 1289, 1230, 1073, 894, 738; **HRMS** (ESI) *m/z* calculated for $C_{26}H_{29}N_2O_2$ [MH$^+$]: 401.2224, found: 401.2232.

***Syn*-dimethyl 1-(pyrrolidin-1-yl)-9,10-dihydro-9,10-ethanoanthracene-11,12-dicarboxylate (*syn*-430eA)**

***Anti*-dimethyl 1-(pyrrolidin-1-yl)-9,10-dihydro-9,10-ethanoanthracene-11,12-dicarboxylate (*anti*-430eA)**

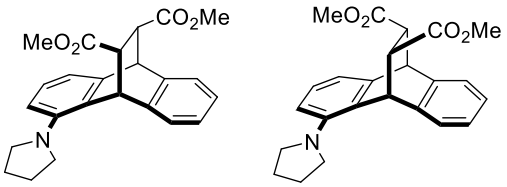

Following general procedure **L**, reaction of anthracene **419e** (200 mg, 809 µmol, 1.0 equiv) and dimethyl fumarate (**A**) (128 mg, 889 µmol, 1.1 equiv) for 24 h afforded after purification by flash column chromatography (DCM to DCM:EA = 19:1) *syn*-**430eA** as a white solid (147 mg, 370 µmol, 46%) and *anti*-**430eA** as a white solid (157 mg, 400 µmol, 50%).

syn-**430eA:** $\mathbf{R_f}$ = 0.77 (DCM:EA = 19:1); **mp** 138 − 139 °C; **^{1}H NMR** (400 MHz, $CDCl_3$) δ_H = 7.52 – 7.47 (m, 1H), 7.42 – 7.39 (m, 1H), 7.31 – 7.22 (m, 2H), 7.16 (dd, *J* = 8.2, 7.2 Hz, 1H), 7.03 (d, *J* = 7.1 Hz, 1H), 6.78 (dd, *J* = 8.3, 1.0 Hz, 1H), 5.46 (d, *J* = 2.9 Hz, 1H), 4.84 (d, *J* = 2.8 Hz, 1H), 3.76 (s, 3H), 3.74 (s, 3H), 3.69 – 3.60 (m, 3H), 3.51 (dd, *J* = 4.7, 2.9 Hz, 1H), 3.36 – 3.28 (m, 2H), 2.25 – 2.13 (m, 2H), 2.10 – 1.98 (m, 2H); **^{13}C NMR** (101 MHz, $CDCl_3$) δ_C = 173.1, 173.0, 146.3, 143.7, 142.5, 140.8, 128.6, 126.9, 126.3, 126.2, 124.7, 123.2, 115.5, 113.7, 52.2, 51.9, 51.8, 47.8, 47.6, 47.4, 43.5, 25.7; **IR** (ν/cm^{-1}): 3052, 3022, 2952, 2870, 1729, 1580, 1479, 1435, 1356, 1259, 1192, 1006, 868, 771; **HRMS** (ESI) *m/z* calculated for $C_{24}H_{26}NO_4$ [MH$^+$]: 392.1856, found: 392.1858.

anti-**430eA:** $\mathbf{R_f}$ = 0.59 (DCM:EA = 19:1); **mp** 106 − 107 °C; **^{1}H NMR** (400 MHz, $CDCl_3$) δ_H = 7.51 – 7.46 (m, 1H), 7.44 – 7.41 (m, 1H), 7.30 – 7.22 (m, 2H), 7.13 (dd, *J* = 8.2, 7.2 Hz, 1H), 6.96 (d, *J* = 7.1 Hz, 1H), 6.84 (dd, *J* = 8.3, 1.0 Hz, 1H), 5.37 (d, *J* = 2.6 Hz, 1H), 4.85 (d, *J* = 2.6 Hz, 1H), 3.81 (s, 3H), 3.78 (s, 3H), 3.61 (dd, *J* = 5.0, 2.6 Hz, 1H), 3.58 – 3.43 (m, 5H), 2.21

– 2.09 (m, 4H); **^{13}C NMR** (101 MHz, $CDCl_3$) δ_C = 173.0, 172.9, 146.0, 142.6, 141.8, 140.7, 130.9, 126.4, 126.2, 126.1, 124.3, 123.6, 116.8, 113.8, 52.2, 52.0, 47.9, 47.6, 47.3, 42.9, 25.4; **IR** (ν/cm^{-1}): 3019, 2955, 2577, 2814, 1729, 1587, 1476, 1435, 1304, 1177, 1010, 872, 782, 738; **HRMS** (ESI) *m/z* calculated for $C_{24}H_{26}NO_4$ [MH^+]: 392.1856, found: 392.1863.

***Exo*-1-(pyrrolidin-1-yl)-9,10-dihydro-9,10-[3,4]furanoanthracene-12,14-dione (*exo*-430eB)**

***Endo*-1-(pyrrolidin-1-yl)-9,10-dihydro-9,10-[3,4]furanoanthracene-12,14-dione (*endo*-430eB)**

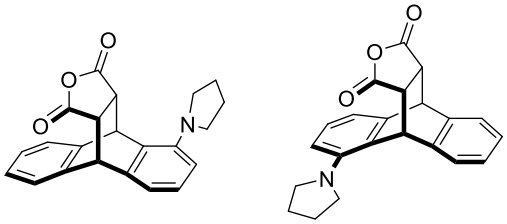

Following general procedure **L**, reaction of anthracene **419e** (200 mg, 809 µmol, 1.0 equiv) and maleic anhydride (**B**) (87.0 mg, 889 µmol, 1.1 equiv) for 30 min afforded a crude mixture of *exo*-**430eB** and *endo*-**430eB** (NMR yield > 99%, ratio *endo*-**430eB**/*exo*-**430eB** = 67:33) as a white solid. During purification by flash column chromatography (DCM to DCM:EA = 19:1) decomposition of both products was observed and only *endo*-**430eB** could be isolated as a white solid (94.0 mg, 272 µmol, 34%).

endo-**430eB: R_f** = 0.63 (DCM:EA = 19:1); **mp** 218 − 219 °C; **^{1}H NMR** (400 MHz, $CDCl_3$) δ_H = 7.40 – 7.30 (m, 2H), 7.24 – 7.15 (m, 2H), 7.06 (t, *J* = 7.7 Hz, 1H), 6.93 (d, *J* = 7.2 Hz, 1H), 6.74 (d, *J* = 8.2 Hz, 1H), 5.29 (d, *J* = 3.1 Hz, 1H), 4.77 (d, *J* = 3.2 Hz, 1H), 3.57 – 3.37 (m, 4H), 3.33 – 3.18 (m, 2H), 2.08 – 1.92 (m, 4H); **^{13}C NMR** (101 MHz, $CDCl_3$) δ_C = 170.9, 170.8, 146.7, 142.4, 138.6, 129.3, 127.6, 127.4, 125.2, 124.8, 116.3, 114.6, 52.2, 48.1, 48.0, 46.1, 42.1, 25.5; **IR** (ν/cm^{-1}): 3026, 2970, 2825, 1859, 1774, 1580, 1476, 1356, 1222, 1077, 928, 756; **HRMS** (EI) *m/z* calculated for $C_{22}H_{19}NO_3$ [M^+]: 345.1359, found: 345.1353.

***Exo*-13-phenyl-4-(pyrrolidin-1-yl)-9,10-dihydro-9,10-[3,4]epipyrroloanthracene-12,14-dione (*exo*-430eC)**

***Endo*-13-phenyl-4-(pyrrolidin-1-yl)-9,10-dihydro-9,10-[3,4]epipyrroloanthracene-12,14-dione (*endo*-430eC)**

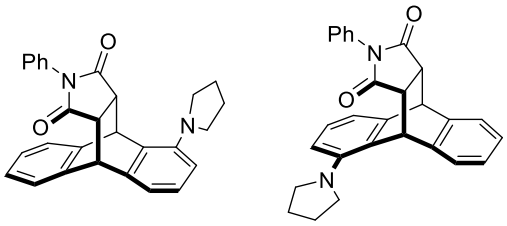

Following general procedure **L**, reaction of anthracene **419e** (200 mg, 809 µmol, 1.0 equiv) and *N*-phenylmaleimide (**C**) (154 mg, 889 µmol, 1.1 equiv) for 30 min afforded an inseparable mixture of *exo*-**430eC** and *endo*-**430eC** (ratio *endo*-**430eC**/*exo*-**430eC** = 67:33) as a white solid (324 mg, 771 µmol, 95%).

Characteristic signals of minor compound *exo*-**430eC** are marked in the proton NMR.

exo-**430eC** and *endo*-**430eC: mp** 177 − 178 °C; **^{1}H NMR** (400 MHz, $CDCl_3$) δ_H =7.50 – 7.13 (m, 13H), 7.05 (q, *J* = 7.5 Hz, 2H), 6.96 (d, *J* = 7.2 Hz, 1H), 6.81^{minor} (t, *J* = 3.7 Hz, 2H), 6.74 (d, *J* = 8.2 Hz, 1H), 6.67^{minor} (d, *J* = 8.3 Hz, 1H), 6.64 – 6.54 (m, 1H), 6.49 (dd, *J* = 7.0, 2.7 Hz, 2H), 5.51^{minor} (d, *J* = 3.2 Hz, 1H), 5.32 (d, *J* = 3.1 Hz, 1H), 4.82 (d, *J* = 3.3 Hz, 1H), 4.80^{minor} (d, *J* = 3.1 Hz, 1H), 3.54 (q, *J* = 7.8 Hz, 1H), 3.44 (q, *J* = 6.9 Hz, 2H), 3.40 – 3.15 (m, 6H), 2.06 – 1.92 (m, 5H), 1.92 – 1.81 (m, 1H); **^{13}C NMR** (101 MHz, $CDCl_3$) δ_C = 176.47, 176.42, 176.3, 176.1, 146.7, 146.5, 143.1, 141.9, 140.0, 139.1, 134.2, 131.7, 131.5, 130.0, 129.1, 129.09, 129.05, 128.7, 128.6, 127.9, 127.3, 127.05, 127.00, 126.66, 126.60, 126.5, 126.4, 126.0, 125.1, 124.7, 124.3, 123.6, 116.3, 116.2, 114.2, 114.1, 52.1, 51.8, 47.2, 47.1, 47.0, 46.5, 46.4, 42.4, 42.1, 25.6, 25.4; **IR** (ν/cm^{-1}): 3067, 2967, 2870, 2825, 2251, 1774, 1707, 1587, 1498, 1382, 1185, 909, 723; **HRMS** (ESI) *m/z* calculated for $C_{28}H_{25}N_2O_2$ [MH^+]: 421.1911, found 421.1913 (rt 2.584 min) and 421.1916 (rt 2.671 min).

Dimethyl 1-(pyrrolidin-1-yl)-1,4-dihydro-1,4-ethenoanthracene-2,3-dicarboxylate (431eD)

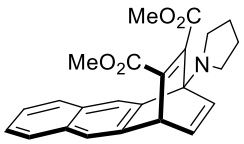

Following general procedure **L**, reaction of anthracene **419e** (282 mg, 1.14 mmol, 1.0 equiv) and DMAD (**D**) (154 µL, 1.25 mmol, 1.1 equiv) for 24 h afforded **431eD** after purification by flash column chromatography (DCM:EA = 19:1) as a white solid (403 mg, 1.03 mmol, 90%).

R_f = 0.33 (DCM:EA = 19:1); **mp** 159 − 160 °C; **^{1}H NMR** (400 MHz, $CDCl_3$) δ_H = 7.89 (s, 1H), 7.77 – 7.68 (m, 2H), 7.63 (s, 1H), 7.45 – 7.39 (m, 2H), 7.07 – 6.99 (m, 2H), 5.38 (dd, *J* = 5.9, 1.9 Hz, 1H), 3.80 (s, 3H), 3.74 (s, 3H), 3.45 – 3.34 (m, 4H), 2.06 – 1.98 (m, 4H); **^{13}C NMR** (101 MHz, $CDCl_3$) δ_C = 168.1, 163.8, 155.2, 142.6, 142.0, 141.8, 139.5, 139.0, 131.05, 131.02, 128.3, 127.2, 126.2, 125.9, 122.0, 121.1, 79.1, 52.7, 52.5, 51.4, 47.3, 26.4; **IR** (ν/cm^{-1}): 3034, 2952, 2870, 2836, 1722, 1628, 1595, 1427, 1312, 1237, 1203, 1110, 1051, 883, 749; **HRMS** (ESI) *m/z* calculated for $C_{24}H_{24}NO_4$ [MH^+]: 390.1700, found: 390.1700.

Methyl 4-(pyrrolidin-1-yl)-9,10-dihydro-9,10-ethenoanthracene-11-carboxylate (*syn*-430eE)

Methyl 1-(pyrrolidin-1-yl)-9,10-dihydro-9,10-ethenoanthracene-11-carboxylate (*anti*-430eE)

Methyl 1-(pyrrolidin-1-yl)-1,4-dihydro-1,4-ethenoanthracene-2-carboxylate (431eE)

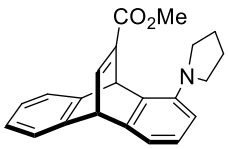

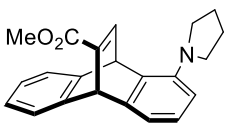

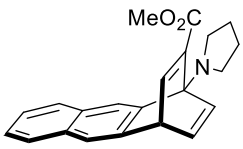

Following general procedure **L**, reaction of anthracene **419e** (200 mg, 809 µmmol, 1.0 equiv) and methyl propiolate (**E**) (79.0 µL, 889 µmol, 1.1 equiv) for 24 h afforded after purification by flash column chromatography (DCM:EA = 19:1 to 3:2) an inseparable mixture of *syn*-**430eE** and *anti*-**430eE** (ratio: *syn*-**430eE**/*anti*-**430eE** = 55:45) as a white solid (67.0 mg, 203 µmol, 25%) and pure **431eE** as a white solid (193 mg, 582 µmol, 72%).

Characteristic signals of minor compound *anti*-**430eE** are marked in the proton NMR.

syn-**430eE** and *anti*-**430eE: R_f** = 0.71 (DCM:EA = 19:1); **mp** 64 − 65 °C; **^{1}H NMR** (400 MHz, $CDCl_3$) δ_H = 7.91 (dd, *J* = 6.2, 1.8 Hz, 1H), 7.87^{minor} (dd, *J* = 6.3, 1.8 Hz, 1H), 7.42 – 7.31 (m, 4H), 7.05 – 6.95 (m, 5H), 6.94 – 6.86 (m, 3H), 6.60^{minor} (d, *J* = 8.1 Hz, 1H), 6.57 – 6.51 (m, 1H), 6.27 (d, *J* = 1.8 Hz, 1H), 5.77^{minor} (d, *J* = 6.3 Hz, 1H), 5.66^{minor} (d, *J* = 1.9 Hz, 1H), 5.21 (d, *J* = 6.2 Hz, 1H), 3.74 (s, 6H), 3.51 – 3.46 (m, 4H), 3.45 – 3.38^{minor} (m, 2H), 3.33 – 3.25^{minor} (m, 2H), 2.07 – 1.93 (m, 8H); **^{13}C NMR** (101 MHz, $CDCl_3$) δ_C = 165.5, 165.3, 150.4, 149.7, 147.2, 146.4, 146.3, 146.04, 146.02, 145.7, 145.14, 145.13, 144.5, 144.3, 134.7, 133.0, 132.4, 131.3, 125.58, 125.51, 124.95, 124.94, 124.8, 124.7, 123.7, 123.4, 123.3, 123.1, 116.4, 115.3, 112.9, 112.7, 52.7, 52.6, 52.1, 51.9, 51.84, 51.82, 51.1, 48.1, 47.1, 25.7, 25.4; **IR** (ν/cm^{-1}): 3063, 2948, 2870, 1707, 1617, 1587, 1435, 1330, 1244, 1214, 1066, 946, 745; **HRMS** (ESI) *m/z* calculated for $C_{22}H_{22}NO_2$ [MH^+]: 332.1645, found: 332.1651 (rt 2.485 min) and 332.1649 (rt 2.555 min).

431eE: R_f = 0.24 (DCM:EA = 3:2); **mp** 84 − 85 °C; **^{1}H NMR** (400 MHz, $CDCl_3$) δ_H = 7.93 (s, 1H), 7.78 – 7.73 (m, 1H), 7.69 – 7.64 (m, 1H), 7.52 (s, 1H), 7.44 – 7.38 (m, 3H), 7.03 – 6.97 (m, 2H), 4.93 – 4.83 (m, 1H), 3.71 (s, 3H), 3.38 – 3.23 (m, 4H), 2.11 – 1.99 (m, 4H); **^{13}C NMR** (101 MHz, $CDCl_3$) δ_C = 166.7, 148.4, 146.1, 144.1, 142.2, 139.6, 138.4, 131.1, 130.8, 128.2, 127.1, 125.9, 125.8, 121.2, 120.5, 52.0, 51.4, 47.5, 26.0; **IR** (ν/cm^{-1}): 3056, 2948, 2866, 1714, 1621, 1580, 1431, 1289, 1226, 1196, 1077, 883, 745; **HRMS** (ESI) *m/z* calculated for $C_{22}H_{22}NO_2$ [MH^+]: 332.1645, found: 332.1650.

1-Phenyl-3-(4-(pyrrolidin-1-yl)anthracen-1-yl)pyrrolidine-2,5-dione (434)

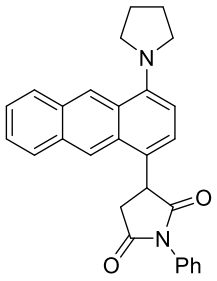

A sealed tube was charged with anthracene **419e** (100 mg, 400 µmol, 1.0 equiv), *N*-phenylmaleimide (**C**) (77.0 mg, 440 µmol, 1.1 equiv), $AlCl_3$ (162 mg, 1.21 mmol, 3.0 equiv) and $CHCl_3$ (5.0 mL). The mixture was dispersed in an ultrasonic bath for 1 min and afterwards stirred at room temperature for 3 h. The reaction was quenched with water (10 mL) and the aqueous phase was extracted with DCM (3×). The combined organic phases were washed with brine (1×), dried over anhydrous Na_2SO_4 and the solvent was removed under reduced pressure.

After purification by flash column chromatography (PE:DCM = 1:2 to DCM), pure **434** was obtained as a brownish solid (106 mg, 250 µmol, 62%).

R_f = 0.63 (DCM); **mp** 94 − 95 °C; **^{1}H NMR** (400 MHz, $CDCl_3$) δ_H = 8.88 (s, 1H), 8.33 (s, 1H), 8.06 – 7.96 (m, 2H), 7.56 – 7.44 (m, 7H), 7.28 (d, *J* = 7.7 Hz, 1H), 6.84 (d, *J* = 7.7 Hz, 1H), 4.95 (dd, *J* = 9.7, 4.8 Hz, 1H), 3.59 (dd, *J* = 18.5, 9.7 Hz, 1H), 3.51 – 3.41 (m, 4H), 3.04 (dd, *J* = 18.5, 4.9 Hz, 1H), 2.11 – 2.05 (m, 4H); **^{13}C NMR** (101 MHz, $CDCl_3$) δ_C = 177.6, 175.4, 148.6, 132.2, 131.6, 130.9, 130.5, 129.4, 128.8, 128.6, 128.0, 127.9, 126.6, 126.2, 125.9, 125.5, 125.3, 121.4, 108.7, 52.9, 43.5, 37.9, 25.0; **IR** (ν/cm^{-1}): 3049, 2963, 2870, 2817, 1777, 1707, 1561, 1498, 1375, 1170, 745, 693; **HRMS** (ESI) *m/z* calculated for $C_{28}H_{25}N_2O_2$ [MH^+]: 421.1911, found: 421.1918.

1-(2,4-Dibromoanthracen-1-yl)pyrrolidine (436)

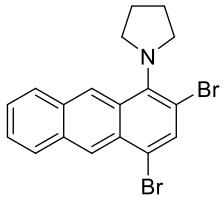

Anthracene **419e** (200 mg, 810 µmol, 1.0 equiv) and NEt_3 (676 µL, 4.85 mmol, 6.0 equiv) were dissolved in DCM (10 mL) and the resulting solution was cooled to 0 °C. NBS (864 mg, 4.85 mmol, 6.0 equiv) was added in portions over a period of 15 min and the reaction mixture was stirred at 0 °C for 5 h. The mixture was washed with saturated K_2CO_3 solution (1×) and the aqueous phase was extracted with DCM (3×). The combined organic phases were dried over anhydrous K_2CO_3 and the solvent was removed under reduced pressure. The crude product was purified by flash column chromatography (PE) to yield **436** as a bright yellow solid (191 mg, 0.47 mmol, 58%).

R_f = 0.52 (PE); **mp** 138 − 139 °C; **^{1}H NMR** (400 MHz, $CDCl_3$) δ_H = 8.80 (s, 1H), 8.73 (s, 1H), 8.09 – 8.03 (m, 2H), 7.92 (s, 1H), 7.57 – 7.50 (m, 2H), 3.53 – 3.48 (m, 4H), 2.23 – 2.18 (m, 4H); **^{13}C NMR** (101 MHz, $CDCl_3$) δ_C = 143.9, 133.6, 133.4, 132.4, 132.3, 130.1, 128.6, 128.5, 127.1, 126.6, 126.4, 124.2, 120.2, 119.0, 50.8, 27.0; **IR** (ν/cm^{-1}): 3052, 2967, 2862, 2814, 2668, 1677, 1595, 1558, 1442, 1293, 1140, 939, 838, 872, 715; **HRMS** (EI) *m/z* calculated for $C_{18}H_{15}NBr_2$ [M^+]: 402.9565, found: 402.9555.

4-Methyl-1-(4-(pyrrolidin-1-yl)anthracen-1-yl)-1,2,4-triazolidine-3,5-dione (438)

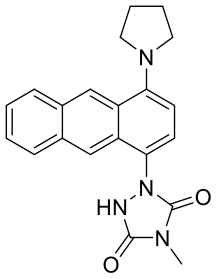

Under nitrogen atmosphere anthracene **419e** (247 mg, 1.00 mmol, 2.0 equiv), NEt_3 (279 µL, 2.00 mmol, 4.0 equiv) and MTAD **437** (57.0 mg, 500 µmol, 1.0 equiv) were dissolved in degassed acetone (5.0 mL) and stirred under irradiation with a green LED (λ = 530 nm) at – 78 °C for 5 h. The solvent was removed under reduced pressure and the crude product was purified by flash column chromatography (DCM to DCM:MeOH = 19:1) to afford **438** as a brownish solid (107 mg, 300 µmol, 60%).

R_f = 0.28 (DCM:MeOH = 19:1); **mp** 191 − 192 °C; **^{1}H NMR** (400 MHz, CD_2Cl_2) δ_H =8.79 (s, 1H), 8.24 (s, 1H), 8.00 – 7.98 (m, 1H), 7.92 – 7.88 (m, 1H), 7.48 – 7.43 (m, 2H), 7.21 (d, *J* = 8.0 Hz, 1H), 6.57 (d, *J* = 8.0 Hz, 1H), 3.51 – 3.45 (m, 4H), 3.12 (s, 3H), 2.07 – 2.01 (m, 4H); **^{13}C NMR** (101 MHz, CD_2Cl_2) δ_C = 155.3, 153.3, 149.9, 132.1, 130.9, 130.0, 129.1, 128.3, 127.1, 126.9, 126.6, 126.0, 125.6, 123.8, 121.3, 107.1, 53.4, 25.79, 25.78; **IR** (ν/cm^{-1}): 3049, 2952, 2866, 1766, 1692, 1617, 1453, 1386, 1323, 1148, 1021, 875, 741; **HRMS** (ESI) *m/z* calculated for $C_{21}H_{21}N_4O_2$ [MH^+]: 361.1659, found: 361.1666.

5 Computational details

All calculations have been conducted with the Gaussian09 E.01 suite of programs[265]. The calculations were carried out at the B3LYP-D3/6-31G**[266] level of theory with Grimme's D3 dispersion correction[267] accounting for long-range dispersion interactions. Stationary points were confirmed as ground or transition states with the computation of the harmonic vibrational frequencies and evaluating the number of imaginary frequencies (0 for ground state, 1 for transition state). IRC calculations were conducted to classify the transition states as the correct ones and moreover, to find potential hints of stepwise processes by analyzing the RMS gradient. Population analyses according to Mulliken[268] and NBO[269] were employed to derive FMO information and provide access to partial charges.

5.1 Thermodynamic data

Table S1. Thermodynamic data for the reaction of anthracenes **419a-e** with DMAD (**D**).

anthracene	9,10-addition				1,4-addition			
	$\Delta G^{\neq[a]}$	$\Delta H^{\neq[a]}$	$\Delta_R G^{[a]}$	$\Delta_R H^{[a]}$	$\Delta G^{\neq[a]}$	$\Delta H^{\neq[a]}$	$\Delta_R G^{[a]}$	$\Delta_R H^{[a]}$
419a	25.7	13.5	–24.6	–39.6	31.9	19.5	–12.4	–27.2
419b	26.7	13.6	–22.7	–38.0	28.1	14.3	–6.9	–22.7
419c	25.0	11.9	–25.6	–41.4	25.0	10.2	–5.1	–21.7
419d	24.4	8.2	–26.8	–42.9	21.6	5.4	–5.0	–21.0
419e[b]	29.1	14.8	–24.8	–40.9	23.1	7.0	–19.7	–2.3

[a] values in [kcal/mol]; [b] values in [kcal/mol] for 5,8-addition: $\Delta G^{\neq} = 36.1$; $\Delta H^{\neq} = 22.0$; $\Delta_R G = -10.8$; $\Delta_R H = -42.3$.

Table S2. Thermodynamic data for the reaction of anthracenes **419a-e** with maleic anhydride (**B**).

anthracene	9,10-addition				1,4-addition (*endo*)			
	$\Delta G^{\neq[a]}$	$\Delta H^{\neq[a]}$	$\Delta_R G^{[a]}$	$\Delta_R H^{[a]}$	$\Delta G^{\neq[a]}$	$\Delta H^{\neq[a]}$	$\Delta_R G^{[a]}$	$\Delta_R H^{[a]}$
419a	23.2	9.8	–8.6	–22.6	31.0	17.5	4.1	–9.9
419b	22.8	8.9	–7.4	–21.9	33.4	19.5	11.4	–3.4
419c	22.1	8.0	–8.5	–23.4	24.8	10.6	14.3	–0.8
419d	19.8	6.1	–10.1	–24.5	17.1	1.2	8.1	–7.5
419e[b,c]	28.5	14.1	–7.3	–21.9	19.5	4.3	7.9	–7.5

[a] values in [kcal/mol]; [b] values in [kcal/mol] for 5,8-addition: $\Delta G^{\neq} = 31.0$; $\Delta H^{\neq} = 17.0$; $\Delta_R G = 4.4$; $\Delta_R H = -10.1$; [c] values for 9,10-addition for *endo* pathway.

Table S3. Thermodynamic data for the reaction of anthracenes **419a-e** with maleic anhydride (**B**).

anthracene	9,10-addition				1,4-addition (*exo*)			
	$\Delta G^{\neq}$[a]	$\Delta H^{\neq}$[a]	$\Delta_R G$[a]	$\Delta_R H$[a]	$\Delta G^{\neq}$[a]	$\Delta H^{\neq}$[a]	$\Delta_R G$[a]	$\Delta_R H$[a]
419a	23.2	9.8	–8.6	–22.6	30.6	17.3	3.9	–10.0
419b	22.8	8.9	–7.4	–21.9	29.9	16.2	10.1	–4.8
419c	22.1	8.0	–8.5	–23.4	22.6	7.8	12.7	–2.5
419d	19.8	6.1	–10.1	–24.5	17.9	2.5	11.5	–3.6
419e[b,c]	22.7	9.0	–7.3	–22.6	17.4	2.3	10.9	–3.5

[a] values in [kcal/mol]; [b] values in [kcal/mol] for 5,8-addition: $\Delta G^{\neq} = 30.4$; $\Delta H^{\neq} = 16.6$; $\Delta_R G = 4.2$; $\Delta_R H = -10.3$; [c] values for 9,10-addition for *exo* pathway.

5.2 Bond orders

The bond orders have been calculated with Pauling's equation (equation 1) with 0.6 as a fitting factor for transition states.[270] As reference, the according product structures were used.

$$BO = n_0 \times e^{\frac{r_0 - r_x}{c}} \qquad (1)$$

With n_0 representing the reference bond order, r_0 representing the reference bond length in Å, r_x representing the examined bond length in Å and c representing a factor with 0.3 for ground states and 0.6 for transition states.

Table S4. Bond lengths in the product structures for **430a-eB** and **431a-eB**.

anthracene	1,4-addition (*exo*)		1,4-addition (*endo*)		9,10-Addition	
	C1 – CA (Å)	C4 – CB (Å)	C1 – CA (Å)	C4 – CB (Å)	C9-CA (Å)	C10-CB (Å)
419a	1.57	1.57	1.57	1.57	1.57	1.57
419b	1.58	1.58	1.59	1.57	1.57	1.57
419c	1.59	1.58	1.63	1.56	1.56	1.57
419d	1.59	1.57	1.59	1.57	1.57	1.57
419e[a,b,c]	1.60	1.57	1.59	1.57	1.57	1.57

[a] for 5,8-addition *endo* product: C5 – CA = 1.57, C8 – CB = 1.57; [b] for 5,8-addition *exo* product: C5 – CA = 1.57, C8 – CB = 1.57; [c] values in table for *exo* 9,10-addition product. Values for *endo* 9,10-product: C9 – CA = 1.57, C10 – CB = 1.57.

Table S5. Bond lengths in the transition state structures for **430a-eB** and **431a-eB**.

anthracene	1,4-addition (*exo*)		1,4-addition (*endo*)		9,10-Addition	
	C1 – CA (Å)	C4 – CB (Å)	C1 – CA (Å)	C4 – CB (Å)	C9-CA (Å)	C10-CB (Å)
419a	2.13	2.13	2.14	2.14	2.19	2.19
419b	2.46	1.86	2.42	1.93	2.17	2.18
419c	2.66	1.85	2.73	1.83	2.15	2.25
419d	2.76	1.86	2.79	1.85	2.16	2.18
419e[a,b,c]	2.75	1.86	2.78	1.86	2.20	2.16

[a] for 5,8-addition *endo* product: C5 – CA = 2.13, C8 – CB = 2.13; [b] for 5,8-addition *exo* product: C5 – CA = 2.14, C8 – CB = 2.14; [c] values in table for *exo* 9,10-addition transition state. Values for *endo* 9,10-transition state: C9 – CA = 2.28, C10 – CB = 2.12.

Table S6. Bond orders after Pauling, calculated after equation 1 for structures **430a-eB** and **431a-eB**.

anthracene	1,4-addition (*exo*)		1,4-addition (*endo*)		9,10-Addition	
	C1 – CA (Å)	C4 – CB (Å)	C1 – CA (Å)	C4 – CB (Å)	C9-CA (Å)	C10-CB (Å)
419a	0.39	0.39	0.39	0.39	0.36	0.36
419b	0.23	0.63	0.25	0.55	0.37	0.36
419c	0.17	0.64	0.16	0.64	0.37	0.32
419d	0.14	0.62	0.14	0.63	0.37	0.36
419e[a,b,c]	0.15	0.62	0.14	0.62	0.35	0.37

[a] for 5,8-addition *endo* product: C5 – CA = 0.39, C8 – CB = 0.39; [b] for 5,8-addition *exo* product: C5 – CA = 0.39, C8 – CB = 0.39 ; [c] values in table for *exo* 9,10-addition transition state. Values for *endo* 9,10-transition state: C9 – CA = 0.31, C10 – CB = 0.40.

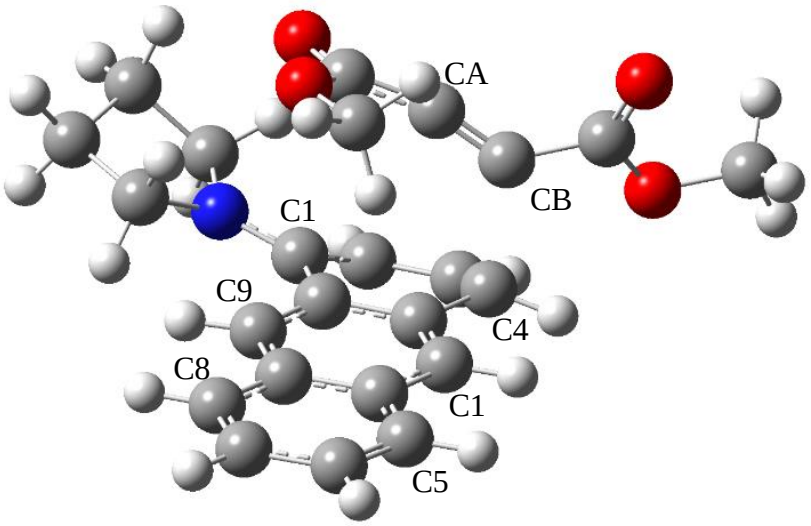

Figure S1. Assignment of the carbon atoms for the calculation of the bond orders.

Table S7. Computed bond lengths in product structures for **430a-eD** and **431a-eD**.

anthracene	**1,4-Addition**		**9,10-Addition**	
	C1 – CA (Å)	C4 – CB (Å)	C9-CA (Å)	C10-CB (Å)
419a	1.54	1.53	1.54	1.54
419b	1.56	1.56	1.53	1.53
419c	1.55	1.53	1.54	1.54
419d	1.56	1.55	1.53	1.53
419e[a]	1.56	1.53	1.54	1.53

[a] for 5,8-addition, values are: C5-CA = 1.53, C8 – CB = 1.54.

Table S8. Computed bond lengths in transition state structures for **430a-eD** and **431a-eD**.

anthracene	1,4-Addition		9,10-Addition	
	C1 – CA (Å)	C4 – CB (Å)	C9-CA (Å)	C10-CB (Å)
419a	2.40	2.04	2.50	2.05
419b	2.76	1.91	2.61	2.03
419c	3.08	1.96	2.26	2.15
419d	3.35	1.94	3.50	1.86
419e[a]	3.18	1.95	2.20	2.31

[a] for 5,8-addition, values are: C5-CA = 2.20, C8 – CB = 2.20.

Table S9. Calculated bond orders in transition state structures for **430a-eD** and **431a-eD**.

anthracene	1,4-Addition		9,10-Addition	
	C1 – CA (Å)	C4 – CB (Å)	C9-CA (Å)	C10-CB (Å)
419a	0.24	0.43	0.20	0.42
419b	0.13	0.56	0.17	0.44
419c	0.08	0.51	0.30	0.36
419d	0.05	0.52	0.04	0.58
419e[a]	0.07	0.50	0.33	0.28

[a] for 5,8-addition, values are: C5-CA = 0.33, C8 – CB = 0.33.

5.3 Marcus Analysis

The data for the intrinsic barrier were calculated after the following equation 2[271]:

$$\Delta G^{\neq}=\Delta G^{\neq\circ}+0.5\Delta_R G+\frac{\Delta_R G^2}{16\Delta G^{\neq\circ}} \qquad (2)$$

With $\Delta G^{\neq}$ representing the activation barrier, $\Delta G^{\neq\circ}$ representing the intrinsic barrier and $\Delta_R G$ representing the driving force.

Table S10. Calculated intrinsic barriers for the reaction of anthracenes **419a-e** with DMAD (**D**).

anthracene	$\Delta G^{\neq}_{9,10}$[a]	$\Delta_R G_{9,10}$[a]	$\Delta G^{\neq\circ}_{9,10}$[a]	$\Delta G^{\neq}_{1,4}$[a]	$\Delta_R G_{1,4}$[a]	$\Delta G^{\neq\circ}_{1,4}$[a]
419a	25.7	–24.6	37.0	31.9	–12.4	37.9
419b	26.7	–22.7	37.2	28.1	–6.9	31.5
419c	25.0	–25.6	35.7	25.0	–5.1	27.5
419d	23.1	–26.8	36.6	21.6	–5.0	24.0
419e[b]	29.1	–24.8	40.6	23.1	–2.3	24.2

[a]values in [kcal/mol]; [b] values in [kcal/mol] for 5,8-position: $\Delta G^{\neq}_{5,8}$ = 36.1 ; $\Delta_R G_{5,8}$ = –10.8, $\Delta G^{\neq\circ}_{5,8}$ = 41.3.

Table S11. Calculated intrinsic barriers for the reaction of anthracenes **419a-e** with maleic anhydride (**B**) (*endo* path for 1,4-addition process).

anthracene	$\Delta G^{\neq}_{9,10}$[a]	$\Delta_R G_{9,10}$[a]	$\Delta G^{\neq\circ}_{9,10}$[a]	$\Delta G^{\neq}_{1,4}$[a]	$\Delta_R G_{1,4}$[a]	$\Delta G^{\neq\circ}_{1,4}$[a]
419a	23.2	−8.6	27.3	31.0	4.1	28.9
419b	22.8	−7.4	26.4	33.4	11.4	27.4
419c	22.1	−8.5	26.2	24.8	14.3	16.9
419d	19.8	−10.1	24.6	17.1	8.1	12.7
419e[b]	28.5	−7.3	33.0	19.5	7.9	15.3

[a]values in [kcal/mol]; [b] values in [kcal/mol] for 5,8-position: $\Delta G^{\neq}_{5,8}$ = 31.0 ; $\Delta_R G_{5,8}$ = 4.4, $\Delta G^{\neq\circ}_{5,8}$ = 28.8.

Table S12. Calculated intrinsic barriers for the reaction of anthracenes **419a-e** with maleic anhydride (**B**) (*exo* path for 1,4-addition process).

anthracene	$\Delta G^{\neq}_{9,10}$[a]	$\Delta_R G_{9,10}$[a]	$\Delta G^{\neq\circ}_{9,10}$[a]	$\Delta G^{\neq}_{1,4}$[a]	$\Delta_R G_{1,4}$[a]	$\Delta G^{\neq\circ}_{1,4}$[a]
419a	23.2	−8.6	27.3	30.6	3.9	28.6
419b	22.8	−7.4	26.4	29.9	10.1	24.6
419c	22.1	−8.5	26.2	22.6	12.7	15.6
419d	19.8	−10.1	24.6	17.9	11.5	11.4
419e[b]	22.7	−7.3	26.2	17.4	10.9	11.3

[a]values in [kcal/mol]; [b] values in [kcal/mol] for 5,8-position: $\Delta G^{\neq}_{5,8}$ = 31.0 ; $\Delta_R G_{5,8}$ = 4.4, $\Delta G^{\neq\circ}_{5,8}$ = 28.8.

5.4 FMO Analysis

The computed orbital energies from the Mulliken analysis were used for the calculation of the HOMO-LUMO gap.

Table S13. FMO Analysis for anthracenes **419a-e** with DMAD (**D**).

anthracene	normal electron demand			inverse electron demand		
	e_{HOMO} (419) (eV)	e_{LUMO} (D) (eV)	$\Delta_{HOMO-LUMO}$ (eV)	e_{HOMO} (D) (eV)	e_{LUMO} (419) (eV)	$\Delta_{HOMO-LUMO}$ (eV)
419a	−5.23		3.74		−1.65	6.24
419b	−4.82		3.33		−1.27	6.62
419c	−4.81	−1.49	3.32	−7.89	−1.40	6.49
419d	−4.37		2.88		−1.12	6.77
419e	−4.68		3.19		−1.38	6.51

Table S14. FMO Analsis for anthracenes **419a-e** with maleic anhydride (**B**).

anthracene	normal electron demand			inverse electron demand		
	e_{HOMO} (419) (eV)	e_{LUMO}(B) (eV)	$\Delta_{HOMO-LUMO}$ (eV)	e_{HOMO} (B) (eV)	e_{LUMO} (419) (eV)	$\Delta_{HOMO-LUMO}$ (eV)
419a	−5.23		2.04		−1.65	6.49
419b	−4.82		1.63		−1.27	6.87
419c	−4.81	−3.19	1.62	−8.14	−1.40	6.74
419d	−4.37		1.18		−1.12	7.02
419e	−4.68		1.49		−1.38	6.76

5.5 NBO Analysis

The partial charges were taken from the NBO analysis. In all cases, the charge from the neighbouring hydrogen atom was added to the charge of the carbon center.

Table S15. Partial charges at the reaction centers for the reaction of anthracenes **419a-e** with DMAD (**D**).

anthr.	1,4-addition				9,10-addition			
	CA	**CB**	**C1**	**C4**	**CA**	**CB**	**C9**	**C10**
419a	−0.023	−0.130	0.049	0.076	−0.132	−0.013	0.074	0.102
419b	−0.025	−0.153	0.410	0.005	−0.130	−0.022	0.083	0.119
419c	−0.060	−0.131	0.269	−0.012	−0.103	−0.052	0.077	0.091
419d	−0.058	−0.148	0.283	−0.022	−0.173	−0.047	0.019	0.125
419e[a]	−0.103	−0.138	0.282	−0.032	−0.123	−0.086	0.068	0.096

[a] Values for 5,8-addition: CA = −0.106, CB = −0.110, C5 = 0.074, C8 = 0.056.

Table S16. Partial charges at the reaction centers for the reaction of anthracenes **419a-e** with maleic anhydride (**B**).

anthr.	1,4-addition (*endo*)				9,10-addition			
	CA	**CB**	**C1**	**C4**	**CA**	**CB**	**C9**	**C10**
419a	−0.086	−0.086	0.075	0.075	−0.083	−0.083	0.102	0.102
419b	−0.150	−0.076	0.403	0.030	−0.087	−0.087	0.118	0.117
419c	−0.201	−0.070	0.273	0.004	−0.083	−0.096	0.107	0.112
419d	−0.222	−0.057	0.293	−0.003	−0.084	−0.084	0.106	0.101
419e[a,b]	−0.214	−0.065	0.287	−0.004	−0.094	−0.078	0.104	0.093

[a] Values for 5,8-addition *endo*: CA = −0.089, CB = −0.087, C5 = 0.074, C8 = 0.074; [b] Values for 9,10-addition are for *endo* case. Values for 9,10-addition *exo*: CA = −0.093, CB = −0.084, C9 = 0.112, C10 = 0.088.

Table S17. Partial charges at the reaction centers for the reaction of anthracenes **419a-e** with maleic anhydride (**B**).

anthracene	1,4-addition (*exo*)			
	CA	**CB**	**C1**	**C4**
419a	−0.079	−0.079	0.074	0.074
419b	−0.142	−0.066	0.414	0.020
419c	−0.185	−0.060	0.272	0.005
419d	−0.201	−0.059	0.284	−0.003
419e[a]	−0.200	−0.057	0.282	−0.002

[a] Values for 5,8-addition *exo*: CA = −0.079, CB = −0.080, C5 = 0.073, C8 = 0.074.

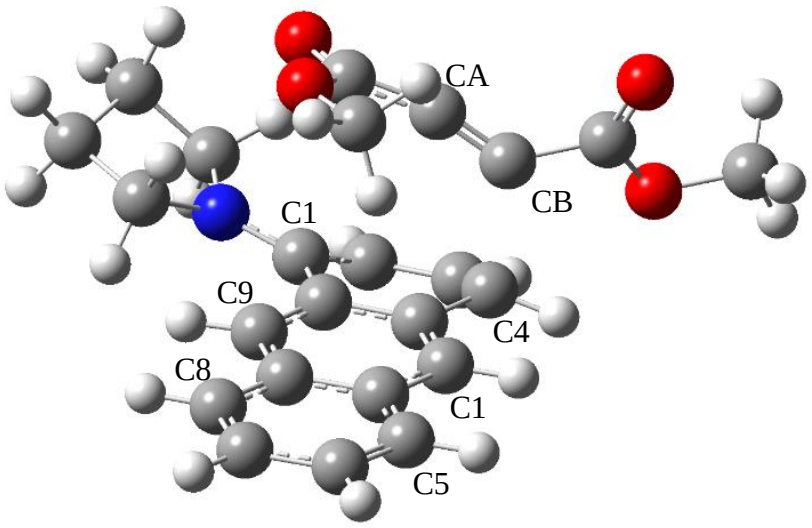

Figure S2. Assignment of the carbon atoms for the calculation of the bond orders.

5.6 IRC plots with DMAD as dienophile

The SCF energy was plotted against the longer critical bond length in the transition state.

IRCs for $R^1 = R^2 = H$ 419a

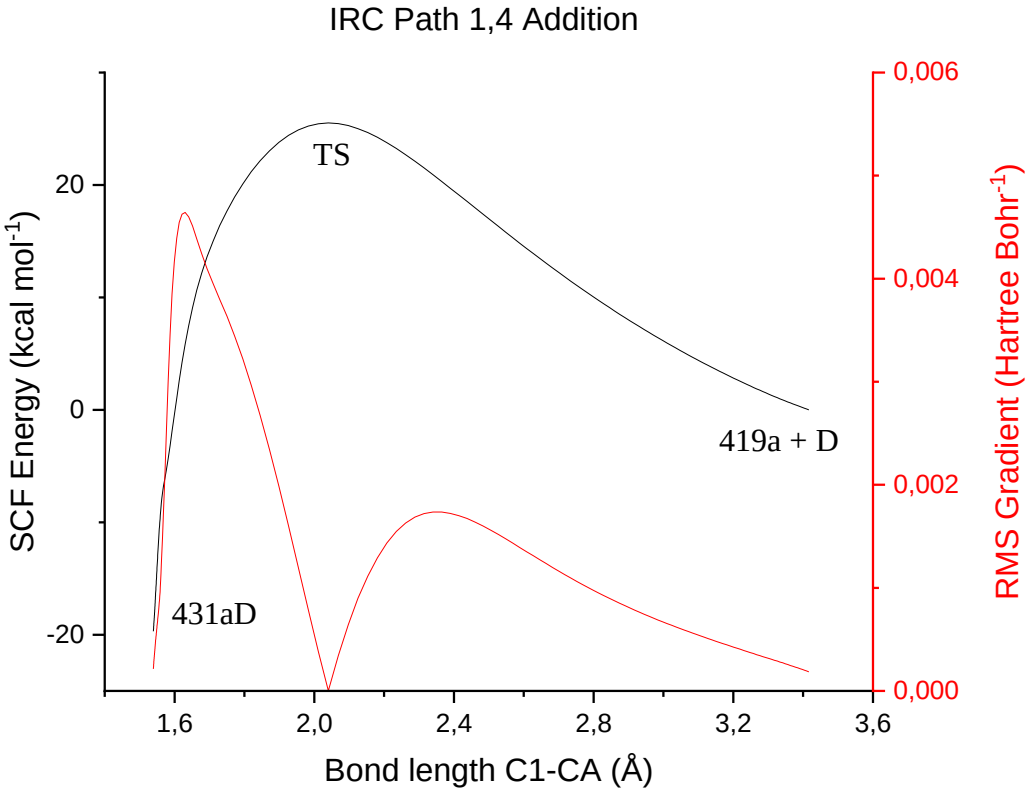

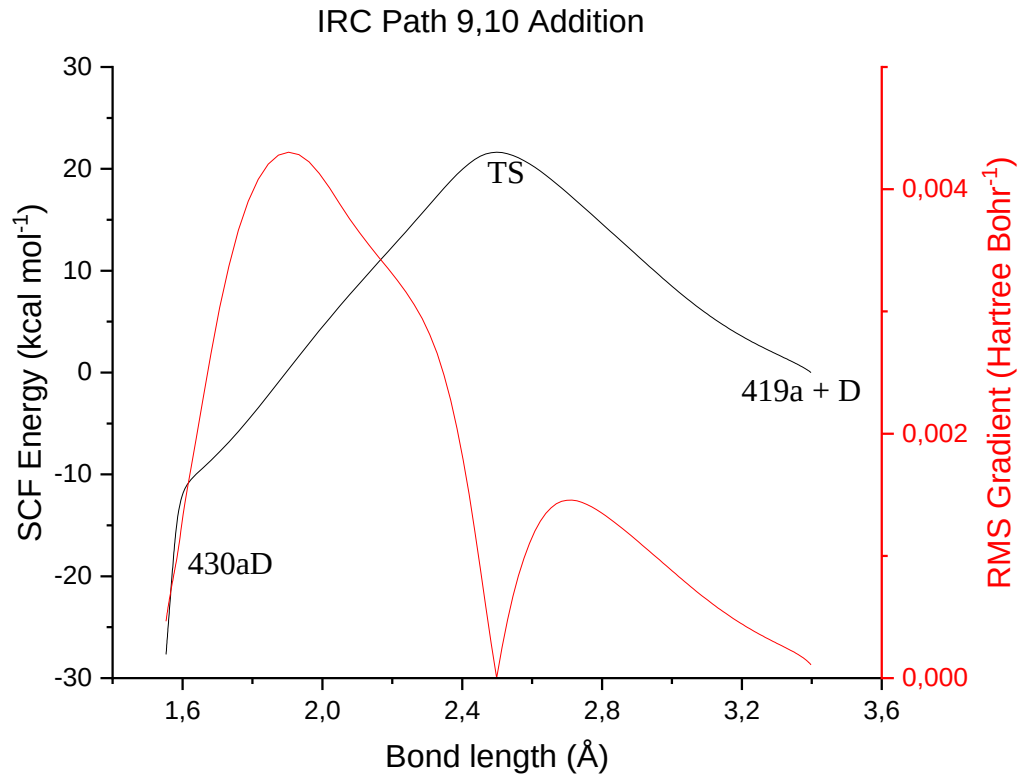

IRCs for $R^1 = R^2 =$ OMe 419b

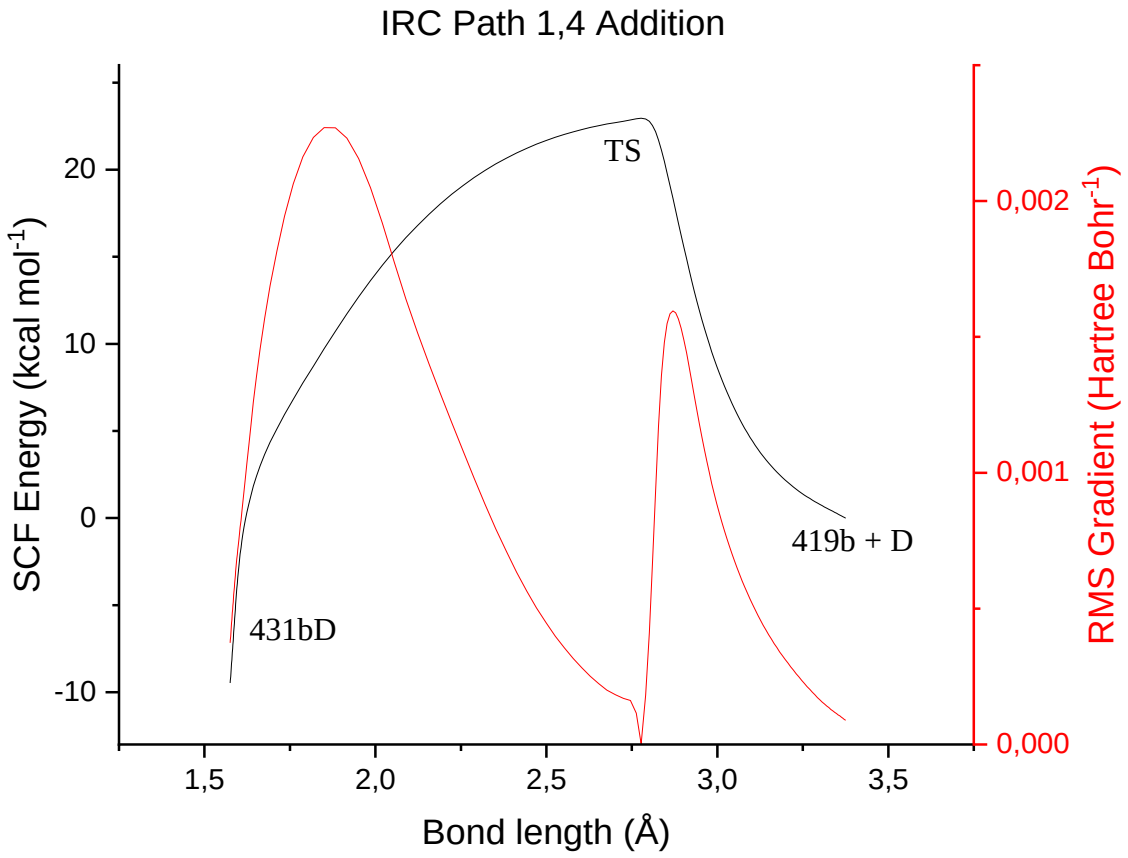

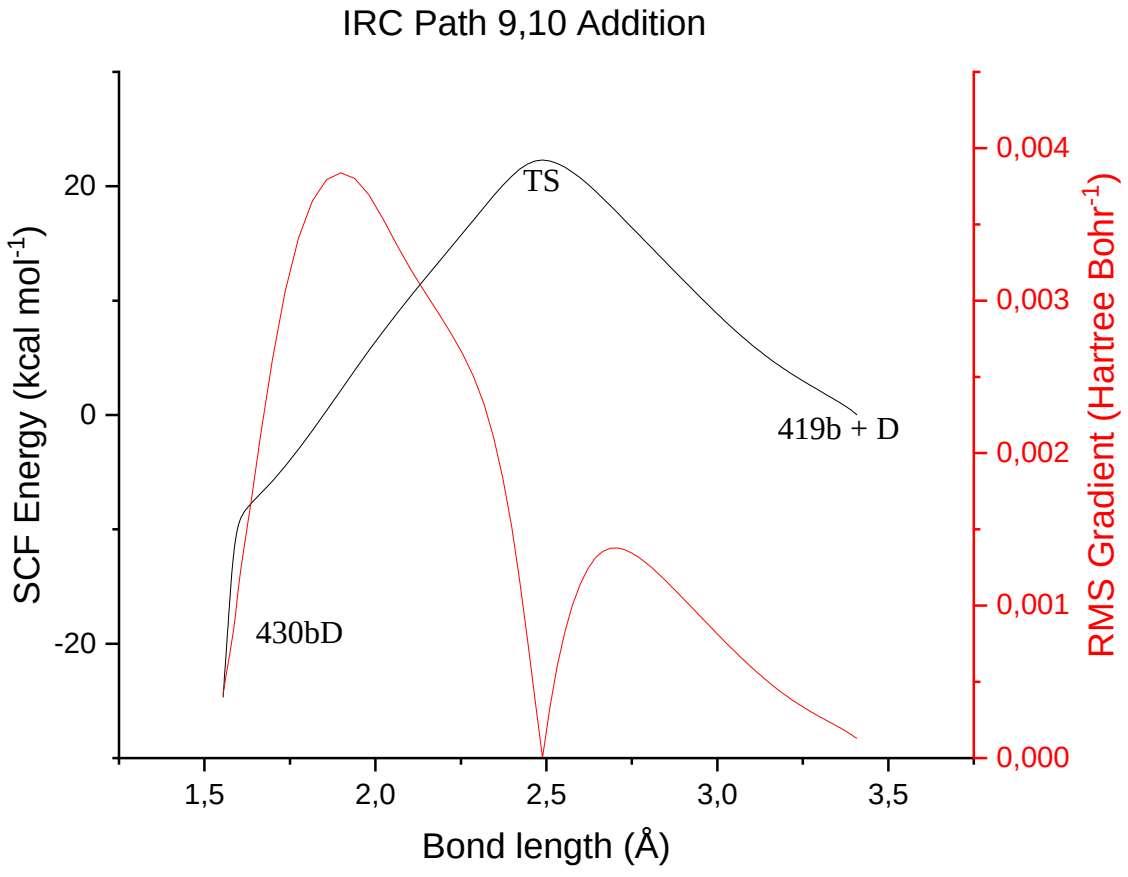

IRCs for $R^1 = R^2 = NMe_2$ 419c

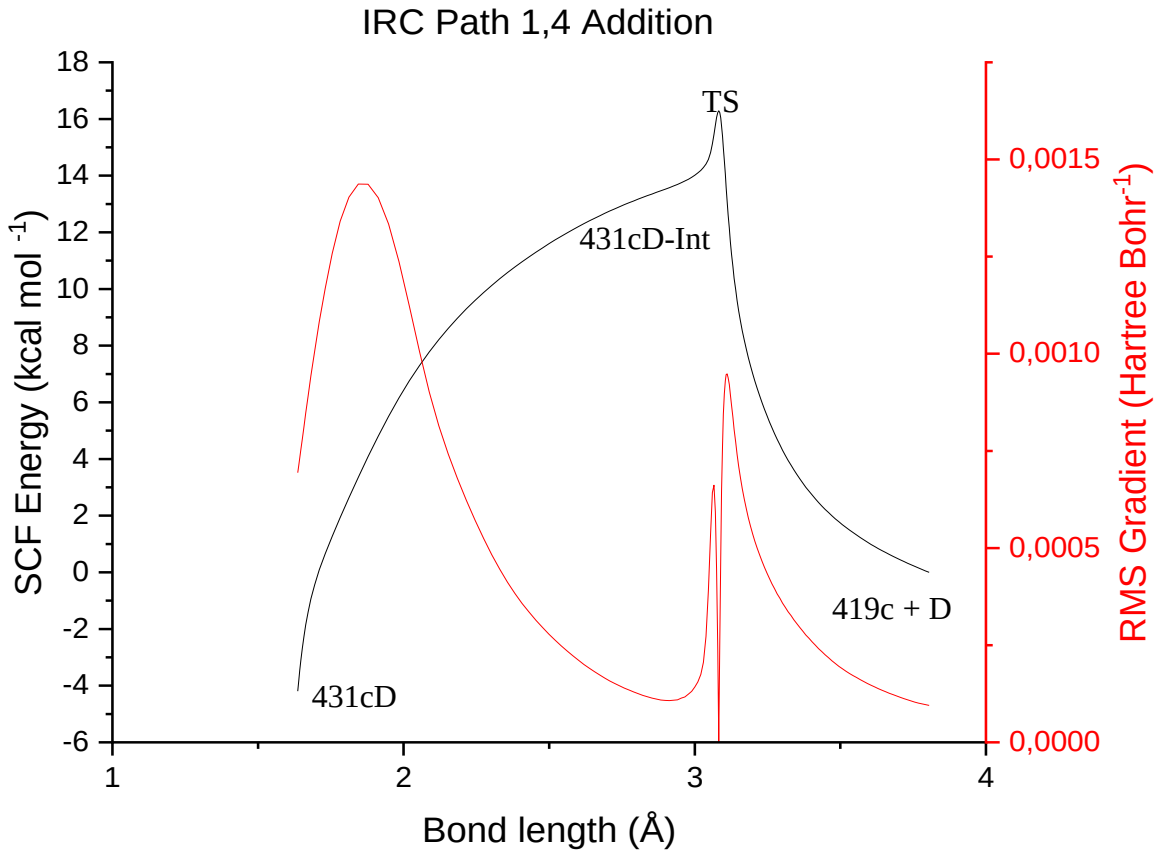

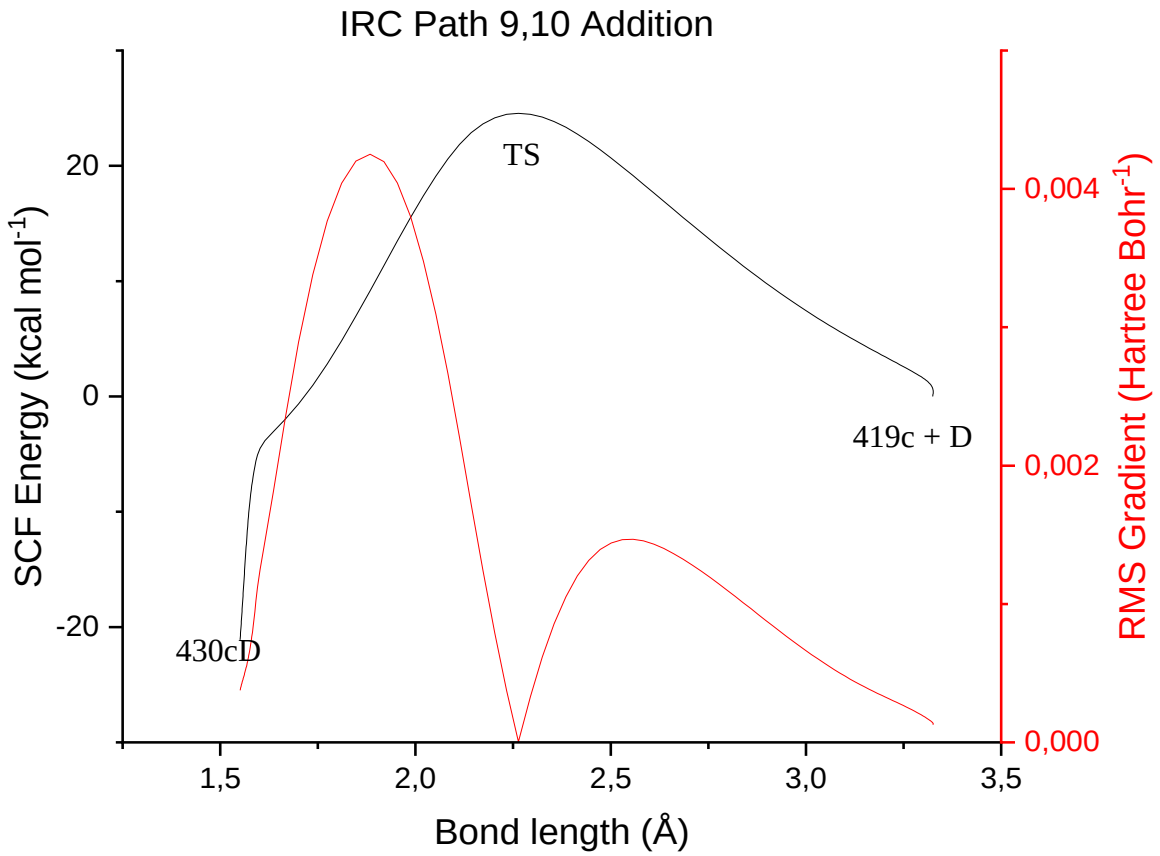

5.7 IRC plots with maleic anhydride as dienophile

Plots for $R^1 = R^2 = H$ 419a

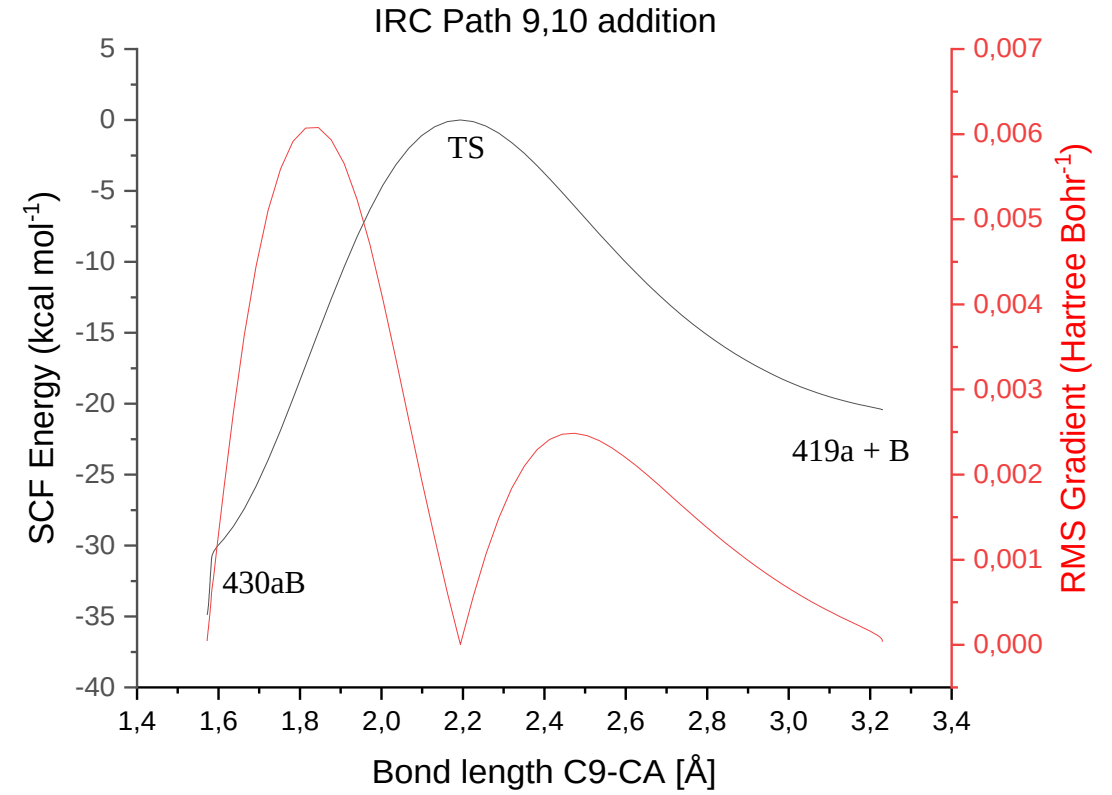

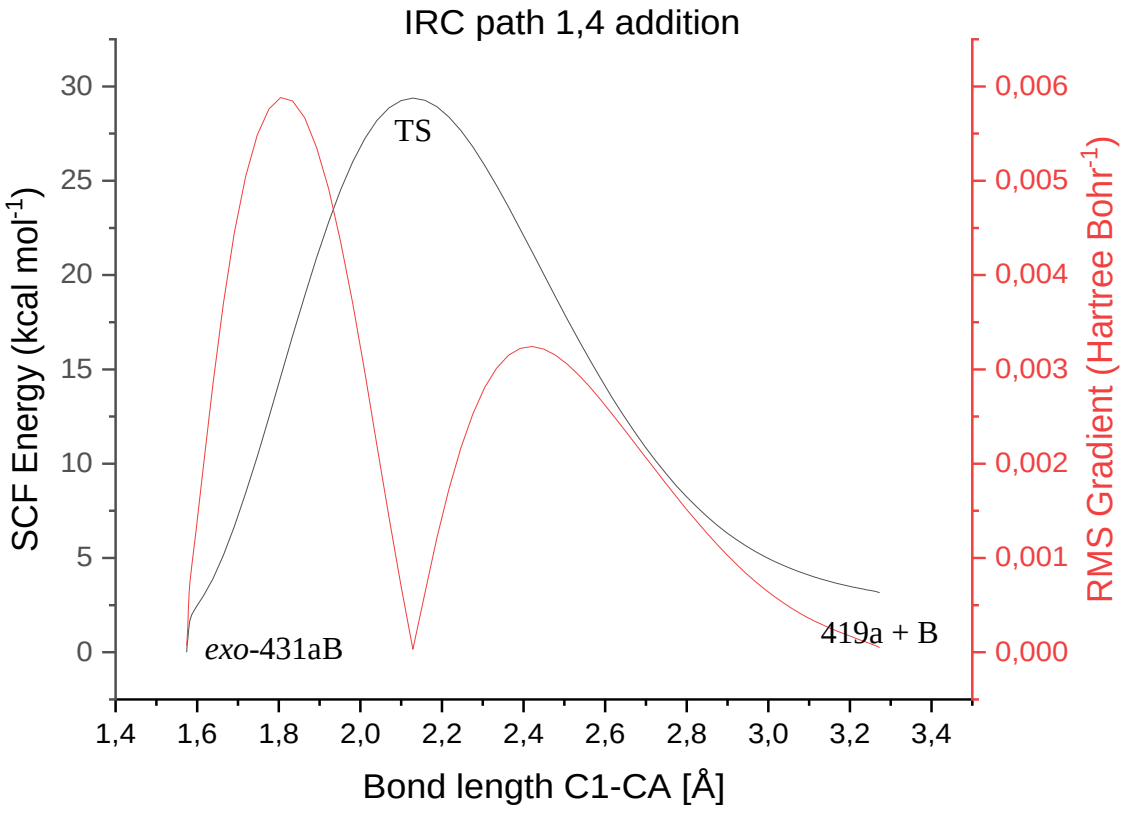

Plots for $R^1 = R^2 =$ OMe 419b

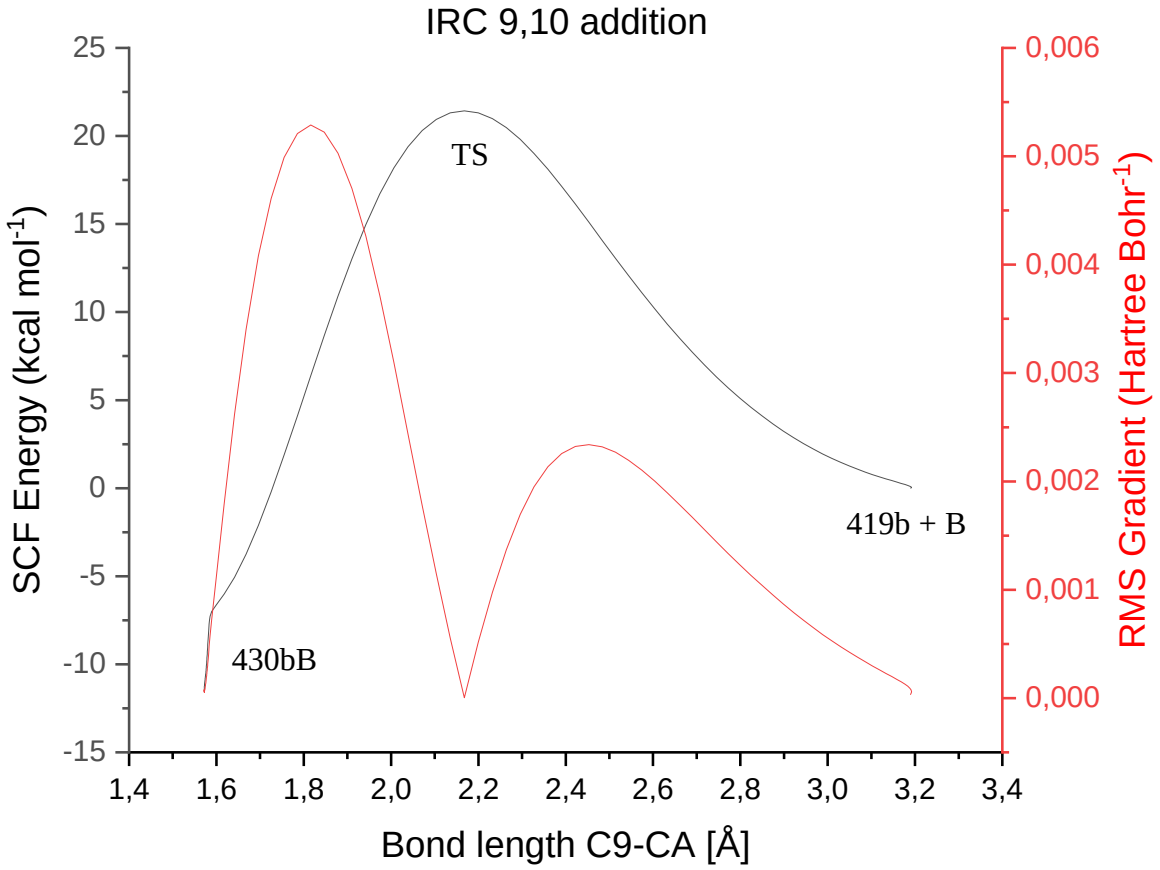

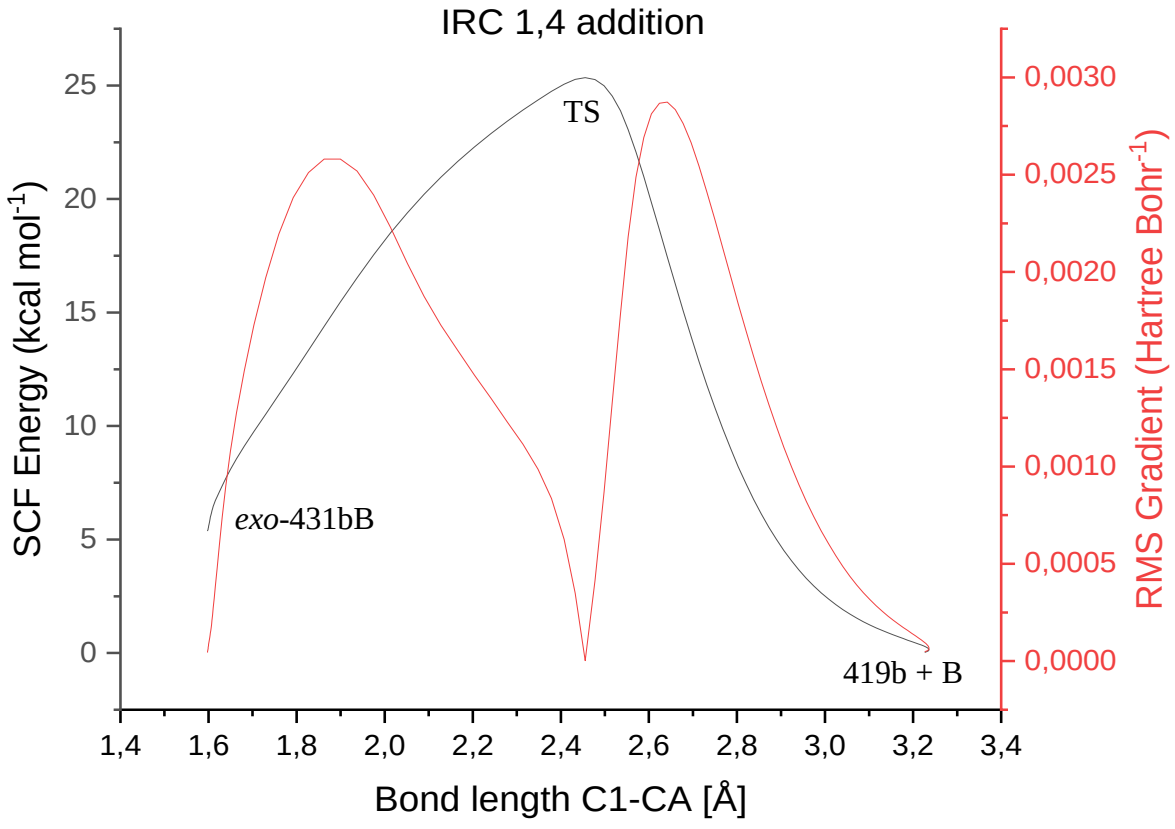

Plots for $R^1 = R^2 = NMe_2$ 419c

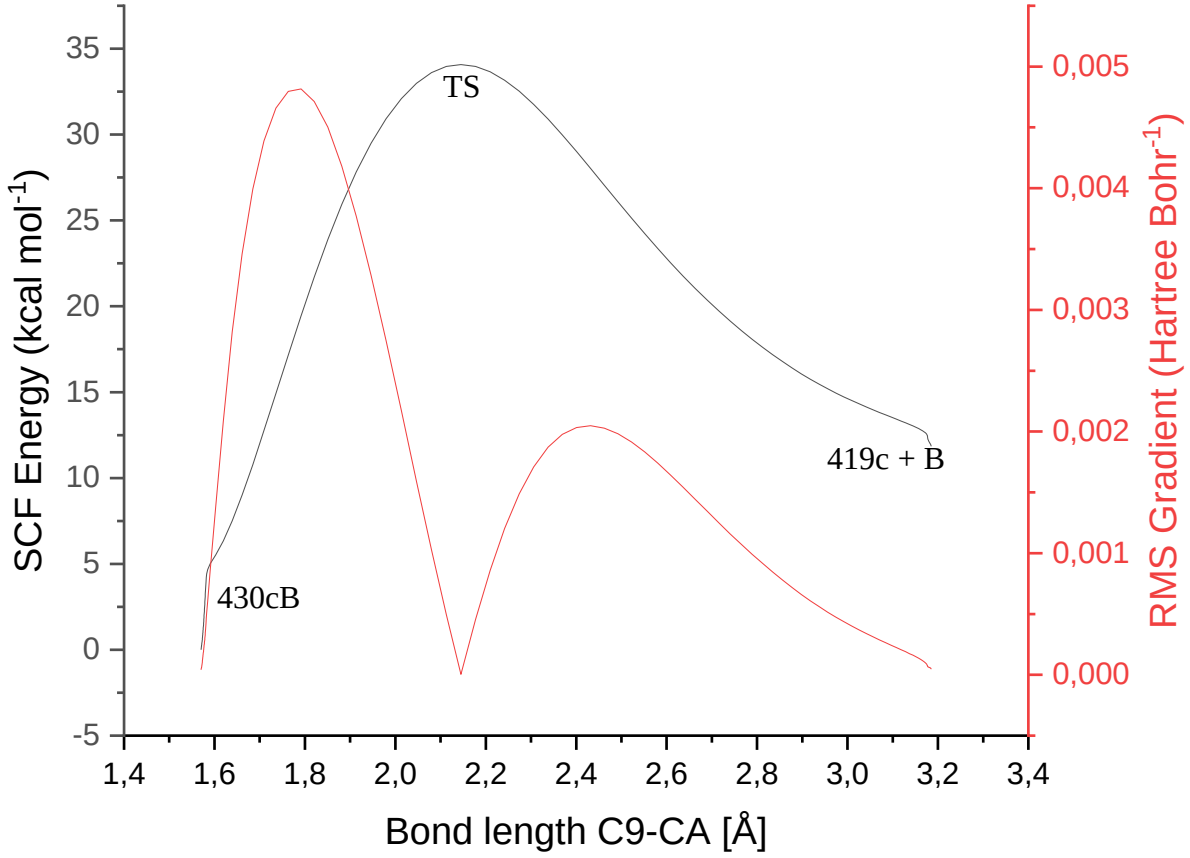

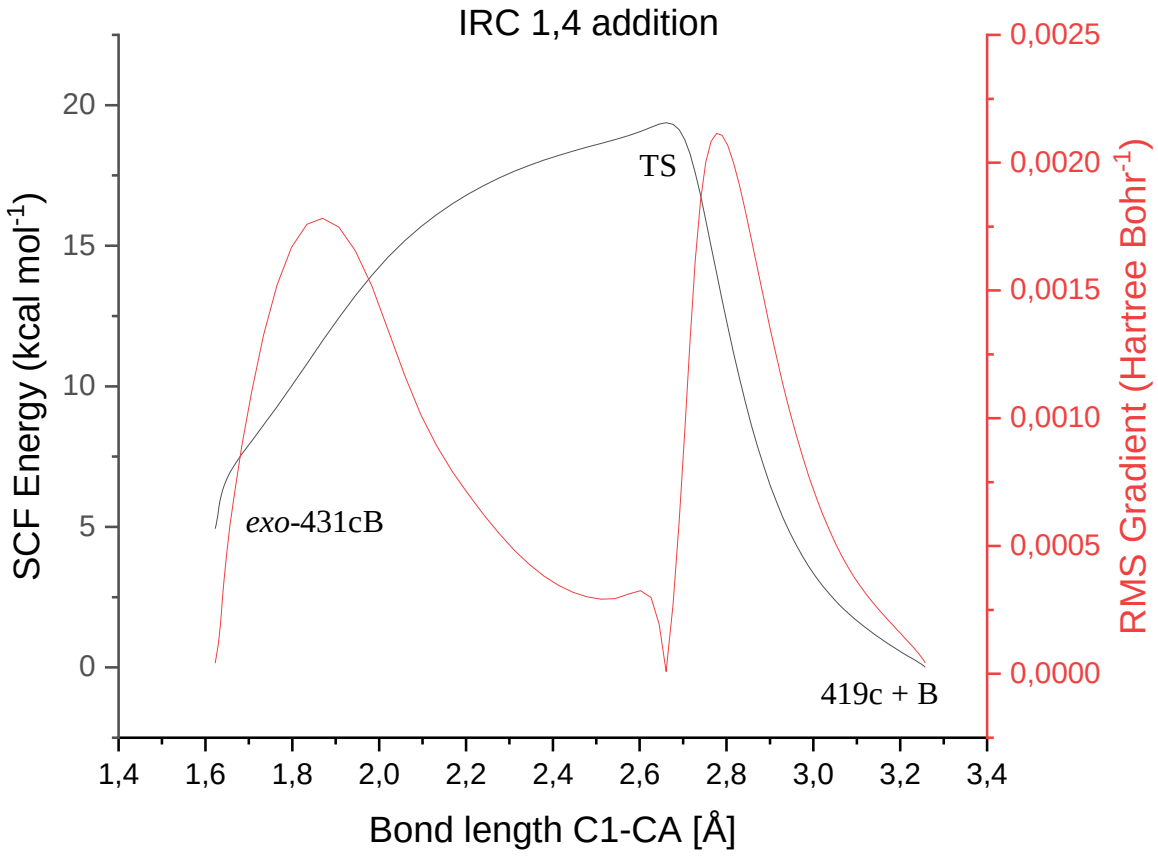

Plots for R^1 = R^2 = Pyrrolidine 419d

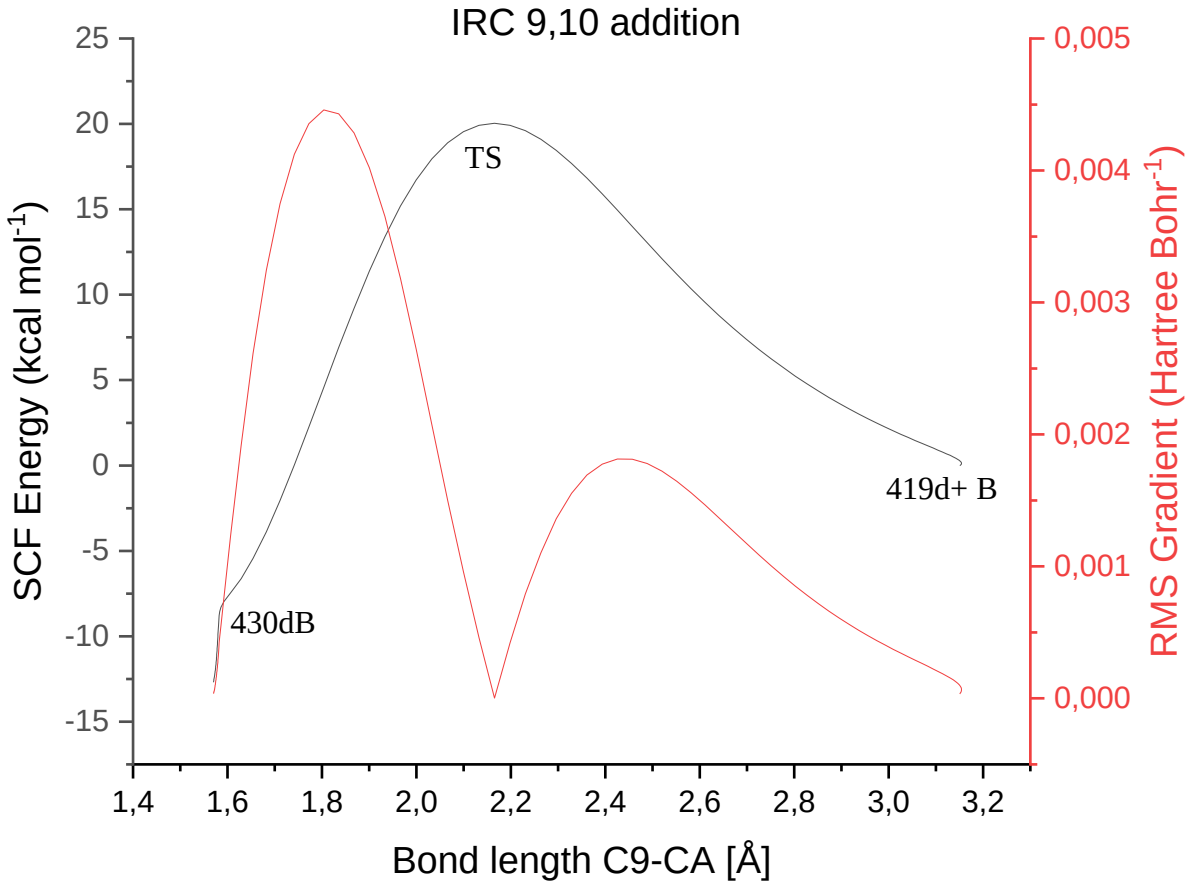

Plots for R^1 = H ; R^2 = Pyrrolidine 419e

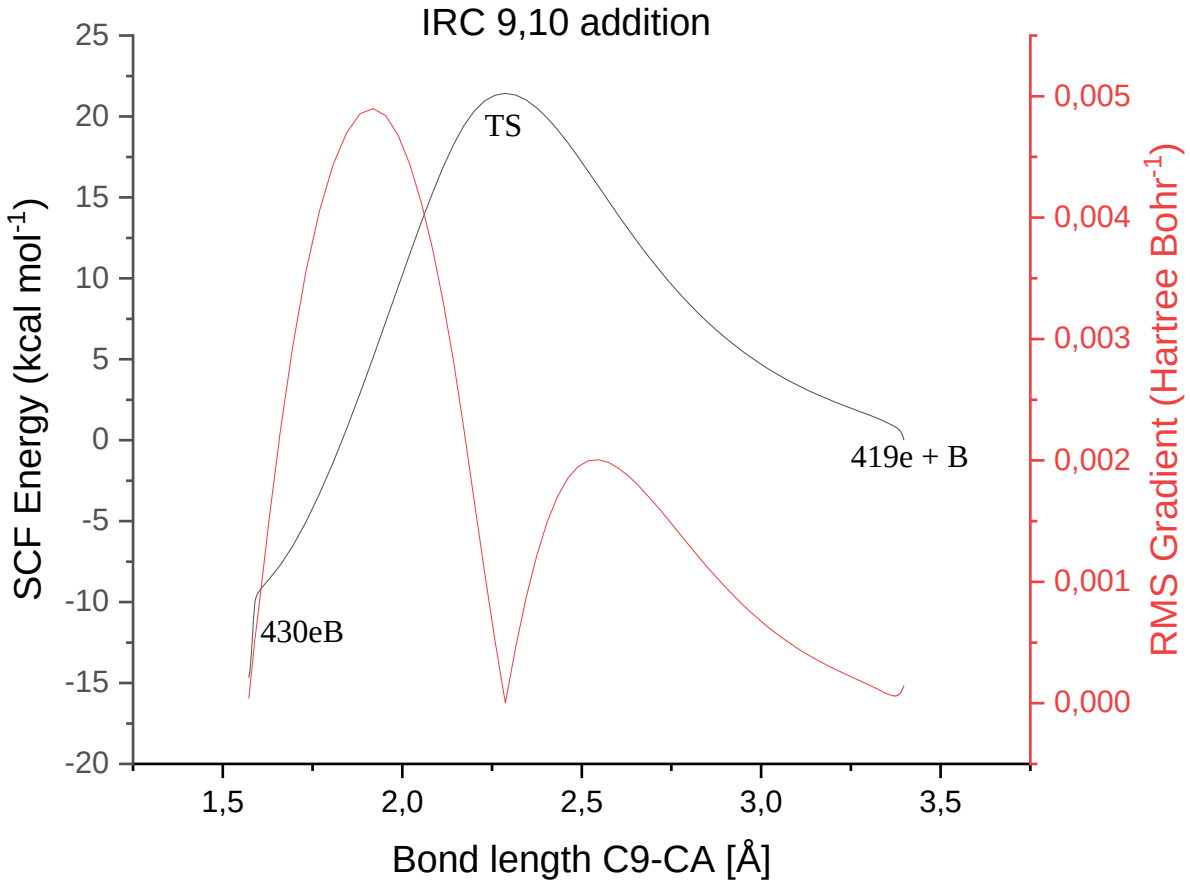

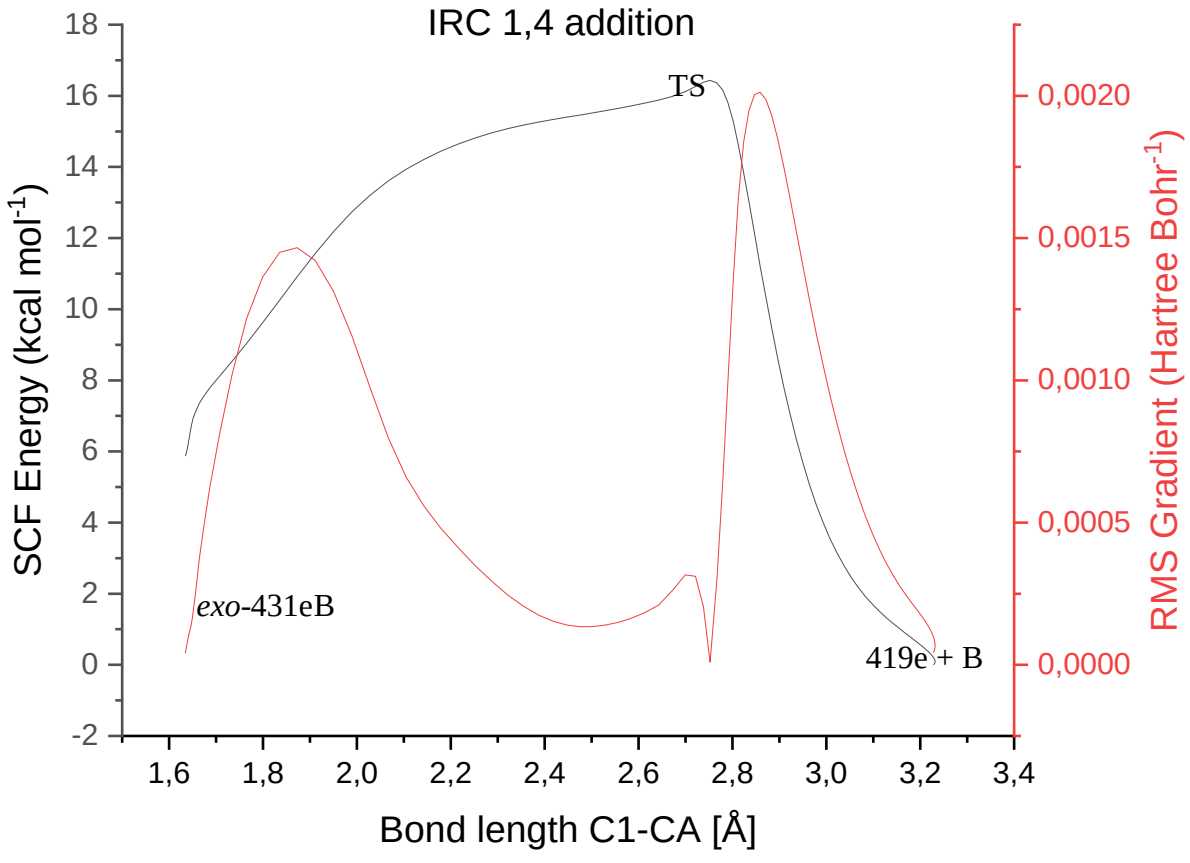

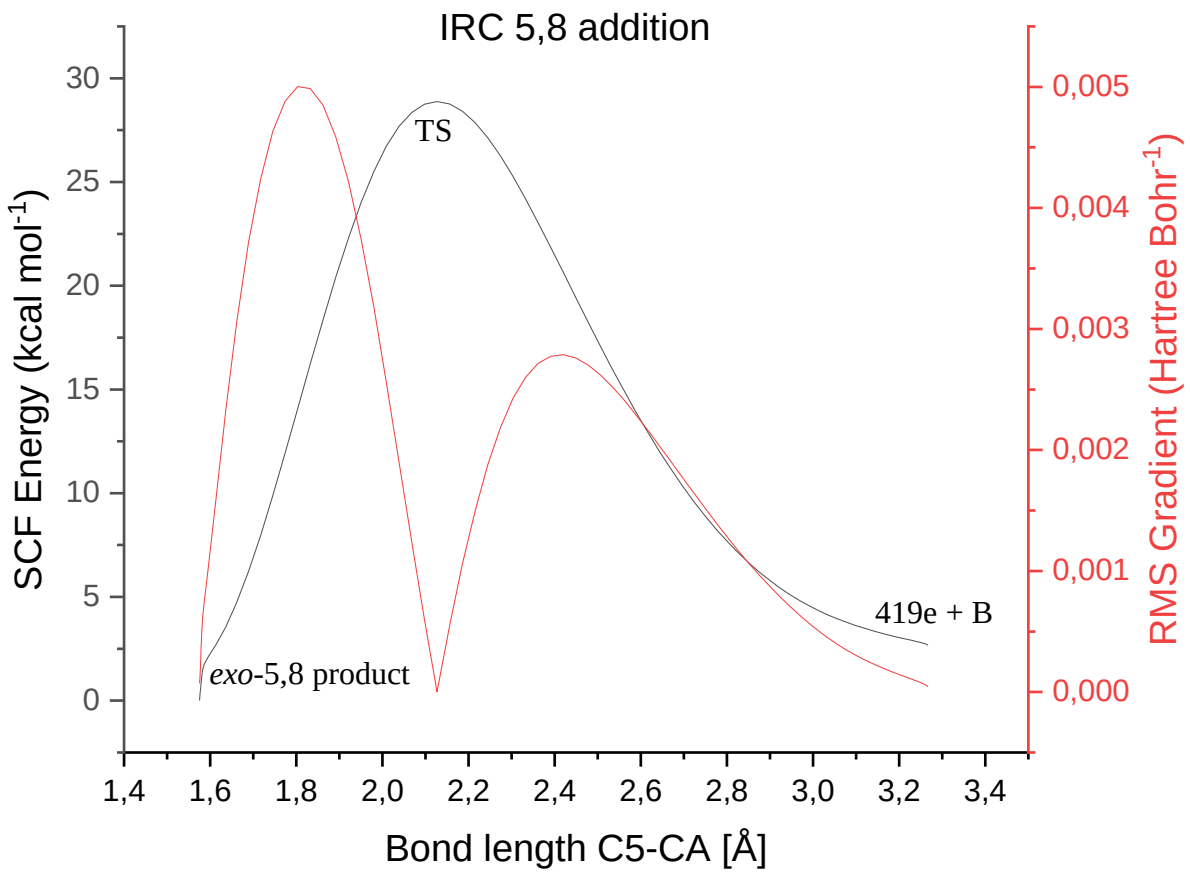
IRC 5,8 addition
SCF Energy (kcal mol-1)
RMS Gradient (Hartree Bohr-1)
Bond length C5-CA [Å]
TS
419e + B
exo-5,8 product
30
25
20
15
10
5
0
0,005
0,004
0,003
0,002
0,001
0,000
1,4
1,6
1,8
2,0
2,2
2,4
2,6
2,8
3,0
3,2
3,4

F Appendix

1 NMR-spectra

^{1}H NMR spectra upper image

^{13}C NMR spectra lower image

Solvent and frequency are given at the spectra.

3a,4,7,7a-Tetrahydro-1*H*-4,7-methanoinden-1-one (22)

^{1}H NMR (400 MHz, $CDCl_3$)

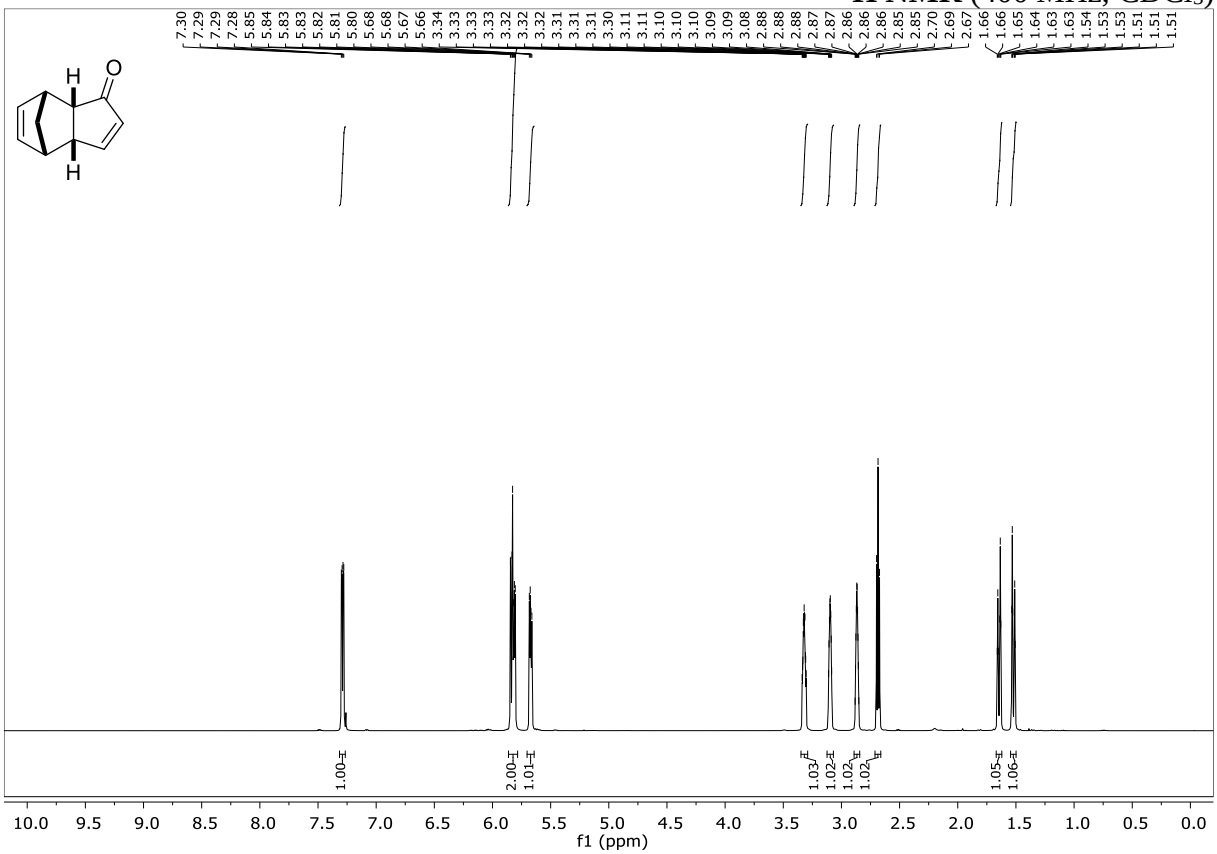

^{13}C NMR (101 MHz, $CDCl_3$)

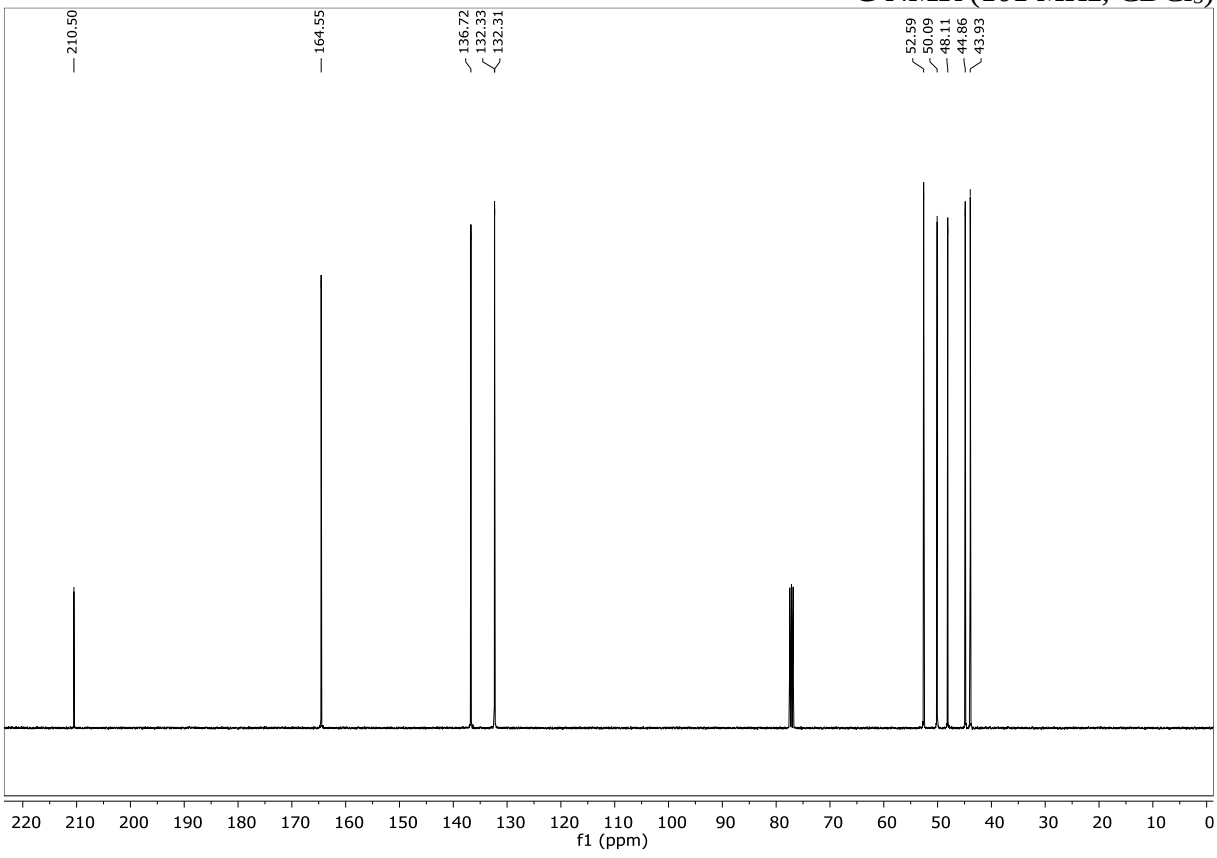

1a,1b,2,5,5a,6a-Hexahydro-6*H*-2,5-methanoindeno[1,2-*b*]oxiren-6-one (313)

^{1}H NMR (400 MHz, $CDCl_3$)

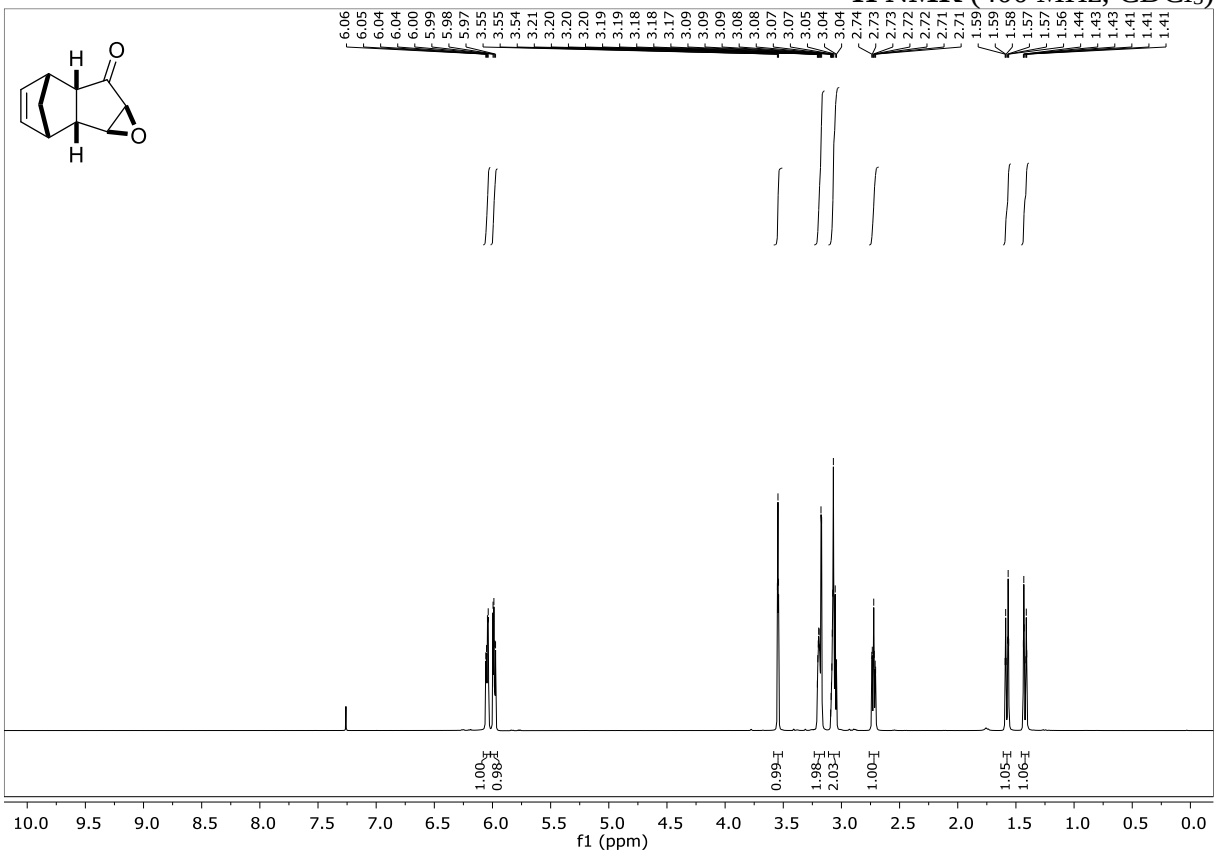

^{13}C NMR (101 MHz, $CDCl_3$)

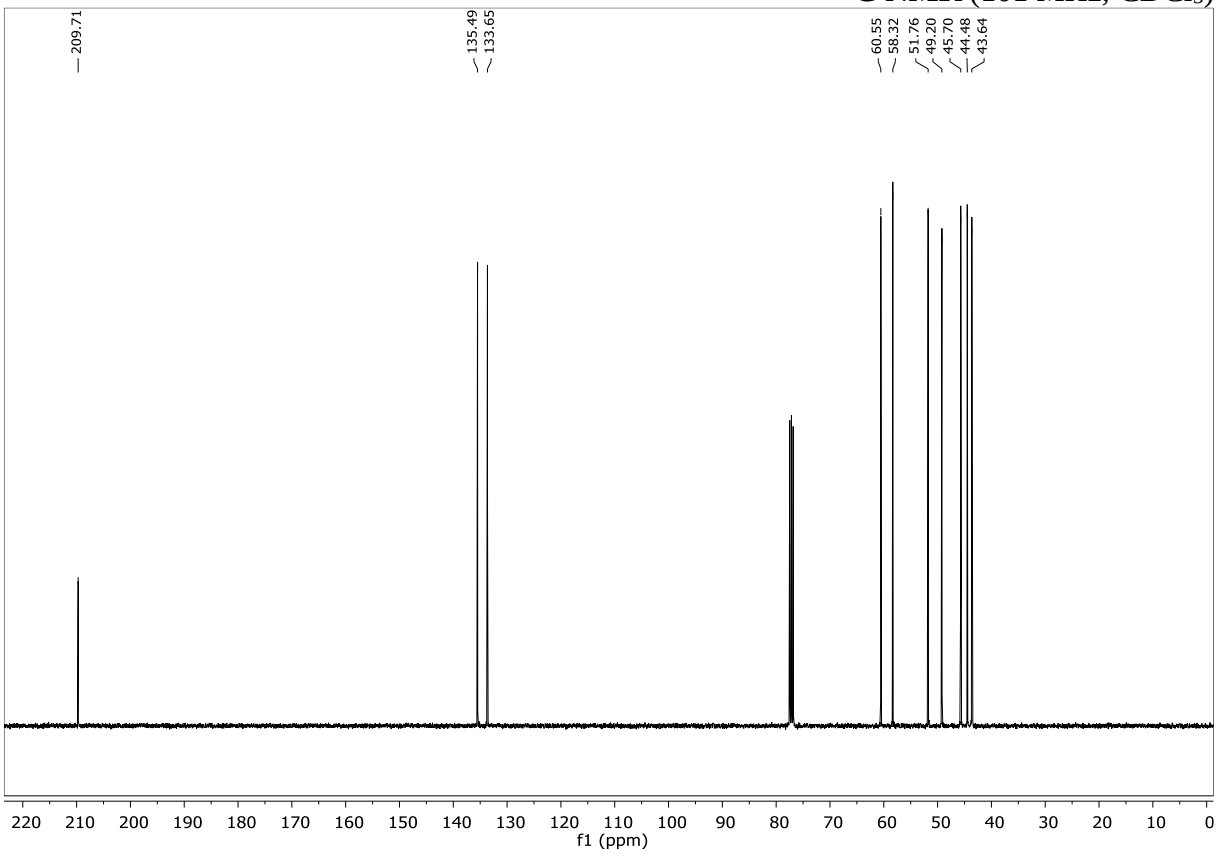

2*H*-Pyran-2-one (1)

^{1}H NMR (400 MHz, $CDCl_3$)

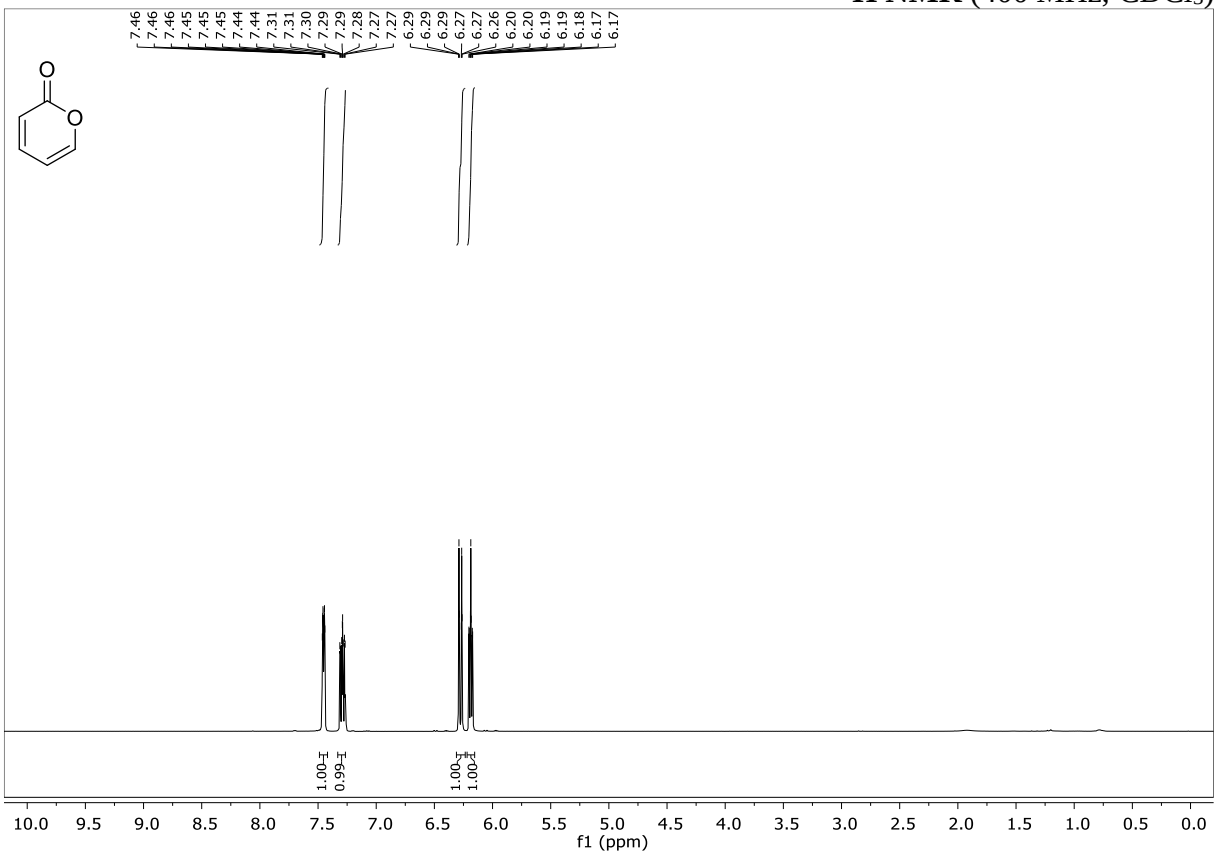

^{13}C NMR (101 MHz, $CDCl_3$)

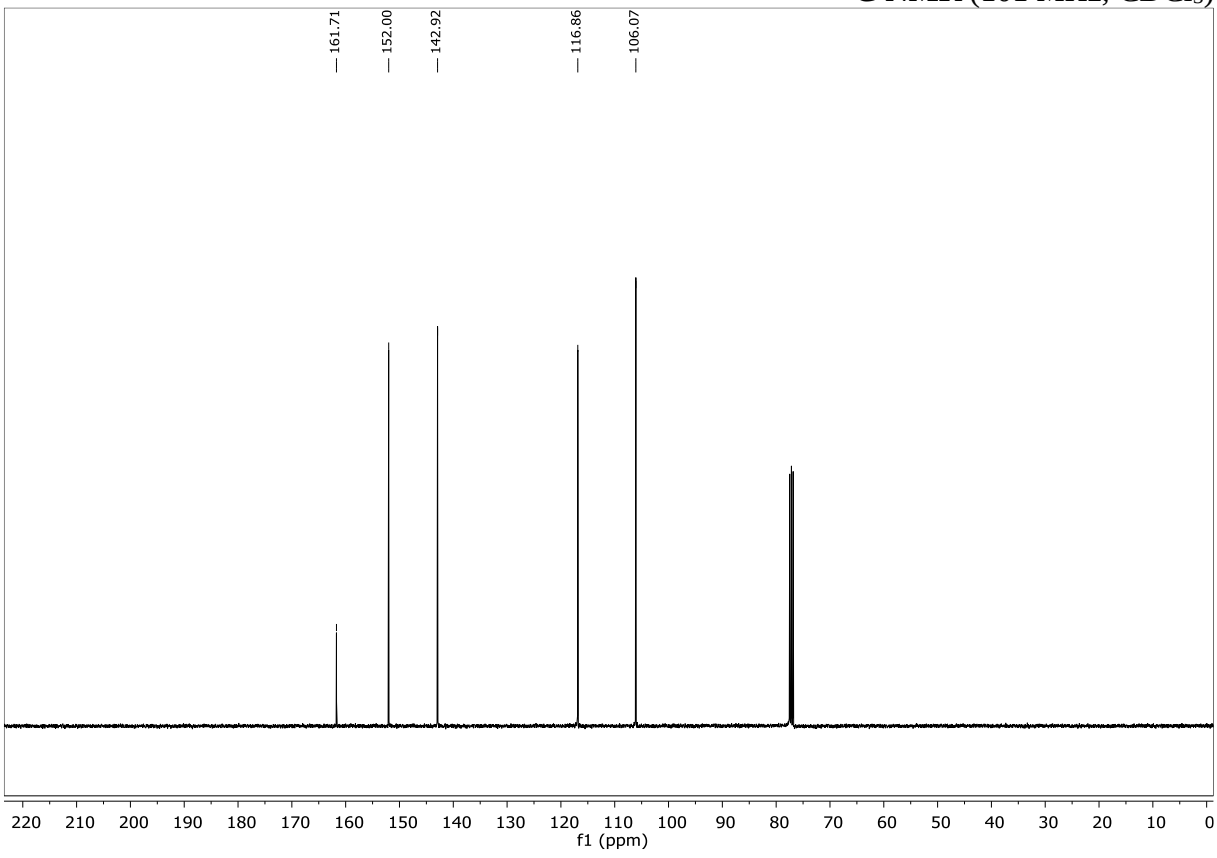

6-(1-Hydroxyethyl)-2*H*-pyran-2-one (26a)

^{1}H NMR (300 MHz, $CDCl_3$)

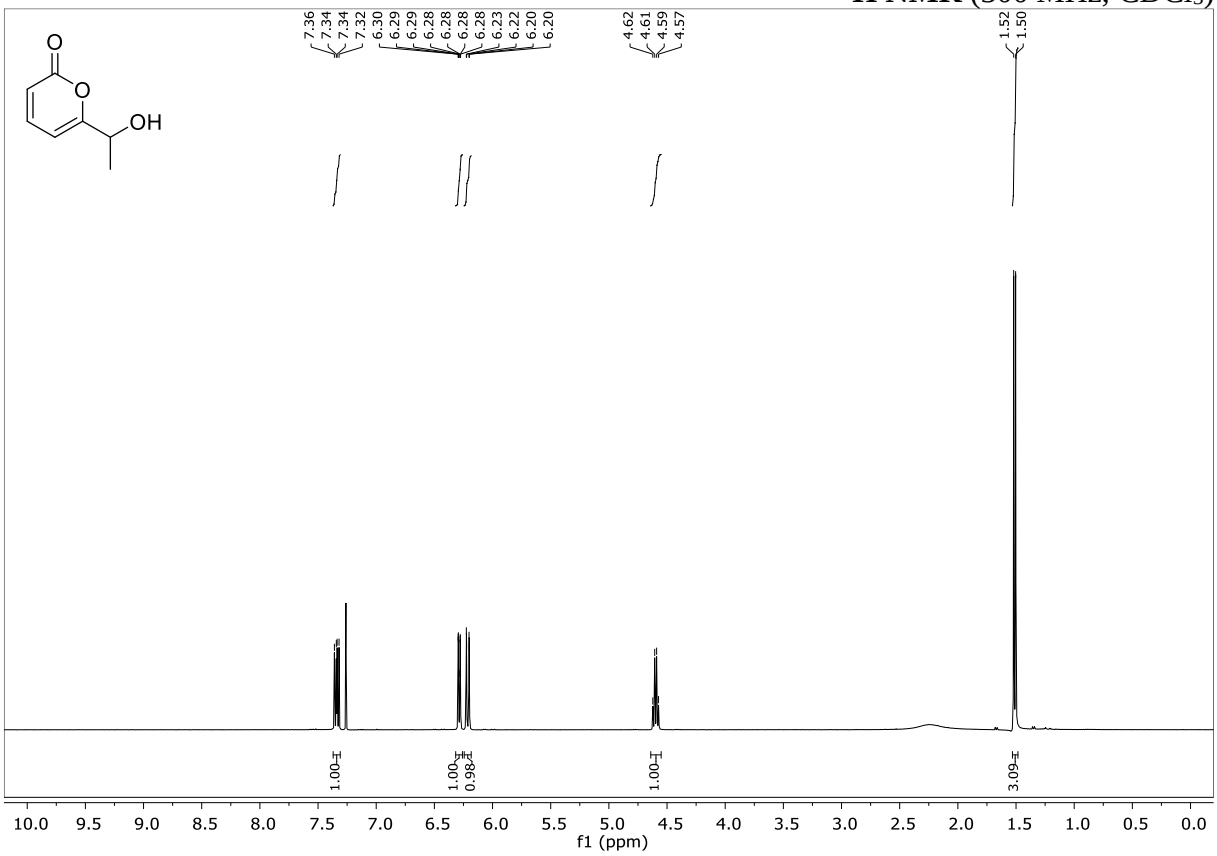

^{13}C NMR (75 MHz, $CDCl_3$)

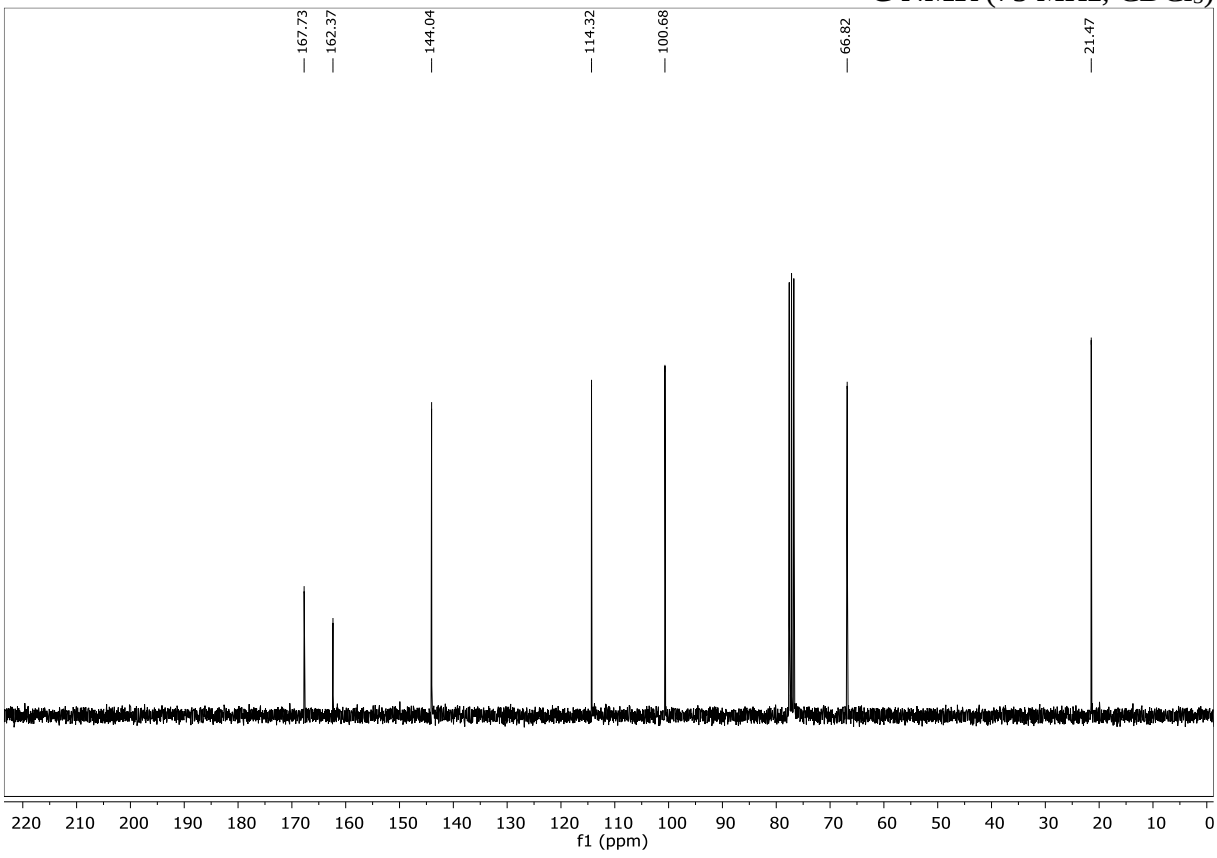

1-(Furan-2-yl)butan-1-ol (314a)

^{1}H NMR (300 MHz, $CDCl_3$)

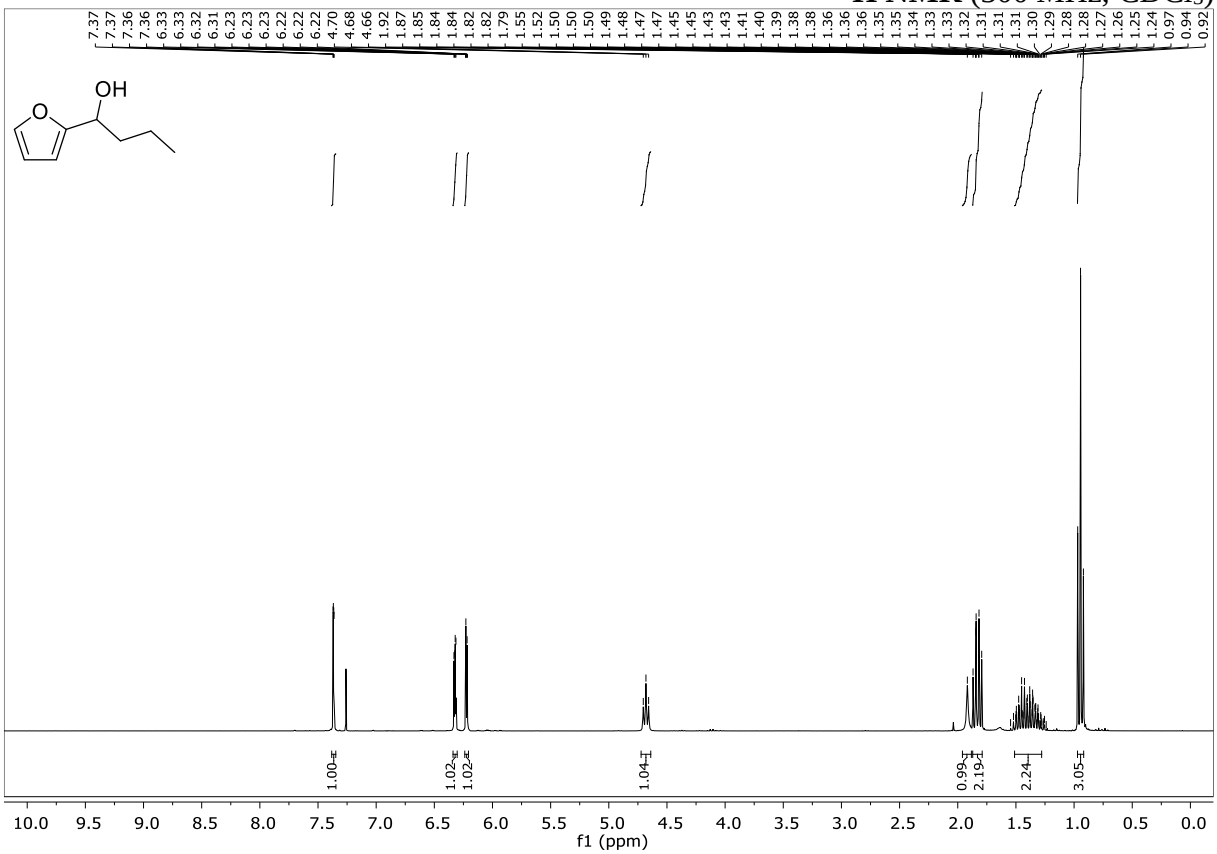

^{13}C NMR (75 MHz, $CDCl_3$)

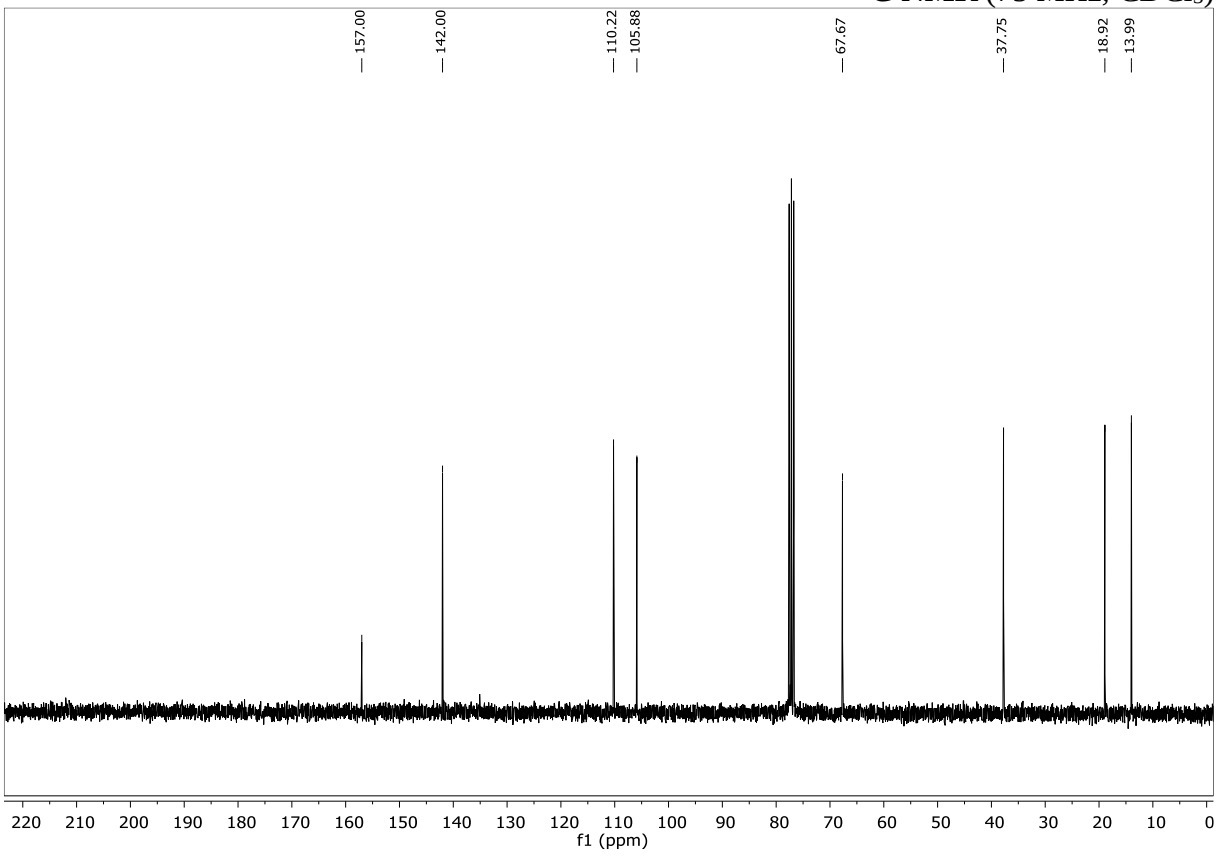

1-(Furan-2-yl)hexan-1-ol (314b)

^{1}H NMR (300 MHz, $CDCl_3$)

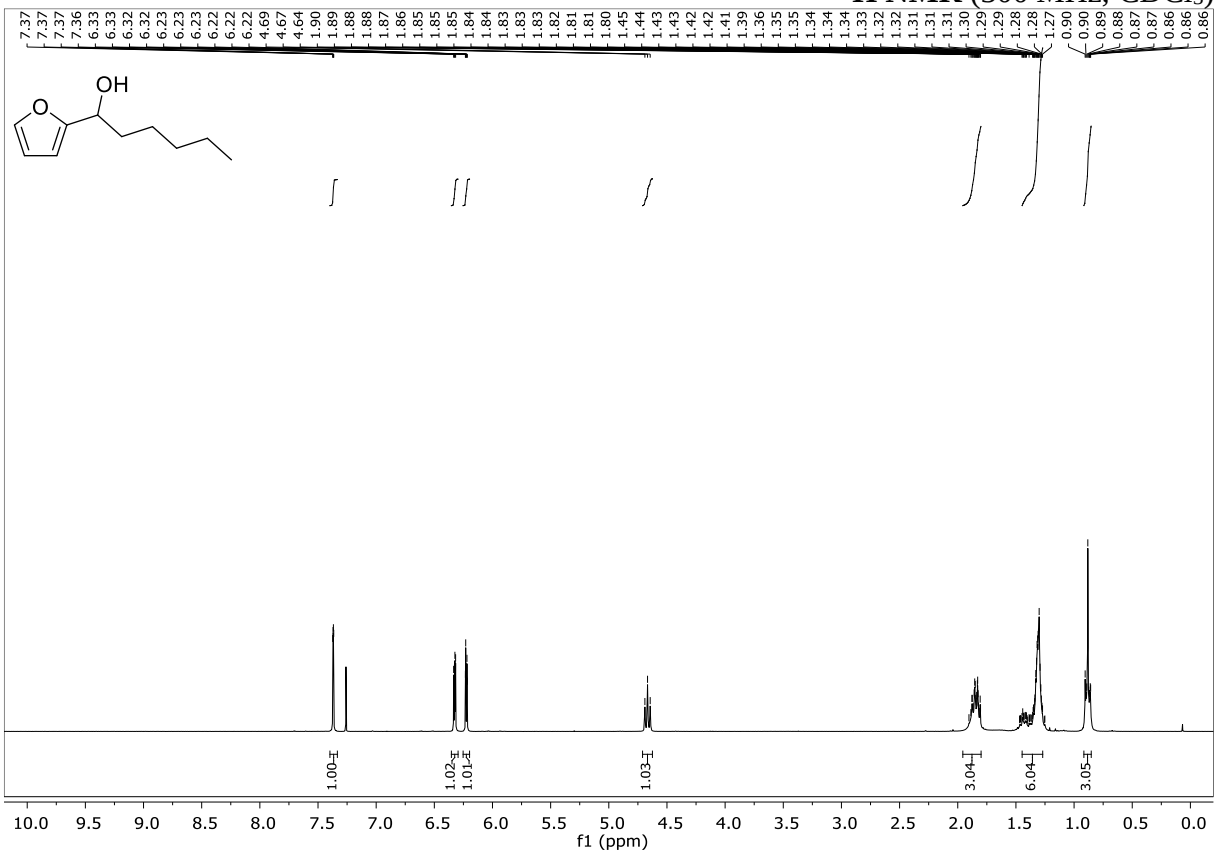

^{13}C NMR (75 MHz, $CDCl_3$)

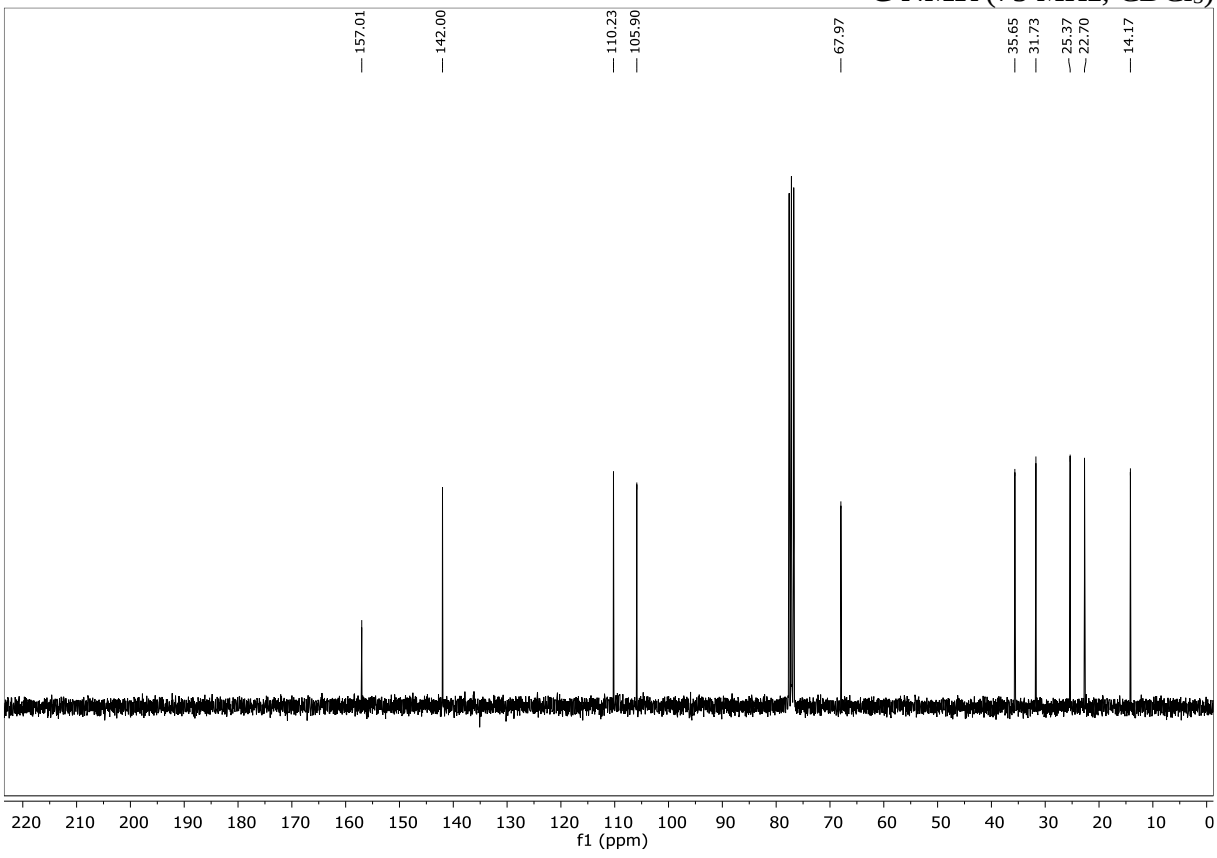

1-(Furan-2-yl)octan-1-ol (314c)

^{1}H NMR (300 MHz, $CDCl_3$)

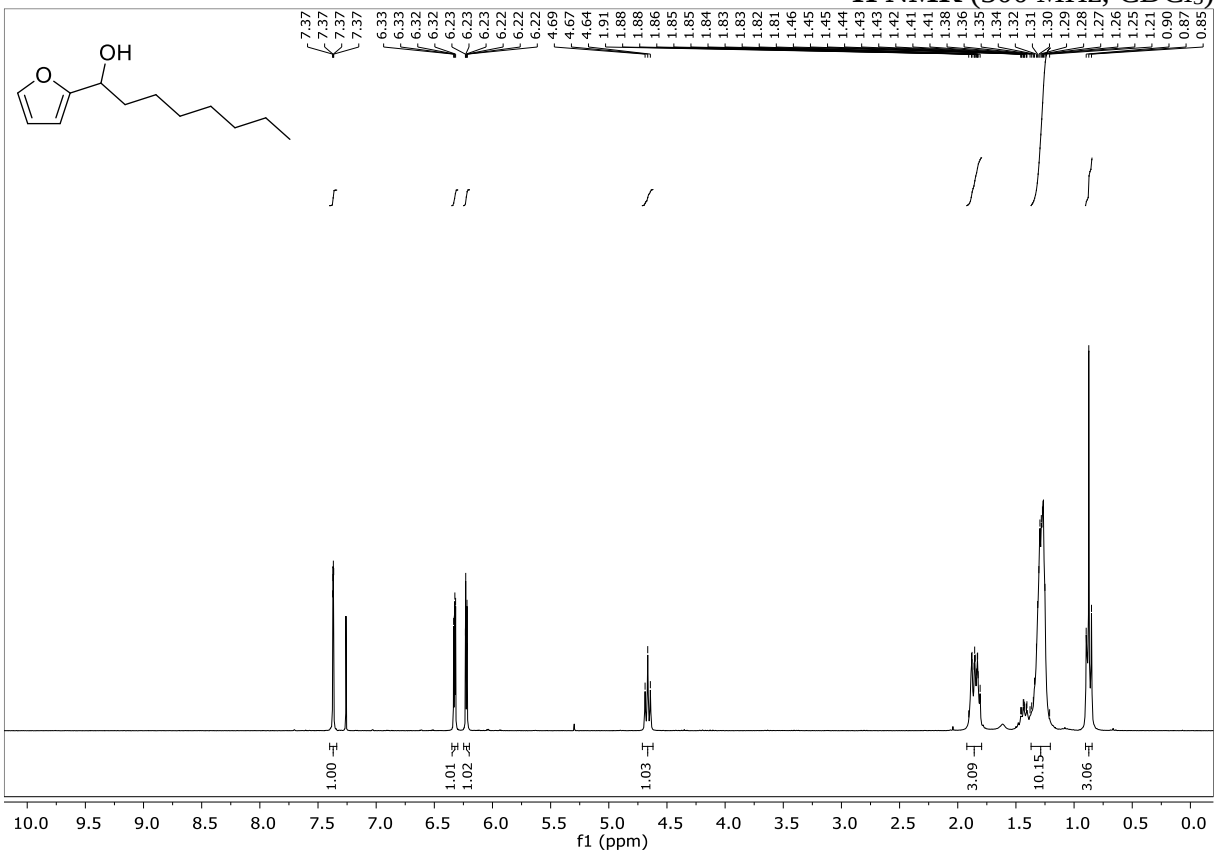

^{13}C NMR (75 MHz, $CDCl_3$)

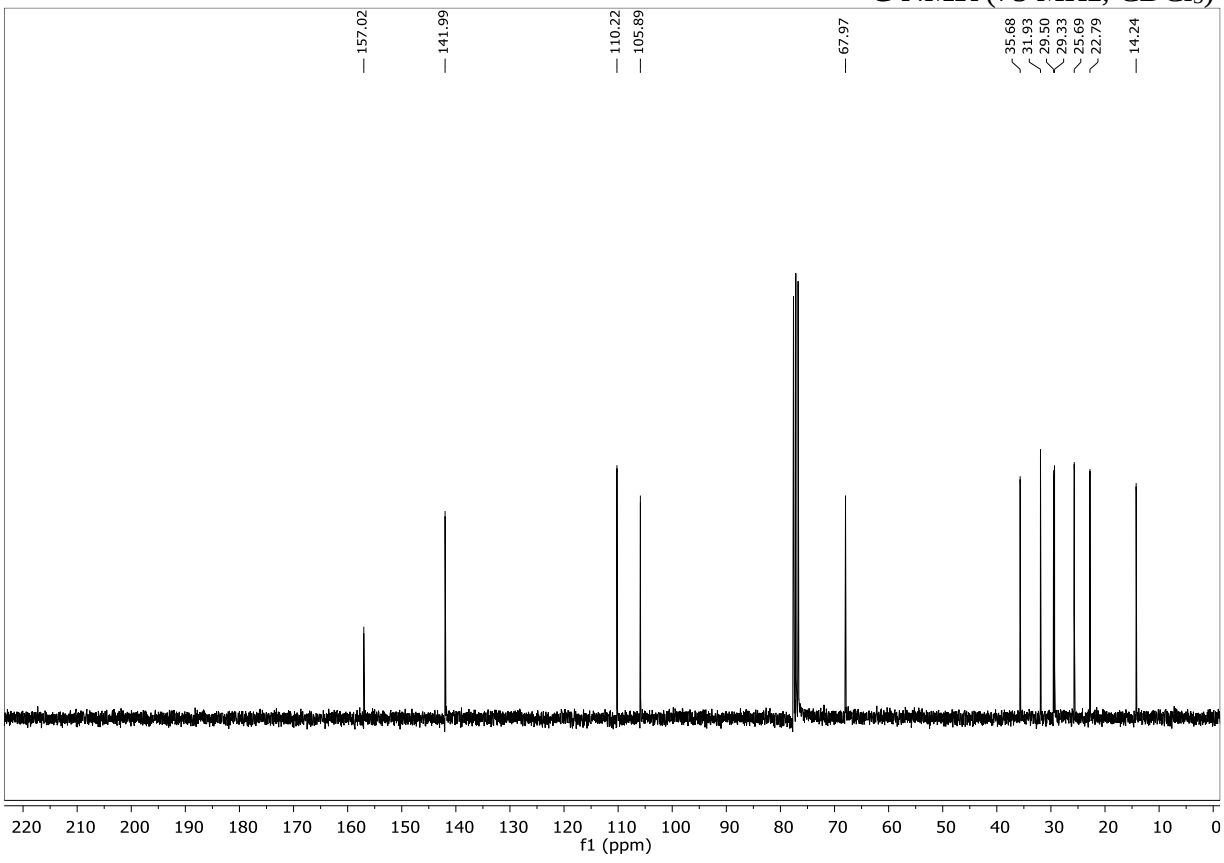

4-Hydroxy-5-propylcyclopent-2-en-1-one (315a)

^{1}H NMR (300 MHz, $CDCl_3$)

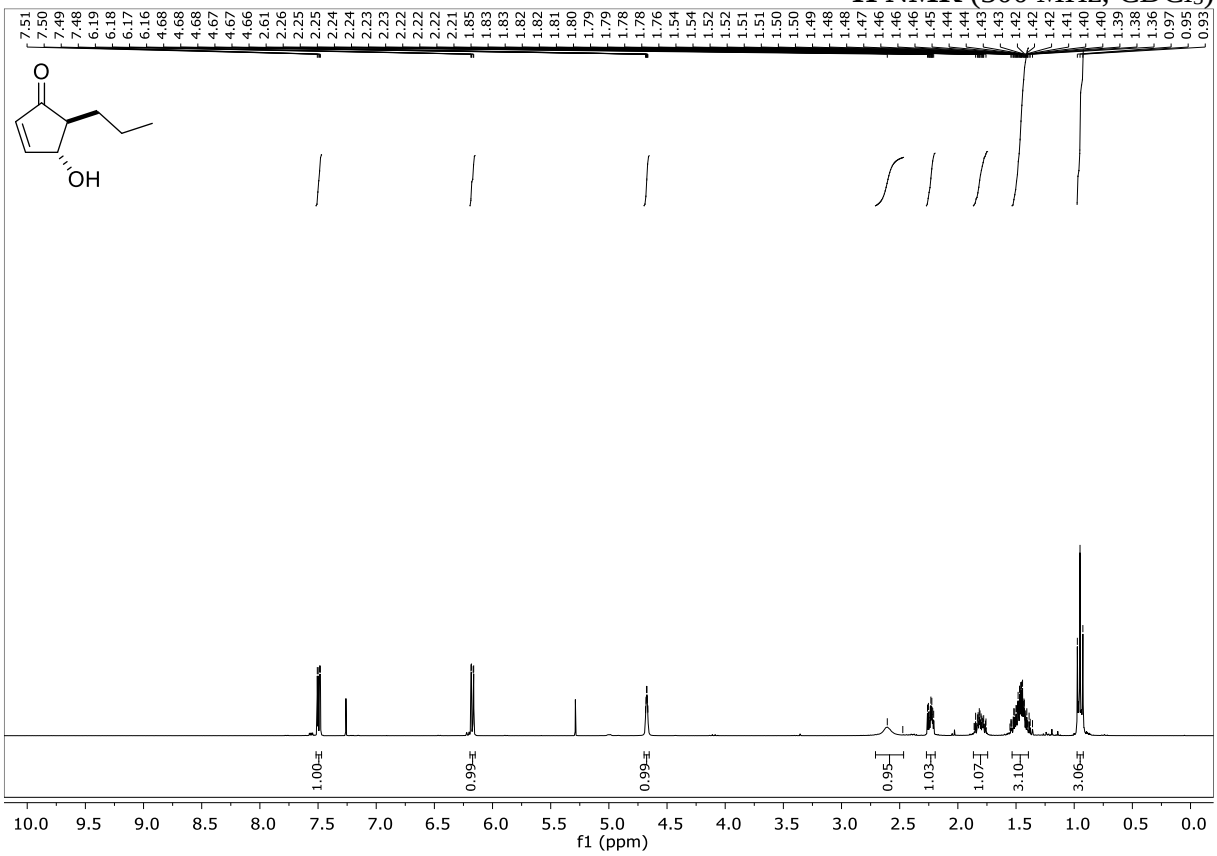

^{13}C NMR (75 MHz, $CDCl_3$)

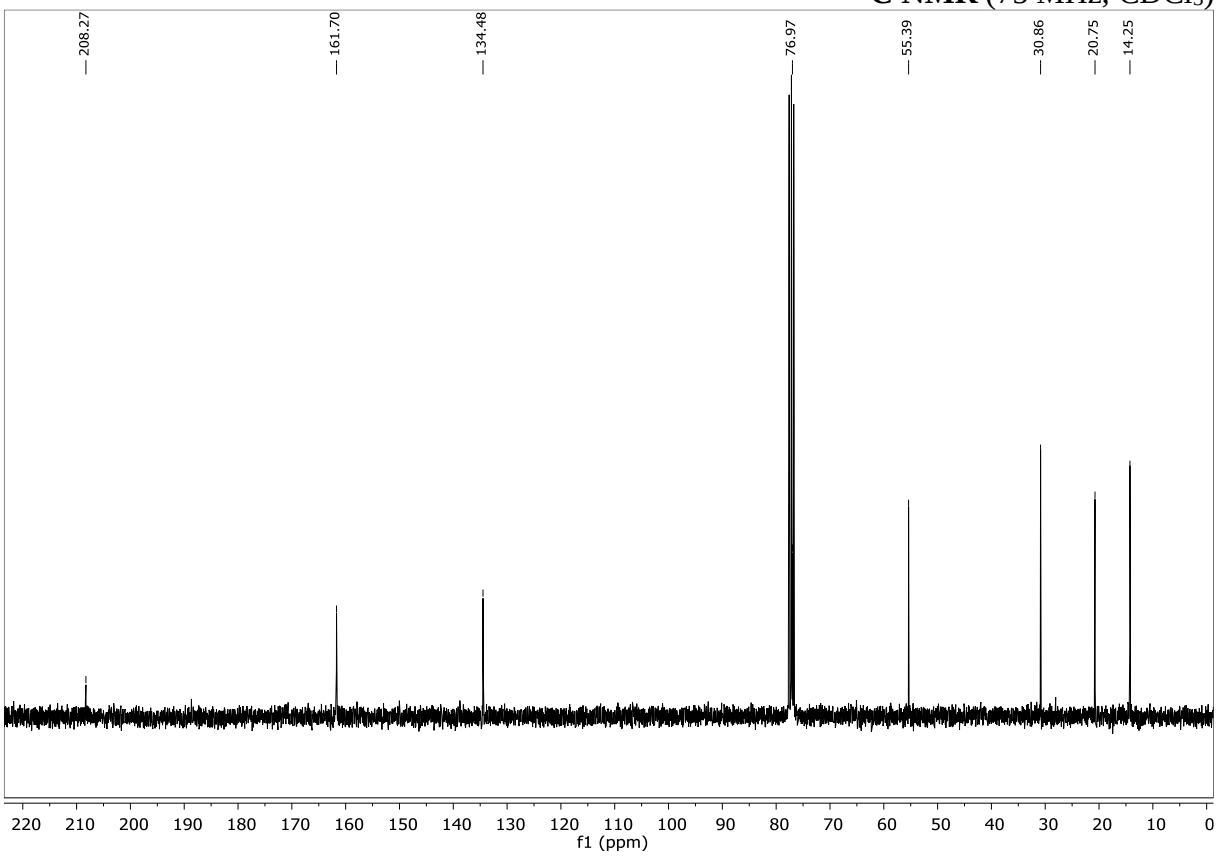

4-Hydroxy-5-pentylcyclopent-2-en-1-one (315b)

^{1}H NMR (400 MHz, $CDCl_3$)

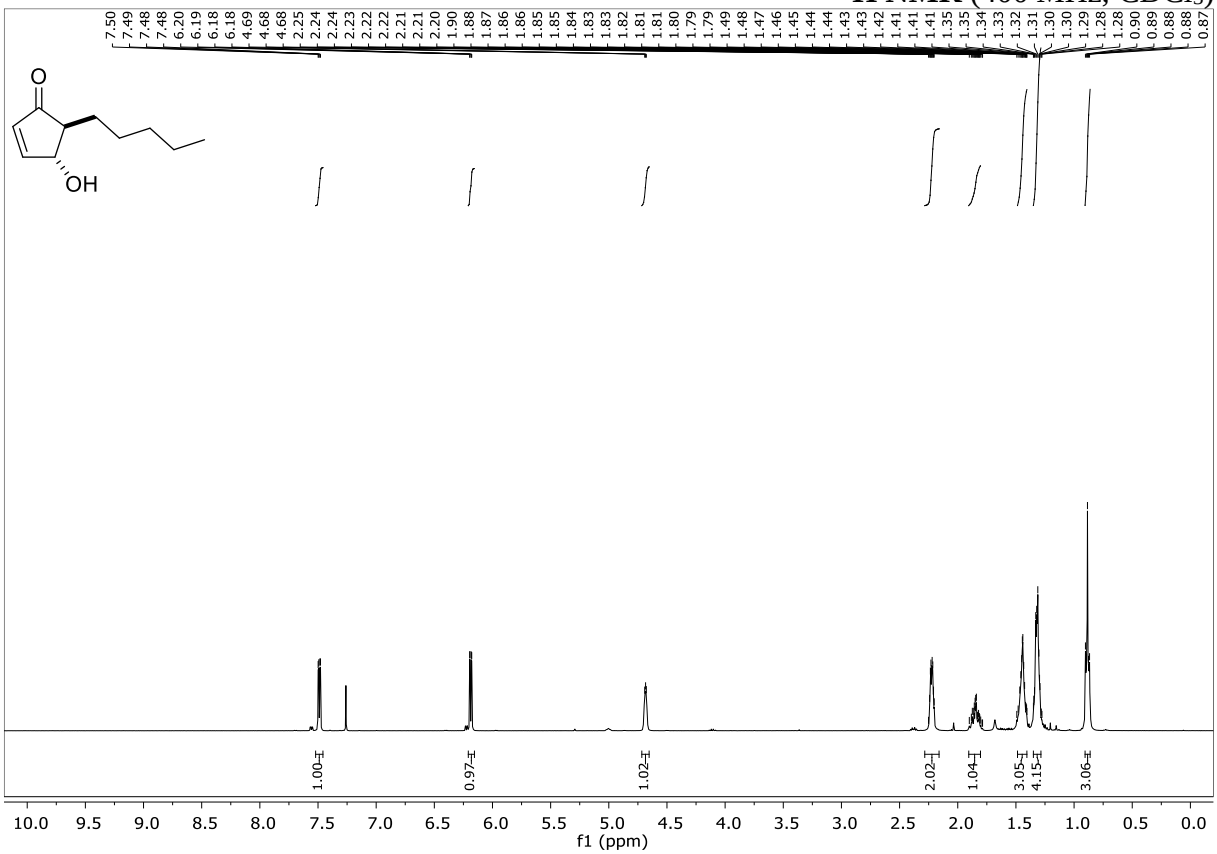

^{13}C NMR (75 MHz, $CDCl_3$)

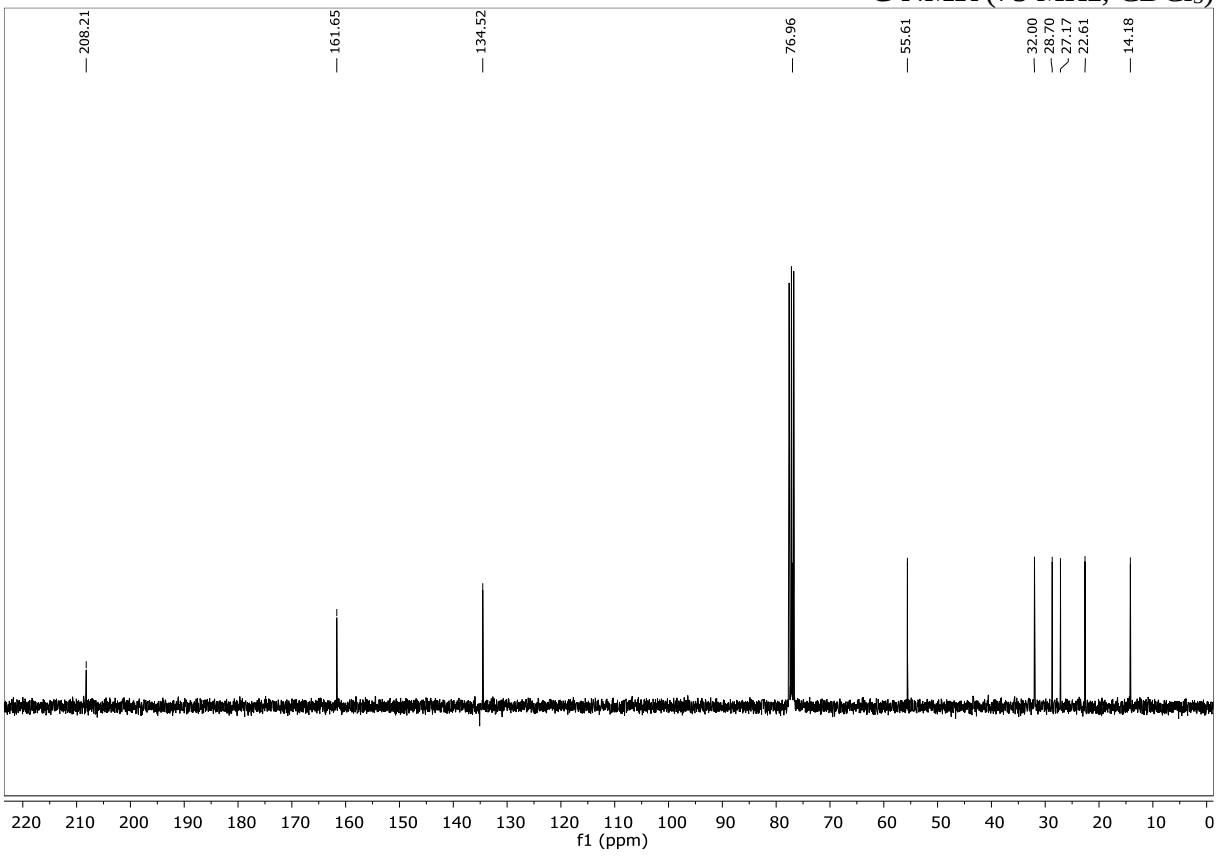

5-Heptyl-4-hydroxycyclopent-2-en-1-one (315c)

^{1}H NMR (300 MHz, $CDCl_3$)

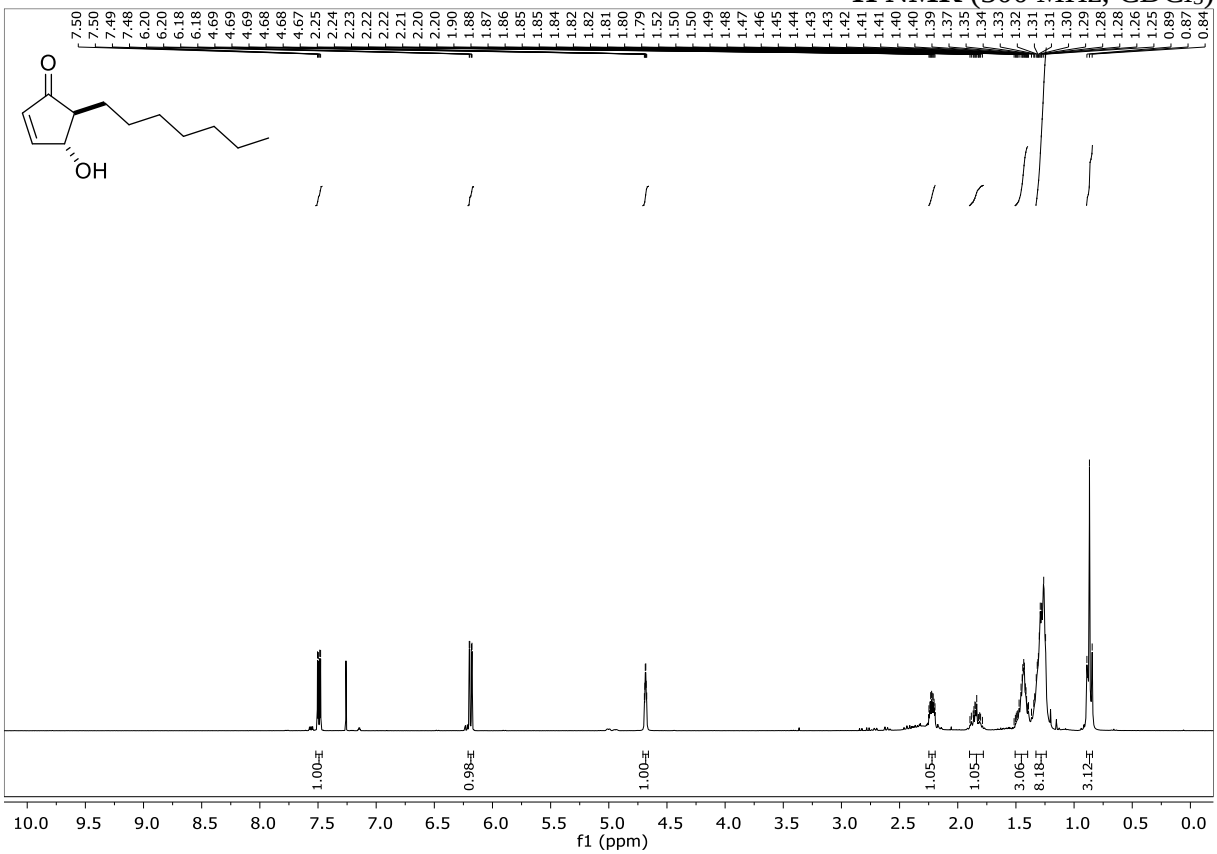

^{13}C NMR (75 MHz, $CDCl_3$)

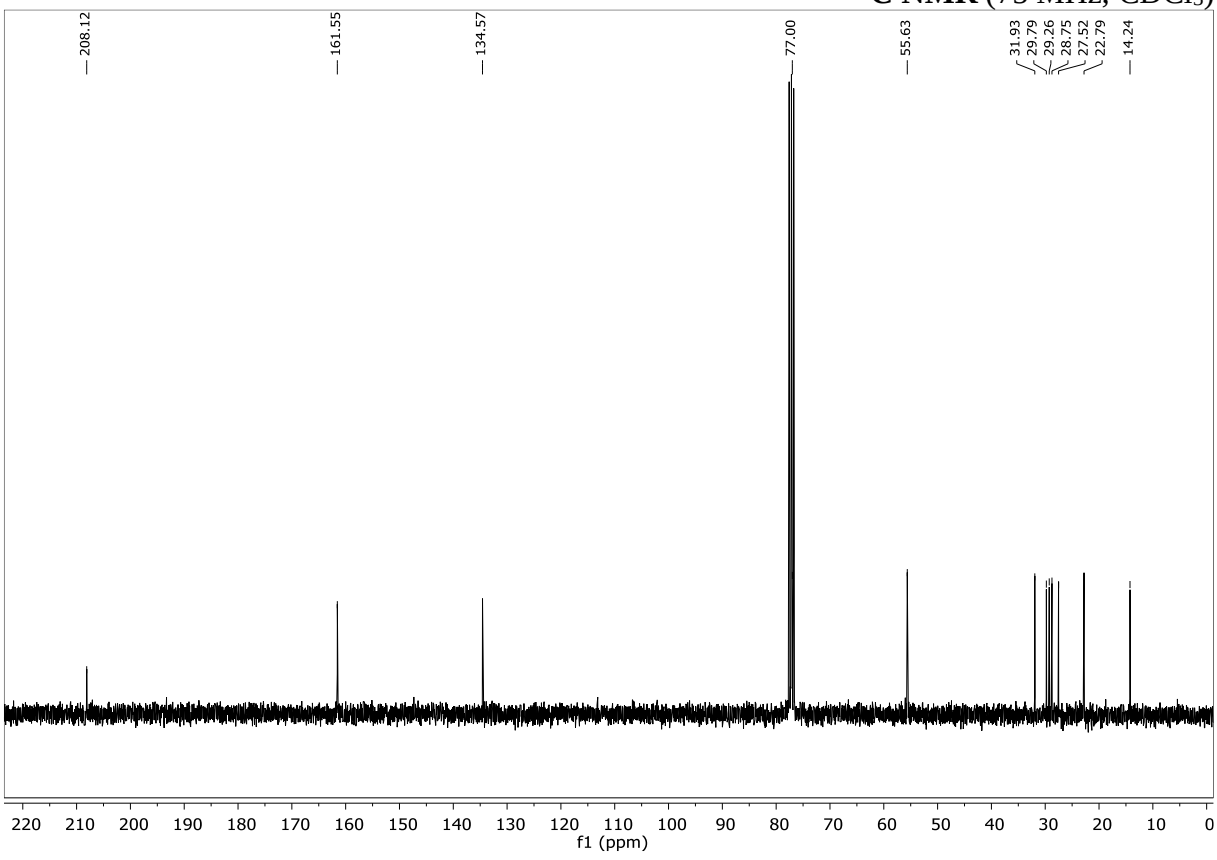

4-Oxo-5-propylcyclopent-2-en-1-yl acetate (316a)

^{1}H NMR (300 MHz, $CDCl_3$)

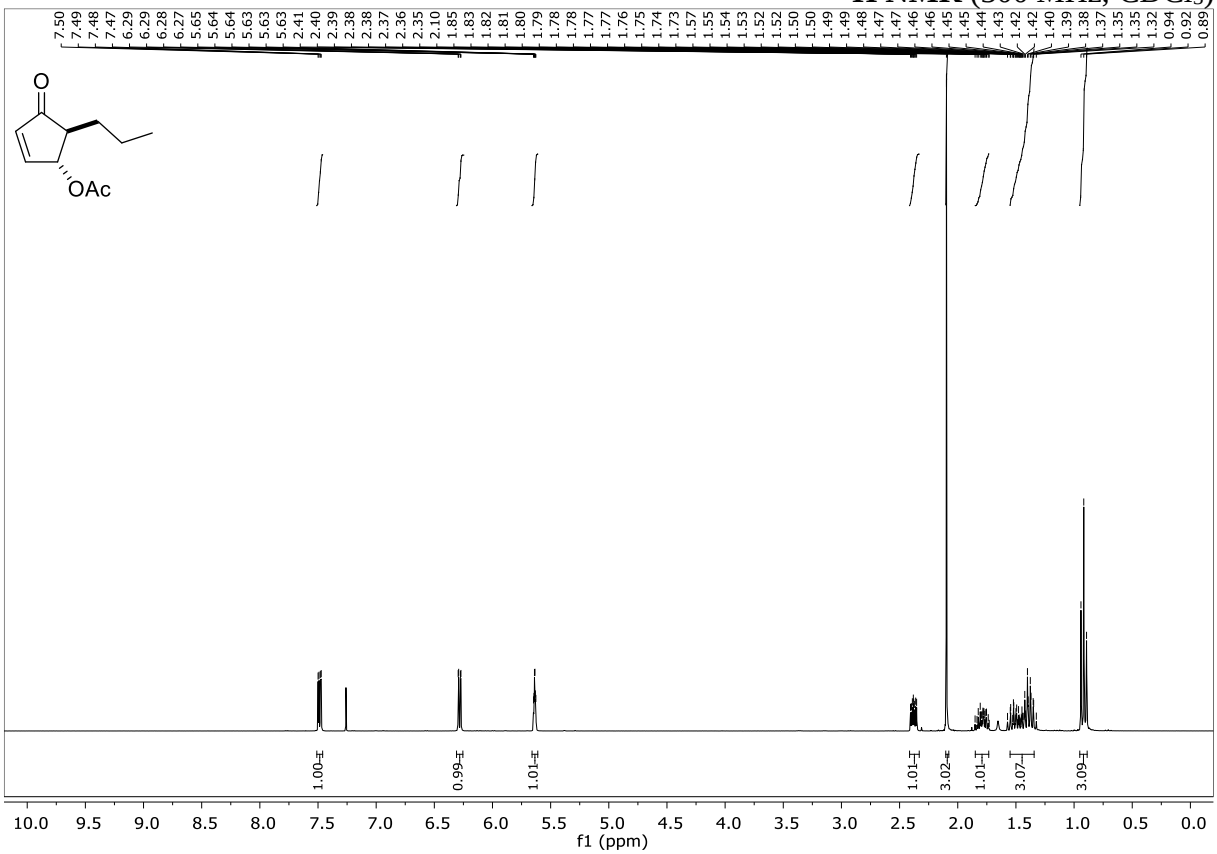

^{13}C NMR (75 MHz, $CDCl_3$)

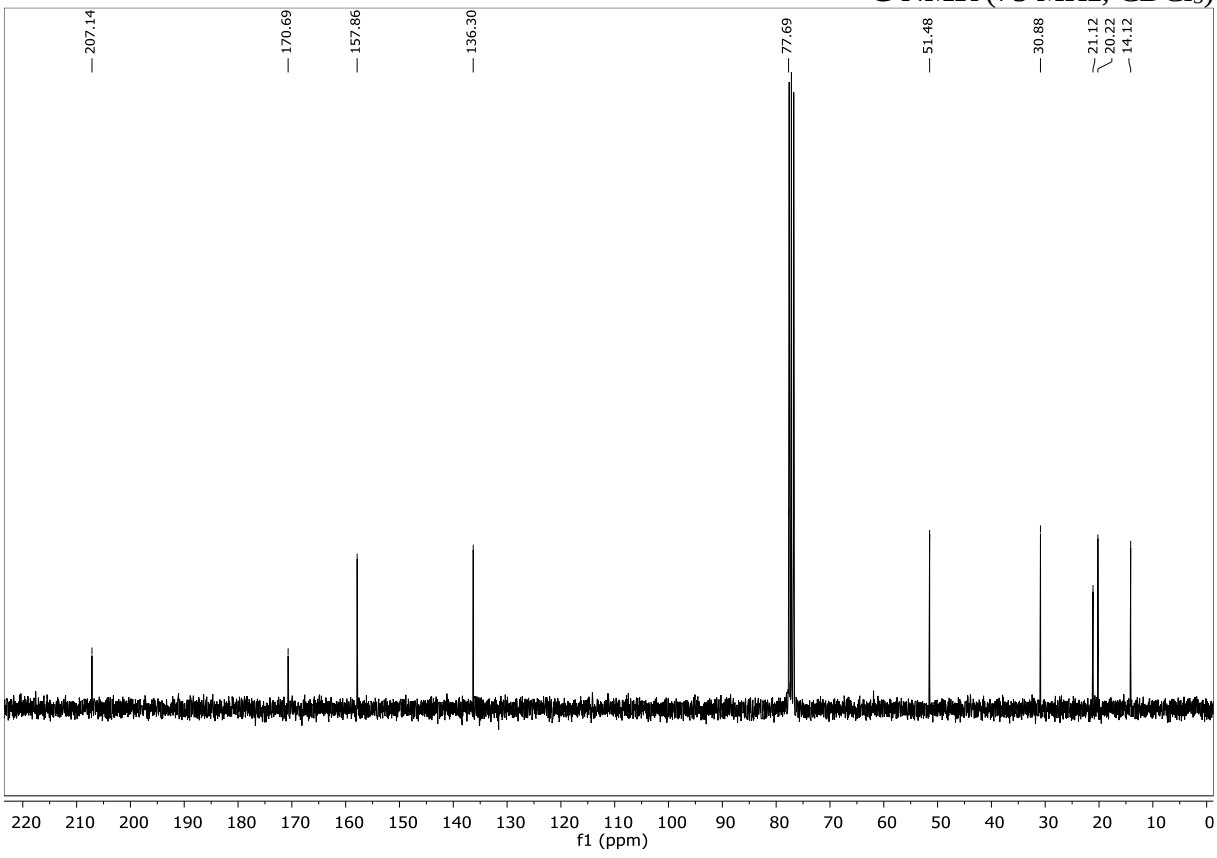

4-Oxo-5-pentylcyclopent-2-en-1-yl acetate (316b)

^{1}H NMR (300 MHz, $CDCl_3$)

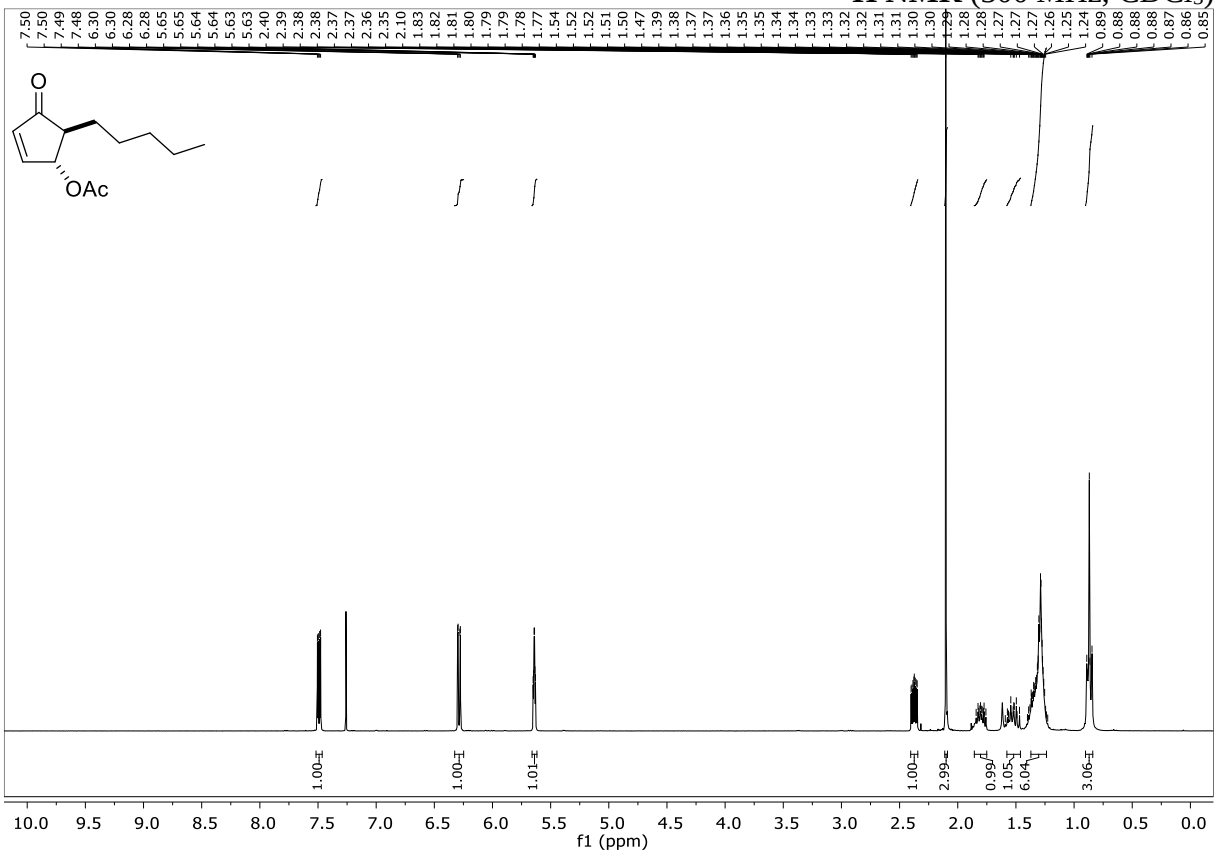

^{13}C NMR (75 MHz, $CDCl_3$)

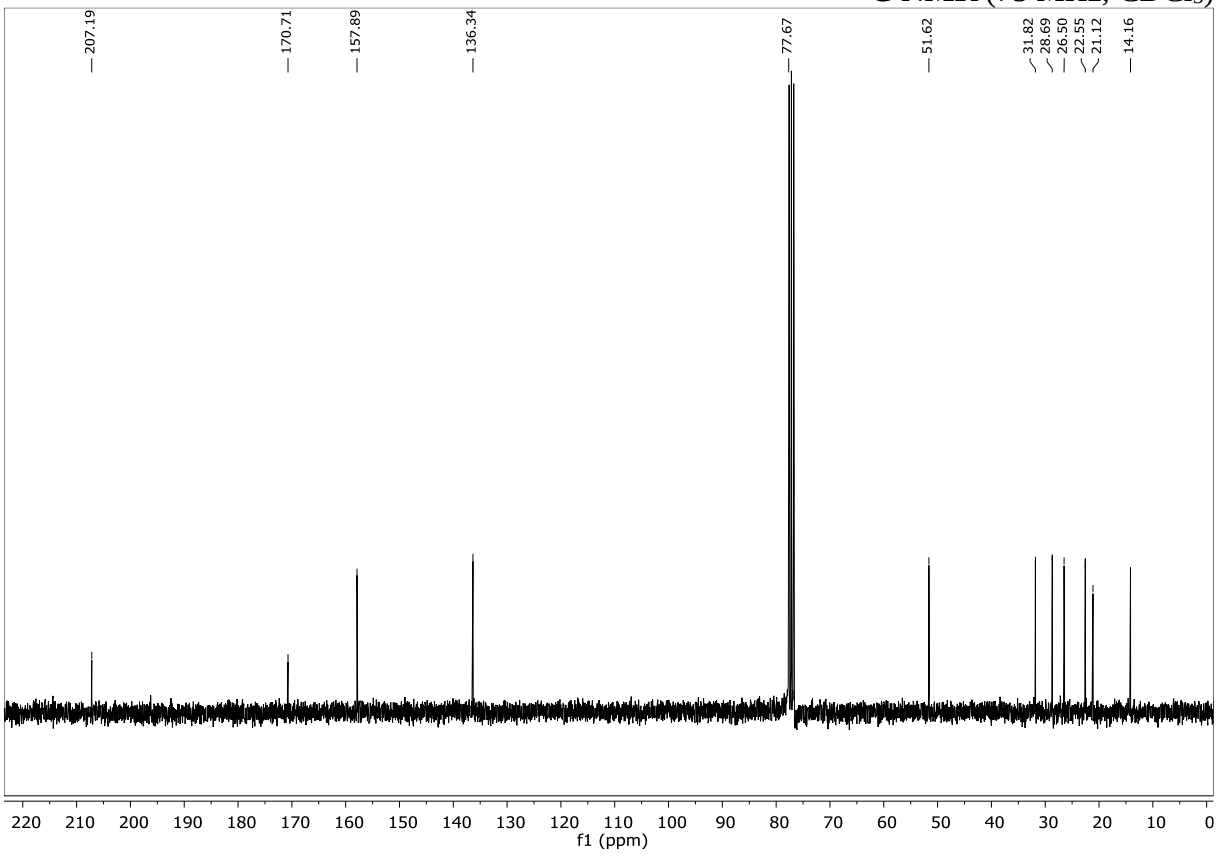

5-Heptyl-4-oxocyclopent-2-en-1-yl acetate (316c)

^{1}H NMR (300 MHz, $CDCl_3$)

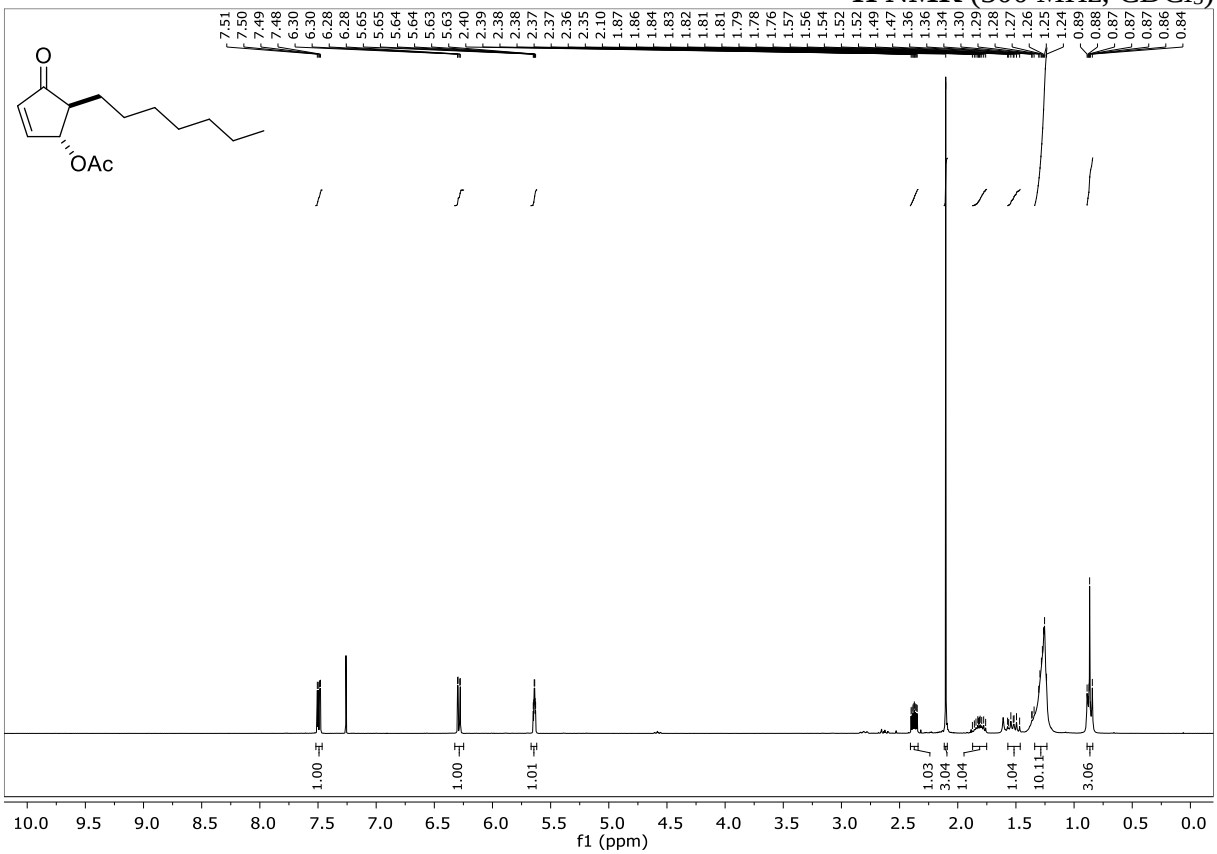

^{13}C NMR (75 MHz, $CDCl_3$)

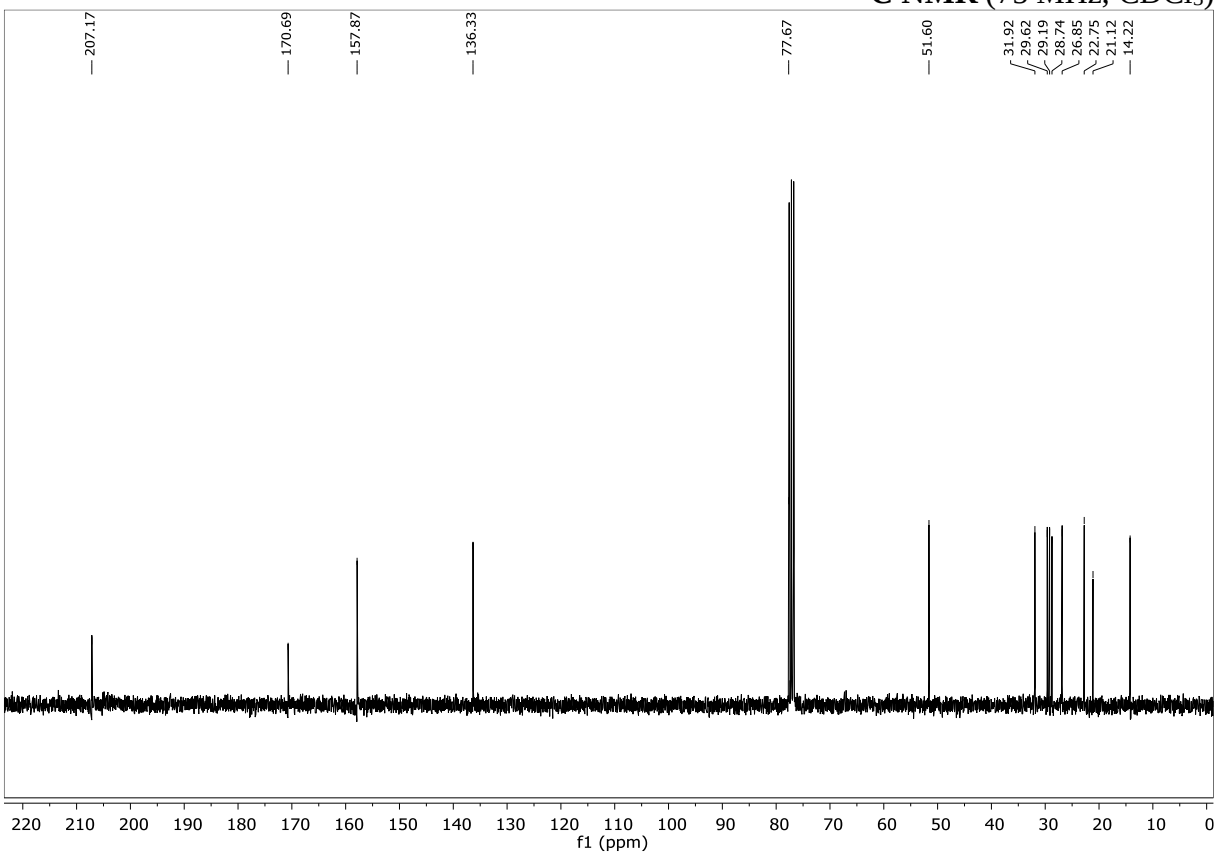

2-Propyl-3a,4,7,7a-tetrahydro-1*H*-4,7-methanoinden-1-one (317a)

^{1}H NMR (300 MHz, $CDCl_3$)

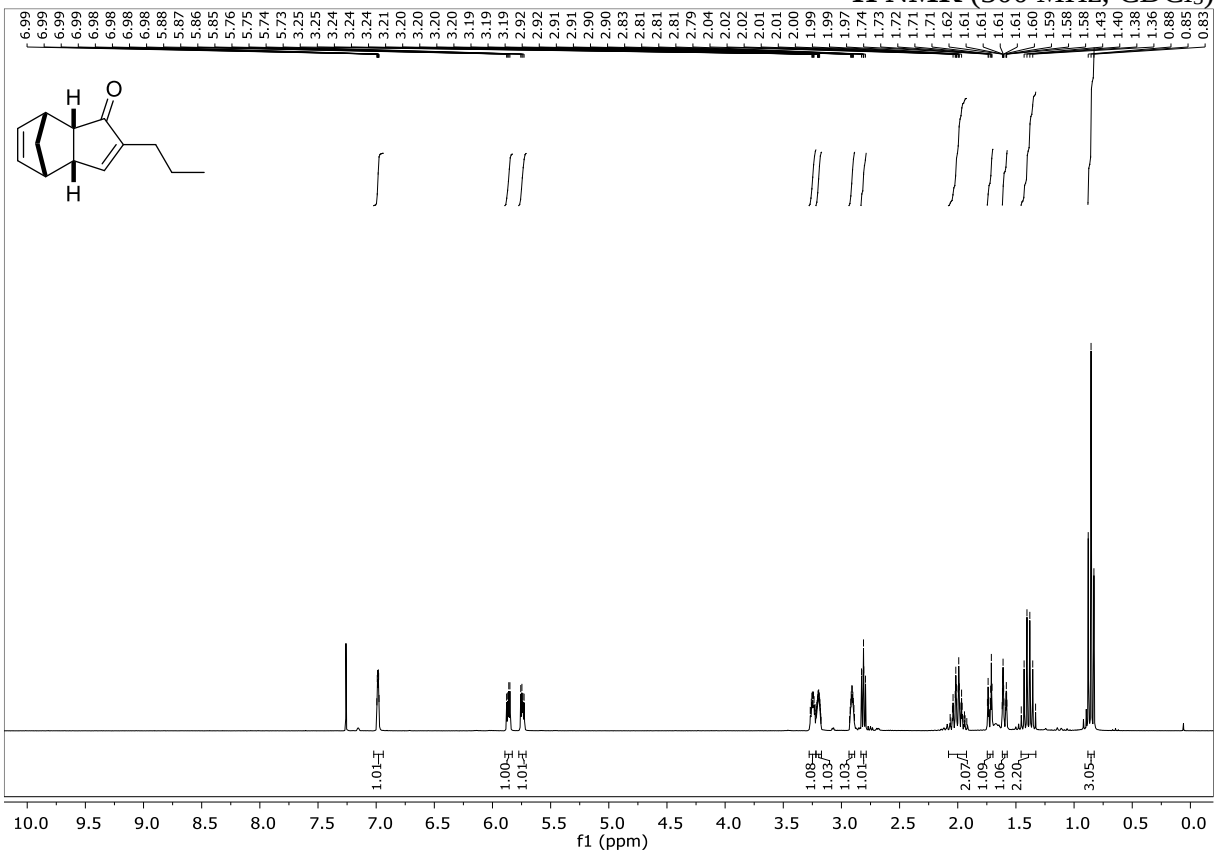

^{13}C NMR (75 MHz, $CDCl_3$)

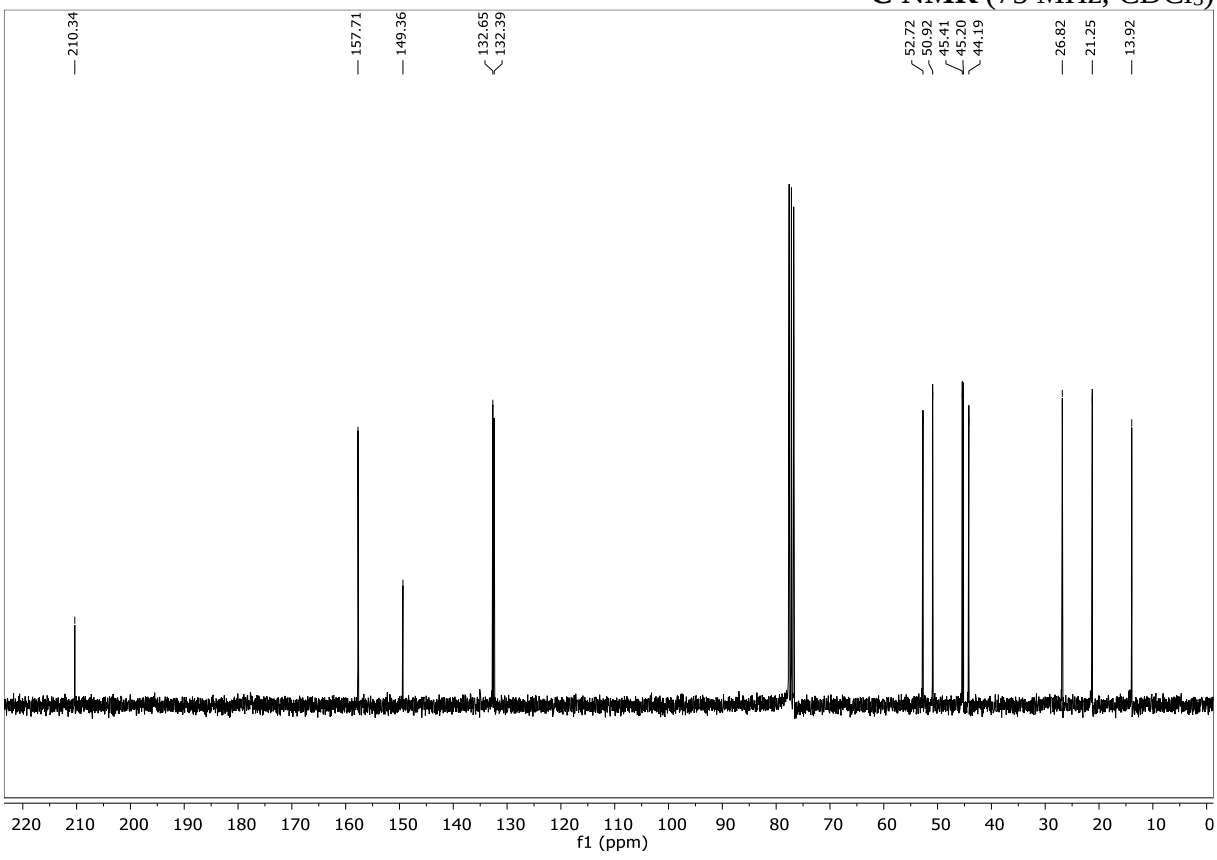

2-Pentyl-3a,4,7,7a-tetrahydro-1*H*-4,7-methanoinden-1-one (317b)

^{1}H NMR (400 MHz, $CDCl_3$)

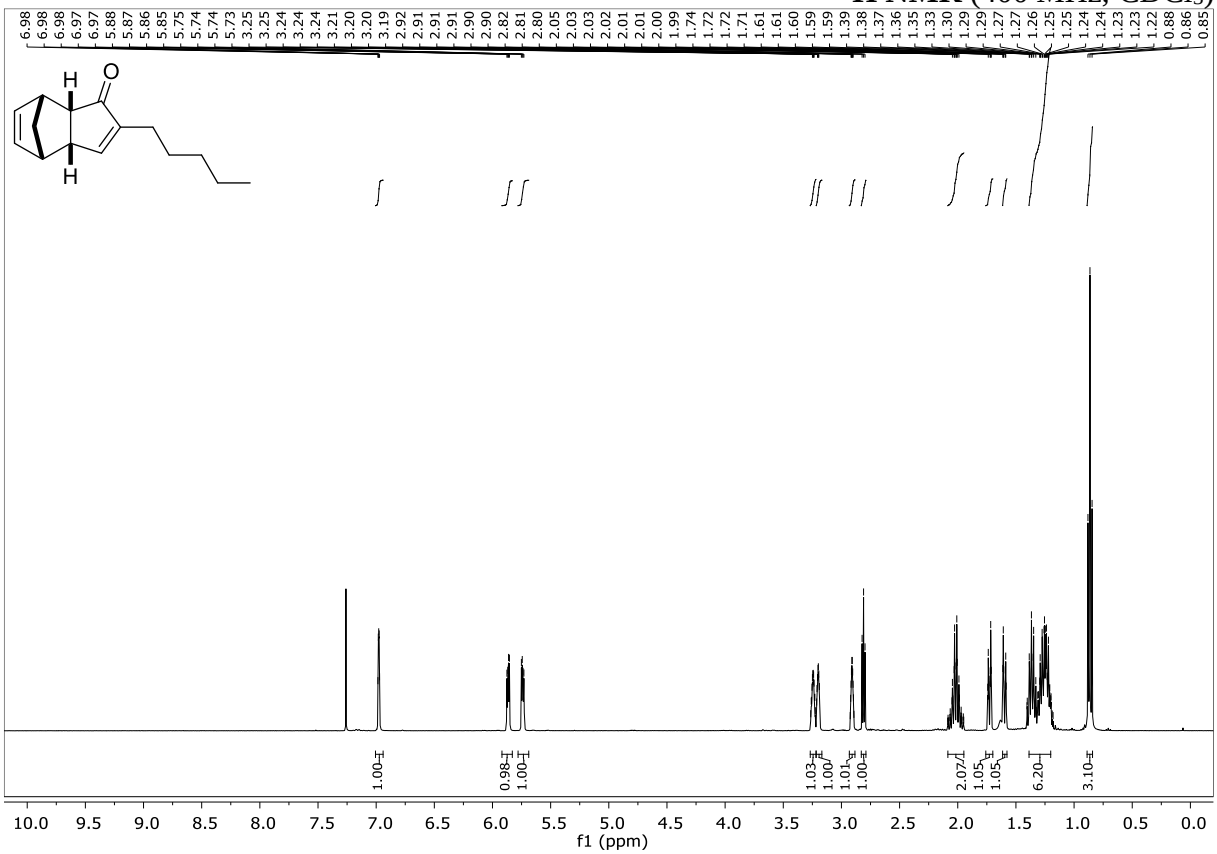

^{13}C NMR (75 MHz, $CDCl_3$)

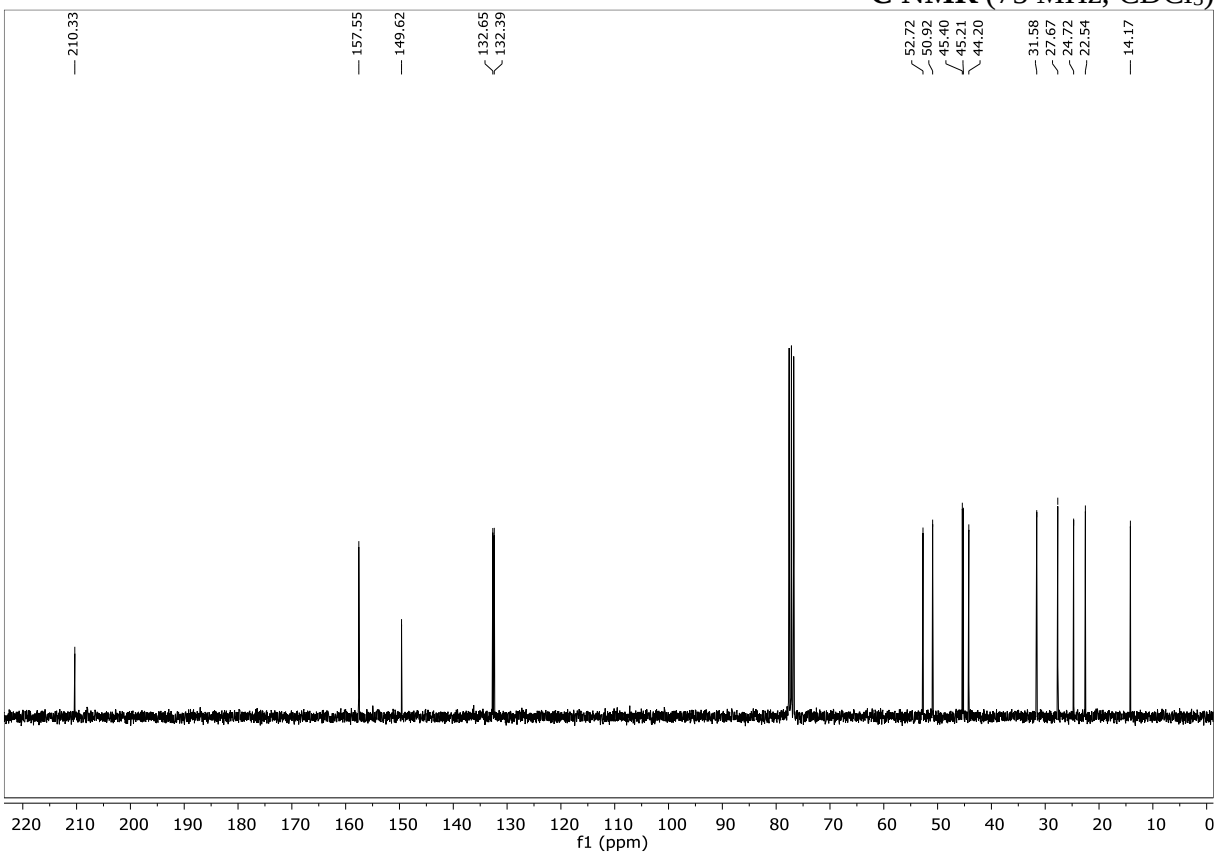

2-Heptyl-3a,4,7,7a-tetrahydro-1*H*-4,7-methanoinden-1-one (317c)

^{1}H NMR (300 MHz, $CDCl_3$)

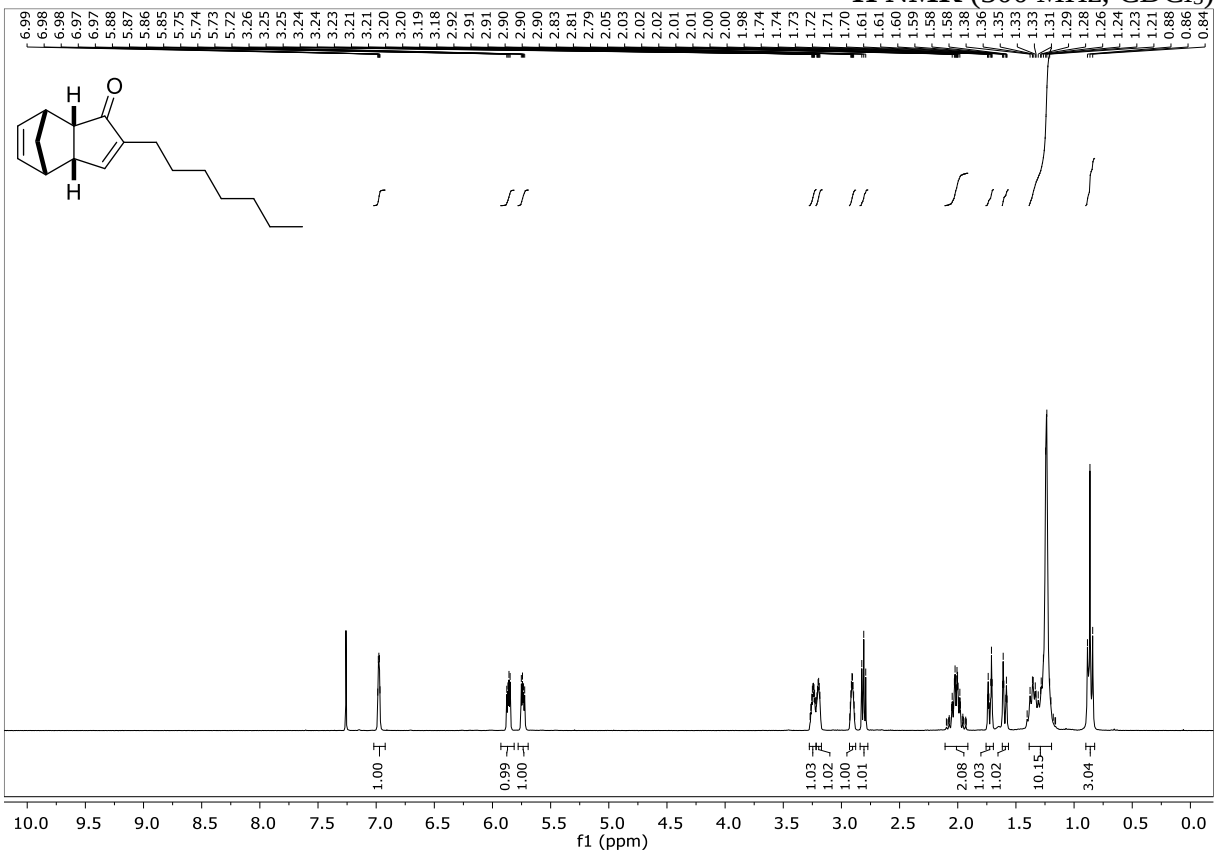

^{13}C NMR (75 MHz, $CDCl_3$)

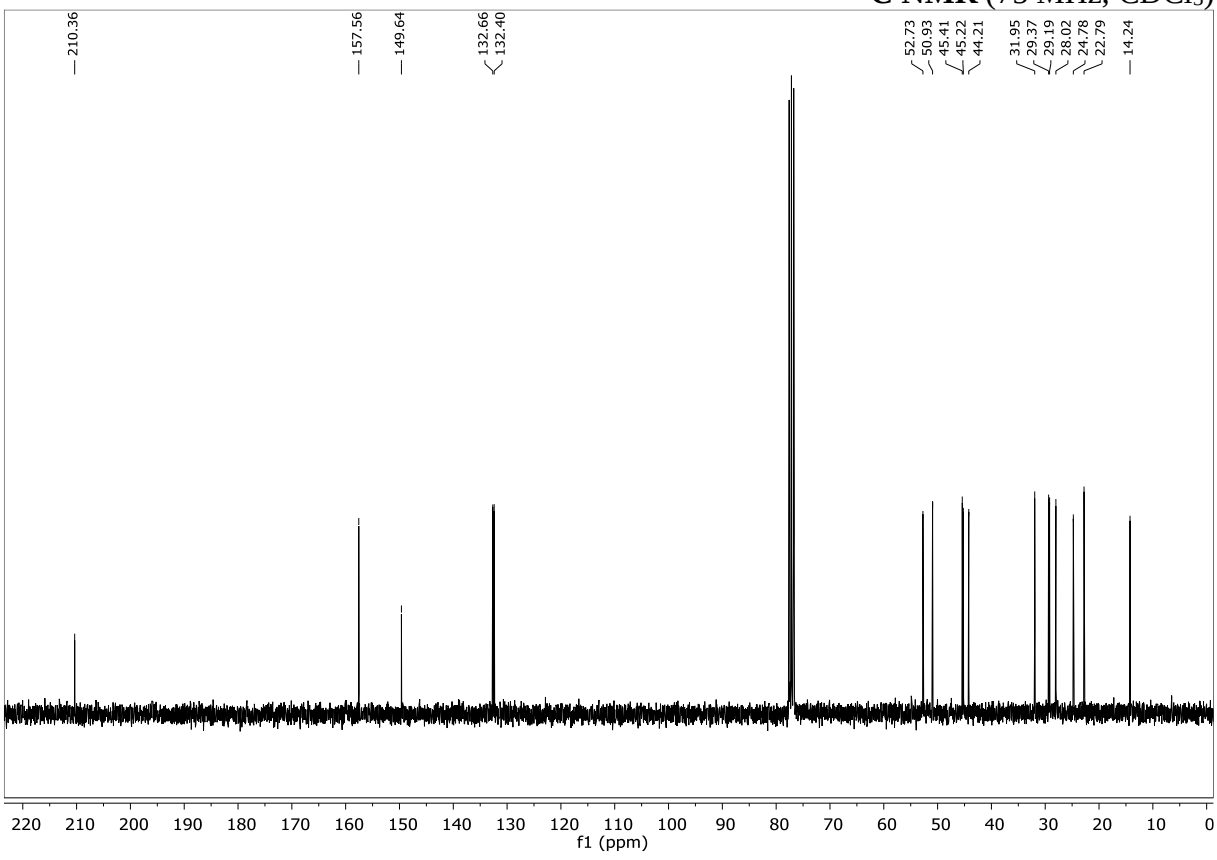

6a-Propyl-1a,1b,2,5,5a,6a-hexahydro-6*H*-2,5-methanoindeno[1,2-*b*]oxiren-6-one (318a)

^{1}H NMR (300 MHz, $CDCl_3$)

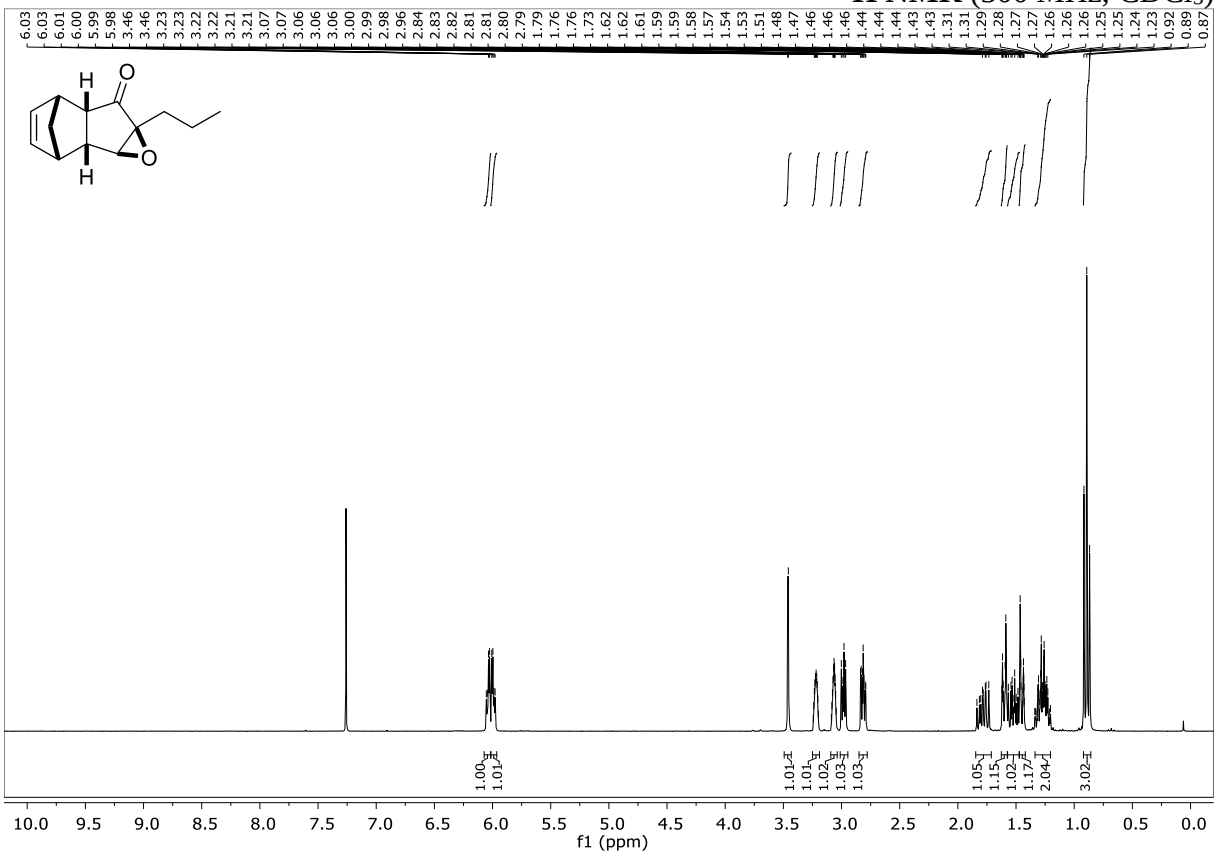

^{13}C NMR (75 MHz, $CDCl_3$)

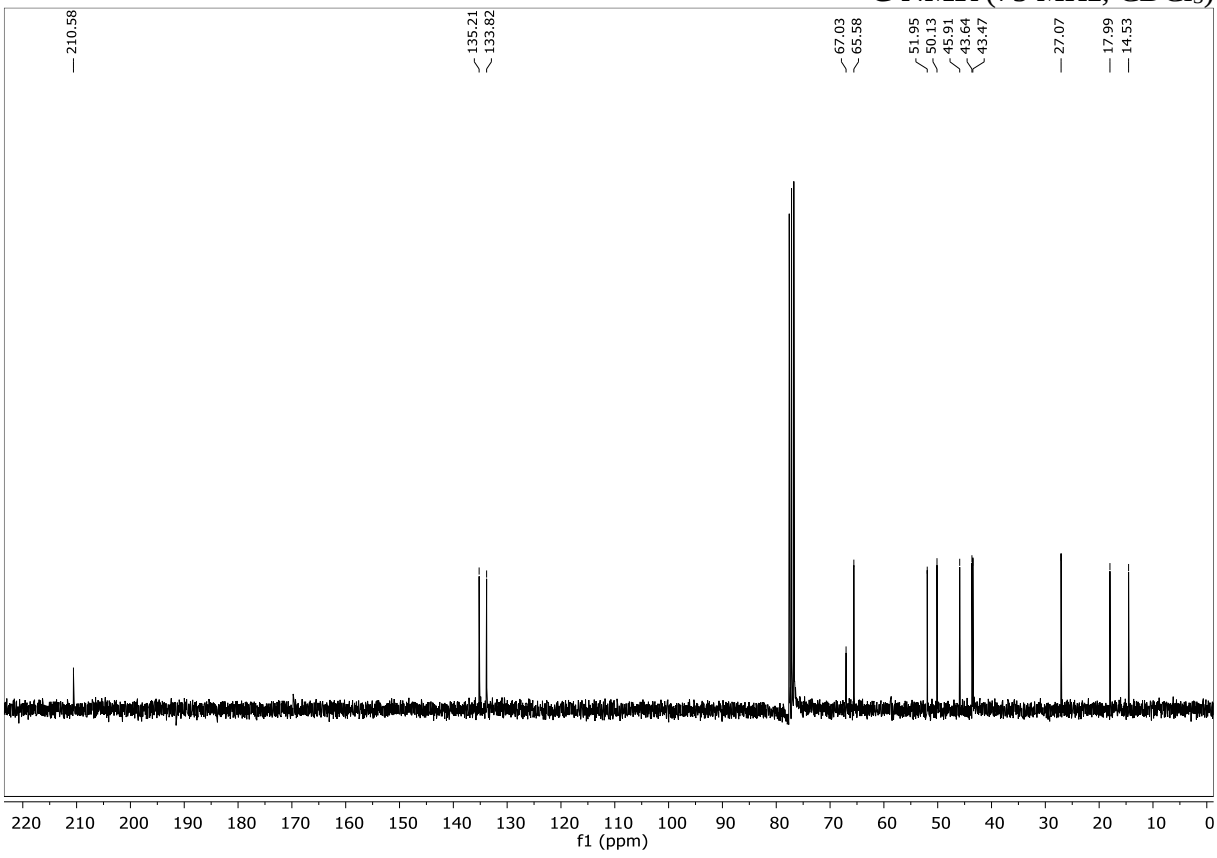

6a-Pentyl-1a,1b,2,5,5a,6a-hexahydro-6*H*-2,5-methanoindeno[1,2-*b*]oxiren-6-one (318b)

^{1}H NMR (300 MHz, $CDCl_3$)

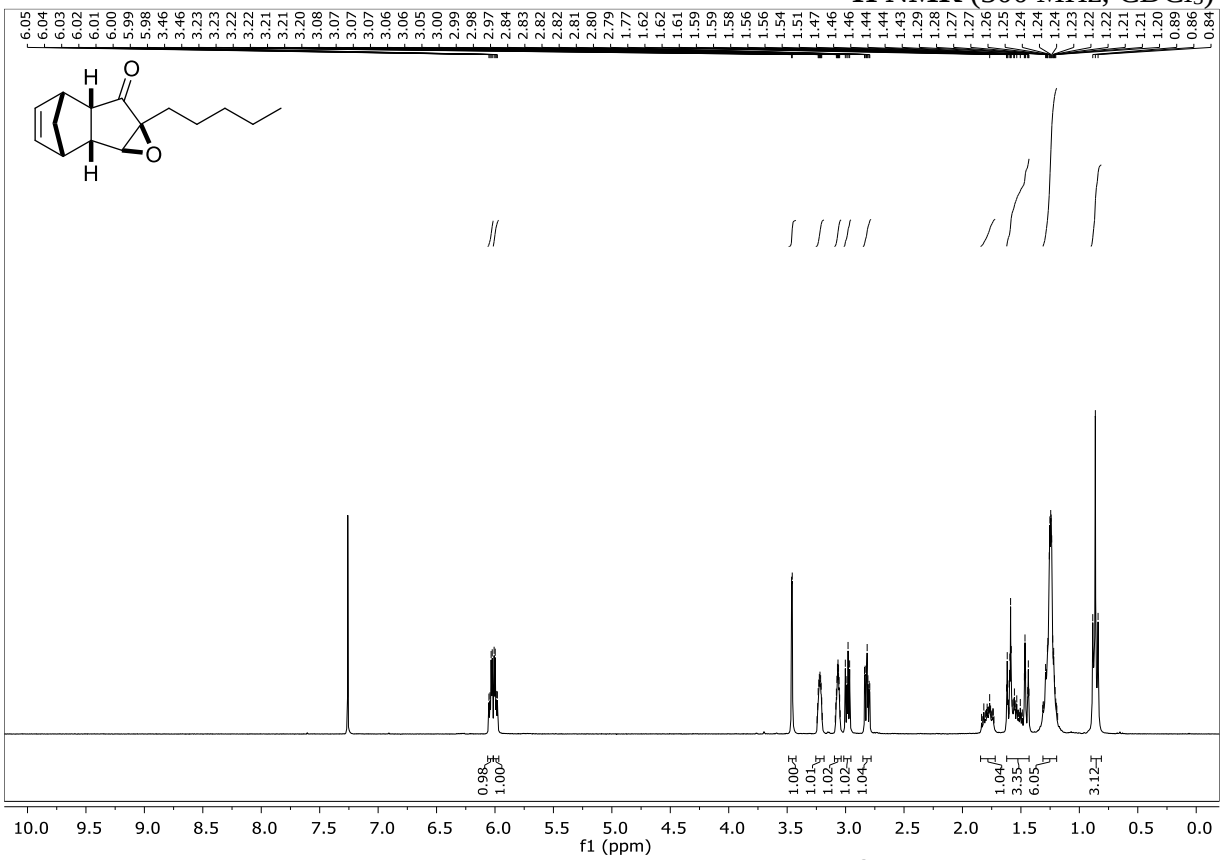

^{13}C NMR (75 MHz, $CDCl_3$)

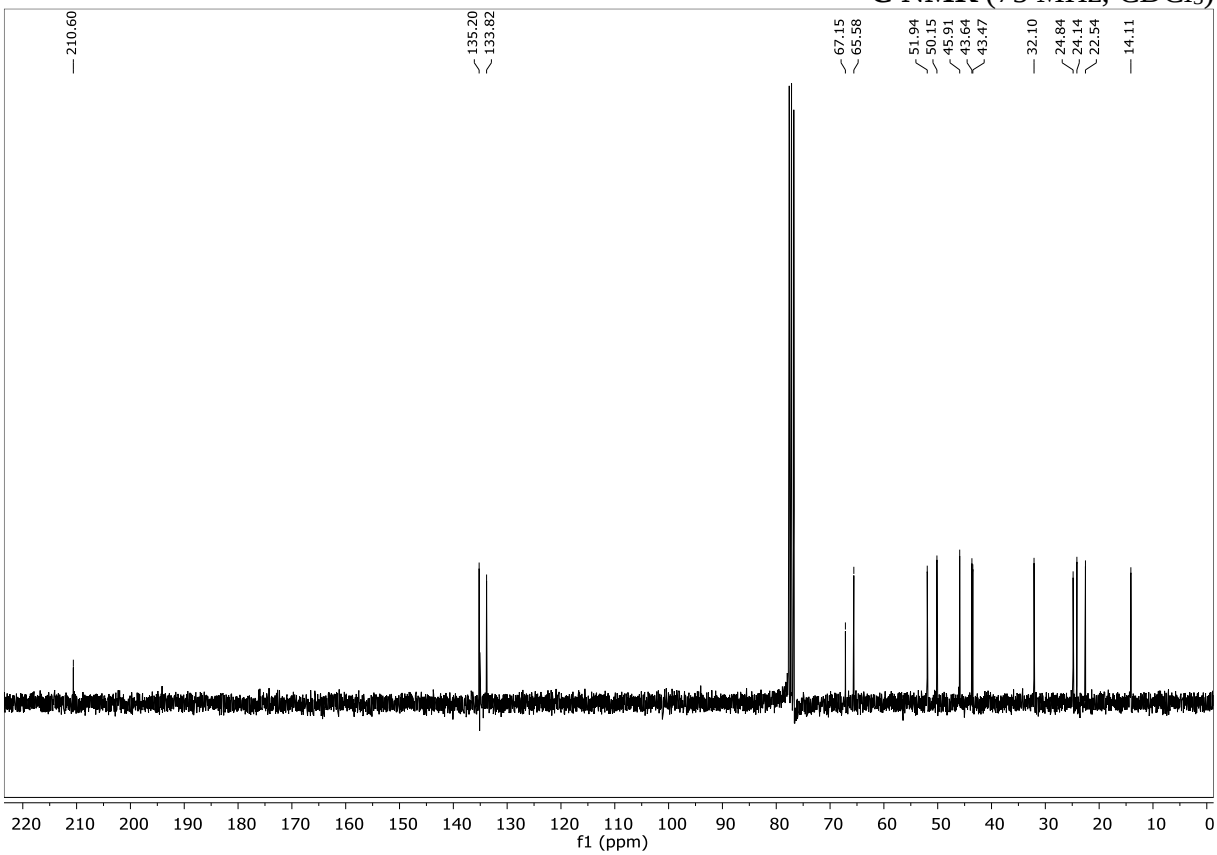

6a-Heptyl-1a,1b,2,5,5a,6a-hexahydro-6*H*-2,5-methanoindeno[1,2-*b*]oxiren-6-one (318c)

^{1}H NMR (300 MHz, $CDCl_3$)

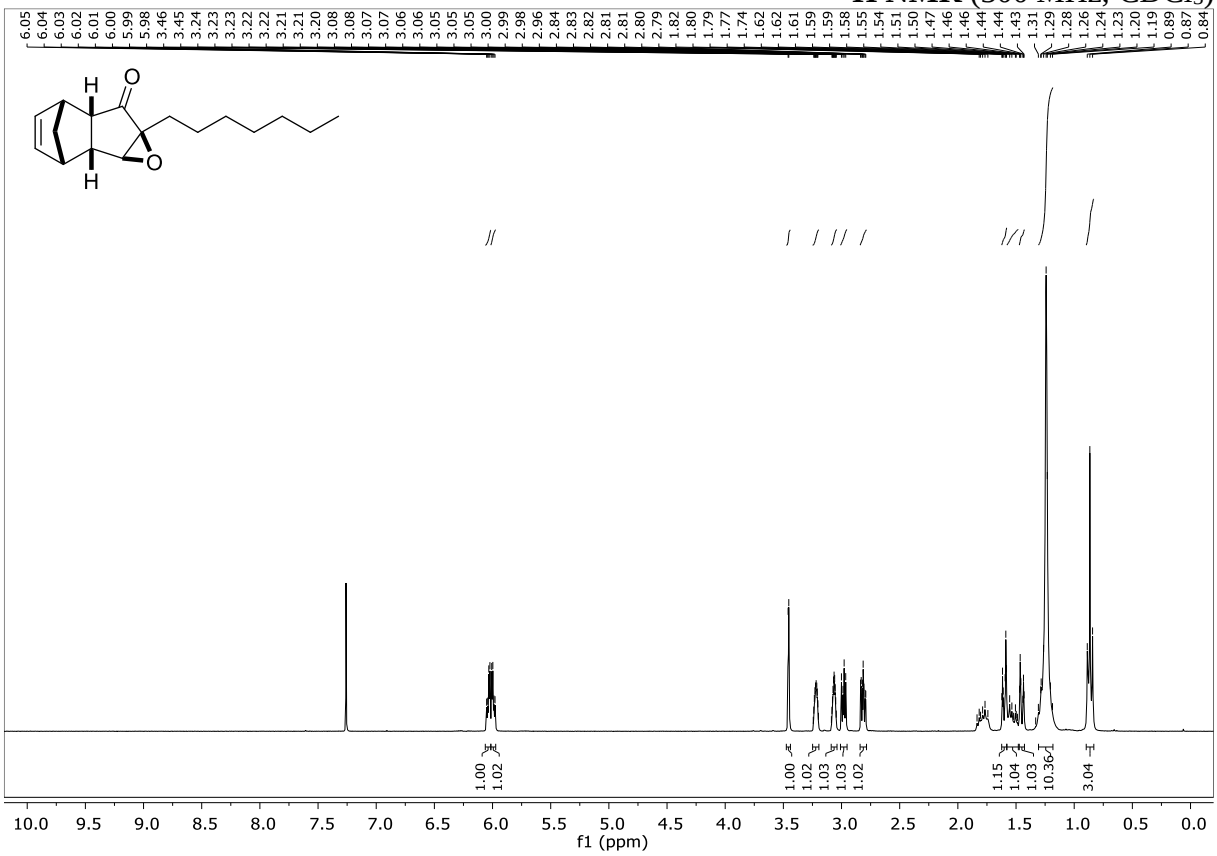

^{13}C NMR (75 MHz, $CDCl_3$)

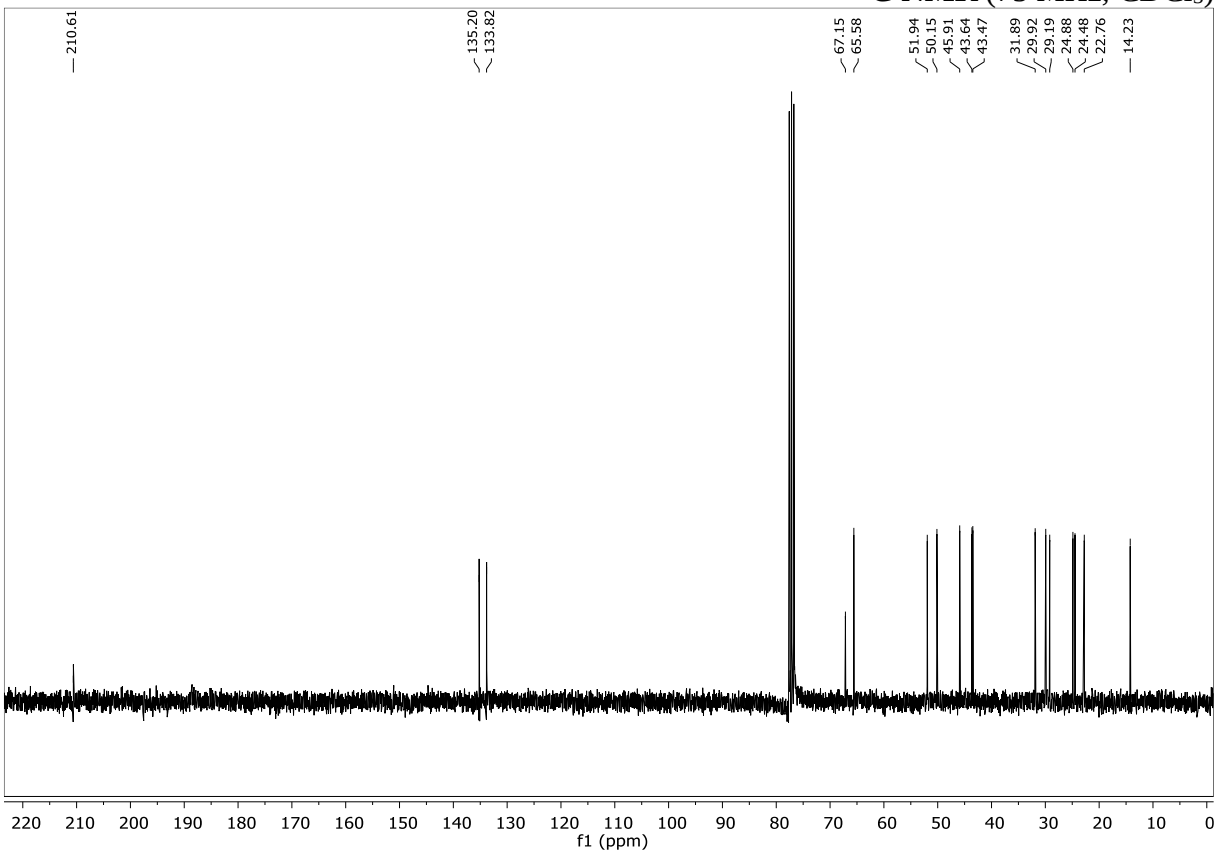

6-propyl-2*H*-pyran-2-one (2a)

^{1}H NMR (300 MHz, $CDCl_3$)

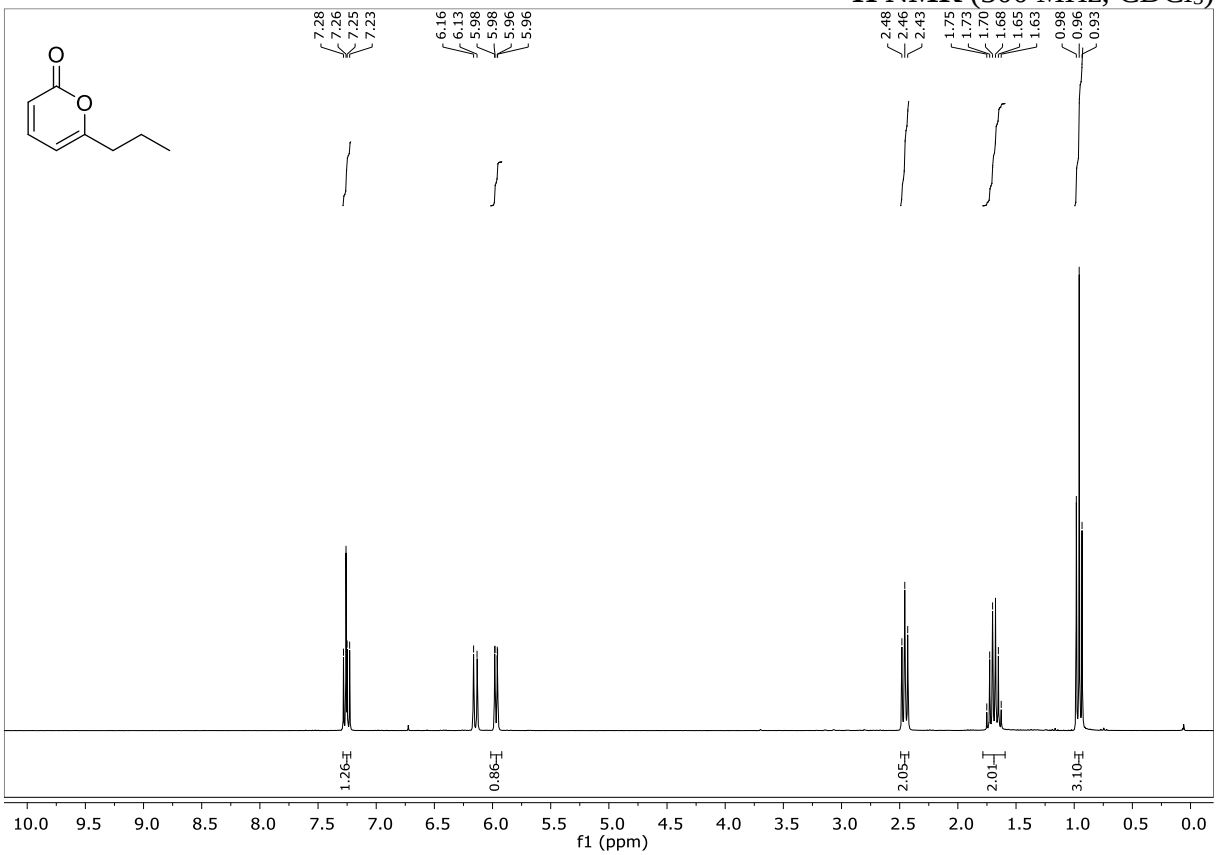

^{13}C NMR (75 MHz, $CDCl_3$)

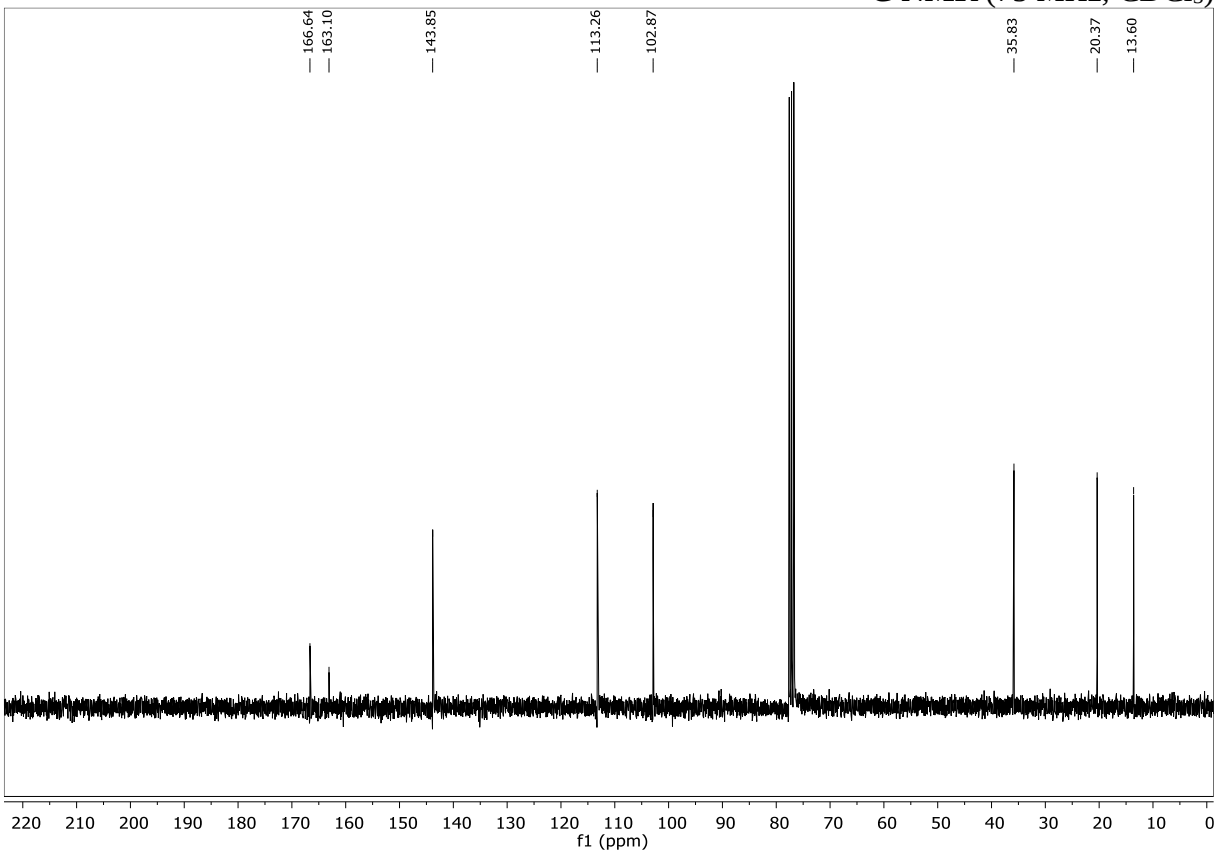

6-Pentyl-2*H*-pyran-2-one (2b)

^{1}H NMR (300 MHz, $CDCl_3$)

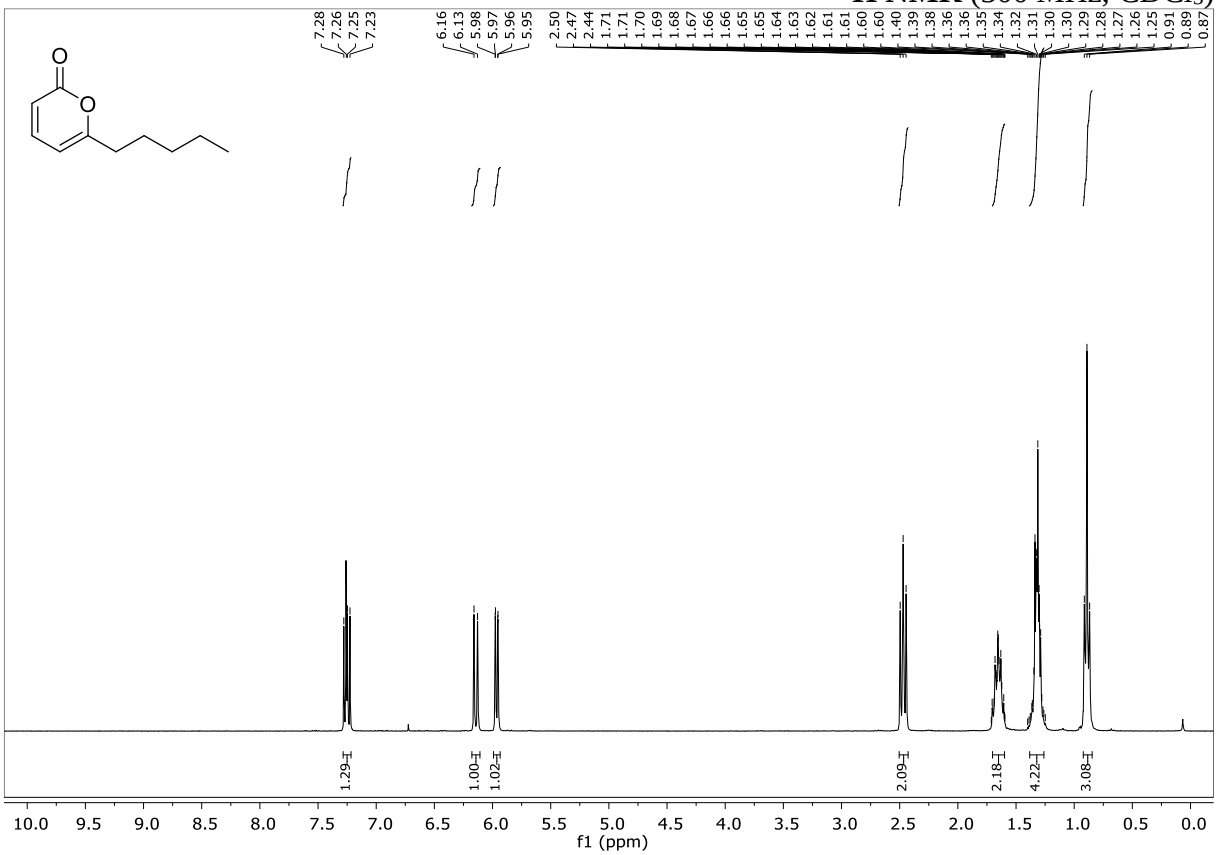

^{13}C NMR (75 MHz, $CDCl_3$)

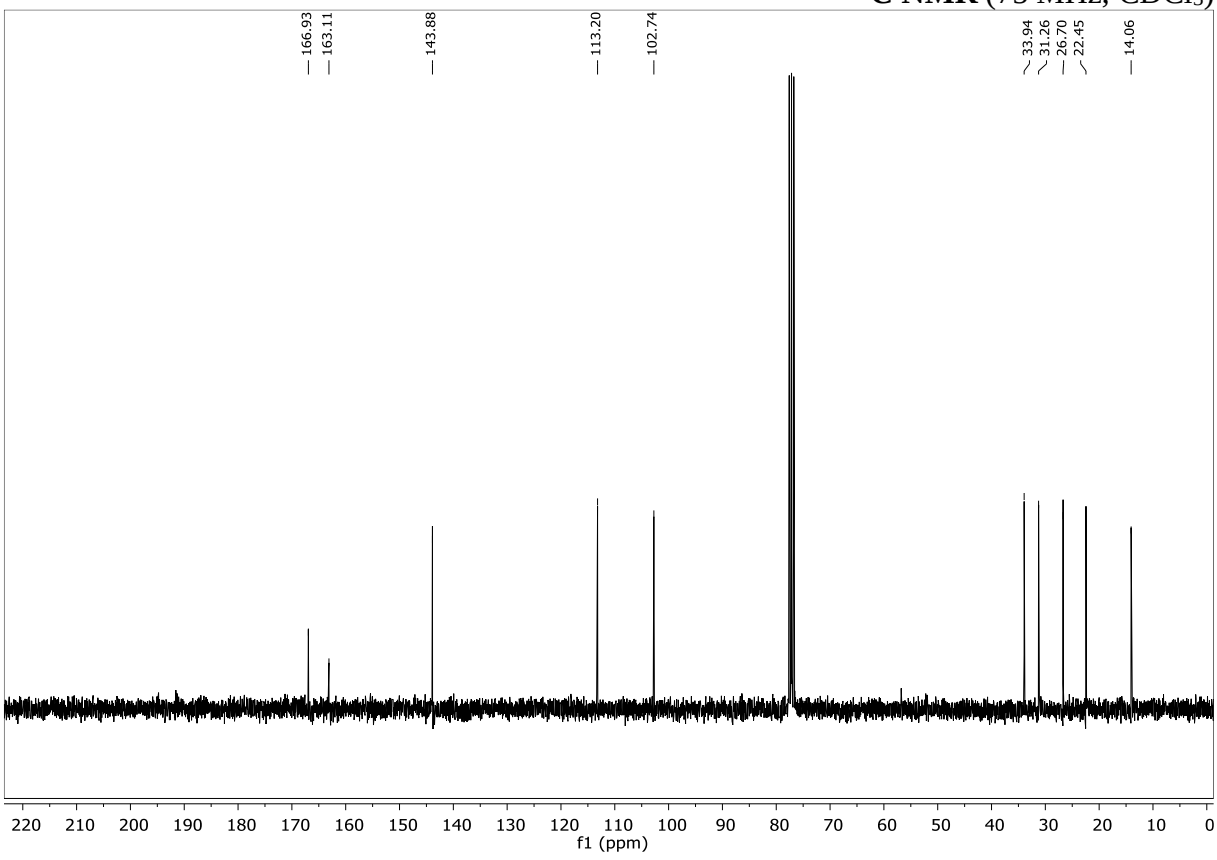

6-Heptyl-2*H*-pyran-2-one (2c)

^{1}H NMR (300 MHz, $CDCl_3$)

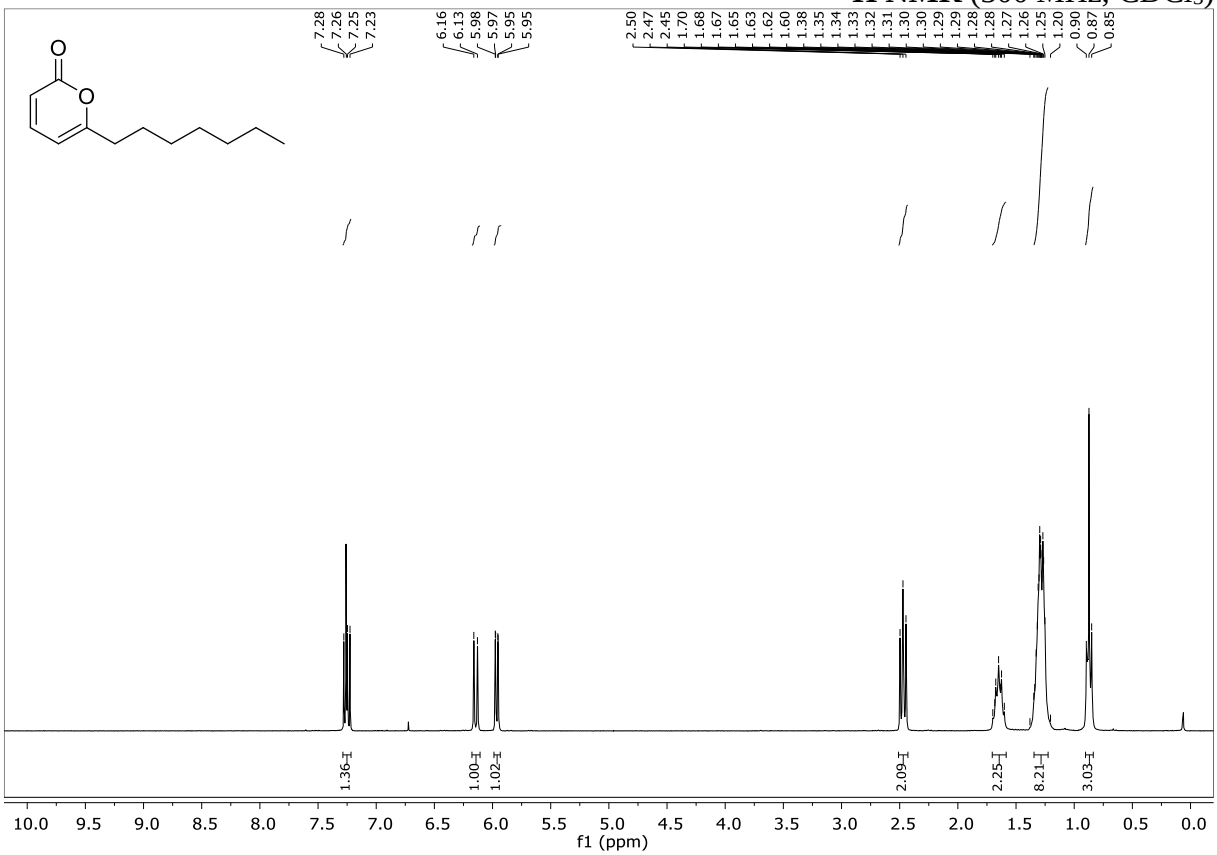

^{13}C NMR (75 MHz, $CDCl_3$)

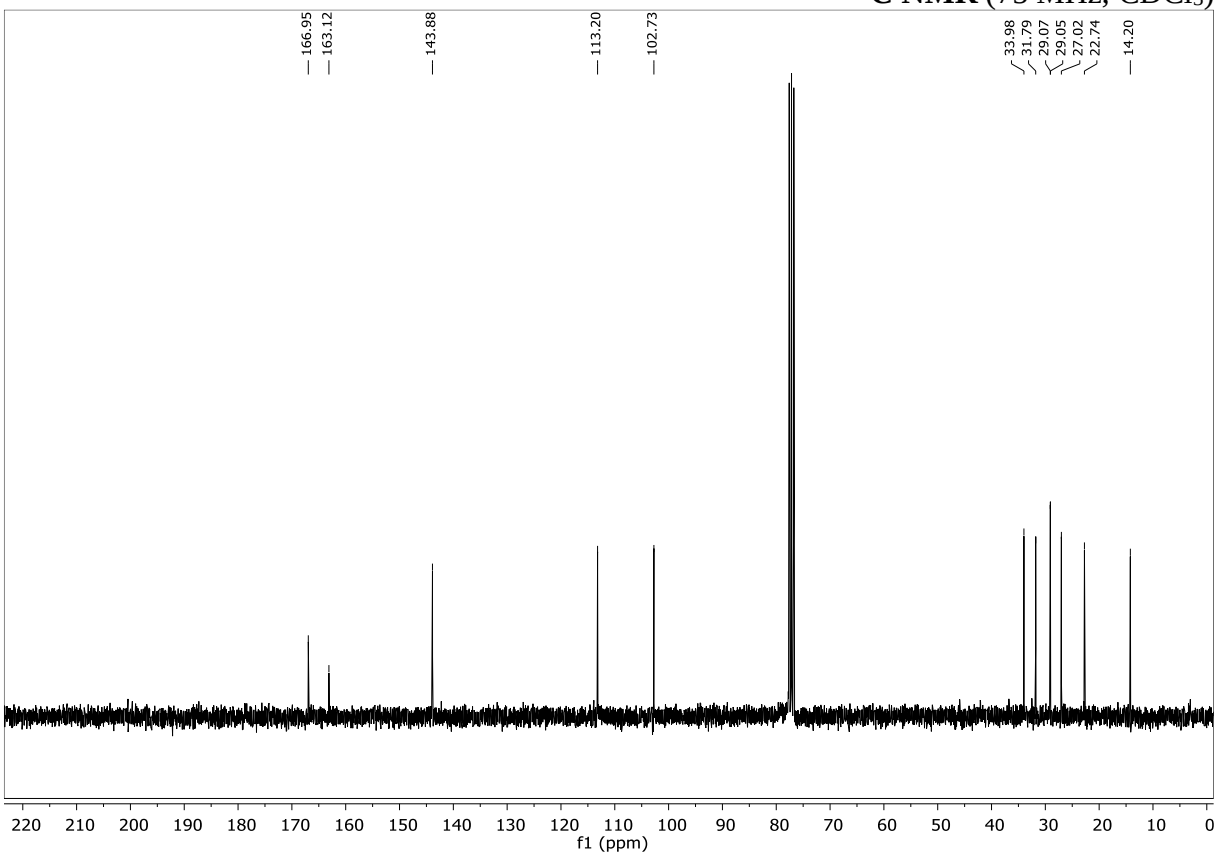

Ethyl (*S*)-1-methyl-3-oxo-1,3-dihydroisobenzofuran-4-carboxylate ((*S*)-342a)

^{1}H NMR (400 MHz, $CDCl_3$)

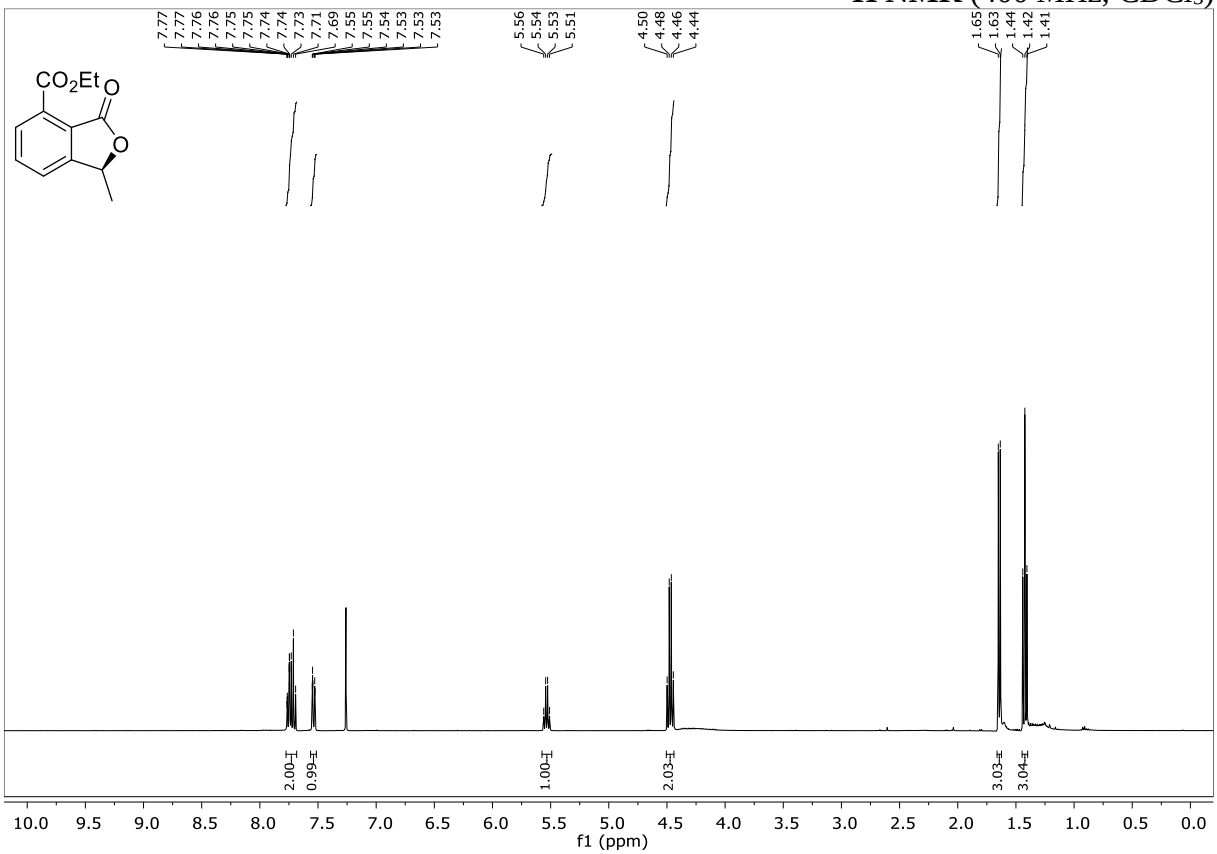

^{13}C NMR (101 MHz, $CDCl_3$)

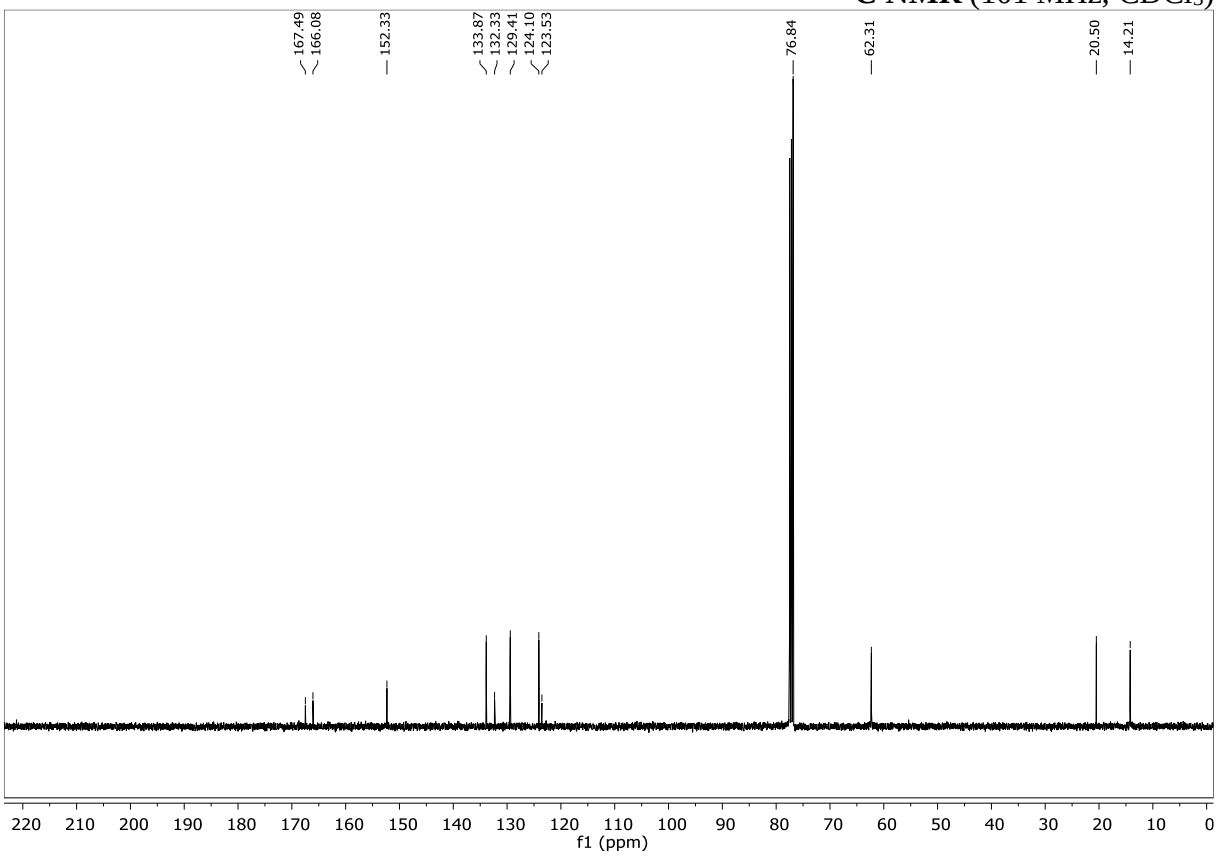

Ethyl 1-butyl-3-oxo-1,3-dihydroisobenzofuran-4-carboxylate (342b)

^{1}H NMR (300 MHz, $CDCl_3$)

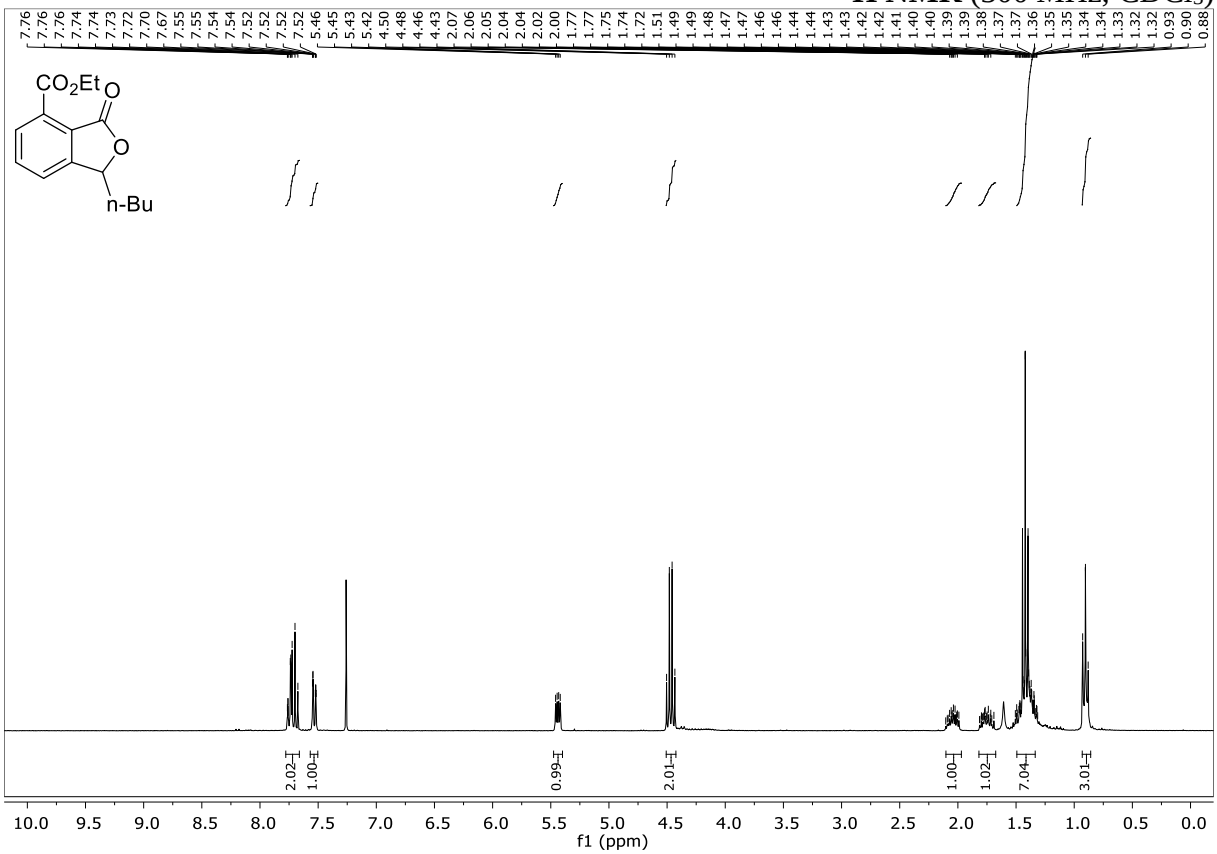

^{13}C NMR (101 MHz, $CDCl_3$)

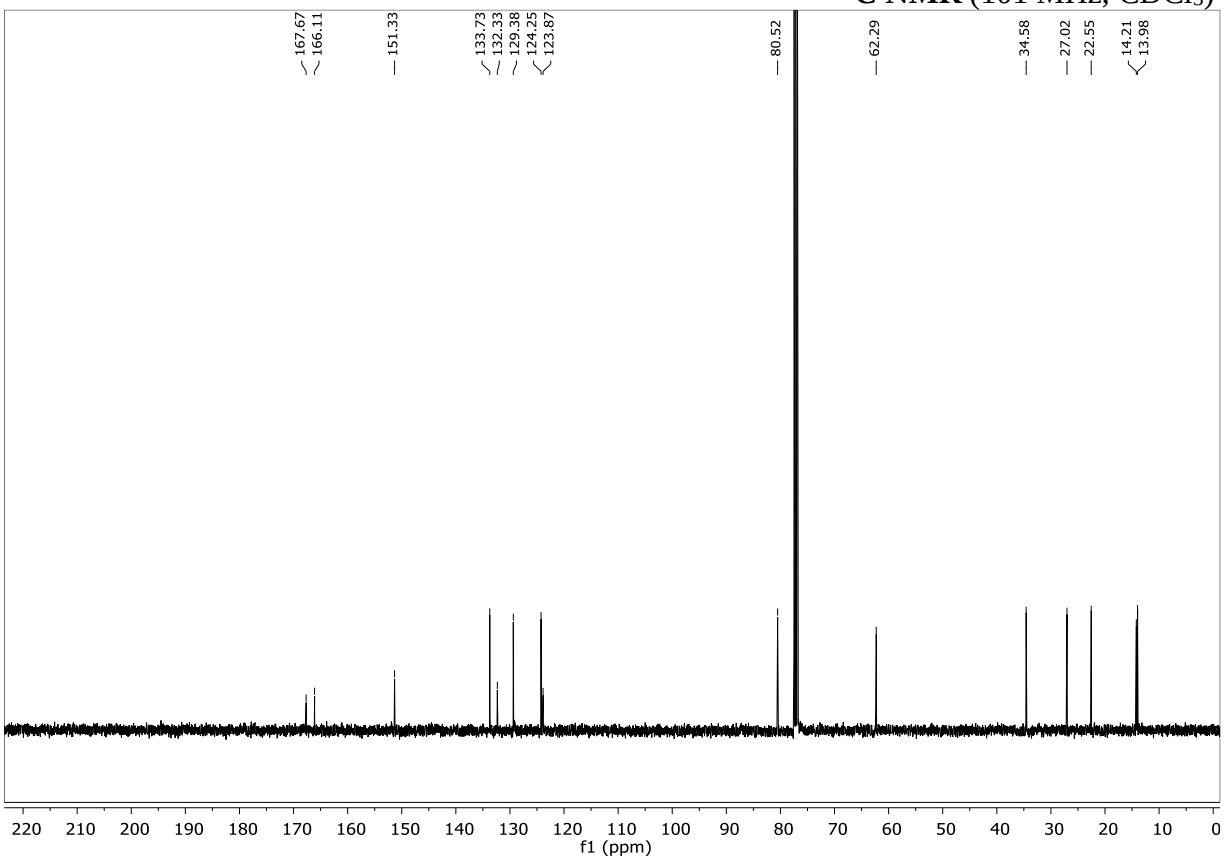

Ethyl 3-oxo-1-phenyl-1,3-dihydroisobenzofuran-4-carboxylate (342c)

^{1}H NMR (300 MHz, $CDCl_3$)

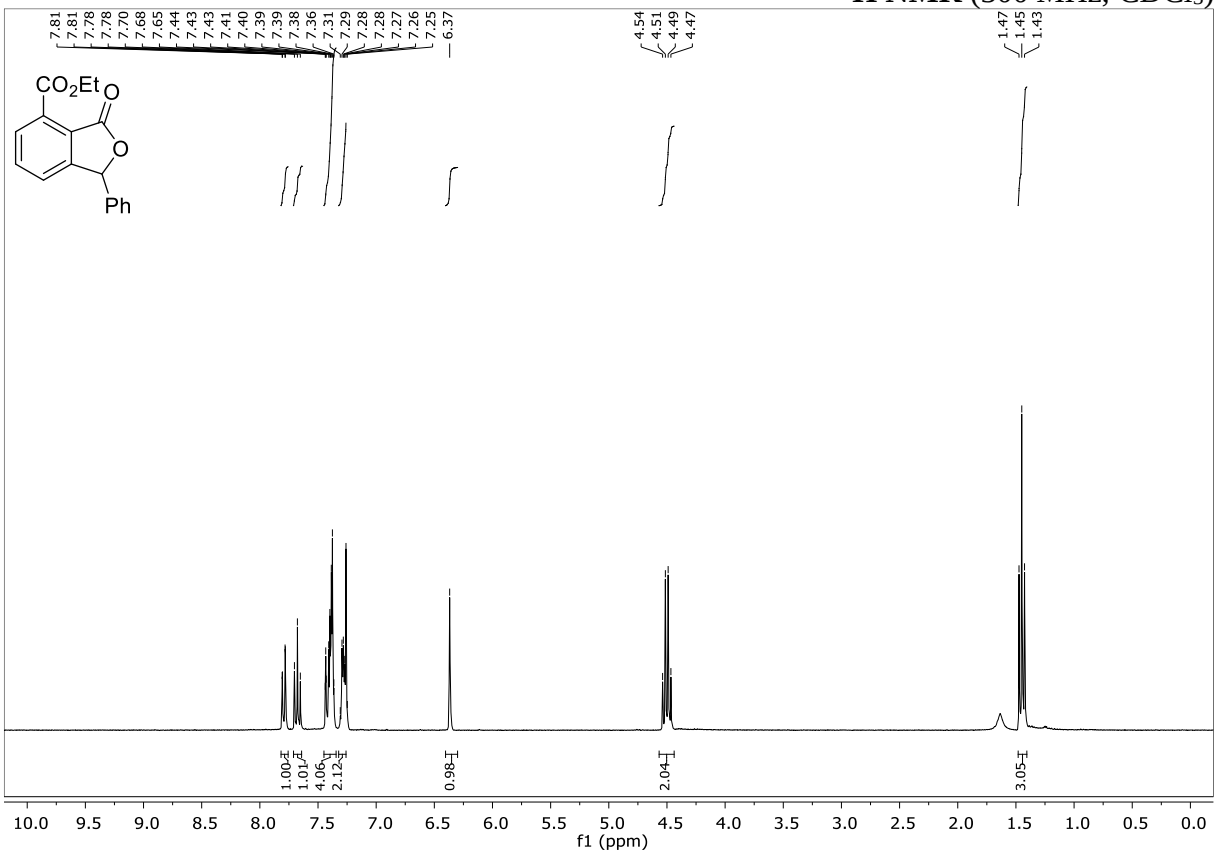

^{13}C NMR (75 MHz, $CDCl_3$)

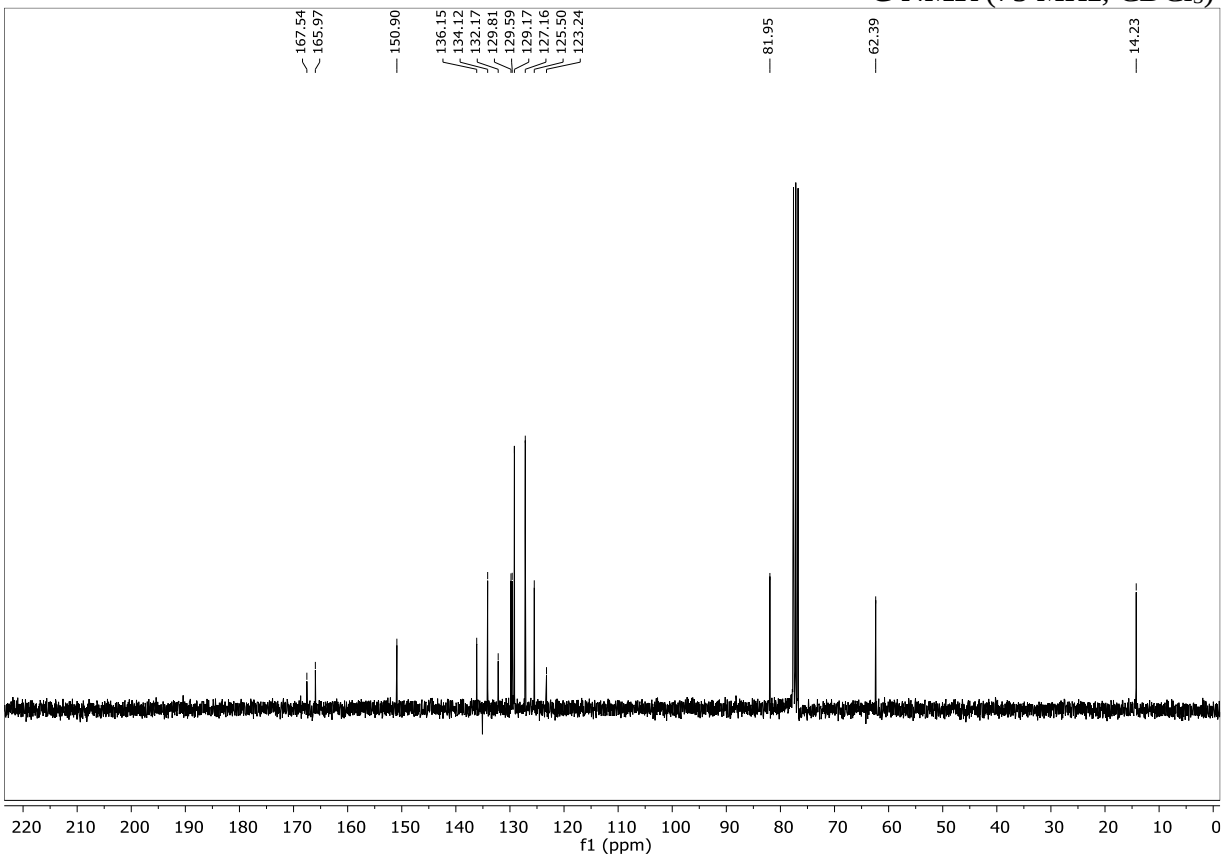

Ethyl 3-(1-hydroxyethyl)benzoate (348a)

^{1}H NMR (400 MHz, $CDCl_3$)

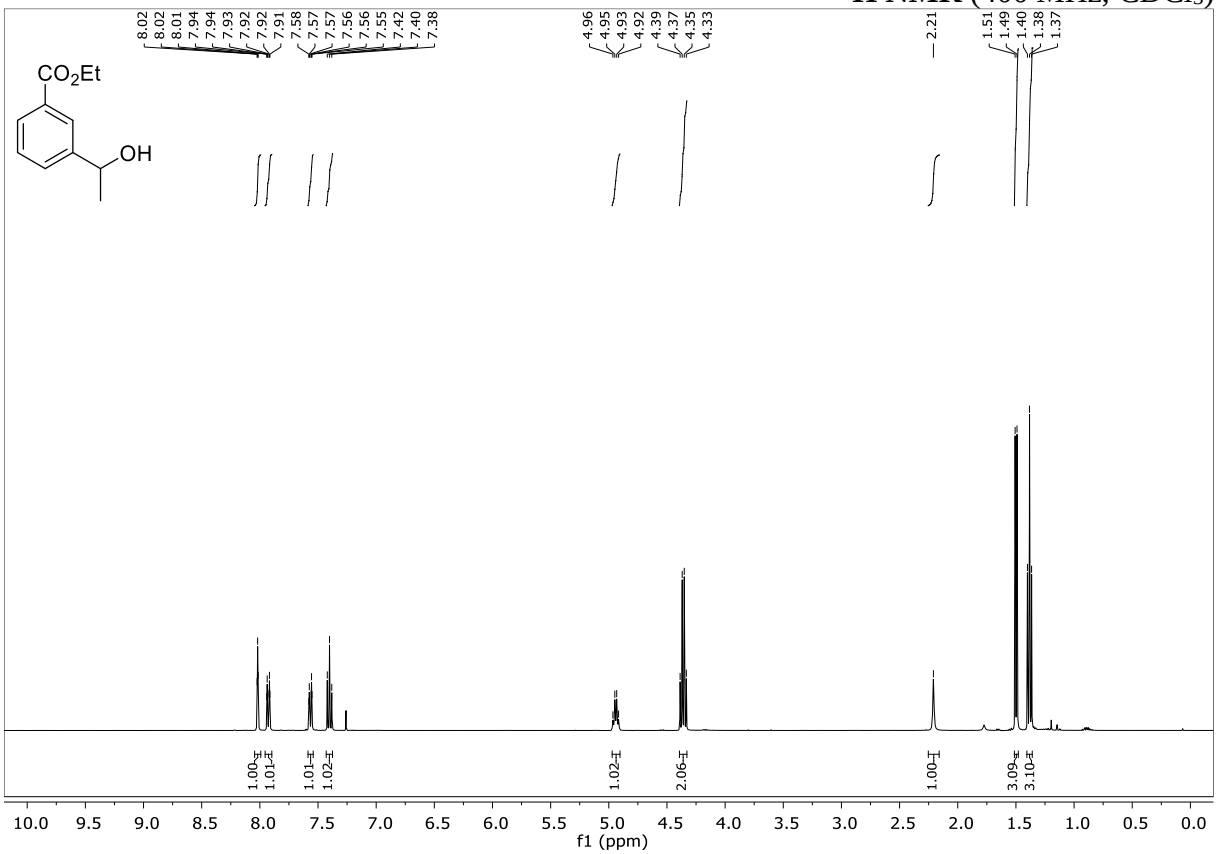

^{13}C NMR (101 MHz, $CDCl_3$)

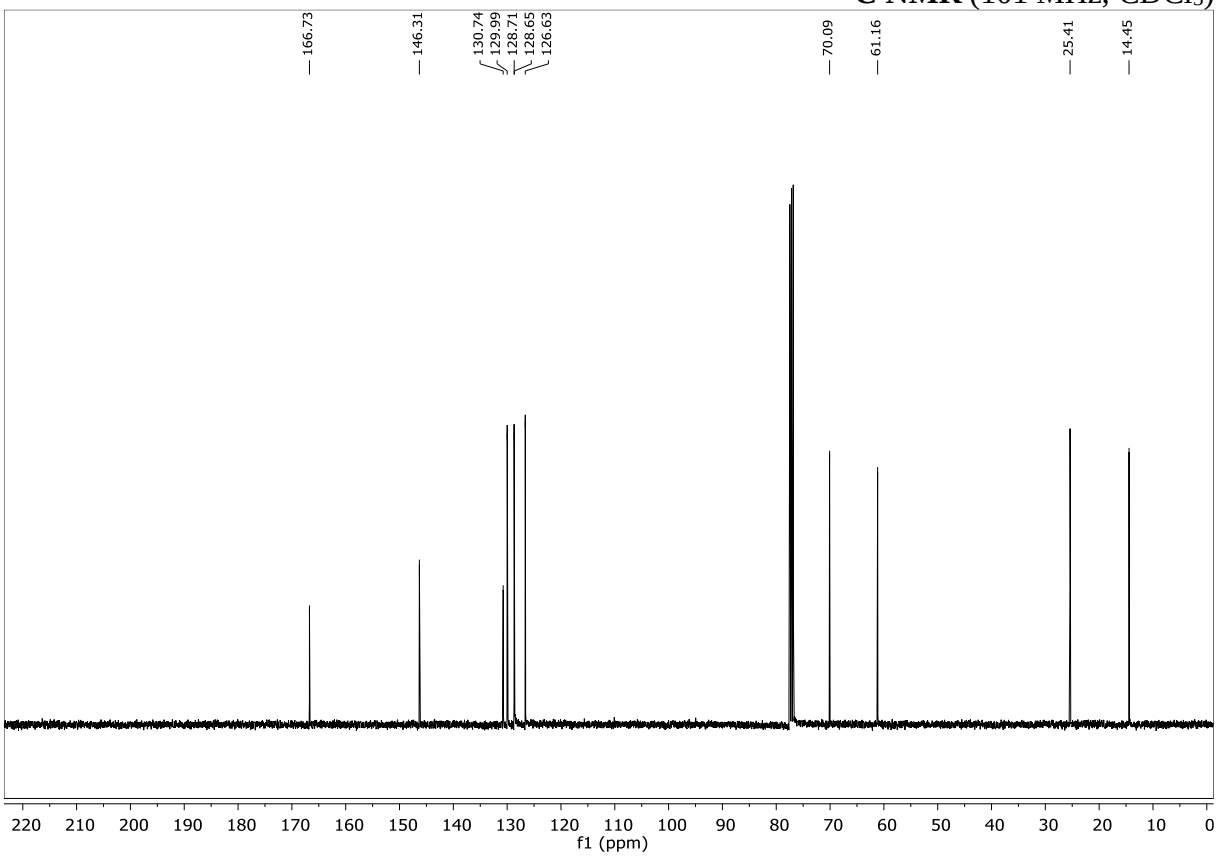

3-Methylisobenzofuran-1(3*H*)-one (326a)

^{1}H NMR (400 MHz, $CDCl_3$)

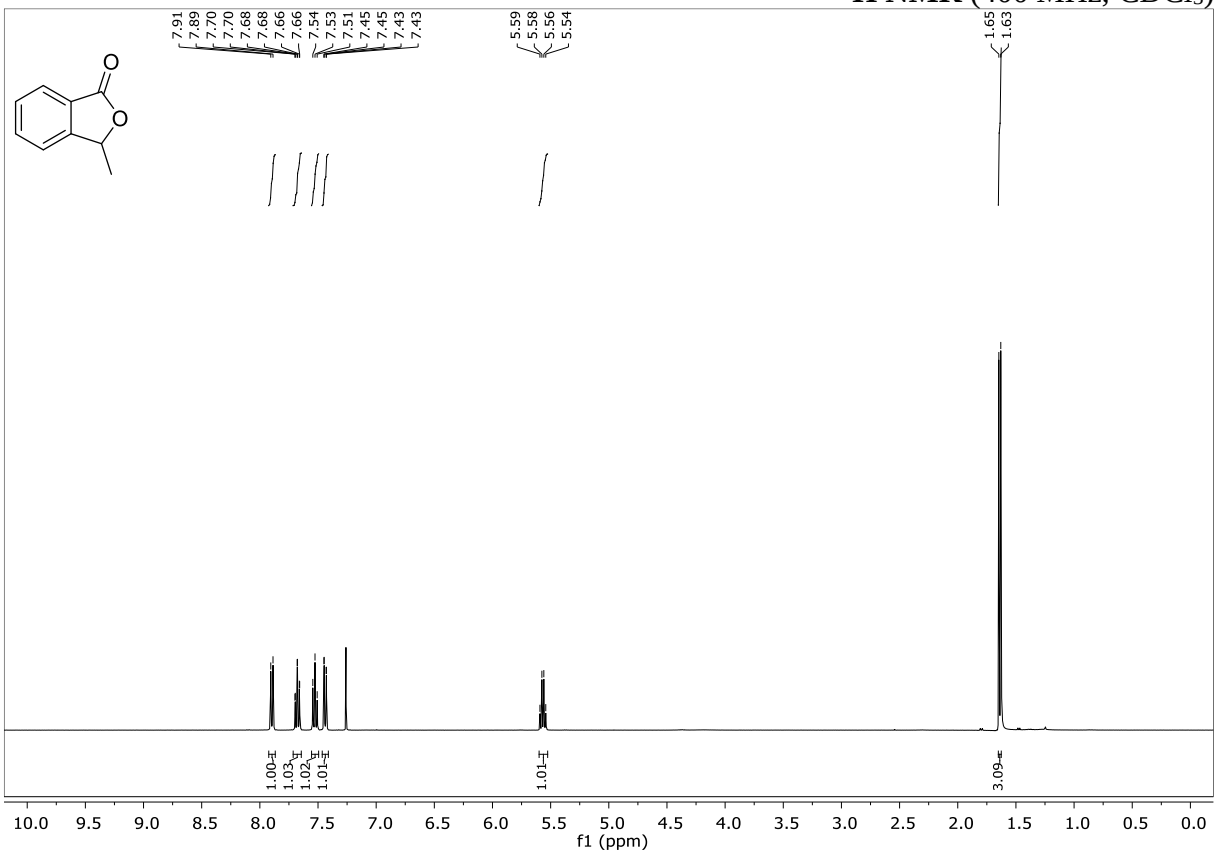

^{13}C NMR (101 MHz, $CDCl_3$)

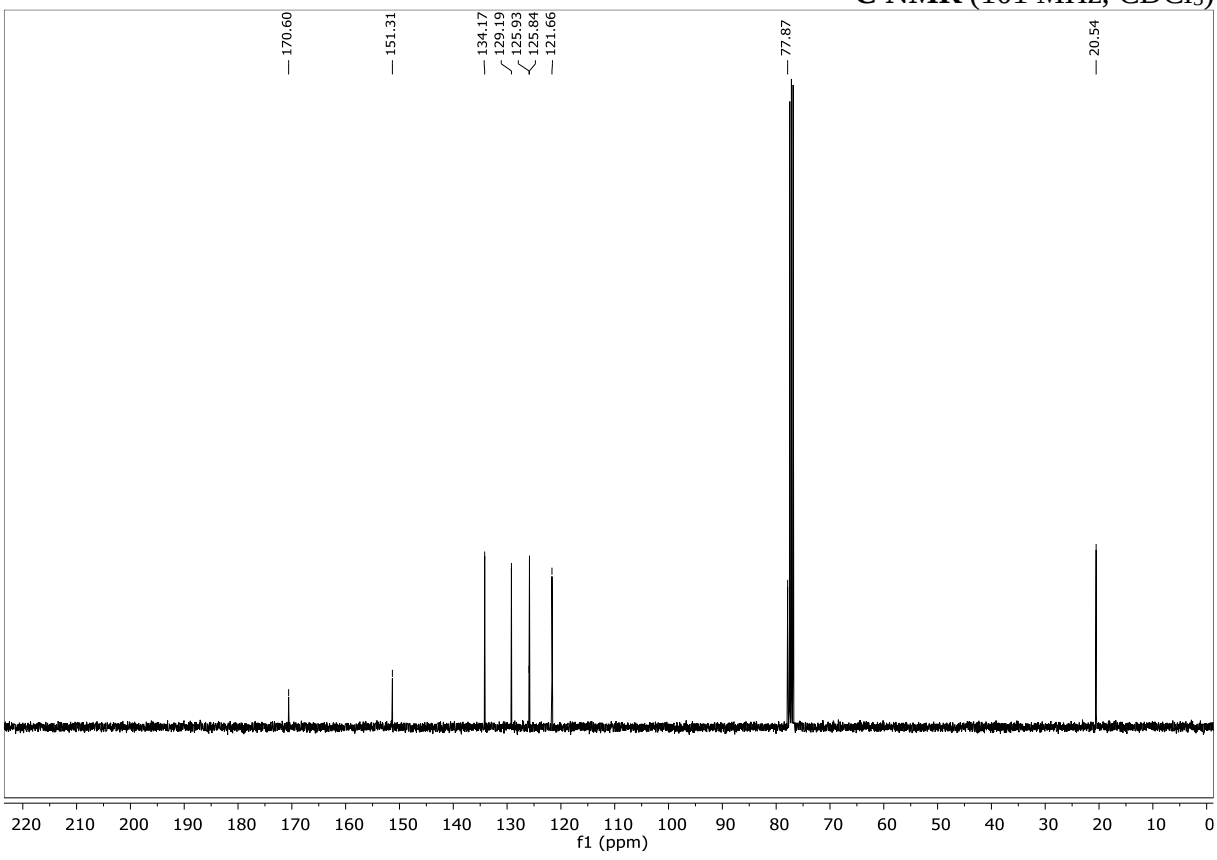

1-(2-Oxo-2*H*-pyran-6-yl)ethyl propiolate (350a)

^{1}H NMR (300 MHz, $CDCl_3$)

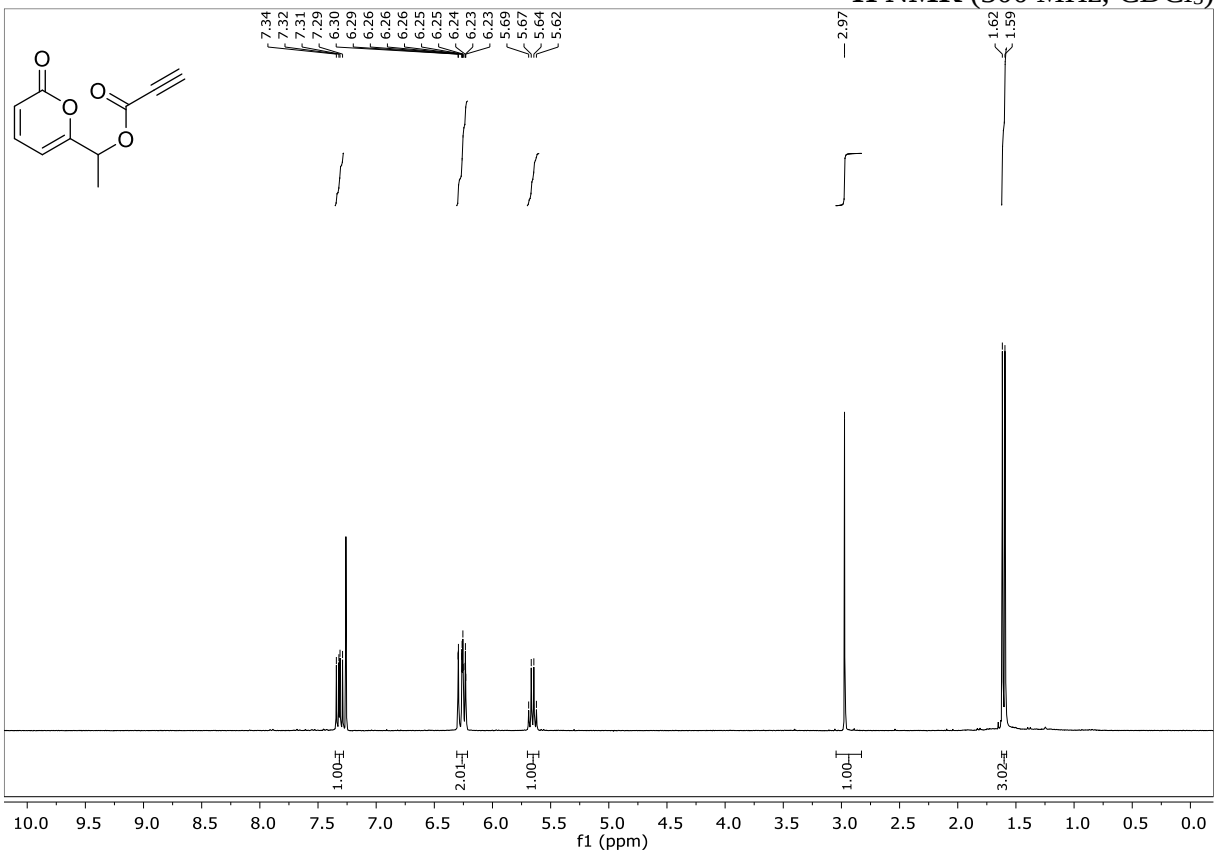

^{13}C NMR (101 MHz, $CDCl_3$)

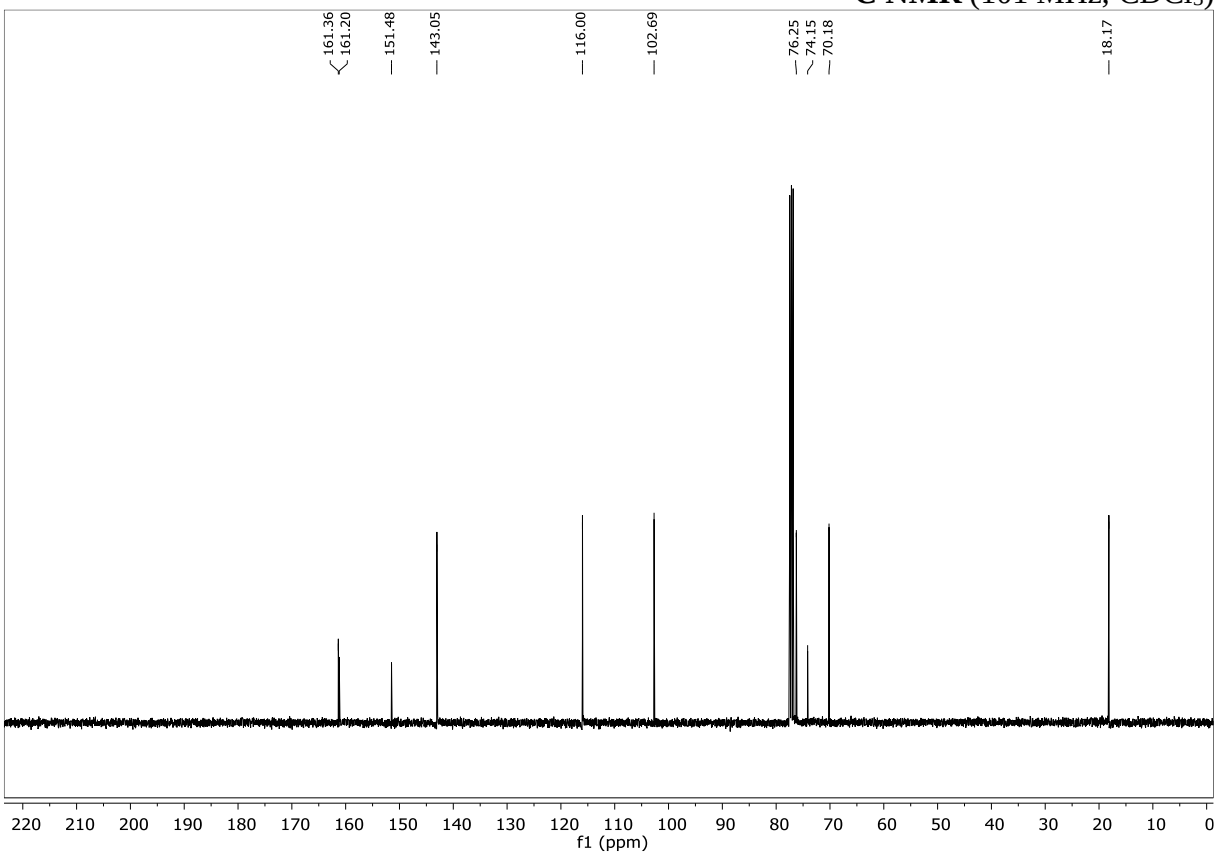

(*R*)-1-(2-Oxo-2*H*-pyran-6-yl)pentyl propiolate) ((*R*)-350b)

^{1}H NMR (300 MHz, $CDCl_3$)

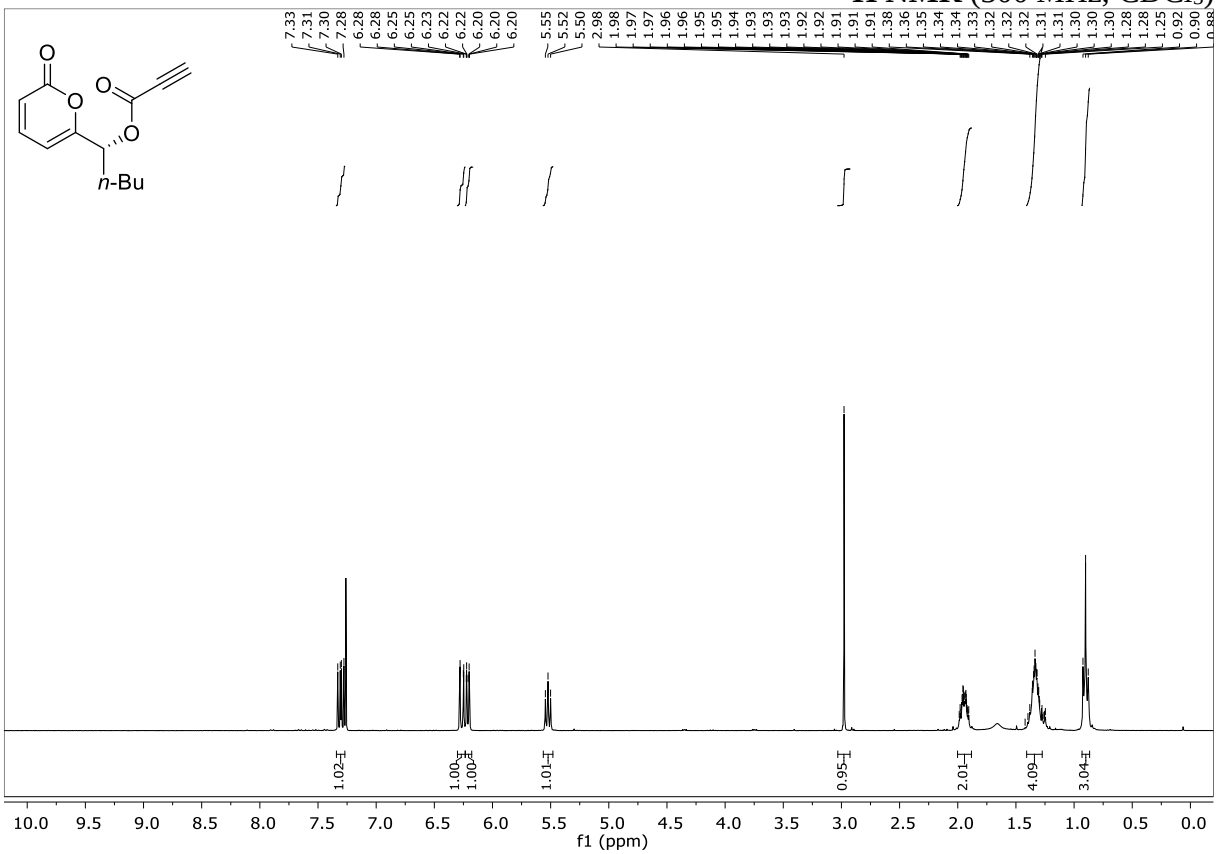

^{13}C NMR (101 MHz, $CDCl_3$)

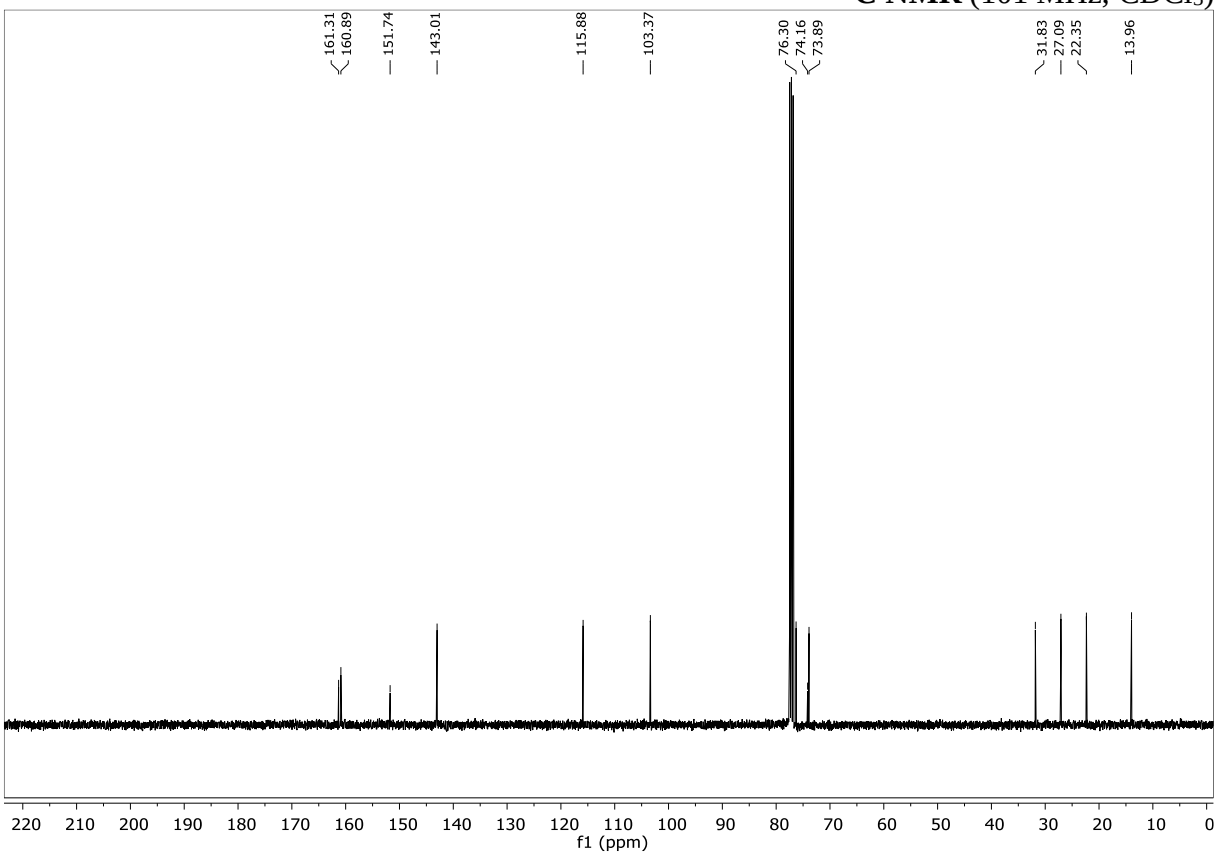

(2-Oxo-2*H*-pyran-6-yl)(phenyl)methyl propiolate (350c)

^{1}H NMR (300 MHz, $CDCl_3$)

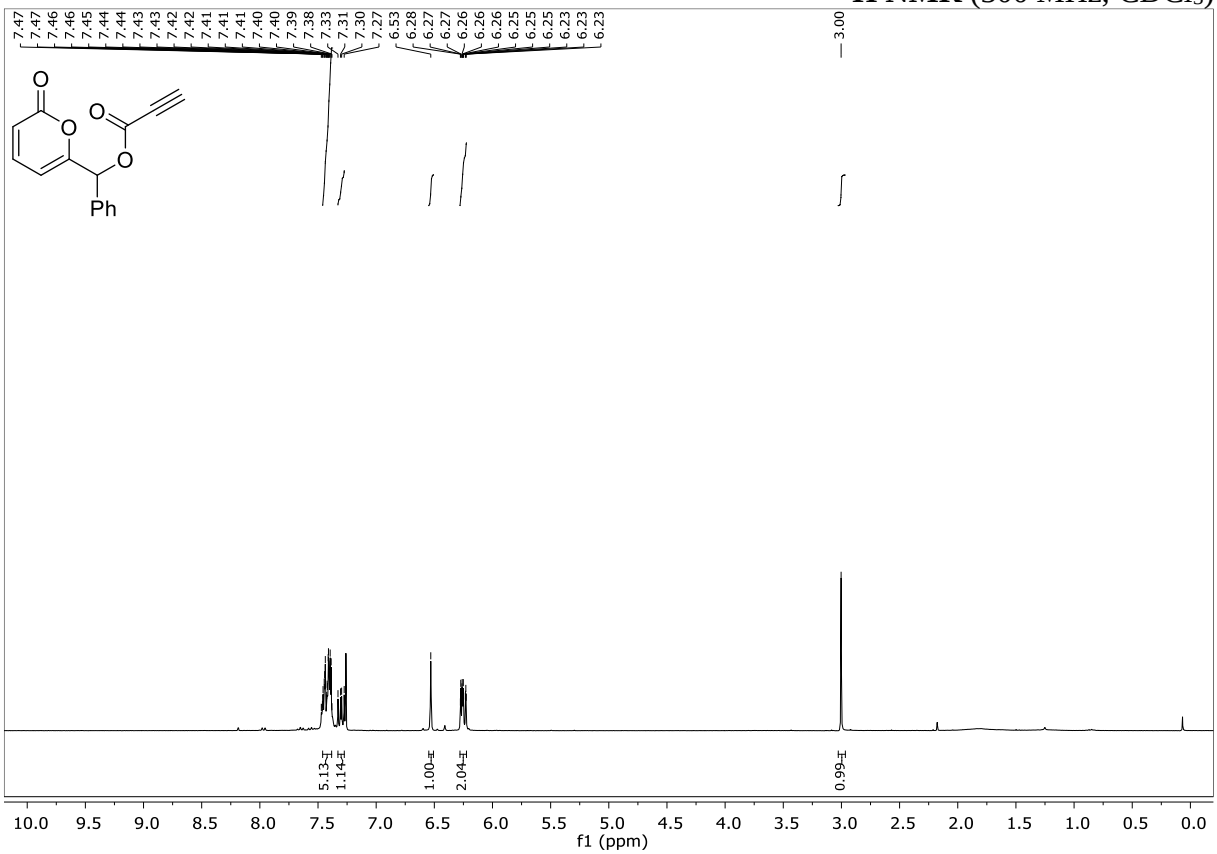

^{13}C NMR (75 MHz, $CDCl_3$)

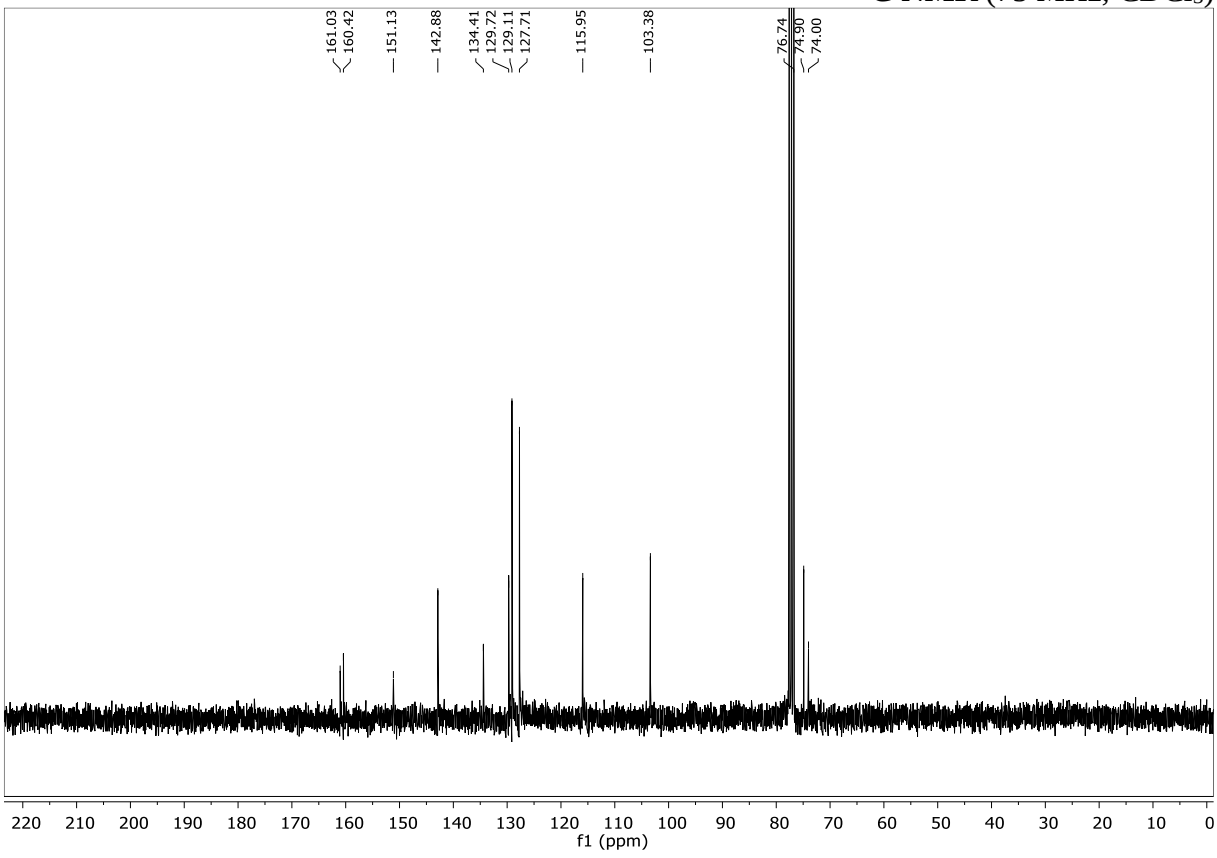

(*R*)-3-Butylisobenzofuran-1(3*H*)-one ((*R*)-326b)

^{1}H NMR (400 MHz, $CDCl_3$)

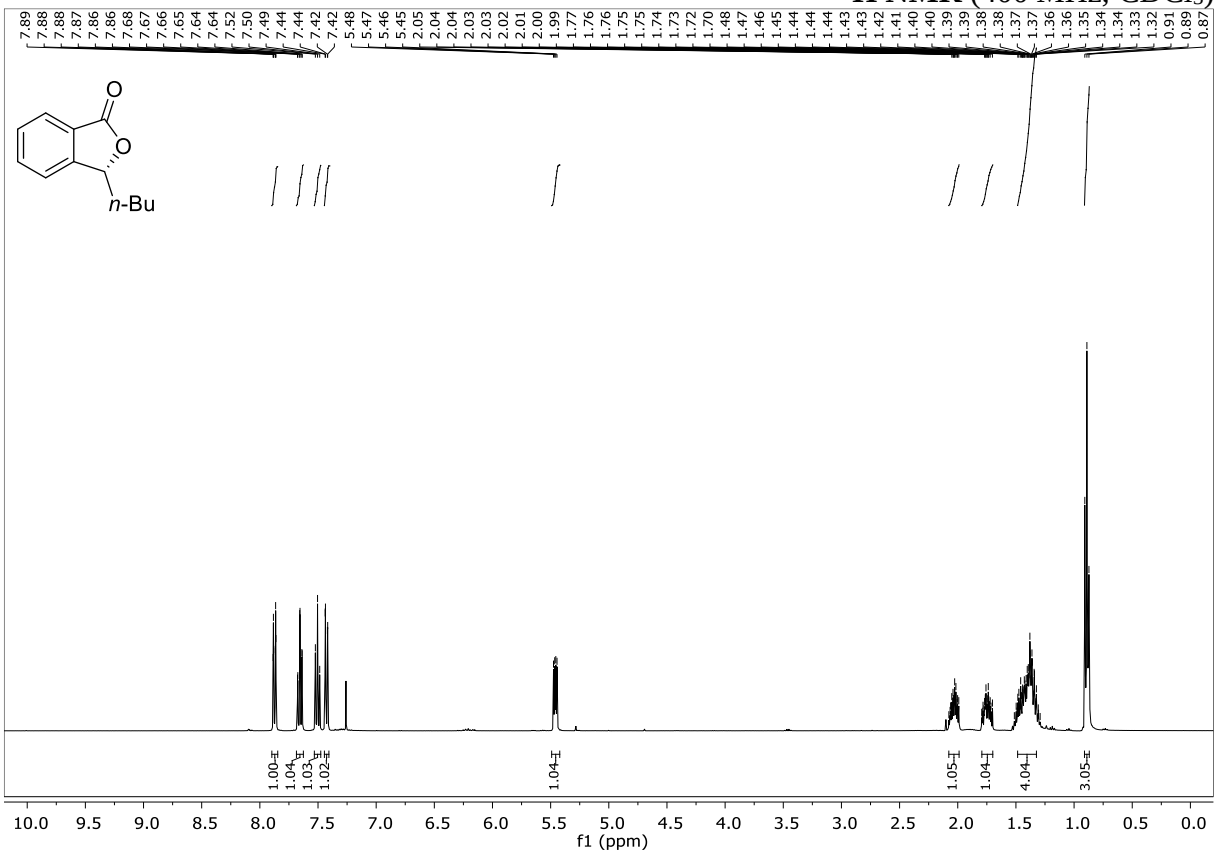

^{13}C NMR (101 MHz, $CDCl_3$)

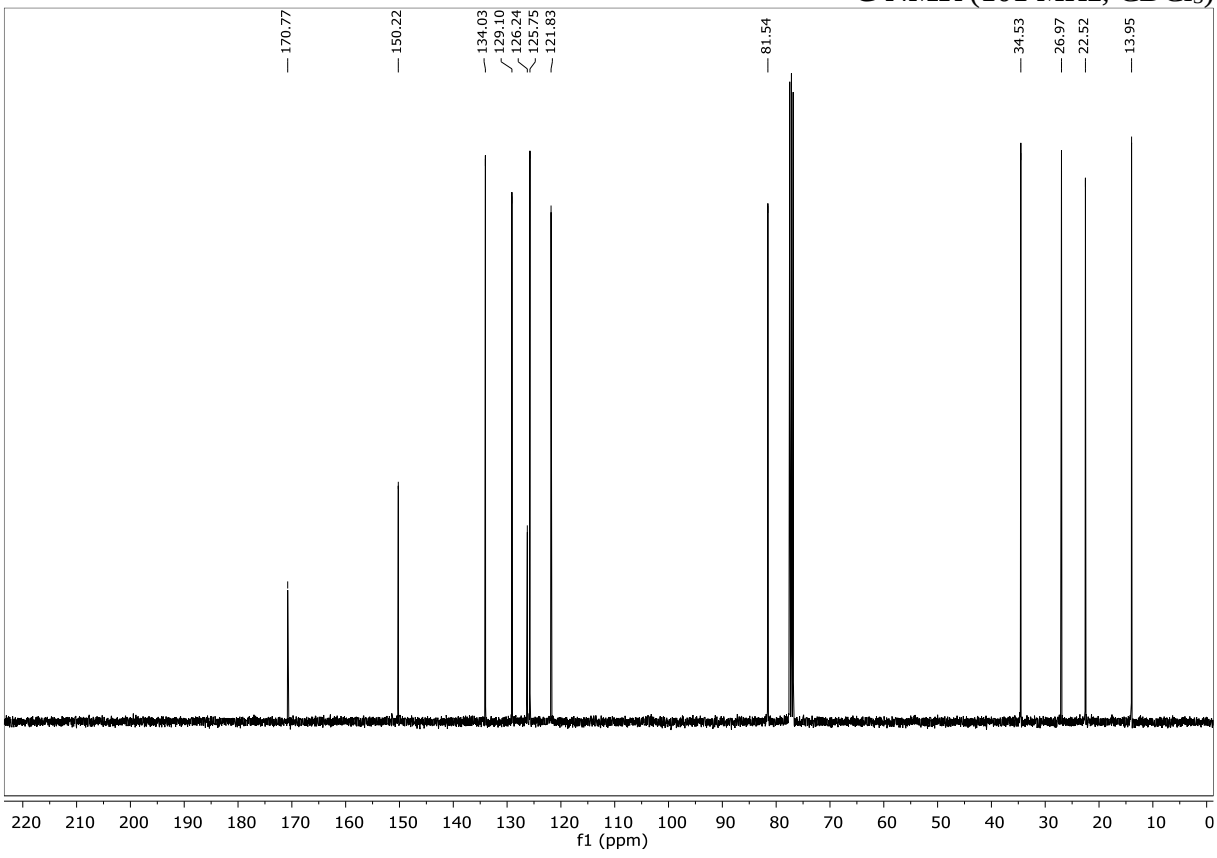

3-Phenylisobenzofuran-1(3*H*)-one (326c)

^{1}H NMR (400 MHz, $CDCl_3$)

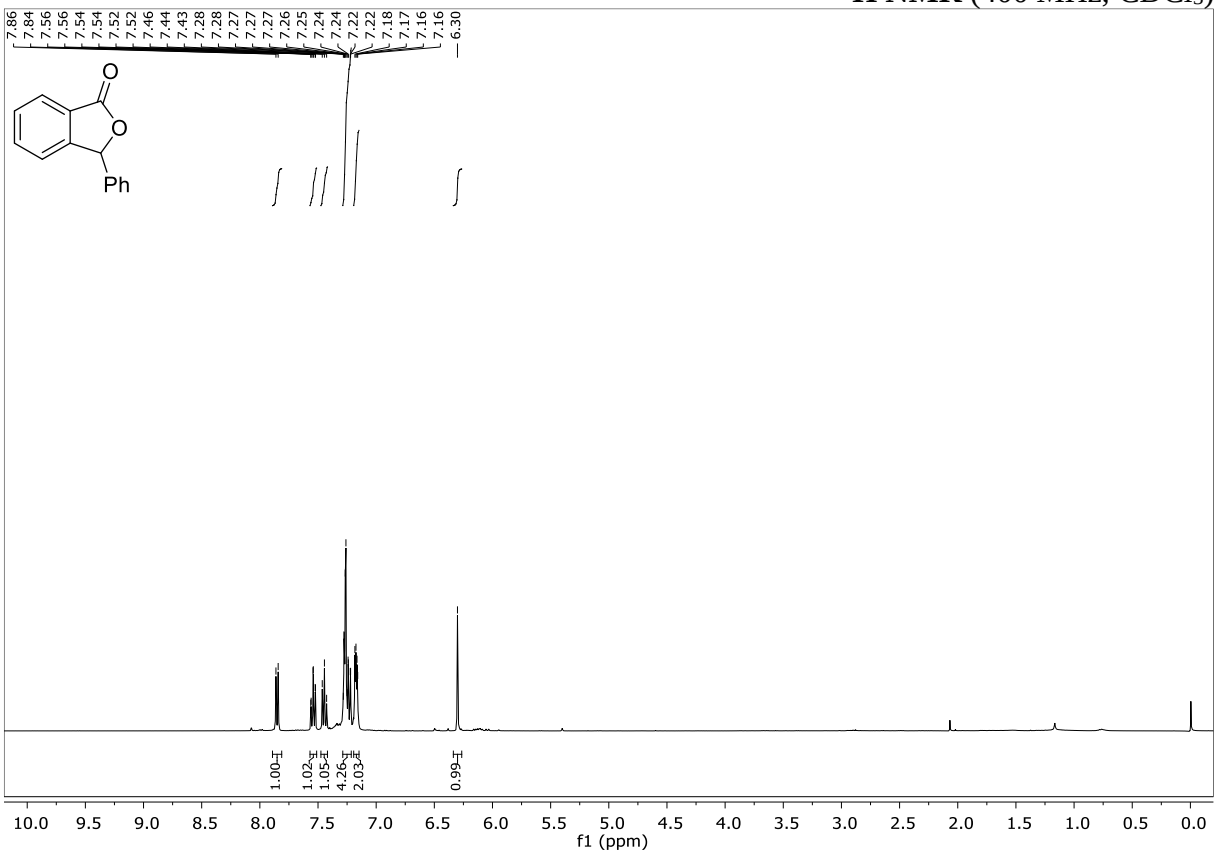

^{13}C NMR (101 MHz, $CDCl_3$)

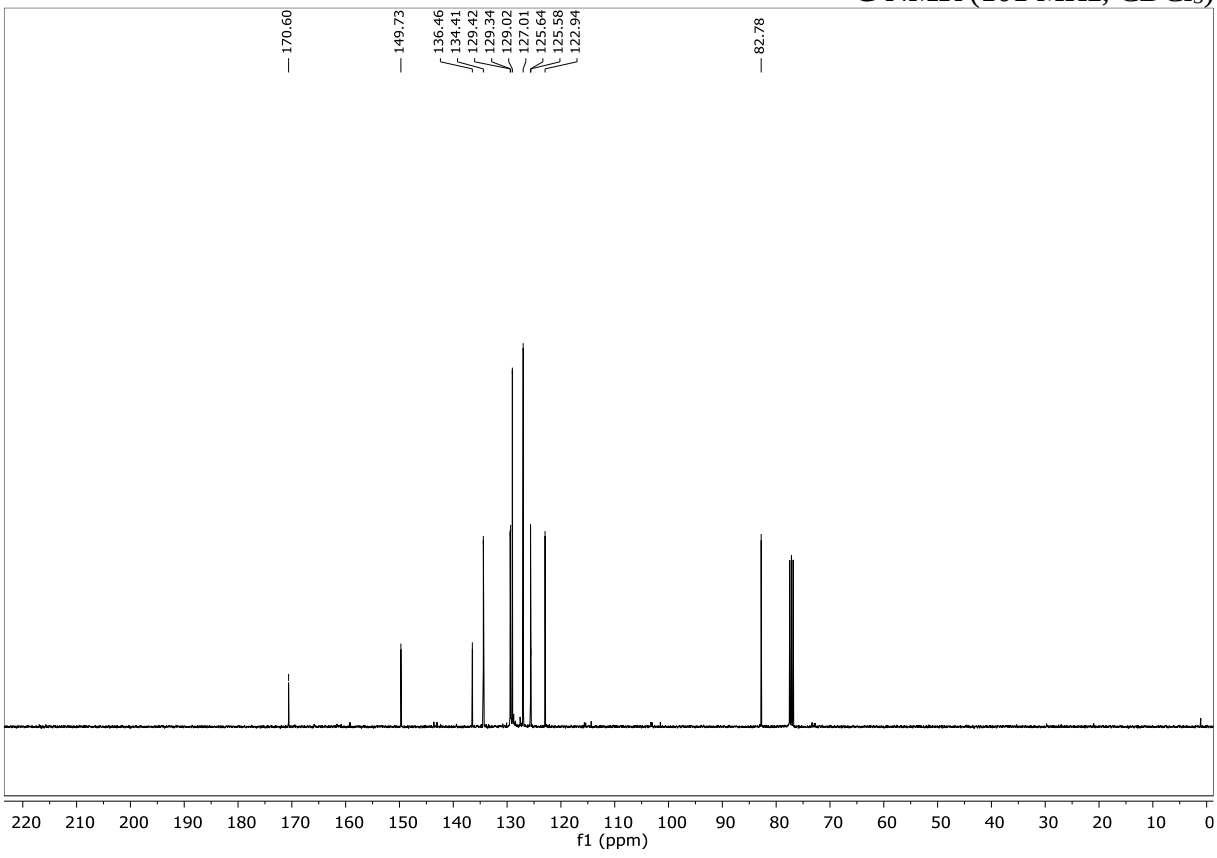

1-(2-Oxo-2*H*-pyran-6-yl)ethyl 3-bromopropiolate (355)

^{1}H NMR (400 MHz, $CDCl_3$)

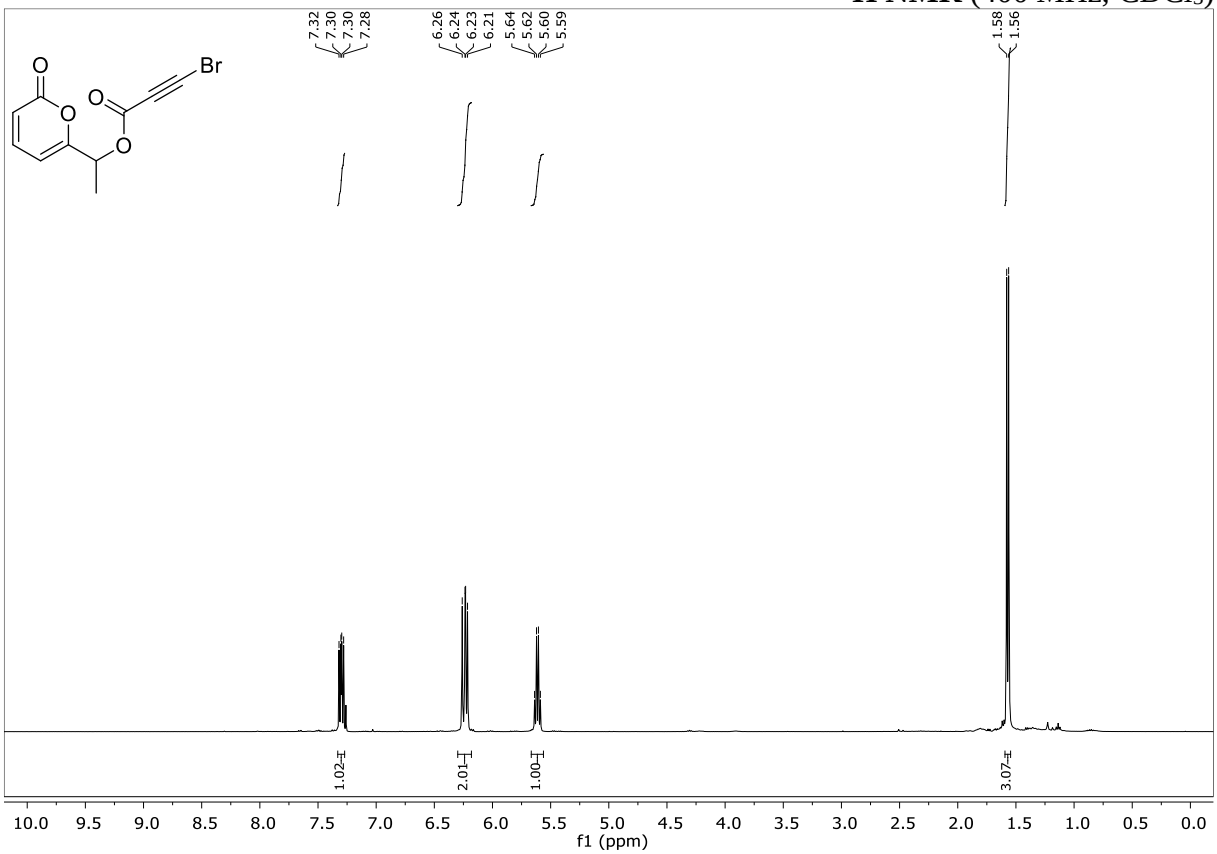

^{13}C NMR (101 MHz, $CDCl_3$)

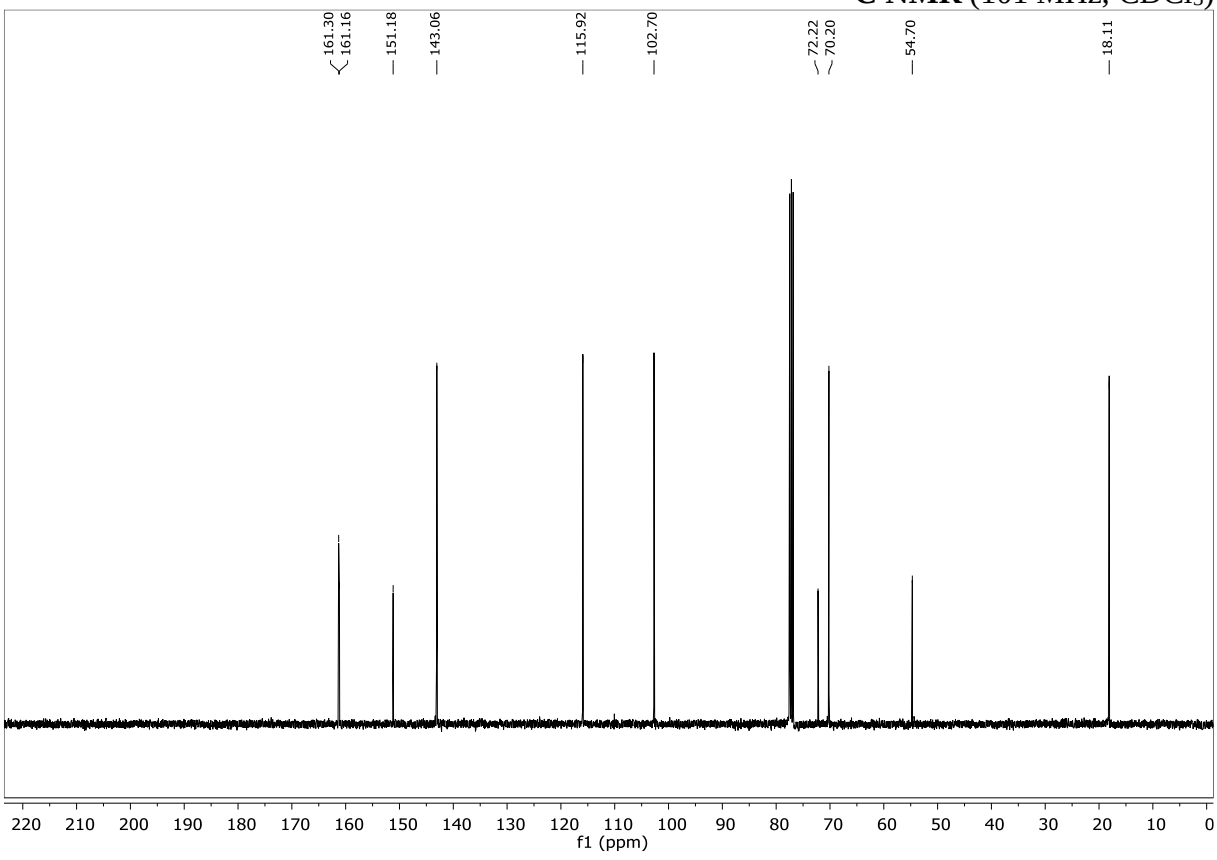

7-Bromo-3-methylisobenzofuran-1(3*H*)-one (354)

^{1}H NMR (400 MHz, $CDCl_3$)

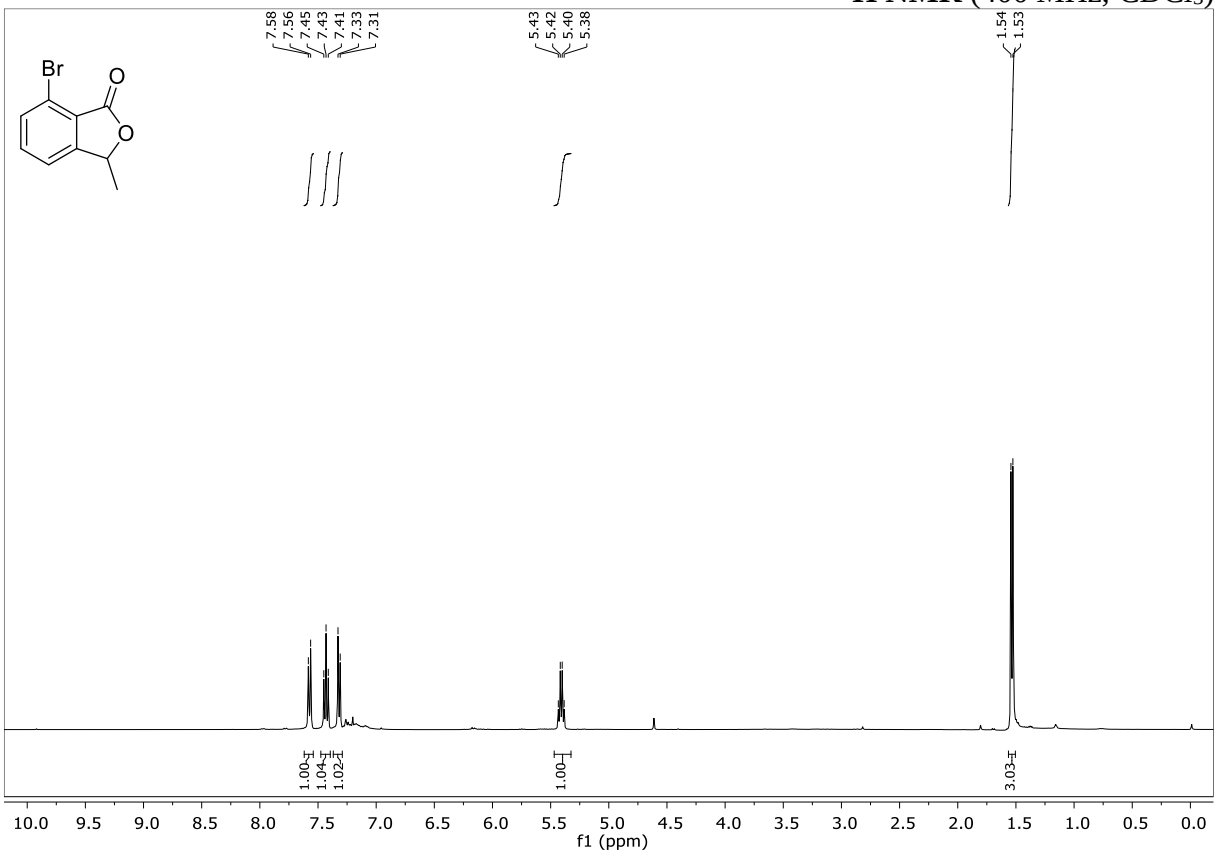

^{13}C NMR (101 MHz, $CDCl_3$)

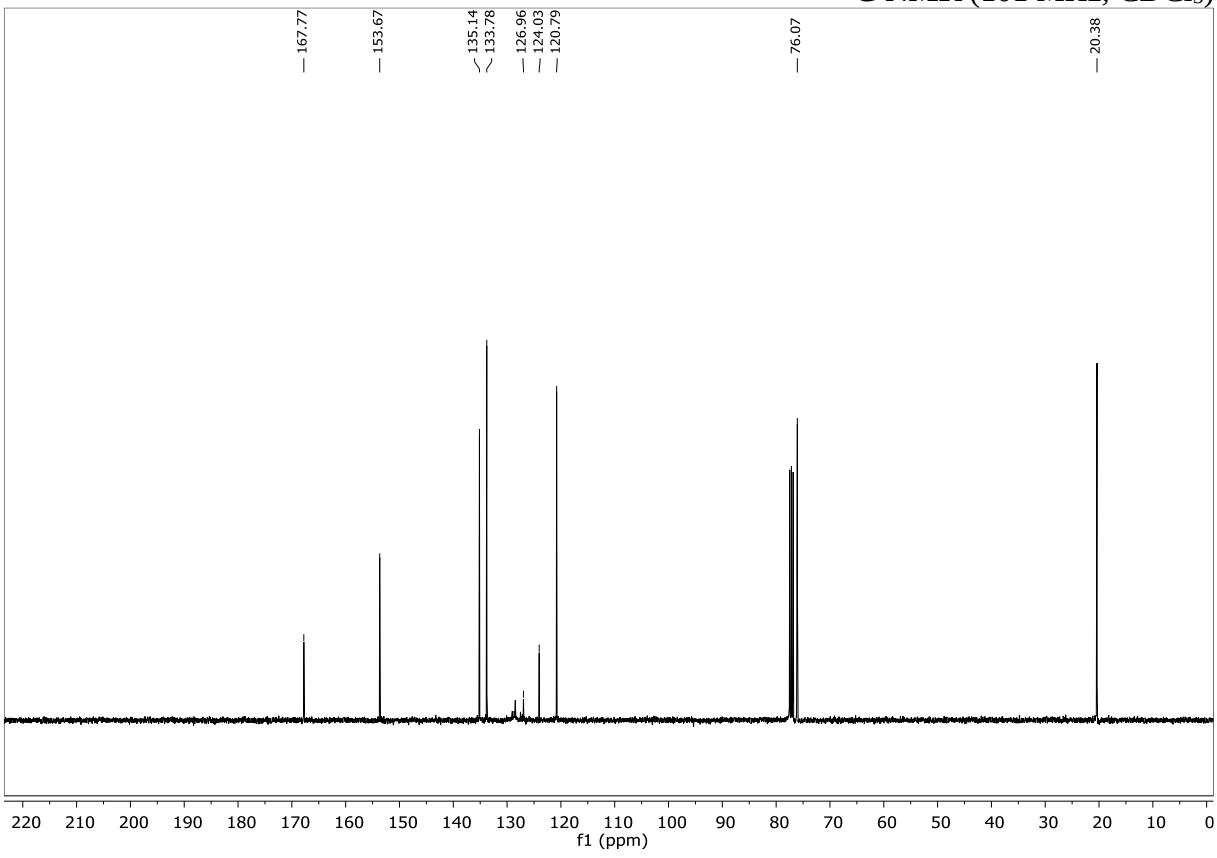

(*Exo*)-4a,5,8,8a-tetrahydro-1*H*-8,5-(epoxymethano)isochromene-1,10-dione (367a)

^{1}H NMR (400 MHz, $CDCl_3$)

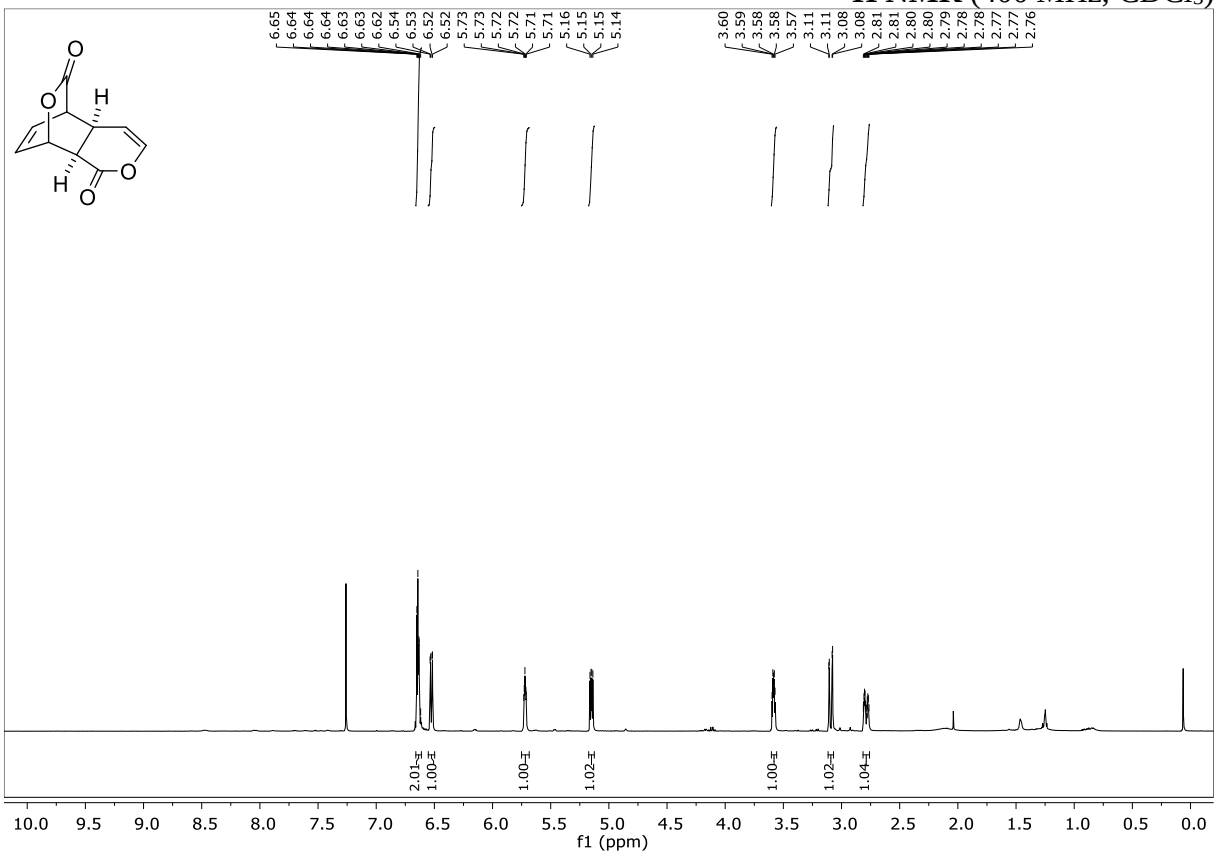

^{13}C NMR (101 MHz, $CDCl_3$)

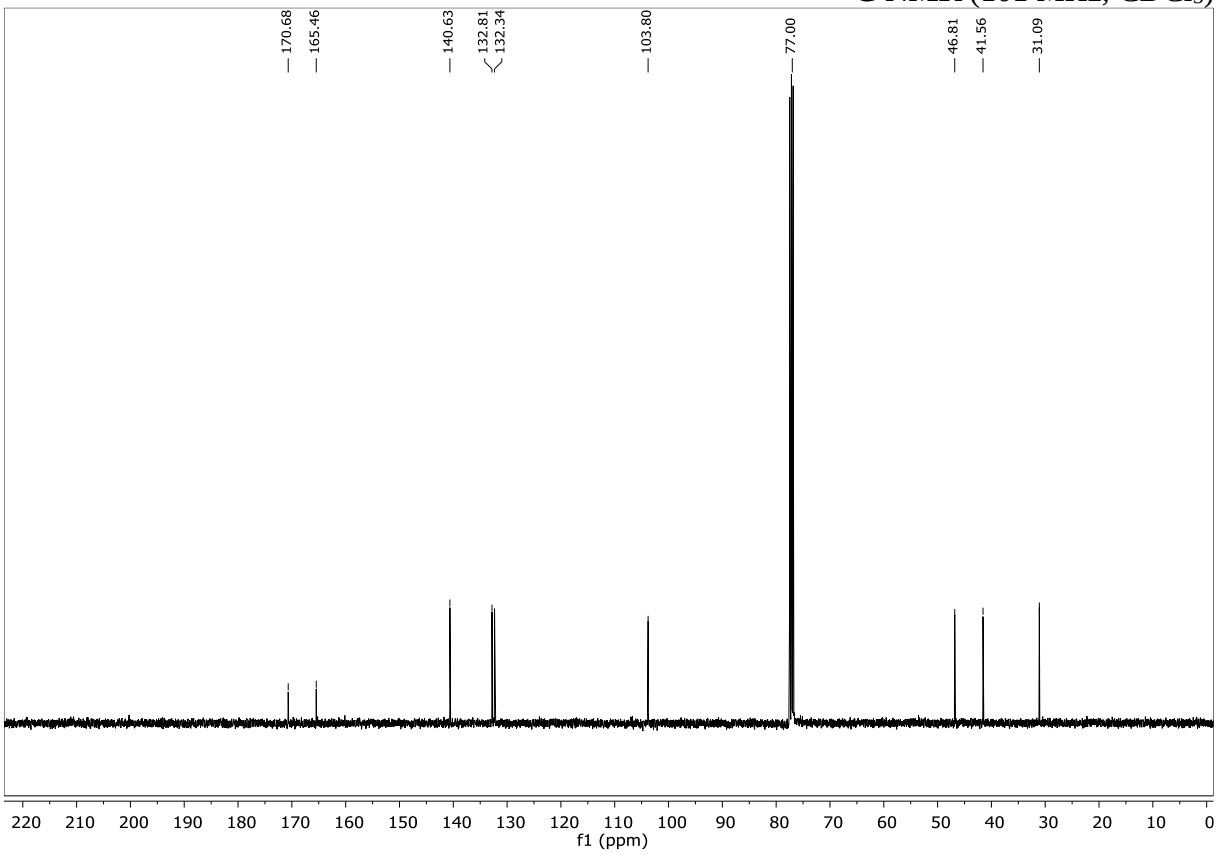

(*Exo*)-4a,5,8,8a-tetrahydro-2*H*-8,5-(epoxymethano)chromene-2,10-dione (367b)

^{1}H NMR (400 MHz, $CDCl_3$)

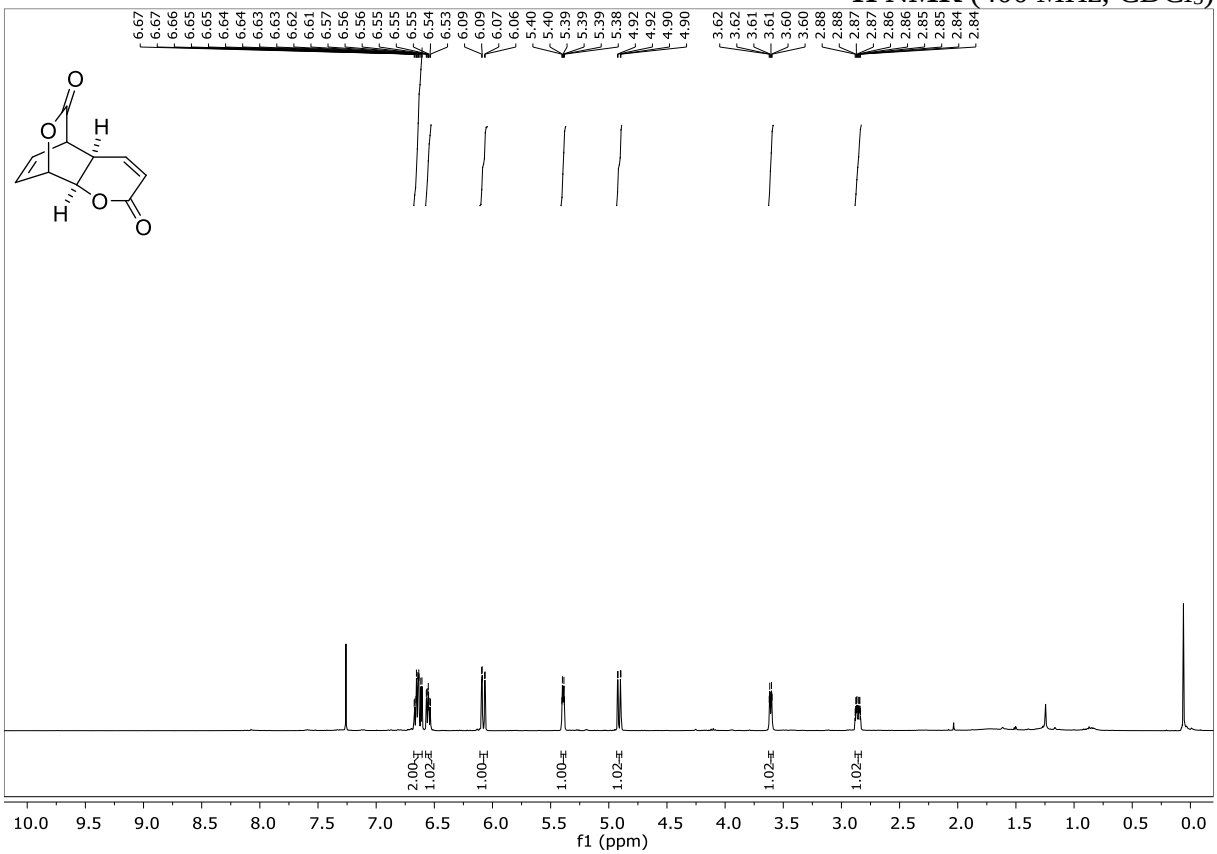

^{13}C NMR (101 MHz, $CDCl_3$)

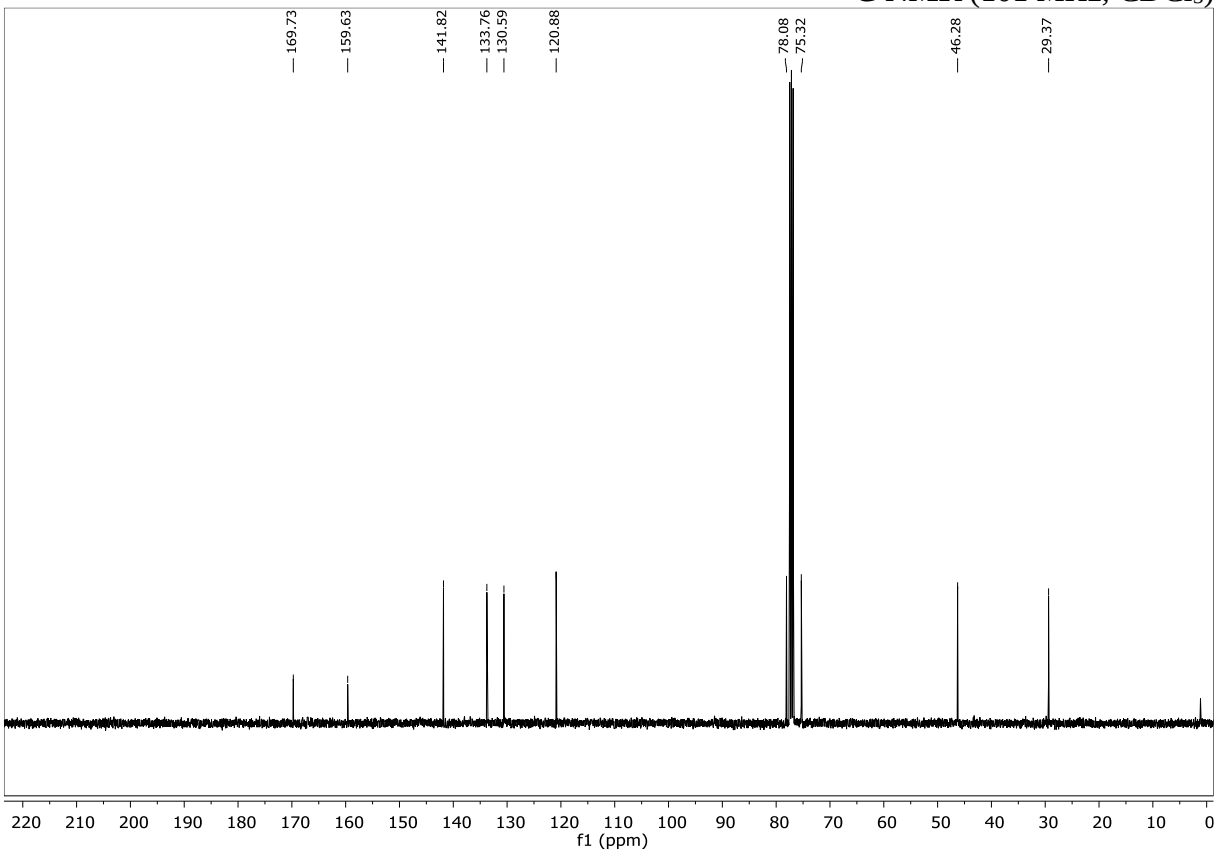

Methyl 3-oxo-7-phenyl-2-oxabicyclo[4.1.0]hept-4-ene-7-carboxylate (377a)

^{1}H NMR (400 MHz, $CDCl_3$)

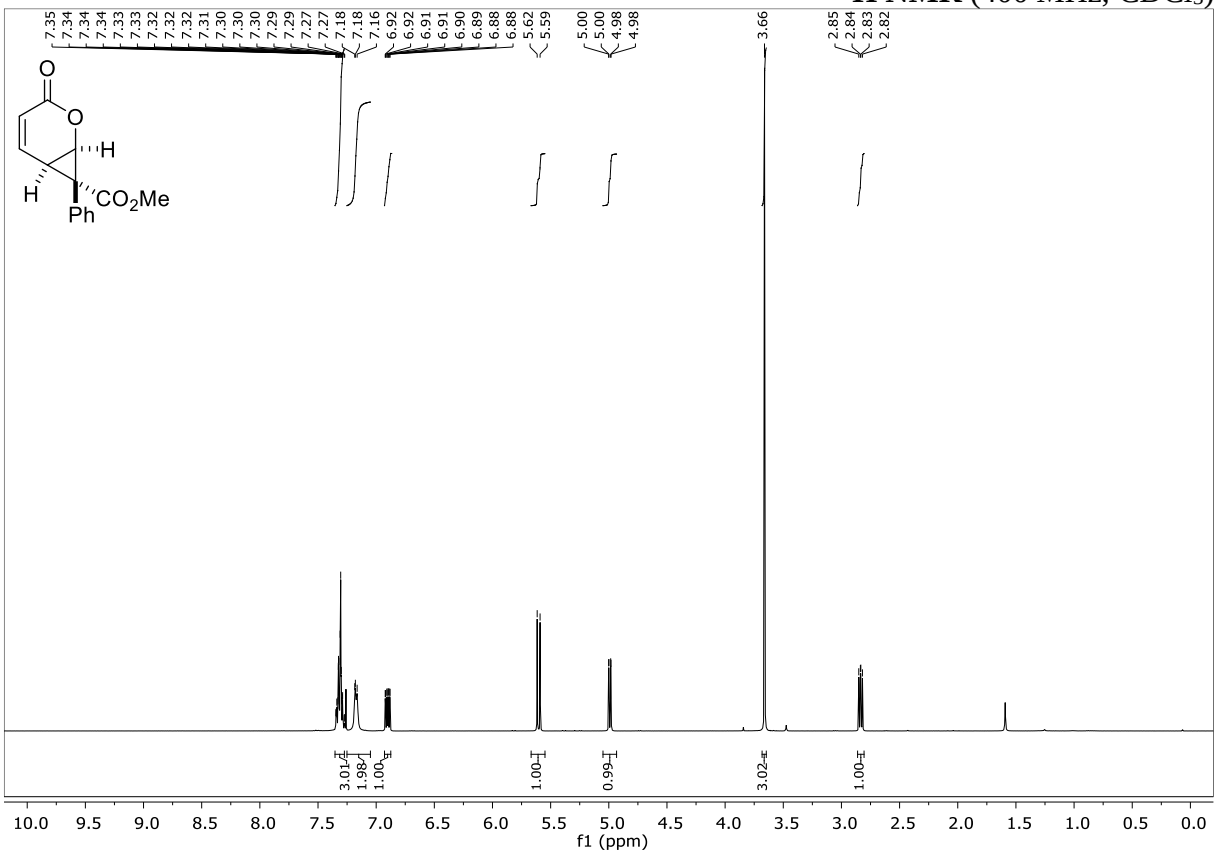

^{13}C NMR (101 MHz, $CDCl_3$)

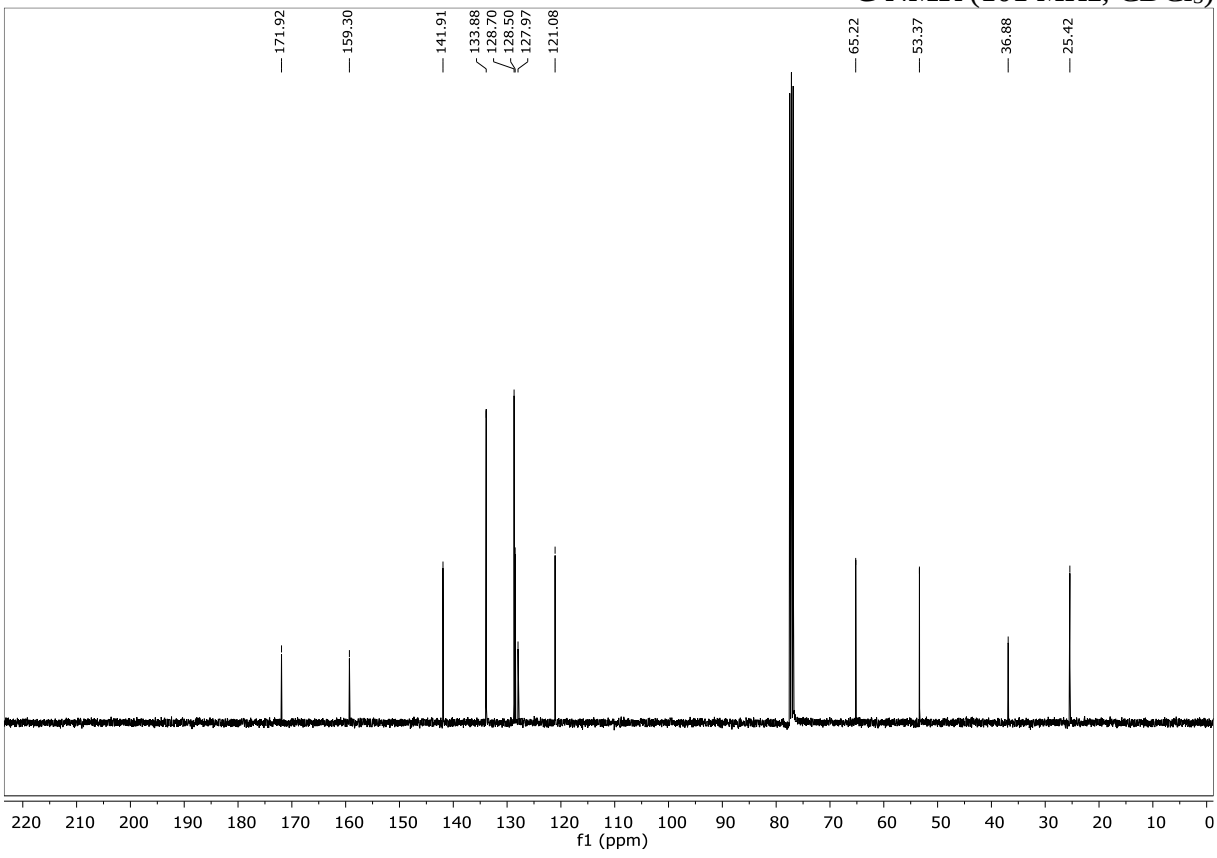

Methyl 3-oxo-7-phenyl-2-tosyl-2-azabicyclo[4.1.0]hept-4-ene-7-carboxylate (377a)

^{1}H NMR (400 MHz, $CDCl_3$)

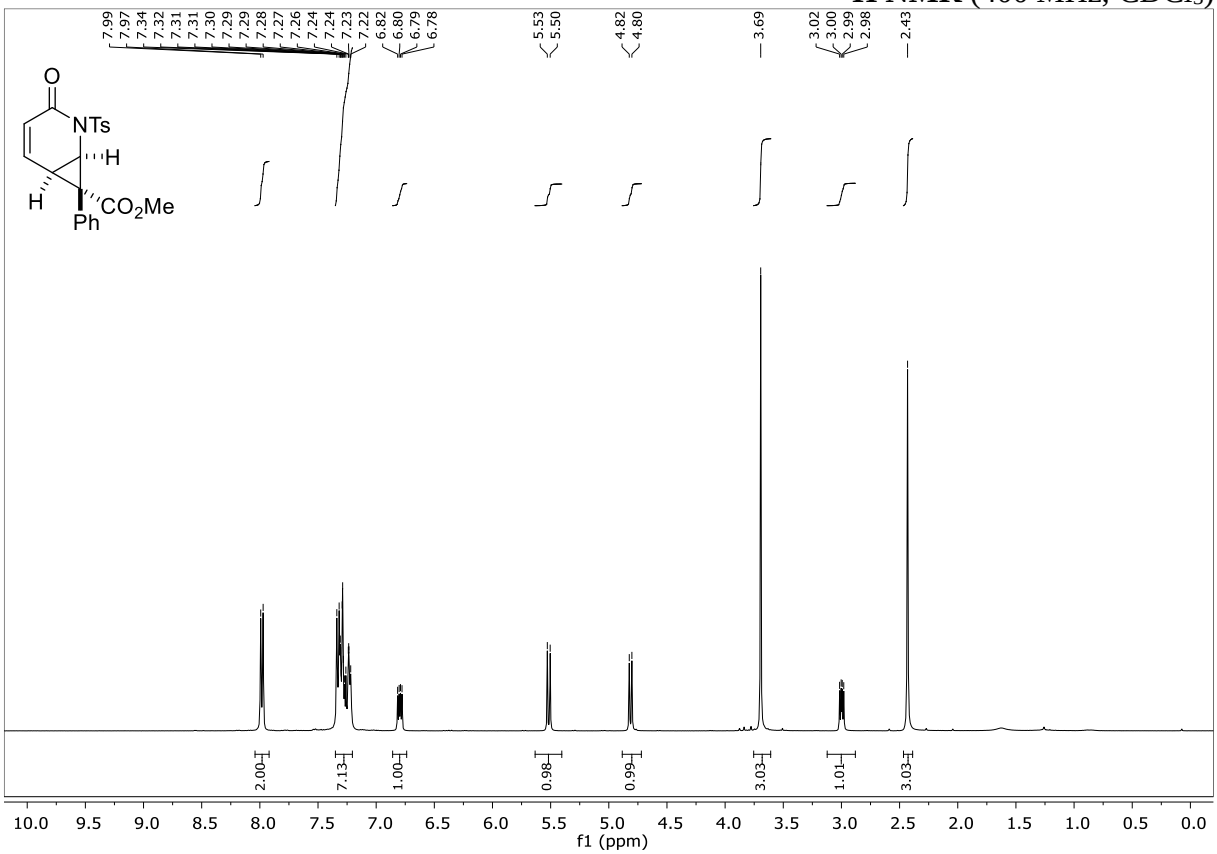

^{13}C NMR (101 MHz, $CDCl_3$)

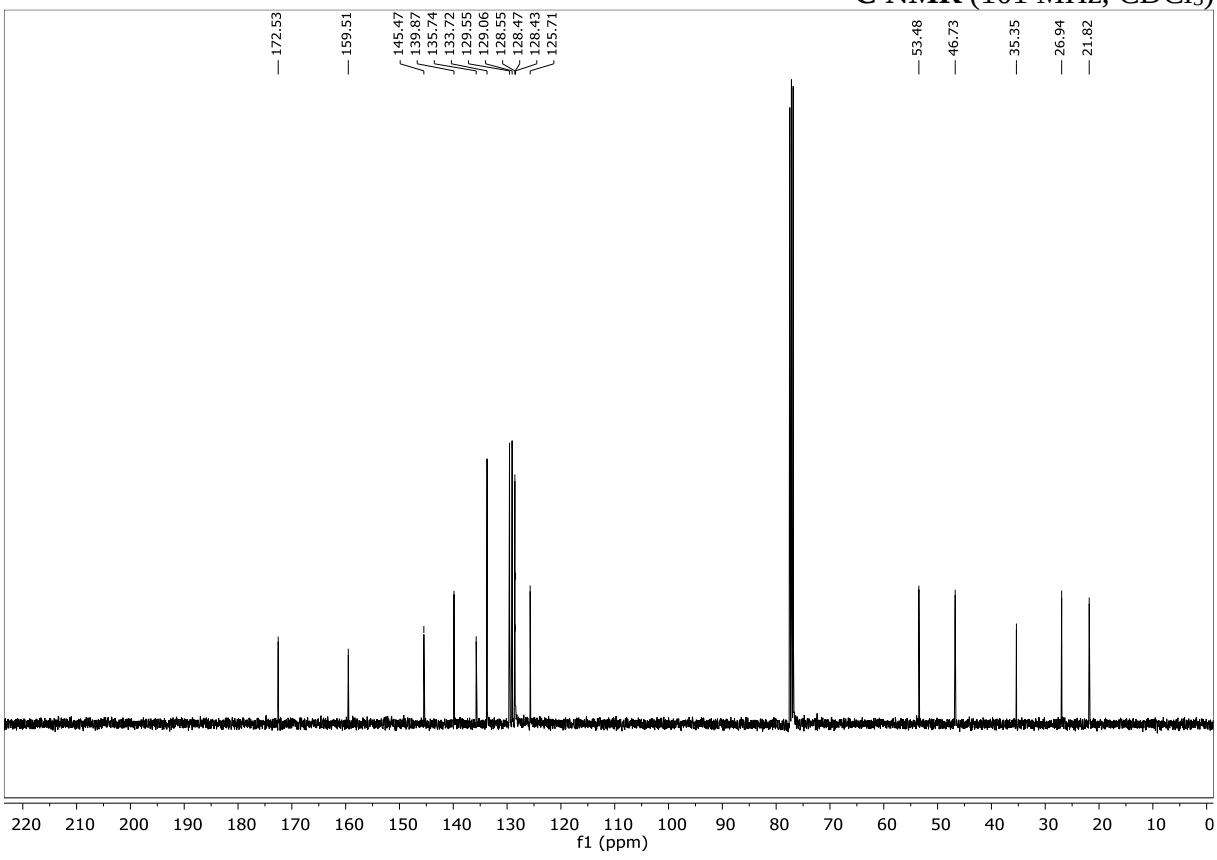

2,2,2-Trichloroethyl 7-(4-bromophenyl)-3-oxo-2-oxabicyclo[4.1.0]hept-4-ene-7-carboxylate (380a)

^{1}H NMR (400 MHz, $CDCl_3$)

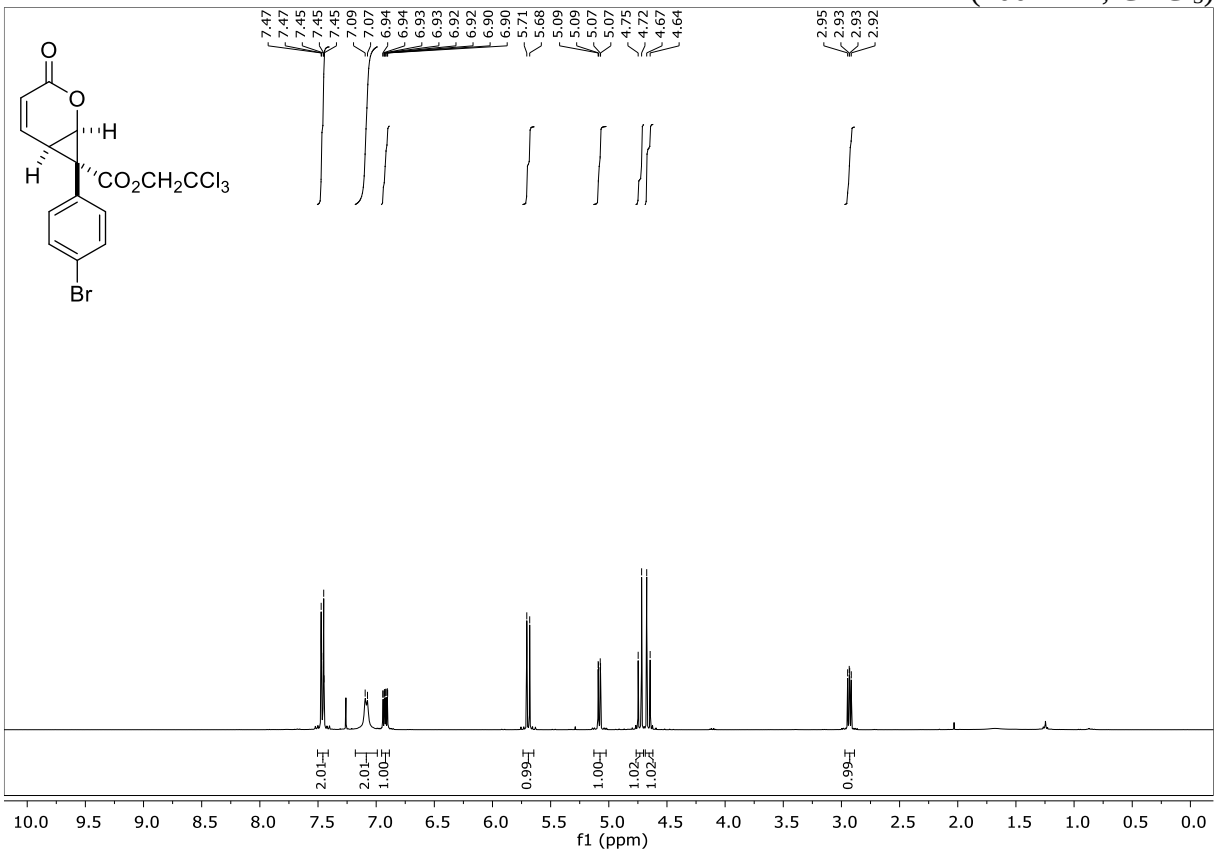

^{13}C NMR (101 MHz, $CDCl_3$)

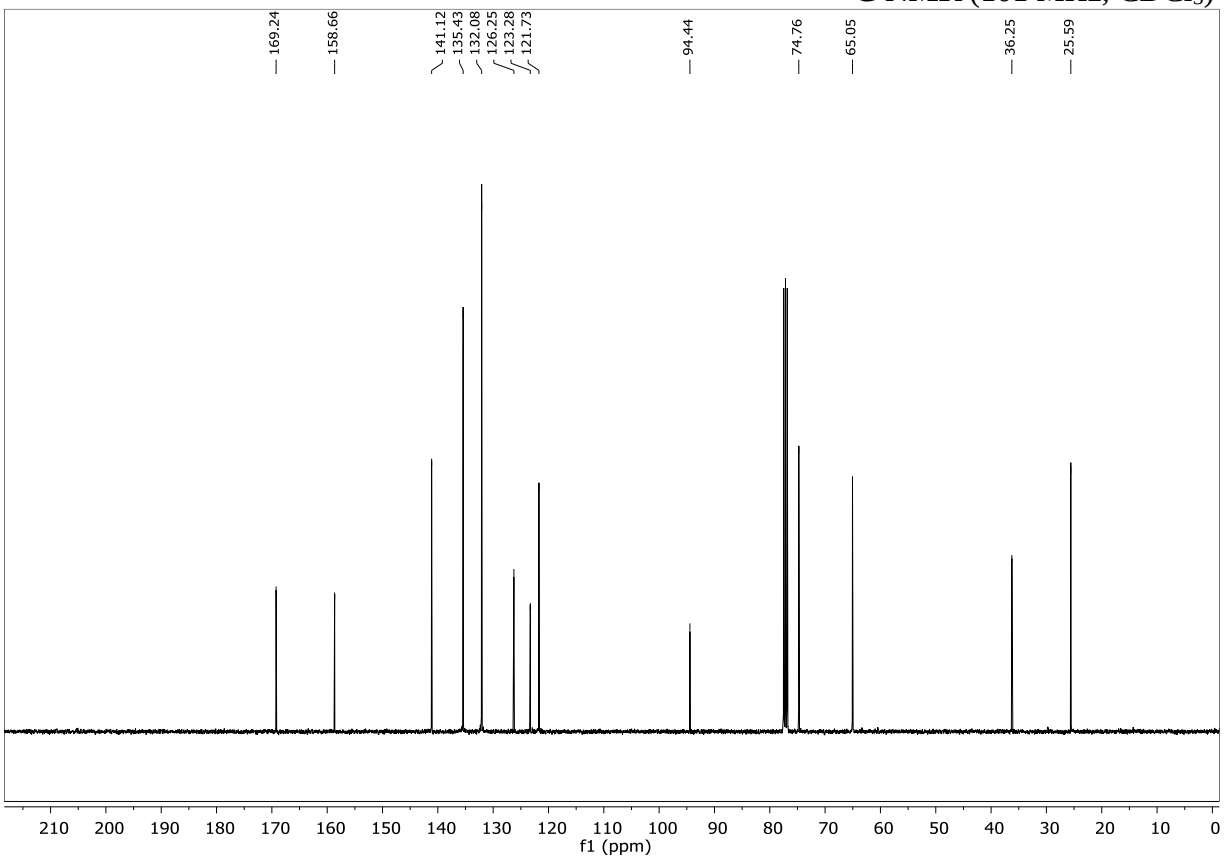

2,2,2-Trichloroethyl 7-(4-bromophenyl)-3-oxo-2-tosyl-2-azabicyclo[4.1.0]hept-4-ene-7-carboxylate (380b)

^{1}H NMR (400 MHz, $CDCl_3$)

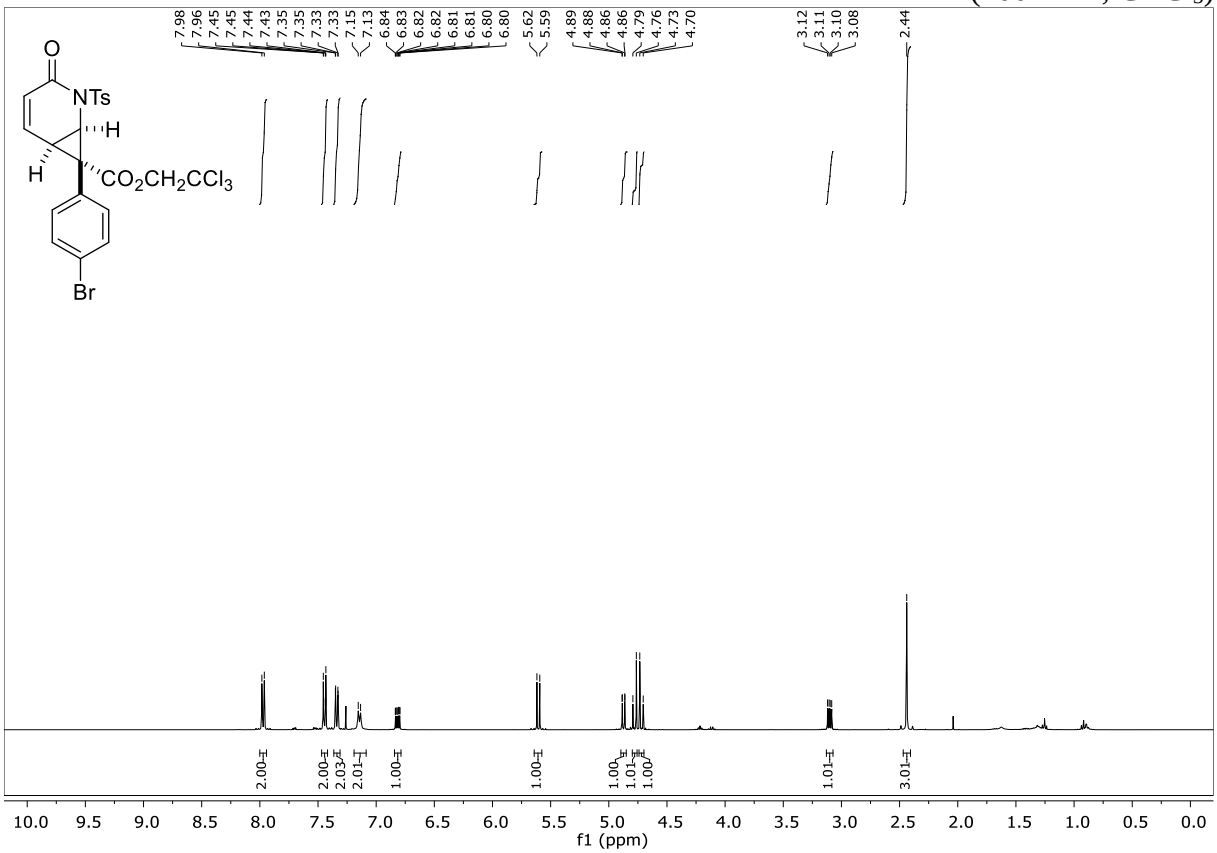

^{13}C NMR (101 MHz, $CDCl_3$)

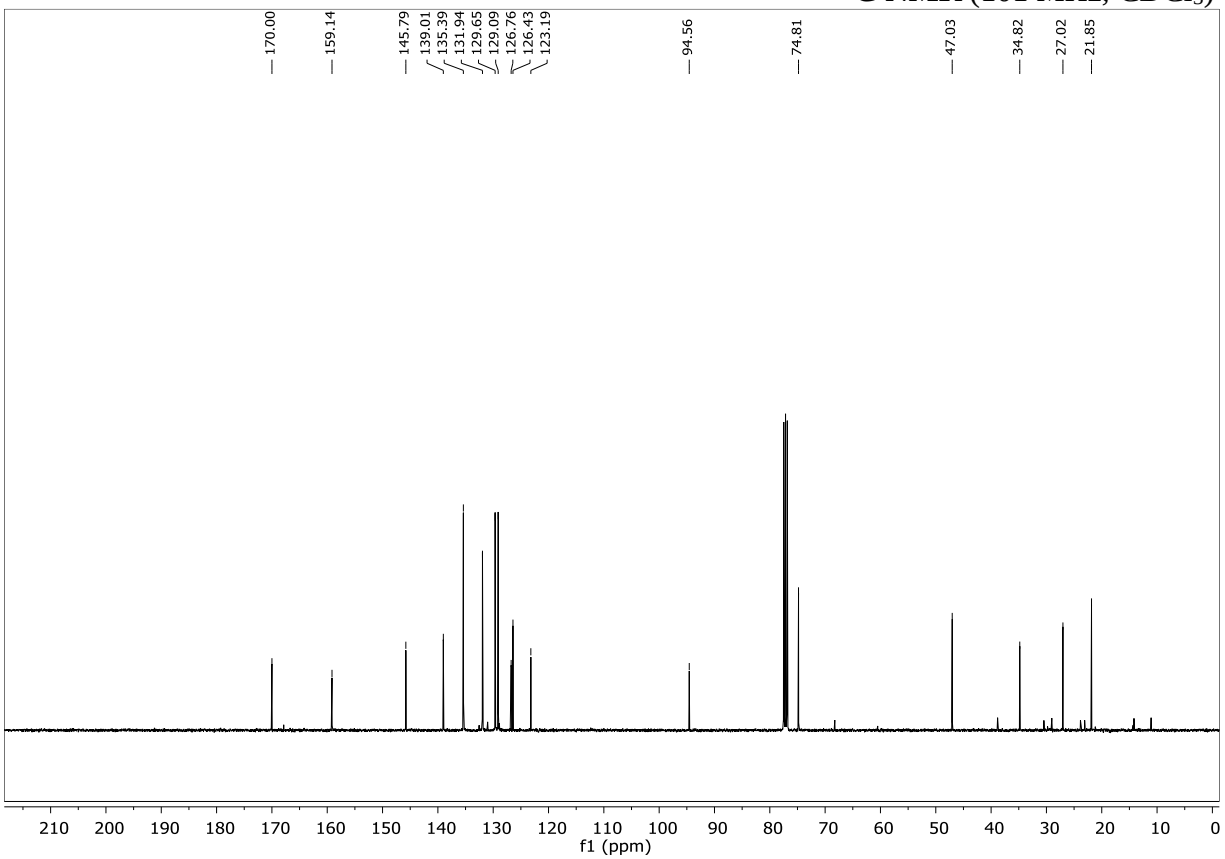

(2-Hydroxy-1-phenylcyclopent-4-ene-1,3-diyl)dimethanol (411)

^{1}H NMR (300 MHz, $CDCl_3$)

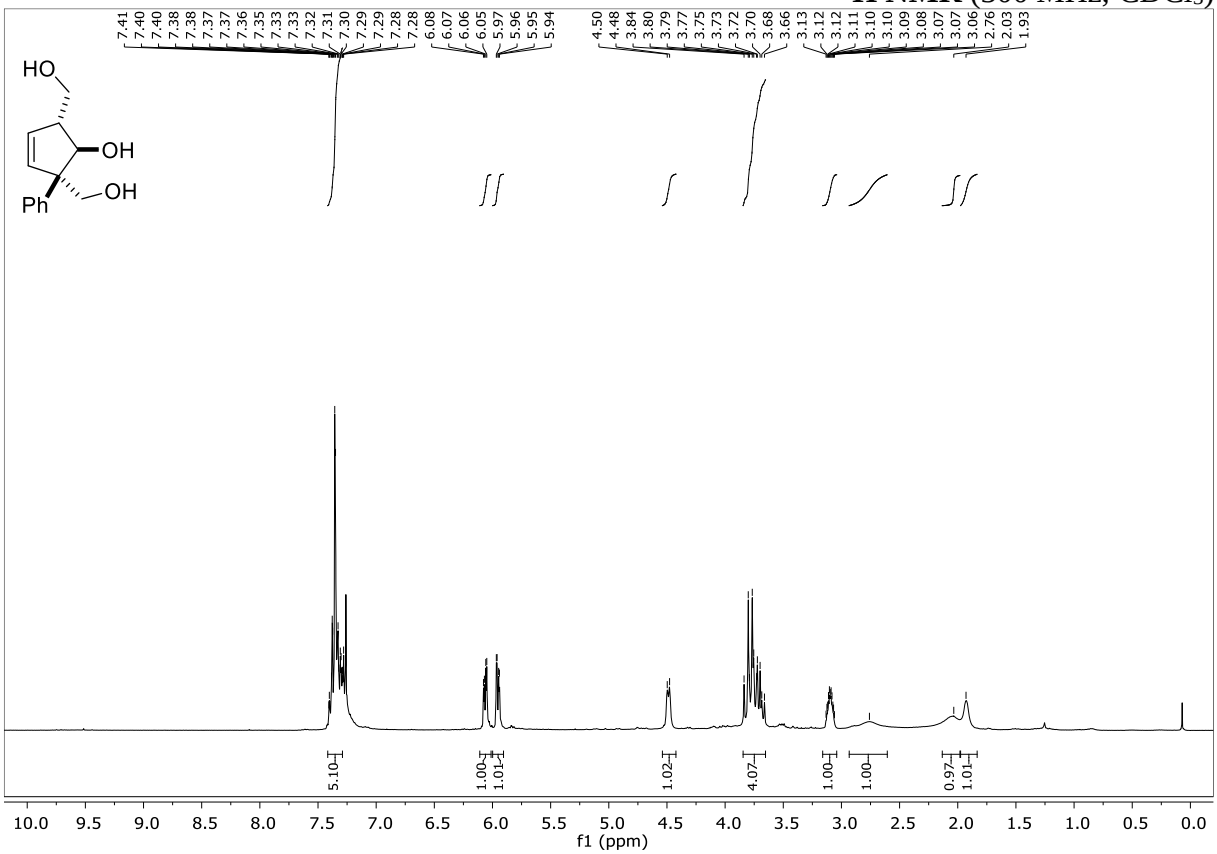

^{13}C NMR (101 MHz, $CDCl_3$)

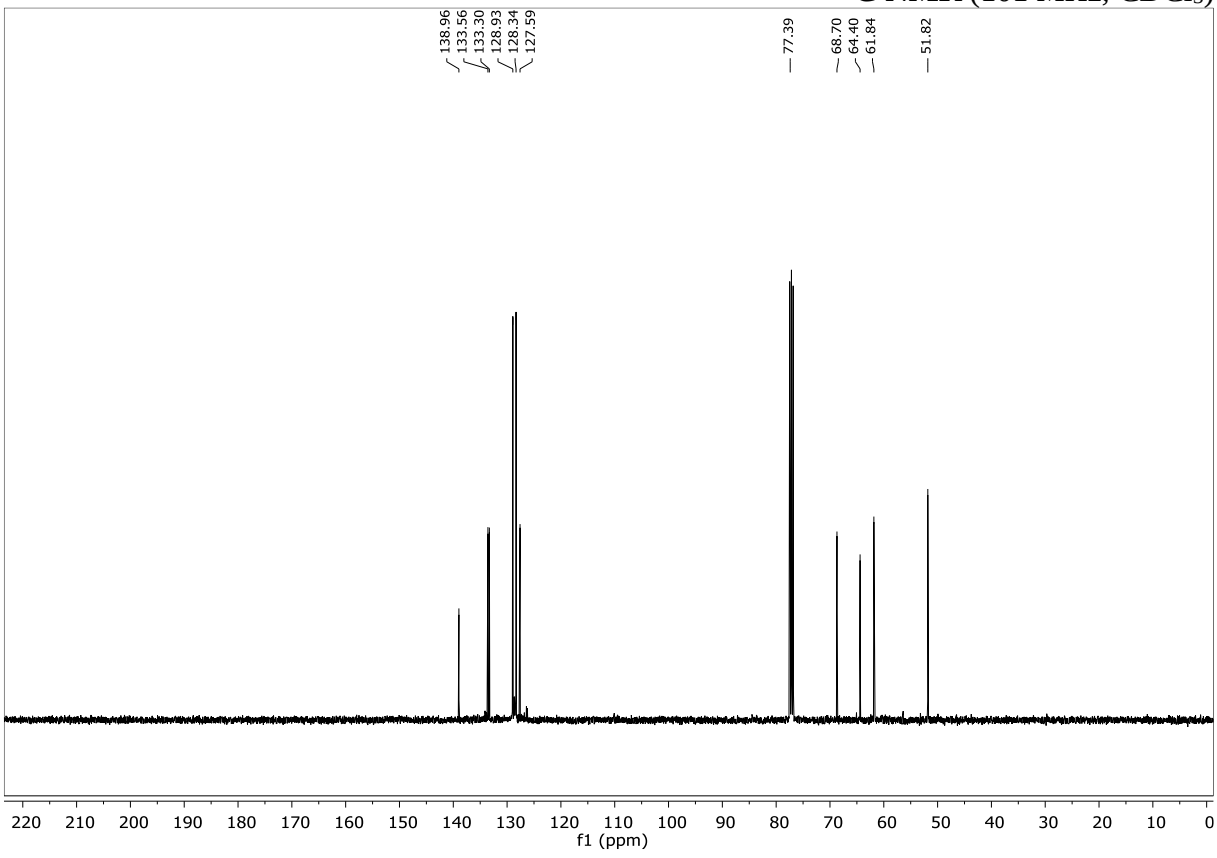

1,5-Dimethoxy-9,10-anthraquinone (427)

^{1}H NMR (300 MHz, $CDCl_3$)

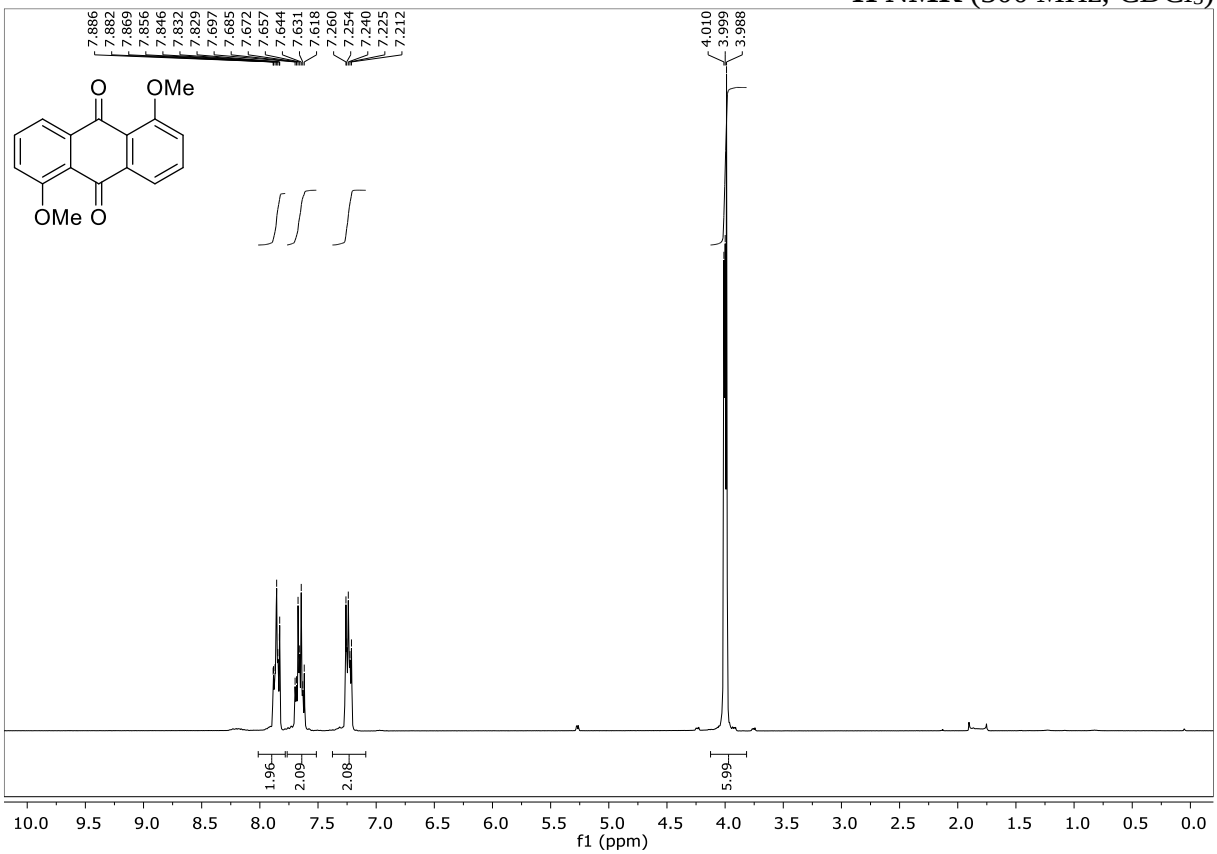

^{13}C NMR (75 MHz, $CDCl_3$)

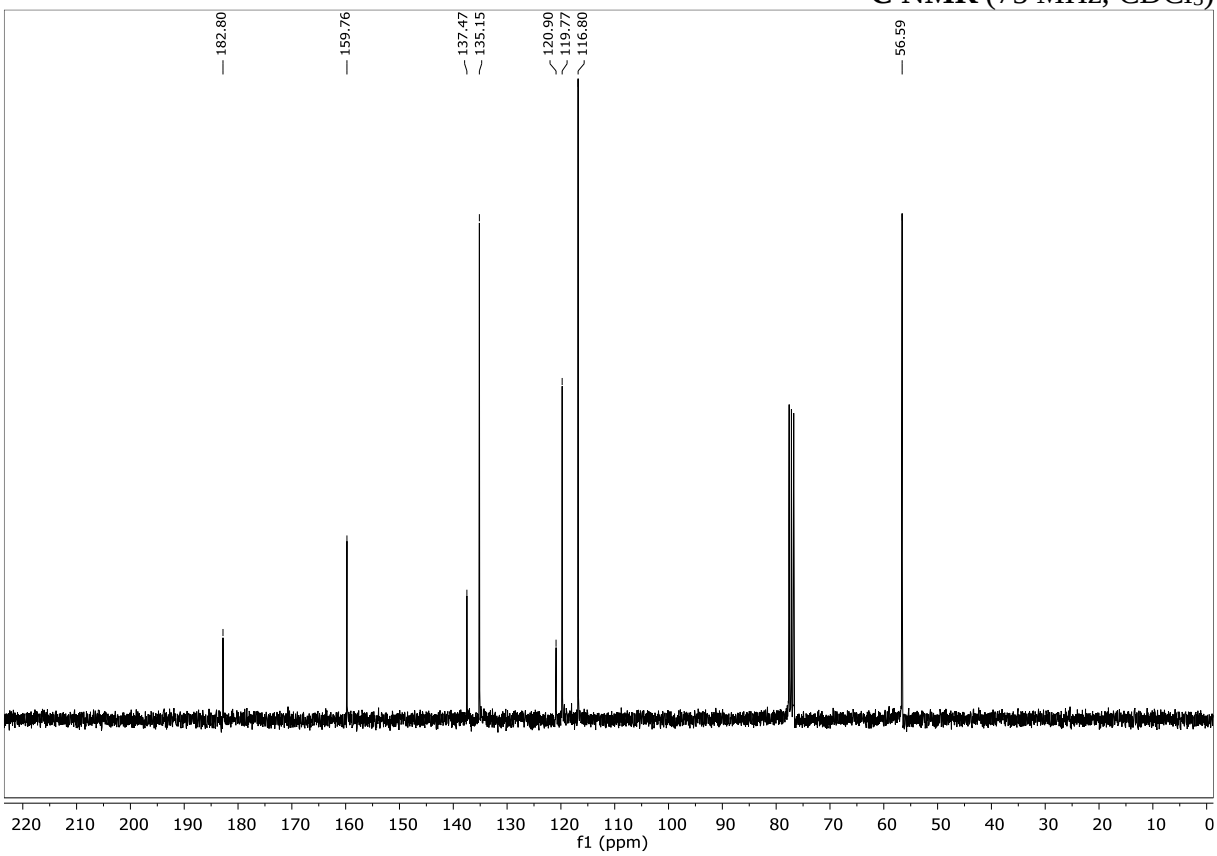

1,5-Bis(*N*,*N*-dimethylamino)anthracene (419c)

^{1}H NMR (300 MHz, $CDCl_3$)

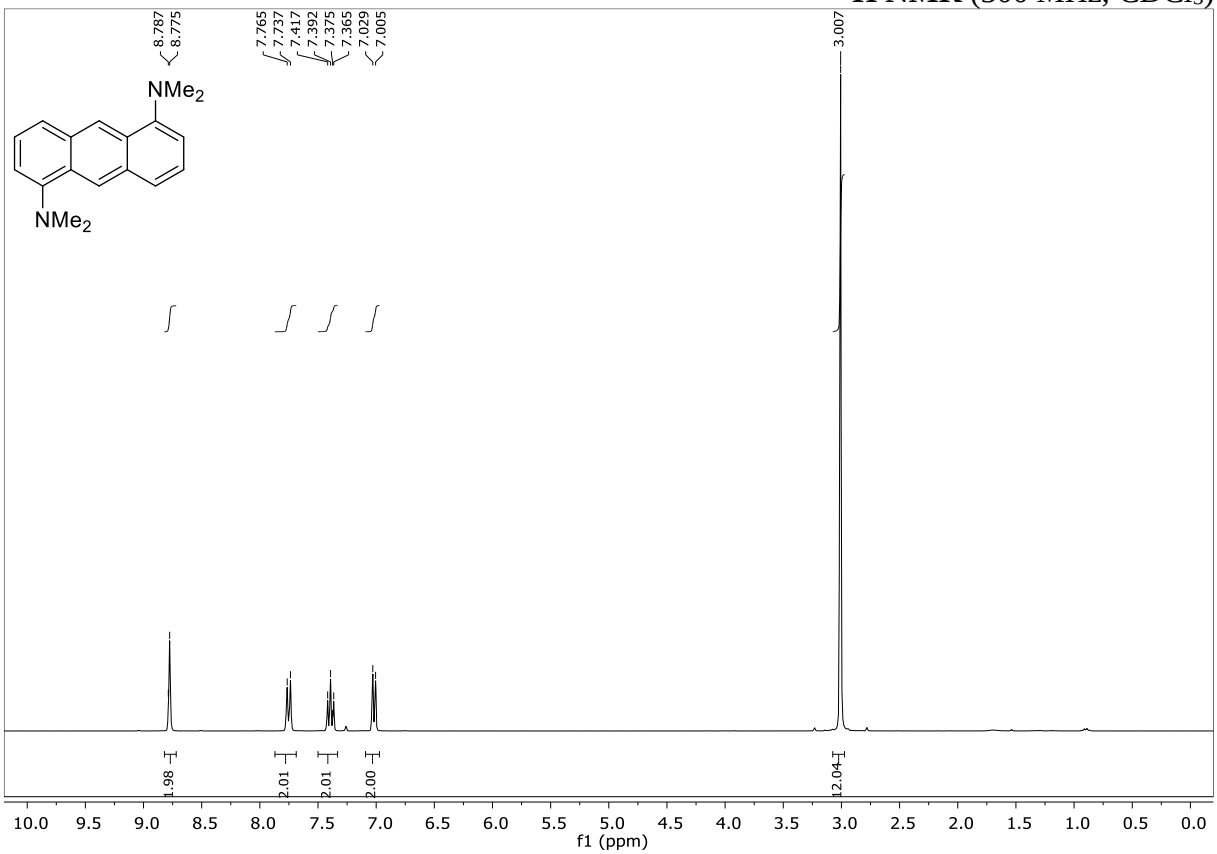

^{13}C NMR (75 MHz, $CDCl_3$)

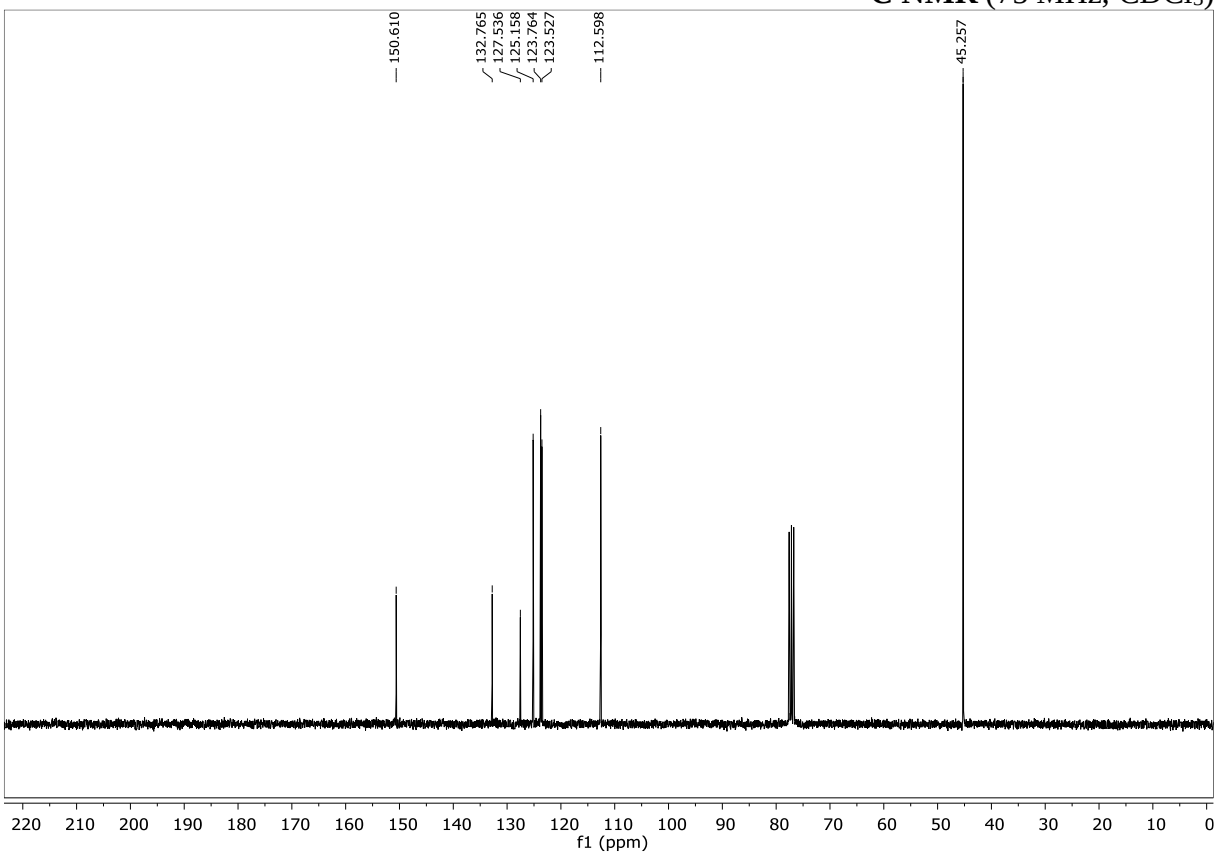

1,5-di(pyrrolidin-1-yl)anthracene (419d)

^{1}H NMR (300 MHz, $CDCl_3$)

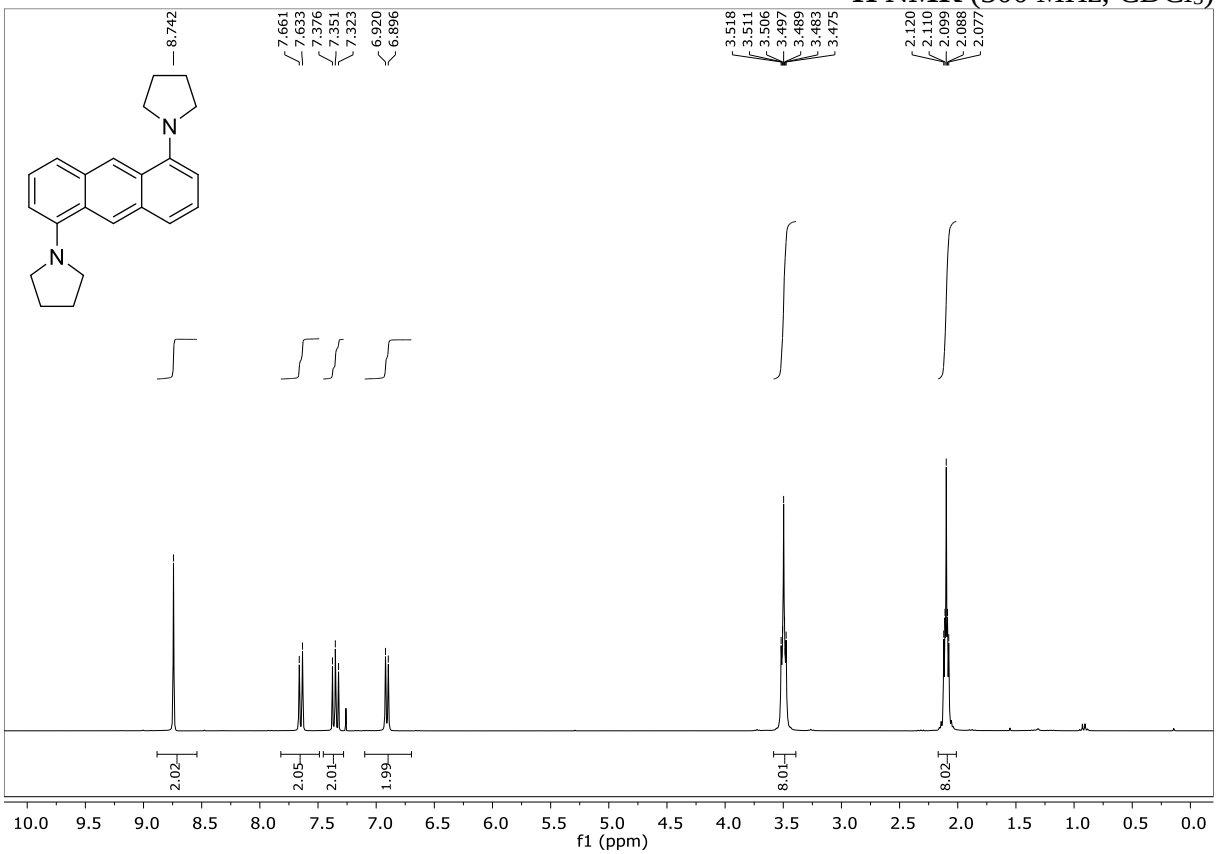

^{13}C NMR (75 MHz, $CDCl_3$)

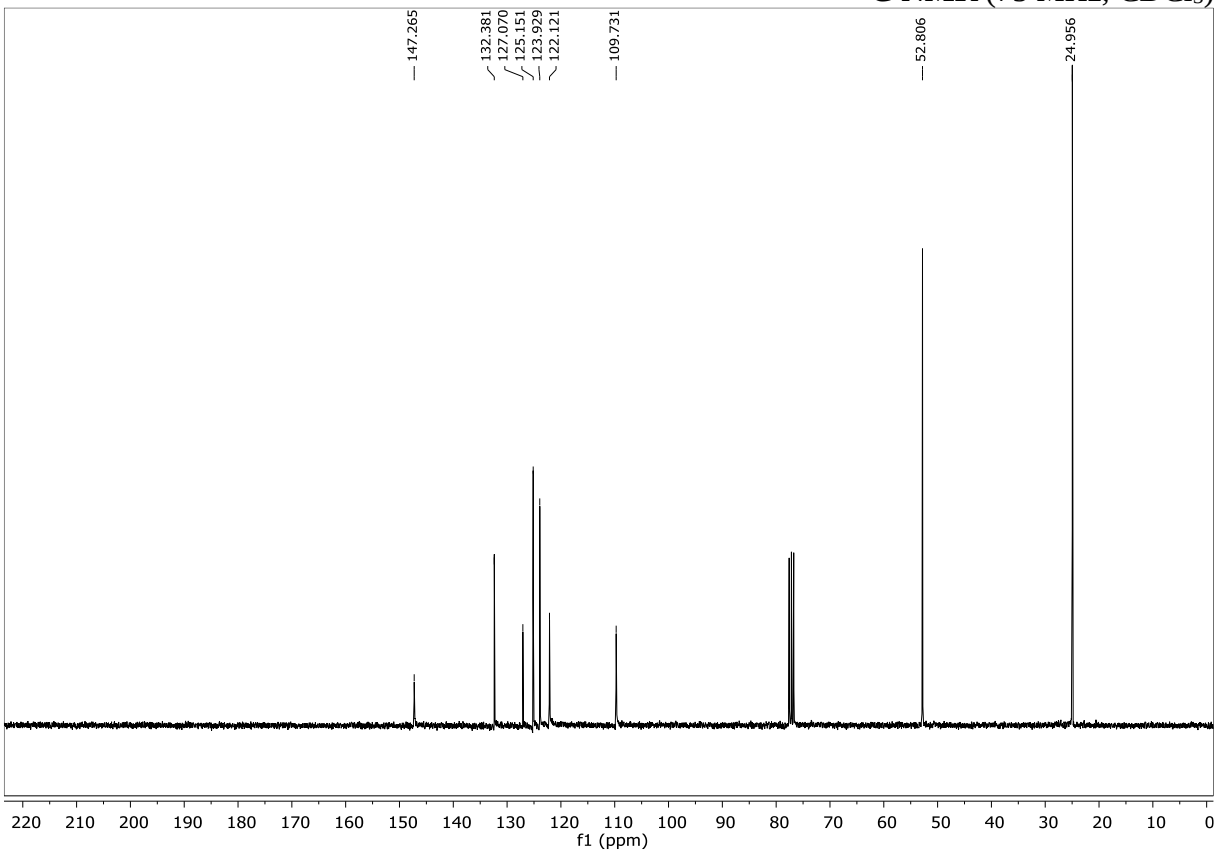

1-(Pyrrolidine-1-yl)anthracene (419e)

^{1}H NMR (400 MHz, $CDCl_3$)

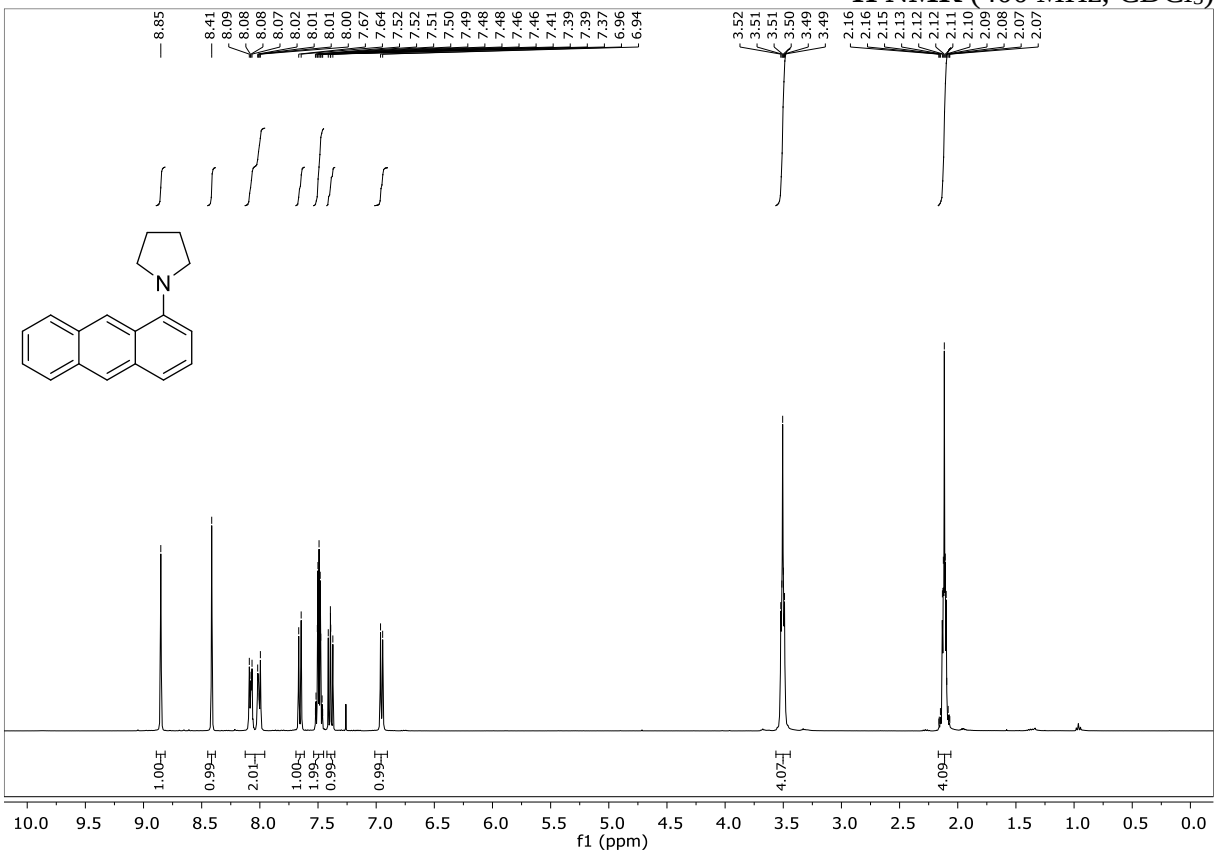

^{13}C NMR (101 MHz, $CDCl_3$)

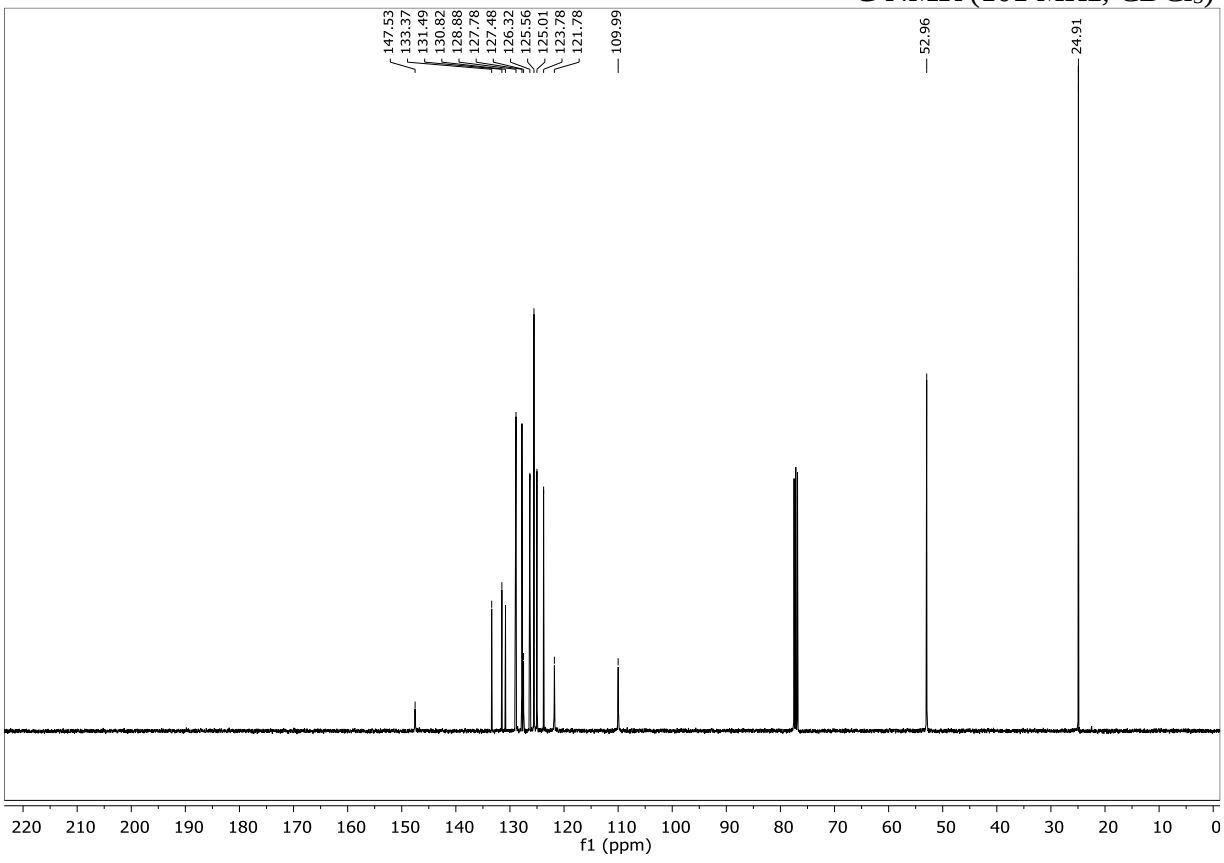

Syn-dimethyl-1,5-dimethoxy-9,10-dihydro-9,10-ethanoanthracene-11,12-dicarboxylate (430bA)

^{1}H NMR (400 MHz, $CDCl_3$)

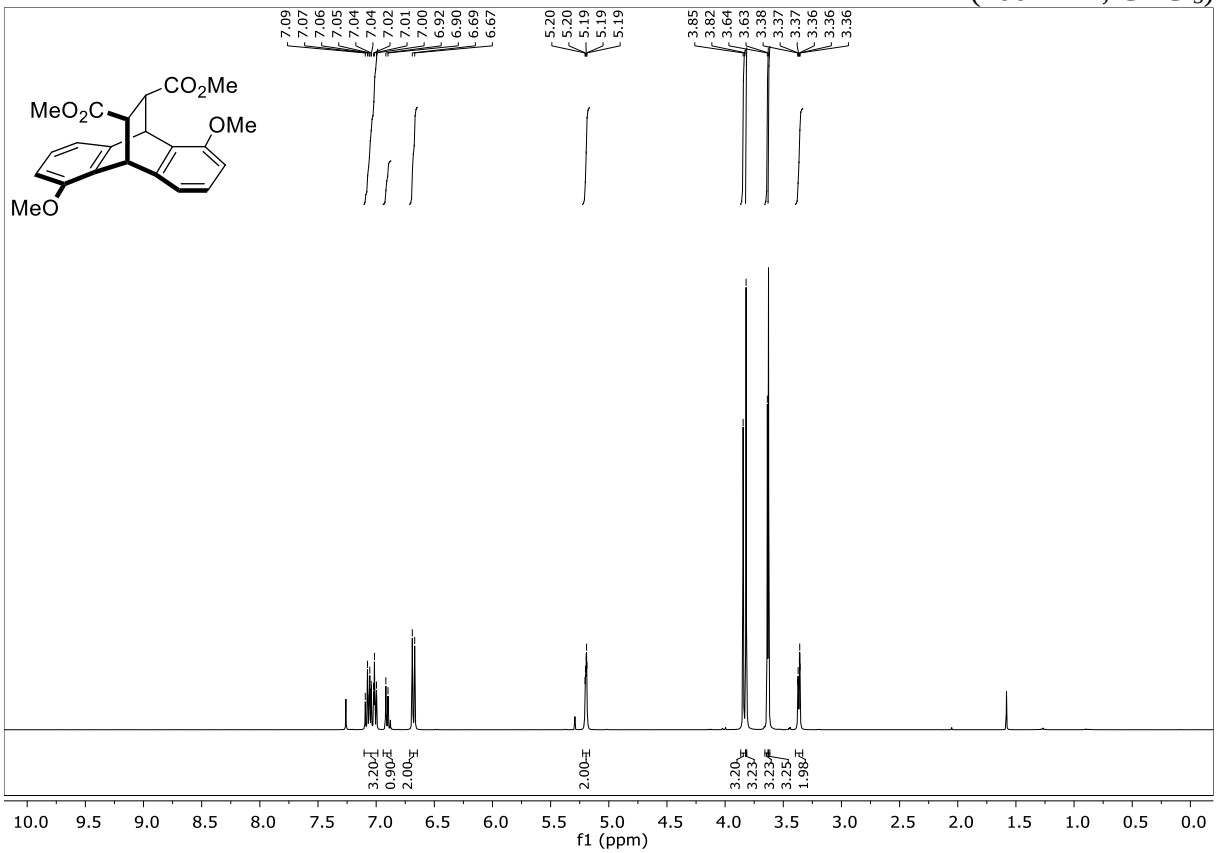

^{13}C NMR (101 MHz, $CDCl_3$)

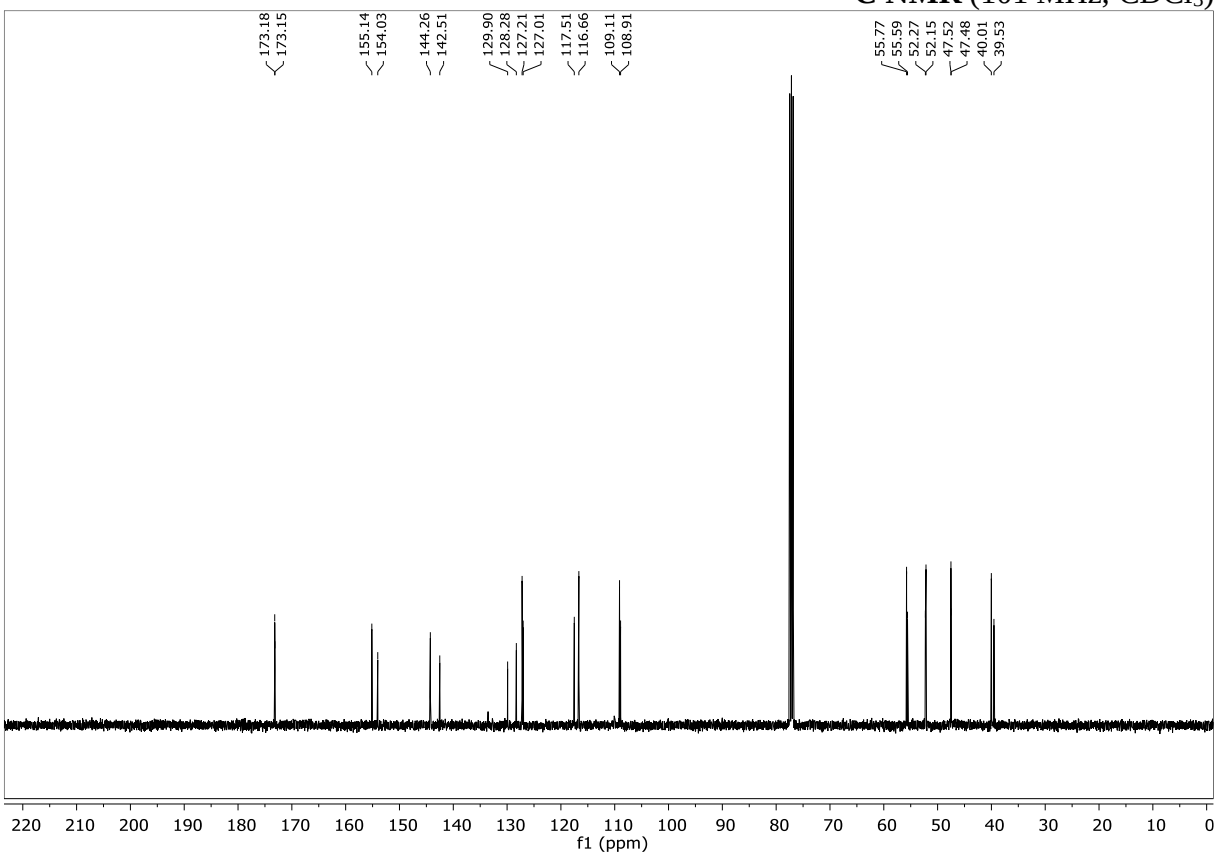

1,5-Dimethoxy-9,10-dihydro-9,10-[3,4]furanoanthracene-12,14-dione (430bB)

^{1}H NMR (400 MHz, $CDCl_3$)

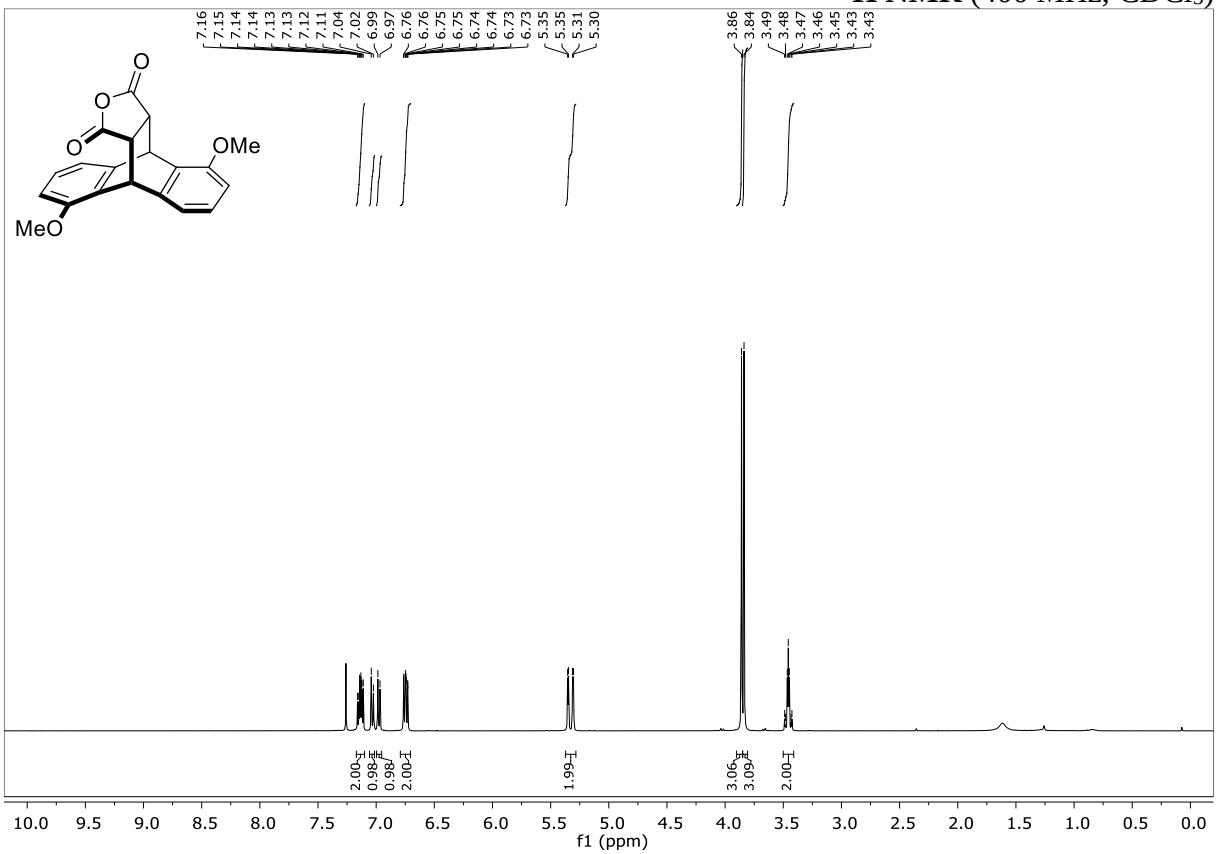

^{13}C NMR (101 MHz, $CDCl_3$)

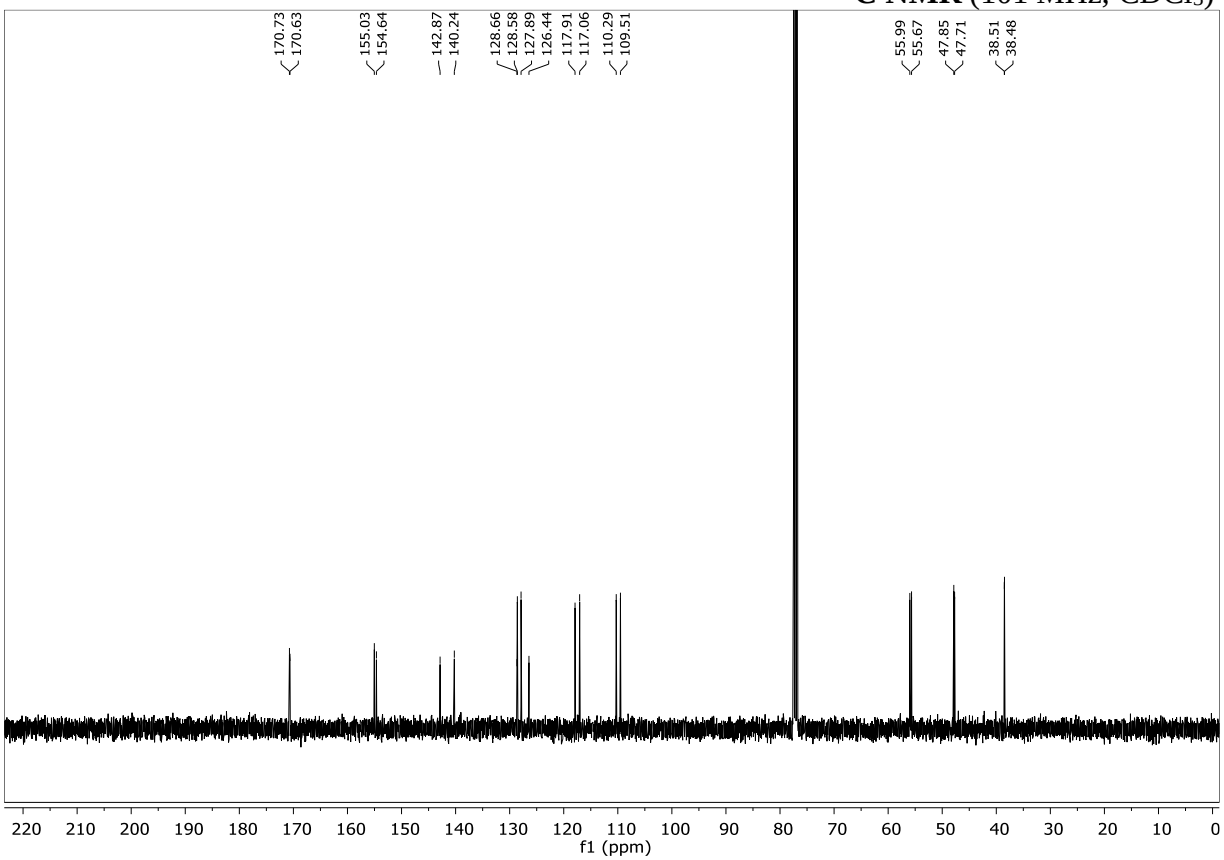

1,5-Dimethoxy-13-phenyl-9,10-dihydro-9,10-[3,4]epipyrroloanthracene-12,14-dione (430bC)

^{1}H NMR (400 MHz, $CDCl_3$)

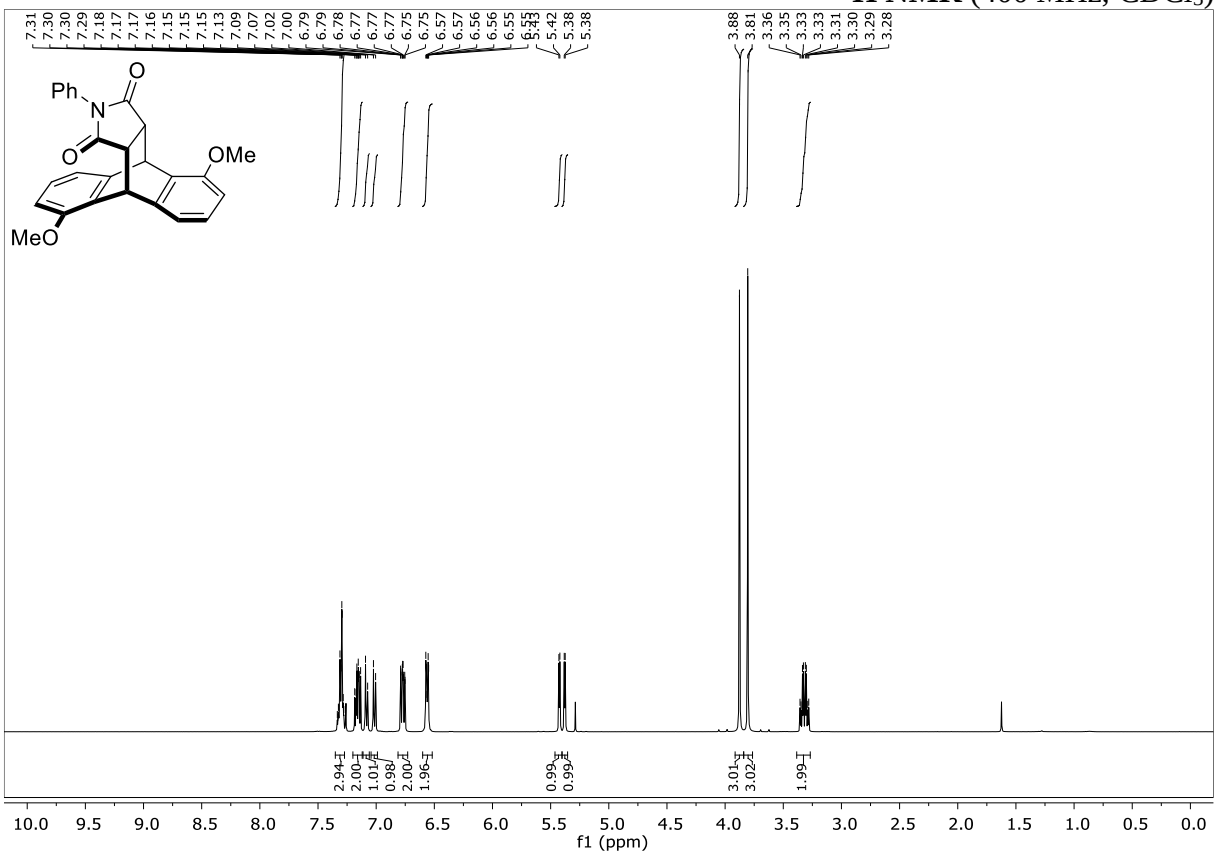

^{13}C NMR (101 MHz, $CDCl_3$)

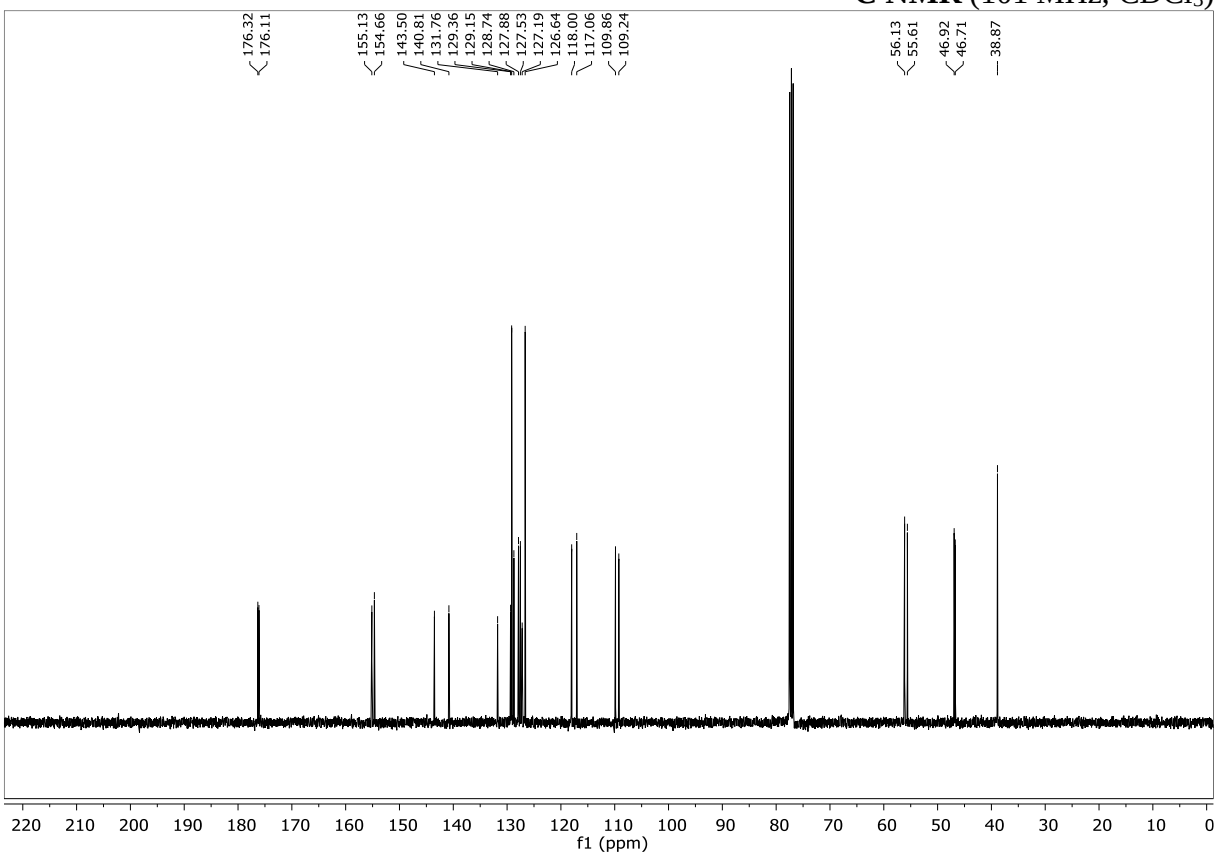

1,5-Bis(dimethylamino)-13-phenyl-9,10-dihydro-9,10-[3,4]epipyrroloanthracene-12,14-dione (430cC)

^{1}H NMR (400 MHz, $CDCl_3$)

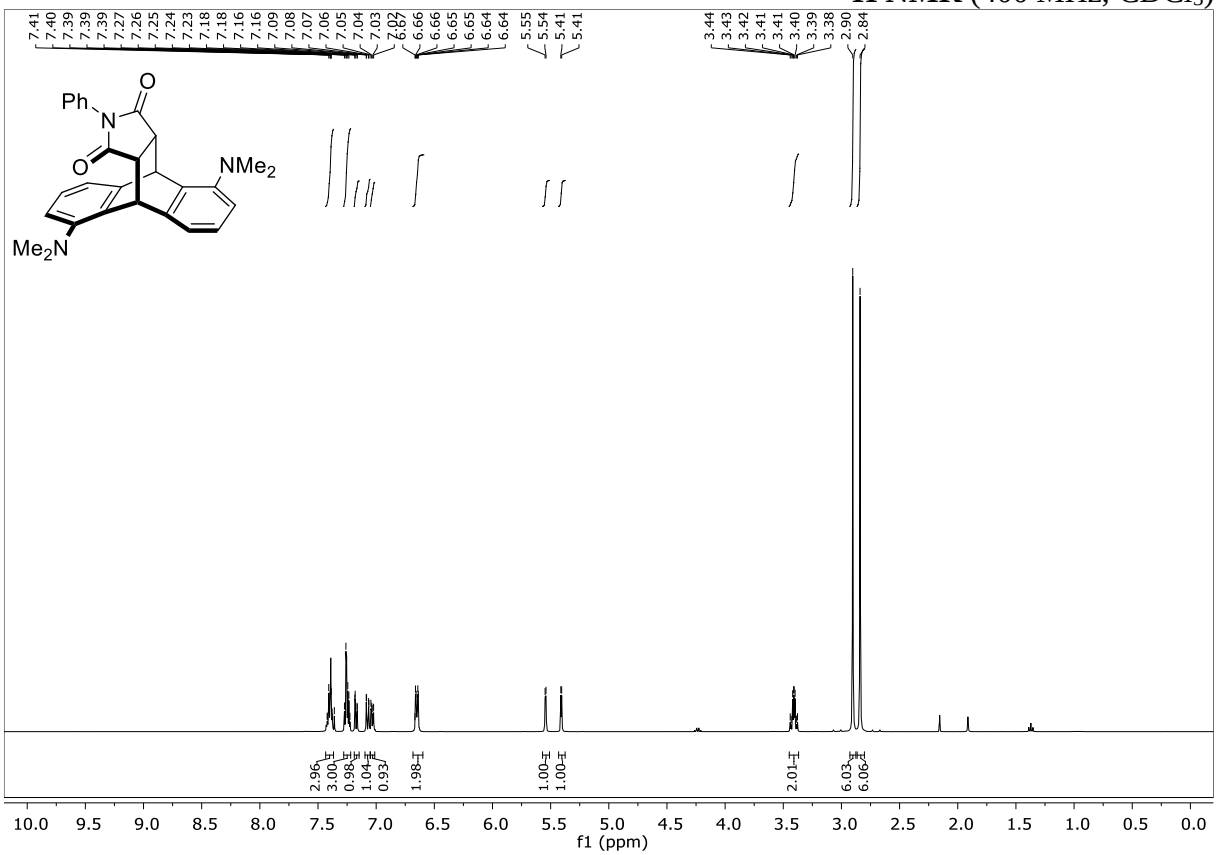

^{13}C NMR (101 MHz, $CDCl_3$)

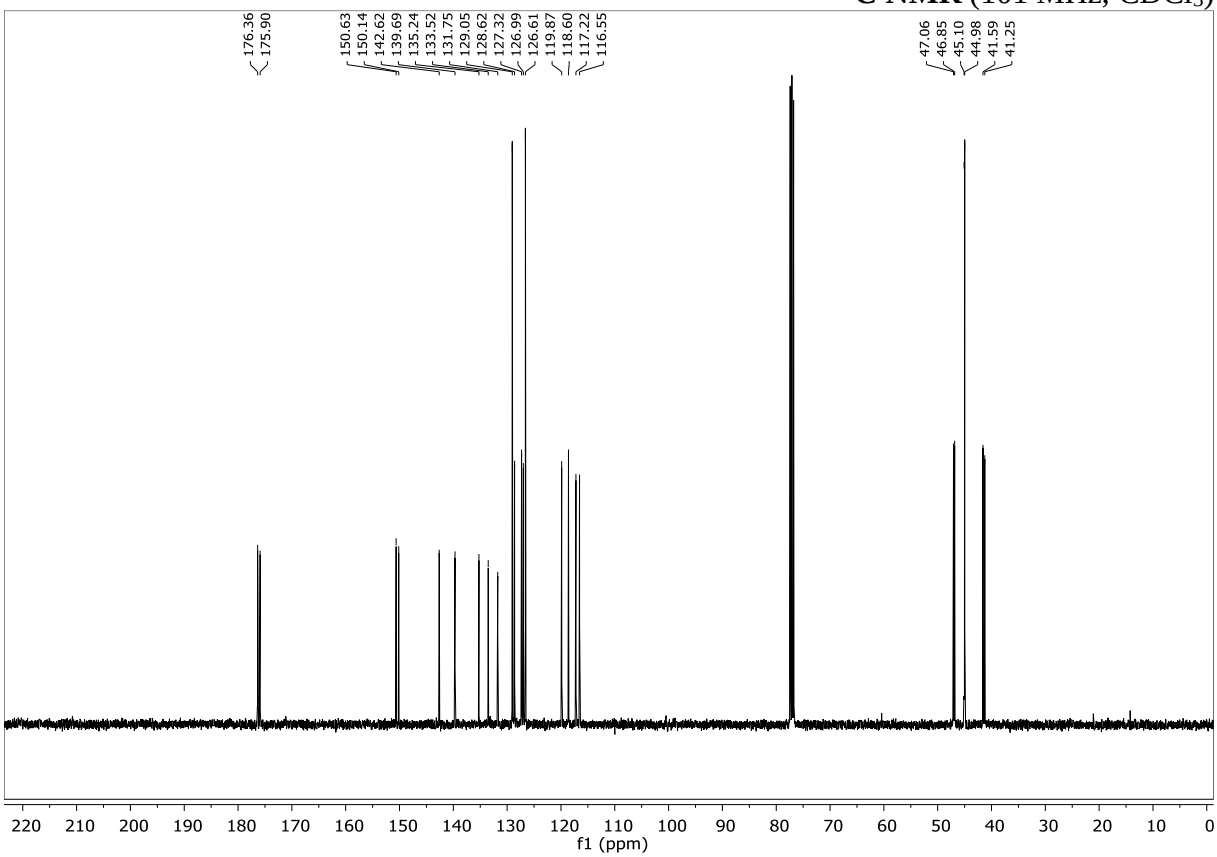

13-Phenyl-1,5-di(pyrrolidin-1-yl)-9,10-dihydro-9,10-[3,4]epipyrroloanthracene-12,14-dione (430dC)

^{1}H NMR (400 MHz, $CDCl_3$)

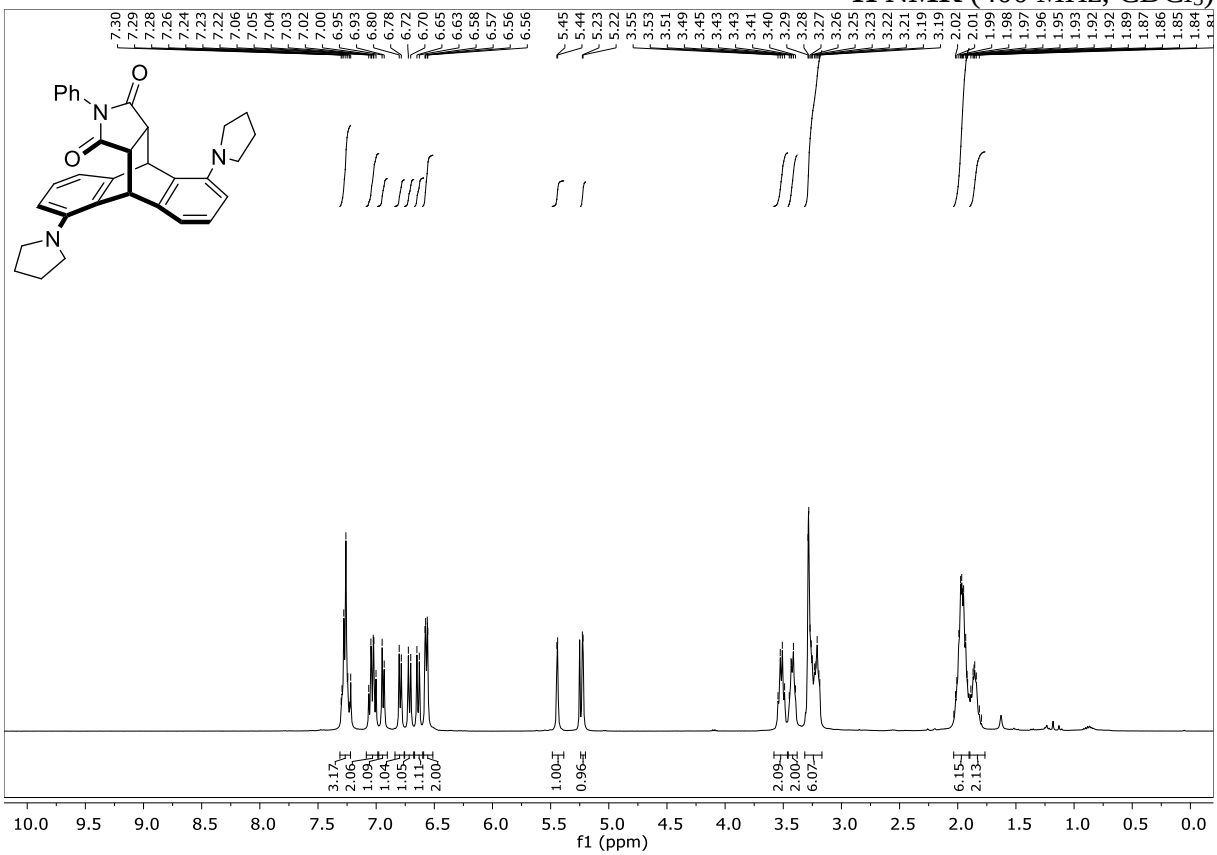

^{13}C NMR (101 MHz, $CDCl_3$)

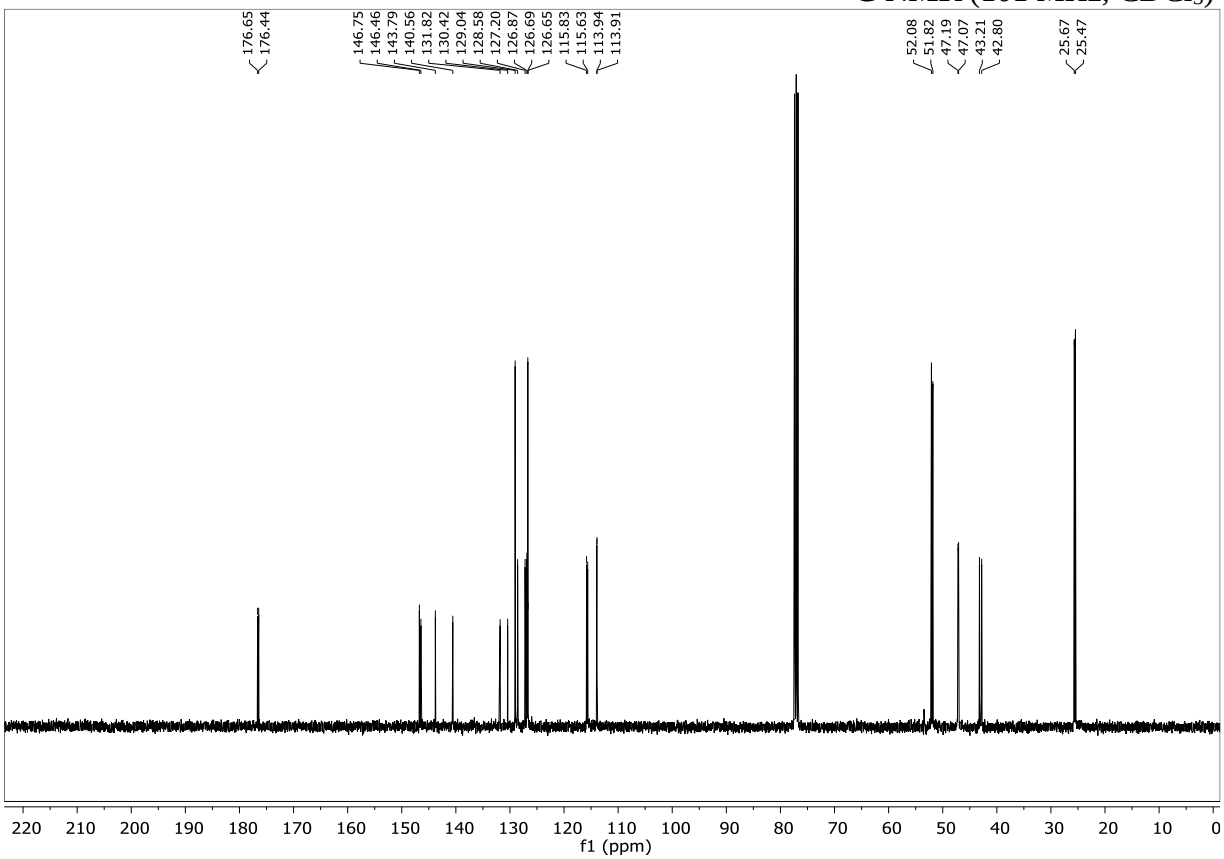

Methyl 1,5-di(pyrrolidin-1-yl)-9,10-dihydro-9,10-ethenoanthracene-11-carboxylate (430dE)

^{1}H NMR (400 MHz, $CDCl_3$)

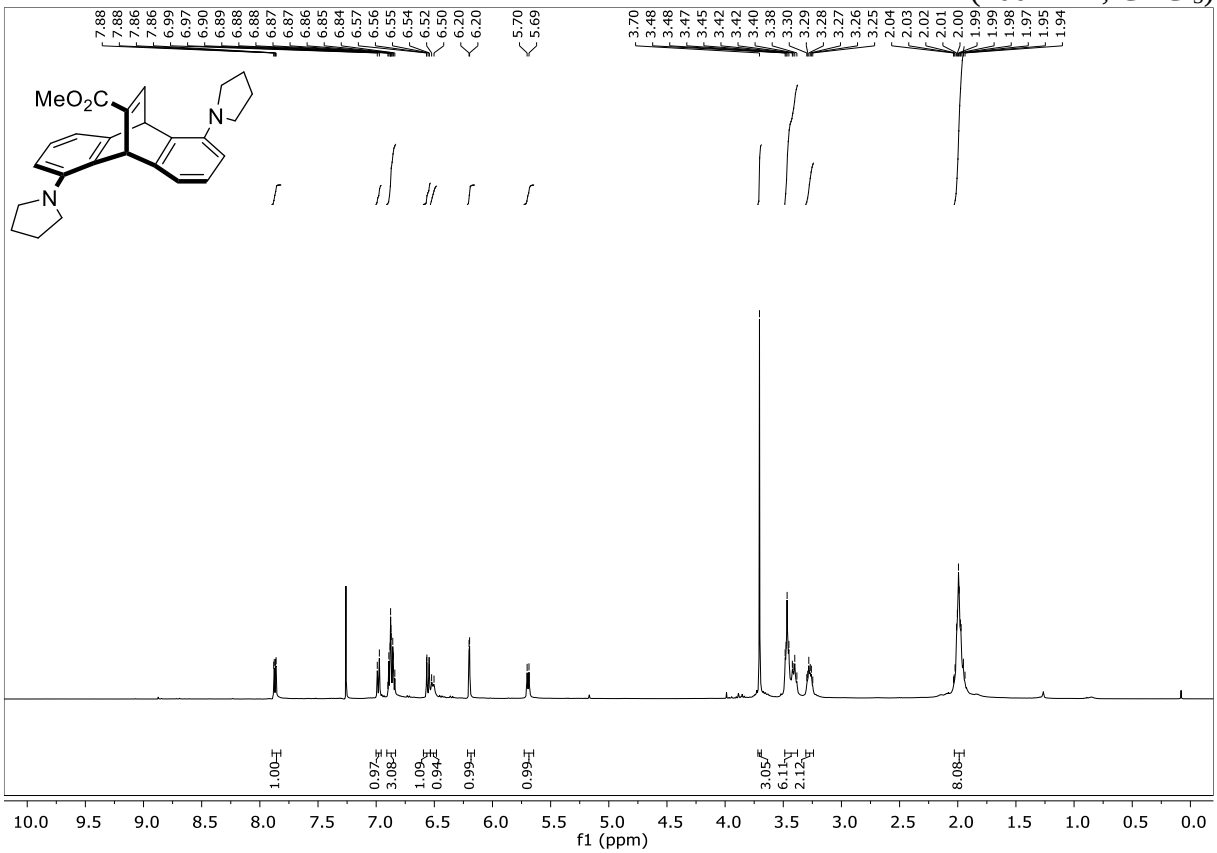

^{13}C NMR (101 MHz, $CDCl_3$)

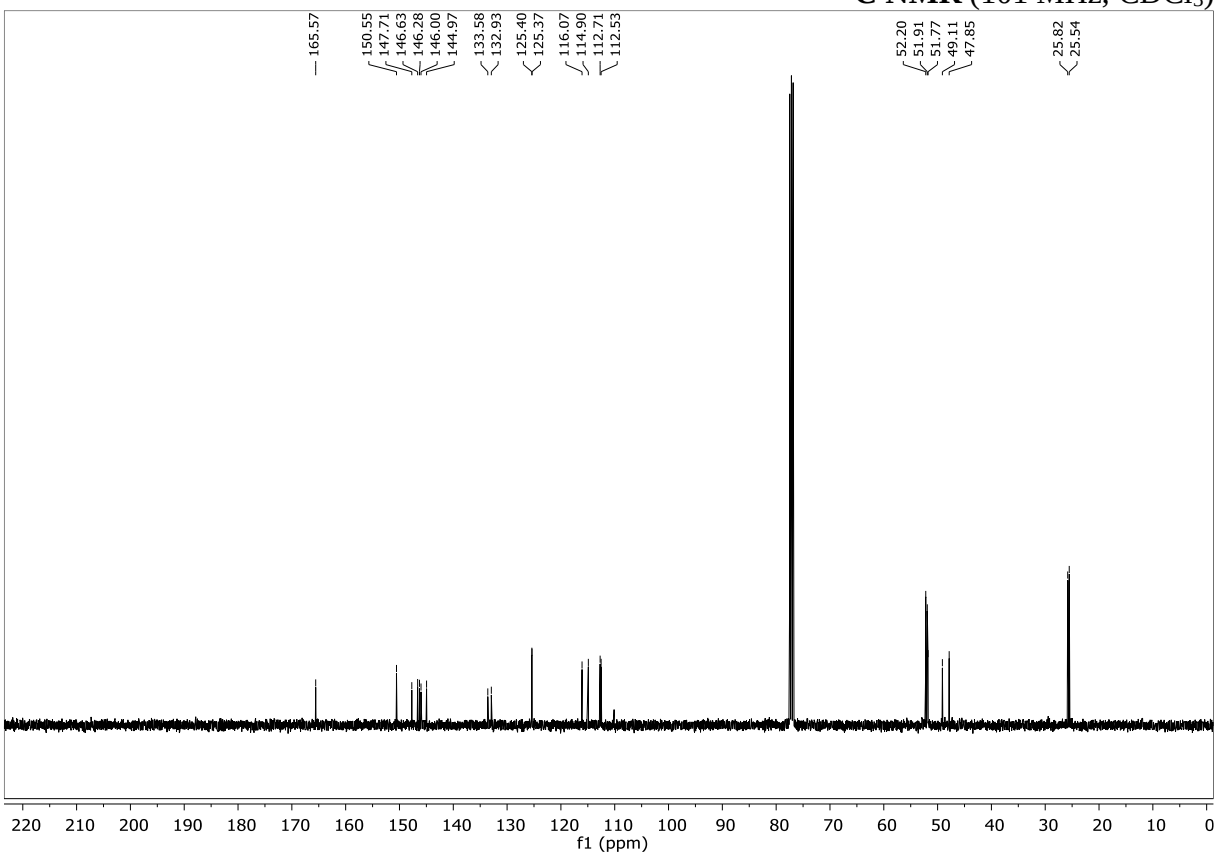

Methyl 1,5-di(pyrrolidin-1-yl)-1,4-dihydro-1,4-ethenoanthracene-2-carboxylate (431dE)

^{1}H NMR (400 MHz, $CDCl_3$)

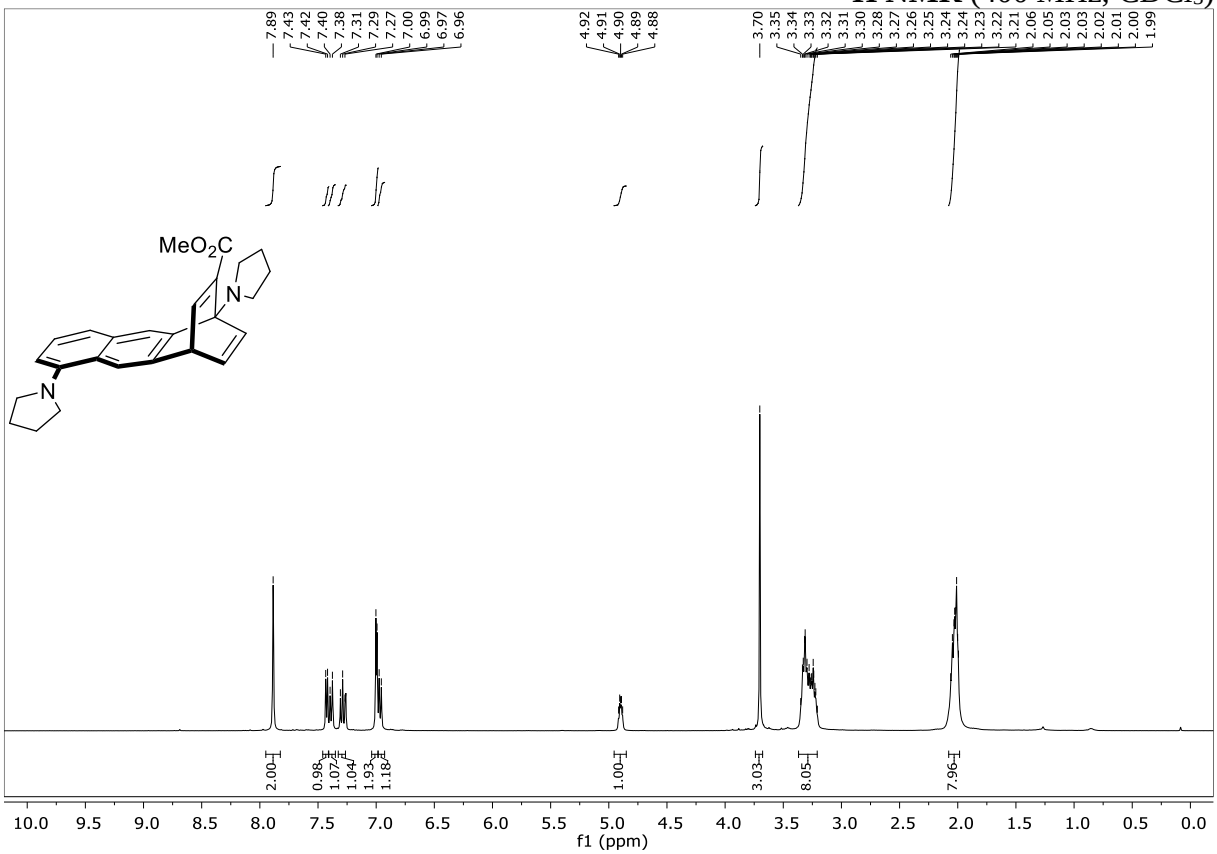

^{13}C NMR (101 MHz, $CDCl_3$)

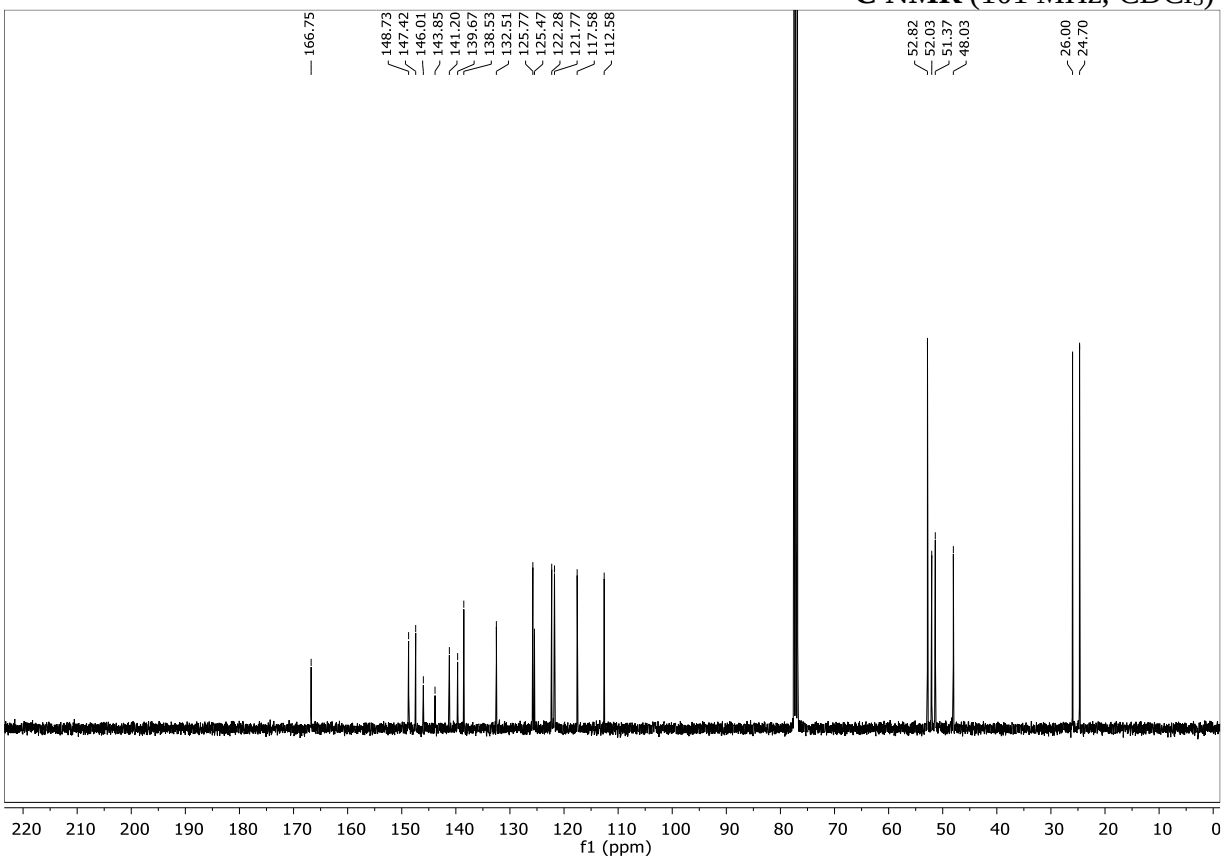

***Syn*-dimethyl 1-(pyrrolidin-1-yl)-9,10-dihydro-9,10-ethanoanthracene-11,12-dicarboxylate (*syn*-430eA)**

^{1}H NMR (400 MHz, $CDCl_3$)

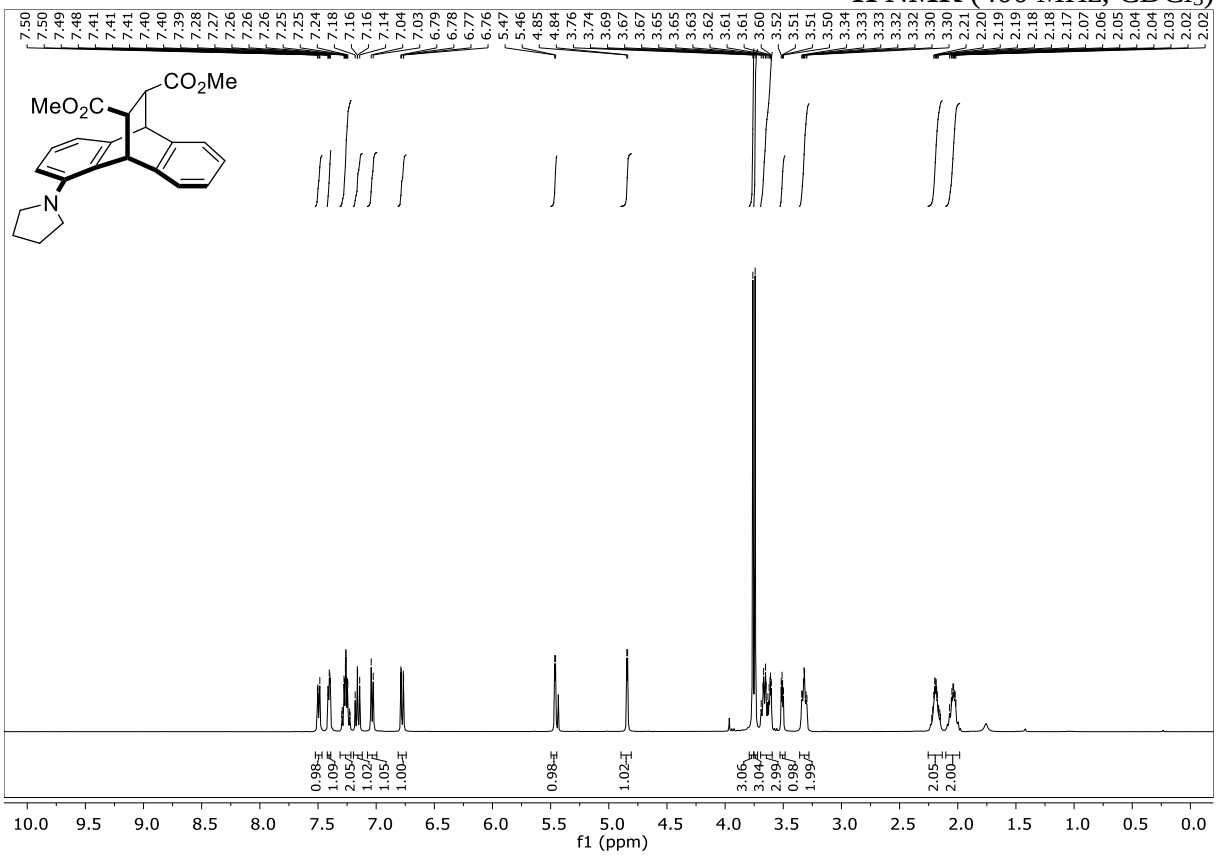

^{13}C NMR (101 MHz, $CDCl_3$)

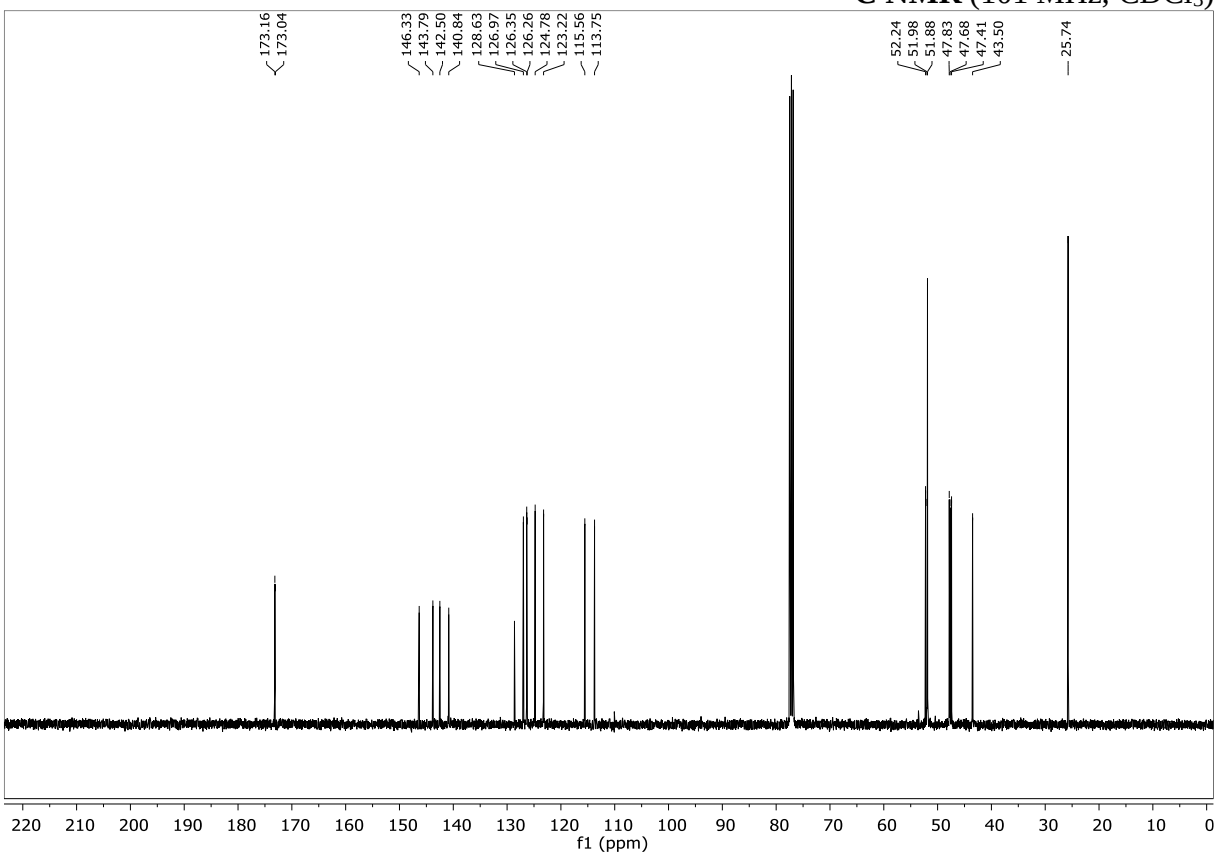

***Anti*-dimethyl 1-(pyrrolidin-1-yl)-9,10-dihydro-9,10-ethanoanthracene-11,12-dicarboxylate (*anti*-430eA)**

^{1}H NMR (400 MHz, $CDCl_3$)

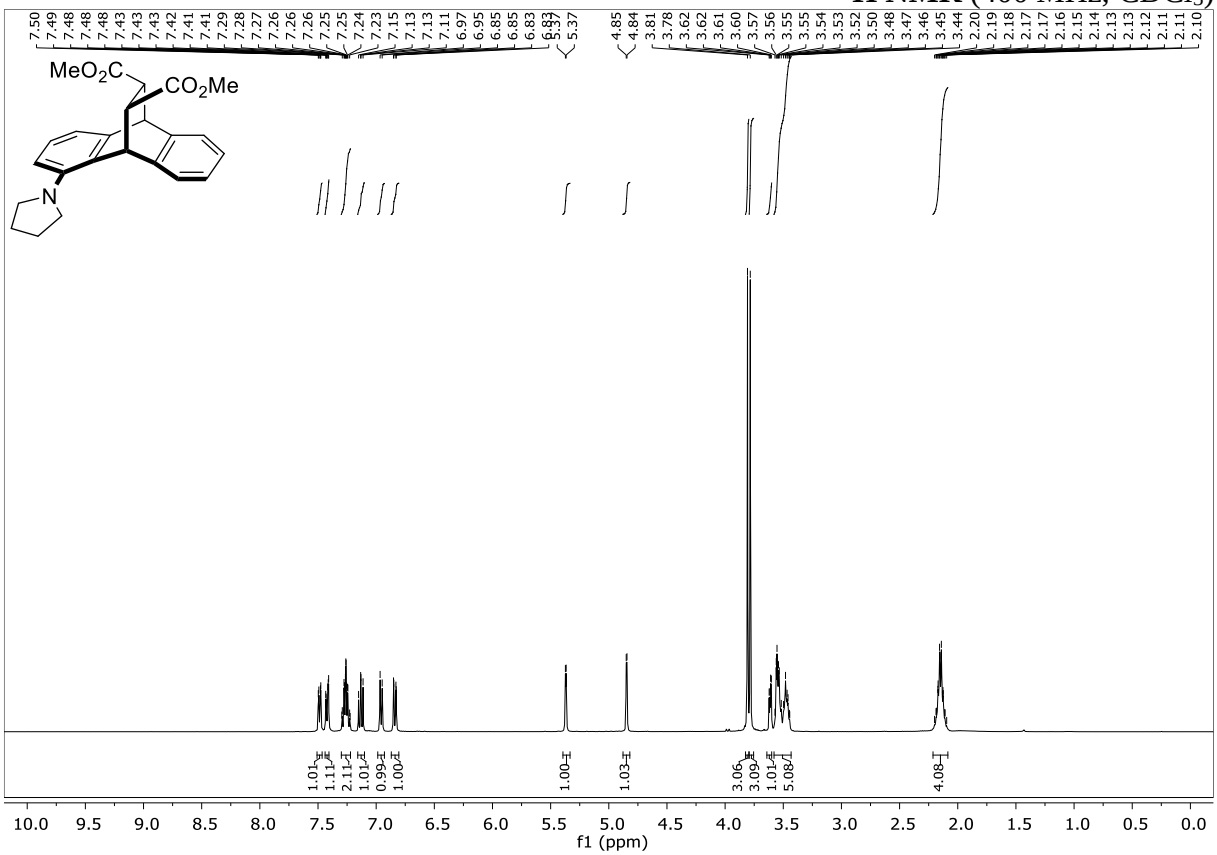

^{13}C NMR (101 MHz, $CDCl_3$)

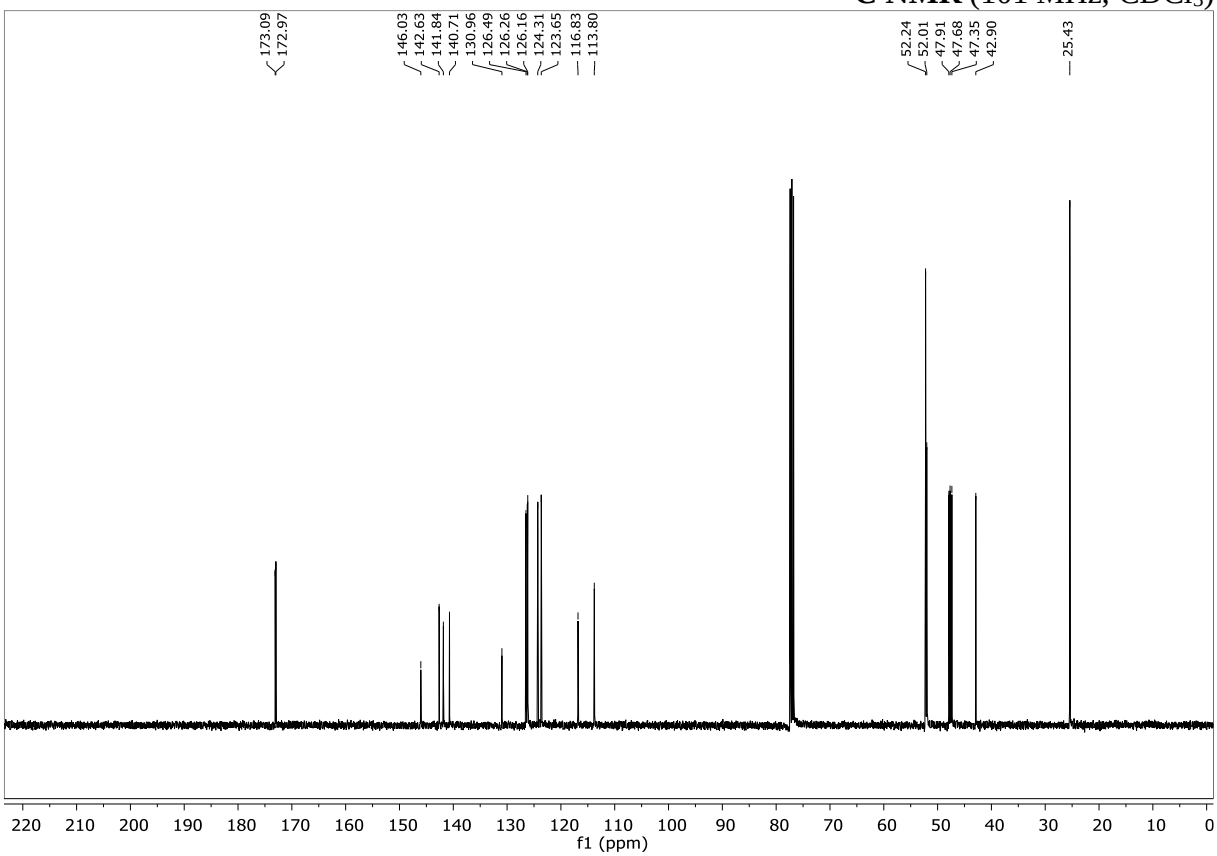

***Endo*-1-(pyrrolidin-1-yl)-9,10-dihydro-9,10-[3,4]furanoanthracene-12,14-dione (*endo*-430eB)**

^{1}H NMR (400 MHz, $CDCl_3$)

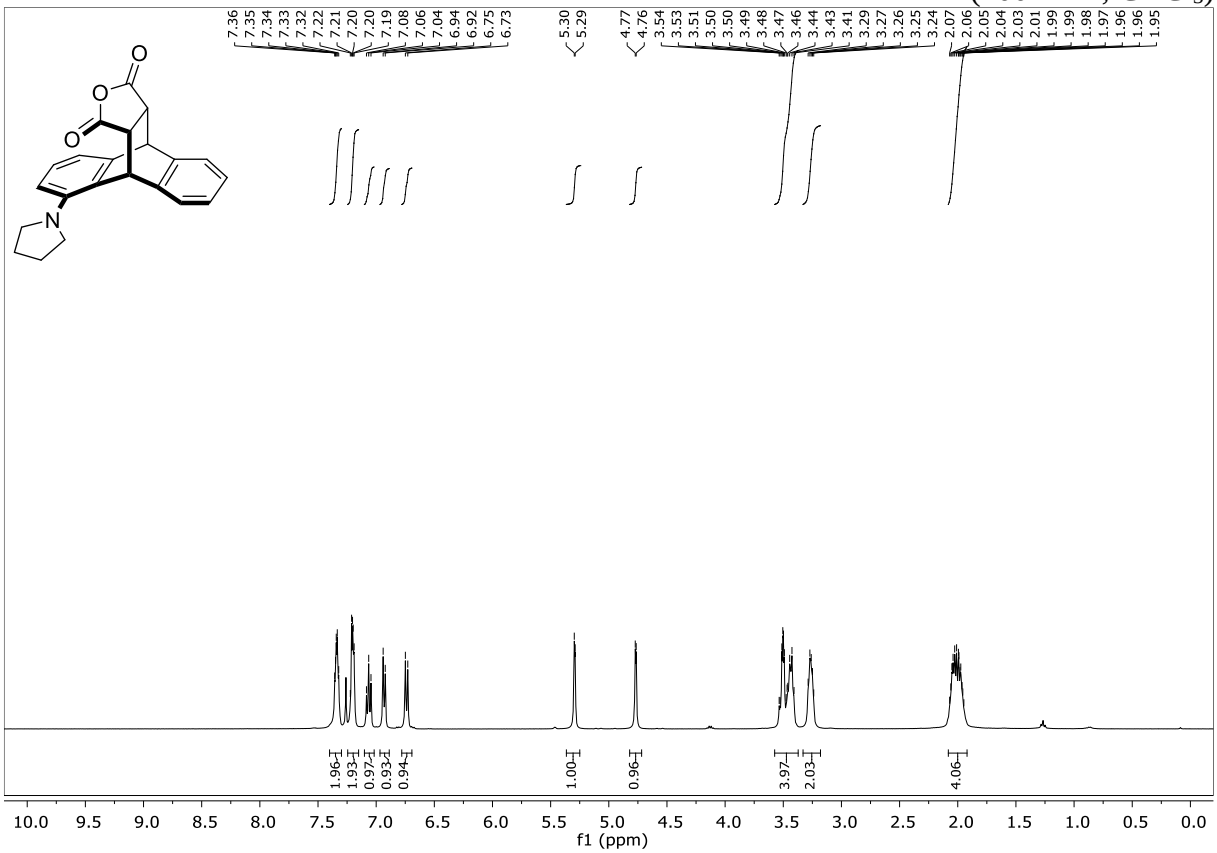

^{13}C NMR (101 MHz, $CDCl_3$)

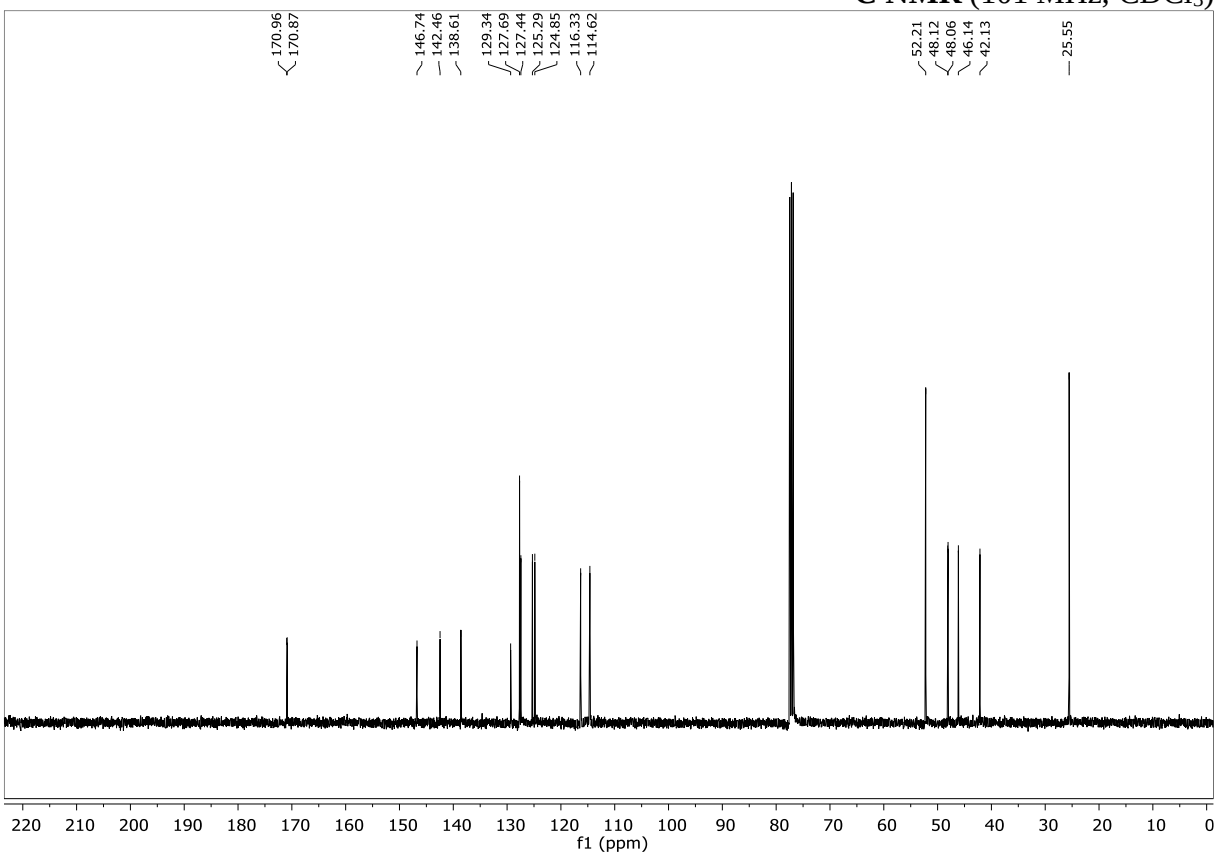

***Exo*/*endo*-13-phenyl-4-(pyrrolidin-1-yl)-9,10-dihydro-9,10-[3,4]epipyrroloanthracene-12,14-dione (*exo*/*endo*-430eC)**

^{1}H NMR (400 MHz, $CDCl_3$)

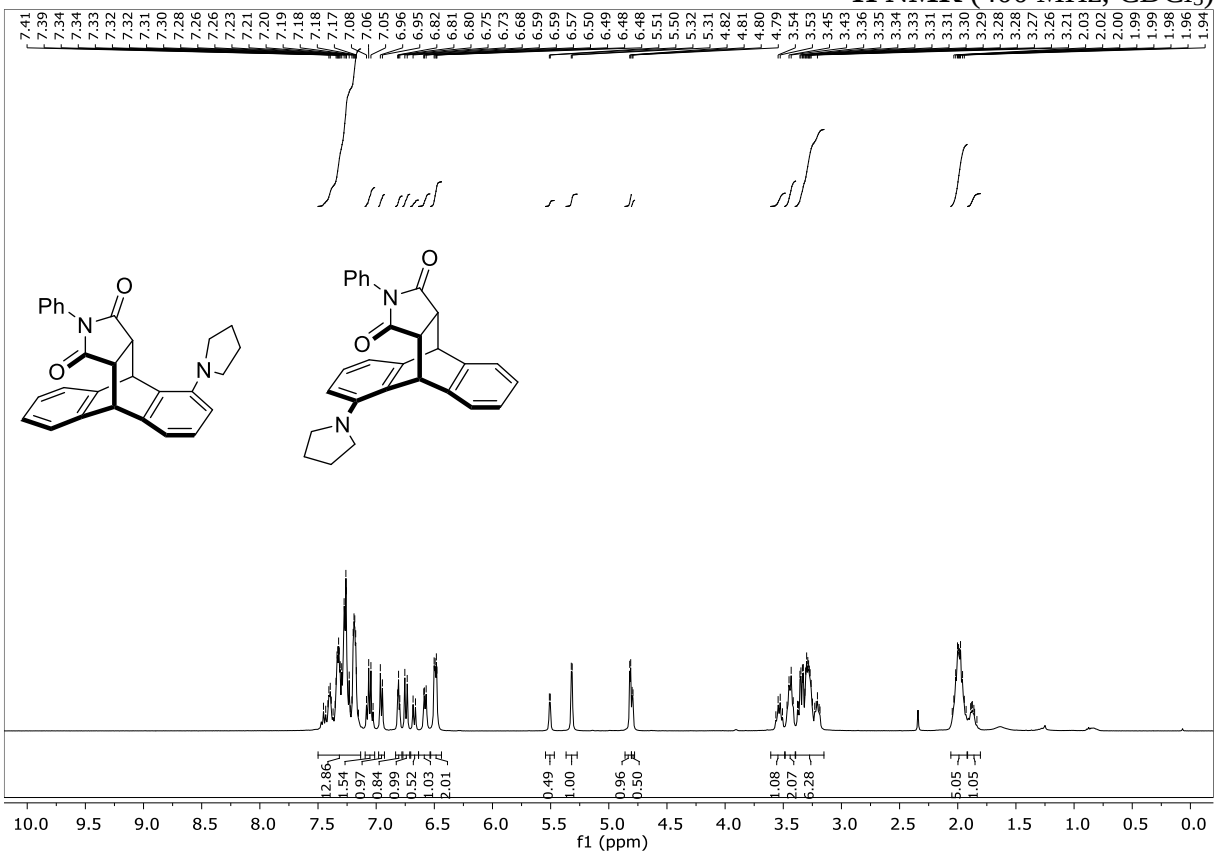

^{13}C NMR (101 MHz, $CDCl_3$)

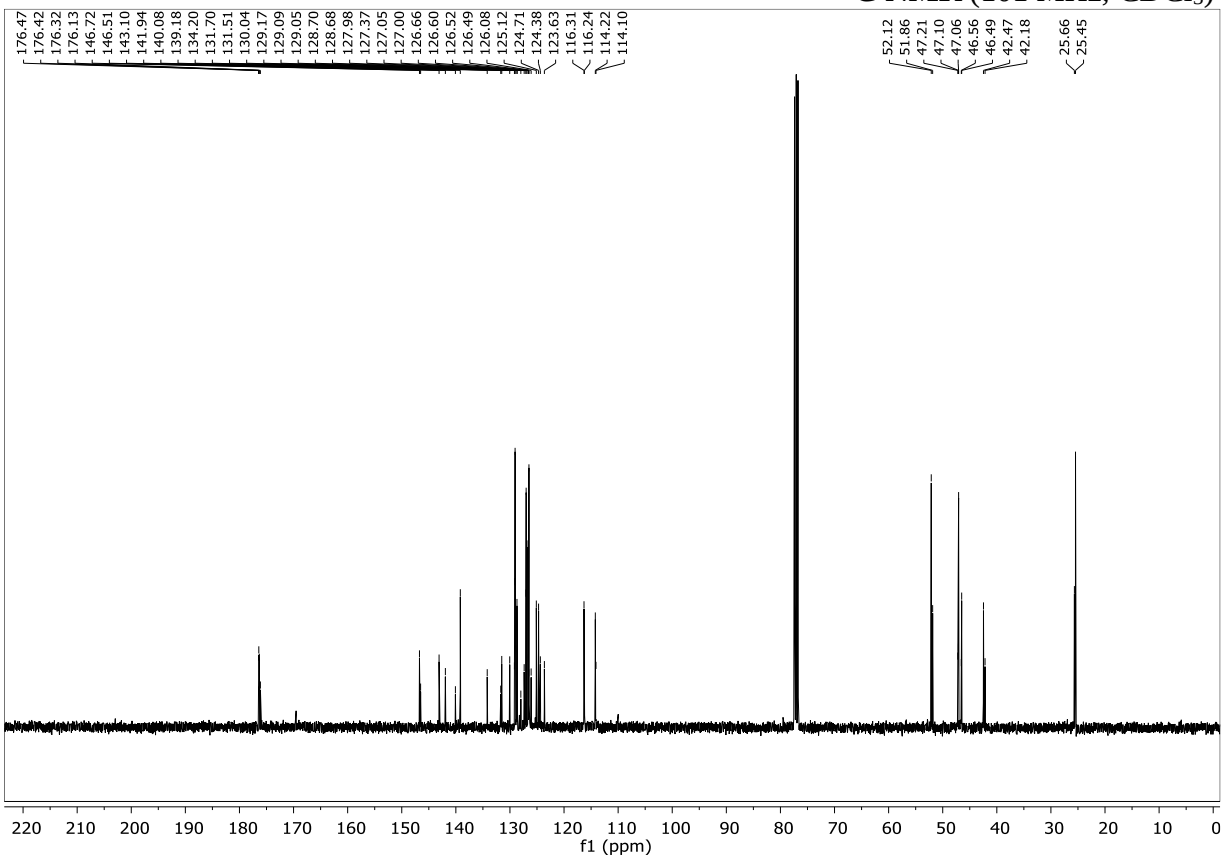

Dimethyl 1-(pyrrolidin-1-yl)-1,4-dihydro-1,4-ethenoanthracene-2,3-dicarboxylate (431eD)

^{1}H NMR (400 MHz, $CDCl_3$)

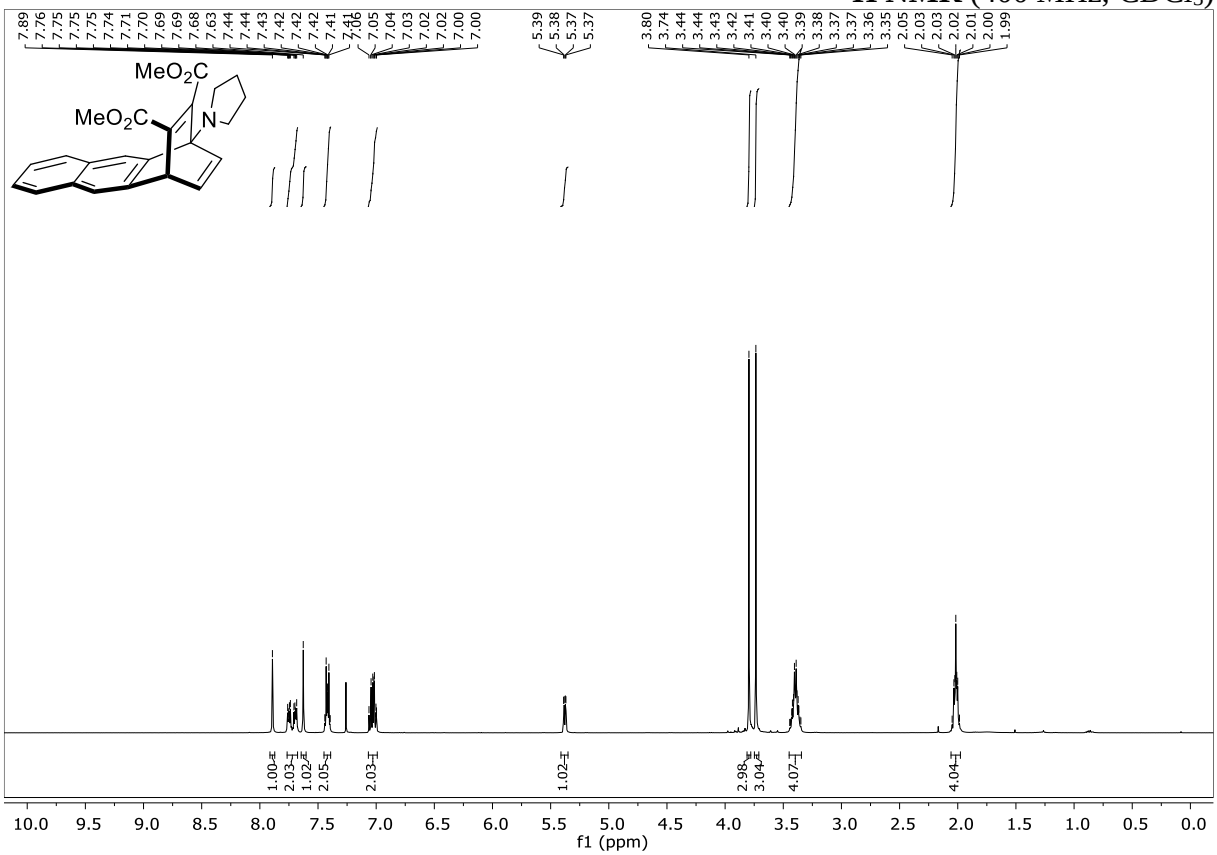

^{13}C NMR (101 MHz, $CDCl_3$)

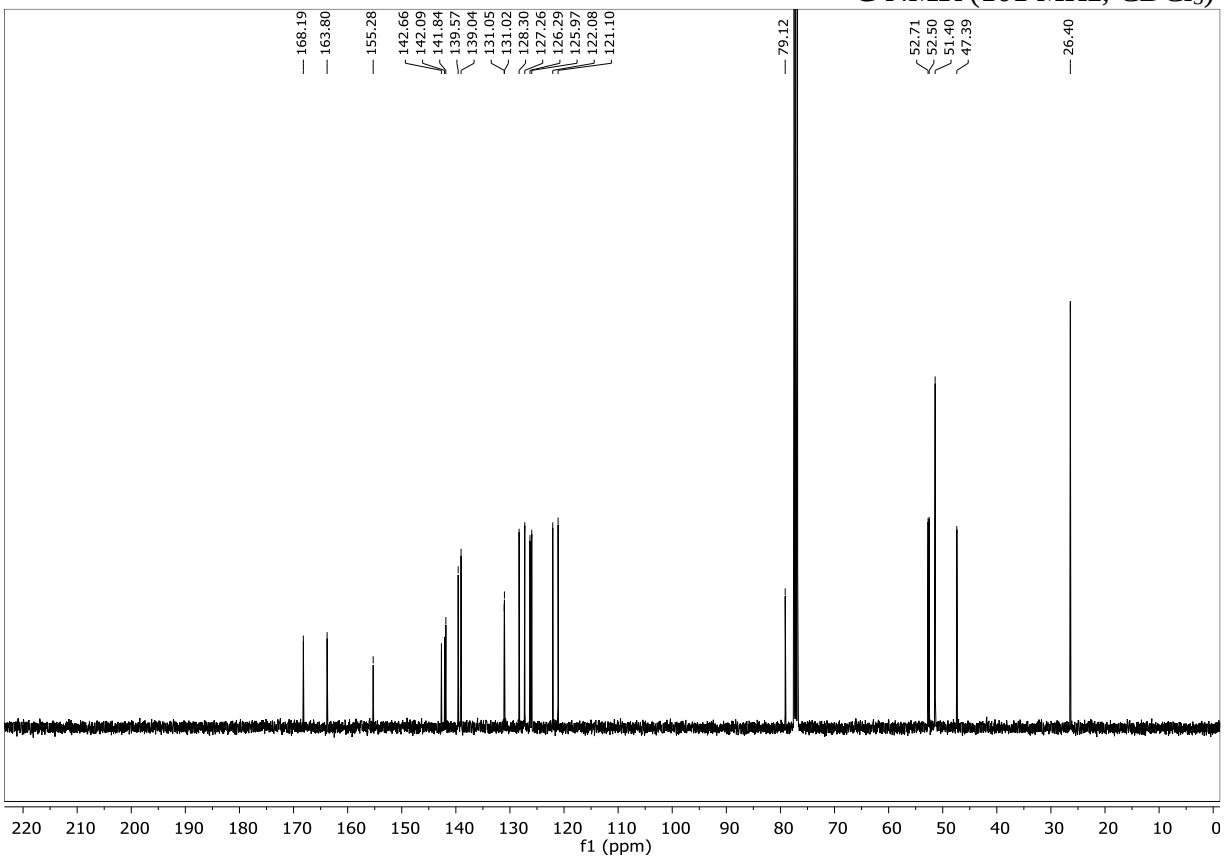

Methyl 4-(pyrrolidin-1-yl)-9,10-dihydro-9,10-ethenoanthracene-11-carboxylate (*syn*-430eE)/(*anti*-430eE)

^{1}H NMR (400 MHz, $CDCl_3$)

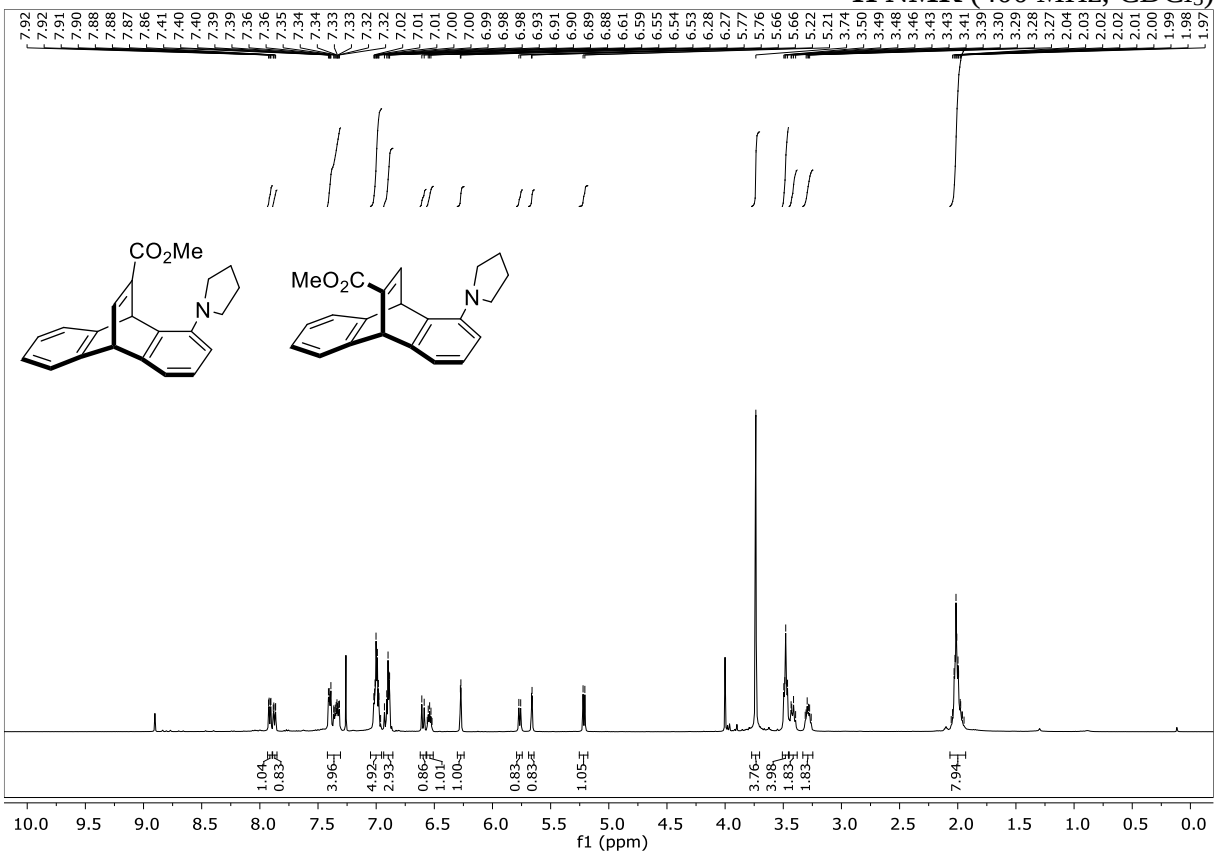

^{13}C NMR (101 MHz, $CDCl_3$)

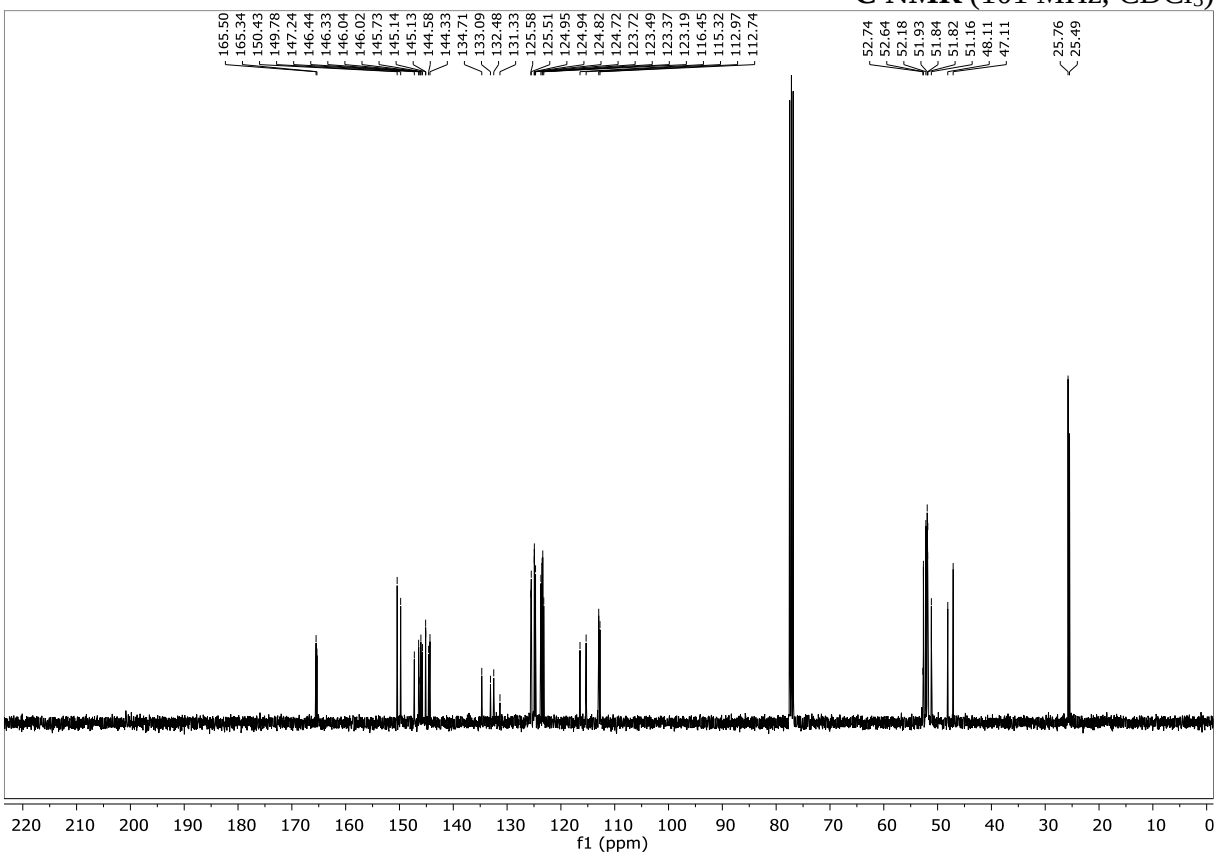

Methyl 1-(pyrrolidin-1-yl)-1,4-dihydro-1,4-ethenoanthracene-2-carboxylate (431eE)

^{1}H NMR (400 MHz, $CDCl_3$)

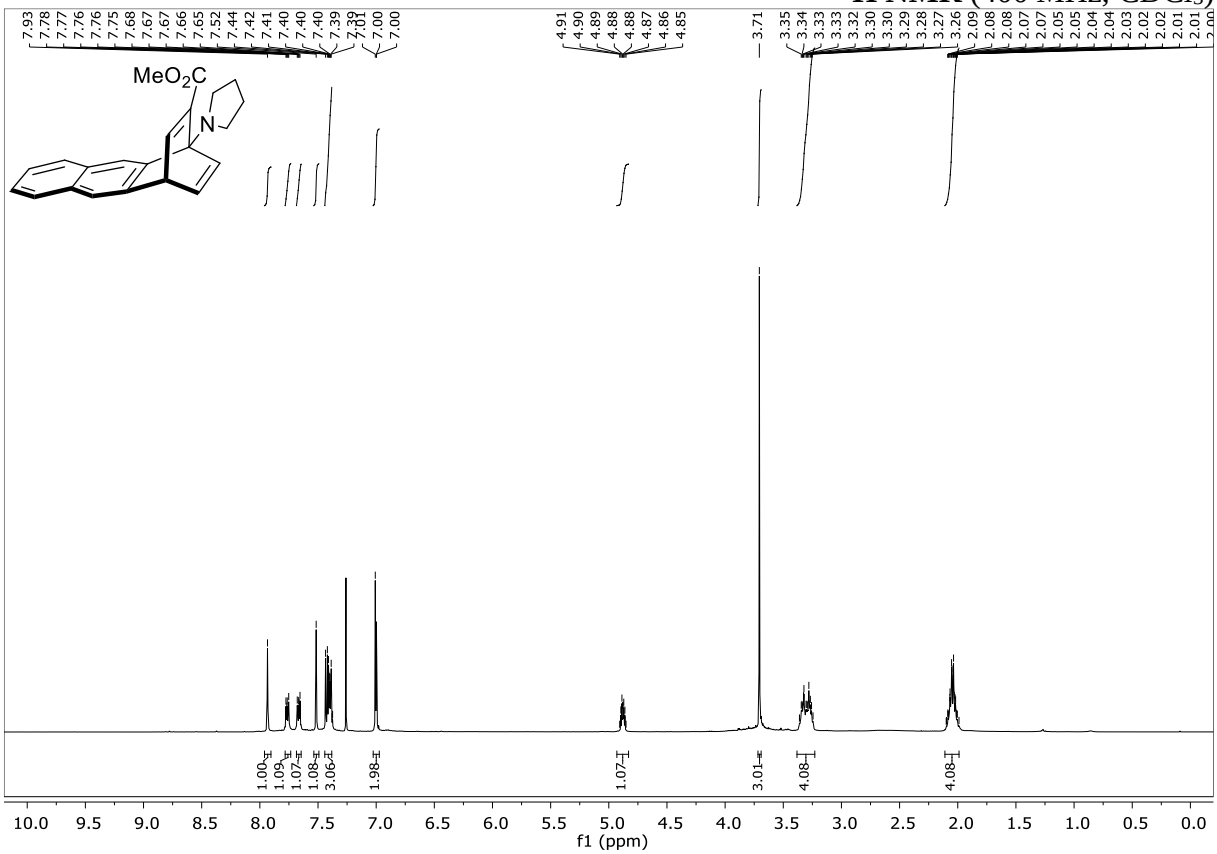

^{13}C NMR (101 MHz, $CDCl_3$)

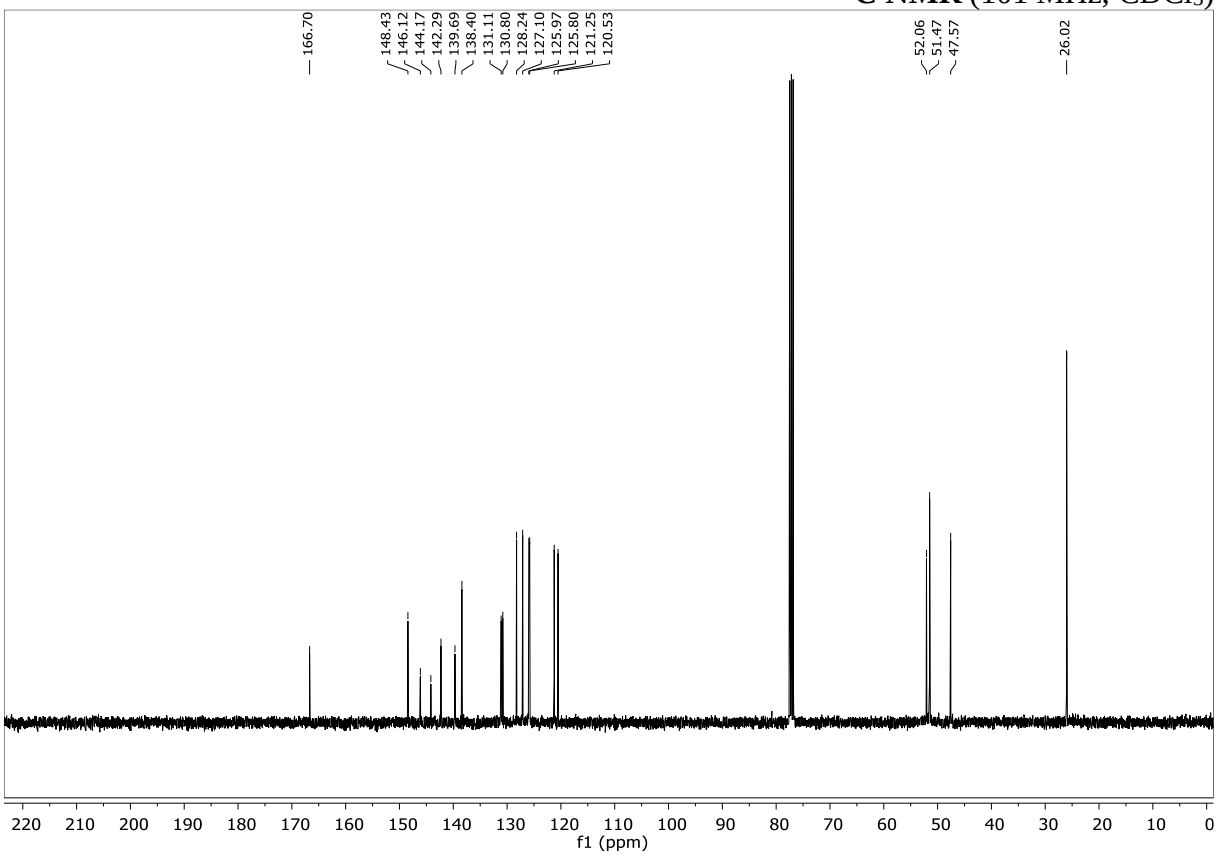

1-Phenyl-3-(4-(pyrrolidin-1-yl)anthracen-1-yl)pyrrolidine-2,5-dione (434)

^{1}H NMR (400 MHz, $CDCl_3$)

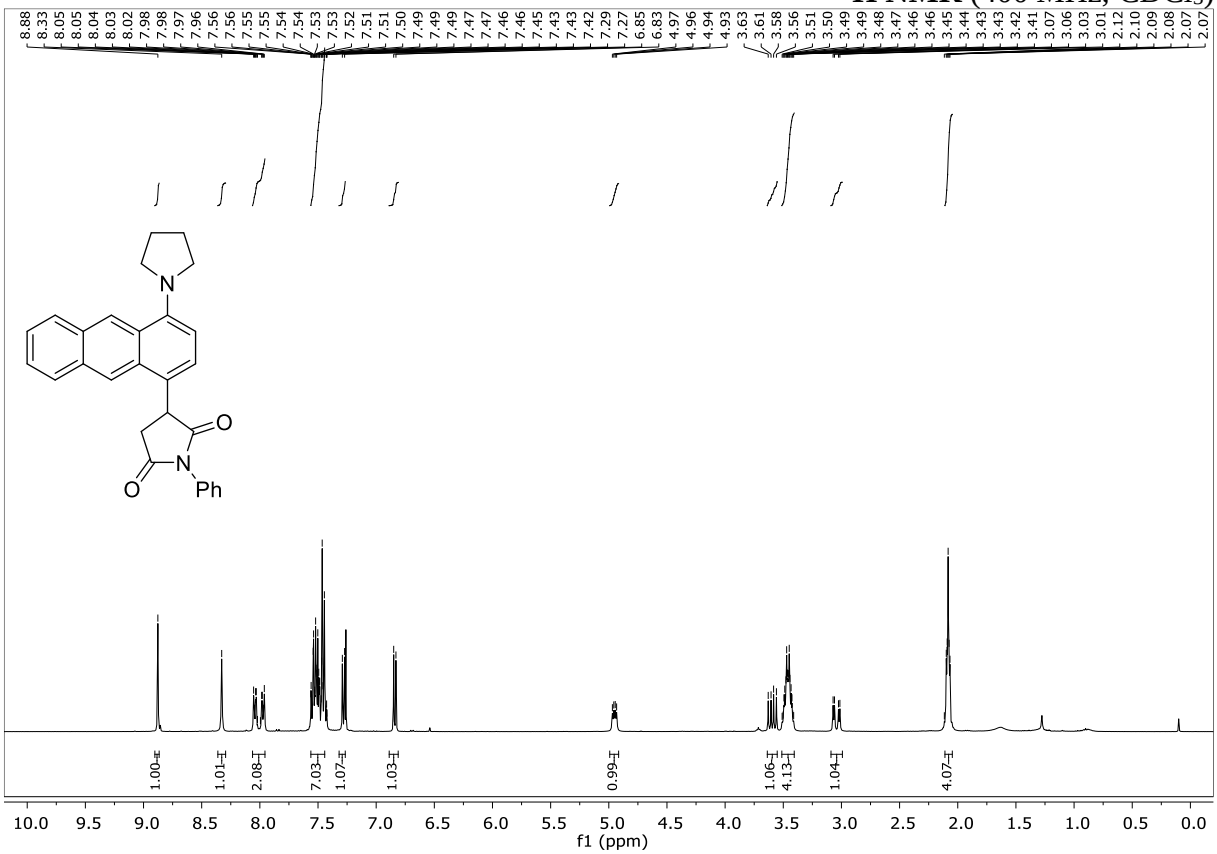

^{13}C NMR (101 MHz, $CDCl_3$)

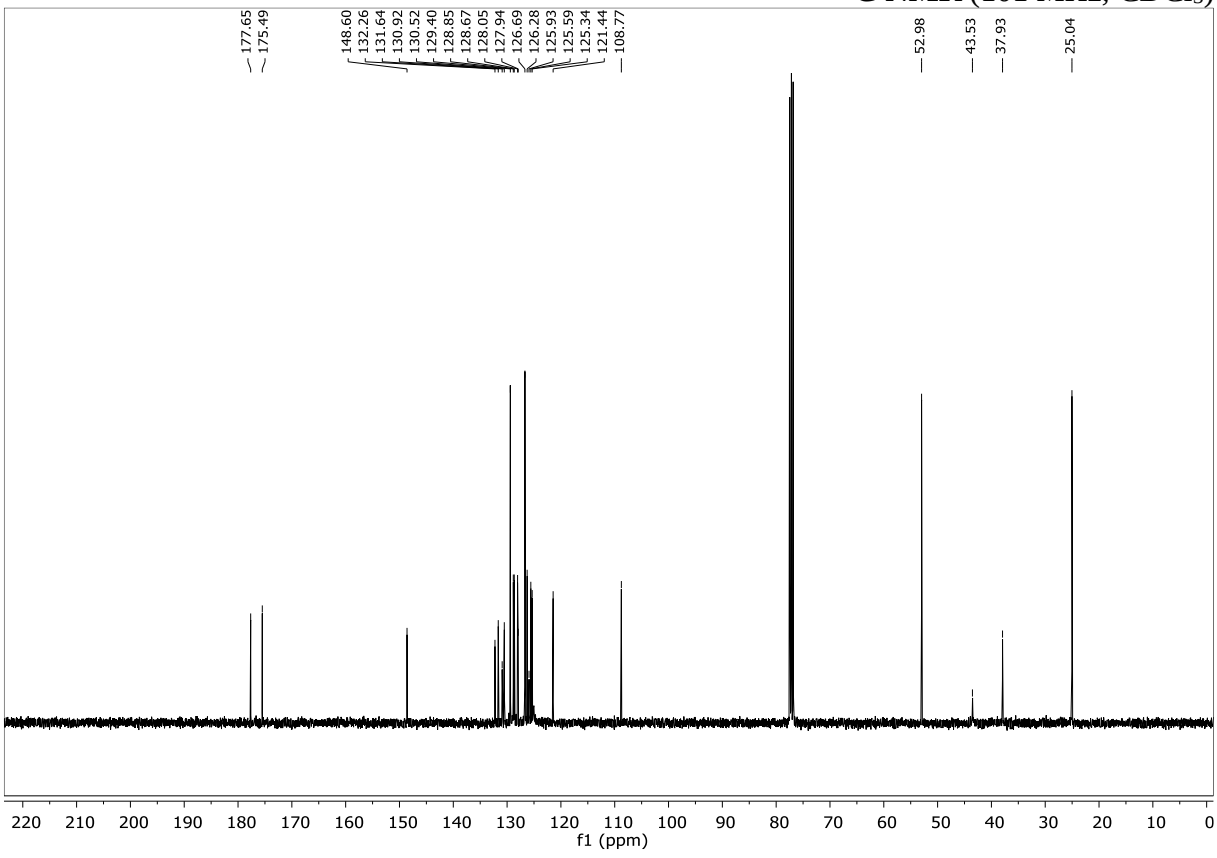

1-(2,4-Dibromoanthracen-1-yl)pyrrolidine (436)

^{1}H NMR (400 MHz, $CDCl_3$)

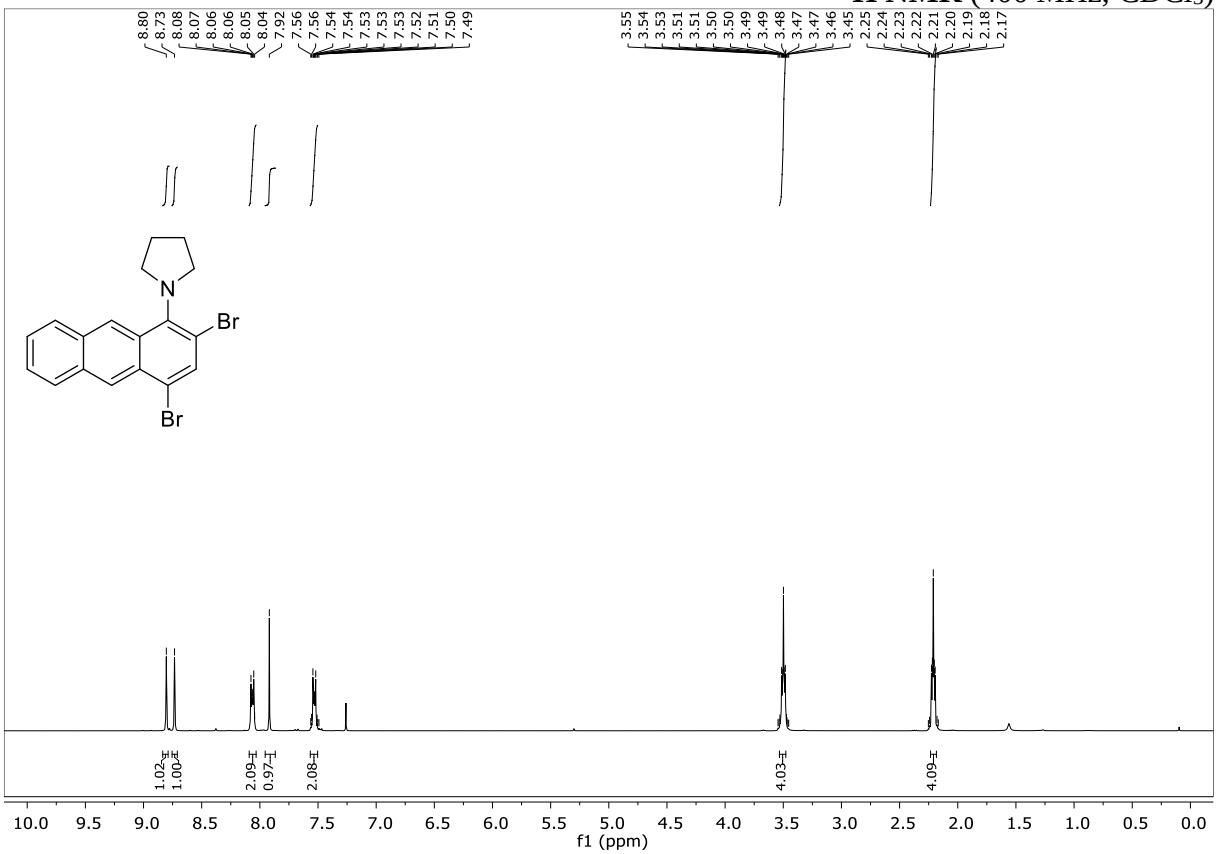

^{13}C NMR (101 MHz, $CDCl_3$)

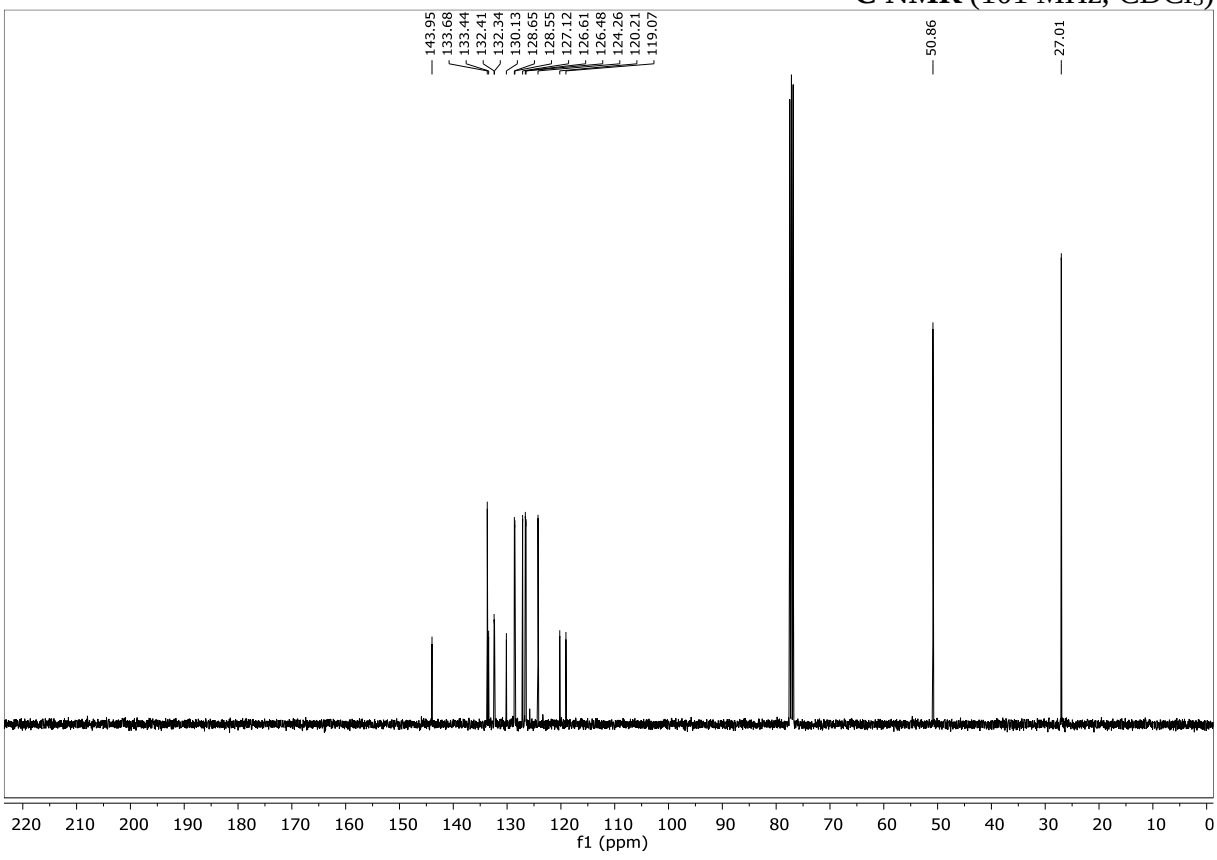

4-Methyl-1-(4-(pyrrolidin-1-yl)anthracen-1-yl)-1,2,4-triazolidine-3,5-dione (438)

^{1}H NMR (400 MHz, CD_2Cl_2)

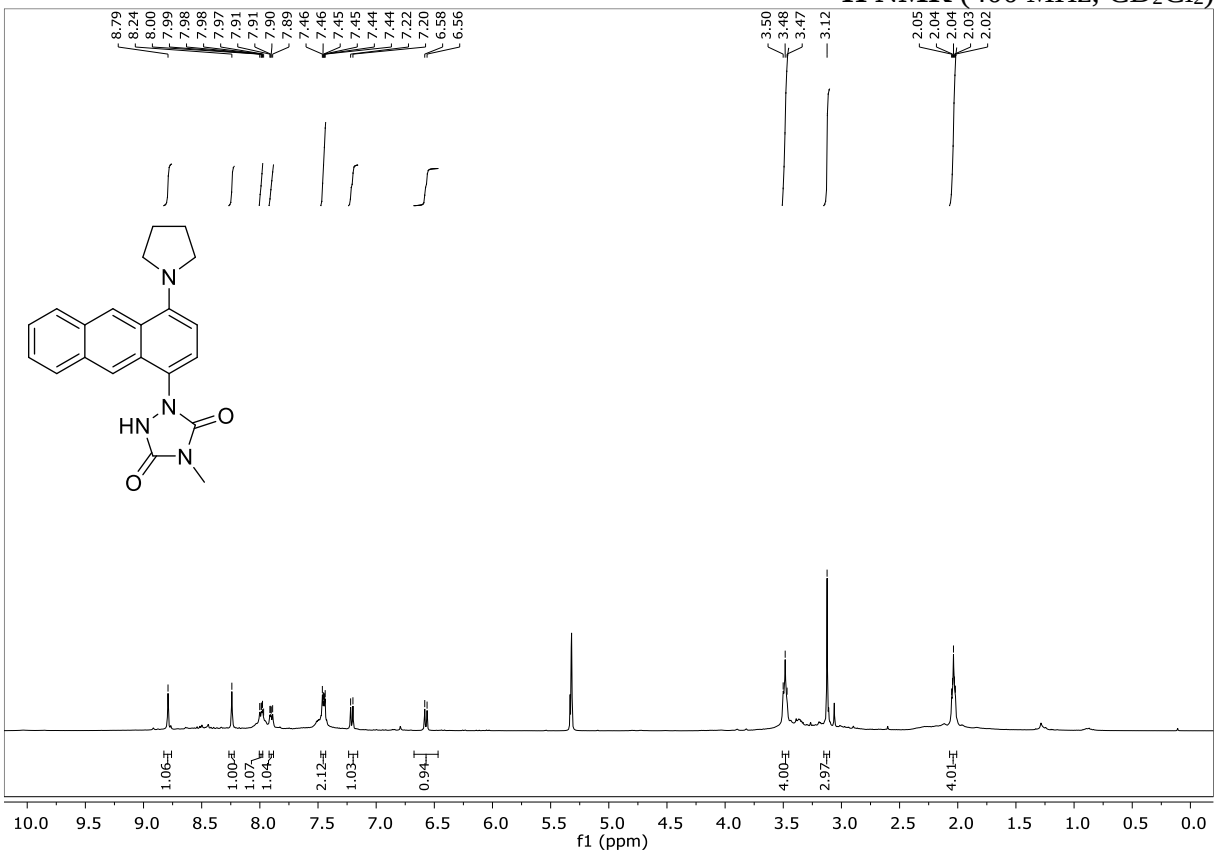

^{13}C NMR (101 MHz, CD_2Cl_2)

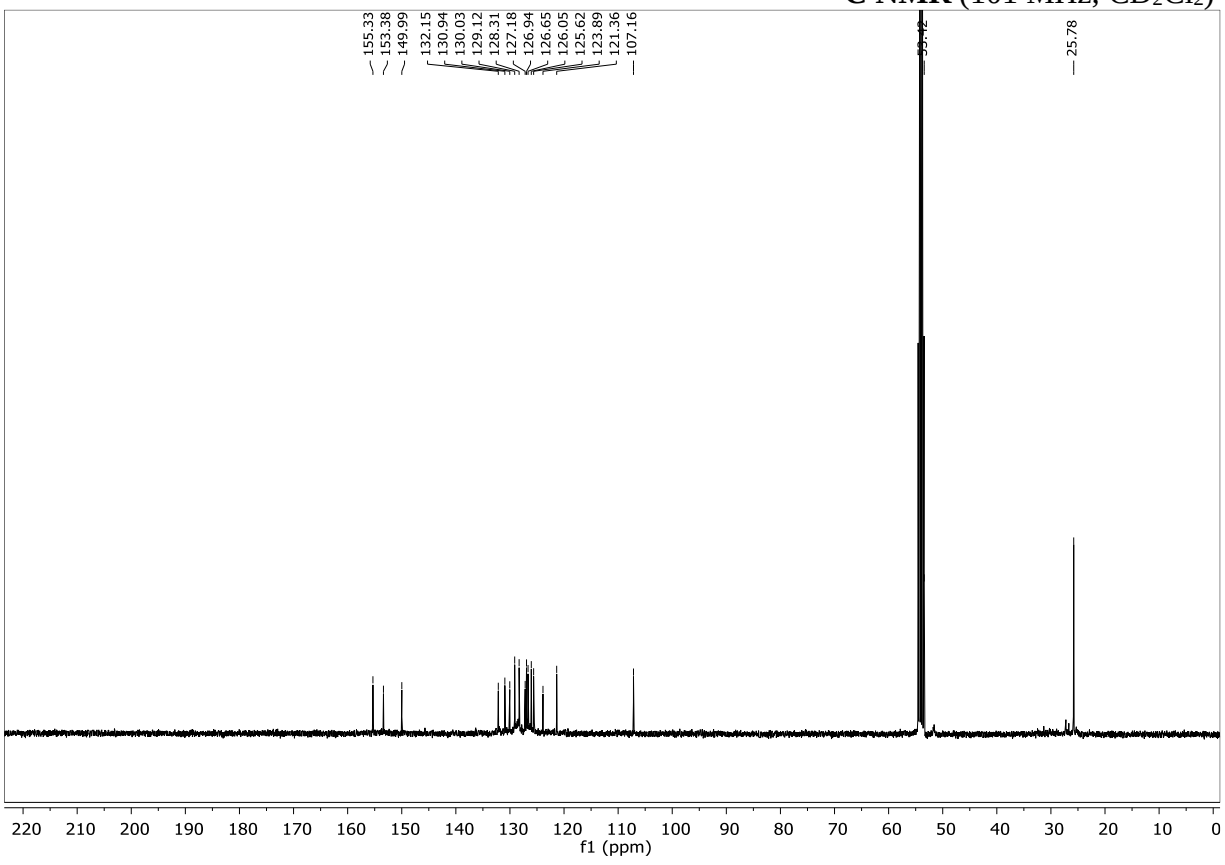

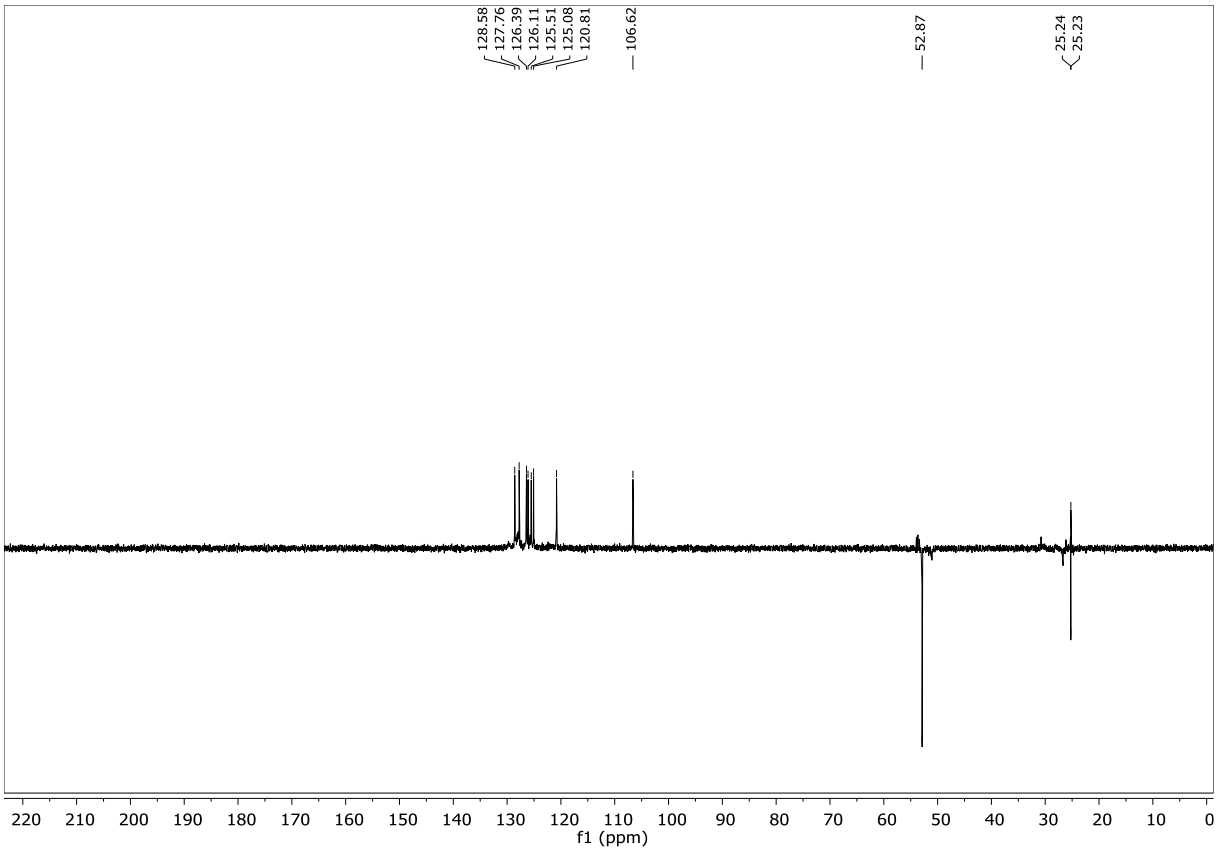
128.58
127.76
126.39
126.11
125.51
125.08
120.81
106.62
52.87
25.24
25.23
220 210 200 190 180 170 160 150 140 130 120 110 100 90 80 70 60 50 40 30 20 10 0
f1 (ppm)

2 GC-spectra

2*H*-Pyran-2-one (1)

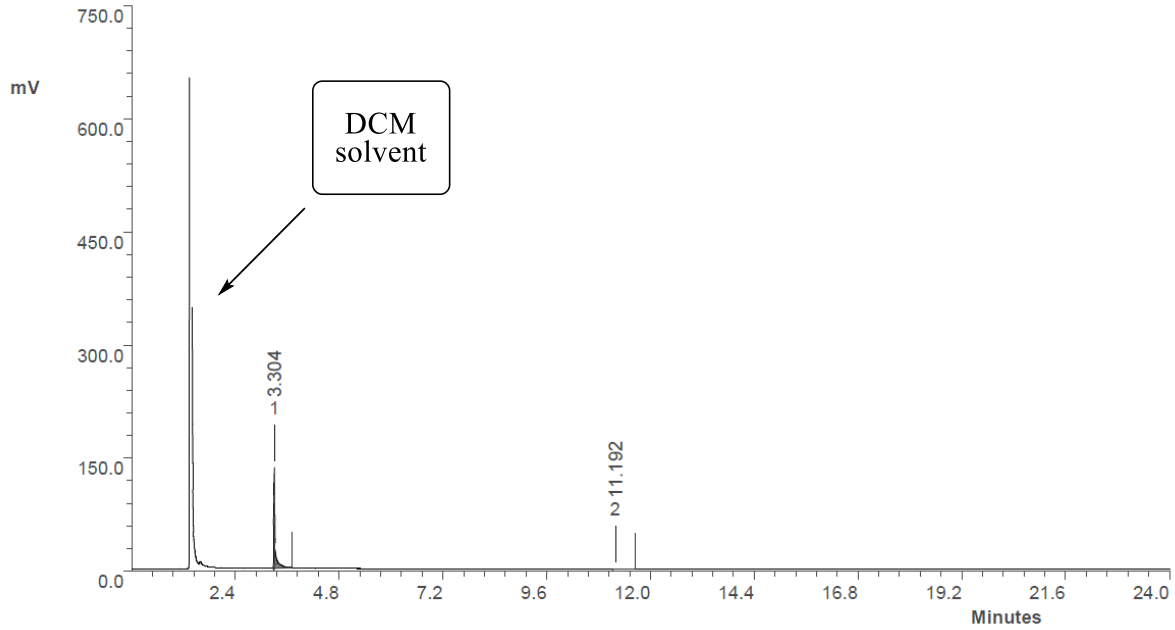

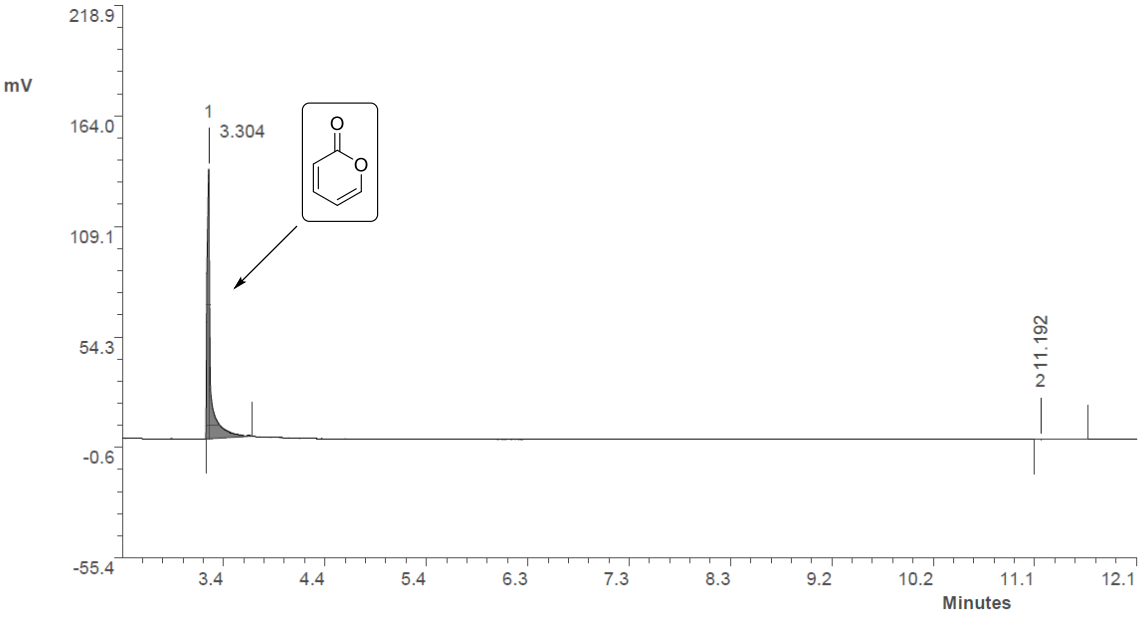

Peak	RT	Area	%Ar	Height
1	3.304	311.528	99.63	133.688
2	11.192	1.157	0.37	0.118

GC-Analysis: purity >99%, RT = 3.304

3 Chiral HPLC data

Ethyl-1-methyl-3-oxo-1,3-dihydroisobenzofuran-4-carboxylate (342a)

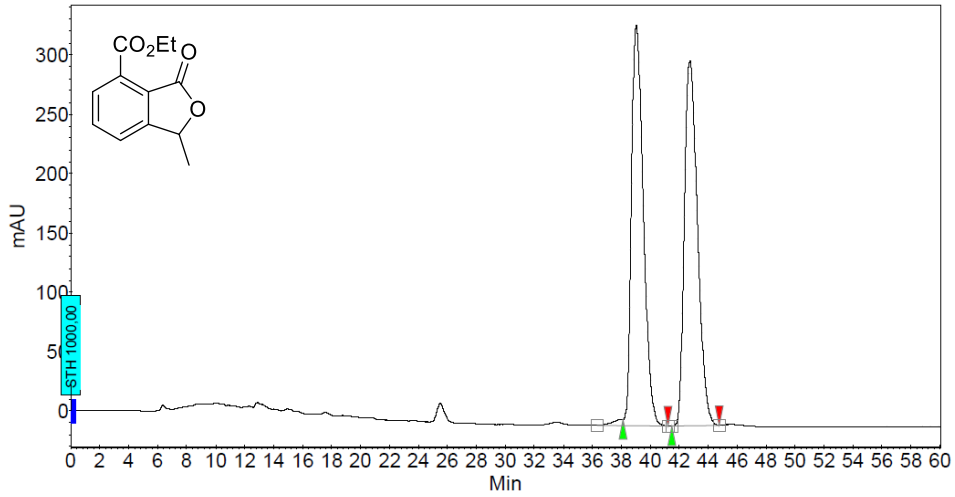

Peak Results :

Index	Name	Time [Min]	Quantity [% Area]	Height [mAU]	Area [mAU.Min]	Area % [%]
2	UNKNOWN	39.04	49.82	337.8	321.2	49.819
1	UNKNOWN	42.73	50.18	308.0	323.6	50.181
Total			100.00	645.7	644.8	100.000

Ethyl (*S*)-1-methyl-3-oxo-1,3-dihydroisobenzofuran-4-carboxylate ((*S*)-342a)

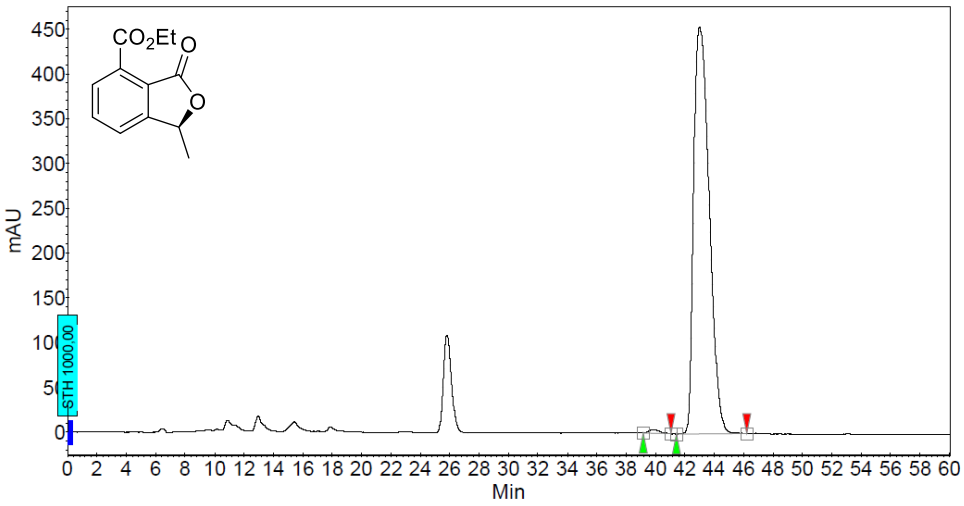

Peak Results :

Index	Name	Time [Min]	Quantity [% Area]	Height [mAU]	Area [mAU.Min]	Area % [%]
2	UNKNOWN	39.89	0.59	4.3	3.3	0.588
1	UNKNOWN	43.01	99.41	454.4	557.2	99.412
Total			100.00	458.7	560.5	100.000

(*R*)-3-Butylisobenzofuran-1(3*H*)-one ((*R*)-326b)

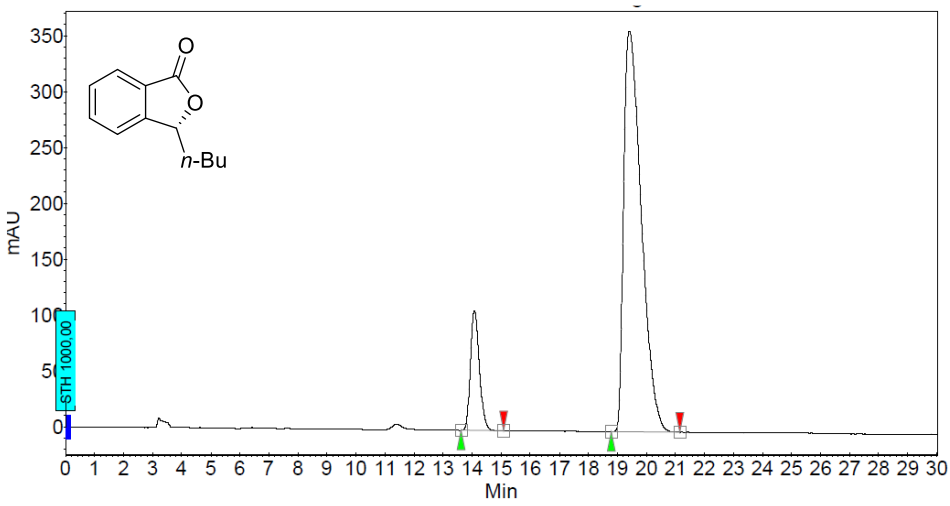

Peak Results :

Index	Name	Time [Min]	Quantity [% Area]	Height [mAU]	Area [mAU.Min]	Area % [%]
1	UNKNOWN	14.08	13.21	107.0	38.4	13.212
2	UNKNOWN	19.42	86.79	358.6	252.3	86.788
Total			100.00	465.6	290.7	100.000

Methyl 3-oxo-7-phenyl-2-oxabicyclo[4.1.0]hept-4-ene-7-carboxylate (377a)

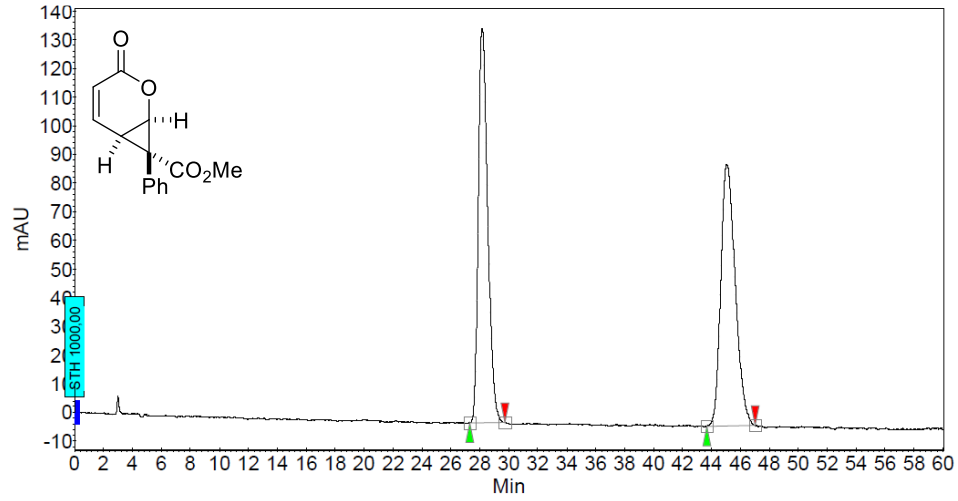

Peak Results :

Index	Name	Time [Min]	Quantity [% Area]	Height [mAU]	Area [mAU.Min]	Area % [%]
1	UNKNOWN	28.16	49.50	137.5	103.7	49.499
2	UNKNOWN	45.05	50.50	91.3	105.8	50.501
Total			100.00	228.8	209.4	100.000

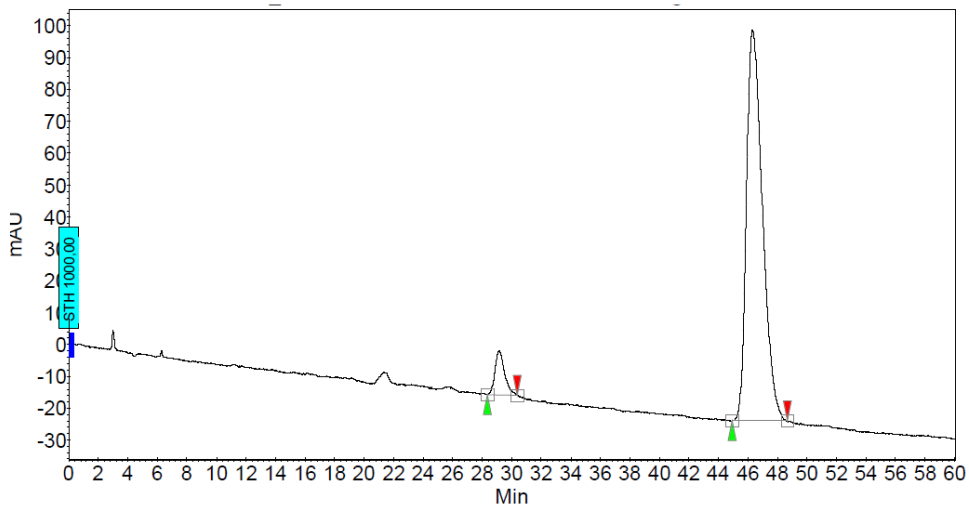

Peak Results :

Index	Name	Time [Min]	Quantity [% Area]	Height [mAU]	Area [mAU.Min]	Area % [%]
1	UNKNOWN	29.15	6.29	13.8	10.3	6.286
2	UNKNOWN	46.32	93.71	122.7	154.3	93.714
Total			100.00	136.4	164.6	100.000

4 X-ray data

X-ray crystallography structure of **367a** (the ellipsoid contour percent probability level is 50%).

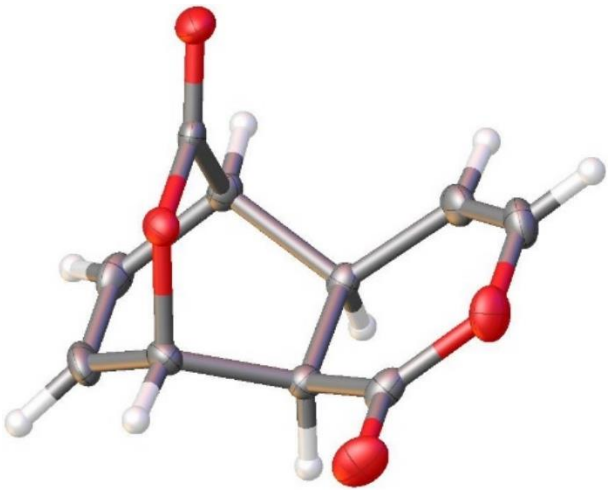

Compound	**Q174**
Formula	$C_{10}H_8O_4$
$D_{calc.}$/ g cm^{-3}	1.546
m/mm^{-1}	1.027
Formula Weight	192.16
Colour	clear colourless
Shape	prism
Max Size/mm	0.33
Mid Size/mm	0.26
Min Size/mm	0.13
T/K	122.99(10)
Crystal System	orthorhombic
Flack Parameter	0.00(6)
Hooft Parameter	-0.01(4)
Space Group	$Pna2_1$
a/Å	12.9535(3)
b/Å	6.90480(10)
c/Å	9.2292(2)
a/°	90
b/°	90
g/°	90
V/Å^3	825.47(3)
Z	4
Z'	1
Q_{min}/°	6.836
Q_{max}/°	75.981
Measured Refl.	13889
Independent Refl.	1732
Reflections Used	1726
R_{int}	0.0345
Parameters	127
Restraints	1
Largest Peak	0.161
Deepest Hole	-0.151
GooF	1.072
wR_2 (all data)	0.0646
wR_2	0.0646
R_1 (all data)	0.0244
R_1	0.0243

X-ray crystallography structure of **367b** (the ellipsoid contour percent probability level is 50%).

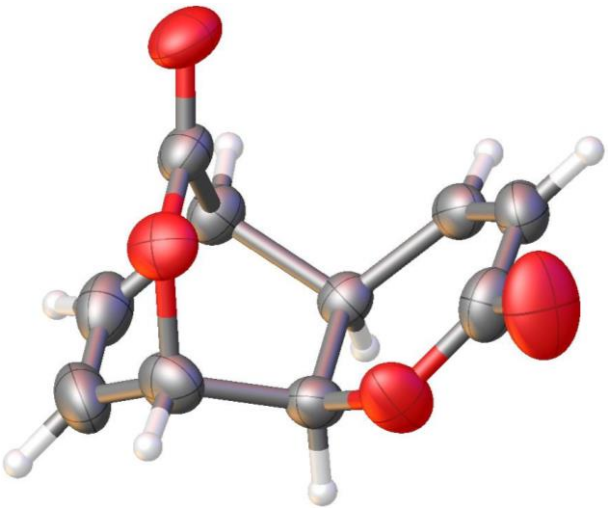

Compound	**Q176**
Formula	$C_{10}H_8O_4$
$D_{calc.}$/ g cm^{-3}	1.520
m/mm^{-1}	1.010
Formula Weight	192.16
Colour	clear colourless
Shape	prism
Size/mm^3	0.27×0.17×0.06
T/K	296.9(7)
Crystal System	monoclinic
Space Group	$P2_1/c$
a/Å	6.4822(2)
b/Å	12.2757(4)
c/Å	10.5683(3)
a/°	90
b/°	93.126(2)
g/°	90
V/Å^3	839.71(4)
Z	4
Z'	1
Wavelength/Å	1.54184
Radiation type	CuK_a
Q_{min}/°	5.528
Q_{max}/°	73.685
Measured Refl.	17038
Independent Refl.	1675
Reflections Used	1481
R_{int}	0.0408
Parameters	127
Restraints	0
Largest Peak	0.190
Deepest Hole	-0.231
GooF	1.066
wR_2 (all data)	0.1010
wR_2	0.0958
R_1 (all data)	0.0419
R_1	0.0371

X-ray crystallography structure of **377a** (the ellipsoid contour percent probability level is 50%).

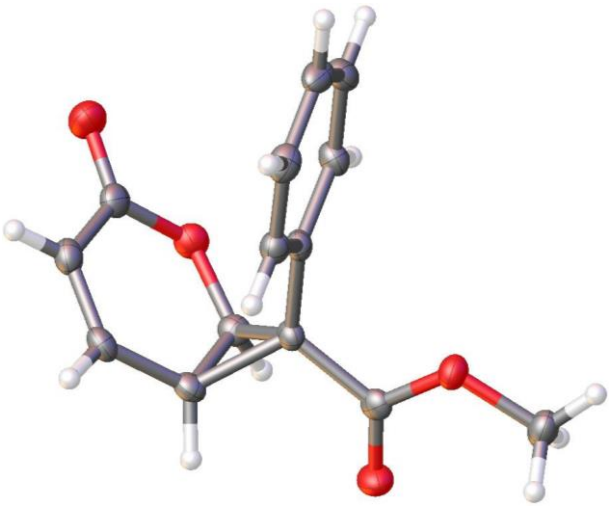

Compound	**S144**
Formula	$C_{14}H_{12}O_4$
$D_{calc.}$/ g cm^{-3}	1.417
□/mm^{-1}	0.867
Formula Weight	244.24
Colour	clear colourless
Shape	prism
Size/mm^3	0.14×0.08×0.04
T/K	122.93(18)
Crystal System	monoclinic
Flack Parameter	-0.02(10)
Hooft Parameter	-0.01(8)
Space Group	$P2_1$
a/Å	8.5849(2)
b/Å	7.83773(17)
c/Å	8.61592(16)
□/°	90
□/°	99.086(2)
□/°	90
V/Å^3	572.46(2)
Z	2
Z'	1
Wavelength/Å	1.54184
Radiation type	Cu K□
□$_{min}$/°	5.199
□$_{max}$/°	74.315
Measured Refl's.	7123
Ind't Refl's	2283
Refl's with I > 2(I)	2203
R_{int}	0.0296
Parameters	164
Restraints	1
Largest Peak	0.187
Deepest Hole	-0.142
GooF	1.065
wR_2 (all data)	0.0735
wR_2	0.0725
R_1 (all data)	0.0297
R_1	0.0283

X-ray crystallography structure of **377b** (the ellipsoid contour percent probability level is 50%).

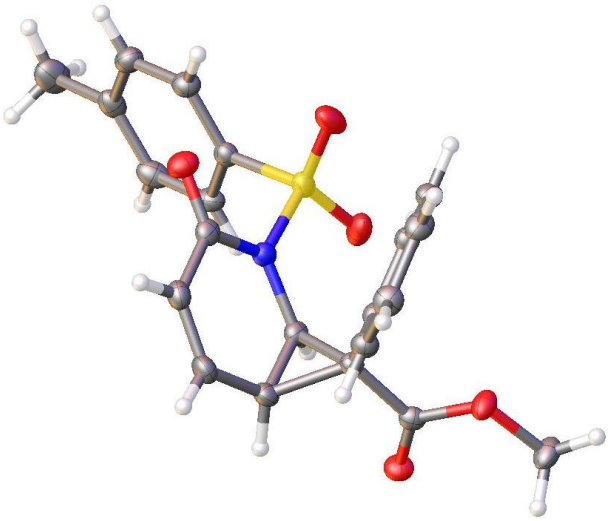

Compound	**S143**
Formula	$C_{21}H_{19}NO_5S$
$D_{calc.}$/ g cm^{-3}	1.409
□/mm^{-1}	1.828
Formula Weight	397.43
Colour	clear colourless
Shape	irregular
Size/mm^3	0.17×0.13×0.06
T/K	123.01(10)
Crystal System	monoclinic
Space Group	$P2_1/c$
a/Å	16.9878(3)
b/Å	15.4001(3)
c/Å	7.23590(15)
□/°	90
□/°	98.2042(19)
□/°	90
V/Å^3	1873.64(6)
Z	4
Z'	1
Wavelength/Å	1.54184
Radiation type	Cu K□
□$_{min}$/°	3.892
□$_{max}$/°	76.011
Measured Refl's.	18181
Ind't Refl's	3861
Refl's with I > 2(I)	3510
R_{int}	0.0218
Parameters	256
Restraints	0
Largest Peak	0.328
Deepest Hole	-0.336
GooF	1.057
wR_2 (all data)	0.0809
wR_2	0.0782
R_1 (all data)	0.0328
R_1	0.0294

X-ray crystallography structure of **431eD** (the ellipsoid contour percent probability level is 50%).

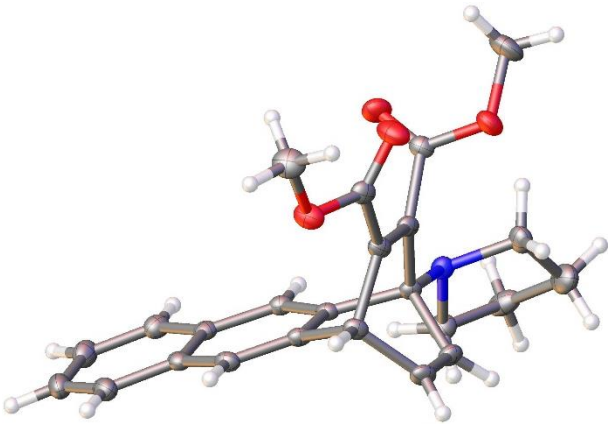

Compound	**R040**
Formula	$C_{24}H_{23}NO_4$
$D_{calc.}$/ g cm^{-3}	1.347
□/mm^{-1}	0.742
Formula Weight	389.43
Colour	clear yellow
Shape	block
Size/mm^3	0.30×0.27×0.20
T/K	122.9(2)
Crystal System	orthorhombic
Flack Parameter	-0.06(5)
Hooft Parameter	-0.05(5)
Space Group	$P2_12_12_1$
a/Å	6.74420(10)
b/Å	7.90290(10)
c/Å	36.0260(3)
□/°	90
□/°	90
□/°	90
V/Å^3	1920.14(4)
Z	4
Z'	1
Wavelength/Å	1.54184
Radiation type	CuK□
□$_{min}$/°	4.910
□$_{max}$/°	74.780
Measured Refl.	22748
Independent Refl.	3901
Reflections Used	3824
R_{int}	0.0300
Parameters	264
Restraints	0
Largest Peak	0.155
Deepest Hole	-0.245
GooF	1.049
wR_2 (all data)	0.0771
wR_2	0.0765
R_1 (all data)	0.0291
R_1	0.0285

5 Curriculum Vitae

Personal data

Name	Michael Leitner
Date of birth	August 1, 1991 in Prien am Chiemsee
Nationality	German
Email	Michael.Leitner@chemie.uni-regensburg.de

Education

Since 11/2016	Ph.D. thesis in the group of Prof. Dr. O. Reiser at the University of Regensburg, Germany
09/2016	Master of Science in chemistry
1/2016-09/2016	Master thesis in the group of Prof. Dr. O. Reiser at the University of Regensburg, Germany
10/2014 – 09/2016	Advanced studies in chemistry, University of Regensburg, Germany
09/2014	Bachelor of science in chemistry
10/2011 – 09/2014	Studies in chemistry, University of Regensburg, Germany
09/2002 – 05/2011	Allgemeine Hochschulreife (A-levels), Ludwig-Thoma-Gymnasium (secondary school), Prien am Chiemsee, Germany

Professional References

Prof. Dr. Oliver Reiser
Institut für Organische Chemie
Universität Regensburg, Universitätsstr. 31
93053 Regensburg, Germany
Phone: 0049 941 943 4631

Conferences

7th EuCheMS Chemistry Congress (26.-30.08.2018), Liverpool, United Kingdom

‘‘*Sustainable synthesis of 3-substituted phthalides*’’ (Poster)

GDCh-Wissenschaftsforum 2017 (10.-14.09.2017), Berlin, Germany

‘‘*Synthesis of 3H-isobenzofuran-1-ones starting from renewable resources*’’ (Poster)

26th ISHC-congress (03.-08.09.2017), Regensburg, Germany

‘‘*Sustainable synthesis of 3-substituted phthalides from pyrones*’’ (Poster)

Regularly Group Seminar Research Report (oral presentation, 15 min)

G References

(1) Newman, D. J.; Cragg, G. M. *J. Nat. Prod.* **2020**, *83*, 770–803.

(2) Dickinson, J. M. *Nat. Prod. Rep.* **1993**, *10*, 71–98.

(3) McGlacken, G. P.; Fairlamb, I. J. S. *Nat. Prod. Rep.* **2005**, *22*, 369–385.

(4) Lee, J. S. *Marine drugs* **2015**, *13*, 1581–1620.

(5) Schäberle, T. F. *Beilstein J. Org. Chem.* **2016**, *12*, 571–588.

(6) Goel, A.; Ram, V. J. *Tetrahedron* **2009**, *65*, 7865–7913.

(7) Pratap, R.; Ram, V. J. *Tetrahedron* **2017**, *73*, 2529–2590.

(8) Wickel, S. M.; Citron, C. A.; Dickschat, J. S. *Eur. J. Org. Chem.* **2013**, *2013*, 2906–2913.

(9) (a) Michinobu, T.; Bito, M.; Yamada, Y.; Tanimura, M.; Katayama, Y.; Masai, E.; Nakamura, M.; Otsuka, Y.; Ohara, S.; Shigehara, K. *Polym. J.* **2009**, *41*, 1111–1116; (b) Kraus, G. A.; Pollock III, G. R.; Beck, C. L.; Palmer, K.; Winter, A. H. *RSC Adv.* **2013**, *3*, 12721.

(10) Baumann, M.; Baxendale, I. R. *Beilstein J. Org. Chem.* **2013**, *9*, 2265–2319.

(11) Sharma, C. P.; Gupta, N. M.; Singh, J.; Yadav, R. A. K.; Dubey, D. K.; Rawat, K. S.; Jha, A. K.; Jou, J.-H.; Goel, A. *J. Org. Chem.* **2019**, *84*, 7674–7684.

(12) Pechmann, H. von. *Liebigs Ann.* **1891**, *264*, 261–309.

(13) Wiley, R. H.; Smith, N. R. *Org. Synth.* **1951**, *31*, 23.

(14) Smith, L. K.; Baxendale, I. R. *React. Chem. Eng.* **2018**, *3*, 722–732.

(15) Leonardi, G.; Li, J.; Righetti, G. I. C.; Truscello, A. M.; Gambarotti, C.; Terraneo, G.; Citterio, A.; Sebastiano, R. *Eur. J. Org. Chem.* **2020**, *2020*, 241–251.

(16) Dobler, D.; Reiser, O. *J. Org. Chem.* **2016**, *81*, 10357–10365.

(17) Tsuda, T.; Morikawa, S.; Sumiya, R.; Saegusa, T. *J. Org. Chem.* **1988**, *53*, 3140–3145.

(18) Louie, J.; Gibby, J. E.; Farnworth, M. V.; Tekavec, T. N. *J. Am. Chem. Soc.* **2002**, *124*, 15188–15189.

(19) Ishii, M.; Mori, F.; Tanaka, K. *Chem. Eur. J.* **2014**, *20*, 2169–2174.

(20) Hou, J.; Ee, A.; Feng, W.; Xu, J.-H.; Zhao, Y.; Wu, J. *J. Am. Chem. Soc.* **2018**, *140*, 5257–5263.

(21) Manikandan, R.; Jeganmohan, M. *Org. Lett.* **2014**, *16*, 652–655.

(22) Larock, R. C.; Doty, M. J.; Han, X. *J. Org. Chem.* **1999**, *64*, 8770–8779.

(23) Mochida, S.; Hirano, K.; Satoh, T.; Miura, M. *J. Org. Chem.* **2009**, *74*, 6295–6298.

(24) Yu, Y.; Huang, L.; Wu, W.; Jiang, H. *Org. Lett.* **2014**, *16*, 2146–2149.

(25) Prakash, R.; Shekarrao, K.; Gogoi, S. *Org. Lett.* **2015**, *17*, 5264–5267.

(26) Yang, Q.-L.; Xing, Y.-K.; Wang, X.-Y.; Ma, H.-X.; Weng, X.-J.; Yang, X.; Guo, H.-M.; Mei, T.-S. *J. Am. Chem. Soc.* **2019**, *141*, 18970–18976.

(27) Kumar, A.; Prabhu, K. R. *J. Org. Chem.* **2020**, *85*, 3548–3559.

(28) Kajita, Y.; Kurahashi, T.; Matsubara, S. *J. Am. Chem. Soc.* **2008**, *130*, 17226–17227.

(29) Matsuda, T.; Suzuki, K. *RSC Adv.* **2014**, *4*, 37138–37141.

(30) Prakash, R.; Shekarrao, K.; Gogoi, S.; Boruah, R. C. *Chem. Commun.* **2015**, *51*, 9972–9974.

(31) Itoh, M.; Shimizu, M.; Hirano, K.; Satoh, T.; Miura, M. *J. Org. Chem.* **2013**, *78*, 11427–11432.

(32) Wu, J.; Wang, D.; Wan, Y.; Ma, C. *Chem. Commun.* **2016**, *52*, 1661–1664.

(33) Zhou, P.; Yang, W.-T.; Rahman, A. U.; Li, G.; Jiang, B. *J. Org. Chem.* **2020**, *85*, 360–366.

(34) Dombray, T.; Blanc, A.; Weibel, J.-M.; Pale, P. *Org. Lett.* **2010**, *12*, 5362–5365.

(35) Chaładaj, W.; Corbet, M.; Fürstner, A. *Angew. Chem. Int. Ed.* **2012**, *51*, 6929–6933.

(36) Luo, T.; Schreiber, S. L. *Angew. Chem. Int. Ed.* **2007**, *46*, 8250–8253.

(37) Sánchez-Larios, E.; Giacometti, R. D.; Hanessian, S. *Eur. J. Org. Chem.* **2014**, *2014*, 5664–5669.

(38) Luo, T.; Dai, M.; Zheng, S.-L.; Schreiber, S. L. *Org. Lett.* **2011**, *13*, 2834–2836.

(39) Wang, Y.; Burton, D. J. *J. Org. Chem.* **2006**, *71*, 3859–3862.

(40) Cherry, K.; Parrain, J.-L.; Thibonnet, J.; Duchêne, A.; Abarbri, M. *J. Org. Chem.* **2005**, *70*, 6669–6675.

(41) Tian, P.-P.; Cai, S.-H.; Liang, Q.-J.; Zhou, X.-Y.; Xu, Y.-H.; Loh, T.-P. *Org. Lett.* **2015**, *17*, 1636–1639.

(42) Ahmad, T.; Qiu, S.-Q.; Xu, Y.-H.; Loh, T.-P. *J. Org. Chem.* **2018**, *83*, 13414–13426.

(43) Qiu, S.-Q.; Ahmad, T.; Xu, Y.-H.; Loh, T.-P. *J. Org. Chem.* **2019**, *84*, 6729–6736.

(44) Fukuyama, T.; Higashibeppu, Y.; Yamaura, R.; Ryu, I. *Organic letters* **2007**, *9*, 587–589.

(45) Kuninobu, Y.; Kawata, A.; Nishi, M.; Takata, H.; Takai, K. *Chem. Commun.* **2008**, 6360–6362.

(46) Grigalunas, M.; Wiest, O.; Helquist, P. *Org. Lett.* **2016**, *18*, 5724–5727.

(47) Huang, J.; Li, L.; Chen, H.; Xiao, T.; He, Y.; Zhou, L. *J. Org. Chem.* **2017**, *82*, 9204–9209.

(48) Bellina, F.; Biagetti, M.; Carpita, A.; Rossi, R. *Tetrahedron* **2001**, *57*, 2857–2870.

(49) Yao, T.; Larock, R. C. *J. Org. Chem.* **2003**, *68*, 5936–5942.

(50) Faizi, D. J.; Issaian, A.; Davis, A. J.; Blum, S. A. *J. Am. Chem. Soc.* **2016**, *138*, 2126–2129.

(51) Yata, T.; Kita, Y.; Nishimoto, Y.; Yasuda, M. *J. Org. Chem.* **2019**, *84*, 14330–14341.

(52) Zhu, X.-F.; Schaffner, A.-P.; Li, R. C.; Kwon, O. *Org. Lett.* **2005**, *7*, 2977–2980.

(53) Yeh, P.-P.; Daniels, D. S. B.; Cordes, D. B.; Slawin, A. M. Z.; Smith, A. D. *Org. Lett.* **2014**, *16*, 964–967.

(54) (a) Kong, X.; Zhang, G.; Yang, S.; Liu, X.; Fang, X. *Adv. Synth. Catal.* **2017**, *359*, 2729–2734; (b) Zheng, P.; Li, C.; Mou, C.; Pan, D.; Wu, S.; Xue, W.; Jin, Z.; Chi, Y. R. *Asian J. Org. Chem.* **2019**, *8*, 1067–1070; (c) Bera, S.; Studer, A. *Synthesis* **2016**, *49*, 121–126; (d) Lang, M.; Jia, Q.; Wang, J. *Chem. Asian. J.* **2018**, *13*, 2427–2430.

(55) Wang, G.; Chen, X.; Miao, G.; Yao, W.; Ma, C. *J. Org. Chem.* **2013**, *78*, 6223–6232.

(56) Xu, L.-C.; Zhou, P.; Li, J.-Z.; Hao, W.-J.; Tu, S.-J.; Jiang, B. *Org. Chem. Front.* **2018**, *5*, 753–759.

(57) Sathishkannan, G.; Srinivasan, K. *Adv. Synth. Catal.* **2014**, *356*, 729–735.

(58) Zhu, Y.; Gong, Y. *J. Org. Chem.* **2015**, *80*, 490–498.

(59) Kim, H. Y.; Oh, K. *Org. Lett.* **2017**, *19*, 4904–4907.

(60) Zhang, W.-Z.; Yang, M.-W.; Lu, X.-B. *Green Chem.* **2016**, *18*, 4181–4184.

(61) Zhou, Y.; Chen, X.; Ling, X.; Rao, W. *Green Chem.* **2019**, *21*, 5611–5615.

(62) Joule, J. A.; Mills, K. *Heterocyclic Chemistry;* A John Wiley & Sons, Ltd., Publication, United Kingdom, 2010.

(63) Vogel, G. *J. Org. Chem.* **1965**, *30*, 203–207.

(64) Sun, C.-L.; Fürstner, A. *Angew. Chem. Int. Ed.* **2013**, *52*, 13071–13075.

(65) Zhuo, C.-X.; Fürstner, A. *Angew. Chem. Int. Ed.* **2016**, *55*, 6051–6056.

(66) Zhuo, C.-X.; Fürstner, A. *J. Am. Chem. Soc.* **2018**, *140*, 10514–10523.

(67) Agarwal, J.; Bayounes, O.; Thorimbert, S.; Dechoux, L. *RSC Adv* **2014**, *4*, 2772–2775.

(68) Plevová, K.; Chang, L.; Martin, E.; Llopis, Q.; Dechoux, L.; Thorimbert, S. *Adv. Synth. Catal.* **2016**, *358*, 3293–3297.

(69) Maji, T.; Tunge, J. A. *Org. Lett.* **2015**, *17*, 4766–4769.

(70) (a) Shimo, T.; Somekawa, K.; Wakikawa, Y.; Uemura, H.; Tsuge, O.; Imada, K.; Tanabe, K. *Bull. Chem. Soc. Jpn.* **1987**, *60*, 621–626; (b) Shimo, T.; Yasuda, M.; Tajima, J.; Somekawa, K. *Heterocycl. Chem.* **1991**, *28*, 745–748.

(71) Corey, E. J.; Streith, J. *J. Am. Chem. Soc.* **1964**, *86*, 950–951.

(72) Williams, J. D.; Otake, Y.; Coussanes, G.; Saridakis, I.; Maulide, N.; Kappe, C. O. *ChemPhotoChem* **2019**, *3*, 229–232.

(73) Frébault, F.; Luparia, M.; Oliveira, M. T.; Goddard, R.; Maulide, N. *Angew. Chem. Int. Ed.* **2010**, *49*, 5672–5676.

(74) Luparia, M.; Oliveira, M. T.; Audisio, D.; Frébault, F.; Goddard, R.; Maulide, N. *Angew. Chem. Int. Ed.* **2011**, *50*, 12631–12635.

(75) Niyomchon, S.; Audisio, D.; Luparia, M.; Maulide, N. *Org. Lett.* **2013**, *15*, 2318–2321.

(76) Souris, C.; Misale, A.; Chen, Y.; Luparia, M.; Maulide, N. *Org. Lett.* **2015**, *17*, 4486–4489.

(77) Souris, C.; Frébault, F.; Patel, A.; Audisio, D.; Houk, K. N.; Maulide, N. *Org. Lett.* **2013**, *15*, 3242–3245.

(78) Chen, Y.; Coussanes, G.; Souris, C.; Aillard, P.; Kaldre, D.; Runggatscher, K.; Kubicek, S.; Di Mauro, G.; Maryasin, B.; Maulide, N. *J. Am. Chem. Soc.* **2019**, *141*, 13772–13777.

(79) (a) Nistanaki, S. K.; Boralsky, L. A.; Pan, R. D.; Nelson, H. M. *Angew. Chem. Int. Ed.* **2019**, *58*, 1724–1726; (b) Gutekunst, W. R.; Baran, P. S. *J. Am. Chem. Soc.* **2011**, *133*, 19076–19079; (c) Gutekunst, W. R.; Gianatassio, R.; Baran, P. S. *Angew. Chem. Int. Ed.* **2012**, *51*, 7507–7510.

(80) Colvin, E. W.; Thom, I. G. *Tetrahedron* **1986**, *42*, 3137–3146.

(81) Imagawa, T.; Sueda, N.; Kawanisi, M. *J. Chem. Soc., Chem. Commun.* **1972**, 388.

(82) Afarinkia, K.; Vinader, V.; Nelson, T. D.; Posner, G. H. *Tetrahedron* **1992**, *48*, 9111–9171.

(83) Diels, O.; Alder, K. *Ann.* **1931**, *490*, 257–266.

(84) Shah, T. K.; Medina, J. M.; Garg, N. K. *J. Am. Chem. Soc.* **2016**, *138*, 4948–4954.

(85) Bronner, S. M.; Bahnck, K. B.; Garg, N. K. *Org. Lett.* **2009**, *11*, 1007–1010.

(86) Kirkham, J. D.; Butlin, R. J.; Harrity, J. P. A. *Angew. Chem. Int. Ed.* **2012**, *51*, 6402–6405.

(87) Habicht, M. H.; Wossidlo, F.; Bens, T.; Pidko, E. A.; Müller, C. *Chem. Eur. J.* **2018**, *24*, 944–952.

(88) Habicht, M. H.; Wossidlo, F.; Weber, M.; Müller, C. *Chem. Eur. J.* **2016**, *22*, 12877–12883.

(89) Wang, Y.; Li, H.; Wang, Y.-Q.; Liu, Y.; Foxman, B. M.; Deng, L. *J. Am. Chem. Soc.* **2007**, *129*, 6364–6365.

(90) Shi, L.-M.; Dong, W.-W.; Tao, H.-Y.; Dong, X.-Q.; Wang, C.-J. *Org. Lett.* **2017**, *19*, 4532–4535.

(91) Zhao, P.; Beaudry, C. M. *Angew. Chem. Int. Ed.* **2014**, *53*, 10500–10503.

(92) Cole, C. J. F.; Fuentes, L.; Snyder, S. A. *Chemical science* **2020**, *11*, 2175–2180.

(93) (a) Markó, I. E.; Chellé-Regnaut, I.; Leroy, B.; Warriner, S. L. *Tetrahedron Lett.* **1997**, *38*, 4269–4272; (b) Markó, I. E.; Evans, G. R. *Tetrahedron Lett.* **1994**, *35*, 2771–2774; (c) Markó, I. E.; Evans, G. R.; Declercq, J.-P. *Tetrahedron* **1994**, *50*, 4557–4574; (d) Posner, G. H.; Carry, J.-C.; Kyoo Lee, J.; Bull, D.S.; Dai, H. *Tetrahedron Lett.* **1994**, *35*, 1321–1324; (e) Posner, G. H.; Dai, H.; Bull, D. S.; Lee, J.-K.; Eydoux, F.; Ishihara, Y.; Welsh, W.; Pryor, N.; Petr, S. *J. Org. Chem.* **1996**, *61*, 671–676; (f) Posner, G. H.; Eydoux, F.; Lee, J. K.; Bull, D.S. *Tetrahedron Lett.* **1994**, *35*, 7541–7544.

(94) Liang, X.-W.; Zhao, Y.; Si, X.-G.; Xu, M.-M.; Tan, J.-H.; Zhang, Z.-M.; Zheng, C.-G.; Zheng, C.; Cai, Q. *Angew. Chem. Int. Ed.* **2019**, *58*, 14562–14567.

(95) (a) Watanabe, S.; Nishikawa, T.; Nakazaki, A. *Org. Lett.* **2019**, *21*, 7410–7414; (b) Wang, N.; Du, S.; Li, D.; Jiang, X. *Org. Lett.* **2017**, *19*, 3167–3170; (c) Liang, X.; Zhou, L.; Min, L.; Ye, W.; Bao, W.; Ma, W.; Yang, Q.; Qiao, F.; Zhang, X.; Lee, C.-S. *J. Org. Chem.* **2017**, *82*, 3463–3481.

(96) Lee, J.-H.; Cho, C.-G. *Org. Lett.* **2018**, *20*, 7312–7316.

(97) Gan, P.; Smith, M. W.; Braffman, N. R.; Snyder, S. A. *Angew. Chem. Int. Ed.* **2016**, *55*, 3625–3630.

(98) Trost, B. M.; Wang, Y. *Angew. Chem. Int. Ed.* **2018**, *57*, 11025–11029.

(99) (a) Trost, B. M.; Schneider, S. *Angew. Chem. Int. Ed. Engl.* **1989**, *28*, 213–215; (b) Zheng, S.; Lu, X. *Org. Lett.* **2009**, *11*, 3978–3981.

(100) Gao, X.; Xia, M.; Yuan, C.; Zhou, L.; Sun, W.; Li, C.; Wu, B.; Zhu, D.; Zhang, C.; Zheng, B.; Wang, D.; Guo, H. *ACS Catal.* **2019**, *9*, 1645–1654.

(101) Liu, K.; Teng, H.-L.; Wang, C.-J. *Org. Lett.* **2014**, *16*, 4508–4511.

(102) Giardinetti, M.; Jessen, N. I.; Christensen, M. L.; Jørgensen, K. A. *Chem. Commun.* **2018**, *55*, 202–205.

(103) Jessen, H. J.; Gademann, K. *Nat. Prod. Rep.* **2010**, *27*, 1168–1185.

(104) Liu, Y.; Zhang, Q.; Chen, L.-H.; Yang, H.; Lu, W.; Xie, X.; Nan, F.-J. *ACS Med. Chem. Lett.* **2016**, *7*, 579–583.

(105) Hu, L.; Feng, H.; Zhang, H.; Yu, S.; Zhao, Q.; Wang, W.; Bao, F.; Ding, X.; Hu, J.; Wang, M.; Xu, Y.; Wu, Z.; Li, X.; Tang, Y.; Mao, F.; Chen, X.; Zhang, H.; Li, J. *J. Med. Chem.* **2020**, *63*, 1051–1067.

(106) Lv, Z.; Sheng, C.; Wang, T.; Zhang, Y.; Liu, J.; Feng, J.; Sun, H.; Zhong, H.; Niu, C.; Li, K. *J. Med. Chem.* **2010**, *53*, 660–668.

(107) Vincetti, P.; Caporuscio, F.; Kaptein, S.; Gioiello, A.; Mancino, V.; Suzuki, Y.; Yamamoto, N.; Crespan, E.; Lossani, A.; Maga, G.; Rastelli, G.; Castagnolo, D.; Neyts, J.; Leyssen, P.; Costantino, G.; Radi, M. *J. Med. Chem.* **2015**, *58*, 4964–4975.

(108) Liu, Z.; Yao, Y.; Kogiso, M.; Zheng, B.; Deng, L.; Qiu, J. J.; Dong, S.; Lv, H.; Gallo, J. M.; Li, X.-N.; Song, Y. *J. Med. Chem.* **2014**, *57*, 8307–8318.

(109) Gorobets, N. Y.; Yousefi, B. H.; Belaj, F.; Kappe, C.O. *Tetrahedron* **2004**, *60*, 8633–8644.

(110) Hammes, G. G.; Lillford, P. J. *J. Am. Chem. Soc.* **1970**, *92*, 7578–7585.

(111) Rawson, J. M.; Winpenny, R. E.P. *Coord. Chem. Rev.* **1995**, *139*, 313–374.

(112) Dimroth, K. *Angew. Chem. Int. Ed.* **1960**, *72*, 331–342.

(113) Moloney, H.; Magnus, N. A.; Buser, J. Y.; Embry, M. C. *J. Org. Chem.* **2017**, *82*, 6279–6288.

(114) Disadee, W.; Lekky, A.; Ruchirawat, S. *J. Org. Chem.* **2020**, *85*, 1802–1822.

(115) Kume, T.; Kojima, T.; Iwasaki, H.; Yamamoto, Y.; Akiba, K. *J. Org. Chem.* **1989**, *54*, 1931–1935.

(116) Mao, B.; Fañanás-Mastral, M.; Feringa, B. L. *Org. Lett.* **2013**, *15*, 286–289.

(117) Ireland, R. E.; McGarvey, G. J.; Anderson, R. C.; Badoud, R.; Fitzsimmons, B. *J. Am. Chem. Soc.* **1980**, *102*, 6178–6180.

(118) Yanai, H.; Kobayashi, O.; Takada, K.; Isono, T.; Satoh, T.; Matsumoto, T. *Chem. Commun.* **2016**, *52*, 3280–3283.

(119) Liu, Q.; Zu, L. *Angew. Chem.* **2018**, *130*, 9649–9653.

(120) Chang, L.; Thorimbert, S.; Dechoux, L. *Org. Biomol. Chem.* **2019**, *17*, 2784–2791.

(121) Palani, V.; Hugelshofer, C. L.; Sarpong, R. *J. Am. Chem. Soc.* **2019**, *141*, 14421–14432.

(122) Kurasawa, K.; Kwon, E.; Kuwahara, S.; Enomoto, M. *Org. Lett.* **2018**, *20*, 4645–4648.

(123) Ohyoshi, T.; Mitsugi, K.; Higuma, T.; Ichimura, F.; Yoshida, M.; Kigoshi, H. *RSC Adv.* **2019**, *9*, 7321–7323.

(124) Liu, Z.; Meinwald, J. *J. Org. Chem.* **1996**, *61*, 6693–6699.

(125) Lee, J.-H.; Kim, W.-S.; Lee, Y. Y.; Cho, C.-G. *Tetrahedron Lett.* **2002**, *43*, 5779–5782.

(126) Gravett, E. C.; Hilton, P. J.; Jones, K.; Péron, J.-M. *Synlett* **2003**, 253–255.

(127) Bellina, F.; Biagetti, M.; Carpita, A.; Rossi, R. *Tetrahedron Lett.* **2001**, *42*, 2859–2863.

(128) Lee, J.-H.; Park, J.-S.; Cho, C.-G. *Org. Lett.* **2002**, *4*, 1171–1173.

(129) Kim, W.-S.; Kim, H.-J.; Cho, C.-G. *J. Am. Chem. Soc.* **2003**, *125*, 14288–14289.

(130) (a) Frébault, F.; Oliveira, M. T.; Wöstefeld, E.; Maulide, N. *J. Org. Chem.* **2010**, *75*, 7962–7965; (b) Kuroda, J.-i.; Inamoto, K.; Hiroya, K.; Doi, T. *Eur. J. Org. Chem.* **2009**,

2009, 2251–2261; (c) Shah, P.; Santana, M. D.; García, J.; Serrano, J. L.; Naik, M.; Pednekar, S.; Kapdi, A. R. *Tetrahedron* **2013**, *69*, 1446–1453.

(131) Nolan, M.-T.; Pardo, L. M.; Prendergast, A. M.; McGlacken, G. P. *J. Org. Chem.* **2015**, *80*, 10904–10913.

(132) Burns, M. J.; Thatcher, R. J.; Taylor, R. J. K.; Fairlamb, I. J. S. *Dalton Trans.* **2010**, *39*, 10391–10400.

(133) Nolan, M.-T.; Bray, J. T.W.; Eccles, K.; Cheung, M. S.; Lin, Z.; Lawrence, S. E.; Whitwood, A. C.; Fairlamb, I. J.S.; McGlacken, G. P. *Tetrahedron* **2014**, *70*, 7120–7127.

(134) Pardo, L. M.; Prendergast, A. M.; Nolan, M.-T.; Ó Muimhneacháin, E.; McGlacken, G. P. *Eur. J. Org. Chem.* **2015**, 3540–3550.

(135) Prendergast, A. M.; Pardo, L. M.; Fairlamb, I. J. S.; McGlacken, G. P. *Eur. J. Org. Chem.* **2017**, *2017*, 5119–5124.

(136) Mackey, K.; Pardo, L. M.; Prendergast, A. M.; Nolan, M.-T.; Bateman, L. M.; McGlacken, G. P. *Org. Lett.* **2016**, *18*, 2540–2543.

(137) Cheng, C.; Chen, W.-W.; Xu, B.; Xu, M.-H. *J. Org. Chem.* **2016**, *81*, 11501–11507.

(138) Zhang, J.; Zhuang, Y.; Ma, Y.; Yang, X.; Szostak, M. *Adv. Synth. Catal.* **2019**, *361*, 5709–5714.

(139) Lah, H. U.; Rasool, F.; Yousuf, S. K. *RSC Adv.* **2015**, *5*, 78958–78961.

(140) Rosenblum, M.; Gatsonis, C. *J. Am. Chem. Soc.* **1967**, *89*, 5074–5075.

(141) Fairlamb, I. J.; Syvänne, S. M.; Whitwood, A. C. *Synlett* **2003**, 1693–1697.

(142) Lin, Q.; Leong, W. K. *Organometallics* **2003**, *22*, 3639–3648.

(143) Rosenblum, M.; North, B.; Wells, D.; Giering, W. P. *J. Am. Chem. Soc.* **1972**, *94*, 1239–1246.

(144) Saura-Llamas, I.; Dalton, D. M.; Arif, A. M.; Gladysz, J. A. *Organometallics* **1992**, *11*, 683–693.

(145) Fairlamb, I. J. S.; Lynam, J. M.; Taylor, I. E.; Whitwood, A. C. *Organometallics* **2004**, *23*, 4964–4969.

(146) Fairlamb, I. J. S.; Lynam, J. M.; Moulton, B. E.; Taylor, I. E.; Duhme-Klair, A. K.; Sawle, P.; Motterlini, R. *Dalton Trans.* **2007**, 3603–3605.

(147) Fairlamb, I. J. S.; Duhme-Klair, A.-K.; Lynam, J. M.; Moulton, B. E.; O'Brien, C. T.; Sawle, P.; Hammad, J.; Motterlini, R. *Bioorg. Med. Chem. Lett.* **2006**, *16*, 995–998.

(148) Sawle, P.; Hammad, J.; Fairlamb, I. J. S.; Moulton, B.; O'Brien, C. T.; Lynam, J. M.; Duhme-Klair, A. K.; Foresti, R.; Motterlini, R. *J. Pharm. Exp. Ther.* **2006**, *318*, 403–410.

(149) Diercks, R.; Arndt, J.-D.; Freyer, S.; Geier, R.; Machhammer, O.; Schwartze, J.; Volland, M. *Chem. Eng. Technol.* **2008**, *31*, 631–637.

(150) (a) Ragauskas, A. J.; Williams, C. K.; Davison, B. H.; Britovsek, G.; Cairney, J.; Eckert, C. A.; Frederick, W. J.; Hallett, J. P.; Leak, D. J.; Liotta, C. L.; Mielenz, J. R.; Murphy, R.; Templer, R.; Tschaplinski, T. *Science* **2006**, *311*, 484–489; (b) Binder, J. B.; Raines, R. T. *J. Am. Chem. Soc.* **2009**, *131*, 1979–1985.

(151) Zhou, C.-H.; Xia, X.; Lin, C.-X.; Tong, D.-S.; Beltramini, J. *Chem. Soc. Rev.* **2011**, *40*, 5588–5617.

(152) Verband der chemischen Industrie e.V. Energiestatistik in Daten und Fakten.

(153) (a) Chapman, O. L.; Hess, T. C. *J. Org. Chem.* **1979**, *44*, 962–964; (b) Morris, M. R.; Waring, A. J. *J. Chem. Commun.* **1969**, 526–527; (c) Klunder, A. J. H.; Bos, W.; Verlaak, J. M. M.; Zwanenburg, B. *Tetrahedron Lett.* **1981**, *22*, 4553–4556; (d) Houwen-Claassen, A. A. M.; Klunder, A. J. H.; Zwanenburg, B. *Tetrahedron* **1989**, *45*, 7134–7148.

(154) (a) Klunder, A. J. H.; Bos, W.; Zwanenburg, B. *Tetrahedron Lett.* **1981**, *22*, 4557–4560; (b) Zhu, J.; Klunder, A. J. H.; Zwanenburg, B. *Tetrahedron* **1994**, *50*, 10597–10610; (c) Zhu, J.; Yang, J.-Y.; Klunder, A. J. H.; Liu, Z.-Y.; Zwanenburg, B. *Tetrahedron* **1995**, *51*, 5847–5870.

(155) Corma, A.; Iborra, S.; Velty, A. *Chem. Rev.* **2007**, *107*, 2411–2502.

(156) Dutta, S.; De, S.; Saha, B.; Alam, M. I. *Catal. Sci. Technol.* **2012**, *2*, 2025.

(157) Mamman, A. S.; Lee, J.-M.; Kim, Y.-C.; Hwang, I. T.; Park, N.-J.; Hwang, Y. K.; Chang, J.-S.; Hwang, J.-S. *Biofuels, Bioprod. Bioref.* **2008**, *2*, 438–454.

(158) Achmatowicz, O.; Bielski, R. *Carbohydrate Research* **1977**, *55*, 165–176.

(159) Piancatelli, G.; Scettri, A.; Barbadoro, S. *Tetrahedron Lett.* **1976**, *17*, 3555–3558.

(160) Ulbrich, K.; Kreitmeier, P.; Reiser, O. *Synlett* **2010**, *2010*, 2037–2040.

(161) Dobler, D. Conversion of 4-hydroxy-2-cyclopentenone derivatives into valuable fine chemicals. Dissertation, Universität Regensburg, Regensburg, 2017.

(162) (a) Zimmermann, H. E.; Grunewald, G. L.; Paufler, R. M. *Org. Synth.* **1966**, *46*, 101–104; (b) Nakagawa, M.; Saegusa, J.; Tonozuka, M.; Obi, M.; Kiuchi, M.; Hino, T.; Ban, Y. *Org. Synth.* **1977**, *56*, 49–52; (c) Izumi, T.; Kasahara, A. *Bull. Chem. Soc. Jpn.* **1975**,

48, 1673–1674; (d) Chidambaram, N.; Satyanarayana, K.; Chandrasekaran, S. *Tetrahedron Lett.* **1989**, *30*, 2429–2432.

(163) Dols, P. P. M.; Klunder, A. J. H.; Zwanenburg, B. *Tetrahedron* **1994**, *50*, 8515–8538.

(164) (a) Eddolls, J. P.; Iqbal, M.; Roberts, S. M.; Santoro, M. G. *Tetrahedron* **2004**, *60*, 2539–2550; (b) Mander, L. N.; Thomson, R. J. *J. Org. Chem.* **2005**, *70*, 1654–1670; (c) Sugahara, T.; Fukuda, H.; Iwabuchi, Y. *J. Org. Chem.* **2004**, *69*, 1744–1747; (d) Takano, S.; Kamikubo, T.; Moriya, M.; Ogasawara, K. *Synthesis* **1994**, *1994*, 601–604; (e) Tanaka, K.; Nakashima, H.; Taniguchi, T.; Ogasawara, K. *Org. Lett.* **2000**, *2*, 1915–1917.

(165) Karpf, M. *Angew. Chem. Int. Ed.* **1986**, *25*, 414–430.

(166) Seybold, G. *Angew. Chem. Int. Ed.* **1977**, *16*, 365–373.

(167) Moss, M. O.; Jackson, R. M.; Rogers, D. *Phytochemistry* **1975**, *14*, 2706–2708.

(168) Amaral, P. A.; Gouault, N.; Le Roch, M.; Eifler-Lima, V. L.; David, M. *Tetrahedron Lett.* **2008**, *49*, 6607–6609.

(169) Soldi, C.; Moro, A. V.; Pizzolatti, M. G.; Correia, C. R. D. *Eur. J. Org. Chem.* **2012**, 3607–3616.

(170) Zhu, J.; Klunder, A. J.H.; Zwanenburg, B. *Tetrahedron* **1995**, *51*, 5099–5116.

(171) Karmakar, R.; Pahari, P.; Mal, D. *Chem. Rev.* **2014**, *114*, 6213–6284.

(172) (a) Beck, J. J.; Chou, S.-C. *J. Nat. Prod.* **2007**, *70*, 891–900; (b) Zhang, H.; Zhang, S.; Liu, L.; Luo, G.; Duan, W.; Wang, W. *J. Org. Chem.* **2010**, *75*, 368–374.

(173) Diao, X.; Deng, P.; Xie, C.; Li, X.; Zhong, D.; Zhang, Y.; Chen, X. *Drug Metab. Dispos.* **2013**, *41*, 430–444.

(174) Zhang, B.; Xu, M.-H.; Lin, G.-Q. *Org. Lett.* **2009**, *11*, 4712–4715.

(175) (a) Kitamura, M.; Ohkuma, T.; Inoue, S.; Sayo, N.; Kumobayashi, H.; Akutagawa, S.; Ohta, T.; Takaya, H.; Noyori, R. *J. Am. Chem. Soc.* **1988**, *110*, 629–631; (b) Everaere, K.; Scheffler, J.-L.; Mortreux, A.; Carpentier, J.-F. *Tetrahedron Lett.* **2001**, *42*, 1899–1901.

(176) Lu, B.; Zhao, M.; Ding, G.; Xie, X.; Jiang, L.; Ratovelomanana-Vidal, V.; Zhang, Z. *ChemCatChem* **2017**, *9*, 3989–3996.

(177) Phan, D. H. T.; Kim, B.; Dong, V. M. *J. Am. Chem. Soc.* **2009**, *131*, 15608–15609.

(178) Tanaka, K.; Osaka, T.; Noguchi, K.; Hirano, M. *Org. Lett.* **2007**, *9*, 1307–1310.

(179) Shinohara, H.; Sonoda, M.; Atobe, S.; Masuno, H.; Ogawa, A. *Tetrahedron Lett.* **2011**, *52*, 6238–6241.

(180) Afarinkia, K.; Vinader, V.; Nelson, T. D.; Posner, G. H. *Tetrahedron* **1992**, *48*, 9111–9171.

(181) Loupy, A.; Maurel, F.; Sabatié-Gogová, A. *Tetrahedron* **2004**, *60*, 1683–1691.

(182) Kappe, C. O. *Angew. Chem. Int. Ed.* **2004**, *43*, 6250–6284.

(183) Ward, D. E.; Souweha, M. S. *Org. Lett.* **2005**, *7*, 3533–3536.

(184) Birkett, S.; Ganame, D.; Hawkins, B. C.; Meiries, S.; Quach, T.; Rizzacasa, M. A. *Org. Lett.* **2011**, *13*, 1964–1967.

(185) Billingsley, K. L.; Buchwald, S. L. *J. Org. Chem.* **2008**, *73*, 5589–5591.

(186) (a) Vijgen, S.; Nauwelaerts, K.; Wang, J.; van Aerschot, A.; Lagoja, I.; Herdewijn, P. *J. Org. Chem.* **2005**, *70*, 4591–4597; (b) Jung, Y.-G.; Lee, S.-C.; Cho, H.-K.; Darvatkar, N. B.; Song, J.-Y.; Cho, C.-G. *Org. Lett.* **2013**, *15*, 132–135; (c) Pfennig, T.; Chemburkar, A.; Johnson, R. L.; Ryan, M. J.; Rossini, A. J.; Neurock, M.; Shanks, B. H. *ACS Catal.* **2018**, *8*, 2450–2463.

(187) Pirkle, W. H.; McKendry, L. H. *Tetrahedron Lett.* **1968**, *9*, 5279–5282.

(188) Kerres, S.; Plut, E.; Malcherek, S.; Rehbein, J.; Reiser, O. *Adv. Synth. Catal.* **2019**, *361*, 1400–1407.

(189) (a) Fehr, M. J.; Consiglio, G.; Scalone, M.; Schmid, R. *J. Org. Chem.* **1999**, *64*, 5768–5776; (b) Huck, W.-R.; Bürgi, T.; Mallat, T.; Baiker, A. *J. Catal.* **2003**, *219*, 41–51.

(190) (a) Hale, K. J.; Hummersone, M. G.; Bhatia, G. S. *Org. Lett.* **2000**, *2*, 2189–2192; (b) Huang, H.; Panek, J. S. *Org. Lett.* **2003**, *5*, 1991–1993; (c) Tarver, J. E.; Joullié, M. M. *J. Org. Chem.* **2004**, *69*, 815–820.

(191) Davies, H. M. L.; Hedley, S. J. *Chem. Soc. Rev.* **2007**, *36*, 1109–1119.

(192) Davies, H. M. L.; Denton, J. R. *Chem. Soc. Rev.* **2009**, *38*, 3061–3071.

(193) Lehner, V.; Davies, H. M. L.; Reiser, O. *Org. Lett.* **2017**, *19*, 4722–4725.

(194) Fu, J.; Wurzer, N.; Lehner, V.; Reiser, O.; Davies, H. M. L. *Org. Lett.* **2019**, *21*, 6102–6106.

(195) Davies, H.; Babal, T.; Liu, W.; Röther, A.; Reiser, O. *Chem. Eur. J.* **2019**.

(196) Pilsl, L. K. A.; Ertl, T.; Reiser, O. *Org. Lett.* **2017**, *19*, 2754–2757.

(197) Schneider, T. F.; Kaschel, J.; Werz, D. B. *Angew. Chem. Int. Ed.* **2014**, *53*, 5504–5523.

(198) Reddy, R. P.; Davies, H. M. L. *J. Am. Chem. Soc.* **2007**, *129*, 10312–10313.

(199) Jurberg, I. D.; Davies, H. M. L. *Chem. Sci.* **2018**, *9*, 5112–5118.

(200) Hiroya, K.; Jouka, R.; Katoh, O.; Sakuma, T.; Anzai, M.; Sakamoto, T. *Arkivoc* **2003**, 232–246.

(201) Davies, H. M. L.; Bruzinski, P. R.; Lake, D. H.; Kong, N.; Fall, M. J. *J. Am. Chem. Soc.* **1996**, *118*, 6897–6907.

(202) Davies, H. M.L.; Bruzinski, P. R.; Fall, M. J. *Tetrahedron Lett.* **1996**, *37*, 4133–4136.

(203) (a) Chhor, R. B.; Nosse, B.; Sörgel, S.; Böhm, C.; Seitz, M.; Reiser, O. *Chem. Eur. J.* **2003**, *9*, 260–270; (b) Gharpure, S. J.; Shukla, M. K.; Vijayasree, U. *Org. Lett.* **2009**, *11*, 5466–5469.

(204) (a) Liu, Z.; Lin, X.; Yang, N.; Su, Z.; Hu, C.; Xiao, P.; He, Y.; Song, Z. *J. Am. Chem. Soc.* **2016**, *138*, 1877–1883; (b) Saito, A.; Yanai, H.; Taguchi, T. *Tetrahedron Lett.* **2004**, *45*, 9439–9442; (c) Yanai, H.; Takahashi, A.; Taguchi, T. *Tetrahedron* **2007**, *63*, 12149–12159.

(205) (a) Brown, M. K.; Degrado, S. J.; Hoveyda, A. H. *Angew. Chem. Int. Ed.* **2005**, *44*, 5306–5310; (b) Fan, X.-Z.; Rong, J.-W.; Wu, H.-L.; Zhou, Q.; Deng, H.-P.; Tan, J. D.; Xue, C.-W.; Wu, L.-Z.; Tao, H.-R.; Wu, J. *Angew. Chem. Int. Ed.* **2018**, *57*, 8514–8518; (c) Khiar, N.; Valdivia, V.; Salvador, Á.; Chelouan, A.; Alcudia, A.; Fernández, I. *Adv. Synth. Catal.* **2013**, *355*, 1303–1307; (d) Le Nôtre, J.; Allen, J. C.; Frost, C. G. *Chem. Commun.* **2008**, 3795–3797; (e) Liang, L.; Su, L.; Li, X.; Chan, A. S.C. *Tetrahedron Lett.* **2003**, *44*, 7217–7220; (f) Liang, L.; Yan, M.; Li, Y.-M.; Chan, A. S.C. *Tetrahedron: Asymmetry* **2004**, *15*, 2575–2578; (g) Maciver, E. E.; Maksymowicz, R. M.; Wilkinson, N.; Roth, P. M. C.; Fletcher, S. P. *Org. Lett.* **2014**, *16*, 3288–3291; (h) Walter, C.; Auer, G.; Oestreich, M. *Angew. Chem. Int. Ed.* **2006**, *45*, 5675–5677.

(206) (a) Aggarwal, V. K.; Emme, I.; Fulford, S. Y. *J. Org. Chem.* **2003**, *68*, 692–700; (b) Bugarin, A.; Connell, B. T. *J. Org. Chem.* **2009**, *74*, 4638–4641; (c) Karur, S.; Hardin, J.; Headley, A.; Li, G. *Tetrahedron Lett.* **2003**, *44*, 2991–2994.

(207) (a) Kitanosono, T.; Xu, P.; Kobayashi, S. *Chem. Asian. J.* **2014**, *9*, 179–188; (b) Ebel, H.; Zeitler, K.; Steglich, W. *Synthesis* **2003**, 101–106; (c) Martínez-Fructuoso, L.; Pereda-Miranda, R.; Rosas-Ramírez, D.; Fragoso-Serrano, M.; Cerda-García-Rojas, C. M.; da Silva, A. S.; Leitão, G. G.; Leitão, S. G. *J. Nat. Prod.* **2019**, *82*, 520–531; (d) Sawant, K. B.; Jennings, M. P. *J. Org. Chem.* **2006**, *71*, 7911–7914.

(208) Wolberg, M.; Dassen, B. H. N.; Schürmann, M.; Jennewein, S.; Wubbolts, M. G.; Schoemaker, H. E.; Mink, D. *Adv. Synth. Catal.* **2008**, *350*, 1751–1759.

(209) Yadav, V. K.; Kapoor, K. K. *Tetrahedron* **1995**, *51*, 8573–8584.

(210) (a) Weisser, R.; Yue, W.; Reiser, O. *Org. Lett.* **2005**, *7*, 5353–5356; (b) Roy, S.; Reiser, O. *Angew. Chem. Int. Ed.* **2012**, *51*, 4722–4725; (c) Garve, L. K. B.; Barkawitz, P.;

Jones, P. G.; Werz, D. B. *Org. Lett.* **2014**, *16*, 5804–5807; (d) Kreft, A.; Jones, P. G.; Werz, D. B. *Org. Lett.* **2018**, *20*, 2059–2062.

(211) Yedoyan, J.; Wurzer, N.; Klimczak, U.; Ertl, T.; Reiser, O. *Angew. Chem. Int. Ed.* **2019**, *58*, 3594–3598.

(212) (a) Yet, L. *Chem. Rev.* **2000**, *100*, 2963–3008; (b) Wei, Y.; Liu, S.; Li, M.-M.; Li, Y.; Lan, Y.; Lu, L.-Q.; Xiao, W.-J. *J. Am. Chem. Soc.* **2019**, *141*, 133–137.

(213) Li, M.; Lin, S.; Dong, Z.; Zhang, X.; Liang, F.; Zhang, J. *Org. Lett.* **2013**, *15*, 3978–3981.

(214) Reissig, H.-U.; Zimmer, R. *Chem. Rev.* **2003**, *103*, 1151–1196.

(215) (a) Danheiser, R. L.; Martinez-Davila, C.; Morin, J. M. *J. Org. Chem.* **1980**, *45*, 1340–1341; (b) Danheiser, R. L.; Bronson, J. J.; Okano, K. *J. Am. Chem. Soc.* **1985**, *107*, 4579–4581; (c) Davies, H. M.L.; Hu, B. *Tetrahedron Lett.* **1992**, *33*, 455–456; (d) McGaffin, G.; Grimm, B.; Heinecke, U.; Michaelsen, H.; Meijere, A. d.; Walsh, R. *Eur. J. Org. Chem.* **2001**, *2001*, 3559–3573; (e) Murray, C. K.; Yang, D. C.; Wulff, W. D. *J. Am. Chem. Soc.* **1990**, *112*.

(216) Davies, H. M. L.; Hu, B. *J. Org. Chem.* **1992**, *57*, 3186–3190.

(217) Bisacchi, G. S.; Chao, S. T.; Bachard, C.; Daris, J. P.; Innaimo, S.; Jacobs, G. A.; Kocy, O.; Lapointe, P.; Martel, A.; Merchant, Z.; Slusarchyk, W. A.; Sundeen, J. E.; Young, M. G.; Colonno, R.; Zahler, R. *Bioorg. Med. Chem. Lett.* **1997**, *7*, 127–132.

(218) (a) Wang, S.-c.; Zhang, X.-q.; Gu, H.-m.; Zhu, X.-y.; Guo, Y.-j. *Org. Prep. Proced. Int.* **2017**, *49*, 568–574; (b) La Clair, J. J. *Angew. Chem. Int. Ed.* **2006**, *45*, 2769–2773; (c) Tsuna, K.; Noguchi, N.; Nakada, M. *Angew. Chem. Int. Ed.* **2011**, *50*, 9452–9455; (d) Tsuna, K.; Noguchi, N.; Nakada, M. *Chem. Eur. J.* **2013**, *19*, 5476–5486.

(219) Schaudt, M.; Blechert, S. *J. Org. Chem.* **2003**, *68*, 2913–2920.

(220) Kress, S.; Weckesser, J.; Schulz, S. R.; Blechert, S. *Eur. J. Org. Chem.* **2013**, *2013*, 1346–1355.

(221) (a) Fringuelli, F.; Taticchi, A. *The Diels Alder reaction*: Selected practical methods; Wiley, Chichester, New York, 2002; (b) Atherton, J.C.C.; Jones, S. *Tetrahedron* **2003**, *59*, 9039–9057.

(222) Wiberg, K. B. *J. Org. Chem.* **1997**, *62*, 5720–5727.

(223) Klanderman, B. H. *J. Am. Chem. Soc.* **1965**, *87*, 4649–4651.

(224) Godinez, C. E.; Zepeda, G.; Mortko, C. J.; Dang, H.; Garcia-Garibay, M. A. *J. Org. Chem.* **2004**, *69*, 1652–1662.

(225) Rigaudy, J.; Thang, K. V. *Compt. Rend.* **1965**, *260*, 2527–2530.

(226) Nikitin, K.; Müller-Bunz, H.; McGlinchey, M. J. *Organometallics* **2013**, *32*, 6118–6129.

(227) Chen, H.; Yao, E.; Xu, C.; Meng, X.; Ma, Y. *Org. Biomol. Chem.* **2014**, *12*, 5102–5107.

(228) Chen, Q.; Chen, H.; Meng, X.; Ma, Y. *Org. Lett.* **2015**, *17*, 5016–5019.

(229) Yoshizawa, M.; Tamura, M.; Fujita, M. *Science* **2006**, *312*, 251–254.

(230) Taylor, R. G. D.; Carta, M.; Bezzu, C. G.; Walker, J.; Msayib, K. J.; Kariuki, B. M.; McKeown, N. B. *Org. Lett.* **2014**, *16*, 1848–1851.

(231) Tius, M. A.; Gomez-Galeno, J.; Zaidi, J. H. *Tetrahedron Lett.* **1988**, *29*, 6909–6912.

(232) Kendall, J. K.; Shechter, H. *J. Org. Chem.* **2001**, *66*, 6643–6649.

(233) Ngoc, V. N. 1,4-Cycloaddition of anthracenes and practical method for the synthesis of chiral diamino alcohols. Dissertation, Universität Regensburg, Regensburg, 2017.

(234) Bouffard, J.; Eaton, R. F.; Müller, P.; Swager, T. M. *J. Org. Chem.* **2007**, *72*, 10166–10180.

(235) (a) Heinrich, M. R.; Klisa, H. S.; Mayr, H.; Steglich, W.; Zipse, H. *Angew. Chem. Int. Ed.* **2003**, *42*, 4826–4828; (b) Held, I.; Villinger, A.; Zipse, H. *Synthesis* **2005**, *2005*, 1425–1430.

(236) Verma, S. M.; Singh, M. D. *J. Org. Chem.* **1977**, *42*, 3736–3740.

(237) Pauling, L. *J. Am. Chem. Soc.* **1947**, *69*, 542–553.

(238) Marcus, R. A. *J. Phys. Chem.* **1968**, *72*, 891–899.

(239) Streitwieser, A.; Heathcock, C. H. *Introduction to Organic Chemistry;* Macmillan, New York, 1981.

(240) (a) Duan, S.; Turk, J.; Speigle, J.; Corbin, J.; Masnovi, J.; Baker, R. J. *J. Org. Chem.* **2000**, *65*, 3005–3009; (b) Cakmak, O.; Erenler, R.; Tutar, A.; Celik, N. *J. Org. Chem.* **2006**, *71*, 1795–1801.

(241) Das, B.; Venkateswarlu, K.; Majhi, A.; Siddaiah, V.; Reddy, K. R. *J. Mol. Catal. A: Chem.* **2007**, *267*, 30–33.

(242) Breton, G. *Adv. Chem. Lett.* **2013**, *1*, 68–73.

(243) Tang, R.-J.; Milcent, T.; Crousse, B. *Eur. J. Org. Chem.* **2017**, 4753–4757.

(244) Southgate, E. H.; Pospech, J.; Fu, J.; Holycross, D. R.; Sarlah, D. *Nat. Chem.* **2016**, *8*, 922–928.

(245) Bouas-Laurent, H.; Desvergne, J.-P.; Castellan, A.; Lapouyade, R. *Chem. Soc. Rev.* **2001**, *30*, 248–263.

(246) Bailey, D.; Williams, V. E. *J. Org. Chem.* **2006**, *71*, 5778–5780.

(247) Bouas-Laurent, H.; Desvergne, J.-P.; Castellan, A.; Lapouyade, R. *Chem. Soc. Rev.* **2000**, *29*, 43–55.

(248) Becker, H.-D.; Becker, H.-C.; Langer, V. *J. Photochem. Photobiol. A* **1996**, *97*, 25–32.

(249) Armarego, W. L. F.; Chai, C. L. L. *Purification of Laboratory Chemicals*, 6th ed.; Elsevier/BH, Oxford, 2009.

(250) Lee, M.; Neukirchen, S.; Cabrele, C.; Reiser, O. *J. Pept. Sci.* **2017**, *23*, 556–562.

(251) Pirtsch, M.; Paria, S.; Matsuno, T.; Isobe, H.; Reiser, O. *Chem. Eur. J.* **2012**, *18*, 7336–7340.

(252) Zheng, Y.; Bian, R.; Zhang, X.; Yao, R.; Qiu, L.; Bao, X.; Xu, X. *Eur. J. Org. Chem.* **2016**, *2016*, 3872–3877.

(253) Fu, L.; Mighion, J. D.; Voight, E. A.; Davies, H. M. L. *Chem. Eur. J.* **2017**, *23*, 3272–3275.

(254) Yamawaki, M.; Tsutsui, H.; Kitagaki, S.; Anada, M.; Hashimoto, S. *Tetrahedron Lett.* **2002**, *43*, 9561–9564.

(255) Qin, C.; Boyarskikh, V.; Hansen, J. H.; Hardcastle, K. I.; Musaev, D. G.; Davies, H. M. L. *J. Am. Chem. Soc.* **2011**, *133*, 19198–19204.

(256) Reddy, R. P.; Lee, G. H.; Davies, H. M. L. *Org. Lett.* **2006**, *8*, 3437–3440.

(257) (a) Breton, G. W.; Turlington, M. *Tetrahedron Lett.* **2014**, *55*, 4661–4663; (b) Cookson, R. C.; Gupte, S. S.; Stevens, I. D. R.; Watts, C. T. *Org. Synth.* **1971**, *51*, 121.

(258) Zhu, J.; Yang, J.-Y.; Klunder, A. J. H.; Liu, Z.-Y.; Zwanenburg, B. *Tetrahedron* **1995**, *51*, 5847–5870.

(259) Pirkle, W. H.; Dines, M. *J. Heterocycl. Chem.* **1969**, *6*, 1–3.

(260) Wang, H.-Y. L.; Qi, Z.; Wu, B.; Kang, S.-W.; Rojanasakul, Y.; O'Doherty, G. A. *ACS Med. Chem. Lett.* **2011**, *2*, 259–263.

(261) Ma, Y.; O'Doherty, G. A. *Org. Lett.* **2015**, *17*, 5280–5283.

(262) Otero, M. P.; Santín, E. P.; Rodríguez-Barrios, F.; Vaz, B.; Lera, Á. R. de. *Bioorg. Med. Chem. Lett.* **2009**, *19*, 1883–1886.

(263) Billington, D. C.; Helps, I. M.; Pauson, P. L.; Thomson, W.; Willison, D. *J. Organomet. Chem.* **1988**, *354*, 233–242.

(264) Carreno, M. C.; Ruano, J. L.; Urbanoy, A. *J. Org. Chem.* **1992**, *57*, 6870–6876.

(265) M. J. Frisch, G. W. Trucks, H. B. Schlegel, G. E. Scuseria, M. A. Robb, J. R. Cheeseman, G. Scalmani, V. Barone, B. Mennucci, G. A. Petersson, H. Nakatsuji, M. Caricato, X. Li, H. P. Hratchian, A. F. Izmaylov, J. Bloino, G. Zheng, J. L. Sonnenberg, M. Hada, M. Ehara, K. Toyota, R. Fukuda, J. Hasegawa, M. Ishida, T. Nakajima, Y. Honda, O. Kitao, H. Nakai, T. Vreven, J. A. Montgomery, Jr., J. E. Peralta, F. Ogliaro, M. Bearpark, J. J. Heyd, E. Brothers, K. N. Kudin, V. N. Staroverov, T. Keith, R. Kobayashi, J.

Normand, K. Raghavachari, A. Rendell, J. C. Burant, S. S. Iyengar, J. Tomasi, M. Cossi, N. Rega, J. M. Millam, M. Klene, J. E. Knox, J. B. Cross, V. Bakken, C. Adamo, J. Jaramillo, R. Gomperts, R. E. Stratmann, O. Yazyev, A. J. Austin, R. Cammi, C. Pomelli, J. W. Ochterski, R. L. Martin, K. Morokuma, V. G. Zakrzewski, G. A. Voth, P. Salvador, J. J. Dannenberg, S. Dapprich, A. D. Daniels, O. Farkas, J. B. Foresman, J. V. Ortiz, J. Cioslowski, and D. J. Fox. *Gaussian 09, Revision E.01;* Gaussian, Inc., Wallingford CT, 2013.

(266) (a) Lee, C.; Yang, W.; Parr, R. G. *Phys. Rev. B* **1988**, *37*, 785–789; (b) Krishnan, R.; Binkley, J. S.; Seeger, R.; Pople, J. A. *J. Chern. Phys.* **1980**, *72*, 650–654; (c) Becke, A. D. *J. Chem. Phys.* **1993**, *98*, 5648–5652.

(267) Grimme, S.; Antony, J.; Ehrlich, S.; Krieg, H. *J. Phys. Chem.* **2010**, *132*, 154104.

(268) Mulliken, R. S. *J. Chem. Phys.* **1955**, *23*, 1833–1840.

(269) (a) NBO Version 3.1, E. D. Glendening, A. E. Reed, J. E. Carpenter, and F. Weinhold as implemented in Gaussian09.E01; (b) Foster, J. P.; Weinhold, F. *J. Am. Chem. Soc.* **1980**, *102*, 7211–7218; (c) Reed, A. E.; Weinstock, R. B.; Weinhold, F. *J. Chem. Phys.* **1985**, *83*, 735–746; (d) Reed, A. E.; Weinhold, F. *J. Chem. Phys.* **1985**, *83*, 1736–1740; (e) Reed, A. E.; Curtiss, L. A.; Weinhold, F. *Chem. Rev.* **1988**, *88*, 899–926.

(270) (a) Pauling, L. *J. Am. Chem. Soc.* **1947**, *69*, 543–553; (b) Houk, K. N.; Gustafson, S. M.; Black, K. A. *J. Am. Chem. Soc.* **1992**, *114*, 8565–8572.

(271) (a) Marcus, R. A. *J. Phys. Chem.* **1968**, *72*, 891–899; (b) Follet, E.; Mayer, P.; Mayr, H. *Eur. J. Org. Chem.* **2016**, *2016*, 4050–4058.

H Acknowledgment

Ich bedanke mich bei Prof. Oliver Reiser für die Überlassung des äußerst interessanten Themas und seine beständige Unterstützung während der gesamten Arbeit.

Ebenfalls großer Dank gebührt Dr. Peter Kreitmeier für seine Hilfe bei technischen und chemischen Problemen sowie für die unzähligen fachlichen, aber besonders auch für die nicht fachlichen Diskussionen. Außerdem bedanke ich mich bei Klaus Döring, Johanes Floß, Roxane Harteis, Helena Konkel und Brigitte Eichenseher für die Unterstützung im Laboralltag.

Vielen Dank an Prof. Julia Rehbein und Patrick Sakrausky für die Durchführung der theoretischen Berechnungen zu den Diels-Alder Reaktionen der Anthracene. Vielen Dank auch an Jiantao Fu (AK Prof. Davies, Atlanta) für seine Kollaboration bei der enantioselektiven Cyclopropanierung der Pyrone und Pyridinone.

Bei allen Mitarbeitern der zentralen Analytik möchte ich mich bedanken. Besonders bedanke ich mich bei den Mitarbeitern der Röntgenstrukturanalyse Dr. Michael Bodensteiner, Dr. Stefanie Gärtner, Sabine Stempfhuber und Birgit Hirscha für die Messung der Kristallstrukturen, sowie Josef Kiermaier und Wolfgang Söllner für die Messung der Massenspektren. Des Weiteren bei den Mitarbeitern der NMR Abteilung Dr. Ilya Shenderovich, Fritz Kastner, Veronica Scheidler, Annette Schramm und Georgine Stühler.

Ein herzliches Dankeschön an unsere Sekretärinnen, Antje Weigert und Michaela Schüle, für aller Hilfe organisatorischer Art.

Herzlichen Dank an alle aktuellen und ehemaligen Mitarbeiter des AK Reisers für die gute Atmosphäre, die schönen Aktivitäten am und außerhalb des Arbeitskreises. Besonders danken möchte ich Verena Lehner, Thomas Ertl, Daniel Dobler, Corina Neumeister, Matthias Gnahn, Benjamin Kastl, Martin Hofman, Saerom Park, Sabine Kerres, Thomas Föll, Simon Budde, Aditya Bhattacharyya, Tobias Babl, Robert Eckl, Peter Ehrnsberger, Christian Eichinger, Sebastian Engl, Sebastian Fischer, Andreas Hartl, Tomislav Krolo, Natalija Moor, Eva Plut, Roxane Harteis, Carina Sonnleitner, Lisa Stadler, Lukas Traub, Andreas Ratzenböck und Thomas Weinbender.

Für das gewissenhafte Korrekturlesen bedanke ich mich herzlichst bei Sebastian Fischer, Sabine Kerres, Sebastian mein Engl, Aditya Bhattacharyya und Tomislav Krolo.

Außerdem danke ich meinen ehemaligen Bachelorstudenten und Forschungspraktikanten Andreas Ratzenböck, Sebastian Hauer, Simon Scheuerer und Fabian Schabenberger.

Vielen lieben Dank an meine Laborkollegen, Sabine Kerres, Thomas Ertl, Robert Eckl, Eva Plut, Tomislav Krolo und Aditya Bhattacharyya für die gute Zusammenarbeit und lustige Zeit im Labor 33.1.19, aber auch dafür, dass ihr meine laute Musik täglich ertragen habt. Mein besonderer Dank gilt hierbei Tom und Sabine, die mich gleich als neues Mitglied im Labor aufgenommen haben und mir eine extreme Hilfe waren. Danke auch für unsere Laborabende und die schöne Zeit außerhalb der Universität.

Liebe Sabine, ich kann dir gar nicht genug danken für deine Unterstützung jeglicher Art und vor allem für deine Freundschaft. Es war ja schon fast Laborehe auf dem ersten Blick. Du hast sehr großen Anteil daran, dass diese Zeit immer unvergessen bleibt.

Tomislav moje sunce, brate moje, hvala. ću uvijek ću biti tvoj heroj. Ich vermisse jetzt schon unsere Tanz- und Gesangseinlagen. Wir sind so richtige Tschucksl. Kad se sjetim, suza krene. Lijepa li si.

An meine Leidgenossen Lisa Stadler, Christian Eichinger, Andreas Hartl, Lukas Traub, Thomas Weinbender und Peter Ehrnsberger ein herzliches Dankeschön. Wir waren ein super Jahrgang und keine Spreu.

Für die schönen Ausflüge, die Konferenzen, die Küchenpartys, die morgendlichen Kaffeepausen, für diese unvergessliche Zeit möchte ich mich herzlich bei Benjamin Kastl, Matthias Gnahn, Lisa Stadler, Sabine Kerres, Peter Ehrnsberger, Thomas Föll, Sebastian Fischer, Sebastian Engl, Carina Sonnleitner und Tomislav Krolo bedanken.

Vielen Dank an die Regensburg Familie Flori, Messut, Resi, Nini, Sebi, Otzi, Schäffer, Luca, Basti, Lisa und Julia für diese Wahnsinnszeit in Regensburg. Egal ob Sport, Grillen oder Fortgehen, es war immer super lustig. Ihr habt die Zeit hier zu was Besonderem gemacht.

Tobi, Kalle, Hias, Michi, Pol, Felix und Nuschey herzliches Merce für alles. Ohne euch wäre alles deutlich schwieriger gewesen und das Leben ganz schön langweilig. Dr. Sepp und Tino auch an euch ein großes Dankeschön. Egal ob Skiausflug oder Raguse-Dachterrasse es ist immer eine super Zeit mit euch. Natürliche bedanke ich mich auch bei allen Biergls und Proseccls. Ihr seid der Wahnsinn. Danke auch an den TuS Prien und seinen Spielern, dass trotz Trainingsmangel immer ein Platz für mich im Team war. Besonders möchte ich mich hier bei Opa, Jochen, Nicolai und Yannick bedanken. TuS ein Leben lang.

Mein größter Dank geht an meine ganze Familie für ihre unerschütterliche Unterstützung. Ohne euch wäre alles nicht möglich gewesen und dafür bin ich euch unendlich dankbar. Danke Baba, Dedo, Oma, Tetkas und Ojkos. Markus und Thomas danke für alles. Ihr seid die besten Brüder, die man sich nur wünschen kann. Mama und Papa, ohne euch wäre ich nie so weit gekommen. Eure unermüdliche Unterstützung ermutigt mich immer wieder meine Ziele zu verfolgen.

I Declaration

Herewith I declare that this present thesis is a presentation of my original work prepared single-handed. Wherever contributions from others are involved, all of them are marked clearly, with reference to the literature, license, and acknowledgment of collaborative research.

Regensburg, July 02, 2020

Michael Leitner